

N° d'ordre :

THESE

présentée à

L'UNIVERSITE DES SCIENCES ET TECHNOLOGIES DE LILLE

pour obtenir le grade de

DOCTEUR EN CHIMIE ORGANIQUE ET MACROMOLECULAIRE

par

Jérôme GROMADA

**Alcoolates de Terres Rares : Synthèse, Caractérisation
et Application à la (Co)-Polymérisation d'Oléfines**

Soutenue le 22 octobre 2003 devant la commission d'examen :

J.-C. BOIVIN	Président
M. BOCHMANN	Rapporteur
A. DEFFIEUX	Rapporteur
F. LEISING	Examinateur
T. MATHIVET	Examinateur
A. MORTREUX	Examinateur
J.-F. CARPENTIER	Examinateur

Acknowledgements

This Ph.D. work was carried out at the “Laboratoire de Catalyse de Lille” under the direction of Professor André Mortreux of Lille University. I would like to express my sincere gratitude and deep appreciation to him for his excellent supervision on this research.

First, I would like to thank Pr. Jean-Claude Boivin of Lille University for chairing my committee.

I am grateful to Pr. Alain Deffieux of Bordeaux University and to Pr. Manfred Bochmann of Norwich (East Anglia) University for their interest in this work and for accepting to be Examiners of this Board.

I also thank Dr. Frédéric Leising of Rhodia Recherches for initiating this fruitful collaboration and for helpful discussions.

I sincerely thank Pr. Jean-François Carpentier of Rennes University for efficiently supervising this thesis. His valuable guidance and constructive criticism have been of importance and influence to me.

I extend my warm thanks to Dr. Thomas Chenal of Lille Univ. and to Dr. Thomas Mathivet of Rhodia Electronics & Catalysis for their kind help and scientific advice.

A special thanks to Pr. Guy Nowogrocki (Lille Univ.) for patiently helping me in resolving X-ray structures. I am also indebted to everyone who gave me technical assistance and expertise for the characterization of the complexes and polymers: Pr. J. W. Ziller (California Univ.; X-ray), A.-M. Cazé (Lille Univ.; SEC), Pr. R. F. Jordan (Chicago Univ.; SEC), N. Djelal (Lille Univ.; DSC), L. Burylo (Lille Univ.; XRD), S. Chlebicki (E.N.S.A.I.T.; preparation of polymer blends), Dr. J.-M. Gloaguen (Lille Univ.; SEM) and Pr. T. Kowalewski (CMU Pittsburgh; AFM).

I undoubtedly want to thank the whole lab staff for their help and all my fellow Ph.D. students for their support and wonderful friendship.

I also thank Rhodia Electronics & Catalysis for financially supporting this thesis.

Last but not least, thanks to Kathelyne.

Table of contents

Introduction.....	16
Chapter 1	
Lanthanide-mediated polymerizations	22
3.Ethylene and α-olefin polymerization.....	24
3.1.Before organometallic catalysis.....	24
3.2.Ziegler-Natta catalysis.....	24
3.3.Metallocene catalysts.....	25
3.4.Post-metallocene catalysts.....	28
3.5.Catalytic systems based on group 3 metals.....	30
3.5.1. <i>Lanthanocene catalysts</i>	30
3.5.1.1.Preliminary studies.....	30
3.5.1.2.Further investigations.....	32
3.5.1.3.Binary lanthanocene catalyst systems.....	35
3.5.1.4.Divalent lanthanocene catalysts.....	36
3.5.2. <i>Ansa-lanthanocene catalysts</i>	36
3.5.3. <i>Monocyclopentadienyl complexes</i>	38
3.5.3.1.Constrained geometry catalysts.....	38
3.5.3.2.Other monocyclopentadienyl complexes.....	39
3.5.3.3.Divalent monocyclopentadienyl complexes.....	40
3.5.4. <i>Chain transfer reactions</i>	41
3.5.4.1.Silanes as chain transfer agent.....	41
3.5.4.2.Thiophene as transfer agent.....	42
3.5.5. <i>Post-lanthanocene catalysts</i>	42
3.5.5.1.Nitrogen-based catalysts.....	43
3.5.5.2.Oxygen-based catalysts.....	47
4.Polymerization of methyl methacrylate initiated by rare earth compounds.....	49
4.1.Introduction.....	49
4.1.1. <i>Anionic polymerization</i>	49
4.1.2. <i>Group transfer polymerization</i>	51
4.1.3. <i>Controlled radical polymerization</i>	51
4.2.Lanthanocene-type catalysts.....	53
4.2.1. <i>Single component initiating systems</i>	53
4.2.1.1.Cyclopentadienyl and pentamethylcyclopentadienyl complexes.....	53
4.2.1.2.Other lanthanocene complexes.....	57
4.2.1.3.Anса-lanthanocene complexes.....	59
4.2.1.4.Half-lanthanocene complexes.....	62
4.2.2. <i>Binary systems</i>	63
4.2.3. <i>Chain transfer reactions in lanthanocene-based MMA polymerizations</i>	65
4.3.Non-metallocene type rare earth metal compounds.....	67
4.3.1. <i>Single component initiating systems</i>	67
4.3.1.1.Allyl complexes.....	67
4.3.1.2.Alkyl-lanthanides.....	68
4.3.1.3.Nitrogen-based ligands.....	69
4.3.1.4.Lanthanide alkoxides.....	70
4.3.1.5.Lanthanide thiolates.....	71

4.3.2. <i>Binary initiating systems</i>	72
4.4. Group 4 organometallic catalyst systems.....	73
4.5. Conclusion.....	75
5. Lanthanide-catalyzed diene polymerization	75
5.1. Introduction.....	75
5.2. Diene polymerization: mechanistic aspect.....	77
5.3. Cis-1,4 lanthanide-based catalyst systems.....	79
<i>5.3.1. Presentation of the catalytic systems</i>	79
<i>5.3.2. General features of the cis-1,4 lanthanide-based catalyst systems</i>	80
<i>5.3.3. Detailed description of Nd(OCOR)3/AlR3/halogen source systems</i>	81
5.3.3.1. Nature of the precursor.....	82
5.3.3.2. Effect of catalyst component addition order.....	82
5.3.3.3. Nature of the active species in Nd(OCOR)3/AlR3/AlEt ₂ Cl.....	83
5.3.3.4. Effect of the concentration of the various components.....	83
<i>5.3.4. Allyl-based catalysts</i>	85
<i>5.3.5. Nitrogen-based ligands</i>	86
<i>5.3.6. Lanthanocene-based catalysts</i>	87
5.4. Trans-1,4 lanthanide-based catalyst systems.....	87
5.5. Styrene-Butadiene copolymerization.....	88
<i>5.5.1. Ternary systems</i>	88
<i>5.5.2. Allyl-based neodymium catalysts</i>	90
<i>5.5.3. Lanthanocene-based catalysts</i>	90
5.6. Conclusion.....	91
Presentation of the research project.....	92
Chapter 2	
Synthesis of lanthanide alkoxides.....	98
7. Synthesis of lanthanide alkoxides and related complexes.....	100
7.1. Introduction.....	100
7.2. Reaction of metal with alcohol.....	101
7.3. Salt metathesis.....	102
<i>7.3.1. In the presence of alcohol</i>	102
<i>7.3.2. In the absence of alcohol</i>	103
7.3.2.1. Lanthanide alkoxides.....	103
7.3.2.2. Lanthanide aryloxides.....	105
7.4. Exchange of organic ligands.....	107
<i>7.4.1. Alcoholysis of tris(amido) complexes</i>	107
7.4.1.1. Lanthanide alkoxides.....	108
7.4.1.2. Lanthanide aryloxides.....	109
7.4.1.3. Lanthanide silyloxides.....	109
7.4.1.4. Functionalized lanthanide alkoxides, aryloxides and silyloxides.....	110
7.4.1.4.1. Alkoxide-based ligands.....	110
7.4.1.4.2. Aryloxide-based ligands.....	110
7.4.1.4.3. Silyloxide-based ligand.....	112
<i>7.4.2. Protonolysis of tris(alkyl) complex</i>	112
<i>7.4.3. Transalkoxylation</i>	113
<i>7.4.4. Carboxylates</i>	113
7.5. Ce(IV) alkoxides: a special case.....	113

7.6.Conclusion.....	114
8.Synthesis of neodymium alkoxides.....	114
8.1.Neodymium tert-butoxides.....	114
8.1.1. <i>Salt metathesis reactions.....</i>	115
8.1.1.1.From anhydrous NdCl ₃ and NaOtBu.....	115
8.1.1.2.From anhydrous NdCl ₃ and MOtBu (M = Li and K) in THF.....	118
8.1.1.3.From NdCl ₃ (THF) ₂ in THF.....	119
8.1.1.3.1.Effect of the reaction time.....	120
8.1.1.3.2.Influence of the neodymium concentration.....	120
8.1.1.4.From NdCl ₃ (THF) ₂ in hexanes.....	121
8.1.1.4.1.Reaction time.....	121
8.1.1.4.2.Neodymium concentration.....	121
8.1.1.5.Conclusions.....	122
8.1.2. <i>Alcoholysis reaction.....</i>	123
8.1.2.1.Reaction in THF.....	123
8.1.2.2.Reaction in non polar solvents.....	123
8.1.2.3.Evolution of Nd ₃ (μ ₃ -OtBu) ₂ (μ ₂ -OtBu) ₃ (OtBu)₄(HOtBu) ₂	124
8.2.Other neodymium tert-alkoxides.....	126
8.2.1. <i>Synthesis of neodymium tert-amyoxyde by salt metathesis.....</i>	126
8.2.2. <i>Synthesis of difunctional tert-alkoxides by alcoholysis reaction.....</i>	129
9.Neodymium aryloxides: a contribution to the reported work.....	132
9.1.Salt metathesis.....	132
9.2.Alcoholysis reaction.....	133
10.Conclusions.....	134
Chapter 3	
Methyl methacrylate polymerization.....	137
12.Methyl methacrylate polymerization: preliminary screening.....	139
13.Optimization of the Nd₃(OtBu)₉(THF)₂/Mg(n-Hex)₂ catalyst system.....	140
13.1.Influence of Nd/Mg ratio.....	140
13.2.Activation temperature.....	143
13.3.Polymerization temperature.....	143
14.Alkylating agent.....	144
15.Neodymium precursor.....	146
16.Proposed mechanism.....	148
17.Conclusion.....	149
Chapter 4	
Ethylene polymerization and diblock copolymerization ethylene-MMA.....	151
19.Ethylene polymerization.....	153
19.1.Introduction.....	153
19.2.Preliminary screening.....	154
19.2.1. <i>Influence of the rare earth metal.....</i>	154

19.2.2. Ethylene polymerization with various Nd alkoxides.....	155
19.2.3. Influence of the synthetic route of neodymium tert-butoxide.....	156
19.3. Ethylene polymerization with Nd ₃ (OtBu) ₉ (THF) ₂ in slurry.....	158
19.3.1. Influence of the nature of the dialkylmagnesium reagent.....	158
19.3.2. Influence of the Nd/Mg ratio.....	159
19.3.3. Influence of activation conditions.....	160
19.3.4. Effect of the polymerization temperature.....	162
19.3.5. Effect of various additives on the polymerization activity.....	162
19.3.6. Polymerization in the presence of transfer agent.....	163
19.3.6.1. Phenylsilane.....	163
19.3.6.2. Molecular dihydrogen.....	164
19.3.7. Effect of further additions of dialkylmagnesium.....	165
19.4. Ethylene polymerization with the precipitated polymer	167
19.4.1. Principle.....	167
19.4.2. Activity of the separated phases.....	167
20. Diblock copolymerizations	169
20.1. Synthesis of olefin-MMA diblock copolymers in the literature.....	169
20.1.1. With lanthanide-based catalysts.....	169
20.1.2. With Group 4 catalysts.....	171
20.1.2.1. Multistep procedures.....	171
20.1.2.2. Two-step procedures.....	173
20.1.3. Indirect method: hydrogenation of polybutadiene	174
20.2. Ethylene-MMA.....	174
20.2.1. Preparation of the copolymers.....	174
20.2.1.1. In situ system.....	175
20.2.1.2. Solid S as initiator.....	175
20.2.2. Morphological characterization.....	175
20.2.3. Application as compatibilizing agent.....	177
20.3. Other diblock copolymerizations.....	178
20.3.1. Ethylene-methyl acrylate diblock copolymerization.....	178
20.3.2. Ethylene-ε-caprolactone diblock copolymerization.....	178
21. Proposed mechanism.....	179
22. Conclusion.....	180
Chapter 5	
Butadiene polymerization	
and diblock copolymerization	
butadiene-glycidyl methacrylate.....	181
24. Introduction.....	183
25. Butadiene homopolymerization.....	183
25.1. With Nd ₃ (OtBu) ₉ (THF) ₂	183
25.1.1. Preliminary results.....	183
25.1.2. Influence of the Nd/Mg ratio.....	185
25.2. With neodymium aryloxides.....	186
25.2.1. Nd(O-2,6-tBu ₂ -4-Me-Ph) ₃ (THF) as precursor.....	186
25.2.2. Nd(O-2,6-tBu ₂ -4-Me-Ph) ₃ as precursor.....	187
26. Butadiene copolymerizations.....	187

26.1. Butadiene-styrene statistical copolymerization.....	187
26.2. Butadiene-glycidyl methacrylate diblock copolymerization.....	189
26.2.1. <i>Initial results: copolymer characterization</i>	190
26.2.2. <i>Copolymerization results</i>	191
27. Mechanistic considerations.....	192
28. Conclusion.....	194
Chapter 6	
Mechanistic study.....	197
1. NMR investigations.....	199
28.1. NMR monitoring of 1/RM.....	199
28.1.1. <i>I/DHM</i>	199
28.1.2. <i>I/MgRR'</i>	201
28.1.3. <i>I/RM systems</i>	202
28.2. "Ln(OtBu)3"/DHM.....	203
28.2.1. <i>Formation of alkenes</i>	203
28.2.2. <i>Evidences for alkyl lanthanide species</i>	204
28.3. "Nd(OR)3"/DHM systems.....	205
28.4. Conclusion.....	206
29. Isolation of active species or intermediates.....	206
29.1. Isolation of metathesis products from "Nd(OR)3"/MgR ₂ systems.....	207
29.2. Isolation of metathesis products from Nd(OAr) ₃ (THF)/MR _z systems.....	214
30. Conclusion.....	217
Concluding remarks.....	220
Experimental section.....	224
32. Solvents and reagents.....	226
33. Analyses.....	227
34. Preparation of lanthanide alkoxides.....	228
34.1. Synthesis of neodymium tert-butoxides.....	228
34.1.1. <i>Nd₃(μ₃-OtBu)₂(μ₂-OtBu)₃(OtBu)4(THF)2 (I)</i>	228
34.1.2. <i>Nd₃(μ₃-OtBu)₂(μ₂-OtBu)₃(OtBu)4(HOtBu)2 (7)</i>	229
34.1.3. <i>Nd₅(μ₅-O)(μ₃-OtBu)4(μ₂-OtBu)4(OtBu)5 (8)</i>	229
34.1.4. <i>Synthesis of neodymium tert-butoxide in hexanes (5) & (6)</i>	230
34.1.5. <i>Various neodymium tert-butoxides prepared by salt metathesis</i>	230
34.2. Other characterized neodymium alk(aryl)oxides.....	230
34.2.1. <i>Nd₃(μ₃-OtAm)₂(μ₂-OtAm)₃(OtAm)4(THF)2 (9)</i>	230
34.2.2. <i>Nd₁₂(OtAm)26Cl₁₁Na•2(Et₂O) (10)</i>	230
34.2.3. <i>Nd₂(OCMe₂CH₂CH₂OMe)₆ (11)</i>	231
34.2.4. <i>Modified synthesis of Nd(O-2,6-tBu₂-4-Me-Ph)₃(THF) (12) and Nd(O-2,6-tBu₂-4-Me-Ph)₃ (13)</i>	232
34.3. Miscellaneous lanthanide alkoxides.....	232
35. MMA polymerization.....	233
35.1. Preparation of the initiator	233

35.2.MMA polymerization.....	233
36.Ethylene homo-polymerization.....	233
36.1.With in situ "Nd(OR)3"/MRz combinations.....	233
36.2.With the isolated solid catalyst S.....	234
36.2.1. <i>Isolation of solid catalyst S.</i>	234
36.2.2. <i>Gas phase ethylene polymerization.</i>	234
36.2.3. <i>Slurry phase ethylene polymerization:</i>	235
37.Diblock ethylene-MMA copolymerization.....	235
37.1.With the in situ system	235
37.2.With the solid S.....	235
38.Butadiene (co)-polymerization.....	236
38.1.Butadiene homo-polymerization.....	236
38.2.Butadiene-styrene statistical copolymerization	236
38.3.Butadiene-GMA diblock copolymerization	236
39.Mechanism section.....	237
39.1.NMR monitoring of 1/MgR2 combinations.....	237
39.2.Synthesis of active species or intermediates.....	237
39.2.1. <i>Nd(μ3-OtBu)2(μ2-OtBu)2(OtBu)Mg2(CH2SiMe3)2(THF)</i> (14).....	237
39.2.2. <i>[(Me3SiCH2)Mg(OtBu)(THF)]</i> (15).....	238
39.2.3. <i>[(n-hex)Mg(O-2,6-tBu2-4-Me-C6H2)]2</i> (16).....	238
39.2.4. <i>Nd(O-2,6-tBu2-4-Me-Ph)2(CH2SiMe3)(THF)2</i> (17).....	239
39.2.5. <i>[(Me3SiCH2)Mg(O-2,6-tBu2-4-Me-Ph)]2</i> (18).....	239
French summary.....	242
1.Introduction.....	244
40.Systèmes catalytiques à base de métaux du groupe 3.....	247
40.1.Polymérisation des α-oléfines non fonctionnalisées.....	247
40.1.1. <i>Catalyseurs lanthanocéniques</i>	247
40.1.2. <i>Systèmes lanthanocéniques binaires</i>	249
40.1.3. <i>Catalyseurs ansa-lanthanocéniques et à géométrie contrainte</i>	249
40.1.4. <i>Réactions de transfert</i>	251
40.1.5. <i>Catalyseurs post-lanthanocéniques</i>	251
40.1.5.1.Complexes porteurs de ligands azotés.....	251
40.1.5.2.Complexes porteurs de ligands oxygénés.....	252
40.2.Polymérisation du méthacrylate de méthyle.....	252
40.2.1. <i>Complexes lanthanocéniques</i>	253
40.2.2. <i>Systèmes lanthanocéniques binaires</i>	254
40.2.3. <i>Complexes ansa-lanthanocéniques</i>	255
40.2.4. <i>Amorceurs post-lanthanocéniques</i>	255
40.2.4.1.Complexes allyliques.....	255
40.2.4.2.Alcoolates de lanthanide.....	256
40.2.4.3.Thiolates de lanthanide.....	256
40.2.5. <i>Systèmes post-lanthanocéniques binaires</i>	256
40.3.Polymérisation du butadiène.....	257
40.3.1. <i>Généralités</i>	257
40.3.2. <i>Caractéristiques générales de la polymérisation 1,4-cis du butadiène</i> 187.....	258

40.3.3. Mécanisme de polymérisation.....	259
40.3.4. Autres systèmes de stéréospécificité 1,4-cis.....	259
40.3.5. Polymérisation 1,4-trans.....	260
40.4. Copolymérisation butadiène-styrène.....	260
40.4.1. Systèmes ternaires.....	260
40.4.2. Systèmes lanthanocéniques.....	261
41. Présentation du projet de recherche.....	262
42. Synthèse d'alcoolates/phénates de lanthanide.....	262
42.1. Etude bibliographique.....	262
42.1.1. Réaction de métathèse ionique.....	263
42.1.2. Alcoolyse de complexes tris(amidure).....	264
42.1.3. Protonolyse de complexes tris(alkyl)lanthanide.....	265
42.1.4. Conclusion.....	265
42.2. Synthèse d'alcoolates de néodyme.....	266
42.2.1. Tertiobutylates de néodyme.....	266
42.2.1.1. Réactions de métathèse ionique.....	266
42.2.1.1.1. A partir de NdCl ₃ /NaOtBu dans divers solvants.....	266
42.2.1.1.2. A partir de NdCl ₃ /MOTBu (M = Li, K) dans le THF.....	268
42.2.1.1.3. A partir de NdCl ₃ (THF) ₂ dans le THF.....	268
42.2.1.2. Alcoolyse du tris(amidure) Nd[N(SiMe ₃) ₂] ₃	270
42.2.2. Autres alcoolates de néodyme.....	271
42.2.2.1. Synthèse du tertioamylate de néodyme par métathèse ionique.....	271
42.2.2.2. Synthèse d'alcoolate tertiaire fonctionnalisé par alcoolyse de Nd[N(SiMe ₃) ₂] ₃	272
42.2.3. Synthèse de phénates de néodyme.....	273
42.3. Conclusion.....	274
43. Polymérisation du méthacrylate de méthyle.....	275
43.1. Résultats préliminaires.....	275
43.2. Optimisation du système catalytique Nd ₃ (OtBu) ₉ (THF) ₉ /DHM.....	275
43.2.1. Influence du rapport Nd/Mg.....	276
43.2.2. Températures d'activation et de polymérisation.....	277
43.3. Nature de l'agent alkylant.....	277
43.4. Nature du précurseur de néodyme.....	278
43.5. Mécanisme proposé.....	279
43.6. Conclusion.....	280
44. Homopolymérisation de l'éthylène et copolymérisation dibloc éthylène-MAM.....	280
44.1. Etude préliminaire des systèmes "Ln(OR) ₃ "/MgR ₂	280
44.2. Polymérisation de l'éthylène en slurry amorcée par Nd ₃ (OtBu) ₉ (THF) ₂	283
44.2.1. Effet de certains additifs sur l'activité de polymérisation.....	285
44.2.2. Polymérisation en présence d'agent de transfert.....	285
44.2.3. Addition de dialkylmagnésium en cours de polymérisation.....	286
44.3. Polymérisation de l'éthylène avec le polymère précipité (S)	286
44.3.1. Principe.....	286
44.4. Copolymérisation dibloc PE-b-PMAM.....	287
44.4.1. Synthèse de copolymères diblocs oléfine-MAM.....	287
44.4.2. Copolymérisation dibloc éthylène-MAM.....	288
44.4.2.1. Système in situ	288

44.4.2.2.Utilisation du solide S comme amorceur de copolymérisation.....	288
44.4.2.3.Etude morphologique.....	288
44.4.2.4.Application comme agent compatibilisant.....	289
44.4.3. <i>Mécanisme</i>	290
45.(Co)-Polymérisation du butadiène.....	291
45.1.Homopolymérisation.....	291
45.1.1.Avec $Nd_3(OtBu)_9(THF)_2$	291
45.1.2.Avec les phénates de néodyme 12 et 13.....	292
45.2.Copolympératation du butadiène.....	293
45.2.1.Copolympératation statistique butadiène-styrène.....	293
45.2.2.Copolympératation dibloc butadiène-méthacrylate de glycidyle.....	294
45.3.Mécanisme	296
46.Etude mécanistique.....	298
46.1.Etude RMN.....	298
46.1.1.Evolution des systèmes " $Ln(OR)_3$ "/DHM ($Ln/Mg = 1,0$).....	298
46.1.2.Evolution des systèmes 1/RM ($Ln/M = 1,0$).....	300
46.2.Cristallisation des espèces actives.....	301
46.2.1.Cristallisation de $Nd(THF)(\mu_3-OtBu)_2(\mu_2-OtBu)_2(OtBu)Mg_2(CH_2TMS)_2$ (14)....	301
46.2.2.Cristallisation de composés issus de systèmes $Nd(OAr)_3(THF)/RM$	304
46.3.Conclusion.....	305
47.Conclusion générale.....	307
Bibliographical references.....	309
Appendix.....	321
Appendix 1. 1H NMR spectrum of 1 in toluene-d8 at various temperatures.....	323
Appendix 2. 13C NMR spectrum of 12 in C6D6 at RT.....	323
Appendix 3. Typical 1H NMR spectrum of PMMA obtained with 1/DHM system (CDCl3, 23 °C)....	324
Appendix 4. Typical 1H NMR spectrum of PE obtained with 1/DHM system (C2D2Cl4, 130 °C)....	324
Appendix 5. DSC chromatogram of PE obtained with 1/DHM system.....	326
Appendix 6. 1H NMR spectrum of phenylsilyl-terminated PE (C2D2Cl4, 130 °C).....	326
Appendix 7. 1H NMR spectrum of PE-b-PMMA prepared with $La_3(OtBu)_9(THF)_2/DHM$ as catalyst system (C2D2Cl4, 130 °C).....	328
Appendix 8. IR spectrum of PE-b-PMMA copolymer (KBr pellets).....	328
Appendix 9. 1H NMR spectrum of PE-b-poly(ϵ -caprolactone) copolymer (C2D2Cl4, 130 °C)....	329
Appendix 10. Typical 1H NMR spectrum of homopolybutadiene obtained with 12/DHM as catalyst system (CDCl3, 23 °C).....	329
Appendix 11. IR spectrum of PE-b-PGA copolymer (KBr pellets).....	330
Appendix 12. Formation and consumption of ethylene monitored by 1H NMR with 1/BEM system (toluene-d8).....	330
Appendix 13. 1H NMR spectrum of $La_3(OtBu)_9(THF)_2/DHM$ mixture (1:1) at 0 °C in toluene-d8..	331
Appendix 14. 1H NMR spectrum of $Y_3(OtBu)_8Cl(THF)_2/DHM$ mixture (1:1) at 20 °C in toluene-d8.....	331
Appendix 15. 1H NMR spectrum of $[(Me_3SiCH_2)Mg(OtBu),(THF)]$ (15) in C6D6 at 23 °C.....	332
Appendix 16. 13C NMR spectrum of $[(Me_3SiCH_2)Mg(OtBu),(THF)]$ (15) in C6D6 at 23 °C....	332
Appendix 17. 1H NMR spectrum of $[(n-Hex)Mg(O-2,6-tBu_2-4-Me-Ph)]_2$ (16) in C6D6 at 23 °C.....	333

Appendix 18. ^{13}C NMR spectrum of [(n-Hex)Mg(O-2,6-tBu2-4-Me-Ph)] ₂ (16) in C6D6 at 23 °C....	
333	
Appendix 19. ^1H NMR spectrum of [(Me ₃ SiCH ₂)Mg(O-2,6-tBu2-4-Me-Ph)] ₂ (18) in C6D6 at 23 °C.....	334
Appendix 20. ^{13}C NMR spectrum of [(Me ₃ SiCH ₂)Mg(O-2,6-tBu2-4-Me-Ph)] ₂ (18) in C6D6 at 23 °C.....	334

Abbreviations

acac	acetylacetone
BD	butadiene
BEM	butylethylmagnesium
brs	broad singlet
concn	concentration
conv.	conversion
Cp	cyclopentadienyl
Cp*	pentamethylcyclopentadienyl
DHM	di- <i>n</i> -hexylmagnesium
DSC	differential scanning calorimetry
Eff.	efficiency
equiv.	equivalent
Flu	fluorenyl
GMA	glycidyl methacrylate
Ind	indenyl
IR	infra-red
Ln	lanthanide
LnN ₃	Ln(N(SiMe ₃) ₂) ₃
m	multiplet
mm	isotactic triad
mmmm	isotactic pentad
M _η	viscosimetric molecular weight
M _n	number-average molecular weight
mr	atactic triad
M _w	weight-average molecular weight
M _w /M _n = MWD	molecular weight distribution
MMA	methyl methacrylate
NMR	nuclear magnetic resonance
nc	not calculated
nd	not determined
PBD	polybutadiene
PE	polyethylene
PP	polypropylene
ppm	part per million
PMMA	poly(methyl methacrylate)
rr	syndiotactic triad
RT	room temperature
SEC	size exclusion chromatography

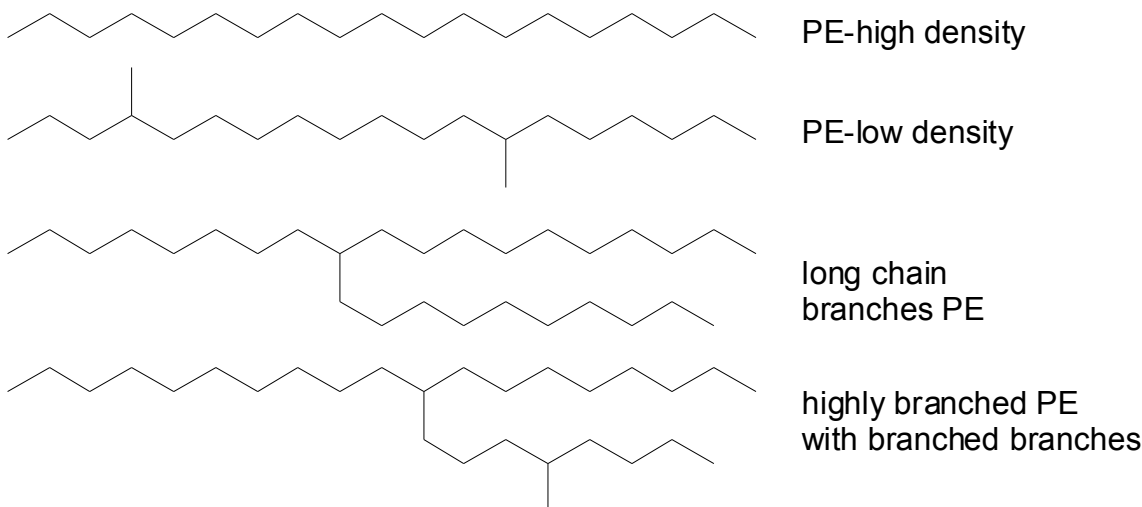
s	singlet
t	triplet
THF	tetrahydrofuran
THP	tetrahydropyran
TMS	trimethylsilyl
TMSM	bistrimethylsilyl magnesium
T _g	glass transition temperature
T _m	melting temperature

Introduction

Since the concepts of high molecular weight polymer and polymerization processes linking together individual small molecules by the mean of covalent bonds proposed by Staudinger in the 1920's,¹ polymer chemistry has known many breakthroughs.

The area of polyolefins has been probably the most concerned by all these great discoveries. The appearance of transition metal polymerization catalysis in the early 1950's has changed the face of the polyolefins industry. While harsh conditions were required for the synthesis of branched low density polyethylene (LDPE), these new catalytic systems enabled the synthesis of high density polyethylene (HDPE) and high molecular weight polypropylene (PP) at low temperature and pressure. The different macromolecular architectures of polyethylenes are depicted in Figure 1.

Figure 1. Macromolecular architectures of polyethylenes.



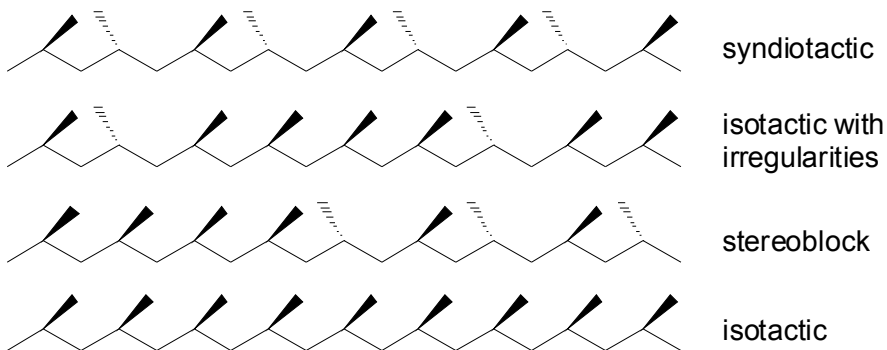
Improvement of these catalysts led to high activities and highly stereospecific polypropylene polymerization. Another significant breakthrough in the polyolefins area is the appearance of homogeneous metallocene catalysts. These molecular catalysts enabled the establishment of direct correlations between catalyst structure and polymer microstructure, and all kinds of stereoregular polyolefins to be synthesized along with high activities (Figure 2).

Nonetheless, after 50 years of development, heterogeneous organometallic polymerization catalysis (Ziegler-Natta catalysis) is still nowadays accountable for the worldwide production of 52 million metric tons of PE and 29 million metric tons of PP; it is evaluated that only ca. 3% of the polyolefins have been produced with metallocene catalysts.²

¹ Staudinger, H. *Helv. Chim. Acta* **1922**, 5, 785.

² Ulbrich, D.; Vollmer, M. S. *Macromol. Mater. Eng.* **2002**, 287, 435-441.

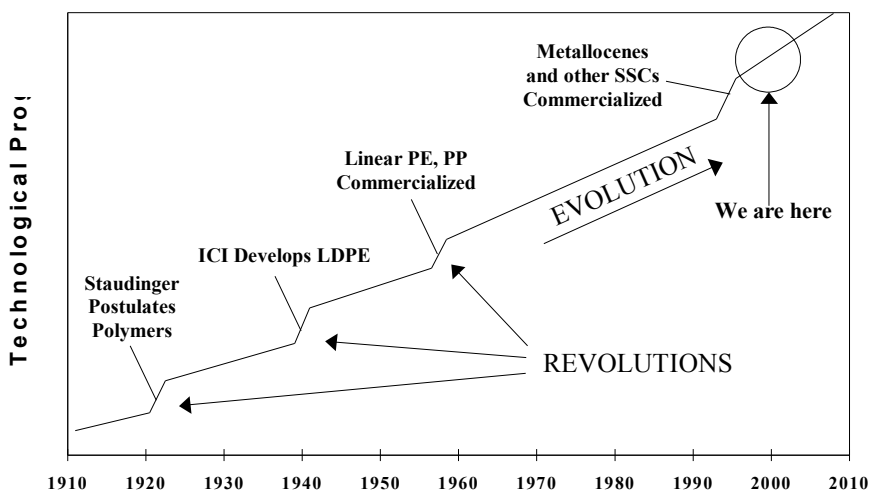
Figure 2. Stereochemistry of metallocene-based poly(α -olefins).



Polyolefin-based materials have found a wide range of application in automotive market (fuel tank...), consumer and industrial packaging (bottles, cans...), consumer products (houseware and leisure articles), pipes, and textile (carpet). The overall resin market estimated at 80 million tons in 2002 is expected to increase at an average annual growth rate of 7%, likely reaching 100 million tons by 2007.

After a century of development, the polymerization of α -olefins is still a subject widely investigated in both academic and industrial research centers and further evolutions are even so expected (Figure 3).

Figure 3. Technology revolution/evolution cycles in the polymer industry.³



In industrial polyolefin research, the goal is not only the optimization of the existing processes with regard to technology but also the development of new polymers with specific properties. Block copolymers represent a subject of broad current research emphasis across the full spectrum of macromolecular chemistry and physics, ranging from development of new synthetic strategies and molecular architectures to application of advanced theoretical methods. The synthesis of block copolymers with polar and non-polar monomers is of particular interest to obtain polymers with a brand new structure and properties profile.⁴ Few

³ Sinclair, K. B. *Macromol. Symp.* **2001**, *173*, 237-261.

⁴ (a) Lodge, T. P. *Macromol. Chem. Phys.* **2003**, *204*, 265-273. (b) Yanjarappa, M. J.; Sivaram, S. *Prog. Polym. Sci.* **2002**, *27*, 1347-1398. (c) Boffa, L. S.; Novak, B. M. *Chem. Rev.* **2000**, *100*, 1479-1493.

examples have been reported for the synthesis of such polar/non-polar copolymers, especially with ethylene and propylene. Up to date, the most promising results in this area were obtained with lanthanocene catalysts.⁵

In this context, we focused our research on the polymerization of olefins and their copolymerization with polar monomers using lanthanide-based systems. In the first chapter, we will show the great potential of lanthanide complexes for olefin polymerization, especially in ethylene and α -olefins, methacrylates and conjugated dienes polymerizations. Then, we will present the synthesis and the characterization of new lanthanide alkoxides, followed by their application in polymerization when combined with a dialkylmagnesium reagent. Finally, a mechanistic study describing the catalytic behavior of these new initiators/catalysts with lanthanocene-like properties will conclude this study.

⁵ (a) Yasuda, H. *J. Organomet. Chem.* **2002**, *647*, 128–138. (b) Hou, Z.; Wakatsuki, Y. *Coord. Chem. Rev.* **2002**, *231*, 1-22.

1.

Chapter 1

Lanthanide-mediated polymerizations

2.

3. Ethylene and α -olefin polymerization

3.1. Before organometallic catalysis

The polymerization of olefins has a long history that started more than one hundred years ago. In 1898, Von Pechmann observed the polymerization of diazomethane leading to linear crystalline polyethylene (HDPE).⁶ Nonetheless, this route never proved viable for industrial production. The first breakthrough in industry occurred in the early 1930's when Fawcett and Gibson at ICI patented the high pressure free radical polymerization of ethylene ($P > 1000$ bar, 200 °C) initiated by traces of oxygen.⁷ Due to chain transfer reactions, short and long alkyl branches were formed, resulting in reduced density and reduced melting temperature with respect to linear polyethylene (Figure 1). This radical process could not be applied for propylene polymerization since only faintly colored viscous liquids were obtained.⁸ However, in 1939 started the first industrial production of LDPE.

3.2. Ziegler-Natta catalysis

Because of the severe polymerization conditions and the exclusive formation of LDPE,⁷ several groups worked on the synthesis of high density PE. Many results had been previously reported, e.g. alkyl lithium and Grignard reagents could polymerize ethylene under 900 atm ethylene pressure in the absence of transition metal catalyst producing HDPE,⁹ but at this time the potential of this polymer was not recognized. Later, scientists came very close to the discovery of catalysts for low-pressure ethylene polymerization. It was only in 1953 that Karl Ziegler at the Max Planck Institute for Coal Research, Mülheim, reported a low-pressure ethylene polymerization catalytic process.¹⁰ When zirconium and/or titanium halides (catalyst) were added together with aluminum alkyls (activator), high molecular weight linear high density polyethylene was formed at atmospheric pressure and room temperature. At the same time, Banks and Hogan at Phillips Petroleum Co. made another important discovery. The use of CrO₃-silica catalysts, which do not require aluminum alkyl activators, enabled ethylene to polymerize, affording HDPE with an attractive combination of properties and easy processing.¹¹ In 1954, Giulio Natta conducted the polymerization of propylene with Ziegler's catalysts.¹² He found that the formed polymer was composed of different diastereoisomers with different physical properties. The diethylether soluble fraction was amorphous and sticky, whereas the heptane insoluble fraction was crystalline with high melting point: isotactic polypropylene. This was the starting point of organometallic polymerization catalysis and a

⁶ Von Pechmann, H. *Ber. Dtsch. Chem. Ges.* **1898**, *31*, 2643.

⁷ Fawcett, E. W.; Gibson, R. O.; Perrin, M. W.; Paton, J. G.; Williams, E. G., GB 471590 (Imperial Chemical Industries Ltd.), **1937**.

⁸ (a) Brown, D. W.; Wall, L. A. *J. Phys. Chem.* **1963**, *67*, 1016-1019. (b) Mortimer, G. A.; Arnold, L. C. *J. Polym. Sci.* **1964**, *A2*, 4247-4253.

⁹ (a) Meerwein, H.; Burnebeit, W. *Ber. Dtsch. Chem. Ges.* **1928**, *61B*, 1845. (b) Hanford, W. E., US 2,377,779 (Du Pont), **1942**. (c) Roedel, M. J., US 2,475,520 (Du Pont), **1944**.

¹⁰ (a) Ziegler, K., US 3579493, **1955**. (b) Ziegler, K.; Holzkamp, E.; Breil, H.; Martin, H. *Angew. Chem.* **1955**, *67*, 426. (c) Ziegler, K.; Martin, H. *Angew. Chem.* **1955**, *67*, 541.

¹¹ Banks, J. P.; Banks, R. L., US 2,825,721 (Phillips), **1953**.

¹² (a) Natta, G.; Pino, P.; Corradini, P.; Danusso, F.; Mantica, E.; Mazzanti, G.; Moraglio, G. *J. Am. Chem. Soc.* **1955**, *77*, 1708-1710. (b) Natta, G. *Angew. Chem.* **1956**, *68*, 393.

second birth for polyolefins industry. These new processes were rapidly industrialized and the next 30 years were devoted to the development and innovations in process technology in order to increase both activity and stereoselectivity. Stereoselective titanium-based magnesium chloride supported catalysts, started end of the 1960's, and enabled higher polymerization activity, eliminating the need for removal of catalyst residue and atactic by-products.¹³ The addition of Lewis bases such as alkyl benzoates, phthalates or alkoxy silanes gave birth to highly stereospecific olefin polymerizations.¹⁴ Now, with $MgCl_2/1,3\text{-diether/TiCl}_4/AlR_3$ catalyst systems, extraordinarily high activities and good stereoselectivities combined with morphology control are achieved in propylene polymerization.¹⁵

3.3. Metallocene catalysts

However, at the early stage of the Ziegler-Natta catalysis, most catalysts were a mixture of active and inactive species producing a blend of polyolefins containing polymers with different molecular weights, end-groups, regio- and stereoselectivities. Since the active species concentration was found to be very low, it was impossible to identify the architectures of the catalytically active sites. Consequently, rational improvement of these catalysts was hopeless. Therefore, most information was gained using organometallic model compounds of formula $(\eta^5\text{-C}_5\text{H}_5)_2\text{TiRCl}$ ($\eta^5\text{-C}_5\text{H}_5 = Cp$) also called metallocene catalysts or single site catalysts (SSC) (in opposition with the multiple site catalysts that are heterogeneous Ziegler's catalysts). The use of these well-defined molecular catalysts was restricted to the mechanistic study given the low observed activity.¹⁶

The formation of the active sites with these catalysts was debated for a long time and now an unambiguous mechanism is generally accepted.¹⁷ The metallic complex reacts with the activator to generate the corresponding cationic alkyl metal.¹⁸ This electron-deficient species is highly reactive and olefins can coordinate and then be inserted into the metal-carbon bond. This coordination-insertion step can repeat itself until occurrence of a transfer or termination reaction (Scheme 1).

¹³ (a) Jeong, T.; Lee, D. H. *Makromol. Chem.* **1990**, *191*, 1487-1496. (b) Albizzati, E.; Giannini, U.; Collina, G.; Noristi, L.; Resconi, L. in "Polypropylene Handbook", E. P. Moore Jr., Ed., Hanser Publishers, Munich **1996**, p11.

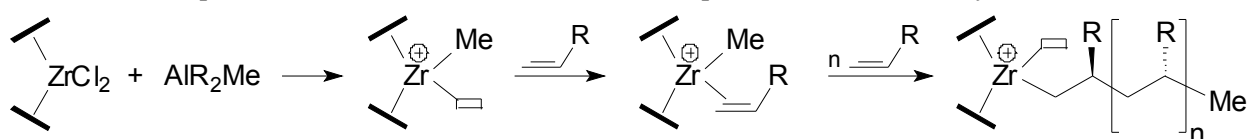
¹⁴ Chadwick, J. C. *Macromol. Symp.* **2001**, *173*, 21-36.

¹⁵ Moore, E. P. Jr., "The rebirth of Polypropylene: Supported Catalysts" Ed., Hanser Publishers, Munich, **1998**.

¹⁶ (a) Pino, P.; Mülhaupt, R. in "Transition Metal Catalyzed Polymerizations – Part A", Vol. 4, R. P. Quirk, Ed., MMI Press Symposium Series, Harwood Academic Publishers, New York **1981**, p1. (b) Fink, G.; Rottler, R.; *Angew. Makromol. Chem.* **1981**, *94*, 25-47.

¹⁷ (a) Cossee, P. J. *Catal.* **1964**, *3*, 80. (b) Arlman, E. J.; Cossee, P. J. *Catal.* **1966**, *5*, 178.

¹⁸ Jordan, R. F. *Adv. Organomet. Chem.* **1991**, *32*, 325.

Scheme 1. Simplified mechanism of formation of active species in metallocene systems.^{17,18}

The accidental discovery of methylaluminoxane (MAO)¹⁹ (from the reaction of trimethyl aluminum and water) as activator for these catalysts in 1976 expanded the frontiers of olefin polymerization well beyond all expectations. Indeed, the discovery of MAO activators was the starting point for the development of many new families of highly active single site catalysts (productivity up to 100,000 kgPE/gZr).²⁰ In addition, for the first time it was possible to establish a direct relationship between catalyst structure and polymer microstructure, i.e., properties (Figure 4).

Thus, beside this high catalytic activity, the stereospecific α -olefin polymerization was also achieved. Brintzinger was the first to report the use of chiral bridged ("ansa") metallocenes for isospecific propene polymerization.²¹ Ewen²² and Kaminsky jointly with Brintzinger²³ demonstrated that MAO-activated homogeneous catalysts were indeed able to produce stereoregular polypropylene. While *meso* *ansa*-metallocenes produced atactic PP, *racemic* ones gave isotactic polypropylene.²⁴ Depth spectroscopic analyses of PP microstructures provided strong experimental evidences for the presence of enantiomeric site control, as well as chain-end control of the stereoselective propene polymerization. Thus, a nearly perfect syndiotactic polypropylene can be obtained using a bridged cyclopentadienyl/fluorenyl zirconocene where the stereocontrol consists of the regularly alternating insertion of olefins at the enantiotopic sites of the C_s -symmetric complex.²⁵ In addition, the synthesis of isotactic-atactic stereoblock polymers was achieved with a C_1 -symmetric catalyst. In this case, the alternated stereospecificity is consistent with an oscillation between achiral and chiral coordination geometries (*rac/C₂*) during the propagation step, a mechanism proposed for the production of stereoblock microstructures.²⁶ The relationship between catalyst symmetry and polymer microstructure is summarized in Figure 4. This concept of single site catalyst was successfully applied to bridged half-sandwich titanium amide complexes known as

¹⁹ (a) Sinn, H.; Mottweiler, R.; Andresen, A; Cordes, H.-G.; Herwig J.; Kaminsky, W.; Merck, A.; Vollmer, H.-J.; Pein, J., DE 2608863 (BASG AG), **1976**. (b) Sinn, H.; Mottweiler, R.; Andresen, A; Cordes, H.-G.; Herwig J.; Kaminsky, W.; Merck, A.; Vollmer, H.-J.; Pein J., DE 2608933 (BASF AG), **1976**.

²⁰ (a) Sinn, H.; Kaminsky, W.; Vollmer, H.-J.; Woldt, R. *Angew. Chem.* **1980**, 92, 396. (b) Sinn, H.; Kaminsky, W. *Adv. Organomet. Chem.* **1980**, 18, 99-149.

²¹ Wild, F. R. W. P.; Zsolnai, L.; Huttner, G.; Brintzinger, H.-H. *J. Organomet. Chem.* **1982**, 232, 233-247.

²² Ewen, J. A. *J. Am. Chem. Soc.* **1984**, 106, 6355-6364.

²³ Kaminsky, W.; Kuelper, K.; Brintzinger, H.-H.; Wild, F. R. W. P. *Angew. Chem.* **1985**, 97, 507-508.

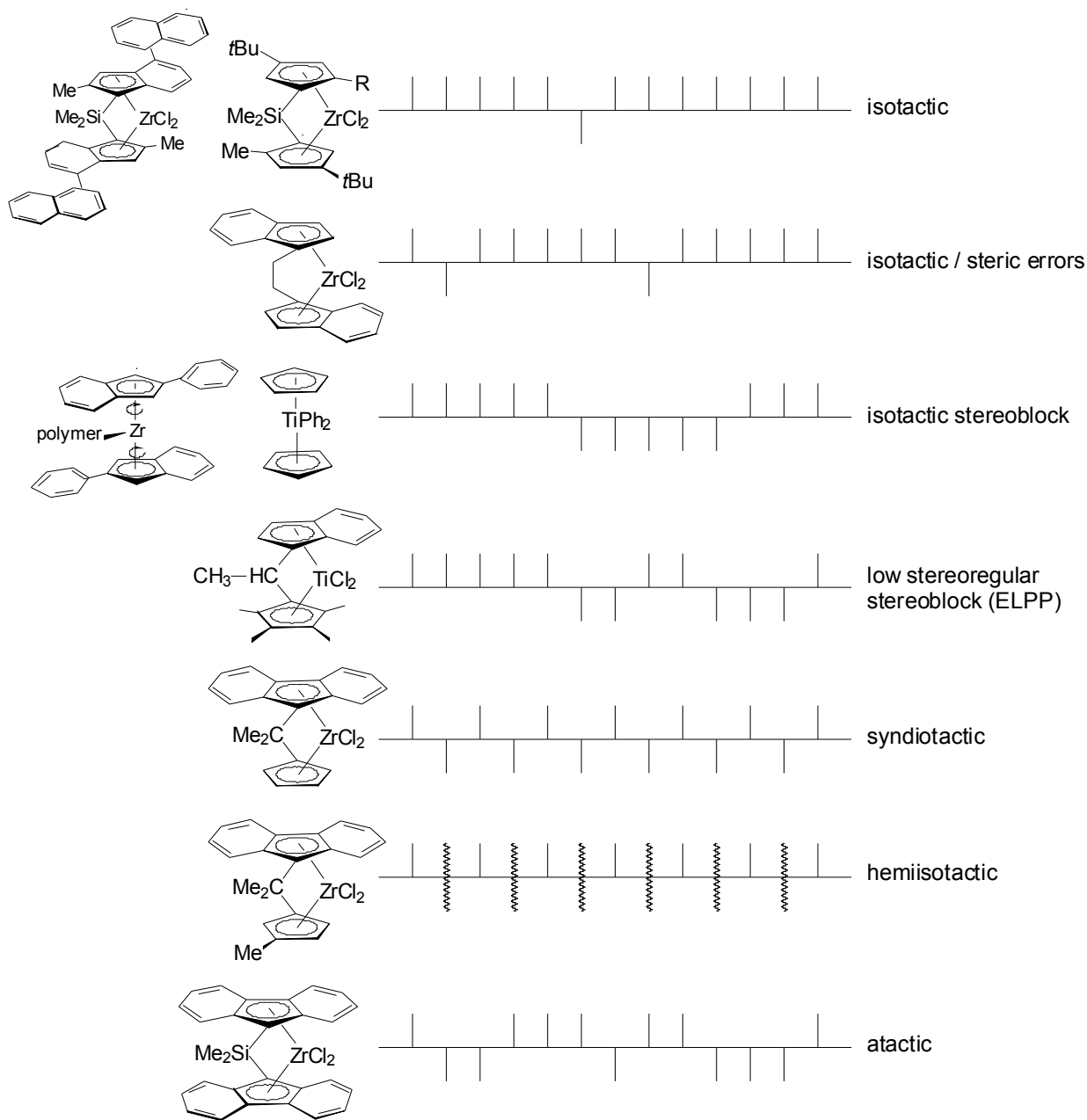
²⁴ (a) Brintzinger, H.-H.; Fischer, D.; Mühlaupt, R.; Rieger, B.; Waymouth, R. M. *Angew. Chem. Int. Ed. Engl.* **1995**, 34, 1143-1170. (b) Bochmann, M. *J. Chem. Soc., Dalton Trans.* **1996**, 255-270. (c) Resconi, L.; Cavallo, L.; Fait, A.; Piemontesi, F. *Chem. Rev.* **2000**, 100, 1253-1345. (d) Angermund, K.; Fink, G.; Jensen, V. R.; Kleinschmidt, R. *Chem. Rev.* **2000**, 100, 1457-1470. (e) Coates, G. W. *Chem. Rev.* **2000**, 100, 1223-1252. (f) Coates, G. W. *J. Chem. Soc., Dalton Trans.* **2002**, 467-475.

²⁵ Ewen, J. A.; Jones, R. L.; Razavi, A.; Ferrara, J. D. *J. Am. Chem. Soc.* **1988**, 110, 6255-6256.

²⁶ Coates, G. W.; Waymouth, R. M. *Science* **1995**, 267, 217-219.

"constrained geometry catalysts" (CGC).²⁷ Thanks to these new catalytic systems, ethylene- α -olefin copolymers with high α -olefin content, cycloolefin copolymers, ethylene-styrene copolymers, syndiotactic polystyrene and long chain branches ethylene copolymers became available.²⁴

Figure 4. Correlation between poly(propylene) architectures and metallocene catalyst structures.²⁸



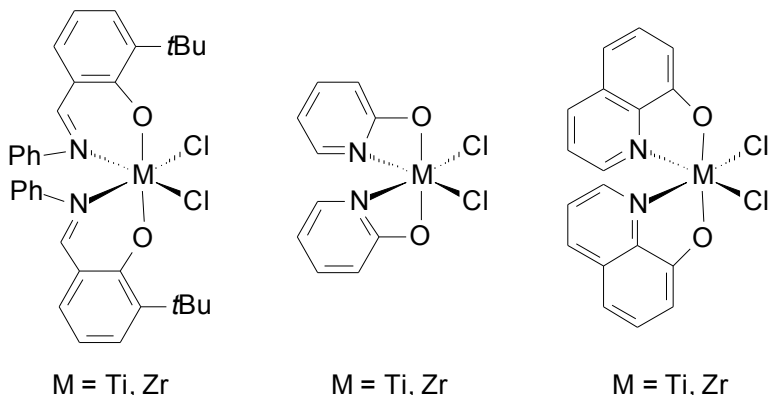
²⁷ McKnight, A. L.; Waymouth, R. M. *Chem. Rev.* **1998**, *98*, 2587-2598.

²⁸ Mühlaupt, R. *Macromol. Chem. Phys.* **2003**, *204*, 289-327.

3.4. Post-metallocene catalysts

More recently it was shown that cyclopentadienyl-free ligands could be employed with Ti and Zr.²⁹ These new ligands can be chosen among chelating nitrogen-based ligands (diamides,³⁰ β -diketiminates,³¹ imino-pyrrolidines,³² amidinates³³...) or chelating alk(aryl) oxides (salicyladiminato³⁴, bis(phenoxy) amine³⁵...), leading to living polymerizations and to well-defined materials (Figure 5).³⁴

Figure 5. Some examples of highly active group 4 post-metallocene catalysts.^{34,35}



The term of *living* polymerization was first defined by Swarc as a chain growth process without chain breaking reactions (transfer and termination).³⁶ Such a polymerization provides end-group control and enables the synthesis of block copolymers by sequential monomer addition. However, it does not necessarily provide polymers with molecular weight control and narrow molecular weight distribution. Additional prerequisites to achieve these goals include that the initiator should be consumed at early stages of polymerization and that initiation step or the exchange between species of various reactivities should be at least as fast

²⁹ (a) Britovsek, G. J. P.; Gibson, V. C.; Wass, D. F. *Angew. Chem. Int. Ed. Engl.* **1999**, *38*, 428-447. (b) Gibson, V. C.; Spitzmesser, S. K. *Chem. Rev.* **2003**, *103*, 283-315.

³⁰ (a) Scollard, J. D.; McConville, D. H. *J. Am. Chem. Soc.* **1996**, *118*, 10008-10009. (b) Scollard, J. D.; McConville, D. H. *Organometallics* **1997**, *16*, 1810-1812. (c) Baumann, R.; Davis, W. M.; Schrock, R. R. *J. Am. Chem. Soc.* **1997**, *119*, 3830-3831. (d) Mehrkhodavandi, P.; Schrock, R. R. *J. Am. Chem. Soc.* **2001**, *123*, 10746-10747.

³¹ For a review on β -diketiminates complexes, see: Bourget-Merle, L.; Lappert, M. F.; Severn, J. R. *Chem. Rev.* **2002**, *102*, 3031-3066.

³² (a) Yoshida, Y.; Matsui, S.; Takagi, Y.; Mitani, M.; Nitabaru, M.; Nakano, T.; Fujita, T.; Kashiwa, T. *Chem. Lett.* **2000**, 1270-1271. (b) Yoshida, Y.; Matsui, S.; Takagi, Y.; Mitani, M.; Nakano, T.; Tanaka, H.; Kashiwa, T.; Fujita, T. *Organometallics* **2001**, *20*, 4793-4799. (c) Dawson, D. M.; Walker, D. A.; Thornton-Pett, M.; Bochmann, M. *J. Chem. Soc., Dalton Trans.* **2000**, 459-466.

³³ Richter, J.; Edelmann, F. T.; Noltemeyer, M.; Schmidt, H. G.; Shmulinson, M.; Eisen, M. S. *J. Mol. Catal. A: Chem.* **1998**, *130*, 149-162.

³⁴ Selected references: (a) Matsui, S.; Mitani, M.; Saito, J.; Tohi, Y.; Makio, H.; Matsukawa, N.; Tagaki, Y.; Tsuru, K.; Nitaburu, M.; Nakano, T.; Fujita, T. *J. Am. Chem. Soc.* **2001**, *123*, 6847-6856. (b) Mitani, M.; Mohri, J.; Yoshida, Y.; Saito, J.; Ishii, S.; Tsuru, K.; Matsui, S.; Furuyama, R.; Nakano, T.; Tanaka, H.; Kojoh, S.-I.; Matsugi, T.; Kashiba, N.; Fujita, T. *J. Am. Chem. Soc.* **2002**, *124*, 3327-3336. (c) Tian, J.; Coates, G. W. *Angew. Chem. Int. Ed. Engl.* **2000**, *39*, 3626-3629. (d) Hustad, P. D.; Tian, J.; Coates, G. W. *J. Am. Chem. Soc.* **2002**, *124*, 3614-3621.

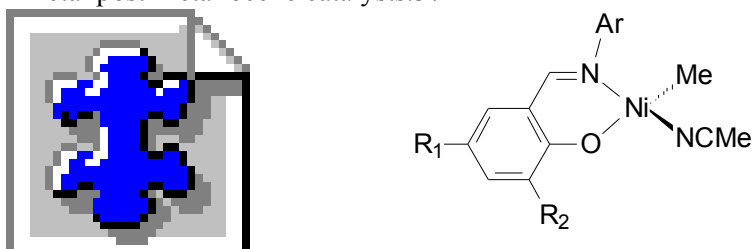
³⁵ (a) Tshuva, E. Y.; Goldberg, I.; Kol, M.; Weitman, H.; Goldschmidt, Z. *Chem. Commun.* **2000**, 379-380. (b) Tshuva, E. Y.; Groysman, S.; Goldberg, I.; Kol, M.; Weitman, H.; Goldschmidt, Z. *Organometallics* **2002**, *21*, 662-670.

³⁶ Swarc, M. *Nature* **1956**, *178*, 1168.

as propagation. If these criteria are met, the term *controlled* polymerization can be used. This term was proposed for systems that provide control of molecular weight and molecular weight distribution but in which chain breaking reactions continue to occur.

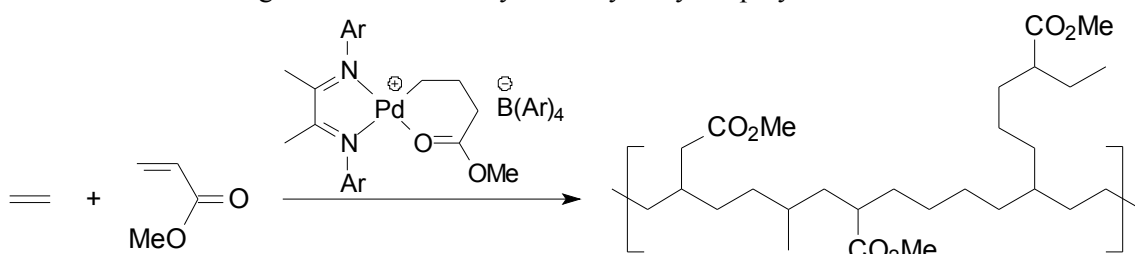
Parallel to this research devoted to group 4 metals, catalysts based on late transition metals with new ligand framework were developed. The foremost findings in this area were the Brookhart-type Ni- and Pd diimine catalysts,³⁷ Brookhart/Gibson-type pyridine-diimine Fe and Co catalysts³⁸ and the activator-free Grubbs iminophenolate Ni catalysts (Figure 6).³⁹ In the latter, the ligands were borrowed to group 4 metals catalysts described by Mitsui.^{32,34}

Figure 6. Late transition-metal post-metallocene catalysts.³⁷⁻³⁹



Most of these catalysts produce branched ethylene polymers, while the pyridine-diimine catalysts of iron and cobalt produce highly linear high density PE and require α -olefin addition to introduce branches. In addition, diimine ligated palladium and nickel complexes are moderately active for the "copolymerization" of ethylene and functional monomers, such as methyl acrylate, yielding in fact a branched polymer with branches terminated by polar moieties, via a chain-walking mechanism (Scheme 2). Effective copolymerization via incorporation of the polar monomer into the polyethylene backbone was achieved by Drent at Shell with a neutral palladium catalyst formed *in situ* by combination of a Pd^(II) precursor modified with di(2-methoxyphenyl)phosphinobenzene-2-sulfonic acid.⁴⁰

Scheme 2. Chain walking mechanism for ethylene-ethyl acrylate polymerization.³⁹



Finally, it must be noted that group 5 and 6 catalysts have been also developed but did not afford any major advantages compared to group 4 and late transitions metals.²⁹

³⁷ Johnson, L. K.; Killian, C. M.; Brookhart, M. *J. Am. Chem. Soc.* **1995**, *117*, 6414-6415.

³⁸ (a) Small, B. L.; Brookhart, M. *J. Am. Chem. Soc.* **1998**, *120*, 7143-7144. (b) Britovsek, G. J. P.; Gibson, V. C; Kimberly, B. S.; Maddox, P. J.; McTavish, S. J.; Solan, G. A.; White, A. J. P.; Williams, D. J. *Chem. Commun.* **1998**, 849-850.

³⁹ Younkin, T. R.; Connor, E. F.; Henderson, J. I.; Friedich, S. K.; Grubbs, R. H.; Bansleben, D. A. *Science* **2000**, *287*, 460-462.

⁴⁰ Drent, E.; Van Dijk, R.; Van Ginkel, R.; Van Oort, B.; Pugh, R. I. *Chem. Commun.* **2002**, 744-745.

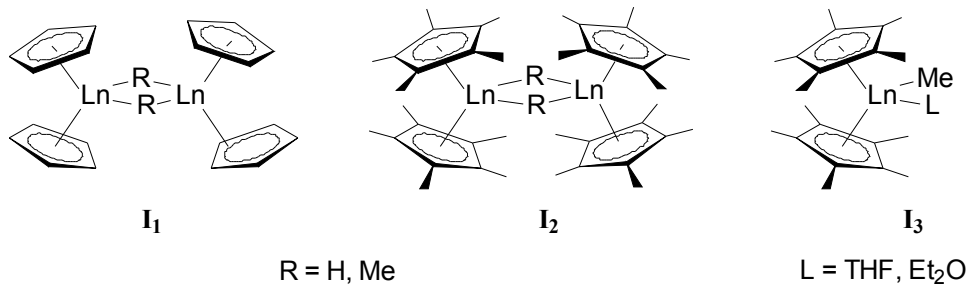
3.5. Catalytic systems based on group 3 metals

Despite the comprehensive research devoted to olefin polymerization catalysis, group 3 metals and lanthanides remain a relatively unexplored part of the transition series in comparison to the work done for group 4 metals. Cyclopentadienyl-based ligands have been largely used in the design of olefin polymerization catalysts. Later, the evolution towards *ansa*-, constrained geometry and Cp-free-ligands was observed. We would like to focus now on the use of such catalysts for olefin polymerization, especially for ethylene and α -olefins, methacrylates and conjugate dienes.

3.5.1. Lanthanocene catalysts

Neutral group 3 bis(cyclopentadienyl) alkyl complexes (typically L_nMR with $L = \eta^5\text{-C}_5\text{H}_5 = \text{Cp}$, $\eta^5\text{-C}_5\text{Me}_5 = \text{Cp}^*$; $n = 2$; $M = \text{Sc}, \text{Y}, \text{Ln}$ and $R = \text{H}$ or alkyl group) are isoelectronic with group 4 cationic alkyl complexes ($[\text{LnMR}]^+$ with $M = \text{Ti}, \text{Zr}, \text{Hf}$) (Figure 7). This analogy has been used in the design of group 3 olefin polymerization catalysts. The main difference is the high intrinsic reactivity of the neutral group 3 complex towards the olefins without preliminary activation. This feature might be a significant economic advantage over the conventional metallocene catalysis, cocatalysts such as trialkylaluminum or MAO becoming useless. In addition, the absence of activation step should enhance the flexibility (faster reaction) of industrial units.

Figure 7. Usual bis(cyclopentadienyl) and bis(pentamethylcyclopentadienyl) lanthanides complexes.



3.5.1.1. Preliminary studies

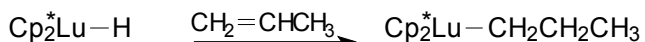
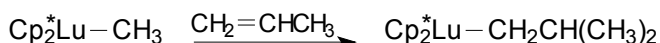
It is probably with this economic aspect in mind that Ballard at ICI developed bis(cyclopentadienyl) alkyl complexes of scandium, yttrium and lanthanide with various Cp ligands for ethylene polymerization.⁴¹ The activity observed was moderate (10-100 kgPE/molLn/atm/h) irrespective of the metal. On the other hand, the substituents on the Cp ring had an influence on the activity: the higher the steric hindrance, the higher the activity and the lower the molecular weight of polymers. This can be correlated to the shortest lifetime of the active species with bulkier substituents and/or to the easier dissociation of the starting dimer precursor due to the greater steric influence.

⁴¹ Ballard, D. G. H.; Courtis, A.; Holton, J.; McMeeking, J.; Pearce, R. *J. Chem. Soc., Chem. Commun.* **1978**, 994-995.

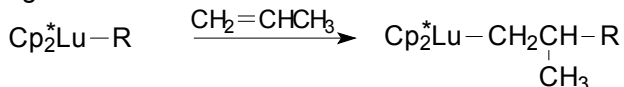
Few years later, a report from Watson *et al.* at DuPont showed that ethylene polymerization with group 3 catalysts was still of interest for industry.⁴² They showed that the complexation of the catalyst (Cp_2^*LuMe)₂ with 1 equimolar quantity of ether could lead to the synthesis of HDPE. But the most interesting results came from the spectroscopic mechanism study of propene insertion, which was at that time one of the clearest experimental model for coordination catalysis of olefin polymerization.⁴³

Scheme 3. Key steps in olefin polymerization catalysis.⁴³

Initiation



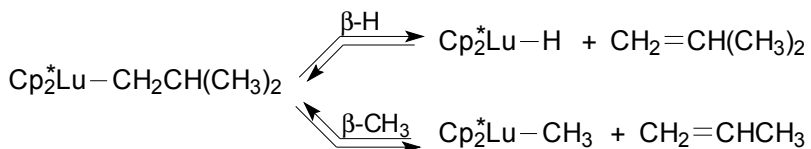
Propagation



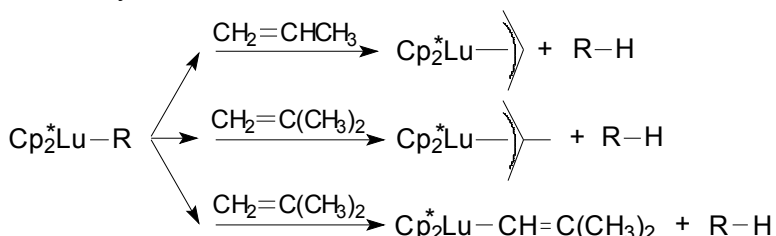
Termination and chain transfer



Termination and chain transfer by olefin extrusion



Termination by C-H activation



Propylene reacts with (Cp_2^*LuMe)₂ to produce only oligomers, indicating that transfer and termination reactions are faster than propagation. It was shown that monomer insertion proceeds regiospecifically into the Lu-CH₃ bond to give exclusively the isobutyl complex. Subsequent insertion into the Lu-isobutyl bond is much slower because of the bulkiness of the alkyl group. Transfer and termination reactions were well identified. The isobutyl complex arising from the first monomer insertion undergoes very slow and reversible β -hydrogen

⁴² (a) Watson, P. L. *J. Am. Chem. Soc.* **1982**, *104*, 337-339. (b) Watson, P. L.; Herskovitz, T. *ACS Symp. Ser.* **1983**, *212*, 459.

⁴³ (a) Watson, P. L.; Roe, D. C. *J. Am. Chem. Soc.* **1982**, *104*, 6471-6473. (b) Watson, P. L.; Parshall, G. W. *Acc. Chem. Res.* **1985**, *18*, 51-56.

elimination to form isobutylene and a lutetium hydride. Simultaneously, a predominant β -methyl extrusion occurs. Both reactions are thermodynamically unfavorable but proceed detectably because other reactions consume the olefinic coproducts. The latter reactions are chain transfer with H₂ and terminations by C-H activation. Abstraction of an allylic methyl C-H from propene or isobutylene gives allylic complexes, which do not react further with propene.

3.5.1.2. Further investigations

Bis(cyclopentadienyl) alkyl complexes of yttrium were first reported by Teuben *et al.*, showing comparable results to those obtained with lutetium.⁴⁴

Further investigations were recently conducted with (Cp₂*YH)₂ by Casey and co-workers.⁴⁵ The authors explained why only propene could not be polymerized using this complex, comparing ethylene, propene and 1-hexene polymerizations. For ethylene polymerization, the insertion of ethylene into the straight metal-alkyl bond is very rapid because of the high reactivity of the monomer and the resulting unbranched alkyl chain. Also, β -hydrogen elimination, the only possibility of transfer reaction, is very slow relative to propagation. For propene, chain extension is slower due to lower monomer reactivity and because of the branched growing alkyl chains that exhibit propagation step approximately 200 times slower than straight alkyl chains. Chain termination by abstraction of an allylic methyl C-H from propene to give η^3 -allyl yttrium complex is much faster than β -hydrogen elimination and occurs at the same rate as propene insertion. For 1-hexene, chain extension is expected to be about as fast as for propene, but termination is much slower because the monomer has only less reactive allylic methylene hydrogens and no reactive allylic methyl groups. The reactivity of (Cp₂*YH)₂ towards C-H bonds decreases in order of allylic CH₃ >> vinyl C-H >> allyl CH₂. Complementary kinetics results reported the existence of three distinct olefin insertion mechanisms with (Cp₂*YH)₂, depending on alkene substitution.

Quantum chemical investigation of the initial steps of yttrium-mediated polymerization of ethylene and propene confirmed experimental information and provided additional clues.⁴⁶ The catalyst chosen for this study was (Cp₂YH)₂. It was shown that the reaction sequence consists of several steps, starting with the formation of an electrostatically bound encounter complex between the catalyst and olefin, followed by the insertion of the monomer into the Y-H bond and finally formation of a Cp₂Y-C₂H₅ or Cp₂Y-C₃H₇ species. For both monomers, several energetic pathways leading to the catalyst-monomer complexes have been identified. The overall reaction is exothermic by 22.2 and 19.5 kcal mol⁻¹ for ethylene and propene, respectively. The formation of a "Y" shape monomer-catalyst complex, which prevents the subsequent insertion of the next incoming monomer unit due to severe steric problems, is the

⁴⁴ Den Haan, K. H.; Wielstra, Y.; Eshuis, J. J. W.; Teuben, J. H. *J. Organomet. Chem.* **1987**, 323, 181-192.

⁴⁵ (a) Casey, P. C.; Tunge, J. A.; Fagan M. A. *J. Organomet. Chem.*, **2002**, 663, 91-97. (b) Casey, P. C.; Tunge, J. A.; Lee, T.-Y.; Carpenetti II, D. W. *Organometallics*, **2002**, 21, 389-396. (c) Casey, P. C.; Tunge, J. A.; Lee, T.-Y.; Fagan, M. A. *J. Am. Chem. Soc.* **2003**, 125, 2641-2651.

⁴⁶ (a) Sändig, N.; Dargel, T. K.; Koch, W. *Z. Anorg. Allg. Chem.* **2000**, 626, 392-399. (b) Sändig, N.; Koch, W. *Organometallics* **2002**, 21, 1861-1869.

hypothesis proposed for explaining the impossibility to polymerize propene with this kind of catalyst.

A similar reactivity towards propene was observed with scandium complexes.⁴⁷ Because of the lower reactivity of scandium derivatives, the elementary steps of polymerization were clearly identified. With excess propene, $\text{Cp}_2^*\text{ScH}(\text{THF})$ led to a stepwise reaction. A rapid insertion into the scandium hydride bond was first observed followed by a slower elimination of propane and generation of a *trans*-propenyl derivative, which is unreactive towards propene. Later, insertion and β -hydrogen elimination in ethylene polymerization was investigated using a series of permethylscandocene alkyls.⁴⁸ Second-order rate constants for ethylene insertion into Sc-C bonds at $-80\text{ }^\circ\text{C}$ have been measured by using ^{13}C NMR spectroscopy. It was shown that the metal-carbon(hydrogen) bond affects the ethylene insertion rate ($\text{Sc-H} >> \text{Sc-CH}_2-(\text{CH}_2)_n-\text{CH}_3 > \text{Sc-}n\text{Pr} > \text{Sc-Et} > \text{Sc-Ph}$). A stronger bond results in a lower insertion rate and stabilizing β -agostic interaction also serves to retard ethylene insertion. The β -hydrogen elimination rate was measured by rapid trapping of Cp_2^*ScH with 2-butyne. The relative order of reactivity is $\text{R= Ph-}p\text{-NMe}_2 > \text{CH}_3 > \text{CH}_2\text{-CH}_3 > \text{Ph} > \text{H} > \text{Ph-}p\text{-CF}_3$ (Table 1).

Table 1. Rate constants for β -Hydrogen elimination of Cp_2^*ScR complexes.⁴⁸

R	T (K)	k (s ⁻¹)
CH_2CH_3	290	3.98×10^{-4}
$\text{CH}_2\text{CH}_2\text{CH}_3$	275	3.01×10^{-4}
$\text{CH}_2\text{CH}_2\text{CH}_2\text{CH}_3$	285	7.63×10^{-4}
$\text{CH}_2\text{CH}_3\text{SiMe}_3$	298	5.38×10^{-6}
$\text{CH}_2\text{CH}_2\text{Ph}$	290	5.23×10^{-4}
$\text{CH}_2\text{CH}_2\text{Ph-}p\text{-CH}_3$	290	1.04×10^{-3}
$\text{CH}_2\text{CH}_2\text{Ph-}p\text{-NMe}_2$	265	3.74×10^{-6}
$\text{CH}_2\text{CH}_2\text{Ph-}p\text{-CF}_3$	295	1.32×10^{-4}

The results reported by Marks *et al.* enabled a nice comparison between late and early lanthanide polymerization chemistry.⁴⁹ They studied the synthesis and application of monomeric bis(pentamethylcyclopentadienyl) hydrocarbyl and dimeric hydride complexes of La, Nd, Sm and Lu. At room temperature and 1 atm of ethylene pressure, the $\text{Cp}_2^*\text{LnCH}(\text{TMS})_2$ complexes ($\text{Ln} = \text{La, Nd and Lu}$) failed to react with ethylene over the course of several hours. However reaction with H_2 under mild conditions gave the corresponding $(\text{Cp}_2^*\text{LnH})_2$ complexes that undergo rapid reaction with ethylene (turnover frequency exceeds 1800 s^{-1}) and present measurable activity even at -80°C . However, this high activity may be

⁴⁷ Thompson, M. E.; Bercaw, J. E. *Pure & Appl. Chem.* **1984**, *56*, 1-11.

⁴⁸ Burger, B. J.; Thompson, M. E.; Cotter, W. D.; Bercaw, J. E. *J. Am. Chem. Soc.* **1990**, *112*, 1566-1577.

⁴⁹ Jeske, G.; Lauke, H.; Mauermann, H.; Swepston, P. N.; Schumann, H.; Marks, T. J. *J. Am. Chem. Soc.* **1985**, *107*, 8091-8103.

observed only for short reaction times and the efficiency of initiation remains modest. The approximate order of reactivity follows decreasing ionic radius: La \geq Nd $>$ Lu (Table 2).

Table 2. Ethylene polymerization by $(Cp^*_2LnH)_2$ compounds: effect of the nature of Ln metal.⁴⁹

Ln	concn (μ M)	time (s)	activity (kg/molLn/atm/h)	$10^{-3} M_n$	M_w/M_n	chains/Ln
La	26	5	1.46×10^5	428	1.97	0.43
Nd	22	5	1.37×10^5	590	1.81	0.32
Lu	25	45	9.72×10^3	250	1.50	0.49

Conditions: reactions carried out in 140 mL of cyclohexane at 25 °C.

However, the kinetics of the process, as well as the molecular weight of the resulting polymers, is limited by mass transport. Insignificant β -H elimination and "low" molecular weight distribution are consistent with the latter ($M_w/M_n \approx 2$) (Table 3). In each case, low initiation efficiency, i.e., formation of less than one polymer chain per metal center is observed. In addition, La and Nd complexes react rapidly with propylene and 1-hexene at –10 °C to yield equal quantities of the disproportionation products i.e. alkane and metal η^3 -alkenyl. Interestingly, the analogous neutral silyl complexes $Cp^*_2NdSiH(SiMe_3)_2$ showed comparable reactivity towards ethylene.⁵⁰

Table 3. Effect of catalyst concentration and reaction time with $(Cp^*_2NdH)_2$.⁴⁹

concn (μ M)	time (s)	activity (kg/molNd/atm/h)	$10^{-3} M_n$	M_w/M_n	chains/Nd
11	10	1.13×10^5	-	-	-
22	5	1.37×10^5	590	1.81	0.32
60	10	3.84×10^4	233	4.46	0.46
60	60	2.32×10^4	-	-	-
60	180	8.23×10^3	-	-	-
22*	600	5.22×10^2	648	1.95	0.13

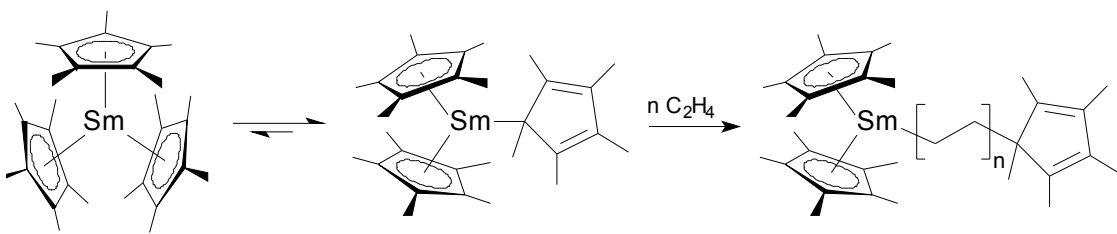
Conditions: reactions carried out in 140 mL of cyclohexane at 25 °C except * at -78 °C.

The sterically very crowded tris(pentamethylcyclopentadienyl) samarium was surprisingly found to be active for ethylene polymerization.⁵¹ Under mild conditions, an ultrahigh molecular weight polymer was obtained; the latter could not be analyzed with the usual analytical techniques ($M_w > 2 \times 10^6$). The authors speculated that one of the ring slips to form a η^1 -C₅Me₅ intermediate, which can then insert ethylene or eliminate tetramethylfulvene to form a catalytically-active Cp^*_2SmH species (Scheme 4).

Scheme 4. Mechanism of ethylene polymerization with a tris(cyclopentadienyl) complex.⁵¹

⁵⁰ Radu, N. S.; Don Tilley, T.; Rheingold, A. L. *J. Am. Chem. Soc.* **1992**, *114*, 8293-8295.

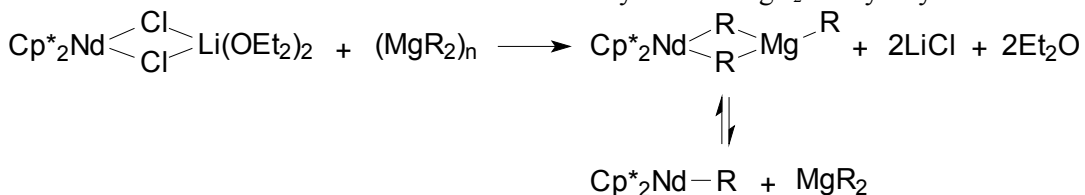
⁵¹ (a) Evans, W. J.; Forrestal, K. J.; Ziller, J. W. *Angew. Chem., Int. Ed. Engl.* **1997**, *36*, 774-776. (b) Evans, W. J.; Forrestal, K. J.; Ansari, M. A.; Ziller, J. W. *J. Am. Chem. Soc.* **1998**, *120*, 2180-2181. (c) Evans, W. J.; Forrestal, K. J.; Ziller, J. W. *J. Am. Chem. Soc.* **1998**, *120*, 9273-9282.



3.5.1.3. Binary lanthanocene catalyst systems

However, these complexes, especially the hydride complexes (Cp_2LnH)₂, are very sensitive, and their synthesis involves a multistep procedure as their handling is arduous. An alternative to circumvent this difficulty is the *in situ* formation of alkyl-lanthanide species from a readily available chlorolanthanocene, e.g. $\text{Cp}^*_2\text{NdCl}_2\text{Li(OEt)}_2$. Combination of the latter with a dialkylmagnesium compound generates an active, stable ethylene polymerization catalytic system in which a living ethylene growth chain transfer reaction between the MgR_2 species and the catalytically active lanthanocene complexes takes place, yielding eventually long chain dialkylmagnesium compounds Mg(PE)_2 with a narrow distribution (Scheme 5).^{52,53}

Scheme 5. Chain transfer reaction with the chloroneodymocene/ MgR_2 catalyst systems.⁵²



The activity are lower than those observed with the corresponding hydrido complexes (activity = 8000 kgPE/molNd/h at 50 °C in cyclohexane)⁵³ however the much more stable active species in the case of the *in situ* system enabled higher productivities. The kinetic and molecular weights depend on the Mg/Nd ratio and polymerization temperature. The initial activity decreases with an increase of this ratio.

It should be noticed that only MgR_2 and $n\text{-BuLi}$ are suitable alkylating agents for this system, neither AlEt_3 , AlEt_2Cl and ZnEt_2 enabled ethylene polymerization to take place. The authors initially presumed that the lower electropositivity of aluminum was insufficient to generate an alkyllanthanide species. However, the possibility of formation of the unreactive $[\text{Cp}^*_2\text{Ln}][\text{AlR}_4]$ species was also mentioned.⁵² Interestingly, AlEt_3 , methylaluminoxane, DIBAL-H/ $n\text{-BuLi}$ (1:1) and NaAlEt_4 were successfully applied with $(\eta^5\text{-}t\text{BuC}_5\text{H}_4)_2\text{Nd}(\mu\text{-Cl})$

⁵² (a) Olonde, X.; Bujadoux, K.; Mortreux, A.; Petit, F., FR 9307180 (ECP Enichem Polymeres France S.A.), **1994**. (b) Pelletier, J.-F.; Bujadoux, K.; Olonde, X.; Adisson, E.; Mortreux, A.; Chenal, T., EP 736536 (Enichem S.P.A., Italy; Université Des Sciences et Technologies De Lille), **1996**. (c) Olonde, X.; Mortreux, A. Petit, F.; Bujadoux, K. *J Mol. Catal.* **1993**, 82, 75-82. (d) Pelletier, J.-F.; Mortreux, A.; Petit, F.; Olonde, X.; Bujadoux, K. In *Catalyst Design for Tailor made Polyolefins*, Soga, K. and Terano, M., Eds, Elsevier, Amsterdam, **1994**, p249. (e) Pelletier, J.-F.; Mortreux, A.; Olonde, X.; Bujadoux, K. *Angew. Chem. Int. Ed. Engl.* **1996**, 35, 1854-1856. (f) Bujadoux, K.; Chenal, T.; Fouga, C.; Olonde, X.; Pelletier, J.-F.; Mortreux, A. In *Metalorganic Catalysts for Synthesis and Polymerization*, Kaminsky, W., Ed, Springer-Verlag, Berlin, **1999**, p590. (g) Bogaert, S.; Carpentier, J.-F.; Chenal, T.; Mortreux, A.; Ricart, G. *Macromol. Chem. Phys.* **2000**, 201, 1813-1822.

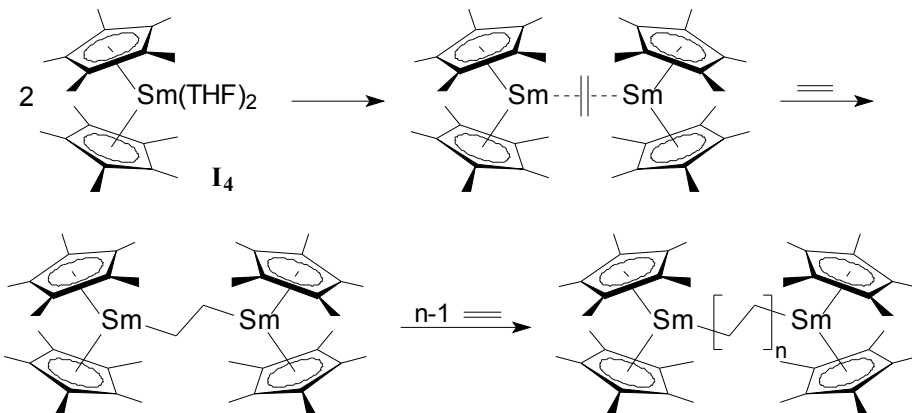
⁵³ Pettijohn, T. M.; Hsieh, H. L., US 5,109,085 (Phillips Petroleum Co., USA). **1992**.

$\text{Li(OEt}_2)_2$ for ethylene (co)-polymerization.⁵⁴ $(\eta^5\text{-tBuC}_5\text{H}_4)_2\text{Nd}(\mu\text{-Cl})_2\text{Li(OEt}_2)_2$ /aluminate systems behave roughly like $\text{Cp}^*\text{NdCl}_2\text{Li(OEt}_2)_2/\text{MgR}_2$ since stable activities were observed along with chain transfer between neodymium and aluminum.

3.5.1.4. Divalent lanthanocene catalysts

The use of cyclopentadienyl-type ligands was not simply restricted to trivalent lanthanides. In the early 1980's, Evans and co-workers reported the synthesis of divalent complexes of formula $(\eta^5\text{-C}_5\text{H}_5)_2\text{ML}_n$ (with L = Et₂O, THF; n = 0, 1, 2; M = Sm, Eu, Yb).⁵⁵ Among these complexes, samarium complex exhibited activity in ethylene polymerization. At this time, the mechanism was unclear. Watson, who worked also on these catalysts, found that only ether-coordinated complexes could polymerize ethylene.^{42,43} Only 15 years later, a mechanism of polymerization with divalent lanthanocenes was reported.⁵⁶ The complexation of one ethylene molecule by two samarium complexes generates after an electron transfer reaction two trivalent alkyl-lanthanocene species linked by a bismethylene bridge, this difunctional initiator acting as two single trivalent species (Scheme 6).

Scheme 6. Ethylene polymerization with divalent lanthanocene catalysts.⁵⁶



3.5.2. Ansa-lanthanocene catalysts

The main limitation of conventional lanthanocene polymerization catalysts is their inefficiency in α -olefin polymerization such as propene, due to the fast and irreversible allylic C-H activation. In order to suppress this side reaction, new sterically demanding ligands were designed. The latter are based on bridged-Cp ligands possessing low Cp-Ln-Cp bite angle (115-117°) in comparison with their analogous unbridged complexes (135-140°), creating additional available space around the metal center, i.e., favoring monomer approach. However, allylic C-H activation remains possible. In addition, the incorporation of bridged ligands affects the electronics configuration due to changes in orbitals overlapping.

Marks *et al.* reported the first *ansa*-lanthanocene complexes in 1985.^{49,57} $[\text{Me}_2\text{Si}(\eta^5\text{-C}_5\text{Me}_4)_2\text{LnH}]_2$ (Ln = Nd, Sm, Lu) were found to be active for propene oligomerization and

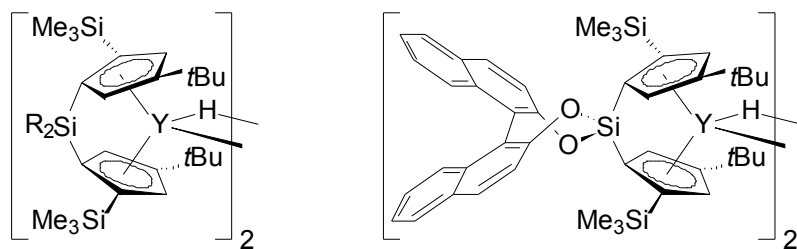
⁵⁴ (a) Barbotin, F.; Boisson, C.; Spitz, R., FR 2,799,468 (Michelin Recherche et Technique S.A.), **1999**. (b) Boisson, C.; Barbotin, F.; Spitz, R.; Congress Organometallic Catalysts and Olefin Polymerization, Oslo, Norway, June **2002**.

⁵⁵ Evans, W. J.; Bloom, I.; Hunter, W. E.; Atwood, J. L. *J. Am. Chem. Soc.* **1981**, *103*, 6507-6508.

⁵⁶ Evans, W. J.; DeCoster, D. M.; Greaves, J. *Macromolecules* **1995**, *28*, 7929-7936.

ethylene-1-hexene copolymerization while 1-hexene homopolymerization was limited to the dimer formation under D₂ atmosphere. Active α -olefin polymerization was observed with the more sterically crowded ligand Me₂Si(2-SiMe₃-4-*t*BuC₅H₂)₂.⁵⁸ The resulting yttrium C₂-symmetric complexes enabled highly isotactic α -olefin polymerization (isotactic pentad *mmmm* > 97%). However, rather low molecular weight polymers were obtained. High molecular weight isotactic polypentene ($M_n = 119,000$, $M_w/M_n = 1.44$ and *mmmm* > 95%) could be obtained by replacing the SiMe₂ bridge by the corresponding binaphthoxysilyl bridge.⁵⁹ These examples of *ansa*-lanthanocene catalysts are depicted in Figure 8.

Figure 8. Examples of *ansa*-lanthanocene catalysts for α -olefin polymerization.⁵⁸⁻⁵⁹



Yasuda *et al.* did a significant work in this area using mono- and bis(silylated)-bridged ligands.⁶⁰ The corresponding samarium and yttrium alkyls and hydrides complexes were tested for ethylene and α -olefin polymerization. They showed that the catalytic activity depends on the nature of the metal, the bulkiness of the ligand and the number of THF molecules coordinated (excess of coordinated THF led to polymerization inhibition). Thus, the activity decreases in the order I₇>I₅>I₈>I₆>I₉, (Figure 9).

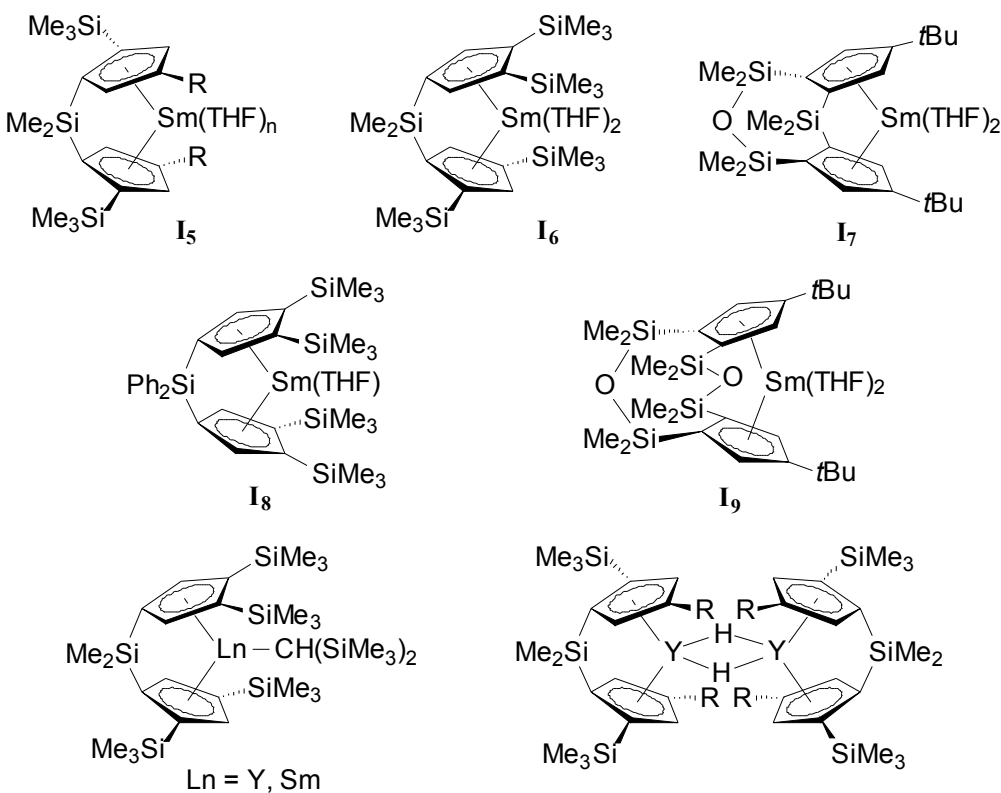
Figure 9. *Ansa*-lanthanocene complexes developed by Yasuda and co-workers.⁶⁰

⁵⁷ (a) Jeske, G.; Laurel, E.; Schock, P.; Swepston, P. N.; Schumann, H.; Marks, T. J. *J. Am. Chem. Soc.* **1985**, *107*, 8103-8110. (b) Mauermann, H.; Swepston, P. N.; Marks, T. J. *Organometallics* **1985**, *4*, 200-202. (c) Marks, T. J.; Mauermann, H., WO 8605788 (Northwestern University, USA) **1986**.

⁵⁸ (a) Wiesenfeldt, H.; Reinmuth, A.; Barsties, E.; Evertz, K.; Brintzinger, H.-H. *J. Organomet. Chem.* **1989**, *369*, 359-370. (b) Roll, W.; Brintzinger, H.-H.; Riegler, B.; Zolk, R. *Angew. Chem. Int. Ed. Engl.* **1990**, *29*, 279.

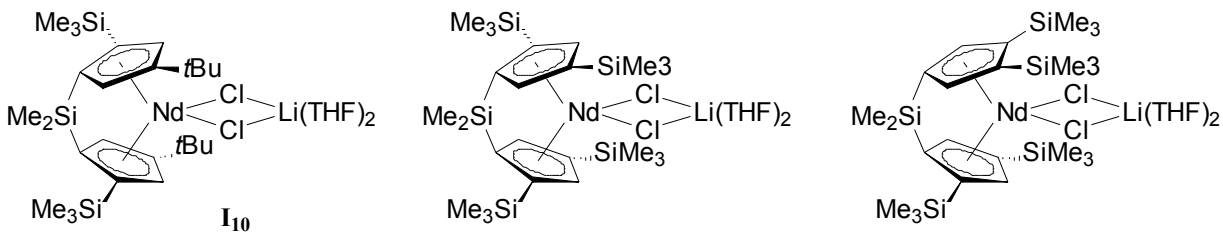
⁵⁹ (a) Mitchell, J. P.; Hajela, S.; Brookhart, K.; Hardcastle, K. I.; Henling, L. M.; Bercaw, J. E. *J. Am. Chem. Soc.* **1996**, *118*, 1045-1053. (b) Gilchrist, J. H.; Bercaw, J. E. *J. Am. Chem. Soc.* **1996**, *118*, 12021-12028.

⁶⁰ (a) Ihara, E.; Nodono, M.; Yasuda, H. *Macromol. Chem. Phys.* **1996**, *197*, 1909-1917. (b) Ihara, E.; Nodono, M.; Katsura, K.; Adachi, Y.; Yasuda, H.; Yamagashira, M.; Hashimoto, H.; Kanehisa, N.; Kai, Y. *Organometallics* **1998**, *17*, 3945-3956. (c) Yasuda, H.; Ihara, E.; Nitto, Y.; Kakehi, T.; Morimoto, M.; Nodono, M. *ACS Symp. Ser.* **1998**, *704*, 149-162. (d) Yasuda, H. *Prog. Polym. Sci.* **2000**, *25*, 573-626. (e) Ihara, E.; Yoshioka, S.; Furo, M.; Katsura, K.; Yasuda, H.; Mohri, S.; Kanehisa, N.; Kai, Y. *Organometallics* **2001**, *20*, 1752-1761.



The use of trivalent *ansa*-chloroneodymium complexes, based on similarly substituted *ansa*-bridged Cp ligands, has been also reported (Figure 10).⁶¹ In combination with a dialkylmagnesium cocatalyst, they afford ethylene and 1-octene polymerizations yielding di (oligoalkyl)magnesium species, which can be finally hydrolyzed to oligomers. The bulky bridged complexes gave significantly more active catalysts for 1-octene oligomerization ($M_n = 400\text{-}1300$, $M_w/M_n = 1.11\text{-}1.65$) than systems based on non-bridged complexes while best results were achieved with I₁₀.

Figure 10. *Ansa*-chlorolanthanocenes used in ethylene and 1-octene oligomerization.⁶¹



3.5.3. Monocyclopentadienyl complexes

3.5.3.1. Constrained geometry catalysts

Concomitantly to *ansa*-lanthanocenes, half-lanthanocenes complexes were explored.⁶² Bercaw and co-workers first reported the use of the amido-monocyclopentadienyl

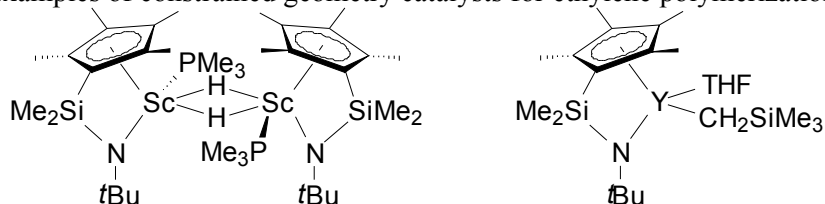
⁶¹ Bogaert, S.; Chenal, T.; Mortreux, A.; Nowogrocki, G.; Lehmann, C. W.; Carpentier, J.-F. *Organometallics* **2001**, *20*, 199-205.

⁶² Arndt, S.; Okuda, J. *Chem. Rev.* **2002**, *102*, 1953-1976.

organoscandium precatalyst for α -olefin polymerization (Figure 11).⁶³ The polymerizations were not stereospecific and rather slow, due to the tendency of the 12 electrons propagating alkyl to associate free trimethylphosphine, deactivating the reactive complex.

Further work from Okuda *et al.* on hydrido and alkyl complexes of yttrium, $[Y(\eta^5:\eta^1-C_5Me_4SiMe_2NCMe_3)(THF)(\mu-H)]_2$ and $[Y(\eta^5:\eta^1-C_5Me_4SiMe_2NCMe_3)(CH_2SiMe_3)(THF)]$ showed that the latter appear to be promising polymerization initiators for both non-polar and polar monomers (Figure 11).⁶⁴ Whereas ethylene is slowly polymerized by the hydrido complex at room temperature to give linear polyethylene ($T_m = 136$ °C), none of α -olefins, dienes, or styrene can be polymerized. In all these cases, stable mono(insertion) products can be isolated. The yttrium hydrido and alkyl complexes are found to polymerize the polar monomers such as *tert*-butyl acrylate and acrylonitrile while efficient and controlled polymerization of styrene could be developed by the use of the monomeric *n*-alkyl complex $[Y(\eta^5:\eta^1-C_5Me_4SiMe_2NCMe_3)\{(CH_2CH_2)_nH\}(THF)]$.

Figure 11. Examples of constrained geometry catalysts for ethylene polymerization.^{63,64}



3.5.3.2. Other monocyclopentadienyl complexes

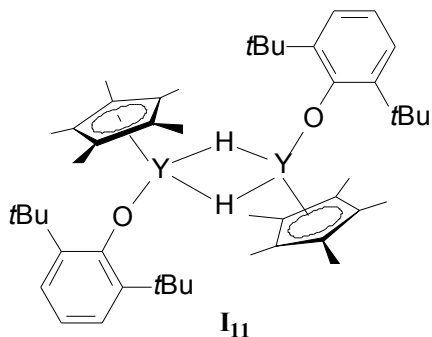
Introduction of an oxygen-Ln bond in α -olefin polymerization catalyst was first reported by Schaverien at Shell company with a half-metallocene complex (Figure 12).⁶⁵ Based on thermodynamic considerations, replacement of pentamethylcyclopentadienyl ligands by hard, electronegative ancillary ligands such as alkoxides is expected to suppress β -H elimination. This phenoxy-Cp complex exhibited high activity in ethylene polymerization, while 1-hexene was stereospecifically and smoothly polymerized ($M_n = 9400$; $M_w/M_n = 1.67$ and $mmmm > 85\%$).

Figure 12. Mixed monocyclopentadienyl-aryloxide complex for α -olefin polymerization.⁶⁵

⁶³ (a) Coughlin, E. B.; Shapiro, P. J.; Bercaw, J. E. *Polym. Prepr. (ACS, Div. Polym. Chem.)* **1992**, *33*, 1226-1227. (b) Piers, W. E.; Shapiro, P. J.; Bunel, E. E.; Bercaw, J. E. *Synlett* **1990**, *74*-84. (c) Bercaw, J. E. *Polym. Prepr. (ACS, Div. Polym. Chem.)* **1991**, *32*, 459-460. (d) Shapiro, P. J.; Bunel, E.; Schaefer, W. P.; Bercaw, J. E. *Organometallics* **1990**, *9*, 867-869. (e) Shapiro, P. J.; Schaefer, W. P.; Labinger, J. A.; Bercaw, J. E.; Cotter, W. D. *J. Am. Chem. Soc.* **1994**, *116*, 4623-4640.

⁶⁴ (a) Arndt, S.; Beckerle, K.; Hultzsch, K. C.; Sinnema, P.-J.; Voth, P.; Spaniol, T. P.; Okuda, J. *J. Mol. Catal. A: Chem.* **2002**, *190*, 215-223. (b) Okuda, J.; Arndt, S.; Beckerle, K.; Hultzsch, K. C.; Voth, P.; Spaniol, T. P. *Organometallic Catalysts and Olefin Polymerization* **2001**, 156-165, and references therein.

⁶⁵ (a) Schaverien, C. J. *Adv. Organomet. Chem.* **1994**, *36*, 283-362. (b) Schaverien, C. J. *J. Mol. Catal.* **1994**, *90*, 177-183. (c) Schaverien, C. J. *Organometallics* **1994**, *13*, 69-82.



Unconventional monocyclopadienyl pyrazinamide derivatives $\text{LnCp}(\text{MS})_2(\text{PzA})_2$ ($\text{Ln} = \text{Nd, Sm, Eu, Tb}$ and $\text{MS} = \text{methanesulfonate}$) and $\text{LnBr}_2\text{CpPzA}$ ($\text{Ln} = \text{Nd, Sm}$) activated with MAO presented catalytic activities of 4-6 kgPE/molLn/atm/h at 70 °C, with Al/Ln ratios of ca. 2000, independently of the lanthanide metal.⁶⁶ The formation of a cationic species by the reaction of MAO with the organolanthanide compound may be responsible for the catalytic activity.

3.5.3.3. Divalent monocyclopentadienyl complexes

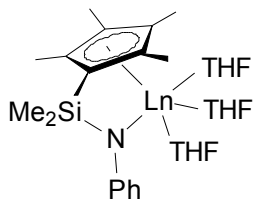
Divalent half-lanthanocenes were studied by Wakatsuki *et al.*⁶⁷ $\text{Me}_2\text{Si}(\text{C}_5\text{Me}_4)(\text{NPh})\text{Yb}(\text{THF})_3$ showed no activity for ethylene polymerization in toluene at room temperature under 1 atm, which is in agreement with the results previously reported for other $\text{Yb}^{(\text{II})}$ complexes.^{57a,68} In contrast, the more reducing $\text{Sm}^{(\text{II})}$ complex $\text{Me}_2\text{Si}(\text{C}_5\text{Me}_4)(\text{NPh})\text{Sm}(\text{THF})$ showed a moderate activity (44.8 kgPE/molSm/h) under the same conditions, to yield linear polyethylene with high molecular weight ($M_n = 7.26 \times 10^5$) and narrow polydispersity ($M_w/M_n = 1.58$) (Figure 13). These polymerization data can be compared with those reported for the $\text{C}_5\text{Me}_5/\text{HNAr-}$, $\text{C}_5\text{Me}_5/\text{HOAr-}$ and $\text{C}_5\text{Me}_5/\text{HPAr-ligated Sm}^{(\text{II})}$ complexes,^{57a} and the more sterically demanding $\text{Me}_2\text{Si}(\text{C}_5\text{Me}_4)(\text{PPh})\text{Sm}(\text{THF})$ complex,^{57c} but are in contrast with those for the samarocene^(II) complex $[(\text{C}_5\text{Me}_5)\text{Sm}(\text{SiH}_3)(\text{THF})(\text{C}_5\text{Me}_5)\text{K}(\text{THF})]_n$ ($M_n = 10,000$ and $M_w/M_n = 3.51$).^{67e}

Figure 13. Divalent half-lanthanocene catalyst for ethylene polymerization.⁶⁷

⁶⁶ (a) Miotti, R. D.; de Souza Maia, A.; Paulino, I. S.; Schuchardt, U.; de Oliveira, W. *Journal of Alloys and Compounds* **2002**, *344*, 92-95. (b) Lavini, V.; Maia, A. S.; Paulino, I. S.; Schuchardt, U.; Oliveira, W. *Inorg. Chem. Commun.* **2001**, *4*, 582-584.

⁶⁷ (a) Hou, Z.; Zhang, Y.; Tezuka, H.; Xie, P.; Tardif, O.; Koizumi, T.; Yamazaki, H.; Wakatsuki, Y. *J. Am. Chem. Soc.* **2000**, *122*, 10533-10543. (b) Hou, Z.; Koizumi, T.-A.; Nishiura, M.; Wakatsuki, Y. *Organometallics* **2001**, *20*, 3323-3328. (c) Tardif, O.; Hou, Z.; Nishiura, M.; Koizumi, T.-A.; Wakatsuki, Y. *Organometallics* **2001**, *20*, 4565-4573. (d) Kaita, S.; Wakatsuki, Y. *Pure Appl. Chem.* **2001**, *73*, 291-294. (e) Hou, Z.; Zhang, Y.; Nishiura, M.; Wakatsuki, Y. *Organometallics* **2003**, *22*, 129-135.

⁶⁸ Trifonov, A. A.; Kirillov, E. N.; Fisher, A.; Edelmann, F. T.; Bochkarev, M. N. *Chem. Commun.* **1999**, 2203-2204.



$\text{Ln} = \text{Yb, Sm}$

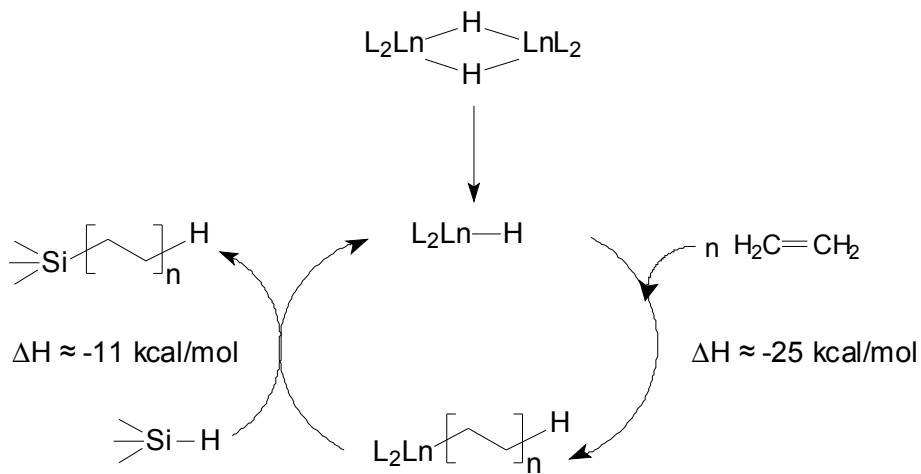
3.5.4. Chain transfer reactions

The efficient catalytic introduction of polar and/or reactive backbone or terminal functional groups into polyolefins via Ziegler-Natta processes currently represents a major scientific and technological challenge. Two major techniques were reported for the terminal mono-functionalization of polyolefins in lanthanocene catalysis.

3.5.4.1. Silanes as chain transfer agent

In addition to the desire of introducing functionalities into the polymer, new efficient and selective chain transfer agents were also sought since only limited and frequently non-selective *in situ* chain transfer means are available for such polymerizations (H_2 , β -H/alkyl elimination, monomer, main group alkyls). The mechanistic study of organolanthanide-catalyzed olefin hydrosilylation led Marks to utilize PhSiH_3 as transfer agent in lanthanocene-catalyzed α -olefin polymerization and copolymerizations.⁶⁹ Based on a Si-H/Ln-C σ -bond metathesis, silyl-terminated polymer chains can be obtained (Scheme 7).

Scheme 7. Chain transfer reaction in the presence of a hydrosilane with lanthanocene catalysts.⁶⁹



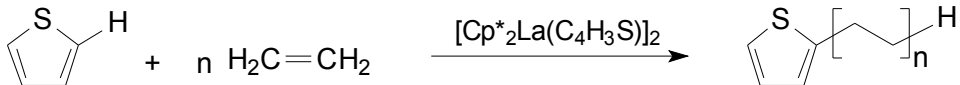
Qualitatively, the polymer molecular weights decrease as the silane concentration increases. This behavior is observed for ethylene homopolymerization but also ethylene-1-hexene and ethylene-styrene copolymerizations. Effective transfer reaction was confirmed by the characteristic PhSiH_2 resonance in ^1H and ^{13}C NMR analyses, except for Lu catalysts for which β -H elimination is the predominant chain transfer reaction.

⁶⁹ (a) Fu, P.-F.; Marks, T. J. *J. Am. Chem. Soc.* **1995**, *117*, 10747-10748. (b) Koo, K.; Fu, P.-F.; Marks, T. J. *Macromolecules* **1999**, *32*, 981-988.

3.5.4.2. Thiophene as transfer agent

Metallocene alkyls and hydrides of the group 3 metals are well-known to readily effect hydrocarbon C-H activation, reducing their efficiency in the polymerization of α -olefins such as propene, as inactive η^3 -allyl species are formed upon chain termination by allylic C-H activation of the monomer.^{42,70} The combination of ethylene polymerization and C-H activation process were supposed to be effective for chain transfer reaction. Teuben reported that ytrocene-mediated ethylene polymerization in the presence of pyridine produced 2-ethyl-pyridine due to the high stability of the first insertion product of ethylene in the Ln-pyridyl bond.⁷¹ When $[\text{Cp}^*_2\text{Y}(\mu\text{-C}_4\text{H}_3\text{S})]_2$ was used (resulting from the thiophene metalation on the 2-position by $[\text{Cp}^*\text{YH}]_2$), the polymerization was very sluggish. However, with the lanthanum analog, the formation of polyethylene with 2-thienyl end-groups was rapidly observed.⁷² ^1H NMR analysis indicated that all the polymer chains are capped on one side by a thienyl group, suggesting that C-H activation was the only chain transfer reaction during the polymerization (Scheme 8).

Scheme 8. Chain transfer reaction in the presence of silane with lanthanocene catalysts.⁷²



3.5.5. Post-lanthanocene catalysts

As shown above, a variety of bis(substituted cyclopentadienyl) alkyl and hydride complexes of rare earth metals have been reported to be active for ethylene polymerization. However, their olefin polymerization efficiency is largely limited to sterically unhindered monomers because of the high degree of steric saturation required to stabilize alkyl and hydride complexes of these large and very reactive metals. With complexes of formula " Cp_2LnR ", any α -olefin polymerization activity reported was rather low. In each case, the activity was lower than the one observed with group 4 catalysts. The appearance of *ansa*-lanthanocene complexes allowed better results, but still the activity remains low and the synthesis of the required ligands and corresponding complexes is tedious.

Consequently, there is considerable interest in developing the chemistry of organometallic yttrium and lanthanide alkyl and hydride complexes involving solubilizing and stabilizing ancillary ligands other than the commonly used cyclopentadienyl ligand. Many types of alternative ancillary ligand systems have been developed including alk(aryl)oxides,⁷³

⁷⁰ (a) Watson, P. L. *J. Chem. Soc., Chem. Commun.* **1983**, 276-277. (b) Evans, W. J.; Ulibarri, T. A.; Ziller, J. W. *Organometallics* **1991**, *10*, 134-142. (c) Booij, M.; Meetsma, A.; Teuben, J. H. *Organometallics* **1991**, *10*, 3246-3252. (d) Booij, M.; Deelman, B. J.; Duchateau, R.; Postma, D. S.; Meetsma, A.; Teuben, J. H. *Organometallics* **1993**, *12*, 3531-3540.

⁷¹ Deelman, B.-J.; Stevels, W. M.; Teuben, J. H.; Lakin, M. T.; Spek, A. L. *Organometallics* **1994**, *13*, 3881-3891.

⁷² (a) Hessen, B.; Ringelberg, S. N.; Meppelder, G.-J.; Teuben, J. H. *Polym. Prep. (ACS, Div. Polym. Chem.)* **2000**, *41*, 397-398. (b) Sinnema, P.-J.; Hessen, B.; Teuben, J. H. *Macromol. Rapid Comm.* **2000**, *21*, 562-566.

⁷³ Anwander, R.; *Top. Curr. Chem.* **1996**, *179*, 151-245, and references therein.

cyclooctatetraenides,⁷⁴ carboranes,⁷⁵ polypyrazolylborates,⁷⁶ amides,⁷⁷ phosphides,⁷⁸ porphyrins,⁷⁹ aza- and oxo-crowns,⁸⁰ benzamidinates,⁸¹ β -diketiminates,⁸² and alkoxyamides.⁸³ This new generation of catalysts will be referred as post-lanthanocenes or Cp-free catalysts. We would like to show here that even if the number of potential alternative ancillary ligands is important, providing a wide unexplored area to the polymer chemist, the reported examples for effective ethylene polymerization using these complexes are not that numerous, and the methodology to obtain post-lanthanocene active olefin polymerization catalysts remains unclear. These complexes will be divided in two categories based on the nature of the ancillary ligand: nitrogen and oxygen-based ligands.

3.5.5.1. Nitrogen-based catalysts

Trofinkenko's tris(pyrazolyl)borates are the focus of much research as a supporting ligand to control steric saturation and reactivity at a variety of metal centers. They display many advantages as a supporting ligand in lanthanide complexes over analogous Cp ligands due to the relative ease of tuning the blocking substituent groups on the 3-position of the pyrazole ring. Modification of these substituents has been shown to effect large changes in the reactivities of metal complexes because of the alteration of steric saturation and electronic character at the metal center.⁸⁴

The use of tris(pyrazolyl)-based ligands for lanthanide-mediated ethylene polymerization was reported by Bianconi and co-workers.⁸⁵ Thus, tris(3,5-dimethyl-1-pyrazolyl)borohydride (Tp^{Me}) complexes of yttrium of general formula [$Tp^{Me}YR_2(THF)_x$] (with R = C₆H₅, CH₂SiMe₃) and similar ones with variously substituted Tp ligands, as well as analogous lanthanide complexes, were found to be very poorly active in ethylene polymerization, yielding linear PE with extremely high molecular weight (Figure 14). The different members of this class of complexes showed variations in polymerization activity. All the Tp^{Me} -Y alkyl and hydride yielded linear PE with M_w, in some cases exceeding 2×10^6 g/mol, with polydispersities ranging from 2.5 to 4.1. In all cases, including the complexes containing the large phenyl and trimethylsilylmethyl groups, the polymerization occurred even though THF remained

⁷⁴ Edelmann, F. T. *New J. Chem.* **1995**, *19*, 535-550, and references therein.

⁷⁵ Reger, D. L.; Knox, S. J.; Lindeman, J. A.; Lebodia, L. *Inorg. Chem.* **1990**, *29*, 416-419.

⁷⁶ (a) Reger, D. L.; Lindeman, J. A.; Lebodia, L. *Inorg. Chem.* **1988**, *27*, 1890-1896. (b) Hasinoff, L.; Takats, J.; Zhang, X.; Bond, A. H.; Rogers, R. D. *J. Am. Chem. Soc.* **1994**, *116*, 8833-8834.

⁷⁷ Anwander, R.; *Top. Curr. Chem.* **1996**, *179*, 33-110, and references therein.

⁷⁸ Rabe, G. W.; Riede, J.; Schier, A. *Inorg. Chem.* **1996**, *35*, 40-45.

⁷⁹ Schaverien, C. J.; Orpen, A. G. *Inorg. Chem.* **1991**, *30*, 4968-4978.

⁸⁰ Lee, L.; Berg, D. J.; Einstein, F. W. *Organometallics* **1997**, *16*, 1819-1831.

⁸¹ (a) Duchateau, R.; van Wee, C. T.; Meetsma, A.; Teuben, J. H. *J. Am. Chem. Soc.* **1993**, *115*, 4931-4932. (b) Duchateau, R.; Meetsma, A.; Teuben, J. H. *Organometallics* **1996**, *15*, 1656-1661. (c) Duchateau, R.; van Wee, C. T.; Meetsma, A.; van Duijnen, P. T.; Teuben, J. H. *Organometallics* **1996**, *15*, 2279-2290. (d) Duchateau, R.; van Wee, C. T.; Teuben, J. H. *Organometallics* **1996**, *15*, 2291-2302.

⁸² (a) Lee, L. W. M.; Piers, W. E.; Elsegood, M. R. J.; Clegg, W.; Parvez, M. *Organometallics* **1999**, *18*, 2947-2949. (b) Hayes, P. G.; Piers, W. E.; Lee, L. W. M.; Knight, L. K.; Parvez, M.; Elsegood, M. R. J.; Clegg, W. *Organometallics* **2001**, *20*, 2533-2544.

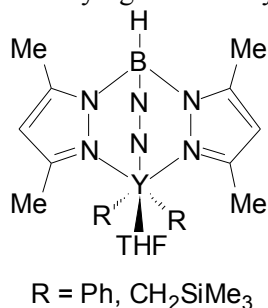
⁸³ Duchateau, R.; Tuinstra, T.; Brussee, E. A. C.; Meetsma, A.; van Duijnen, P. T.; Teuben, J. H. *Organometallics* **1997**, *16*, 3511-3522.

⁸⁴ Hillier, A. C.; Liu, S. Y.; Sella, A.; Elsegood, M. R. J. *Journal of Alloys and Compounds* **2000**, *303-304*, 83-93.

⁸⁵ (a) Bianconi, P. A. *Book of Abstracts, 211th ACS National Meeting, New Orleans, LA, March 24-28 1996*, (b) Long, D. P.; Bianconi, P. A. *J. Am. Chem. Soc.* **1996**, *118*, 12453-12454.

coordinated to the initial yttrium complexes. The highest activity was observed with $\text{Tp}^{\text{Me}}\text{YCl}_2$ (THF)/ $2t\text{-BuLi}$ as catalytic system. The use of tris(3-phenyl-1-pyrazolyl) borohydride (Tp^{Ph}) results in even smaller quantities of polymer, showing that the steric hindrance at the metal center affects the extent of polymerization. Although these findings were the first results regarding Cp-free lanthanide-based catalyst for ethylene polymerization, this area was not further investigated. The relative limited stability of Tp ligands might be a likely explanation.⁸⁶

Figure 14. Tris(pyrazolyl)borate as ancillary ligand for ethylene polymerization.⁸⁵



The reactivity of yttrium triazacyclononane-based lanthanide complexes towards olefins has been reported. The tris(alkyl) complexes (1,4,7-trimethyl-1,4,7-triazacyclononane) LnCH_3 ($\text{Ln} = \text{Sc, Y}$) were found unreactive towards ethylene (Figure 15).⁸⁷ However, activation of the scandium compound with either $[\text{PhNMe}_2\text{H}][\text{B}(\text{C}_6\text{F}_5)_4]$ or $\text{B}(\text{C}_6\text{F}_5)_3$ resulted in slow ethylene polymerization and 1-pentene oligomerization ($M_n = 4000$ and $M_w/M_n = 1.32$) irrespective of the activator.

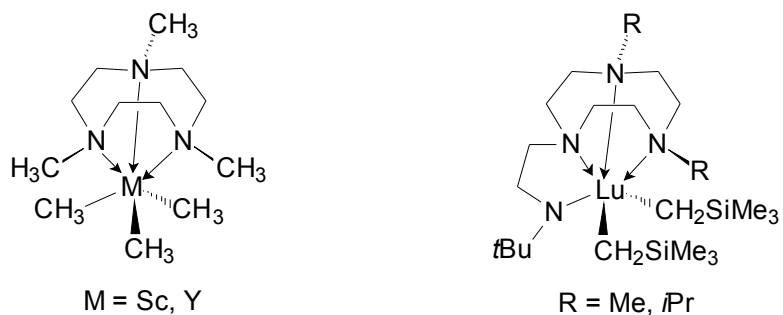
More recently, the synthesis of the $[\text{N,N}'\text{-R}_2\text{-1,4,7-triazacyclononane-N''-(CH}_2\text{CH}_2\text{)NtBu}]$ $\text{Y}(\text{CH}_2\text{SiMe}_3)_2$ ($\text{R} = i\text{Pr}$ or Me) afforded the formation of a cationic active species for ethylene polymerization after reaction with the Brönsted acid activator $[\text{PhNMe}_2\text{H}][\text{B}(\text{C}_6\text{F}_5)_4]$ (Figure 15).⁸⁸ The polymerizations were performed under 5 bar ethylene pressure in toluene solution at various temperatures for 10-15 minutes. Increasing the reaction temperature enhanced the productivity (up to 1800 kgPE/molY/atm/h), concomitantly with higher polydispersities. A likely explanation for this observation might be the thermal transformation of the initial cationic alkyl complex into another species that is also active in the polymerization of ethylene.

Figure 15. Triazacyclononane-based complexes for ethylene polymerization.^{87,88}

⁸⁶ Domingo, A.; Elsegood, M. R. J.; Hillier, A. C.; Lin, G.; Liu, S. Y.; Lopes, I.; Marques, N.; Maunder, G. H.; McDonald, R.; Sella, A.; Steed, J. W.; Takats, J. *Inorg. Chem.* **2002**, *41*, 6761-6768.

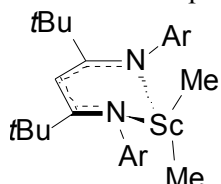
⁸⁷ Hajela, S.; Schaefer, W. P.; Bercaw, J. E. *J. Organomet. Chem.* **1997**, *532*, 45-53.

⁸⁸ (a) Bambirra, S.; Van Leusen, D.; Meetsma, A.; Hessen, B.; Teuben, J. H. *Abstracts of Papers, 222nd ACS National Meeting, Chicago, IL, United States, August 26-30, 2001*. (b) Bambirra, S.; van Leusen, D.; Meetsma, A.; Hessen, B.; Teuben, J. H. *Chem. Commun.* **2001**, 637-638.



Another example of pseudo-cationic catalyst for ethylene polymerization was reported by Piers *et al.* Preliminary results on β -diketiminato "nacnac" dialkyl scandium complexes showed that one of the dibenzyl derivatives may be activated with $\text{B}(\text{C}_6\text{F}_5)_3$ to form an ion pair.⁶³ The X-ray structure of this complex shows that the counteranion $[\text{PhCH}_2\text{B}(\text{C}_6\text{F}_5)_3]^-$ is strongly η^6 -coordinated to the cationic scandium center, a feature that explains the lack of reactivity towards olefins. Given the usual activity observed with such cationic species, development of bulkier nacnac donor with *t*Bu groups was undertaken to avoid such coordination (Figure 16).⁸⁹ Activation of the dimethyl or dichloro precursors with $\text{B}(\text{C}_6\text{F}_5)_3$ or $[\text{Ph}_3\text{C}][\text{B}(\text{C}_6\text{F}_5)_4]$ gave effective catalysts for ethylene polymerization. In slurry batch reactor at 50 °C, polymer with relatively high molecular weights ($\approx 1 \times 10^6$ g/mol) and polydispersities consistent with a single site catalysis model ($M_w/M_n < 2$) are obtained. Activities are slightly lower when the dichloride precursor is used, indicating a slower alkylation of the scandium center. Overall, the activities approach those observed for lanthanocene catalysts, demonstrating once more that scandium cations can be highly effective catalysts for ethylene polymerization.

Figure 16. β -diketiminato dialkyl scandium complexes for ethylene polymerization.⁸⁹



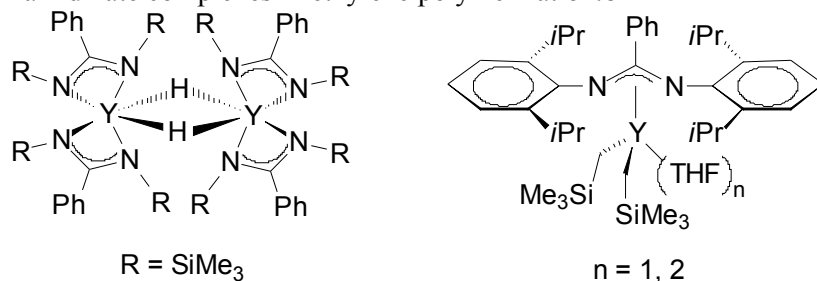
Bis(benzamidinato)yttrium alkyls complexes $[\text{PhC}(\text{NSiMe}_3)_2]_2\text{YCH}_2\text{Ph}\cdot\text{THF}$ and $[(\text{PhC}(\text{NSiMe}_3)_2)\text{Y}(\mu\text{-H})]_2$ were previously reported to be moderately active in ethylene polymerization but inactive towards propylene and 1-hexene when employed as neutral catalyst.^{81d} Under rather drastic conditions (55 °C, 70 bar ethylene pressure), the hydride complex exhibits low activity (4 kgPE/molY/h); the activity noticed with the benzyl derivative was even lower. It seems that either activation of the precatalysts by dissociation or precomplexation of ethylene is unfavorable in these complexes. This was explained as the consequence of the high ionic character of these bis(benzamidinato)yttrium compounds, which causes the yttrium orbitals to contract strongly, making them less available to interact with the incoming olefin.

Very recently, Bambirra *et al.* reported that the monobenzamidinate yttrium dialkyl complex $[\text{PhC}(\text{NAr})_2]\text{Y}(\text{CH}_2\text{SiMe}_3)_2(\text{THF})$ ($\text{Ar} = 2,6$ -diisopropylphenyl), when activated with

⁸⁹ Hayes, P. G.; Piers, W. E.; McDonald, R. *J. Am. Chem. Soc.* **2002**, *124*, 2132-2133.

$[\text{PhNMe}_2\text{H}][\text{B}(\text{C}_6\text{F}_5)_4]$, polymerizes ethylene yielding PE with low polydispersity (Figure 17).⁹⁰ The polymerizations were carried out in toluene solution at 50 °C under 5 bar ethylene pressure for 5 to 30 minutes. Under these conditions, the polymerizations exhibit a living character. Narrow molecular weight distribution along with the formation of one polymer chain per yttrium are evidences for this living nature, and prove the absence of the usual β -H elimination reaction with this catalytic system. The activities are rather high although it slightly decreases with the reaction time (from 1040 kgPE/molY/atm/h over 5 min to 400 kgPE/molY/atm/h over 30 min). The combination of the bis-THF adduct $[\text{PhC}(\text{NAr})_2]\text{Y}(\text{CH}_2\text{SiMe}_3)_2(\text{THF})_2$ with $[\text{PhNMe}_2\text{H}][\text{B}(\text{C}_6\text{F}_5)_4]$ did not result in effective ethylene polymerization. The bonding of the second THF molecule to the cationic metal species is sufficiently strong to suppress catalytic activity. However, in the presence of an excess of partially hydrolyzed tris(isobutyl)aluminum as scavenger, an effective ethylene polymerization was observed. Lower molecular weights are obtained and the formation of 5 polymer chains per yttrium atom was calculated, irrespective of the reaction time. This observation is in agreement with transfer of the polymer chain from the group 3 metal to the main group metal and vice-versa, and where chain termination by β -H elimination is insignificant.

Figure 17. Benzamidinate complexes in ethylene polymerization.^{81^d,90}

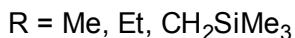
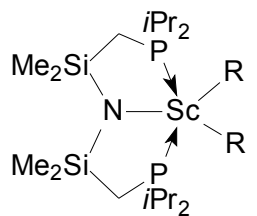


New five-coordinate scandium diphosphine dialkyl complexes $\text{ScEt}_2[\text{N}(\text{SiMe}_2\text{CH}_2\text{PiPr}_2)_2]$ and $\text{Sc}(\text{CH}_2\text{SiMe}_3)_2[\text{N}(\text{SiMe}_2\text{CH}_2\text{PiPr}_2)_2]$ revealed to be active in olefin polymerization (Figure 18).⁹¹ The hard amido donor group is necessary to anchor the ligand to this electropositive metal center and this forces the phosphine donors to bind by virtue of their proximity. The reaction of ethylene with these bis(hydrocarbyl) complexes resulted in the formation of polyethylene. Unfortunately, the nature of the catalytically active species could not be determined and no report on the activity was mentioned.

Figure 18. Scandium diphosphine dialkyl complexes for ethylene polymerization.⁹¹

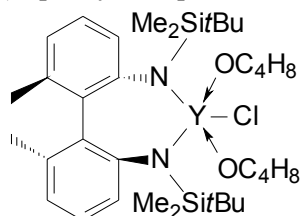
⁹⁰ Bambirra, S.; Van Leusen, D.; Meetsma, A.; Hessen, B.; Teuben, J. H. *Chem. Commun.* **2003**, 522-523.

⁹¹ Fryzuk, M. D.; Giesbrecht, G.; Rettig, S. J. *Organometallics* **1996**, 15, 3329-3336.



Finally, a very low polymerization activity was observed with C_2 -symmetric bis(silylamido)biphenyl yttrium complexes⁹² (Figure 19) while surprisingly [NON]YR(THF) complexes were inert towards ethylene ($[NON]^{2-} = [(tBu-d_6-N-o-C_6H_4)_2O]^{2-}$).⁹³ A catalytic activity was expected since the latter would be isoelectronic of the group 4 catalyst efficient for the living polymerization of 1-hexene.⁹⁴ Exposure of the chloro-complex to ethylene (5.5 bar) in the presence of MAO (500 equiv.) in toluene produced 0.06 g of polyethylene. Use of the corresponding alkyl complex did not allow higher activity. As postulated previously, steric hindrance, coordinate THF and high ionicity in the bonding might be the causes for such low reactivity towards olefins.

Figure 19. Low activity bis(silylamido)biphenyl complex in ethylene polymerization⁹²



3.5.5.2. Oxygen-based catalysts

Beside the nitrogen-based post-lanthanocene catalysts, alk(aryl)oxide ligands seem also attractive because they offer strong metal oxygen bonds which can stabilize complexes of these electropositive metals. However, relatively few examples of oxygen-based post-lanthanocene catalysts have been reported to be effective catalysts for ethylene polymerization.

Among the dozen of structurally well-defined cyclopentadienyl-free lanthanide alkyl-aryloxide complexes that have been described to date, only the neutral dialkyl-aryloxide complex $[Y\{CH(SiMe_3)_2\}_2(O-2,6-tBu_2C_6H_3)(THF)_2]$ (**I₁₂**) has shown very low ethylene polymerization activity under 5 bar ethylene pressure in toluene solution (9×10^{-3} kgPE/molY/atm/h at RT) (Figure 20).⁹⁵ No polymer characteristics were available. This poor ability for ethylene polymerization is rather surprising since alkoxy ligands are expected to render the metal center more electron-deficient and more Lewis acidic.

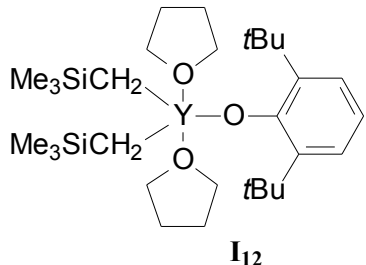
Figure 20. Sole well-defined mixed alkyl-aryloxy complex active in ethylene polymerization.⁹⁵

⁹² Gountchev, T. I.; Don Tilley, T. *Organometallics* **1999**, *18*, 2896-2905.

⁹³ Graf, D. D.; Davis, W. M.; Schrock, R. R. *Organometallics* **1998**, *17*, 5820-5824.

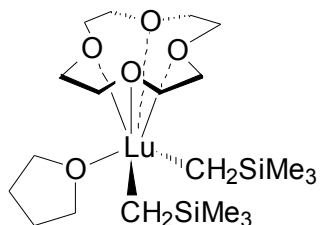
⁹⁴ Baumann, R.; Davis, W. M.; Schrock, R. R. *J. Am. Chem. Soc.* **1997**, *119*, 3830-3831.

⁹⁵ Evans, W. J.; Broomhall-Dillard, R. N. R.; Ziller, J. W. *J. Organomet. Chem.* **1998**, *569*, 89-97.



As it was observed with nitrogen-based complexes, cationic complexes seem to exhibit higher activities. Okuda *et al.* have reported that some lutetium alkyl cations, bearing crown ether as oxygenated ligands, are very active for ethylene polymerization.⁹⁶ These complexes have the general formula $[\text{Lu}(\text{CH}_2\text{SiMe}_3)_2(\text{CE})(\text{THF})_n][\text{B}(\text{CH}_2\text{SiMe}_3)(\text{C}_6\text{H}_5)_3]$ with CE = [12]-crown-4, n = 1; CE = [15]-crown-5 and [18]-crown-6, n = 0 (Figure 21). The anions were shown to be non-coordinating and the cation formation from alkyl abstraction was possible under mild conditions with triphenylborane, the use of the more electrophilic perfluorinated triphenylborane being not required. This indicates a high reactivity of the complex, high reactivity observed towards olefins since a significant ethylene polymerization was noticed. Unfortunately, no data are available concerning either the polymerization conditions or the polymer characteristics.

Figure 21. Crown ether as ancillary ligand for dialkyl lutetium complexes.⁹⁶



Binary catalytic systems composed of a rare earth calix[n]arene (n = 4, 6, 8 and rare earth metals = La, Nd, Sm, Dy, Y) complexes and Al(*i*Bu)₃ were found to be effective homogeneous catalysts for ethylene polymerization.⁹⁷ Linear high molecular weight polymers ($M_n > 5 \times 10^5$) with melting temperatures ranging from 128 to 136 °C were obtained along with moderate activities (up to 56 kgPE/molNd/h). Neodymium calix[n]arenes activities decrease in the order: C₆Nd > C₄Nd > C₈Nd. Although rare earth elements are very similar in chemical properties, their catalytic activities in ethylene polymerization are quite different depending on the ligand. A maximum of activity was noticed at 80 and 120 °C for respectively C₄Nd and C₆Nd. However, the molecular weight of the polymer decreased with an increase in reaction temperature due to the enhanced β-H transfer reaction at higher temperatures. AlEt₃ and Al(*i*Bu)₂H proved to be efficient cocatalysts with C₆Nd for ethylene polymerization while no polymer was produced with Al(*i*Bu)₂Cl as cocatalyst.

⁹⁶ Arndt, S.; Spaniol, T. P.; Okuda, J. *Chem. Commun.* **2002**, 896-897.

⁹⁷ Chen, Y.; Zhang, Y.; Shen, Z; Kou, R.; Chen, L. *Eur. Polym. J.* **2001**, 37, 1181-1184.

The oligomerization of 1-octene with lanthanide carboxylates or phosphonates associated with AlR_3 in CCl_4 as solvent was reported in the early 1990's.⁹⁸ The best results were obtained with a catalytic system based on neodymium naphtenate associated with AlEt_3 in CCl_4 . The use of other chlorinated solvents does not bring dramatic changes in the polymerization characteristics and the catalytic activity of early rare earth elements seems to be slightly higher than that of late ones (with $\text{Nd}(\text{naph})_3$ activity = 2.5 kgPO/molNd/h at 50 °C). It was found that the catalyst aged for the same time at room temperature gave better results than the one aged at 60 °C. Maximum conversion and molecular weight were obtained at Al/Nd mol ratio in the range 6-8. In addition, chain-transfer reactions were evidenced in 1-octene polymerization with $\text{Nd}(\text{naph})/\text{AlEt}_3$ as catalytic system. The observed kinetics first order with respect to monomer concentration and the presence of double bonds in the polymer agree with the latter.

4. Polymerization of methyl methacrylate initiated by rare earth compounds

4.1. Introduction

The polymerization of methacrylates, and especially methyl methacrylate, has been studied for decades. This class of monomer has the ability to be polymerized by anionic, group transfer, radical and coordinative-anionic (organometallic) methods. Now, research focuses on their controlled stereospecific polymerization to achieve high molecular weight polymers with low polydispersity. Syndiotactic poly(methacrylates) are especially the subject of many investigations because of their improved thermo-physical properties.

4.1.1. Anionic polymerization

In anionic polymerization, secondary side reactions of alkyl methacrylates arise from the possible nucleophilic attack of the active species (ester enolates) on the ester group of both the monomer and the polymer chain (back-biting). Another problem is the tendency of ester enolates to aggregate to dimers or tetramers; the slow exchange between aggregated and non-aggregated ion pairs most often causes a significant broadening of the molecular weight distribution.

Generally, optimum conditions for improving the living character of alkyl methacrylates polymerization include the use of bulky initiators, polar solvent (e.g. THF), and low temperature (< -60 °C). The reactivity and aggregation properties of anionic species can be also modulated by coordination with Lewis acidic ligands such as alkali metal alkoxides,⁹⁹ Li

⁹⁸ Yang, M.; Zhang, X.; Li, J.; Shen, Z. *J. Polym. Sci., Part A: Polym. Chem.* **1992**, *30*, 63-69.

⁹⁹ (a) Lochmann, L.; Rodova, M.; Trekoval, J. *J. Polym. Sci (Chem. Ed.)* **1974**, *12*, 2091-2094. (b) Lochmann, L.; Pokorny, J.; Trekoval, J.; Alder, H. J.; Berger, W. *Makromol. Chem.* **1983**, *184*, 2021-2031. (c) Lochmann, L.; Müller, A. H. E. *Makromol. Chem.* **1990**, *191*, 1657-1664. (d) Janata, M.; Lochmann, L.; Vlcek, P.; Dybal, J.; Müller, A. H. E. *Makromol. Chem.* **1992**, *193*, 101-112. (e) Janata, M.; Lochmann, L.; Müller, A. H. E. *Makromol. Chem.* **1993**, *194*, 625.

alkoxyalkoxides,¹⁰⁰ Li salts (LiCl, LiClO₄),¹⁰¹ Li silanlates,¹⁰² as well as Al-alkyls.¹⁰³ With the latter examples and the use of metal-free initiators,¹⁰⁴ the effect of the cation on the ion pair association and the degree of termination is nowadays well documented.¹⁰⁵ Recent years have witnessed considerable efforts to polymerize alkyl methacrylates under suitable conditions for process scaling-up, i.e. at temperatures above 0 °C in hydrocarbon media, keeping all the advantages of a living polymerization. The controlled anionic polymerization of methyl methacrylate in toluene at 20 °C was first achieved using an initiator system consisting of a lithiated ester enolate and an alkali metal *tert*-butoxide as ligand.^{99a,b} The living isotactic polymerization of MMA in toluene at 0 °C with *n*-BuLi-siloxane systems has recently been reported.¹⁰² Besides the innumerable studies devoted to organolithium initiators, the use of alkylmagnesium initiators in the anionic polymerization of alkyl methacrylates is more restricted. It is known that *t*-BuMgBr•Et₂O causes no side reaction in the polymerization of MMA in toluene at -78 °C and forms highly isotactic polymer (mm > 95%) with narrow molecular weight distribution ($M_w/M_n < 1.2$).¹⁰⁶

Table 4. Characteristics of conventional initiators for syndiotactic PMMA.¹⁰⁷

initiator	temp. (°C)	$10^{-3} M_n$	M_w/M_n	tacticity (%)			conversion (%)
				rr	rm	mm	
CH ₃ (CH ₂) ₄ CPh ₂ Li	-78	10	1.18	83.8	15.1	1.1	100
(piperidinyl)MgEt	-78	29	2.17	91.0	7.6	1.4	93
<i>i</i> BuMgBr ^b	-110	15	1.84	94.3	5.7	0.0	12

¹⁰⁰ (a) Wang, J. S.; Jérôme, R.; Bayard, P.; Patin, M.; Teyssié, P. *Macromolecules* **1994**, *27*, 4635-4638. (b) Maurer, A.; Marcarian, X.; Müller, A. H. E.; Navarro, C.; Vuillemin, B. *Polym. Prepr. (ACS, Div. Polym. Chem.)* **1997**, *38*, 467-468.

¹⁰¹ (a) Fayt, R.; Forte, R.; Jacobs, C.; Jérôme, R.; Ouhadi, T.; Teyssié, P.; Varshney, S. K. *Macromolecules* **1987**, *20*, 1442-1444. (b) Baskaran, D.; Sivaram, S. *Macromolecules* **1997**, *30*, 1869-1874. (c) Baskaran, D.; Müller, A. H. E.; Sivaram, S. *Macromolecules* **1999**, *32*, 1356-1361.

¹⁰² (a) Zundel, T.; Teyssié, P.; Jérôme, R. *Macromolecules* **1998**, *31*, 2433-2439. (b) Zundel, T.; Zune, C.; Teyssié, P.; Jérôme, R. *Macromolecules* **1998**, *31*, 4089-4092.

¹⁰³ (a) Hatada, K.; Ute, K.; Tanaka, K.; Okamoto, Y.; Kitayama, T. *Polym. J.* **1986**, *18*, 1037. (b) Hatada, K.; Kitayama, T.; Ute, K.; Masuda, E.; Shinozaki, T.; Yamamoto, M. *Polym. Prepr. (ACS, Div. Polym. Chem.)* **1988**, *29*, 54-55. (c) Ballard, D. G. H.; Bowles, R. J.; Haddleton, D. M.; Richards, S. N.; Sellens, R.; Twose, D. L. *Macromolecules* **1992**, *25*, 5907-5913. (d) Haddleton, D. M.; Muir, A. V. G.; O'Donnell, J. P.; Richards, S. N.; Twose, D. L. *Macromol. Symp.* **1995**, *91*, 91. (e) Seebach, D.; Pietzonka, T. *Angew. Chem.* **1993**, *105*, 741. (f) Wang, J. S.; Teyssié, P.; Heim, P.; Vuillemin, B., EP 95400861.1, **1995**. (g) Schlaad, H.; Schmitt, B.; Müller, A. H. E.; Jüngling, S.; Weiss, H. *Macromolecules* **1998**, *31*, 573-577. (h) Schlaad, H.; Schmitt, B.; Müller, A. H. E. *Angew. Chem., Int. Ed.* **1998**, *37*, 1389-1391.

¹⁰⁴ Leading references for metal-free initiators of anionic polymerization of alkyl methacrylates: (a) Reetz, M. T.; Ostarek, R. *Chem. Commun.* **1988**, 213-214. (b) Raj, D. J. A.; Wadgaonkar, P. P.; Sivaram, S. *Macromolecules* **1992**, *25*, 2774-2776. (c) Zagala, A. P.; Hogen-Esch, T. E. *Macromolecules* **1996**, *29*, 3038-3039. (d) Baskaran, D.; Müller, A. H. E. *Macromolecules* **1997**, *30*, 1869-1874.

¹⁰⁵ (a) Müller, A. H. E. In *Comprehensive Polymer Science*; G. Allen, J. C. Bevington Eds.; Pergamon, Oxford, U.K., **1988**; p 387. (b) Warmkessel, J.; Kim, J.; Quirk, R.; Brittain, W. *Polym. Prepr. (ACS, Div. Polym. Chem.)* **1994**, *35*, 589-590.

¹⁰⁶ (a) Hatada, K.; Ute, K.; Tanaka, K.; Kitayama, T.; Okamoto, Y. *Polym. J.* **1985**, *17*, 977. (b) Hatada, K.; Ute, K.; Tanaka, K.; Okamoto, Y.; Kitayama, T. *Polym. J.* **1986**, *18*, 1037. (c) Nakano, N.; Ute, K.; Okamoto, Y.; Matsuura, Y.; Hatada, K. *Polym. J.* **1989**, *21*, 935. (d) Hatada, K. *J. Polym. Sci., Part A: Chem.* **1999**, *37*, 245-260.

¹⁰⁷ Yasuda, H.; Yamamoto, H.; Yamashita, M.; Yokota, K.; Nakamura, A.; Miyake, S.; Kai, Y.; Kanehisa, N. *Macromolecules* **1993**, *26*, 7134-7143.

mVBzMgBr ^c	-110	14	1.19	96.6	3.1	0.3	19
Ph ₃ P·AlMe ₃	-93	28	1.63	94.9	4.6	0.5	70
AlEt ₃ ·TiCl ₄	-78	109	4.58	90.3	9.0	0.7	89

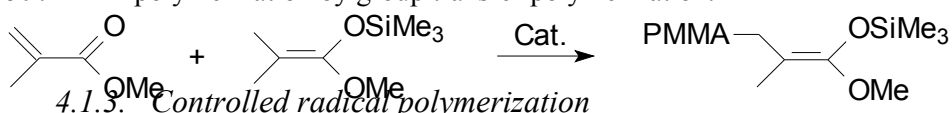
[MMA]₀/[initiator]₀ = 10-50. ^a Reaction time, 24 h. Solvent, toluene. ^b Solvent, THF. ^c Vbz = vinylbenzyl.

The typical initiating systems reported for the synthesis of highly syndiotactic PMMA are bulky alkyl lithium CH₃(CH₂)₄CPh₂Li,¹⁰⁸ Grignard reagents in THF^{106c} and some AlR₃ complexes (Table 4).¹⁰⁹ Although the first initiator reacted rapidly with MMA in THF at -78 °C, the molecular weight reached only 10,000 g/mol with M_w/M_n = 1.18, while it gave isotactic polymer in toluene. Isobutylmagnesium bromide and *m*-vinylbenzylmagnesium chloride in THF at -110 °C, also yielded highly syndiotactic polymer, but M_n remained as low as 14,000-18,000 and the conversions were quite low.¹¹⁰ AlEt₃·PR₃ complexes gave high syndiotacticity, but not a high molecular weight.

4.1.2. Group transfer polymerization

Ketene silyl acetal/nucleophilic agent systems initiate the living polymerization of alkyl methacrylates (Scheme 9). These well-known Group-Transfer systems developed by Webster yield living polymers with atactic sequences at relatively high temperatures.¹¹¹ Me₂C=C(OMe)-OSiR₃ and R₂POSiMe₃ can be used as initiators, and tris(dimethylamino)sulfonium bifluoride and nBuN⁺CN⁻ are frequently used as catalysts. For example, the polydispersity of the resulting PMMA was 1.06 for M_n = 3800, and 1.15 for M_n = 6300.

Scheme 9. MMA polymerization by group transfer polymerization.¹¹¹



More recently, different "controlled/living" radical polymerization methods (CRP) were reported for methacrylates polymerization.¹¹² These methods are based on establishing a rapid dynamic equilibrium between a minute amount of growing free radicals and a large majority of dormant species. The dormant species may be halides (P_n-X), as in atom transfer radical polymerization (ATRP),¹¹³ thioesters (P_n-X²) as in reversible addition fragmentation chain

¹⁰⁸ Cao, Z. K.; Okamoto, Y.; Hatada, K. *Kobunshi Ronbunshu* **1986**, *43*, 857.

¹⁰⁹ Abe, H.; Imai, K.; Matsumoto, M. *J. Polym. Sci., Part C*, **1968**, *C23*, 469.

¹¹⁰ Hatada, K.; Nakanishi, H.; Ute, K.; Kitayama, T.; Okamoto, Y. *Polym. J.* **1986**, *18*, 581. For related studies with Grignard and dialkylmagnesium reagents, see: (a) Allen, P. E. M.; Bateup, B. O. *Eur. Polym. J.* **1978**, *14*, 1001-1010. (b) Allen, P. E. M.; Mair, C. *Eur. Polym. J.* **1983**, *20*, 697-705. (c) Matsuzaki, K.; Tanaka, H.; Kanai, T. *Makromol. Chem.* **1981**, *182*, 2905-2918. (d) Soum, A.; D'Accorso, N.; Fontanile, M. *Makromol. Chem., Rapid Commun.* **1983**, *4*, 471-477.

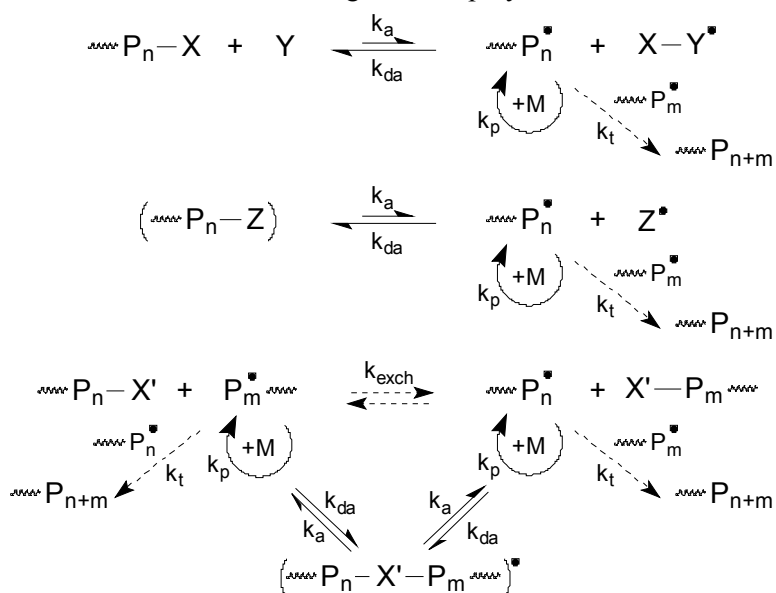
¹¹¹ (a) Webster, O. W.; Hertler, W. R.; Sogah, D. Y.; Farnham, W.; Rajanbabu, T. V. *J. Am. Chem. Soc.* **1983**, *105*, 5706-5708. (b) Sogah, D. Y.; Hertler, W. R.; Webster, O. W.; Cohen, G. M. *Macromolecules* **1987**, *20*, 1473-1488. (c) Webster, O. W. *Science* **1991**, *251*, 887.

¹¹² (a) "Controlled Radical Polymerization"; Matyjaszewski, K., Ed.; American Chemical Society: Washington, DC **1998**; Vol.685. (b) "Controlled/living Radical Polymerization: Progress in ATRP, NMP, and RAFT"; Matyjaszewski, K., Ed.; American Chemical Society: Washington, DC **2000**; Vol.685. (c) Matyjaszewski, K.; Davis, T. P. *Handbook of Radical Polymerization*; John Wiley and Sons, Inc., Hoboken, **2002**.

¹¹³ (a) Matyjaszewski, K.; Xia, J. *Chem. Rev.* **2001**, *101*, 2921-2990. (b) Kamigaito, M.; Ando, T.; Sawamoto, M. *Chem. Rev.* **2001**, *101*, 3689-3746.

transfer processes (RAFT),¹¹² or alkoxylamines (P_n-Z) as in nitroxide-mediated polymerizations (NMP).¹¹⁴ Free radicals may be generated by the spontaneous thermal process (NMP, RAFT) or via a catalyzed reaction (ATRP). All the CRP methods include activation and deactivation steps. Generated free radicals propagate with monomer (M) and terminate, as in conventional free-radical polymerization. Thus, although termination occurs, under appropriate conditions its contribution will be small and these radical polymerizations behave as nearly living or controlled systems (Scheme 10). However, these reactions can not be considered as metal-catalyzed processes.

Scheme 10. Mechanism for controlled/"living" radical polymerization.¹¹²



Both ATRP and RAFT techniques appeared to be efficient for controlled polymerization of alkyl methacrylates. In ATRP, a large range of catalysts is available (based on Ru, Cu, Ni, Fe, Pd and Rh) for MMA polymerization and most of the polymerizations were carried out in solution at temperatures ranging from 50 to 90 °C. Under these conditions, well-defined PMMA can be prepared within the molecular weight range from 1000 to 180,000. RAFT proved to be also a valuable technique for MMA polymerization. Again, in solution at temperatures ranging from 60 to 90 °C, a controlled polymerization of MMA can be observed. In this case, lower molecular weights are reported. However, up to now, these techniques did not allow the control of the stereospecificity of the polymerization. The polymers prepared from ATRP and RAFT feature the same microstructure as polymers prepared by free-radical polymerization, i.e. syndiotacticity content below 70%. Despite many attempts to control the stereochemistry of the polymerization (chiral-auxiliary control, control with Lewis acids, with solvents), no relevant results have been reported so far for the highly syndiotactic living radical polymerization of MMA.¹¹⁵

¹¹⁴ Hawker, C. J.; Bosman, A. W.; Harth, E. *Chem Rev.* **2001**, *101*, 3661-3688.

¹¹⁵ Matsumoto, A. In *Handbook of Radical Polymerization*; Matyjaszewski, K.; Davis, T. P. Ed. ; John Wiley and Sons, Inc., Hoboken, **2002**, 691-774.

4.2. Lanthanocene-type catalysts

At the same time, despite significant progress observed in the different polymerization methods, new initiating systems were still under investigation. Thus in the early 1990's, lanthanide-based catalysts proved to be efficient *initiators* for highly syndiotactic MMA polymerization. We would like to give here an overview of the different types of complexes that exhibit an activity in MMA polymerization, based on the nature of their ligands, separating single and multicomponent systems.

4.2.1. Single component initiating systems

4.2.1.1. Cyclopentadienyl and pentamethylcyclopentadienyl complexes

The first synthesis of high molecular weight poly(methyl methacrylate) with extremely low polydispersity was reported in 1990 by Yasuda *et al.*¹¹⁶ These results were abundantly described in multiple reviews on the use of rare earth compounds as polymerization initiator.¹¹⁷ It was shown initially that trivalent organolanthanide complexes of the type M(C₅Me₅)₂R (M = Y, Sm, Yb, Lu; R = H, Me), previously applied successfully in olefin polymerization,^{41,42} initiated living polymerization of MMA, leading to highly syndiotactic polymers with very narrow polydispersity ($M_w/M_n < 1.04$) and high molecular weight ($M_n > 100,000$) (Table 5).

The polymerizations proceeded very rapidly and were complete in a short period of time (< 2 h). With [SmH(C₅Me₅)₂]₂, M_n of polymers increased linearly in proportion to the conversion irrespective of catalyst concentration and M_w/M_n values remained very low ($M_w/M_n < 1.05$). However, the initiator efficiency is function of the catalyst concentration and nature of the ligand. Values higher than 90% were observed for [MMA]₀/[catalyst]₀ < 500 (0.2 mol %) while the efficiency decreases to 80% when the initiator concentration is lowered to 0.1 mol %. This result is ascribable to undesired side reactions with trace amounts of water or oxygen. The bulkiness of the Cp ligand is also very important. With [YMe(C₅H₅)₂]₂ the initiator efficiency decreased to 60%. This result can be compared to the lowest activity observed with C₅H₅ in ethylene polymerization.⁴¹ Examination of the temperature dependence of syndiotacticity with [SmH(C₅Me₅)₂]₂ as initiator showed that it increases from 77 to 95% by changing the temperature from 40 to –95 °C.

Table 5. Characterization of monodisperse poly(MMA) synthesized by [SmH(C₅Me₅)₂]₂.¹¹⁶

polymerization temp. (°C)	MMA/initiator charged (mol/mol)	10 ⁻³ M_n	M_w/M_n	rr (%)	conversion (%) (reaction time, h)
40	500	55	1.03	77.3	99 (1)
25	500	57	1.02	79.9	99 (1)

¹¹⁶ Yasuda, H.; Yamamoto, H.; Yokota, K.; Miyake, S.; Nakamura, A. *J. Am. Chem. Soc.* **1992**, *114*, 4908-4910.

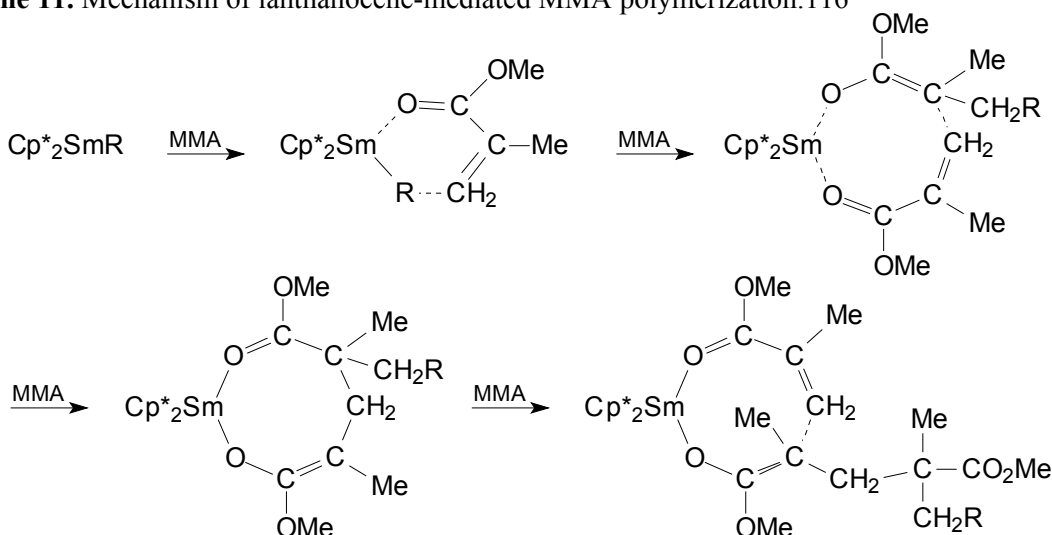
¹¹⁷ (a) Yasuda, H.; Tamai, H. *Prog. Polym. Sci.* **1993**, *18*, 1097-1139. (b) Yasuda, H.; Ihara, E. *Macromol. Chem. Phys.* **1995**, *196*, 2417-2441. (c) Yasuda, H.; Ihara, E.; Hayakawa, T.; Kakehi, T. *J. Macromol. Sci., Pure Appl. Chem.* **1997**, *A34*, 1929-1944. (d) Yasuda, H.; Ihara, E. *Adv. Polym. Sci.* **1997**, *133*, 53-101. (e) Yasuda, H.; Ihara, E. *Bull. Chem. Soc. Jpn.* **1997**, *70*, 1745-1767. (f) Yasuda, H.; Ihara, E.; Nitto, Y.; Kakehi, T.; Morimoto, M.; Nodono, M. *ACS Symp. Ser.* **1998**, *704*, 149-162. (g) Yasuda, H. *Top. Organomet. Chem.* **1999**, *2*, 255-283.

0	500	58	1.02	82.4	99 (1)
0	1500	215	1.03	82.6	93 (2)
-78	500	82	1.04	93.1	97 (17)

^a Reaction conditions : solvent, toluene; solvent/[M₀] = 10 vol/vol.

Estimation of the lifetime of the growing chains was studied by sequential monomer addition at timed intervals. At 0 °C, all the chains remained living after 1 h and 60% after 10 h. Such a long life has not been observed for any type of living polymerization of polar monomers. The mechanism involved in this initiating system was also investigated. Deuterolysis of the reaction product at 0 °C between [SmH(C₅Me₅)₂]₂ and 1 or 2 equivalent(s) of MMA, and hydrolysis of the reaction of SmD(C₅Me₅)₂ with MMA were indicative of the formation of a 1:2 adduct with either Sm-enolate or Sm- α -carbon bond. Isolation of the eight-membered ring (C₅Me₅)₂Sm(MMA)₂H as crystals was the undeniable proof for the Sm-enolate intermediate.¹¹⁶ This isolated complex was shown to be the true active polymerization species. These results allowed the authors to propose the following polymerization mechanism (Scheme 11). In the initiation step, the hydride should attack the CH₂ group of the MMA to generate a transient Sm-O-C-(OCH₃)=C(CH₃)₂ species, and then the incoming MMA molecule may participate in a 1,4-addition to afford the eight-membered ring intermediate. Then in the propagation step, the growing polymer chain may attack another MMA molecule, liberating the coordinated ester group. Syndiotactic polymerization should occur by repeating these reactions with alternative coordination site changes or rather by steric repulsion of the monomer methyl groups. This coordinative mechanism was expected. Indeed, nearly the same results were obtained in toluene, THF, Et₂O, benzene or hexane with SmMe(C₅Me₅)₂ and YbMe(C₅Me₅)₂(OEt₂) as initiating systems while the solvent is known to affect dramatically anionic polymerizations.

Scheme 11. Mechanism of lanthanocene-mediated MMA polymerization.¹¹⁶



$\text{LnMe}(\text{C}_5\text{Me}_5)_2(\text{THF})$ ($\text{Ln} = \text{Sm, Yb, Lu}$), $\text{Ln}(\text{C}_5\text{Me}_5)_2(\mu\text{-Me})_2\text{AlMe}_2$ ($\text{Ln} = \text{Yb, Lu, Y}$) and $[\text{YMe}(\text{C}_5\text{H}_5)_2]_2$ act also as initiators for living MMA polymerization. As previously stated, a lower syndiotacticity and a relatively significant temperature dependence were observed with $\text{LnR}(\text{C}_5\text{H}_5)_2$ complexes as compared with $\text{LnR}(\text{C}_5\text{Me}_5)_2$. Polymerizations carried out with $\text{Ln}(\text{C}_5\text{Me}_5)_2(\mu\text{-Me})_2\text{AlMe}_2$ complexes exhibit also a living behavior along with high syndiotacticity, suggesting the concomitant formation of $\text{LnR}(\text{C}_5\text{Me}_5)_2$ species produced by the attack of MMA and liberation of AlMe_3 .¹¹⁷ From this study, it was found that the rate of polymerization increased as follows: $\text{Sm} > \text{Y} > \text{Yb} > \text{Lu}$ in direct line with the order of the ionic radii (Sm (1.11 Å) > Y (1.06 Å) > Yb (0.86 Å) > Lu (0.85 Å)) as observed in ethylene polymerization.⁴⁹

Higher alkyl methacrylates (ethyl, isopropyl and *tert*-butyl) can be also polymerized in a living fashion with $[\text{SmH}(\text{C}_5\text{Me}_5)_2]_2$ or $\text{LuMe}(\text{C}_5\text{Me}_5)_2(\text{THF})$. The observed M_w/M_n values were again low (< 1.05). In these cases, the syndiotacticity and conversion decreased by reducing the bulkiness of the alkyl group (Table 6).

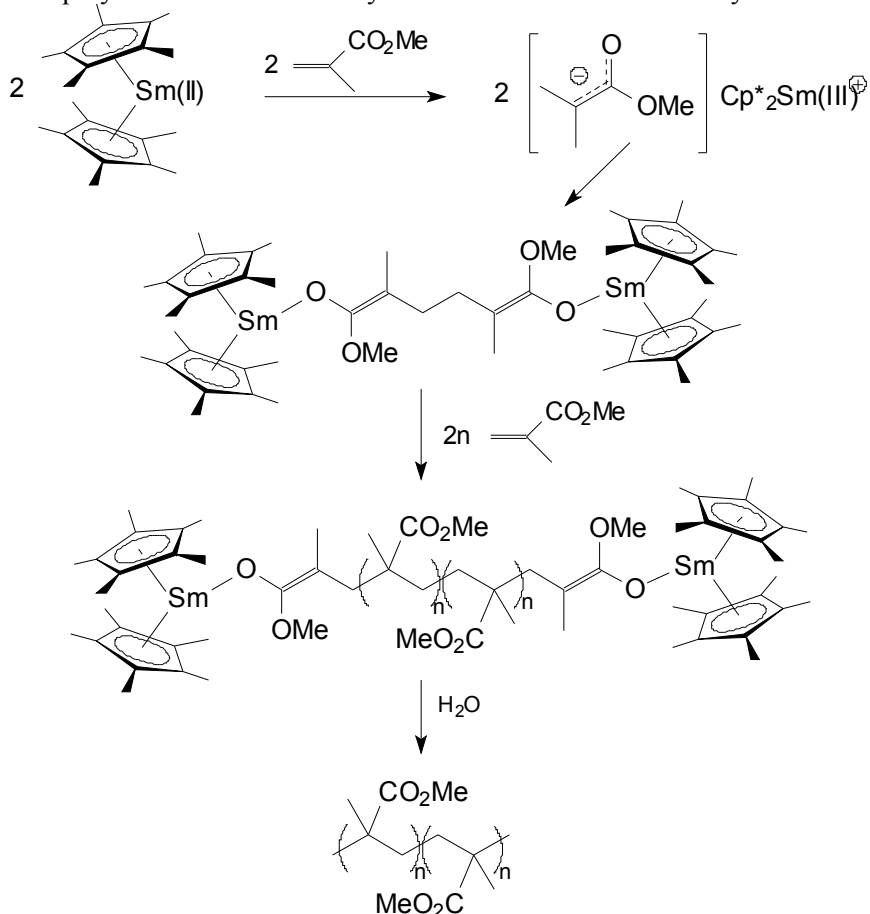
Table 6. Organolanthanide initiated polymerization of alkyl methacrylates.^{117c}

initiator	monomer	$10^{-3} M_n$	M_w/M_n	rr (%)	conv. (%)
$[\text{SmH}(\text{C}_5\text{Me}_5)_2]_2$	MMA	57	1.03	82.4	98
	EtMA	80	1.03	80.9	98
	<i>i</i> PrMA	70	1.03	77.3	90
	<i>t</i> BuMA	63	1.42	77.5	30

Polymerization conditions: 0 °C in toluene, $[\text{monomer}]_0/[\text{initiator}]_0 = 500$.

Divalent organolanthanide complexes were also successfully used. $\text{Ln}(\text{C}_5\text{Me}_5)_2(\text{THF})$ ($\text{Ln} = \text{Sm, Yb}$) provided highly syndiotactic PMMA with a living character.¹⁰⁷ However, the initiation efficiency is rather low. The latter is 30% and 21% for 0.2 and 0.1 mol%, respectively. The stoichiometric reaction of $\text{Ln}(\text{C}_5\text{Me}_5)_2(\text{THF})$ with MMA resulted in a complex mixture. Thus, the real mechanism could not be elucidated. However, given the features of the polymerizations, the authors estimated that the active species should be an $\text{Ln}^{(III)}$ analog generated during the reaction. The re-examination of these systems by Boffa and Novak allowed a better understanding of the mechanism with divalent compounds.¹¹⁸ They showed that under rigorous exclusion of air and water, $[\text{Sm}(\text{C}_5\text{Me}_5)_2]_2$ is a good initiator for MMA polymerization. The mechanism proceeds via the formation of a $\text{Sm}^{(III)}$ bis-initiator. The samarocene catalyst undergoes one-electron transfer to a MMA molecule forming a radical anion. Subsequent dimerization of these radical anions gives a bimetallic bis(enolate), which then acts to initiate the polymerization (Scheme 12). They also confirmed this hypothesis by using a preformed well-characterized bis(allyl) samarocene.

¹¹⁸ (a) Novak, B. M.; Boffa, L. S. *Polym. Prepr. (ACS, Div. Polym. Chem.)* **1994**, 35, 528-529; (b) Boffa, L. S.; Novak, B. M. *Macromolecules* **1994**, 27, 6993-6995. (c) Novak, B. M.; Boffa, L. S., WO 9521873, (University of California, USA), 1995.

Scheme 12. MMA polymerization initiated by a divalent lanthanocene catalyst.^{118b}

Using lanthanocene catalysts, Yasuda and co-workers have also reported the efficient living polymerization of lactones^{117a,119} and alkyl acrylates¹²⁰. With $[\text{SmMe}(\text{C}_5\text{Me}_5)_2]$ as initiator, lactone polymerizations are initiated by the formation of an acetal; ring opening follows. This process has been confirmed by ^{13}C NMR studies of stoichiometric reaction products. Polymerizations of alkyl acrylates present a living character but no stereospecificity (Table 7). Lower steric hindrance of the α -proton compared to the methyl group of methacrylates may explain this absence of stereospecificity. Contrary to methacrylates, the rate of polymerization increases with the bulkiness of the ester group in the order butyl > ethyl > methyl. True living anionic polymerizations of alkyl acrylates have never been reported because chain transfer or termination reactions due to the high sensitivity of the acidic α -proton. In this sense, trivalent organolanthanide initiators exhibit a special feature.

Table 7. Polymerization of alkyl acrylates initiated by organolanthanide complexes.^{117e}

¹¹⁹ Yasuda, H.; Yamamoto, H.; Takemoto, Y.; Yamashita, M.; Yokota, K.; Miyake, S.; Nakamura, A. *Makromol. Chem., Macromol. Symp.* **1993**, 67, 187-201.

¹²⁰ Ihara, E.; Morimoto, M.; Yasuda, H. *Macromolecules* **1995**, 28, 7886-7892.

initiator	monomer	$10^{-3} M_n$	M_w/M_n	tacticity (%)			conversion (%)	initiator efficiency (%)
				rr	rm	mm		
[SmMe(C_5Me_5) ₂ (THF)]	MeA	48	1.04	30	50	20	99	89
	EtA	55	1.04		51	49	94	86
	<i>n</i> BuA	70	1.05	28	53	19	99	91
	<i>t</i> BuA	15	1.03	27	47	26	99	79

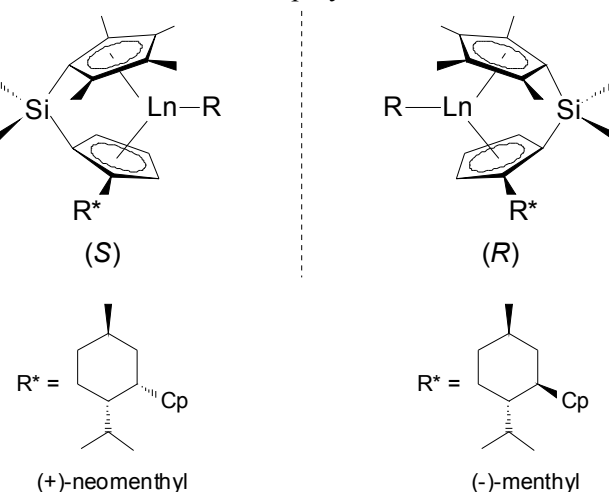
Polymerization conditions: 0 °C in toluene, [monomer]₀/[initiator]₀ = 500.

By taking advantage of these versatile living systems, various types of copolymers (random, block) with both polar and non-polar monomers were obtained using adequate experimental conditions. The copolymerization of non-polar with polar monomers using lanthanocene initiators was also successful and will be studied in detail in chapter 4.117.¹²¹

4.2.1.2. Other lanthanocene complexes

The highly syndiotactic MMA polymerization with an achiral organolanthanide complex raised the intriguing question of whether methacrylate polymerizations might be subject to enantiomorph site control via a chiral-ligand template. Using various hydride, hydrocarbyl and amide catalysts, Marks *et al.* showed that *C₁*-symmetric catalysts bearing the (+)-neomenthyl chiral auxiliary produced isotactic PMMA with isotacticity increasing with decreasing temperature.¹²² In sharp contrast, the catalysts bearing the (-)-menthyl chiral auxiliary produces syndiotactic polymers with stereoregularities close to the ones of parent achiral complexes.

Figure 22. First chiral lanthanocenes in MMA polymerization.¹²²



In addition, it was shown that the mechanism of stereoregulation is independent of the precatalyst R group. Indeed, PMMA microstructure was identical with (*R,S*)-(neomenthylCp) YR (R = CH(TMS)₂, H) complexes. Also, for the first time, amide lanthanocenes (typically

¹²¹ Yasuda, H.; Furo, M.; Yamamoto, H.; Nakamura, A.; Miyake, S.; Kibino, N. *Macromolecules* **1992**, *25*, 5115-5116.

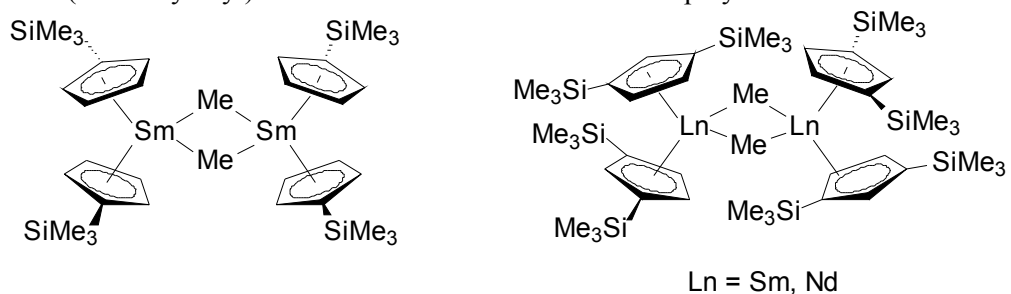
¹²² Giardello, M. A.; Yamamoto, Y.; Brard, L.; Marks, T. J. *J. Am. Chem. Soc.* **1995**, *117*, 3276-3277.

used for the hydroamination/cyclization of amino alkenes¹²³) (*(R)* and (*S*)-(methylCp)LuN (TMS)₂ and (*R*)-(neomenthylCp)La(N(TMS)₂) were employed for MMA polymerization. The mechanism involved with the amido and alkyl lanthanocene complex was assumed to be the same. However, the polydispersity of PMMA from the chiral and achiral hydrocarbyl and amide precatalysts are larger than the corresponding hydrides. It is reasonable to think that a slower initiation step is responsible for such behavior since it is expected that kinetics of initiation should be sensitive to the steric encumbrance and operational nucleophilicity of R.

Cp*-based catalysts have a great potential for olefin polymerization and especially methacrylates polymerization. However, the high cost of production of the Cp* ligand by itself is not compatible with a practical use in industry; and unfortunately complexes based on the non-substituted cyclopentadienyl ligand are known to be less effective to perform living polymerizations. Consequently, new lanthanocene initiating systems were synthesized to examine their ability for performing such living polymerizations.

Bis- and tetra(trimethylsilyl) substituted alkyl lanthanocene complexes were reported by Yasuda and co-workers (Figure 23).¹²⁴

Figure 23. (Trimethylsilyl) substituted lanthanocene for MMA polymerization.¹²⁴



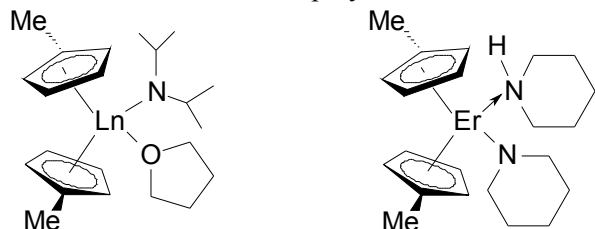
The polymerizations carried out in the absence of cocatalyst proceed in high yield to result in the formation of syndiotactic polymers with narrow molecular weight distribution from -40 to -78 °C, whereas it increases with raising the polymerization temperature (1.3 > M_w/M_n > 1.8 above 0 °C). Syndiotacticity increases with decreasing temperature (rr = 86-90% at -78 °C) but remains lower than the one observed with [SmH(C₅Me₅)₂]₂. In addition, the catalytic activity of these complexes is poor as compared with that of [SmH(C₅Me₅)₂]₂, especially at high temperature, even if the initiator efficiency was much improved.

¹²³ Giardello, M. A.; Conticello, V. P.; Brard, L.; Gagne, M. R.; Marks, T. J. *J. Am. Chem. Soc.* **1994**, *116*, 10241-10254.

¹²⁴ Satoh, Y.; Ititake, N.; Nakayama, Y.; Okuno, S.; Yasuda, H. *J. Organomet. Chem.* **2003**, *667*, 42-52.

High catalytic activities were observed with lanthanide amides (Figure 24). The use of bis(methylcyclopentadienyl)diisopropylamido and bis(methylcyclopentadienyl)piperidino lanthanide complexes was reported by Shen and co-workers.¹²⁵

Figure 24. Amido lanthanocenes in MMA polymerization.¹²⁵



The polymerizations performed in toluene at 0 °C exhibit a good catalytic activity for both initiators. These activities are much higher than that of the chiral organolanthanide amide used by Marks.¹²² The authors assumed that the difference in steric hindrance and the operational nucleophilicity of the amido group may be the reasons for such discrepancy. The piperidino complex afforded syndiotactic-rich PMMA with low polydispersity and high molecular weight below 0 °C ($rr = 87.1\%$, $M_w/M_n = 1.11$ and $M_n = 229,000$ at -78 °C). Increasing the polymerization temperature resulted in a dramatic broadening of the molecular weight distribution ($M_w/M_n = 2.02$ at 25 °C) along with a decrease of the syndiotacticity ($rr = 76.5\%$). $(MeC_5H_4)_2YbN(iPr)_2(THF)$ did not provide low polydispersity PMMA even at very low temperature while the syndiotacticity observed at -78 °C is relatively high ($rr = 87.5\%$). However, the efficiency of initiation is poor (Eff. < 10%). The main difference between these complexes is the difference of activity among their lanthanide analogs. For the piperidino complex, the activity decreases with an increase of ionic radius of the metal, while the opposite is observed with the diisopropylamido complex. The real reason for such a difference remains unclear.

4.2.1.3. *Ansa*-lanthanocene complexes

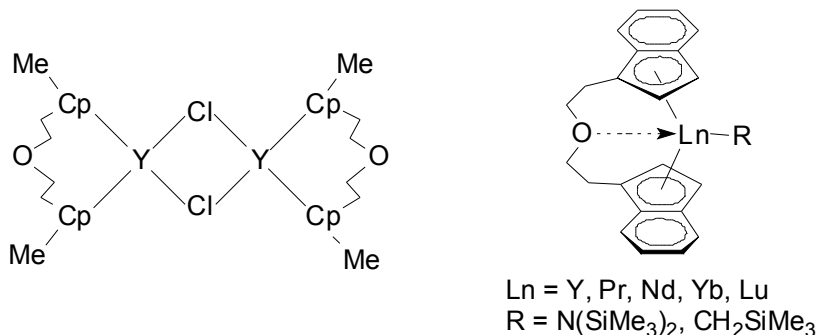
Ansa-lanthanocene complexes were also employed for MMA polymerization. Surprisingly, the *ansa*-lanthanocene chloride $[O(C_2H_4C_5H_3CH_3)_2]LnCl$ ($Ln = Y, Nd, Sm$) was found to be an effective initiator for MMA polymerization in the absence of cocatalyst, in bulk and in toluene solution at temperature above 20 °C (Figure 25).¹²⁶ Syndiotactic PMMAs with monodisperse molecular weight distribution were obtained ($rr = 70\%$; $M_w/M_n = 1.4-1.8$), with an activity increasing in the order $Nd > Sm > Y$. Increasing the polymerization temperature from 20 to 80 °C led to higher yields and molecular weights, and lower syndiotacticities. The molecular weight increased gradually within 25 h, suggesting a slow initiation process and a long lifetime. However, the activity displayed by these initiators was low and the mechanism remains undetermined.

¹²⁵ (a) Mao, L.; Shen, Q.; Sun, J. *J. Organomet. Chem.* **1998**, 566, 9-14. (b) Mao, L.; Shen, Q. J.; *J. Polym. Sci., Part A: Polym. Chem.* **1998**, 36, 1593-1597.

¹²⁶ Sun, J.; Pan, Z.; Zhong, Y.; Hu, W.; Yang, S. *Eur. Polym. J.* **2000**, 36, 2375-2380.

Rac-1,1'-(3-oxapentamethylene)-bridged bis(indenyl) *ansa*-lanthanidocenes reported by Qian and co-workers gave high molecular weight PMMA with a high isotactic content when the polymerization is performed at low temperature (Figure 25).¹²⁷

Figure 25. Oxa-bridged lanthanocene complexes in MMA polymerization.^{126,127}



Bridged fluorenyl (Flu) cyclopentadienyl as ligand for MMA polymerization was largely investigated. Yasuda initially reported that one of the C-bridged alkyl complexes, $[\text{Me}_2\text{C}(2,7-t\text{Bu}_2\text{-Flu})(\text{Cp})]\text{YCH}(\text{TMS})_2$, induced syndiotactic polymerization ($\text{rr} = 75\text{-}78\%$).^{117e} Thus, high molecular weight polymer with moderate polydispersity was obtained at 0 °C ($M_n = 512,000$; $M_w/M_n = 1.66$). The use of the unsubstituted silylene-bridged C_s -symmetric amide complex, $[\text{Me}_2\text{Si}(\text{Flu})(\text{Cp})]\text{YN}(\text{TMS})_2$, by Do *et al.* led to the formation of isotactic PMMA ($\text{mm} = 56\text{-}58\%$) in very low yield (5-10%).¹²⁸

Qian *et al.* have also reported the use of Si-bridged fluorenyl cyclopentadienyl lanthanocene complexes for MMA polymerization. They first employed C_s -symmetric silylene-bridged fluorenyl cyclopentadienyl organolanthanide amide and hydrocarbyl derivatives $\text{Me}_2\text{Si}(\text{Flu})(\text{Cp})\text{LnE}(\text{TMS})_2$ ($\text{E} = \text{N, CH}$; $\text{Ln} = \text{Dy, Er}$) and investigated the relation between the structures of the rare earth metal complexes and their activity towards MMA (Figure 26).¹²⁹ All these C_s -symmetric complexes show comparable high initiating activity (60-100%) and high syndiotacticity (60-83%). These results are quite different from those reported by Youngkin with yttrium as metal center, i.e. high isotacticity with $[(\text{C}_5\text{Me}_4)\text{Flu}]\text{YN}(\text{TMS})_2$.¹²⁸ When the temperature was lowered, the conversion and stereoregulation for the polymerization with amide group increased, while those 2 features decreased with hydrocarbyls. Then they used the carbon-bridged $[\text{Ph}_2\text{C}(\text{Flu})(\text{Cp})]\text{LuN}(\text{TMS})_2$ complex (Figure 26).¹³⁰ The observed activity was very low. This initiator did not show any activity at -78 °C while 12% conversion was obtained after 2 h at 0 °C. The initiation efficiency was very low (10%) giving a syndiotactic-rich PMMA with high polydispersity ($\text{rr} = 59\%$; $M_w/M_n = 2.27$). The low activity was ascribed to the slow initial 1,4-addition of the $\text{Ln}-\text{N}(\text{TMS})_2$ functionality to MMA compared with those of $\text{Ln}-\text{alkyl}$.

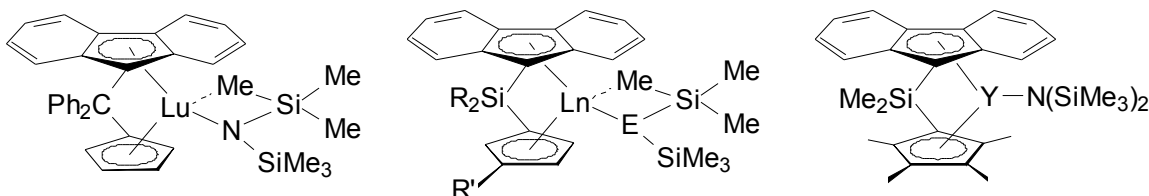
¹²⁷ Qian, C.; Zou, G.; Chen, Y.; Sun, J. *Organometallics* **2001**, *20*, 3106-3112.

¹²⁸ Lee, M. H.; Hwang, J.-W.; Kim, Y.; Kim, J.; Han, Y.; Do, Y. *Organometallics* **1999**, *18*, 5124-5129.

¹²⁹ Nie, W.; Qian, C.; Chen, Y.; Jie, S. *J. Organomet. Chem.* **2002**, *647*, 114-122.

¹³⁰ Qian, C.; Nie, W.; Chen, Y.; Jie, S. *J. Organomet. Chem.* **2002**, *645*, 82-86.

Figure 26. Fluorenyl-based ligand in MMA polymerization.¹²⁸⁻¹³⁰



Divalent catalysts

Interestingly, the bis(indenyl) lanthanide^(II), $(1\text{-SiMe}_3\text{Ind})_2\text{Yb}(\text{THF})$, produced stereoblock PMMA (sb-PMMA) where syndio- and isotactic blocks are alternated along the polymeric chain.¹³¹ The formation of sb-PMMA was attributed to the competing conjugate addition of monomer molecules; inversion of the metallocene conformation resulting from the indenyl rotation around the ligand-metal axis as it was already described for the formation of elastomeric stereoblock polypropylene with $(2\text{-PhInd})_2\text{ZrCl}_2/\text{MAO}$.¹³² However, this suggestion is not sufficient for the formation of sb-polymers. A necessary condition is comparable population of syndiospecific *meso*-conformation and isospecific *rac*-conformation, as well as fast switch from one conformation to another. In a more recent paper, Cadenas *et al.* studied four complexes in sb-MMA polymerization.¹³³ Only $(1\text{-SiMe}_3\text{Ind})\text{Yb}(\text{THF})$ was shown effective for this purpose. The corresponding phenyl-substituted complex was found less reactive and less stable because of the greater electron withdrawing effect of the phenyl group. $(1,3\text{-}(\text{SiMe}_3)_2\text{Ind})\text{Yb}$ was inactive due to its high steric hindrance while the more accessible metal center in $(1,3\text{-}(\text{SiMe}_3)_2\text{Ind})\text{LaMe}(\text{THF})$ enables highly isotactic MMA polymerization at -40 °C.

More recently, new ytterbium^(II) complexes bearing two substituted indenyl ligands (Figure 27) were found to act as single component catalysts for MMA polymerization in dimethoxyethane, but not in toluene and THF.¹³⁴ In this case, the produced PMMA is mainly syndiotactic and the stereochemistry does not seem to be affected by the temperature while activity increases as the polymerization temperature decreases. However, temperatures below -45 °C result in low activities. Moreover, it was shown that the larger the substituent of the indenyl ligand, the higher the catalytic activity of the catalyst.

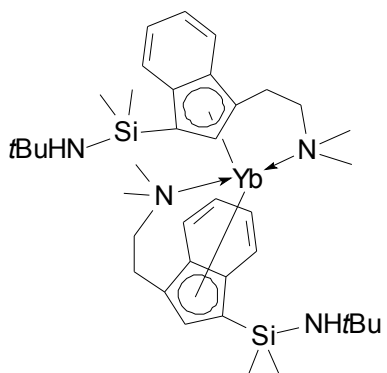
Figure 27. Bis(indenyl)Yb^(II) complexes for MMA polymerization.¹³⁴

¹³¹ Knjazhanski, S. Y.; Elizalde, L.; Cadenas, G.; Bulychev, B. M. *J. Polym. Sci., Part A: Polym. Chem.* **1998**, *36*, 1599-1606.

¹³² Maciejewski, P. J. L.; Agoston, T.; Lal, T. K.; Waymouth, R. M. *J. Am. Chem. Soc.* **1998**, *120*, 11316-11322.

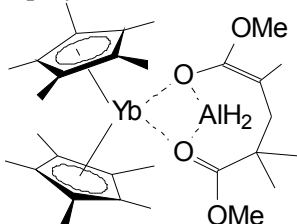
¹³³ Knjazhanski, S. Y.; Lopez-Gonzalez, H. R.; Larios-Lopez, L.; Cadenas, G. *Polym. Prepr. (ACS, Div. Polym. Chem.)* **2000**, *41*, 1294-1295.

¹³⁴ Sheng, E.; Wang, S.; Yang, G.; Zhou, S.; Cheng, L.; Zhang, K.; Huang, Z. *Organometallics* **2003**, *22*, 684-692.



Heterobimetallic complexes of some bivalent ytterbocenes with aluminum ("alane" complexes) $L_2YbAlH_3(NEt)_3$ ($L = C_5Me_5$, 1-SiMe₃Ind, 9-SiMe₃Flu) were found to afford stereospecific polymerization of methyl methacrylate (Figure 28).¹³⁵

Figure 28. Alane complex for MMA polymerization.¹³⁵



The apparent activities of these initiators were estimated to be a few times greater than those of their monometallic analogues $L_2Yb(THF)$. A mechanistic study showed that the polymerization proceeds via the formation of an active intermediate $L_2YbAlH_2[OC(OMe)=C(Me)CH_2C(Me)_2(CO_2Me)]$ arising from the 1,4-addition of MMA to an Al–H bond followed by Michael conjugate addition of a second monomer molecule as it is observed with monometallic lanthanocene complexes. Reactions performed at low temperature (-40 °C) yield high molecular weight polymers (up to 970,000 g/mol) with high syndiotacticity (rr = 93%) with C_5Me_5 as ligand. Isotactic-rich PMMA (mm = 75%) is obtained with indenyl and fluorenyl based ligands. More recently, the activation of MMA with alanes was also reported for zirconocene-mediated MMA polymerization.¹³⁶

4.2.1.4. Half-lanthanocene complexes

The half-lanthanocene complex $La(C_5Me_5)[CH(SiMe_3)_2]_2$ was found to be active for the polymerization of polar monomers (Figure 29).¹³⁷ The polymerizations were carried out in toluene at various temperatures. Effective polymerizations were observed from -78 to 20 °C to give syndiotactic-rich PMMA in high yield. The resulting molecular weights showed sufficiently high values with low polydispersities, $M_w/M_n < 1.23$. However, a low initiation efficiency was noticed, the latter decreasing with the temperature (Eff. = 25% at 20 °C; Eff. =

¹³⁵ Knjazhanski, S. V.; Elizalde, L.; Cadenas, G.; Bulychev, B. M. *J. Organomet. Chem.* **1998**, *568*, 33-40.

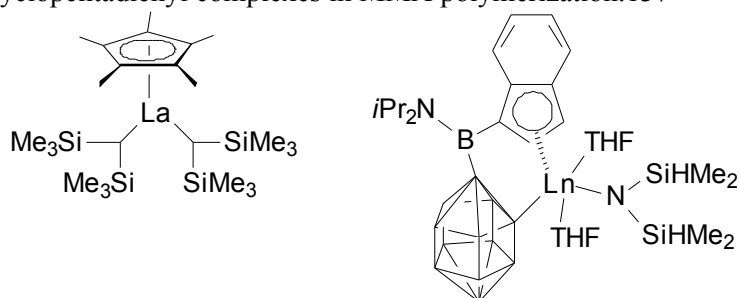
¹³⁶ Bolig, A. D.; Chen, E. Y.-X. *J. Am. Chem. Soc.* **2001**, *123*, 7943-7944.

¹³⁷ Tanaka, K.; Furo, M.; Ihara, E.; Yasuda, H. *J. Polym. Sci., Part A: Polym. Chem.* **2001**, *39*, 1382-1390.

6% at -78°C). This initiating system exhibits many similarities with conventional lanthanocene catalysts such as $[\text{SmH}(\text{C}_5\text{Me}_5)_2]_2$. Unsuccessful attempt to copolymerize MMA and styrene indicates that the polymerization using this half-lanthanocene complex follows the anionic-coordinative polymerization mechanism previously described for $[\text{SmH}(\text{C}_5\text{Me}_5)_2]_2$.

Finally, a particular neodymium complex, bearing new boron-bridged ligands incorporating both indenyl and carboranyl moieties, was found to be an active initiator for MMA polymerization in toluene, affording syndiotactic-rich PMMA (Figure 29).¹³⁸

Figure 29. Monocyclopentadienyl complexes in MMA polymerization.^{137,138}



4.2.2. Binary systems

The use of chlorolanthanocene (e.g. Cp*₂NdCl₂Li(OEt)₂) in combination with a dialkylmagnesium reagent was investigated for MMA polymerization as it was for ethylene. Unfortunately, the results were not so good since limited monomer conversion with broad molecular weight distribution were observed ($M_w/M_n = 6.7$).¹³⁹ This low activity was attributed to the bulkiness and/or the stability of the bimetallic Nd-Mg species. The creation of highly active species from the chloroneodymocene was possible with the use of *n*-BuLi as co-reagent.¹³⁹ Indeed, in toluene solution at 0°C , for Nd/Li molar ratios 1.2-2.0, pseudo-living highly syndiotactic MMA polymerization takes place ($M_w/M_n = 1.75$ and rr = 86%). The controlled character of the polymerization was checked by sequential addition of monomer, and by observation of the linear increase of the molecular weight with the initial monomer concentration, keeping the polydispersity constant.

Interestingly, the chlorolanthanocene/magnesium reagent was more successful for Yasuda *et al.* The chlorocomplexes I₁₃ and I₁₄ (Figure 30) tested in the presence of methyl magnesium chloride (1.1 equiv.) gave acceptable catalytic activities (90% conversion at -78°C) with high molecular weights ($M_n = 58,000\text{-}65,000$) and rather low polydispersities ($M_w/M_n = 1.33\text{-}1.35$).¹²⁴ However, these catalyst systems prepared *in situ* exhibit lower performances than the corresponding hydrocarbyl complexes regarding the polymer yield, molecular weight, polydispersity and syndiotacticity, probably due to the side reactions and/or anionic polymerization initiated by the Grignard reagent.

¹³⁸ Zi, G.; Li, H.-W.; Xie, Z. *Organometallics* **2002**, *21*, 1136-1145.

¹³⁹ Ph.D. Thesis, Fouga, C., Université de Lille, **1997**.

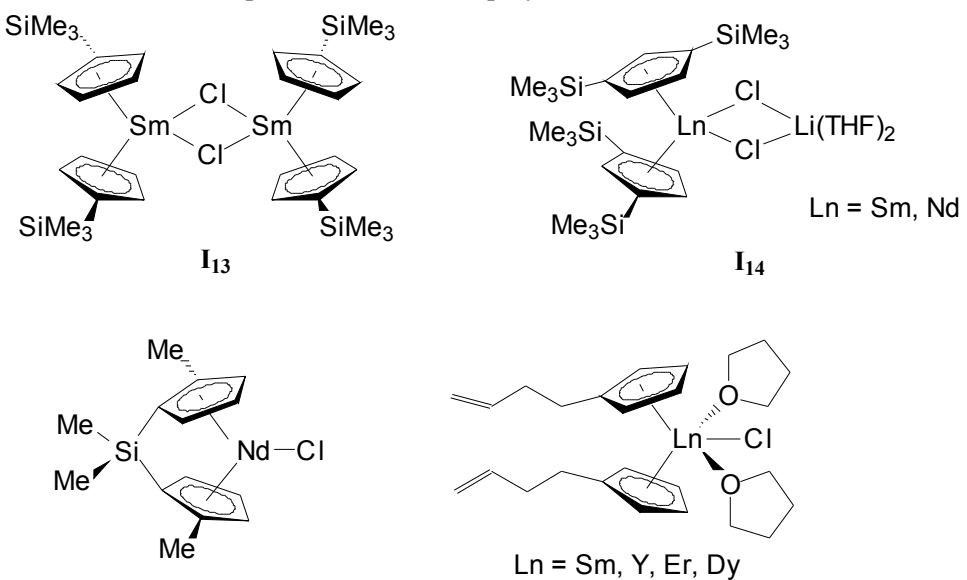
The silylene-bridged complex $\text{Me}_2\text{Si}(\text{CpSiMe}_3)_2\text{NdCl}$ activated by *n*-BuMgCl at low molar ratio (1:12) was successfully used for MMA polymerization (Figure 30).¹⁴⁰ This catalytic system was shown to be active in toluene at 40 °C, producing very high molecular weight PMMA ($M_w = 790,000 \text{ g/mol}$) with moderate polydispersities ($M_w/M_n = 1.80\text{-}2.18$). ^{13}C NMR analysis indicates that the polymer was syndiotactic-rich ($rr = 50\text{-}60\%$).

Finally, the complex $(\text{CH}_2=\text{CHCH}_2\text{CH}_2\text{C}_5\text{H}_4)_2\text{LnCl}(\text{THF})_2$ ($\text{Ln} = \text{Sm, Y, Dy, and Er}$) in association with an excess of $\text{Al}(i\text{Bu})_3$ showed a certain activity for the bulk polymerization of MMA (Figure 30).¹⁴¹ At low catalyst concentration, this system gave 70% conversion yielding a syndiotactic-rich PMMA ($rr = 62\%$) with very high molecular weight ($M_n = 1,650,000$).

¹⁴⁰ Sun, J.; Pan, Z.; Yang, S. *J. Appl. Polym. Sci.* **2001**, 79, 2245-2250.

¹⁴¹ Bala, M. D.; Huang, J.; Zhang, H.; Qian, Y.; Sun, J.; Liang, C. *J. Organomet. Chem.* **2002**, 647, 105-113.

Figure 30. Chlorolanthanocene precursors in MMA polymerization.^{124,140,141}

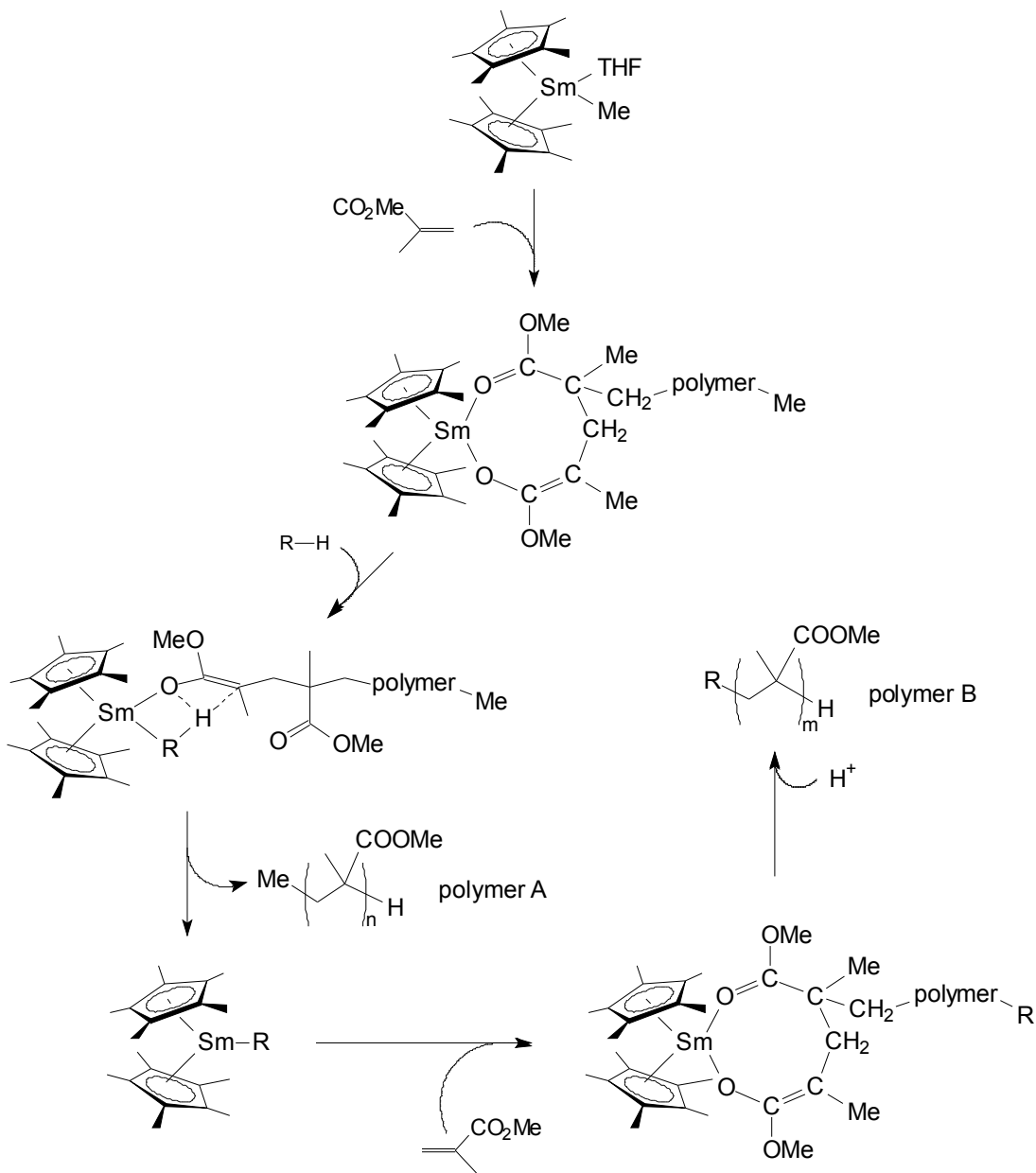


4.2.3. Chain transfer reactions in lanthanocene-based MMA polymerizations

As shown above, organolanthanide compounds initiate the rapid syndiotactic polymerization of MMA, resulting in high molecular weight polymers with low polydispersity, high yield and in a wide range of polymerization conditions. However, reactions using these initiators have several defects especially the need of severe experimental conditions and the coloration of the molded polymer. Also, from an industrial point of view, a controlled chain transfer reaction would be of considerable interest because it would enable the elimination of the above-mentioned flaws and reduce the product costs of the expensive organometallic initiators. So, it is not surprising to observe results from industrial research in this area. Indeed, in 1997, Mitsubishi Rayon Co., Ltd. filed a patent application on the use of chain transfer agents for MMA polymerization initiated by lanthanocene complexes.¹⁴² These transfer agents are organic compounds containing a reactive hydrogen atom such as thiols (*t*BuSH) and enolisable ketones (acetophenone, 4-methyl-2-pentanone). More detailed results were published few years later.¹⁴³ An efficient chain transfer agent would first react with an active bond between lanthanide^(III) and enolate at a living chain end of PMMA. As a result of the reaction, polymer A is eliminated from living chain end and initiator consisting of Ln^(III) cation and anionic form of the chain transfer agent is regenerated. Then the regenerated initiator must be able to reinitiate MMA polymerization, yielding polymer B (Scheme 13).

¹⁴² Yanagase, A.; Tone, S.; Tokimitsu, T.; Nodono, M. WO 9804595 (Mitsubishi Rayon Co., LTD) 1999.

¹⁴³ Nodono, M.; Tokimitsu, T.; Makino, T.; Yanagase, A. *Macromol. Chem. Phys.* **2000**, 201, 2282-2288.

Scheme 13. Chain transfer reaction in lanthanocene-mediated MMA polymerization.¹⁴³

Consequently, chain transfer agents were found in a series of organic acids. Among them, only ketone and thiol compounds were efficient as chain transfer agent as described in the prior patent.¹⁴² Methylisobutylketone (MIBK), acetophenone and *tert*-butyl thiol revealed to be the most suitable. Ketones showed higher reinitiation efficiency than thiols, however higher turnover numbers were observed with thiols because of the absence of possible initial catalyst deactivation. Indeed, initial formation of lanthanide alkoxide, useless for MMA polymerization, can be obtained with ketones. The turnover number of using acetophenone was relatively lower than that with MIBK. This would be due to the difference of the reinitiation efficiency, the latter depending on the character of the deprotonated chain transfer agent anion. The stereoregularity of the PMMA was not dependent on the use of *tert*-BuSH, suggesting that the propagation with *tert*-BuSH proceeds in the same manner as without. To

summarize, organic acids were used as chain transfer agents in the lanthanocene-mediated polymerization of MMA. The electronic character of these organic acids and the active bond in regenerated initiators would determine the reactivity of chain transfer agents. With efficient chain transfer agents, the reduction of the amount of expensive organometallic initiator and reduction of the coloration of PMMA were observed.

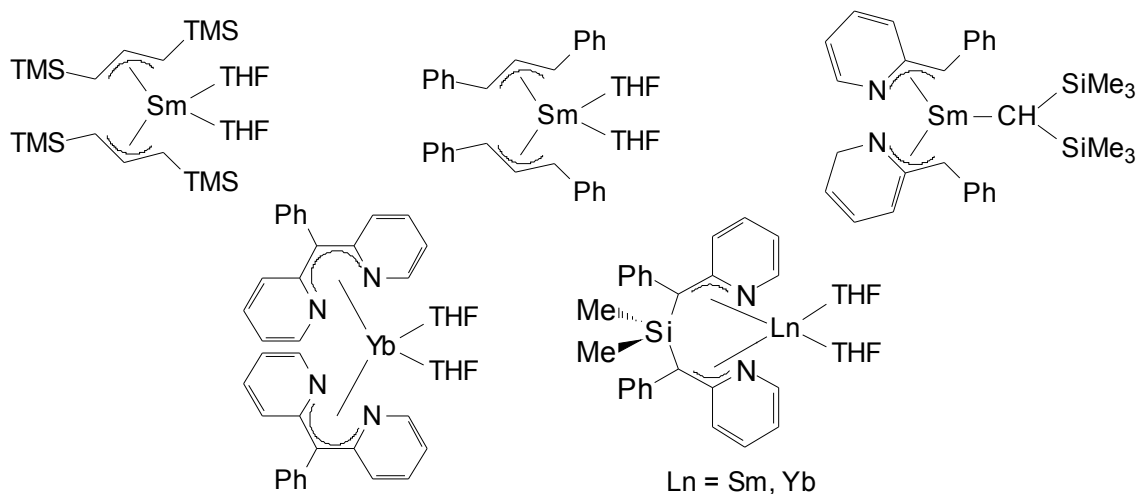
4.3. Non-metallocene type rare earth metal compounds

4.3.1. Single component initiating systems

4.3.1.1. Allyl complexes

As it was observed for olefin polymerization, only a limited number of non-metallocenes type rare earth metal complexes has been reported for MMA polymerization. The activity of some allyl-, aza-allyl- and diaza-pentadienylanthanide complexes for MMA polymerization was evaluated by Yasuda *et al.*¹⁴⁴ The trivalent allyl-Sm complexes showed relatively low catalytic activity and gave low molecular weight polymers with rather broad molecular weight distributions; the isotacticity is also low. In contrast to these allyl initiators, divalent aza-allyl and diaza-pentadienylanthanide complexes exhibit high catalytic activities. The highest activity was obtained with $\text{Yb}[(\text{C}_5\text{H}_4\text{N})_2\text{CPh}]_2(\text{THF})_2$, which affords high molecular weight isotactic-rich PMMA with two polymer populations with narrow polydispersity ($M_n = 53,400$ and $M_w/M_n = 1.02$; $M_n = 25,600$ and $M_w/M_n = 1.02$) at -78°C . Diaza-pentadienylanthanide complexes gave highly isotactic PMMA (mm = 83-88%), but with high polydispersities.

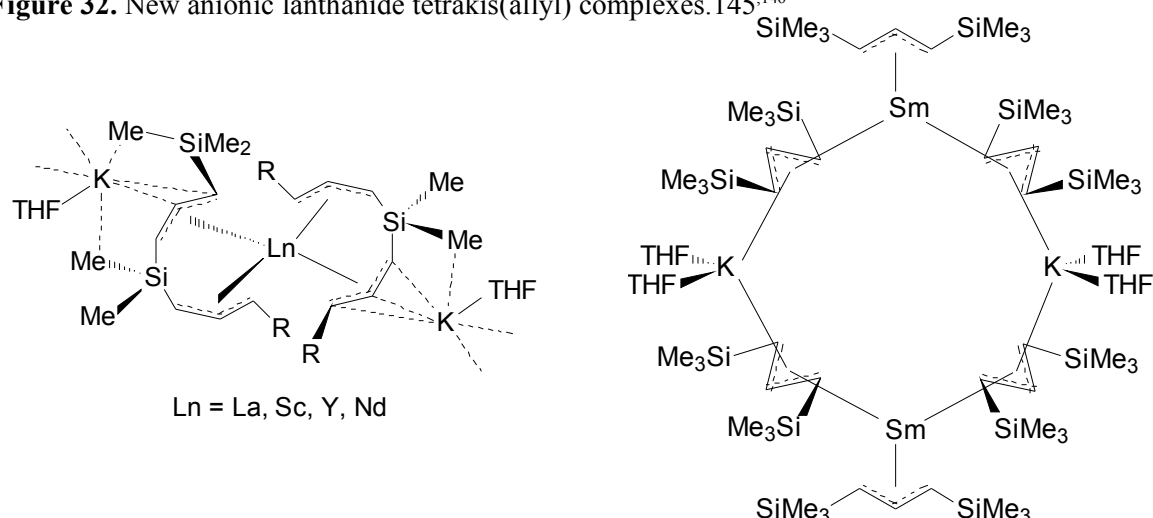
Figure 31. Allyl complexes in MMA polymerization.¹⁴⁴



¹⁴⁴ Ihara, E.; Koyama, K.; Yasuda, H.; Kanehisa, N.; Kai, Y. *J. Organomet. Chem.* **1999**, *574*, 40-49.

More recently, Bochmann *et al.* described the synthesis and the utilization of a new class of anionic $\text{Ln}^{(\text{III})}$ tetrakis(allyl) complexes for MMA polymerization (Figure 32).¹⁴⁵ The best results were obtained with the yttrium derivative, showing turnover numbers up to 86,000 (molMMA/molY/h) when the polymerization is conducted in the presence of toluene at 0 °C. High molecular weight PMMA ($M_w = 100,000$ to 636,000) with rather high polydispersity ($M_w/M_n = 2.2\text{-}3.6$) is thus produced. In addition, the stereochemistry of the polymer (atactic PMMA) is independent of the polymerization temperature. An anionic mechanism was proposed although the observed tacticities do not match with those previously reported in the literature for other anionic polymerization systems. Correspondingly, the allyl-bridged dimer $[\text{Sm}(\text{C}_3\text{H}_3(\text{SiMe}_3)_2)_3\{\mu\text{-K}(\text{THF})_2\}]_2$ exhibits high efficiency for MMA polymerization producing a polymer having comparable features to the polymer produced by the lanthanates described hereabove.¹⁴⁶

Figure 32. New anionic lanthanide tetrakis(allyl) complexes.^{145,146}



4.3.1.2. Alkyl-lanthanides

Some homoleptic alkyl complexes showed activity for methacrylate polymerization. Yasuda reported the use of trivalent and divalent complexes. In his effort to find new stereospecific initiator for MMA polymerization, he found that the bulky alkyl ytterbium^(II) $[(\text{Me}_3\text{Si})_3\text{C}]_2\text{Yb}$ produced a highly isotactic PMMA ($\text{mm} = 97\%$) in a high yield (Figure 33).¹⁴⁷ The polymer had a high molecular weight ($M_n = 500,000$ g/mol) and a low polydispersity ($M_w/M_n = 1.1$). The work done with 2,6-dialkoxyphenyllanthanoid complexes was less successful (Figure 33). Among the different complexes synthesized, only the lithium-containing complex exhibits a low activity along with a poor stereospecificity while the lithium free analog is completely inactive.¹⁴⁸

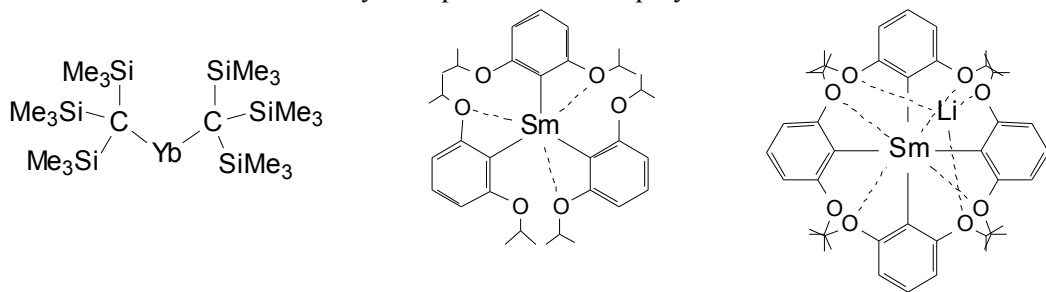
¹⁴⁵ Woodman, T. J.; Schormann, M.; Bochmann, M. *Organometallics* **2003**, 22, 2938-2943.

¹⁴⁶ Woodman, T. J.; Schormann, M.; Hughes, D. L.; Bochmann, M. *Organometallics* **2003**, 22, 3028-3030.

¹⁴⁷ Yasuda, H.; Ihara, E.; Nitto, Y.; Kakehi, T.; Morimot, M.; Nodono, M. *ACS Symp. Ser.* **1998**, 704, 149-162.

¹⁴⁸ Ihara, E.; Adachi, Y.; Yasuda, H.; Hashimoto, H.; Kanehisa, N.; Kai, Y. *J. Organomet. Chem.* **1998**, 569, 147-157.

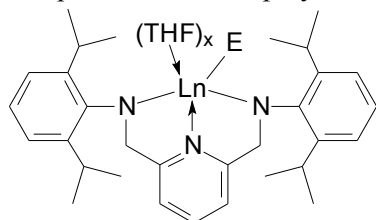
Figure 33. Divalent and trivalent alkyl complexes in MMA polymerization.^{147,148}



4.3.1.3. Nitrogen-based ligands

A series of new monomeric complexes derived from the 2,6-bis(((2,6-diisopropylphenyl)amino)methyl)pyridine ligand ($\text{H}_2\text{BDPPPyr}$) was reported to be effective single component initiators for the living polymerization of MMA ($M_w/M_n < 1.5$), affording mainly atactic polymer at ambient temperature (Figure 34).¹⁴⁹ Interesting results were obtained with the scandium complex while the corresponding complexes of the larger metal centers lutetium and yttrium showed negligible monomer conversion with broad polydispersities. It was also noticed that the nature of the initiating group (alkyl vs. amide) does not influence molecular weights or molecular weight distributions.

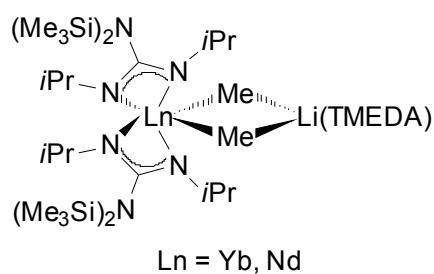
Figure 34. $\text{H}_2\text{BDPPPyr}$ -based complexes for MMA polymerization.¹⁴⁹



$$E = NR_2, CH_2SiMe_3$$

Recently, lanthanide^(III) bis(guanidinate) derivatives were reported to be active for MMA polymerization (Figure 35).¹⁵⁰ However, the activity remained rather low and the polymer did not show any interesting features ($M_w/M_n > 2$ and no stereospecificity).

Figure 35. Bis(guanidinate) complex in MMA polymerization.¹⁵⁰



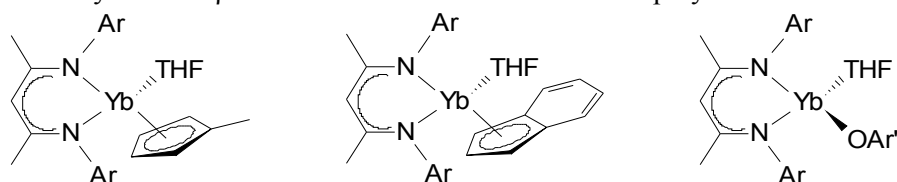
¹⁴⁹ Estler, F.; Eickerling, G.; Herdtweck, E.; Anwander, R. *Organometallics* **2003**, 22, 1212-1222.

¹⁵⁰ Luo, Y.; Yao, Y.; Shen, Q.; Yu, K.; Weng, L. *Eur. J. Inorg. Chem.* **2003**, 318-323.

Tetracoordinate lanthanide amides $[(\text{Me}_3\text{Si})_2\text{N}]_3\text{Ln}(\mu\text{-Cl})\text{Li}(\text{THF})_3$ ($\text{Ln} = \text{Nd, Sm, Eu}$) can act as single-component MMA polymerization initiators in both polar and non-polar solvents.¹⁵¹ Under optimized polymerization conditions (THF, 0 °C), these initiators yielded high molecular weight PMMA with moderate syndiotacticity ($M_n = 50,000\text{-}100,000$ and $rr = 50\text{-}65\%$) and good conversion. It should be noticed that the corresponding triscoordinate complexes $[(\text{Me}_3\text{Si})_2\text{N}]_3\text{Ln}$ showed a poor activity under the same conditions (conversion < 1%). The related amido silyloxy complexes $[\text{Na}(12\text{-crown-4})_2][\text{Yb}(\text{N}(\text{SiMe}_3)_2)_3(\text{OSiMe}_3)]$ gave high molecular weight with rather low polydispersity in toluene solution ($M_n = 1,400,000$ and $M_w/M_n = 1.34$) but with pretty low activity.¹⁵² Tacticity values were not reported.

Finally, divalent ytterbium complexes supported by a β-diketiminate ligand exhibit good catalytic activity for MMA polymerization (Figure 36).¹⁵³ In toluene solution, the conversions are in the range 80-100% at -20 °C yielding atactic PMMA. Molecular weights and molecular weight distributions were not provided, but the authors suggest that the polymerization proceeds via the formation of a trivalent bis-initiator as reported for the divalent lanthanocene.^{118b}

Figure 36. Divalent ytterbium β-diketiminate derivatives for MMA polymerization.¹⁵³



4.3.1.4. Lanthanide alkoxides

Okamoto *et al.* have reported the first example of polymerization of methacrylic esters initiated through Meerwein-Ponndorf-Verley (MPV) reduction.¹⁵⁴ In these polymerizations, the lanthanoid metal does not act as the active center but generates the active species (Scheme 14). Thus, lanthanide isopropoxides ($\text{Ln} = \text{Ce, La}$) synthesized following Kagan's method¹⁵⁵ were used as catalyst for the polymerization of MMA in toluene or THF. The particularity of these alkoxides is their Li-content. According to careful analyses, the cerium salt obtained by Kagan's method could have the formula $[\text{Ce}(\text{O}i\text{Pr})_3(\text{LiO}i\text{Pr})_{12}(\text{LiCl})_{2\text{-}3}]$. The presence of lithium in the complex is imperative since Li-free lanthanide alkoxide are inefficient for MMA polymerization. The MPV mechanism was confirmed by detection of acetone during the polymerization and by analysis of PMMA oligomers by field desorption mass spectrometry, which showed that the polymerization was initiated by hydride anion resulting from the MPV reaction.

¹⁵¹ Zhou, S.-L.; Wang, S.-W.; Yang, G.-S.; Liu, X.-Y.; Sheng, E.-H.; Zhang, K.-H.; Cheng, L.; Huang, Z.-X. *Polyhedron* **2003**, *22*, 1019-1024.

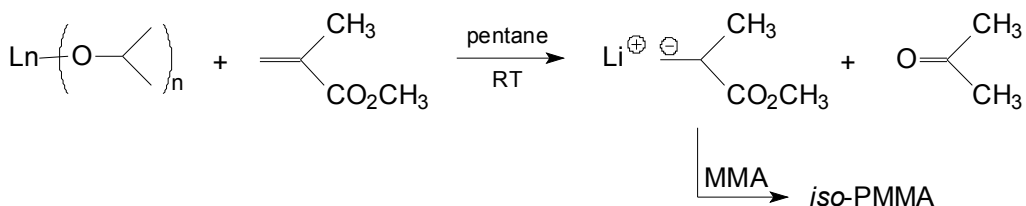
¹⁵² Karl, M.; Seybert, G.; Massa, W.; Harms, K.; Agarwal, S.; Maleika, R.; Stelter, W.; Greiner, A.; Heitz, W.; Neumüller, B.; Dehnicke, K. *Z. Anorg. Allg. Chem.* **1999**, *625*, 1301-1309.

¹⁵³ Yao, Y.; Zhang, Y.; Zhang, Z.; Shen, Q.; Yu, K. *Organometallics* **2003**, *22*, 2876-2882.

¹⁵⁴ Habaue, S.; Yoshikawa, M.; Okamoto, Y. *Polym. J.* **1995**, *27*, 986-992.

¹⁵⁵ Lebrun, A.; Namy, J.-L.; Kagan, H. B. *Tetrahedron Lett.* **1991**, *32*, 2355-2358.

Scheme 14. MMA polymerization initiated by "Ln(O*i*Pr)₃".¹⁵⁴



In toluene, cerium tris(isopropoxide) gave rise to PMMA in good yield. The obtained polymers were mainly isotactic and possessed high polydispersities ($\text{mm} = 80\%$; $M_w/M_n = 1.9\text{-}2.6$). In THF, a change in the tacticity of the polymer was observed, even at low temperature ($\text{rr} = 53\%$). These tacticities are similar to those of the corresponding polymer prepared with butyllithium, where the counterion controls the stereoregularity of the polymer.¹⁰⁴ This suggests that the polymerization initiated by MPV follows the same propagation mechanism as alkylolithium initiated anionic polymerizations.

4.3.1.5. Lanthanide thiolates

Well-defined $\text{Ln}^{(\text{II})}$ and $\text{Ln}^{(\text{III})}$ arenethiolates were studied as initiators for the polymerization of MMA. The reactions were performed in toluene or THF solution.¹⁵⁶ Benzenethiolate lanthanide^(III) complexes gave syndiotactic polymers ($\text{rr} = 70\text{-}82\%$) with high initiation efficiency and moderate polydispersity ($M_w/M_n = 1.34\text{-}1.77$). In this case, the $4[\text{mm}][\text{rr}]/[\text{mr}]^2$ values are close to 1.0, indicating a chain end control mechanism.²² Hydrolysis of the 1:1 reaction of $\text{Sm}(\text{SPh})_3(\text{HMPA})_3$ (HMPA = hexamethylphosphoramide) and MMA in THF proved that the polymerization was initiated by the insertion of MMA into the Ln-S bond, generating a lanthanoid enolate species similar to the polymerization mechanism described with Cp^*_2LnR . This mechanism is in agreement with the much lower activity of the thiolate complexes compared to Cp^*_2LnR ; this behavior might be attributed to the larger bond disruption enthalpy of the Ln-S bond than that of the Ln-C bond.¹⁵⁷ Addition of a strongly coordinated HMPA ligand changes the stereospecificity of the polymerization in toluene with $\text{Sm}(\text{SAr}')_3(\text{Py})_3$ ($\text{Ar}' = 2,4,6\text{-trisisopropylphenyl}$ and $\text{py} = \text{pyridine}$) and enables lower polydispersities to be obtained. The donative coordination of such bulky ligands to the metal center might weaken the Ln-S bonds to accelerate the initiation step. Also, the bulkiness significantly delays the propagation reaction, resulting in polymers with a relatively narrow molecular weight distribution. The polymerization rate was enhanced with addition of three equivalents of $\text{MeAl}(\text{dbmp})_2$ vs. Ln ($\text{dbmp} = 2,6\text{-}tert\text{-butyl-4-phenoxide}$), keeping roughly the same level of stereoregularity than the corresponding Al-free systems. Highly syndiotactic PMMA with high molecular weight and low polydispersity was obtained at low temperature with $\text{Sm}(\text{SPh})_3(\text{HMPA})_3/\text{MeAl}(\text{dbmp})_2$ (0°C , $\text{rr} = 87\%$). It has to be noticed that $[\text{Eu}(\text{SAr}')(\mu\text{-SAr}')(\text{THF})_3]_2$ shows a different selectivity giving isotactic PMMA. In this case, the $2[\text{rr}]/[\text{mr}]$ value of the obtained polymer is 1.05, indicating an enantiomeric site control, i.e., the mechanism of stereocontrol of $\text{Ln}^{(\text{II})}$ and $\text{Ln}^{(\text{III})}$ arenethiolate complexes are different.

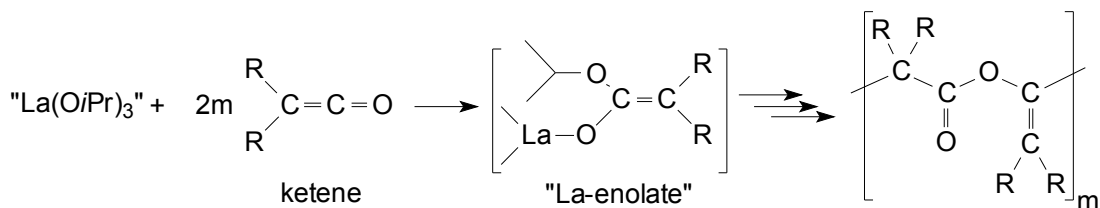
¹⁵⁶ Nakayama, Y.; Shibahara, T.; Fukumoto, H.; Nakamura, A. *Macromolecules* **1996**, *29*, 8014-8016.

¹⁵⁷ Nolan, S. P.; Stern, D.; Marks, T. J. *J. Am. Chem. Soc.* **1989**, *111*, 7844-7853.

4.3.2. Binary initiating systems

Prepared from lanthanum metal and isopropanol, lanthanum isopropoxide combined with diethylketene forms also a good initiator for MMA polymerization.¹⁵⁸ Indeed, *in situ* prepared "La(O*i*Pr)₃" enabled Et₂CCO polymerization at room temperature proceeding via the formation of an enolate intermediate (Scheme 15).¹⁵⁹ This intermediate was assumed to be identical to the one described in lanthanocene-mediated MMA polymerizations.^{117e}

Scheme 15. MMA polymerization initiated by "La(O*i*Pr)₃"/ketene catalyst system.¹⁵⁸



Consequently, the La-enolate obtained from the reaction of "La(O*i*Pr)₃" and Et₂CCO was successfully employed as initiator, while "La(O*i*Pr)₃" has not such ability to initiate MMA polymerization.¹⁵⁴ However, the methods of synthesis of the isopropoxides are different in these two studies. The synthetic route to lanthanide alkoxides can strongly influence their structure, i.e. their catalytic behavior, as it will be demonstrated later. In the presence of an excess of ketene, a diblock copolymer poly(ketene-*b*-methacrylate) could be obtained at room temperature with moderate molecular weight and monodisperse molecular weight distribution ($M_n = 12,900$ and $M_w/M_n = 1.6$). The diblock nature of the copolymer was confirmed by double-detection SEC analyses.

Since the first results regarding the highly syndiotactic living polymerization of MMA with organolanthanocene complexes, a series of new rare earth coordination catalytic systems for methacrylates polymerization has been successfully developed. However, only a limited amount of this research was reported in journal of international audience. Thus, numerous multi-component initiating systems for MMA polymerizations such as Nd(P₂₀₄)₃/Al(*i*Bu)₃, Nd(P₂₀₄)/Al(*i*Bu)₃/CCl₄, Nd(O*i*Pr)₃/Al(*i*Bu)₃, Y(acac)₃/Al(*i*Bu)₃/BuLi and Ln(acac)₃/BuMgCl, were found in the Chinese literature.¹⁶⁰ However, we will focus only on the results presented in English language since we can rightfully believe that the most relevant results should be reported in the international scientific language.

Consequently, to our knowledge, only two catalytic systems have been fully described. The first one consists of the combination of an oxygen-based neodymium precursor with

¹⁵⁸ Sugimoto, H.; Inoue, S. *Polym. Prepr. (ACS, Div. Polym. Chem.)* **2000**, 41(1), 424-425.

¹⁵⁹ Sugimoto, H.; Kato, M.; Inoue, S. *Macromol. Chem. Phys.* **1997**, 198, 1605-1610.

¹⁶⁰ For example: (a) Sun, J. Q.; Wang, G. M.; Shen, Z. Q. *Chin. J. Appl. Chem.* **1993**, 10(4), 1-5. (b) Liu, J. F.; Sun, J. Q., Shen, Z. Q. *Chem. Res. Chin. Univ.* **1993**, 9(2), 148-152. (c) Sun, J. Q. *Chem. Res. Chin. Univ.* **1997**, 13(4), 344-349. (d) Sun, J. Q. Pan, Z. D. *Chin. J. Appl. Chem.* **1997**, 14(2), 1-4.

n-butyllithium.¹⁶¹ The precursor was chosen between Nd(P₂₀₄)₃, Nd(acac)₃ and Nd(naph)₃ (P₂₀₄ = [CH₃(CH₂)₃CH(C₂H₅)CH₂O]₂P(O)OH; naph = naphtenate). However, the polymerization study was performed only with Nd(naph)₃ since the latter in combination with *n*-BuLi gave the best results (highest conversions and molecular weights). As the Li/Nd ratio increased, the conversion, the molecular weight, and the isotacticity increased considerably. The optimum Li/Nd molar ratio was estimated to be 11 in this system. Study of the temperature effect showed that the higher the temperature, the lower the conversion and the molecular weight of the PMMA; best results being obtained below 0 °C. Polar solvents inhibited the polymerization. Effect of aging time and temperature were also investigated. Optimized conditions are a minimum aging time of 30 minutes at 0 °C. A PMMA can be obtained in high yield at low temperature with viscosity average molecular weight M_η = 2.2×10⁶, mm = 60%.

The second system studied is composed of Nd(P₂₀₄)₃ in association with di-*n*-butylmagnesium (*n*-Bu₂Mg) and *N,N,N',N'*-tetramethylenediamine (TMEDA).¹⁶² This catalytic system exhibited a greater activity in the presence of HMPA or DMSO as third component, producing high molecular weight PMMA (M_η = 1.4×10⁶). The catalytic activity was influenced by the order of addition of the catalysts components. The optimum addition order is Nd(P₂₀₄)₃ followed by *n*-Bu₂Mg and then TMEDA. It was shown that both the yield and the molecular weight reached a maximum for TMEDA/Mg = 1. Keeping this molar ratio constant, the highest molecular weight (M_η = 1.4×10⁶) was obtained for Mg/Nd = 12. In toluene solution, conversion, molecular weight and isotacticity increased as temperature decreased from 60 to -18 °C. The highest isotacticity was obtained at 0 °C (mm = 65%). The nature of the metal center was investigated and La, Ce, Nd, Sm, Gd, Er and Y phosphonates were tested. A great difference between the rare earths was observed but no general trend could be given.

In these different studies, no data were provided concerning the number-average molecular weights or the molecular weight distributions. Consequently, it is difficult to attribute a living character to these polymerizations and to compare these catalytic systems with the existing ones.

4.4. Group 4 organometallic catalyst systems

The first results regarding the use of group 4 metals for MMA polymerization were reported nearly in the same time as the lanthanocene-based catalysts. Thus, although the persistent disadvantage of interaction of Lewis basic monomers with the electrophilic metal center of group 4 catalyst, the first controlled MMA polymerization initiated by group 4 catalyst was reported in the early 1990's. Collins and co-workers showed that a combination of neutral Cp₂ZrMe₂ and the cationic zirconocene [Cp₂ZrMe(THF)][B(Ph)₄] affords syndiotactic-rich polymerization of MMA by a chain-end controlled propagation step (rr = 80%, M_n = 120,000 and M_w/M_n = 1.2-1.3).¹⁶³ Further work indicated that the polymerization

¹⁶¹ Liu, J.; Shen, Z. Q.; Sun, J. Q. *Eur. Polym. J.* **1996**, *32*, 883-886.

¹⁶² Jiang, L.; Shen, Z. Q.; Zhang, Y. *Eur. Polym. J.* **2000**, *36*, 2513-2516.

¹⁶³ Collins, S.; Ward, D. G. *J. Am. Chem. Soc.* **1992**, *114*, 5460-5462.

proceeds via a neutral zirconocene enolate species.¹⁶⁴ Later, Soga *et al.* reported the highly syndiotactic MMA polymerization with $\text{Cp}_2\text{ZrMe}_2/\text{B}(\text{C}_6\text{F}_5)_3$ or $\text{Ph}_3\text{CB}(\text{C}_6\text{F}_5)_4/\text{ZnEt}_2$ ¹⁶⁵ and the isotactic polymerization of MMA catalyzed by *rac*-Et-(Ind)₂ZrMe₂/ $\text{B}(\text{C}_6\text{F}_5)_3/\text{ZnEt}_2$.¹⁶⁶ In these systems, MMA required to be pre-aged with ZnEt₂ for polymerization to occur. In comparison with Collins systems, these polymerizations are rather slow (24 h vs. 1h). Again, a chain-end control was proposed to explain the stereospecific character of the polymerizations. More recently, Gibson showed that highly isotactic PMMA (mm = 95%) could be prepared by activation of *rac*-Et-(Ind)₂ZrMe₂ in the absence of ZnEt₂.¹⁶⁷ The key point is the order of addition of the various components in order to form properly the well-defined active species. Thus, the two-component system composed of a dimethylzirconocene and a Lewis acid activator can initiate controlled and rapid formation of PMMA as long as the active species is formed before monomer addition. If not, the Lewis basic monomer binds to the alkyl abstractor, rendering it ineffective.

The first stereospecific polymerization of MMA with a single-component catalyst was recently reported.¹⁶⁸ Further investigation on the use of single-component systems showed that the control of the stereospecificity could be obtained via catalyst symmetry.¹⁶⁹ Indeed, $[\text{Me}_2\text{CCpIndZrMe}(\text{THF})][\text{BPh}_4]$ gives highly isotactic PMMA while $[\text{Me}_2\text{CCp}_2\text{ZrMe}(\text{THF})][\text{BPh}_4]$ is syndiospecific at low temperature. Finally, Chen *et al.* recently achieved the syndiotactic MMA polymerization (rr = 80.7 %) at room temperature using a monoalkyl, chiral-at-metal, constrained geometry titanium complex activated by Al(C₆F₅)₃ (Figure 37).¹⁷⁰

¹⁶⁴ (a) Collins, S.; Ward, D. G.; Suddaby, K. H. *Macromolecules* **1994**, *27*, 7222-7224. (b) Li, Y.; Ward, D. G.; Reddy, S. S.; Collins, S. *Macromolecules* **1997**, *30*, 1875-1883.

¹⁶⁵ (a) Soga, K.; Deng, D.; Yano, T.; Shiono, T. *Macromolecules* **1994**, *27*, 7938-7940. (b) Shiono, T.; Saito, T.; Saegusa, N.; Hagihara, H.; Ikeda, T.; Deng, H.; Soga, K. *Macromol. Chem. Phys.* **1998**, *199*, 1573-1579.

¹⁶⁶ Deng, D.; Shiono, T.; Soga, K. *Macromolecules* **1995**, *28*, 3067-3073.

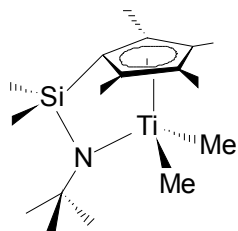
¹⁶⁷ Cameron, P. A.; Gibson, V. C.; Graham, A. J. *Macromolecules* **2000**, *33*, 4329-4335.

¹⁶⁸ Nguyen, H.; Jarvis, A. P.; Lesley, M. J. G.; Kelly, W. M.; Reddy, S. S.; Taylor, N. J.; Collins, S. *Macromolecules* **2000**, *33*, 1508-1510.

¹⁶⁹ Frauenrath, H.; Keul, H.; Höcker, H. *Macromolecules* **2001**, *34*, 14-19.

¹⁷⁰ Jin, J.; Wilson, D. R.; Chen, E. Y.-X. *Chem. Commun.* **2002**, 708-709.

Figure 37. Monoalkyl, chiral-at-metal, titanium complex for syndiotactic MMA polymerization.¹⁷⁰



4.5. Conclusion

MMA polymerization has benefited from the intensive development of new lanthanide complexes. Disappointingly for the researchers, most of the complexes did not show the expected catalytic activity in ethylene and α -olefin polymerizations and thus, MMA polymerization was a useful alternative application for the latter. In this context, nearly all the existing types of complexes (inorganic and organometallic) have been evaluated for the stereospecific polymerization of MMA, targeting high molecular weight PMMA with low polydispersity. Presently, none of the reported initiating system could afford better results than the initial Cp-based systems described by Yasuda. Consequently, the discovery of new catalyst systems, more active and/or more stereospecific is still hypothetical. However, the quest of new, cheap, readily accessible catalysts might still be very challenging and surely the best way to go.

5. Lanthanide-catalyzed diene polymerization

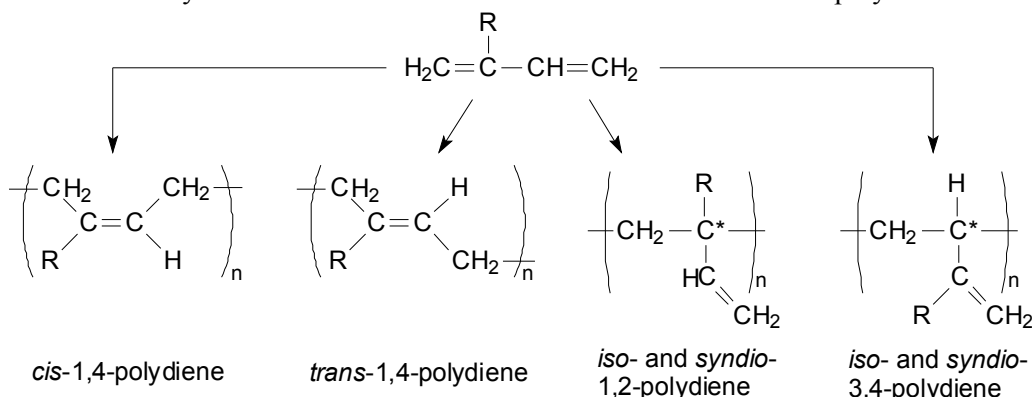
5.1. Introduction

Stereospecific polymerization catalysis of conjugated dienes is of considerable interest from both scientific industrial point of view. From butadiene and isoprene -the industrially most important 1,3-dienes- in comparison with the polymerization of olefins many more structurally different stereoregular polymers can be derived. Thus, by 1,4-polymerization of each of these dienes, a *cis* or a *trans* isomer can be obtained. If the dienes are 1,2-polymerized, a chiral carbon with a vinyl group arises. And, as observed for α -olefin polymerizations, isotactic or syndiotactic polymer can be formed. In the case of substituted dienes like isoprene, a 3,4-polymerization can additionally take place. The formation of another isotactic or syndiotactic structure is also possible in this case (Figure 38).

To synthesize the different stereoregular dienes, the appropriate combination of regio- and stereoselectivity must be realized in the polymerization course. Among the different isomeric forms, *cis*-1,4 polybutadiene is the most important because of its natural rubber-like properties which can be employed in tire industry. Many review articles and book chapters were

published concerning the lanthanide-catalyzed stereospecific diene polymerization, and the reader will find there a complete overview of the subject.¹⁷¹

Figure 38. Structurally different stereoisomers observed in substituted diene polymerization.



The large-scale technical synthesis is carried out as solution polymerization with organometallic complexes of Ziegler-Natta type containing titanium, cobalt, nickel, or neodymium in aromatic or aliphatic hydrocarbons at 50–70 °C (Table 8). In each case, a ternary catalytic system of high activity and selectivity is used. It should be noted that lithium alkyls are also applied to produce *cis*-1,4 polybutadiene in aliphatic hydrocarbons by anionic polymerization.^{171c}

Table 8. Ziegler-Natta type catalysts applied technically for the *cis*-1,4 polymerization of butadiene.^{171c}

Catalytic system	M (mg/L)	PBD (kg/gM)	<i>cis</i> (%)
TiCl ₄ /I ₂ /Al(<i>i</i> Bu) ₃ (1/1.5/8)	50	4-10	93
Co(OCOR) ₂ /H ₂ O/AlEt ₂ Cl (1/10/200)	1-2	40-160	96
Ni(OCOR) ₂ /BF ₃ .OEt ₂ /AlEt ₃ (1/7.5/8)	5	30-90	97
Nd(OCOR) ₃ /AlEt ₂ Cl/Al(<i>i</i> Bu) ₂ H	10	7-15	98

M = transition metal; PBD = polybutadiene

Although Co-based catalyst systems are still the most widely used due to their high activity and relatively high selectivity, Nd-based catalysts are of particular interest since they give typically a higher *cis* microstructure (up to 99%), and exhibits a pseudo-living character which is very rare with Ziegler-Natta catalysts. This high stereoregularity provides excellent dynamic

¹⁷¹ (a) “Ullmann’s Encyclopedia of Industrial Chemistry”, 5th edition, vol. A4, VCH, Weinheim (1993) p22. (b) L. Porri, A. Giarrusso, In *Comprehensive Polymer Science*: G.C. Eastmond, A. Ledwith, S. Russo, P. Sigwalt, Eds. Pergamon Press: Oxford, U.K. 4 (1989) p53. (c) R. Taube, G. Sylvester, “Stereospecific Polymerization of Butadiene or Isoprene”, in “Applied Homogeneous Catalysis with Organometallic compounds”, B. Cornils, W.A. Herrmann, Eds., 2nd Ed., vol. 1, VCH, Weinheim-New York-Basel-Cambridge-Tokyo, 2002, pp. 285-315. (d) Porri, L.; Ricci, G.; Shubin, N. *Macromol. Symp.* **1998**, 128, 53-61. (e) Porri, L.; Ricci, G.; Giarrusso, A.; Shubin, N.; Lu, Z. *ACS Symp. Ser.* **2000**, No 749, 15-30.

properties, especially higher tensile strength, lower heat buildup and better abrasion resistance.¹⁷² In addition, low branching and vinyl content of the polymer as well as its broad molecular weight distribution contribute to a higher processability. Moreover, the pseudo-living character allows the introduction of many polar functional groups into polybutadiene for surface modification and for extending its application to tires.

Since the early discoveries of binary lanthanide-based catalytic systems ($\text{LnX}_3/\text{AlR}_3$) and ternary systems ($\text{Ce}(\text{OCOR})_3/\text{AlR}_3/\text{AlR}_2\text{Cl}$) in the 1960's, many other stereospecific lanthanide-based catalyst systems have been developed.¹⁷³ These systems were largely studied, and we would like to present firstly the different existing catalytic systems, followed by the general trend observed with these catalysts. Then, we will discuss in more details Nd-carboxylates-based systems and the last developments (mechanistic, catalysts...) reported in this area. But before the presentation of the catalyst systems, it seems fundamental to give the general mechanistic principles for stereospecific diene polymerization.

5.2. Diene polymerization: mechanistic aspect

The elucidation of the catalytic reaction mechanism and the structure-reactivity relationships proceeded much more slowly than the development of the catalyst systems. For Natta and Soga, the coordination mode of the monomer is essential.¹⁷⁴ *Trans*-1,4 polymer is formed from unidentately coordinated monomer while bidentate coordination leads to *cis*-1,4 polymer. In the mid 1960's, Wilke and Porri showed that allyl-transition metal complexes can catalyze the butadiene polymerization stereoselectively and quite probably represent the real catalysts.¹⁷⁵ The allyl insertion mechanism was proven directly by NMR spectroscopy to be the principle catalytic reaction for chain growth in diene polymerization.¹⁷⁶

Dolgoplosk proposed a stereoregulation based on the structure of the last monomer unit (chain control mechanism). The *anti*- π -allylic structure favors the *cis* units whereas the *syn* one favors the formation of the *trans* units.¹⁷⁷ A mechanistic study devoted to lanthanide-catalyzed polymerization was reported more recently.¹⁷⁸

For these metals, it has been proven by X-ray structure analysis and NMR spectroscopic studies that the allyl anions in all the allyl-lanthanide complexes are η^3 -coordinated. The allyl-lanthanide bond is strongly polar, but with a quite high covalent contribution due to the higher ionic charge on the metal. As a result of this strong allyl-lanthanide bond, the C-C bond

¹⁷² Witte, J. *Angew. Makromol. Chem.* **1981**, *94*, 119-146.

¹⁷³ (a) Robinson, I. M.; Schreyer, R. C., US 3,118,864 (Du Pont), **1964**. (b) Shen, T.-C.; Gung, C.-Y.; Chung, C.-C.; Ouyang, J. *Sci. Sin.* **1964**, *13*, 1339.

¹⁷⁴ (a) Natta, G.; Porri, L.; Carbonaro, A. *Makromolek. Chem.* **1964**, *77*, 126-138. (b) Soga, K.; Shiono, T.; Sano, T.; Yamamoto, K. *Polym. Prepr., Jpn.* **1982**, *31*, 1445.

¹⁷⁵ (a) Wilke, G.; Bogdanovic, B.; Hardt, P.; Heimbach, P.; Keim, W.; Kröner, M.; Oberkirch, W.; Tanaka, K.; Steinrucke, E.; Wlater, D.; Zimmermann, H. *Angew. Chem. Int. Ed. Engl.* **1966**, *5*, 151. (b) Porri, L.; Natta, G.; Gallazzi, M. C. *J. Polym. Sci. C* **1967**, *16*, 2525.

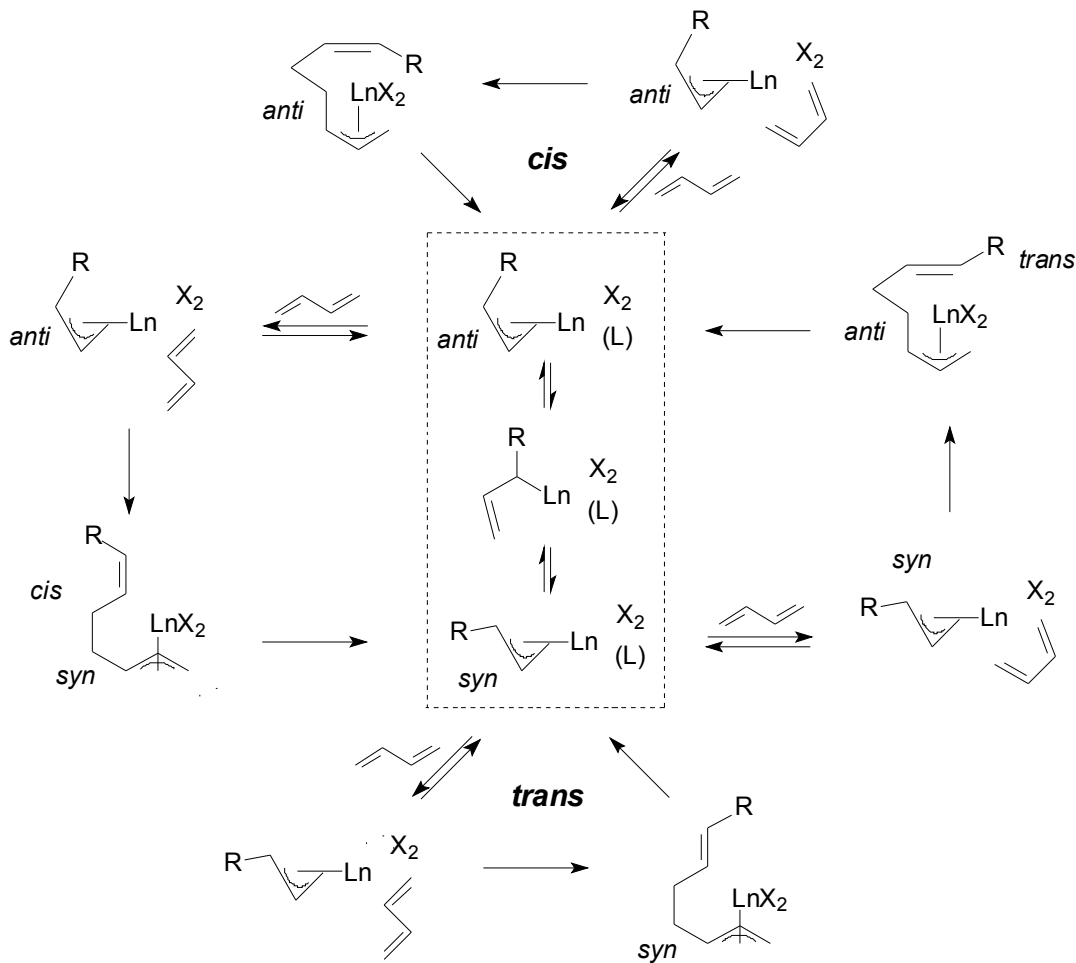
¹⁷⁶ Warin, R.; Teyssié, P.; Bourdaudurq, P.; Dawans, F. *J. Polym. Sci., Polym. Lett.* **1973**, *11*, 177-183.

¹⁷⁷ Dolgoplosk, B.A.; Beilin, S.I.; Korshak, Y.V.; Makovetsky, K.L.; Tinyakova, E.I. *J. Polym. Sci., Part A-1* **1973**, *11*, 2569-2590.

¹⁷⁸ Taube, R.; Windisch, H.; Maiwald, S. *Macromol. Symp.* **1995**, *89*, 393-409.

formation between the allyl anion and the butadiene can only proceed with π -coordinated butadiene according to the σ -allyl insertion mechanism by the energetically favored C(1)-C(1) interaction. Any interaction of the σ -bonded butenyl anion via the C(3) atom with non-coordinated butadiene from the solution is practically impeded by the strong polarizing effect of the $\text{Ln}^{(\text{III})}$ ion, which shifts the negative charge mainly to the directly bonded C(1) atom and strongly decreases the nucleophilicity at the C(3) atom. Therefore, in contrast to allyl-alkali metal compounds, almost no 1,2-polymerization is observed with Ln-based catalysts. If the 1,4-polymerization is realized by the σ -allyl insertion mechanism, then the butenyl group in the *anti* and in the *syn* structure should be practically equally reactive and the *cis-trans* selectivity can be determined by the different modes of butadiene coordination in the butenyl-lanthanide complex. In accordance with the *anti-cis* and *syn-trans* correlation and under the assumption that the insertion step is more rapid than the *anti-syn* isomerization, the *trans* units are obtained from η^2 -coordinated butadiene in its stable single *trans* configuration by *syn* insertion while the η^4 -*cis*-coordinated butadiene provides the *cis* units via *anti* insertion. This mechanism is summarized in Scheme 16.

Scheme 16. General reaction scheme for allyl-lanthanide-catalyzed butadiene polymerization.^{171c}



5.3. *Cis*-1,4 lanthanide-based catalyst systems

5.3.1. Presentation of the catalytic systems

Given the numerous reports on the *cis*-1,4 lanthanide-mediated polymerization of dienes, it would be too long to give precise data on each particular catalytic system. Consequently, we found more judicious to gather all the existing systems, based on their components and, then, discuss the general trends observed in diene polymerizations.

Up to the mid-1990's, more than 95% of the lanthanide-containing catalytic systems were constituted of oxygenated-based ligand and could be simply divided into three categories.

The first group is composed of binary systems where the initial lanthanide compound is represented by its halide LnX_3 or a complex compound of the halide, $\text{LnX}_3 \cdot \text{L}_n$ where L is an electron donor organic ligand. The latter was preferred due to its higher activity (higher solubility). The most commonly used ligands were alcohols,¹⁷⁹ THF,¹⁸⁰ and phosphoric acid.^{179a} In combination with a tris(alkyl)aluminum, polydienes with a high *cis*-1,4 content are produced.

The second group is composed of a lanthanide salt that does not contain halogen atom such as carboxylates: $\text{Ln}(\text{OCOR})_3$, alkylphosphates: $\text{Ln}(\text{O}_3\text{POR})_3$, alkoxides: $\text{Ln}(\text{OR})_3$ or a chelate compound. The salts of mono- and dicarboxylic acids C₁-C₂₂ were used but primarily only carboxylates which possess sufficient solubility in hydrocarbons, i.e., naphthenates,¹⁸¹ versatates,¹⁸² and octanoates¹⁸³ were employed. Among the phosphate derivatives, tributylphosphate has been recently used.¹⁸⁴ In the lanthanide alkoxide systems " $\text{Ln}(\text{OR})_3$ ", the radical R may contain from 1 to 20 carbon atoms, preferably not less than 4, and the linear chain R yields higher activities than the corresponding branched chains.¹⁸⁵ The major chelate compounds are represented by the β -diketonates based on acetyl or benzoyl acetone. To this lanthanide salt, an organoaluminum compound and an halogenating agent are added to observe *cis*-1,4 polymerization of butadiene. Among the halogenating agents, alkylaluminium halides, alkylmagnesium halides, alkyltitanium halides and organic halides were used. However, alkylaluminium and organic halides are the most frequently met.^{172,182} The catalytic systems of this group possess the same *cis*-1,4 stereospecificity as the systems based on the lanthanide halides.

¹⁷⁹ (a) Shen, Z.; Ouyang, J.; Wang, F.; Hu, Z.; Yu, F.; Qian, N. *J. Polym. Sci. Chem. Ed.* **1980**, *18*, 3345-3357.
(b) Srinivasa Rao, G. S.; Updhyay, V. K.; Jain, R. C. *Angew. Makromol. Chem.* **1997**, *251*, 193-205. (c) Srinivasa Rao, G. S.; Updhyay, V. K.; Jain, R. C. *J. Appl. Polym. Sci.* **1999**, *71*, 595-602.

¹⁸⁰ Yang, J. H.; Tsutsui, M.; Shen, Z.; Bergbreiter, D. E. *Macromolecules* **1982**, *15*, 230-233.

¹⁸¹ Wang, F.; Bolognesi, A.; Immirzi, A.; Porri, L. *Makromolek. Chem.* **1981**, *182*, 3617-3623.

¹⁸² Wilson, D. J. *Polym. Int.* **1996**, *39*, 235-242.

¹⁸³ Ricci, G.; Italia, S.; Cabassi, F.; Porri, L. *Polym. Commun.* **1987**, *28*, 223.

¹⁸⁴ Sigaeva, N. N.; Usmanov, T. S.; Budtov, V. P.; Spivak, S. I.; Zaikov, G. E.; Monakov, Y. B. *J. Appl. Polym. Sci.* **2002**, *87*, 358-368.

¹⁸⁵ Dong, W.; Masuda, T. J. *Polym. Sci., Part A: Polym. Chem.* **2002**, *40*, 1838-1844.

The third group is composed of a lanthanide compound containing mixed ligands, of which at least one is an halogen, in combination with a tris(alkyl)aluminum. A typical example is the system $(CF_3COO)_2NdCl(Et_2O)_2/AlR_3$.¹⁸⁶

The preliminary results reported on the use of allyl derivatives for the *trans*-1,4 polymerization of butadiene will be presented in a separated chapter together with the later reports from Taube and co-workers. Indeed, these well-defined complexes have the singular behavior of exhibiting both *cis* and *trans* stereospecificities.

5.3.2. General features of the *cis*-1,4 lanthanide-based catalyst systems¹⁸⁷

Conditions of polymerization

Various solvents were used in these polymerizations: aliphatic, cycloaliphatic and aromatic hydrocarbons. The solvent did not affect the stereospecificity of the polymerization. However, higher molecular weight polymers were obtained in aliphatic solvents along with higher polymerization rates. The difference of activity might be ascribed to the faster propagation rate in aliphatic solvents compared to aromatic solvents. Solvents such as toluene may enter the coordination sphere of the lanthanide, i.e., the active center, and thereby influence its reactivity and also stability.

Although diene polymerization has been patented over a very wide range of temperatures (from -60 to 150 °C), the typical polymerization temperatures are in the range 20-60 °C. Above this temperature, thermal decomposition of the catalyst ensues, especially in aliphatic solvents. The polymer molecular weight decreases with the temperature while the *cis*-1,4 stereospecificity remains unchanged.

Molecular weights and polydispersity

Generally, high molecular weight polymers are obtained by lanthanide-catalyzed polymerization ($M_n = 100,000\text{-}2,000,000$). The molecular weight distribution is often bimodal and broad ($M_w/M_n > 3.0$) suggesting the presence of multiple active sites for the polymerization. The formation and the nature of the active species in these catalyst systems are still under investigation and not yet fully understood.

Stereoregulation

In the polymerization of butadiene, the microstructure of the polymer depends neither on the composition of the catalytic systems nor on the conditions of polymerization, as mentioned above. The polybutadiene chain almost entirely consists of *cis*-1,4 units (> 95%). The mechanism for stereospecific polymerization of dienes has been described in 5.2.

Nature of the lanthanide

¹⁸⁶ Jin, Y.-T.; Sun, Y.-F.; Ouyang, J. *Chem. Abstr.* **1980**, *93*, 150747h.

¹⁸⁷ (a) Marina, N.G.; Monakov, Y. B.; Rafikov, S. R.; Gadaleva, K. K. *Polym. Sci. U.S.S.R.* **1984**, *26*, 1251 and references therein. (b) Wilson, D. J. *Makromol. Chem. Macromol. Symp.* **1993**, *66*, 273-288.

Some general patterns can be discerned for all these catalysts: Neodymium-containing catalysts were found to be the most active, as it was already noted in the very first reports.¹⁷³ Europium-containing systems were inactive because of its exposure to reducing agents such as AlR₃, while the reduction to the divalent state does not occur completely in the case of samarium since a little activity could be observed.

Nature of the halogen

Depending on the nature of the halogen, the catalytic systems line up in the following activity series: Cl > Br >> I > F. The influence of the halogen atom on the polymerization activity is evidently connected to a certain extent with the completeness of halogenation of the lanthanide and, hence, with the number of active sites formed. However, the microstructure of the polymer does not depend on the nature of the halogen. The usual halogenating compounds are AlR₂Cl, AlRCl₂ and alkyl halides. Typically, the best results are obtained for molar ratios [Cl]₀/[Nd]₀ ≥ 2.

Structure of the alkyl aluminum component

It was rapidly noticed that variation in the alkyl radicals in AlR₃ in the lanthanide-catalyzed diene polymerization had an appreciable effect on the activity of the catalyst. Activity series for the organoaluminum compounds depends on the nature of the catalytic system. For the catalytic systems of group 2, the following activity series have been established:



while the latter is somehow inverted for LnCl₃-R'OH/AlR₃ systems:



The difference of activity observed reflects most probably the level of formation of active sites, i.e. the degree of association of the organoaluminum compound. Generally, a molar ratio [AlR₃]₀/[Nd]₀ ≥ 20 is used, and [Al]₀/[Nd]₀ ≥ 100 when the organoaluminum is an aluminoxane derivative. The nature of the alkylaluminum does not affect the stereoregulating capacity of the catalyst. On the other hand, the organoaluminum compound exerts a considerable effect on the molecular weight of the polymers. Rise in the organoaluminum concentration leads to a fall in molecular weight indicating chain transfer reaction between aluminum and lanthanide species. DIBAL-H revealed to be a more effective transfer agent while an increase in the length of the radicals in AlR₃ promotes an increase of the molecular weight. This aspect will be reviewed more precisely later.

5.3.3. Detailed description of Nd(OCOR)₃/AlR₃/halogen source systems

Now, we would like to focus on the most widely studied and industrially used catalytic systems: Nd(OCOR)₃/AlR₃/halogen source. Indeed, a real controversy exists concerning these

systems, and it would be interesting to give a more detailed description, based on the latest publications in this field.

5.3.3.1. Nature of the precursor

First, it has to be borne in mind that neodymium carboxylates have complex structures, in part due to the synthetic route used for their preparation. Indeed, neodymium carboxylates are usually prepared by reaction of an aqueous solution of neodymium chloride or neodymium nitrate with an aqueous sodium carboxylate solution, followed by extraction with an organic solvent. Because of these experimental conditions and the 8- to 12-coordination ability of Nd, neodymium carboxylates (NdV) can not be found as a monomeric structure. MALDI-TOF mass spectroscopic studies showed that these precursors are converted to oligomeric structures by abundant surrounding ligands such as water, chloride, sodium carboxylates and hydroxide. Thus, dimeric and tetrameric structures were clearly identified.¹⁸⁸ It is generally accepted that the formation of the active species arises from halogenation and alkylation of the neodymium carboxylate. Consequently, it is assumed that more accessible monomeric structure would lead to more active catalysts. Thus, the use of well-defined monomeric Nd(neodecanoate)₃ (neodecanoic acid) (NdVH), prepared by ligand exchange between an excess of neodecanoic acid in chlorobenzene, leads eventually to higher activities (Table 9).¹⁸⁸ Comparison with the traditional NdV/AlR₃/AlEt₂Cl and NdCl₃(THF)₂/AlR₃ systems evidenced that the more aggregated the catalyst, the lower the activity.

Table 9. Effect of neodymium catalyst on the catalytic activity.¹⁸⁸

Catalyst	Activity (kg/molNd/h)
NdCl ₃ (THF) ₂ /AlR ₃	0.2×10^2
NdV/AlR ₃ /AlEt ₂ Cl	4.3×10^2
NdVH/AlR ₃ /AlEt ₂ Cl	25.0×10^2

Conditions: [BD]₀ = 3.3 M; [Nd]₀ = 10⁻⁴ mol/100 g BD; [Nd]₀/[AlEt₂Cl]₀/[DIBAL-H]₀/[Al(iBu)₃]₀ = 1/3/10/40 in cyclohexane, 60 °C for 2 h.

5.3.3.2. Effect of catalyst component addition order

The order of addition of the different components of this catalytic system affects the nature of the catalyst.¹⁸⁹ Component addition order influences the homogeneity/stability of the catalyst. Only the order AlR₃/NdV/AlEt₂Cl and NdV/AlR₃/AlEt₂Cl gave catalysts which did not precipitate after 20 h; other addition orders led to precipitate formation after 20 h or immediately. It was clearly demonstrated that at least two different types of active sites operate in these systems. Initial fast polymerization occurs on insoluble particles which may not be visible to the naked eye. Further, slow polymerization occurs at the second type of soluble catalyst site. This second type of chain growth proceeds in a steady pseudo-living fashion. Since rapid polymerization with heterogeneous active sites will lead to extremely

¹⁸⁸ Kwag, G. *Macromolecules* **2002**, *35*, 4875-4879.

¹⁸⁹ Wilson, D. J.; Jenkins, D. K. *Polymer* **1992**, *27*, 407-411.

high molecular weight polymer, the molecular weight distribution of the final polymer is somewhat broad.

5.3.3.3. Nature of the active species in Nd(OCOR)₃/AlR₃/AlEt₂Cl

In this effort to understand the mechanism of formation of the active species, Evans worked also on the synthesis of well-defined neodymium carboxylates (neodymium dimethylbutyrate = NdV').¹⁹⁰ Assuming that the active species is formed by pre-reaction with the halogen source, followed by alkylation with the tris(alkyl)aluminum, he tried to isolate an intermediate species from NdV'/AlEt₂Cl mixtures (1/5). After removing Et₂Al(OCOR) from the resulting solution, all he could crystallize from a THF solution was the neodymium trichloride NdCl₃(THF)₄, while different analytical measurements showed that the mother liquor responds to the formula Nd₂AlCl₅C₁₃H₂₂. This result was consistent with the literature view that the purpose of the halogen source is to prepare NdCl₃.^{171d-e} Unfortunately, it was not possible to fully characterize species of formula Nd₂AlCl₅C₁₃H₂₂. However, it was shown that the latter polymerizes quickly isoprene upon addition of only 1 equiv. of Al(iBu)₃ while an excess of organoaluminum compound and few hours are necessary to observe the same monomer conversion with NdCl₃(THF)₄. The reduced activity of the latter system is, as expected, due to the presence of the coordinating base. A recent study of this system using synchrotron X-ray absorption (XANES and EXAFS experiments) and UV-Vis spectroscopies concludes that the Nd-based catalyst originates from the contact Nd³⁺-C bond having both covalent and ionic character.¹⁹¹ In addition, the presence of chlorine atoms in the catalyst was also proved. The presence of aluminum in the active species has been previously reported, but for the ternary system Nd(O*i*Pr)₃/AlEt₃/AlEt₂Cl. X-ray analysis of crystals grown from this system after few months showed the presence of two different kinds of neodymium active centers, i.e. two different neodymium environments with a neodymium-carbon bond.¹⁹²

It has to be noted that halogenation of neodymium is not necessary to observe diene polymerization with NdV. The simple system composed of MAO and NdV is effective for *cis*-1,4 butadiene polymerization. However, polymerization activity can be observed only for [MAO]₀/[NdV]₀ > 100 and the addition of a chloride source (*t*-BuCl) allows higher *cis*-1,4 content (99% in the presence of *t*-BuCl vs. 91% without) and higher activity, especially for polymerization temperatures below 60 °C.¹⁸² These results are consistent with the higher activity of chloride-containing systems.

5.3.3.4. Effect of the concentration of the various components

To discuss this point, we will refer to two recent papers where the catalytic system NdV/DIBAL-H/AlEt₂Cl was deeply studied.¹⁹³ The reactions were carried out either in hexane at 60 °C or in cyclohexane at 70 °C.

¹⁹⁰ Evans, W. J.; Giarikos, D. G.; Ziller, J. W. *Organometallics* **2001**, *20*, 5751-5758.

¹⁹¹ Kwag, G.; Lee, H.; Kim, S. *Macromolecules* **2001**, *34*, 5367-5369.

¹⁹² Shan, C.; Lin, Y.; Ouyang, J.; Fan, Y.; Yang, G. *Makromol. Chem.* **1987**, *188*, 629-635.

¹⁹³ (a) Friebe, L.; Nuyken, O.; Windisch, H.; Obrecht, W. *Macromol. Chem. Phys.* **2002**, *203*, 1055-1064. (b) Quirk, R. P.; Kells, A. M.; Yunlu, K.; Cuif, J.-P. *Polymer*, **2000**, *41*, 5903-5908.

Effect of AlEt_2Cl

The rate of polymerization exhibits a maximum for $[\text{AlEt}_2\text{Cl}]_0/[\text{NdV}]_0 = 2$, value that is in agreement with most of the literature data. At this molar ratio, the number of active sites created is maximum. When $[\text{AlEt}_2\text{Cl}]_0/[\text{NdV}]_0 > 2$, a decrease in the polymerization rate was observed, which might be explained by the formation of insoluble NdCl_3 . *Cis*-1,4 content increases from 92.5% to 96.2% with increasing the ratio $[\text{AlEt}_2\text{Cl}]_0/[\text{NdV}]_0$ from 0.5 to 4. Simultaneously, the *trans* content decreases from 6.6% to 2.7%; the 1,2 content remaining constant.

Effect of DIBAL-H

DIBAL-H acts simultaneously as a scavenger for impurities, a catalyst activator and a control agent for molar masses. No polymerization is observed below the critical threshold level of $[\text{DIBAL-H}]_0/[\text{NdV}]_0 < 10$. Above this ratio, the rate of polymerization increases within a narrow window of $10 < [\text{DIBAL-H}]_0/[\text{NdV}]_0 < 20$. Above this ratio, [DIBAL-H] does not affect the rate of polymerization anymore. The molecular weights increase linearly with conversion as would be expected for a living polymerization. In addition, the slopes of the M_n -conversion plots decrease with increasing $[\text{DIBAL-H}]_0/[\text{NdV}]_0$. This is clear evidence for the controlling effect of DIBAL-H on molecular weights. Further investigation showed that the number of polymer chains generated per Nd exceeds 1 and depends on the amount of DIBAL-H. Consequently, aluminum is unambiguously involved in the generation of polymer chains. In fact, living polymer chains might be transferred from Nd onto Al, while at the same time Nd species are formed with either isobutyl or hydrogen attached. As these new Nd species are active in the polymerization, more than one polymer chain will be generated per Nd. This chain transfer from Nd to Al is reversible during the course of the polymerization, thus polymer chains attached to Al can be back-transferred to Nd and reactivated; Al with attached polymer can be considered as a dormant species. As the molecular weight distribution does not increase with conversion it has to be concluded that this chain transfer reaction is fast relative to propagation.

An increase in $[\text{DIBAL-H}]_0$ results in an increasing *trans*-1,4 content and a corresponding decrease in the *cis*-1,4 content. The impact of the $[\text{DIBAL-H}]_0/[\text{NdV}]_0$ ratio can be explained by a reduction of the number of available coordination sites in the presence of an excess of DIBAL-H, resulting in a decreased η^4 -coordination of butadiene, i.e. an increase of the *trans*-1,4 content.

Effect of water

Cuif *et al.* studied the effect of water. They showed that the total amount of water affects the catalytic behavior. The conversion is seen to rise to a maximum as the molar ratio of water to Nd increased from 0.008 to 0.11. Water may interact with DIBAL-H to generate aluminoxane-type species, promoting the polymerization at $[\text{H}_2\text{O}]_0/[\text{NdV}]_0 < 0.11$. A decrease of the molecular weight values (from $M_n = 560,000$ to $M_n = 230,000$) and a narrowing of the molecular weight distribution (from $M_w/M_n = 6.7$ to $M_w/M_n = 3.5$) were coupled with this

increase in activity. These effects may be due to an increase of active center concentration or to an increase of chain transfer reactions. At higher water concentrations, lower conversion along with higher M_n and M_w/M_n values are observed, due to the inefficient alkylation of DIBAL-H or reduced chain transfer reactions.

Now that the traditional lanthanide-based catalyst systems used for diene polymerization have been fully described, we would like to focus on the latest developments in this field.

5.3.4. *Allyl-based catalysts*

Preliminary results from Mazzei with the well-defined organometallic complex $\text{Li}(\text{Nd}(\eta^3\text{-allyl})_4)(\text{dioxane})_{1.5}$ in butadiene polymerization showed that the latter was efficient for the *trans*-1,4 polymerization (70-90%) without cocatalyst.¹⁹⁴ Moreover, the addition of THF to the catalytic solution led to the 1,2-polymerization of butadiene. According to these results, an allyl-neodymium compounds is the active species in the butadiene polymerization, and using such organometallic complexes will favor the mechanistic study of such systems.

The contribution of Taube and co-workers in this direction is important. First, they have re-investigated the complex $\text{LiNd}(\text{allyl})_4$.¹⁹⁵ The initial findings were corroborated but it was also shown that this stereospecific *trans*-1,4 single-component catalyst gave birth to a stereospecific *cis*-1,4 catalyst upon addition of 2 equivalents of AlEt_2Cl (*cis*-1,4 = 93%). Further developments were observed with the use of the neutral complexes $[\{\text{La}(\eta^3\text{-allyl})_3(\eta^1\text{-C}_4\text{H}_8\text{O}_2)\}_2(\mu\text{-C}_4\text{H}_8\text{O}_2)]$ and $[\text{Nd}(\eta^3\text{-allyl})_3(\mu\text{-C}_4\text{H}_8\text{O}_2)]_n$ ($\text{C}_4\text{H}_8\text{O}_2$ = 1,4-dioxan). These complexes catalyze the *trans*-1,4 polymerization of butadiene in toluene with a moderate selectivity (82-83%). By addition of a Lewis acid such as AlEt_2Cl , AlEtCl_2 or MAO, catalysts for the *cis*-1,4 polymerization are obtained. The solvate-free complex $\text{Nd}(\eta^3\text{-allyl})_3$ catalyzes also the *trans*-1,4 polymerization of butadiene in toluene at 50 °C with a selectivity of 80-85%.¹⁹⁶ For the first time, it was shown that the average molecular weight of the polymer increased linearly with monomer conversion like in a living polymerization; the polydispersity being correspondingly low ($M_w/M_n < 1.3$). The formation of 2 or 3 polymer chains per Nd was experimentally observed and explained using a reaction model based on the successive formation of two catalyst complexes, a bis- and a tris(polybutadienyl)-neodymium^(III) complex. These compounds catalyze the chain growth in dependence of the extent and the mode of butadiene coordination according to the π -allyl insertion mechanism. However, the catalytic activity and the *cis* selectivity can be improved by combination with aluminoxanes as cocatalyst.¹⁹⁷ In this case, a mono(polybutadienyl)neodymium^(III) complex is formed, producing one polymer chain per Nd center, and the *cis* selectivity resulting from the $\eta^4\text{-cis}$ coordination of the monomer. Recently, the combination of a pre-formed tris(polybutadienyl) neodymium complex with 2 equivalents of AlR_2Cl led to the formation of a structurally

¹⁹⁴ Mazzei, A. *Makromol. Chem. Suppl.* **1981**, 4, 61-72.

¹⁹⁵ Taube, R.; Maiwald, S.; Sieler, J. *J. Organomet. Chem.* **1996**, 513, 37-47.

¹⁹⁶ Maiwald, S.; Weißenborn, H.; Sommer, C.; Müller, G.; Taube, R. *J. Organomet. Chem.* **2001**, 640, 1-9.

¹⁹⁷ Maiwald, S.; Weißenborn, H.; Windisch, H.; Sommer, C.; Müller, G.; Taube, R. *Macromol. Chem. Phys.* **1997**, 198, 3305-3315.

uniform catalyst complex for the *cis*-1,4 polymerization of dienes.¹⁹⁸ The use of AlMe₂Cl in toluene at 50 °C gives rise to high catalytic activity (36,000 molBD/molNd/h) and a *cis* selectivity over 90%. In addition to the low polydispersity ($M_w/M_n = 1.3$), it was found that only one polymer chain was formed per Nd center.

When the mono- and bis(allyl) neodymium chloride complexes, Nd(η^3 -allyl)Cl₂•(THF)₂ and Nd(η^3 -allyl)₂Cl•(THF)_{1.5} are combined with MAO, the activity can be further increased and a *cis* selectivity of more than 95% can be achieved.¹⁹⁹ Kinetics studies indicate that a mono(polybutadienyl)bis(butadiene)neodymium^(III) complex with two complexed alkylaluminoxanate anions might be the catalyst. The latter produces a *cis*-1,4 polybutadiene via *anti* insertion of the η^4 -*cis* coordinated monomer. A living-like polymerization behavior was again observed.

5.3.5. Nitrogen-based ligands

Recently, the amide-based catalyst system Nd(N(SiMe₃)₂)₃/Al(iBu)₃/AlEt₂Cl (Nd(N(SiMe₃)₂)₃ = NdN3) was reported to be at least as efficient in butadiene polymerization as the classical ternary NdV-based systems.²⁰⁰ High activity is observed even at low catalyst concentration (1,350 kgBD/molNd/h), the behavior being attributed to the monomeric structure of the amido-complex. As it was noticed for NdV systems, the highest activity was observed for a molar ratio [AlEt₂Cl]₀/[NdN3]₀ = 2 in heptane solution. The regioselectivity of butadiene insertion does not depend on the ratio [AlEt₂Cl]₀/[NdN3]₀, however, a decrease in the *cis*-1,4 content is noticed for [AlEt₂Cl]₀/[NdN3]₀ > 2 (*cis*-1,4 > 95%). The [Al(iBu)]₀/[NdN3]₀ ratio influences the catalyst activity but barely modifies the stereospecificity of the polymer. Increasing the ratio from 10 to 40 allows a gain of activity (×3).

¹⁹⁸ Maiwald, S.; Sommer, C.; Muller, G.; Taube, R. *Macromol. Chem. Phys.* **2002**, *203*, 1029-1039.

¹⁹⁹ Maiwald, S.; Sommer, C.; Müller, G.; Taube, R. *Macromol. Chem. Phys.* **2001**, *202*, 1446-1456.

²⁰⁰ Boisson, C.; Barbotin, F.; Spitz, R. *Macromol. Chem. Phys.* **1999**, *200*, 1163-1166.

5.3.6. Lanthanocene-based catalysts

Single-component lanthanide metallocene complexes, such as (Cp^*_2LnR) ($R = Me, H$) or $Cp^*_2Sm(THF)_2$ are known to be efficient catalysts for ethylene and MMA polymerizations. However, these complexes are almost completely inactive for polymerization of dienes due to the easy formation of too stable η^3 -allyl complexes. These complexes did not allow further monomer insertion. For example, Evans described that the divalent samarium complex **I₄** reacts with butadiene yielding a stable dimeric samarium^(III) μ -allyl complex which is not active for diene polymerization.²⁰¹ Nevertheless, Wakatsuki and co-workers showed that when a cocatalyst such as MMAO (modified methylalumininoxane containing isobutylalumininoxane) is used, **I₄** can efficiently polymerize butadiene.²⁰² In toluene solution at 50 °C, high molecular weight polymer with a rather high activity is noticed (370 g/molSm/h) and high *cis*-1,4 stereospecificity (98.8%) is obtained. The major difference with the traditional binary and ternary systems is the rather low polydispersity ($M_w/M_n = 1.8$).

When $Al(iBu)_3/\{[Ph_3C][B(C_6F_5)_4]\}$ is used in place of MMAO, the polymerization proceeds smoothly, keeping the same level of activity and stereospecificity (*cis*-1,4 = 95%). The best results were obtained with the bimetallic precursor $(C_5Me_5)_2Sm[(\mu\text{-}Me)AlMe_2(\mu\text{-}Me)]_2Sm(C_5Me_5)_2$. Although this complex was inactive alone or upon activation with $[Ph_3C][B(C_6F_5)_4]$, its activation with $[Ph_3C][B(C_6F_5)_4]$ and a slight excess of $AlMe_3$ brought about rapid polymerization. In this case, a very high *cis*-1,4 content (99.5%) was obtained at -20 °C.

Spitz *et al.* reported similar results under heterogeneous conditions with neodymium complexes supported on modified silica.²⁰³ Thus, the reaction of neodymium complex $Nd(\eta^6-C_6H_5Me)(AlCl_4)_3$ formed *in situ* with the modified silica affords highly active and stereospecific butadiene polymerization: activity up to 1200 gPBD/gCata/h and *cis*-1,4 content superior to 99%.

Finally, Wakatsuki *et al.*, using a gadolinium catalyst, have recently reported a very high *cis*-1,4 stereospecificity.²⁰⁴ The cationic complex $[(C_5Me_5)_2Ln][B(C_6F_5)_4]$ ($Ln = Pr, Nd, Gd$) was found to be very active for *cis*-1,4 butadiene polymerization. High molecular weight polymers ($M_n = 100,000$ -400,000) and rather low polydispersities ($M_w/M_n = 1.41$ -1.73) were observed. Contrary to the general trend, the highest activity was observed with gadolinium complex which exhibits a nearly perfect *cis*-1,4 stereospecificity (> 99.9%) at -78 °C.

5.4. Trans-1,4 lanthanide-based catalyst systems

It would be impossible to conclude this part without reviewing the highly stereospecific *trans*-1,4 diene polymerization. Even if the *cis*-1,4 stereospecificity is from far the most important for dienes polymerization due to the improved physical properties of the resulting polymer, various catalyst systems producing butadiene rubber with a high *trans*-1,4 content were also reported.²⁰⁵ Among them, we can find (allyl)neodymium-based catalysts already largely described and the catalyst system composed of neodymium or didymium versatate

²⁰¹ Evans, W. J.; Ulibarri, T. A.; Ziller, J. W. *J. Am. Chem. Soc.* **1990**, *112*, 2314-2324.

²⁰² Kaita, S.; Hou, Z.; Wakatsuki, Y. *Macromolecules* **1999**, *32*, 9078-9079.

²⁰³ Barbotin, F.; Spitz, R.; Boisson, C. *Macromol. Rapid Commun.* **2001**, *22*, 1411-1414.

²⁰⁴ Kaita, S.; Hou, Z.; Nishiura, M.; Doi, Y.; Kurazumi, J.; Wakatsuki, Y. *Macromol. Rapid Commun.* **2003**, *24*, 179-184.

(didymium refers to a rare earth mixture containing approximately 72% Nd, 20% La and 8% Pr) and di-*n*-butylmagnesium. With the latter, the rate of polymerization is low since 60% conversion is reached within 16 h at 50 °C in hexane solution ($[BD]_0/[Ln]_0 = 7000$). Doubling the catalyst concentration did not allow higher conversions. The catalyst ratio is very important and a critical ratio $[Mg]_0/[NdV]_0 = 10$ must be used for optimal results. The molecular weights are rather low ($M_{peak} = 50,000\text{-}80,000$) and the molecular weight distributions surprisingly narrow with $M_w/M_n = 1.5$. The *trans*-1,4 content, up to 97%, can be slightly increased by addition of a small amount of THF (6 equiv. vs. Nd). As it was observed for most of the catalyst systems reported, the molecular weight increases linearly with conversion up to about 50%, suggesting an initial living character.

5.5. Styrene-Butadiene copolymerization

Random copolymers of butadiene and styrene are widely utilized commercially as styrene-butadiene-rubbers (SBR). Being produced via radical or anionic polymerization, the stereocontrol of the polybutadiene microstructure has not been possible in these systems. These copolymers are of great interest in the synthetic rubber industry. For example, the latter can find wide industrial application in tire applications. However, the ideal copolymer should have a high molecular weight with a high *cis*-1,4 content and ca. 25 mol% of styrene. Unfortunately, the usual methods of preparation do not lead to such a high *cis*-1,4 content in the material.²⁰⁶ Consequently, a number of studies have been devoted to the synthesis of SBR with high *cis*-1,4 content using transition metal catalysts. Even if many examples of Ni-, Co- and Ti-based catalysts have been reported,²⁰⁷ we will focus here only on lanthanide-based catalysts and will classify them according to the components of the system.

5.5.1. Ternary systems

Many studies have been carried out on the use of ternary systems for styrene-butadiene copolymerization. The best results were obtained with the systems based on carboxylates salts. Other oxygenated ligands such as alkoxides and acetylacetone were reported to be inefficient due to low styrene incorporation. Indeed, in these cases, styrene coordination to the metal center is favored and competes with insertion.²⁰⁸

The most studied catalyst system is formed, as it was observed for butadiene polymerization, by $Ln(OCOR)_3/AlEt_2Cl/AlR_3$, and the most complete investigation is due to

²⁰⁵ (a) Jenkins, D.K. *Polymer* **1985**, *26*, 147-151. (b) Chigir, N. N.; Sharaev, O. K.; Tinyakova, E. I.; Dolgoplosk, B. A. *Chem. Abstr.* **1983**, *98*, 126695x. (c) Chigir, N. N.; Guzman, I. S.; Sharaev, O. K.; Tinyakova, E. I.; Dolgoplosk, B. A. *Chem. Abstr.* **1982**, *97*, 56281n. (d) Maiwald, S.; Weißenborn, H.; Sommer, C.; Muller, G.; Taube, R. *J. Organomet. Chem.* **2001**, *640*, 1-9.

²⁰⁶ Tate, P.; Bethea, T. W. In *Encyclopedia of Polymer Science and Engineering*, Vol. 7, 2nd Edition, Wiley Interscience Publication, John Wiley & Sons, Inc.: New York, **1985**, p537.

²⁰⁷ (a) Gehrke, K.; Harwart, M. *Plast. Kautsch.* **1993**, *40*, 356. (b) Oehme, A.; Gebauer, U.; Gehrke, K. *Macromol. Rapid Commun.* **1995**, *16*, 563-569. (c) Zambelli, A.; Proto, A.; Longo, P.; Oliva, P. *Macromol. Chem. Phys.* **1994**, *195*, 2623-2631.

²⁰⁸ Kobayashi, E.; Kaita, S.; Aoshima, S.; Furukawa, J. *J. Polym. Sci., Part A: Polym. Chem.* **1995**, *33*, 2175-2182.

Kobayashi and co-workers who studied both homo- and copolymerization of butadiene and styrene using $\text{Ln}(\text{OCOR})_3/\text{AlEt}_2\text{Cl}/\text{Al}(i\text{Bu})_3$ ($\text{Ln} = \text{Pr, Nd, Gd, Dy, Yb}$ and $\text{R} = \text{CF}_3, \text{CCl}_3, \text{CHCl}_2, \text{CH}_3$) as catalyst systems.²⁰⁹ The results obtained in butadiene homopolymerization are consistent with the general trend previously presented.

Copolymerizations were conducted with $\text{Ln}(\text{OCOR})_3/\text{AlEt}_2\text{Cl}/\text{Al}(i\text{Bu})_3$ (1/2/25) in hexane at 50 °C. The highest activities and styrene incorporation were noticed with neodymium-based catalysts and especially $\text{Nd}(\text{OCOCCl}_3)_3$. The reactions performed with various styrene feed showed that the activity, molecular weights and *cis*-1,4 content decrease with increasing styrene feed. The distribution of styrene units was demonstrated by SEC measurements, equivalent molecular weight distributions using a UV or refractive index detector were observed (Table 10).

Table 10. Copolymerization of BD and St with $\text{Nd}(\text{OCOCCl}_3)_3/\text{AlEt}_2\text{Cl}/\text{Al}(i\text{Bu})_3$ in hexane.²⁰⁹

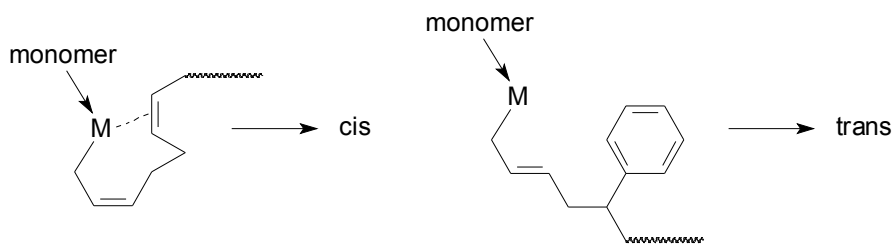
St feed ratio (mol %)	Polymn time (min)	Yield (%)	<i>cis</i> -1,4 (%)	St content (%)	M_w (g/mol)
10	5	8.6	94.4	2.3	81,000
20	10	5.8	85.9	4.7	53,000
50	30	7.2	75.1	27.9	32,000
80	45	8.2	63.8	69.8	10,000
90	45	8.3	55.4	71.1	2,000

Conditions: T = 50 °C; $[\text{BD}]_0 + [\text{St}]_0 = 4 \text{ M}$; $[\text{Nd}]_0 = 10^{-3} \text{ M}$ and $\text{Nd}(\text{OCOCCl}_3)_3/\text{AlEt}_2\text{Cl}/\text{Al}(i\text{Bu})_3$ (1/2/25).

In order to explain the relatively fast decrease of the *cis*-1,4 content with increasing styrene content, Kobayashi *et al.* applied the back-biting model to the *cis*-1,4 polymerization. Indeed, in this model, the coordination between the central metal of the catalyst and the double bond of the penultimate unit of the growing polymer chain is very important for *cis*-1,4 stereospecificity. In the case of copolymerization with styrene, because the penultimate styrene unit hardly coordinates to the central metal, the growing polymer terminal butadiene unit should configurate not to the *cis*-1,4 form but to the *trans*-1,4 form (Figure 39). Moreover, the precise diad analysis of the copolymer microstructure by ^{13}C NMR indicated that the *cis*-1,4 content in both styrene-butadiene and butadiene-butadiene diads decreased with increasing styrene content in the copolymer. Since the *cis*-1,4 content remains constant irrespective of the styrene content with Ni catalysts, the authors proposed that stereospecificity control is not only due to the coordination of the penultimate or antepenultimate unit but to a long range coordination effect. In conclusion, this system gave comparable results to Ni-based catalysts but with lower molecular weights.

Figure 39. Back-biting reaction in butadiene polymerization.²⁰⁹

²⁰⁹ (a) Kobayashi, E.; Kaita, S.; Aoshima, S.; Furukawa, J. *J. Polym. Sci., Part A: Polym. Chem.* **1994**, *32*, 1195-1198. (b) Kobayashi, E.; Kaita, S.; Aoshima, S.; Sakakibara, S.; Furukawa, J. *J. Polym. Sci., Part A: Polym. Chem.* **1996**, *34*, 3431-3434. (c) Kobayashi, E.; Hayashi, N.; Aoshima, S.; Furukawa, J. *J. Polym. Sci., Part A: Polym. Chem.* **1998**, *36*, 241-247.



Other groups worked on the use of neodymium carboxylates for the butadiene styrene copolymerization.

Gehrke *et al.* showed that the Nd(octanoate)₃/CCl₄/Al(*i*Bu)₃ system allows copolymer with high *cis*-1,4 content to be synthesized. However, the styrene content remained very low.^{207a}

More recently, Shen and co-workers have reported the use of ternary systems based on carboxylates and phosphonates.²¹⁰ Typically, the Nd(naph)₃/Al(*i*Bu)₂Cl/Al(*i*Bu)₃ and Nd(P₅₀₇)₃/Al(*i*Bu)₂Cl/Al(*i*Bu)₃ (P₅₀₇ = mono(2-ethylhexyl)-2-ethylhexyl phosphonate) gave, in toluene solution at 50 °C, a copolymer with a moderate styrene content but with high *cis*-1,4 content (92-93%). This content is independent of the styrene content in the copolymer and much higher than the one observed by Kobayashi for the same styrene content (for example: *cis*-1,4 = 75.1% for St = 27.9%). Consequently another mechanism for the polymerization stereospecificity shall be proposed. However, a closer look at the ¹³C NMR spectra of the polymers indicates that these systems are not that different from Kobayashi's ones, and the molecular weight of the copolymers are still low.

Replacement of the tris(alkyl)aluminum by a dialkylmagnesium reagent with lanthanide phosphonates allows higher activities but with lower *cis*-1,4 content (*cis*-1,4 = 85-88%).²¹¹ The results with the optimized system Nd(P₅₀₇)₃/Mg(*n*-Bu)₂/CHCl₃ showed that the incorporation of styrene in the copolymer is low compared to the existing systems.

5.5.2. Allyl-based neodymium catalysts

The different allyl-neodymium complexes reported for butadiene polymerization were also applied to butadiene styrene copolymerization.²¹² The copolymer styrene content is always low irrespective of the styrene feed. As it was noticed in butadiene homopolymerization, in the absence of cocatalyst, the neutral tris(allyl)neodymium complex produces a copolymer with a high *trans*-1,4 content, while a high *cis*-1,4 content can be obtained with the same neodymium precursor when the latter is activated by MAO or a borate. However, these systems are definitely less active than those based on lanthanide carboxylates.

5.5.3. Lanthanocene-based catalysts

Using the highly active catalyst system composed of (C₅Me₅)₂Sm[(μ -Me)AlMe₂(μ -Me)]₂Sm(C₅Me₅)₂ activated by [Ph₃C][B(C₆F₅)₄]/AlMe₃, Wakatsuki *et al.* achieved the synthesis of

²¹⁰ Zhang, Q.; Li, W.; Shen, Z. *Eur. Polym. J.* **2002**, *38*, 869-873.

²¹¹ Zhang, Q.; Ni, X.; Shen, Z. *Polym. Int.* **2002**, *51*, 208-212.

²¹² Windisch, H.; Sylvester, G.; Taube, R.; Maiwald, S.; Giesemann, J.; Rosenstock, T., WO 0185814 (Bayer Aktiengesellschaft, Germany), **2001**.

high molecular weight statistical butadiene-styrene copolymers.²¹³ Styrene and *cis*-1,4 contents seem to be analogous to the carboxylates systems even if a slightly lower *cis*-1,4 content is observed for high styrene content (Table 11). The authors put forward the back-biting reaction to explain this loss of *cis*-1,4 stereospecificity with increasing styrene content. In addition, the rather low polydispersity at low styrene feed increases with increasing styrene content due to a likely loss of the living character in the incorporation of styrene, while the molecular weights decrease. However, the M_n values are much higher as compared to related systems.

Table 11. Copolymerization of BD and St with (C₅Me₅)₂Sm[(μ-Me)AlMe₂(μ-Me)]₂Sm(C₅Me₅)₂ activated by [Ph₃C][B(C₆F₅)₄]/Al(*i*Bu)₃.213

St feed ratio (mol %)	Polymn time (h)	Yield (%)	<i>cis</i> -1,4 (%)	St content (%)	M _n (g/mol)	M _w /M _n
40	0.5	21	94.6	4.6	101,000	1.41
50	1	22	95.1	7.2	78,600	1.59
60	6	20	91.7	11.4	73,900	1.69
70	12	23	87.4	19.1	39,700	1.75
80	50	21	80.3	33.2	23,400	2.23

Conditions: [BD]₀ + [St]₀ = 6 M; [Nd]₀ = 3 × 10⁻⁵ M; [Al(*i*Bu)₃]₀/[Nd]₀ = 3 and [[Ph₃C][B(C₆F₅)₄]]₀/[Nd]₀ = 1; in toluene at 50 °C.

5.6. Conclusion

Transition metal catalysts have proved to be efficient catalysts for highly stereospecific *cis*-1,4 polymerization of dienes. In particular, neodymium-based catalysts produce polymers with higher *cis*-1,4 content, i.e. with the best physical properties. Transition metal-catalyzed styrene-butadiene polymerization allows also high *cis*-1,4 stereospecificity. Lanthanide-based systems were shown to be the most promising giving high *cis*-1,4 and styrene contents. However, an important decrease of the molecular weight comes along styrene incorporation. Since high molecular weights are targeted, these low molecular weights remain a real drawback.

²¹³ Kaita, S.; Hou, Z.; Wakatsuki, Y. *Macromolecules* **2001**, 34, 1539-1541.

Presentation of the research project

The first chapter was an introduction to the lanthanide-catalyzed polymerizations, showing the great potential of these organometallic/inorganic complexes in polymerization catalysis. However, it must be mentioned that lanthanide complexes are also very efficient initiators for lactones, lactides, epoxides and isocyanates polymerizations.¹¹⁷ In addition, divalent and trivalent lanthanides are widely employed in organic and asymmetric synthesis in reactions such as Oppenauer oxidation, asymmetric nitroaldol and Michael reactions.²¹⁴

In our literature study, we showed that the trivalent lanthanide hydride and alkyl complexes stabilized by two cyclopentadienyl-type ligands, "Cp₂LnR", offer high efficiency in polymerizing ethylene and also polar monomers. More recently, the development of substituted cyclopentadienyl ligands and/or introduction of indenyl, fluorenyl ligands allowed the stereospecific polymerization of α -olefins and methacrylates.

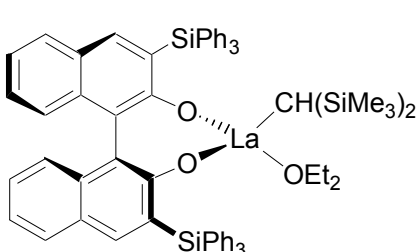
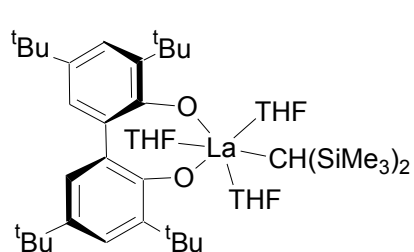
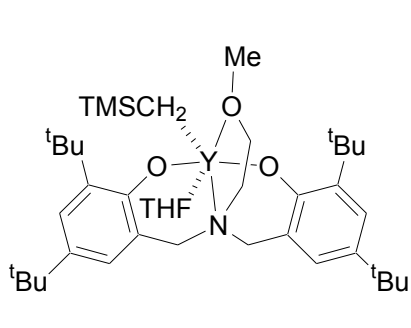
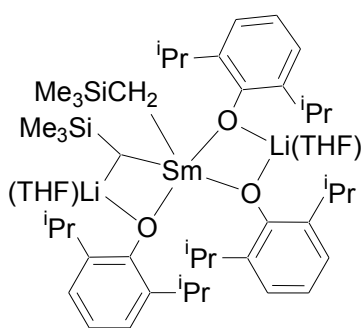
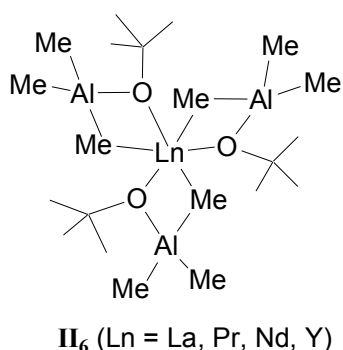
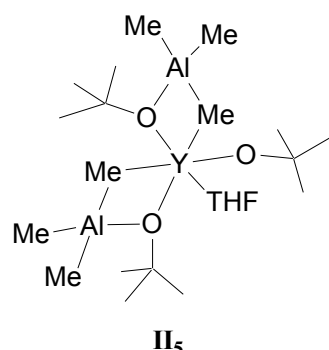
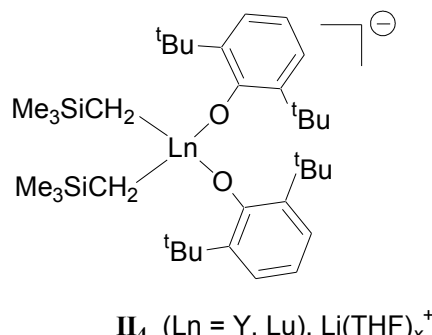
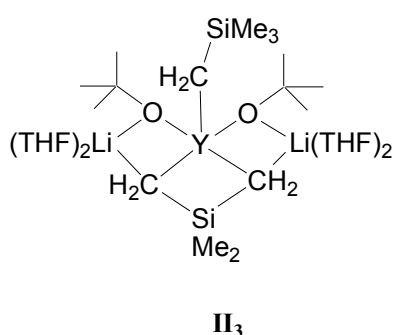
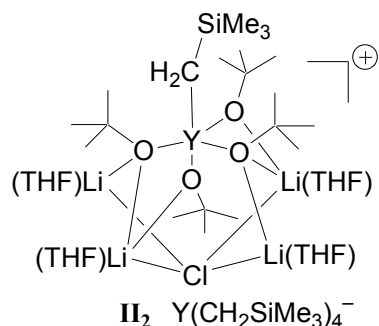
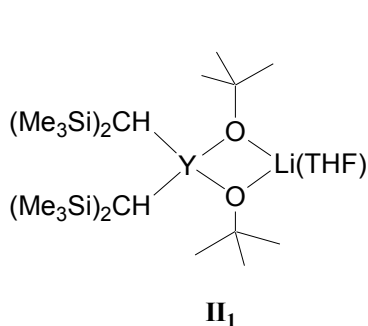
Because of the permanent search for new-generation polymerization catalysts, a considerable interest in developing related organolanthanide complexes involving ancillary ligands other than the commonly used cyclopentadienyl-type ligands exists. These are the so-called post-metallocene catalysts. In this respect, the synthesis of well-defined complexes, bearing ligands such as tris(pyrazolyl)borate, alk(aryl)oxides, amides, oxo-crown ethers, benzamidinates, β -diketiminates, were developed and some of these complexes were found to give highly active catalysts for ethylene and/or MMA polymerization. However, examples of versatile post-lanthanocene catalyst systems presenting a real activity/stereospecificity are quite rare. In this context, it is obvious that the development of new efficient lanthanide-based catalyst systems for ethylene, methacrylate and diene (co)-polymerizations is very challenging.

Literature shows that hard, electronegative π -donor ligands such as alkoxides/aryloxides are particularly attractive because they offer strong metal–oxygen bonds that are expected to stabilize complexes of these electropositive lanthanide metals. Also, the great variety of these ligands conveniently obtained from alcohols allows considerable variation in steric and electronic features.⁷³ The efficient use in polymerization of organolanthanide complexes with alkoxide co-ligands was first achieved with the *mixed* Cp-aryloxide system [Y(C₅Me₅)(O-2,6-*t*Bu₂C₆H₃)(μ -H)]₂ (**I₁₁**) that is active for the polymerization of ethylene and higher α -olefins.⁶⁵ Recently, other mixed Cp-aryloxide complexes of samarium^(II) appeared to be active for the polymerization and block-copolymerization of ethylene and styrene.^{67^{a,d}}

On the other hand, only a few examples of structurally well-defined cyclopentadienyl-free lanthanide alkyl-alk(aryl)oxides have been reported (Figure 40).

²¹⁴ (a) Steel, P. G. *J. Chem. Soc., Perkin Trans. 2001*, **1**, 2727–2751. (b) *Lanthanides: Chemistry and Uses in Organic Synthesis*, Ed. S. Kobayashi, Springer-Verlag, Berlin, 1999.

Figure 40. Examples of well-defined mixed alkyl-alk(aryl)oxide complexes.



Routes involving lanthanide **II₉** complexes with bulky aryl oxide ligands have been found quite reliable for the preparation of these species; in contrast, alkyl/*tert*-butoxide metathesis

reactions proved rather complicated and unpredictable. Studies by Evans *et al.* have shown that the direct combination of LiOtBu, LiCH(SiMe₃)₂ and YCl₃ in THF yielded complex **II₁**.²¹⁵ The analogous reaction from LiCH₂SiMe₃ instead of LiCH(SiMe₃)₂ left *ate* (salt) complex **II₂** in which nearly complete ligand segregation has occurred.²¹⁶ The neutral dialkyl-aryloxide **I₁₂** (see Chapter 1 §3.5.5.2) and the anionic dialkyl-diaryloxide complexes **II₄** were similarly obtained from treatment of LnCl₃ with LiO-2,6-*t*Bu₂C₆H₃ and the adequate lithiated reagent.²¹⁷ Complex $[(\eta^5\text{-indenyl})(\text{OtBu})(\mu_2\text{-OtBu})\text{Y}]_2$ underlies rapid exchange reaction with LiCH₂SiMe₃ to give the mixed alkyl/alkoxide five-coordinate yttrium complex **II₃** featuring two bridging methylene groups of a ($\mu\text{-CH}_2$)₂SiMe₂ moiety.²¹⁸ A varied range of products, including **II₅** and **II₆**, have been obtained by treatment of Y₃(OtBu)₇Cl₂(THF)₂ with the strong Lewis acid AlMe₃ that acts as a powerful disrupting reagent.²¹⁹ Homoleptic mixed-metal complexes **II₆** were independently synthesized as sole products from Ln₃(OtBu)₉ (Ln = Pr, Nd, Y) and AlMe₃.²²⁰ Though the first neutral homoleptic f-element alkyls Ln{CH(SiMe₃)₂}₃ (Ln = La, Sm) have been prepared by the alkylation of the monomeric aryloxide Ln(O-2,6-*t*Bu₂C₆H₃)₃ with 3 equiv. of LiCH(SiMe₃)₂ in hydrocarbon solution,²²¹ the addition of 2 equiv. of LiCH(SiMe₃)₂ to Sm(O-2,6-*i*Pr₂C₆H₃)₃(THF)₂ gives mixed complex **II₇**, probably because of THF ligation, sterically less bulky *i*Pr groups and enhanced solubility of the Li-aryloxide.²²² Mononuclear binaphtholato complex **II₉** and the less sterically hindered biphenolato complex **II₁₀** were prepared through mild protonolysis of La{CH(SiMe₃)₂}₃ and the chelating diols.²²³ A similar synthetic route was applied for the preparation of **II₈**.²²⁴ The catalytic potential of this complex was assessed in ethylene polymerization (4 bar, RT). After a prolonged time, no polymer could be recovered. The authors ascribed this lack of reactivity to the presence of coordinated THF molecules that might block the active sites. In fact, of all of these mixed alkyl-alkoxy lanthanide species, only **I₁₂** has been reported to exhibit very low ethylene polymerization activity (9.10⁻³ kgPE/molY/atm/h at RT).²¹⁷ This is rather surprising since alkoxy ligands are expected to render the metal center more electron-deficient and more Lewis acidic.

Further to our successful work devoted to *in situ* alkylation of chlorolanthanocene precursors with dialkylmagnesium or alkyllithium reagents as alternative, efficient combinations for respectively ethylene and MMA polymerizations,^{52,139} we have undertaken a study aimed at replacing chlorolanthanocenes by homoleptic alkoxide lanthanides. Although much data have been collected to date on alkoxide complexes of rare earth elements, most of them have focused on yttrium, lanthanum and lutetium because these metals provide

²¹⁵ Evans, W. J.; Broomhall-Dillard, N. R.; Ziller, J. W. *Organometallics* **1996**, *15*, 1351-1355.

²¹⁶ Evans, W. J.; Shreeve, J. L.; Broomhall-Dillard, N. R.; Ziller, J. W. *J. Organomet. Chem.* **1995**, *501*, 7-11.

²¹⁷ Evans, W. J.; Broomhall-Dillard, N. R.; Ziller, J. W. *J. Organomet. Chem.* **1998**, *569*, 89-97.

²¹⁸ Evans, W. J.; Boyle, T. J.; Ziller, J. W. *J. Organomet. Chem.* **1993**, *462*, 141-148.

²¹⁹ Evans, W. J.; Boyle, T. J.; Ziller, J. W. *J. Am. Chem. Soc.* **1993**, *115*, 5084-5092.

²²⁰ Biagini, P.; Lugli, G.; Abis, L.; Millini, R. *J. Organomet. Chem.* **1994**, *474*, C16-C18.

²²¹ Hitchcock, P. B.; Lappert, M. F.; Smith, R. G.; Bartlett, R. A.; Power, P. P. *J. Chem. Soc. Chem. Commun.* **1988**, 1007-1009.

²²² Clarck, D. L.; Gordon, J. C.; Huffman, J. C.; Watkin, J. G.; Zwick, B. D. *Organometallics* **1994**, *13*, 4266-4270.

²²³ Schaverien, C. J.; Meijboom, N.; Orpen, A. G. *J. Chem. Soc. Chem. Commun.* **1992**, 124-126.

²²⁴ Cai, C.-X.; Toupet, L.; Lehmann, C. W.; Carpentier, J.-F. *J. Organomet. Chem.* **2003**, *in press*.

diamagnetic compounds characterizable by NMR. In this study we have chosen to work with neodymium because this metal has given some of the most active group 3 metallocene based catalysts for olefin polymerization. Considering the complexity of the alkoxo chemistry of lanthanides, we felt essential to obtain primarily structural information on the alkoxide materials we would use as precursors for polymerization. Hence, the manuscript will be organized as follows:

In a first part, we will give an overview on the synthesis of lanthanide alk(aryl)oxides followed by our results on the preparation and the structural investigation of some new neodymium complexes having simple and functionalized *tert*-alkoxide ligands. In a second part we will show that some of these compounds act as efficient inorganic pre-catalysts, once combined with dialkylmagnesium compounds, for the pseudo-living syndiotactic polymerization of methyl methacrylate, the controlled polymerization of ethylene and its diblock copolymerization with MMA; and the pseudo-living polymerization of 1,3-butadiene and its diblock copolymerization with methacrylates. Finally, insights into the mechanistic aspects of the formation of active species and polymerization reactions will be discussed in the last chapter.

Chapter 2

Synthesis of lanthanide alkoxides

6.

7. Synthesis of lanthanide alkoxides and related complexes

7.1. Introduction

Metal alkoxides in high oxidation states, and related compounds such as aryloxides or metallosiloxanes, are versatile molecular precursors of oxides of high purity and high tech materials, by chemical routes, hydrolysis and subsequent polycondensation reaction, or pyrolysis. Their interest stems from their ability to form homogeneous solutions in a large variety of solvents and in the presence of other alkoxides or metallic derivatives. The development of numerous inorganic materials by the organic sol-gel process or metal-organic chemical vapor deposition (MOCVD), based on simple or complex multicomponent oxides, was motivated by a wide palette of technological applications for high-tech ceramics (electronics, insulators, piezoelectric materials..), chemical applications related to separation problems (membranes or filters) and heterogeneous catalysis.²²⁵ The reactions taking place in this process are quite complicate but a good knowledge of the structure of the precursors and the intermediates in solution might give increased possibilities of tailoring the properties of the ceramic products. In addition, the need for new volatile or soluble metal alkoxides which could serve as precursors for MOCVD or sol-gel process prompted several workers to search new compounds and especially mononuclear, homoleptic compounds.²²⁶ Lanthanide alkoxides were particularly investigated since the discovery of high temperature superconducting ceramics based on $\text{YBa}_2\text{Cu}_3\text{O}_7$.²²⁷ More recently, the sol-gel processing of rare-earth metal ion containing glasses as bulk and wave-guide materials has received considerable interest. Consequently, the development of lanthanide alkoxides chemistry was boosted, their use in catalytic reactions remaining a side application.

We would like to present briefly the principal synthetic routes for the synthesis of lanthanide alkoxides and related ligands. As it will be seen, when the large "oxophilic" lanthanide is exposed to commercially available simple alcohols, oligomerization occurs. These ligands tend to act as bridging ligand and the degree of agglomeration is dependent of the steric bulk of the ligand and its electronic situation. For example, the bridging tendency is directly proportional to the pKa values. We will describe the less commonly used methods as well as the traditional routes which are the salt metathesis from lanthanide halide precursors and the silylamide route, i.e., the alcoholysis of the tris(trimethylsilyl)amido derivative ($\text{Ln}(\text{N}(\text{SiMe}_3)_2)_3 = \text{LnN3}$). An exhaustive list of lanthanide complexes described up to 1996 can be found in two different comprehensive reviews.^{73,228}

²²⁵ Chandler, C. D.; Rogers, C.; Hampden-Smith, M. J. *Chem. Rev.* **1993**, *93*, 1205-1241.

²²⁶ (a) Hubert-Pfalzgraf, L. G. *New J. Chem.* **1987**, *11*, 663-675. (b) Bradley, D. C. *Chem. Rev.* **1989**, *89*, 1317-1322. (c) Caulton, K. G.; Hubert-Pfalzgraf, L. G. *Chem. Rev.* **1990**, *90*, 969-995.

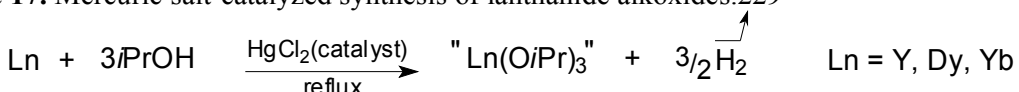
²²⁷ Bednorz, J. G.; Müller, K. A.; Takashige, M. *Science* **1987**, *236*, 73.

²²⁸ Mehrotra, R. C.; Singh, A.; Tripathi, U. M. *Chem. Rev.* **1991**, *91*, 1287-1303.

7.2. Reaction of metal with alcohol

This method was described in the late 1960's by Mazdiyasni *et al.*²²⁹ Their attempts to prepare lanthanide isopropoxide from anhydrous metal halides and alcohol using anhydrous ammonia, as it was already reported for group 4 metals, produced only chloride contaminated products with low yields. Their objective being the preparation of chloride-free metal alkoxides for vapor deposition on refractory substrates, they applied the synthetic method first employed by Adkins and Cox for the preparation of aluminum isopropoxide.²³⁰ This method consists of the reaction of the metal in the refluxing alcohol in the presence of a catalytic amount of mercuric chloride (Scheme 17).

Scheme 17. Mercuric salt-catalyzed synthesis of lanthanide alkoxides.²²⁹



This reaction allows lanthanide isopropoxides to be synthesized in high yields (> 75%). The products were characterized by elemental analysis, IR spectroscopy and X-ray diffraction of powder, suggesting a dimeric structure of the yttrium isopropoxide. This synthetic route was re-investigated later by Caulton and co-workers in order to determine the solid-state structure of this yttrium alkoxide.²³¹ The results of the single-crystal X-ray diffraction structure determination revealed that the elemental composition established earlier was erroneous and that the compound was the pentanuclear $\text{Y}_5(\mu_5\text{-O})(\mu_3\text{-O}i\text{Pr})_4(\mu_2\text{-O}i\text{Pr})_4(\text{O}i\text{Pr})_5$ complex, composed of a highly regular square-based pyramidal arrangement of five $\text{Y}^{(\text{III})}$ centers, with a single O^{2-} ligand. The alkoxide ligands are of three structural types: four triply bridging, four doubly bridging and five terminal. Molecular and basically isostructural oxo-alkoxides $\text{Ln}_5\text{O}(\text{O}i\text{Pr})_{13}$ ($\text{Ln} = \text{Nd}$ and Gd) were also synthesized by salt metathesis of LnCl_3 and $\text{KO}i\text{Pr}$, in combination with stoichiometric hydrolysis, in isopropanol-containing solvents. The erbium analog was obtained as coproduct of the reaction of $15\text{KO}i\text{Pr} + \text{H}_2\text{O} + \text{Al}(\text{O}i\text{Pr})_3$ with 5 ErCl_3 , in a toluene-isopropanol mixture.²³² A similar pentanuclear lanthanum complex $\text{La}_5(\mu_5\text{-O})(\mu_3\text{-O}t\text{Bu})_4(\mu_2\text{-O}t\text{Bu})_4(\text{O}t\text{Bu})_5$ was obtained by refluxing $\text{La}(\text{O}t\text{Bu})_9(t\text{BuOH})_2$ in toluene.²³³

In addition, the reaction between neodymium chips and isopropanol led also to the isolation of the first example of a trigonal bipyramidal metal oxoalkoxide $\text{Nd}_5(\text{O})(\text{O}i\text{Pr})_{13}(i\text{PrOH})_2$, which has been characterized by microanalysis and IR spectroscopy, as well as by X-ray diffraction.²³⁴ The molecule corresponds to a trigonal bipyramidal oxoalkoxide $\text{Nd}_5(\mu_5\text{-O})(\mu_3\text{-O}i\text{Pr})_2(\mu_2\text{-O}i\text{Pr})_6(\text{O}i\text{Pr})_5(i\text{PrOH})_2$ in which all metals achieve hexacoordination. The two alcohol molecules are linked to the same neodymium center, thus leading to distortion of the M_5O_{16} core.

²²⁹ (a) Mazdiyasni, K. S.; Lynch, C. T.; Smith, J. S. *Inorg. Chem.* **1966**, *5*, 342-346. (b) Brown, L. M.; Mazdiyasni, K. S. *Inorg. Chem.* **1970**, *9*, 2783-2786.

²³⁰ Adkins, H.; Cox, F. W. *J. Am. Chem. Soc.* **1938**, *60*, 1151-1159.

²³¹ Poncelet, O.; Sartain, W. J.; Hubert-Pfalzgraf, L. G.; Folting, K.; Caulton, K. G. *Inorg. Chem.* **1989**, *28*, 263-267.

²³² Kritikos, M.; Wijk, M.; Moustakimov, M.; Westin, G. *J. Chem. Soc., Dalton Trans.* **2001**, 1931-1938.

²³³ Daniele, S.; Hubert-Pfalzgraf, L. G.; Hitchcock, P. B.; Lappert, M. F. *Inorg. Chem. Comm.* **2000**, *3*, 218-220.

²³⁴ Helgesson, G.; Jagner, S.; Poncelet, O.; Hubert-Pfalzgraf, L. G. *Polyhedron* **1991**, *10*, 1559-1564.

7.3. Salt metathesis

Salt metathesis refers to the reaction between a lanthanide tris(halide) and an alkali-metal alkoxide as it is summarized in Scheme 18.

Scheme 18. General scheme for the salt metathesis reaction.



7.3.1. In the presence of alcohol

The very first salt metathesis syntheses of metal alkoxides were conducted in the corresponding alcohol.²³⁵ Thus, butoxides and isopropoxides of La, Pr, and Nd were prepared by the reaction of the lanthanide trichloride with the corresponding NaOR in butanol and isopropanol respectively. Neodymium and praseodymium were claimed to be monomeric in benzene solution, while gadolinium and erbium would be tetrameric. Then, the preparation of Pr, Nd, and La methoxides and isopropoxides was described. The methoxides were obtained as precipitates by treating the corresponding chlorides with LiOMe in MeOH, filtering, and washing the precipitates with dry MeOH to remove LiCl.²³⁶ This synthetic route was not really successful due to the low yield of the reactions (50%). Mazdiyasni who suggested the chlorine-contamination of these alkoxides also observed this low yield.²²⁹ Characterization of these products was not provided. In the same time, the reaction between anhydrous scandium trichloride and methanol was reported.²³⁷

Again, these earlier results were re-investigated. Andersen *et al.* characterized the neodymium isopropoxide by X-ray crystal structure determination.²³⁸ He found correspondingly to earlier reports the presence of chlorine atoms in the structure, structure far more complex than the previously suggested monomeric one. Indeed, the crystal grown from a toluene solution responds to the formula Nd₆(OCH(CH₃)₂)₁₇Cl. In this complex, the six neodymium atoms form a trigonal prism centered about the chlorine atom. Six isopropoxide groups are terminal, nine are edge bridging and two are bridging a trigonal face of the prism yielding six two-coordinate, nine three-coordinate and two four-coordinate oxygen atoms, respectively.

Kagan who used the resulting alkoxides in organic synthesis developed a similar route.¹⁵⁵ Okamoto *et al.* also applied these alkoxides in MMA polymerization.¹⁵⁴ The synthesis consists of the reaction of LnCl₃ in suspension in a pentane/isopropanol mixture with *n*-BuLi. However, alkoxides were not isolated from the reaction mixtures, which were used without purification in their different applications.

²³⁵ (a) Misra, S. N.; Misra, T. N.; Kapoor, R. N.; Mehrotra, R. C. *Chem. Ind.* **1963**, 120. (b) Misra, S. N.; Misra, T. N.; Mehrotra, R. C. *Aust. J. Chem.* **1968**, 21, 797-800.

²³⁶ Misra, S. N.; Misra, T. N.; Mehrotra, R. C. *Proc. Nucl. Radiation Chem. Symp.* **1965**, 15-19.

²³⁷ Zeit. Anorg. Allg. Chem. **1963**, 325, 67-71.

²³⁸ Andersen, R. A.; Templeton, D. H.; Zalkin, A. *Inorg. Chem.* **1978**, 17, 1962-1965.

The preparation of lanthanide alkoxides using this synthetic route was not further studied except, as mentioned above, by Kritikos and co-workers who prepared neodymium and gadolinium isopropoxides by reaction of LnCl_3 and $\text{KO}i\text{Pr}$, in combination with stoichiometric hydrolysis, in isopropanol-containing solvents.²³²

7.3.2. In the absence of alcohol

7.3.2.1. Lanthanide alkoxides

The results that followed involve reactions between anhydrous lanthanide trichlorides and alkali-metal alkoxides in an alcohol-free solvent, typically THF or toluene. Most of the work must be attributed to Evans and co-workers who developed the chemistry of lanthanides *tert*-butoxide, and especially the yttrium chemistry.

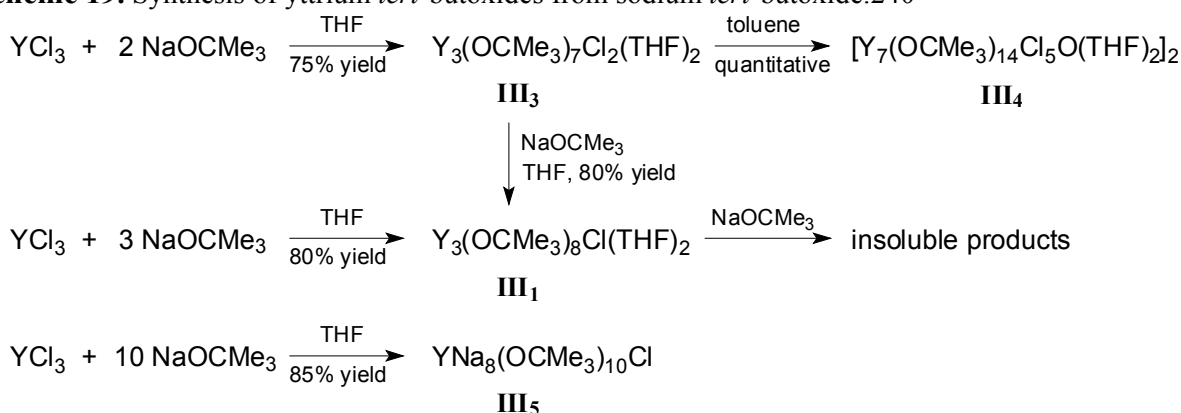
YCl_3 reacts with 3 equivalents of $\text{NaO}t\text{Bu}$ in THF at room temperature to form $\text{Y}_3(\mu_3\text{-O}t\text{Bu})(\mu_3\text{-Cl})(\mu_2\text{-O}t\text{Bu})_3(\text{O}t\text{Bu})_4(\text{THF})_2$ (**III₁**) in 80% yield.²³⁹ X-ray analysis shows that the complex contains a trigonal-planar arrangement of yttrium atoms with $\mu_2\text{-O}t\text{Bu}$ groups along the edges of a Y_3 triangle, a $\mu_3\text{-O}t\text{Bu}$ ligand on one side on the plane and a $\mu_3\text{-Cl}$ on the other, each yttrium being six-coordinate. The reaction conducted in the presence of *tert*-butyl alcohol leads to the formation of an isomer of **III₁**, which was not crystallographically identified. However, spectroscopic and analytical data agreed on the formula $\text{Y}_3(\mu_3\text{-O}t\text{Bu})(\mu_3\text{-Cl})(\mu_2\text{-O}t\text{Bu})_3(\text{O}t\text{Bu})_4(\text{THF})_2$. When the larger metal lanthanum is used, $\text{La}_3(\mu_3\text{-O}t\text{Bu})_2(\mu_2\text{-O}t\text{Bu})_3(\text{O}t\text{Bu})_4(\text{THF})_2$ (**III₂**) is formed directly; $\text{O}t\text{Bu}$ ligand being triply bridged. This trimetallic framework will appear to be the basic structural unit in lanthanide *tert*-butoxide chemistry.

Indeed, when YCl_3 reacts with 2 equivalents of $\text{NaO}t\text{Bu}$ under the same conditions, the isostructural $\text{Y}_3(\mu_3\text{-O}t\text{Bu})(\mu_3\text{-Cl})(\mu_2\text{-O}t\text{Bu})_3(\text{O}t\text{Bu})_3(\text{Cl})(\text{THF})_2$ (**III₃**) is obtained. Addition of 1 equivalent of $\text{NaO}t\text{Bu}$ to **III₃**, allows the replacement of the terminal chloride ligand to yield **III₁**. In toluene under nitrogen atmosphere over a period of 2 weeks, **III₃** converts into $\text{Y}_{14}(\text{O}t\text{Bu})_{28}\text{Cl}_{10}\text{O}_2(\text{THF})_4$ (**III₄**) in quantitative yield.²⁴⁰ In fact this complex is composed of four trimetallic units that have structures similar to **III₃**. The reaction of YCl_3 with 4 equiv. of $\text{NaO}t\text{Bu}$ gives insoluble products whereas with a large excess of $\text{NaO}t\text{Bu}$ a soluble nanometallic *tert*-butoxide mixed-metal complex (**III₅**) is obtained.²⁴¹ However, to obtain high yields in this reaction, the isolation procedure is very important. The synthesis of these yttrium *tert*-butoxides is summarized in Scheme 19.

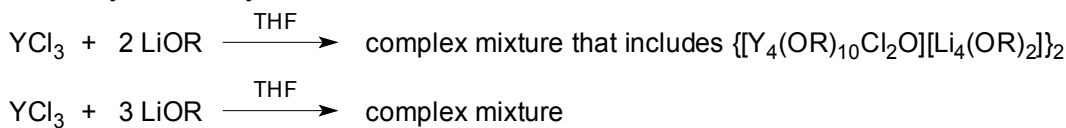
²³⁹ Evans, W. J.; Sollberger, M. S.; Hanusa, T. P. *J. Am. Chem. Soc.* **1988**, *110*, 1841-1850.

²⁴⁰ Evans, W. J.; Sollberger, M. S. *Inorg. Chem.* **1988**, *27*, 4417-4423.

²⁴¹ Evans, W. J.; Sollberger, M. S.; Ziller, J. W. *J. Am. Chem. Soc.* **1993**, *115*, 4120-4127.

Scheme 19. Synthesis of yttrium *tert*-butoxides from sodium *tert*-butoxide.²⁴⁰

The nature of the metal in the alkali-metal alkoxide is also of prime importance. The reaction of yttrium trichloride with 2 equivalents of LiOtBu did not yield **III**₃ as observed with NaOtBu but to a more complex mixture from which the tetranuclear ($[\text{Y}_4(\mu_3\text{-OtBu})_2(\mu_2\text{-OtBu})_4(\text{OtBu})_4(\mu_5\text{-O})(\text{Cl})_2\text{Li}_4((\mu_2\text{-OtBu})_2)]_2$) complex could be isolated (Scheme 20).²³⁹ The formation of an *ate* complex with lithium alkali-metal precursors is not so surprising since a similar behavior was already reported for the synthesis of lanthanide phenoxides (*vide infra*).²⁴²

Scheme 20. Synthesis of yttrium *tert*-butoxides from lithium *tert*-butoxide.²⁴⁰

Finally, the first cationic *tert*-butoxide complexes were obtained by reaction of AgBPh₄ with **III**₃. The formation of two main products was observed depending on the experimental conditions. At 0 °C, the formation of $[\text{Y}_3(\mu_3\text{-OtBu})(\mu_3\text{-Cl})(\mu_2\text{-OtBu})_3(\text{OtBu})_3(\text{THF})_3][\text{BPh}_4]$ is favored while a major unexpected dinuclear complex $\{[\text{Y}_2(\mu_2\text{-Cl})(\mu_2\text{-OtBu})_2(\text{OtBu})_2(\text{THF})_4][\text{BPh}_4]\}$ is obtained at room temperature.²⁴³

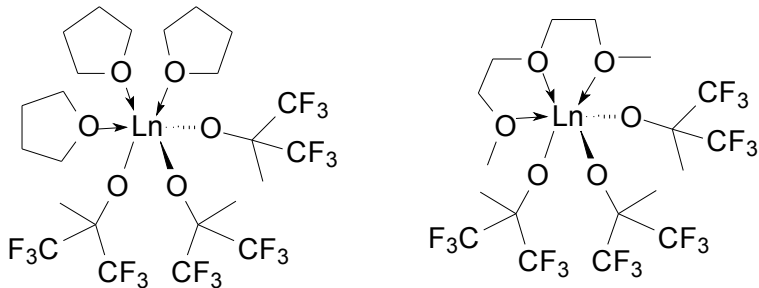
The chemistry of tertiary fluorinated ligands was also investigated. The exchange of CH₃ in *tert*-butoxide ligand by CF₃ groups results in a useful synergism with respect to oligomerization/volatility behavior. Increased intermolecular repulsions, which commonly appear in fluorinated systems, affect the volatility of the resulting alkoxide complexes. In addition to the significantly enlarged CF₃ group compared to the CH₃ group, steric saturation of electrophilic metal centers can be accomplished by intramolecular close Ln--F(CF₃) contacts. The electron withdrawing effect of the CF₃ group generates a less basic alkoxide resulting in a lower bridging tendency. This combination renders an Ln-O bond of increased ionic character and hence an electrophilic metal in a redox-stable environment.

²⁴² Lappert, M. F.; Singh, A.; Atwood, J. L.; Hunter, W. E. *J. Chem. Soc., Chem. Commun.* **1981**, 1191-1193.

²⁴³ Evans, W. J.; Olofson, J. M.; Ziller, J. W. *J. Am. Chem. Soc.* **1990**, *112*, 2308-2314.

Fluorinated lanthanide alkoxides can be prepared from anhydrous LnCl_3 and alcohol in the presence of ammonia. The coordination of ammonia to the metal center could be observed. The solubility of unsolvated fluorinated alkoxide depends on the number of ligand methyl groups. The potential alkoxide bridges are readily disrupted in the presence of coordinating solvents like THF, Et_2O to yield dimeric and even monomeric complexes. For example, $\text{Ln}(\text{hftb})_3(\text{THF})_3$ ($\text{Ln} = \text{La}, \text{Y}$ and hftb = hexafluoro-*tert*-butoxy) and $\text{Y}(\text{hftb})_3(\text{diglyme})$ show the typical six-coordination for *tert*-butoxyde derivatives, where two sets of ligands are disposed in a *fac*-octahedral configuration (Figure 41).²⁴⁴

Figure 41. Examples of mononuclear fluorinated lanthanide *tert*-butoxides.²⁴⁴



Finally, examples of preparation of complexes with functionalized ligands by salt metathesis are rather rare. So, it is interesting to note that the reactions of LnCl_3 ($\text{Ln} = \text{Y}, \text{Nd}$) with the bidentate highly-hindered phosphine-functionalized ligand $\text{LiOC}(t\text{Bu})_2\text{CH}_2\text{PMe}_2$ has been reported to be straightforward, resulting in the formation of six-coordinate species. The bidentate nature of the ligand probably impedes the formation of *ate* complex largely observed using lithium alkoxides.

These examples show that, with simple ligands such as OtBu or $\text{O}i\text{Pr}$, polymetallic complexes that often incorporate chloride and/or oxide ligands are formed instead of simple $\text{Ln}(\text{OR})_3$ species. We will see now that fully characterized monomeric and/or homoleptic $\text{Ln}(\text{OR})_3$ complexes can be obtained with aryloxide ligands.

7.3.2.2. Lanthanide aryloxides

The first structurally identified lanthanide aryloxides were reported by Lappert *et al.*²⁴² Before that, only insoluble, involatile and presumably oligomeric aryloxides based on unsubstituted 4-methyl phenols were synthesized and not so well characterized. The 2,6-substitution was then investigated. The 2,6-substitution pattern will reveal to be effective because the alkyl groups are directed towards the metal center and impose a steric coordination number onto the metal which is comparable to the Cp^* ligand.

As mentioned earlier, *ate* complexes were obtained by reaction of lanthanide trichloride with 3 equivalents of lithium aryloxide. Thus, with the very bulky $\text{LiO}-2,4,6-(t\text{Bu})_3\text{C}_6\text{H}_2$ ligand, the mononuclear $[\text{Ln}(\text{Cl})(\text{OAr})(\mu_2-\text{Cl})_2\text{Li}(\text{THF})_2]$ is formed in THF while the synthesis conducted in toluene led to $[\text{Ln}(\text{Cl})(\text{OAr})(\mu_2-\text{OAr})_2]$.²⁴² With the sodium salt, *ate* complexes

²⁴⁴ (a) Bradley, D. C.; Chudzynska, H.; Hursthouse, M. B.; Motevalli, M. *Polyhedron* **1993**, *12*, 1907-1918. (b) Bradley, D. C.; Chudzynska, H.; Hursthouse, M. B.; Motevalli, M. *Polyhedron* **1994**, *13*, 7-14.

can be obtained when the stoichiometry between the reagents is not respected. Thus, when LnCl_3 ($\text{Ln} = \text{Y, Sm, Er, and Yb}$ and $\text{Ar} = 2,6\text{-}t\text{Bu}_2\text{-}4\text{-Me-C}_6\text{H}_2$) reacts with 2 equivalents of NaOAr in THF at room temperature, a bis(aryloxo) lanthanide chloride $\text{Ln(OAr)}_2\text{Cl}(\text{THF})_2$ can be obtained.²⁴⁵ In the presence of 4 equivalents of NaOAr , NdCl_3 affords a new *ate* complex $[(\text{ArO})_4\text{Nd}][\text{Na}(\text{THF})_6]$.²⁴⁶ More surprisingly, the reaction of anhydrous neodymium chloride with 3 equivalents of potassium 2,6-diisopropylphenoxy in THF solution allows the formation of the salt $\text{K}[\text{Nd(OAr)}_4]$ in good yield.²⁴⁷ X-ray characterization showed that the potassium cation displays an unusual bis(η^6 -arene) interaction, making up a quasi-one dimensional infinite chain. This behavior is unprecedented since alkali-metal cations are usually primarily coordinated to the oxygen anion of alkoxide ligand, as it was observed in the *ate*-aryloxide complexes resulting from reaction of one equivalent of sodium or potassium aryloxide with a preformed lanthanide aryloxide $\text{Y(OAr)}_3(\text{THF})_3$ ($\text{Ar} = 2,6\text{-Me}_2\text{C}_6\text{H}_3$) in THF or THF/DME.²⁴⁸

Homoleptic lanthanide aryloxides can be obtained using different synthetic routes.²⁴⁹ By salt metathesis, LnCl_3 reacts with 3 equiv. of $\text{NaO-2,6-tBu}_2\text{-4-Me-C}_6\text{H}_2$ to produce the four-coordinated THF-adduct $\text{Ln(OAr)}_3\text{THF}$, which can be converted into the three-coordinate solvent-free complex Ln(OAr)_3 by sublimation. (the silylamine route can also lead to the formation of the solvent-free complex; this synthetic route will be exemplified in §7.4.1.2.) However, it must be noticed that the preparation of monuclear complexes is sensitive to the experimental procedure as shown in Scheme 21.

When the less bulky $\text{NaO-(2,6-Me}_2\text{-C}_6\text{H}_3$ is used instead of the sterically crowded *tert*-butyl derivatives, halide- and oxide-free $[\text{Y(OAr)}_3(\text{solvent})_n]_m$ complexes with enough steric flexibility to achieve five- or six-coordination and to form bridged bimetallic species were obtained.²⁵⁰ Depending on the experimental procedure, the easily interconverted $\text{Y(OAr)}_3(\text{THF})_3$ and $[\text{Y}(\mu_2\text{-OAr})(\text{OAr})_2(\text{THF})]_2$ complexes can be prepared in good yield. This 2,6-methyl substituted phenol yields intermediate structures, in terms of nuclearity, compared to the insoluble and likely oligomeric aryloxides obtained with unsubstituted 2,6-positions, and the monomeric complex obtained with the bulky 2,6-*t*Bu₂ aryloxide derivatives.

²⁴⁵ Yao, Y.-M.; Shen, Q.; Zhang, Y.; Xue, M.-Q.; Sun, J. *Polyhedron* **2001**, *20*, 3201-3208.

²⁴⁶ Zhang, L.-L.; Yao, Y.-M.; Luo, Y.-J.; Shen, Q.; Sun, J. *Polyhedron* **2000**, *19*, 2243-2247.

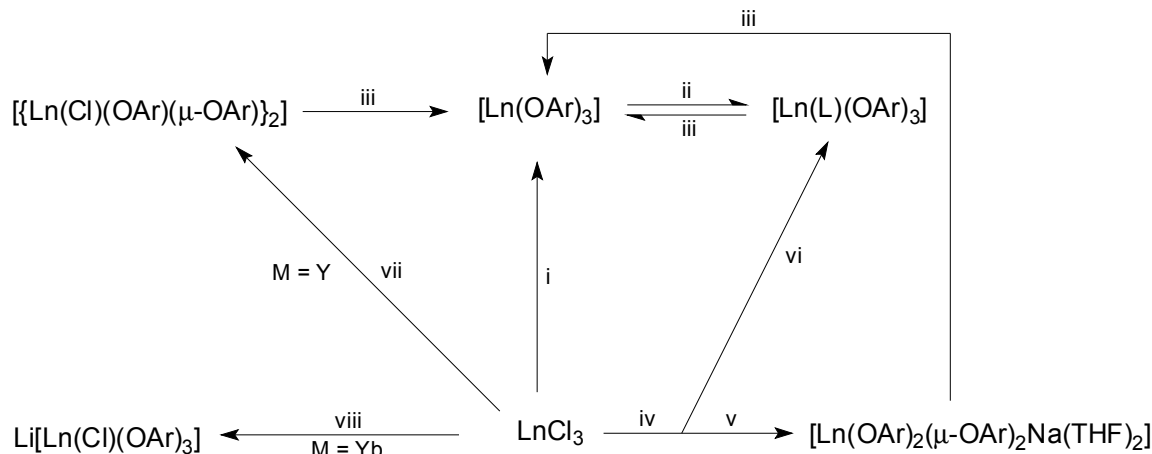
²⁴⁷ Clark, D. L.; Watkin, J. G.; Huffman, J. C. *Inorg. Chem.* **1992**, *31*, 1556-1558.

²⁴⁸ Evans, W. J.; Ansari, M. A.; Ziller, J. W.; Khan, S. I. *J. Organomet. Chem.* **1998**, *553*, 141-148.

²⁴⁹ (a) Hitchcock, P. B.; Lappert, M. F.; Singh, A. *J. Chem. Soc., Chem. Commun.* **1983**, 1499-1501. (b) Lappert, M. F.; Singh, A.; Smith, R. G. *Inorg. Synth.* **1990**, *27*, 164-168.

²⁵⁰ Evans, W. J.; Olofson, J. M.; Ziller, J. W. *Inorg. Chem.* **1989**, *28*, 4309-4311.

Scheme 21. General scheme for the synthesis of lanthanide (2,6-*t*Bu₂-4-Me)aryloxides.²⁴⁹



i, 3 NaOAr(OEt₂), THF, reflux, > 36 h; **ii**, L = THF or P(O)Ph₃, benzene, 20 °C, 18 h; **iii**, sublime in vacuo; **iv**, 3 NaOAr(OEt₂), THF, 20 °C, 16 h, then successive reflux, 24 h, solvent removal in vacuo, pentane and filtration; **v**, precipitate from **iv**; **vi**, filtrate from **iv**; **vii**, 3 [Li(μ-OAr)(OEt₂)₂], toluene, 20 °C, 72 h then successive reflux, 24 h, solvent removal in vacuo; **viii**, 3 [Li(μ-OAr)(OEt₂)₂], toluene, 20 °C, 48 h then successive reflux, 36 h, solvent removal in vacuo.

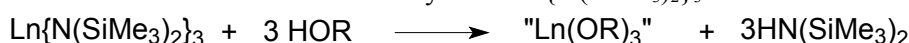
Besides these results on trivalent complexes, it must be noticed that the preparation of well-defined strongly reducing divalent lanthanide aryloxides was also reported. The reaction of YbI₂ or LnI₂(THF)₂ (Ln = Sm, Eu or Yb) respectively in Et₂O or THF, with 2 equivalents of KO-2,6-*t*Bu₂-4-Me-C₆H₂ conducts to Yb(OAr)₂(OEt₂)₂ and Ln(OAr)₂(THF)₃ in good yield.²⁵¹ Only the europium complex was structurally fully characterized showing a distorted trigonal-bipyramidal conformation. However, the relatively low stability of such compounds limits their preparation.

7.4. Exchange of organic ligands

7.4.1. Alcoholytic of tris(amido) complexes

This reaction consists of the addition of alcohols, phenols or silanols to a lanthanide tris (amido) complex as shown in Scheme 22.

Scheme 22. General reaction scheme for alcoholytic of Ln{N(SiMe₃)₂}₃.



The use of well-defined and readily accessible Ln(N(SiMe₃)₂)₃²⁵² (LnN3) and Ln(N(SiHMe₂)₂)₃(THF)₂²⁵³ complexes makes the experimental procedure rather simple due to the high volatility of the liberated amine, avoiding the fastidious filtration or centrifugation steps of the salt metathesis reactions. And as it will be seen, this method proved more advantageous

²⁵¹ Van den Hende, J. R.; Hitchcock, P. B.; Holmes, S. A.; Lappert, M. F.; Leung, W.-P.; Mak, T. C. W.; Prashar, S. *J. Chem. Soc., Dalton Trans.* **1995**, 1427-1433.

²⁵² Bradley, D. C.; Ghotra, J. S.; Hart, F. A. *J. Chem. Soc., Dalton Trans.* **1973**, 1021-1023. Original report on the synthesis of LnN3. Multiple modified experimental procedures were lately published.

²⁵³ Wedler, M.; Gilje, J. W.; Pieper, U.; Stalke, D.; Noltemeyer, M.; Edelmann, F. T. *Chem. Ber.* **1991**, 124, 1163-1165.

for the preparation of lanthanide alkoxides, especially for homoleptic and functionalized derivatives.

7.4.1.1. Lanthanide alkoxides

This synthetic route is the most convenient to obtain halide-free complexes and for the introduction of very bulky or functionalized-alkoxides. Consequently, the absence of reports concerning simple aliphatic alkoxides is not so surprising. To our knowledge, only one paper deals with the preparation of lanthanide *tert*-butoxide using this method. Addition of an excess of tertiary alcohol to LnN_3 ($\text{Ln} = \text{Y}, \text{La}$) in a benzene solution at room temperature conducts to the formation of the trimetallic $\text{La}(\mu_3\text{-O}t\text{Bu})_2(\mu_2\text{-O}t\text{Bu})_3(\text{O}t\text{Bu})_4(t\text{BuOH})_2$ complex (**III**₆).²⁵⁴ The overall molecular structure is similar to that reported by Evans for lanthanum *tert*-butoxide.²³⁹ The substitution of the coordinated *tert*-butyl alcohol molecules by THF, leading to **III**₂, is possible by refluxing **III**₆ in THF. A similar structure is proposed with *tert*-amyl alcohol while a dimeric structure is suggested with higher tertiary alcohols such as HOCMe_2iPr , $\text{HOCMeEt}i\text{Pr}$, and HOCEt_3 .

Further work was devoted to the synthesis of lanthanide alkoxides with highly hindered tertiary aliphatic alcohols such as the tris(*tert*-butyl)methanol since its steric requirements are usually compared to those of Cp ligands which are capable of forming mononuclear complexes. It was initially shown that the introduction of sterically demanding ligands in lanthanoid metal complexes depends on the metal-ion size and on the more precise composition of the lanthanoid precursor, and not only on the size of the new ligand as it was generally accepted. Thus, the reaction of LnN_3 ($\text{Ln} = \text{Nd}, \text{Dy}$) with 3 equiv. of $\text{HOCiPr}(t\text{Bu})_2$ in acetonitrile yielded different crystallization products.²⁵⁵ The light (large) lanthanide neodymium yielded the dimeric $\text{Nd}_2(\text{OR})_6(\text{NCMe})$ structure while the heavier (small) dysprosium formed the mononuclear $\text{Dy}(\text{OR})_3(\text{NCMe})_2$ complex. Interestingly, tris(*tert*-butyl)methanol does not react with LnN_3 of the late (small) lanthanoid metals. However, fast and clean reactions occur with the sterically less demanding $\text{Ln}[\text{N}(\text{SiHMe}_2)_2]_3$ derivatives yielding new homoleptic mononuclear $\text{Ln}[\text{OC}(t\text{Bu})_3]_3(\text{THF})$ with practically all metals of this group of elements. X-ray crystal structural determination was made for yttrium and neodymium complexes.^{253,256} These results are in direct line with the clean synthesis of the unsolvated complex $\text{Ce}[\text{OC}(t\text{Bu})_3]_3$ from CeN_3 and the corresponding alcohol reported by Stecher and co-workers.²⁵⁷ They showed that this cerium complex is quite thermosensitive and proposed a mechanism for its decomposition into $[\text{Ce}(\text{O})(\text{OCH}t\text{Bu}_2)_3]_2$ and isobutylene.²⁵⁸

The synthesis of similar $\text{Ln}(\text{OCH}t\text{Bu}_2)_3$ by direct alcoholysis of LnN_3 was reported but without any structural data.²⁵⁹ Few additional examples of well-characterized simple lanthanide alkoxides such as $\text{Nd}(\text{OCHiPr})_6(\text{THF})_2$ and $\text{Ln}(\text{OCH}_2t\text{Bu})_{12}$ ($\text{Ln} = \text{La}, \text{Nd}$) prepared

²⁵⁴ Bradley, D. C.; Chudzynska, H.; Hursthause, M. B.; Motavalli, M. *Polyhedron* **1991**, *10*, 1049-1059.

²⁵⁵ Herrmann, W. A.; Anwander, R.; Scherer, W. *Chem. Ber.* **1993**, *126*, 1533-1539.

²⁵⁶ Herrmann, W. A.; Anwander, R.; Munck, F. C.; Scherer, W.; Dufaud, V.; Huber, N. W.; Artus, G. R. J. Z. *Naturforsch., B: Chem. Sci.* **1994**, *49*, 1789-1797.

²⁵⁷ Stecher, H. A.; Sen, A.; Rheingold, A. L. *Inorg. Chem.* **1988**, *27*, 1130-1132.

²⁵⁸ Stecher, H. A.; Sen, A.; Rheingold, A. L. *Inorg. Chem.* **1989**, *28*, 3280-3282.

²⁵⁹ Herrmann, W. A.; Anwander, R.; Kleine, M.; Scherer, W. *Chem. Ber.* **1992**, *125*, 1971-1979.

by alcoholysis were also reported. Interestingly, the latter showed the presence of agostic Ln--H-C interactions in the solid state.²⁶⁰

7.4.1.2. Lanthanide aryloxides

The use of this synthetic method for the preparation of lanthanide^(III) aryloxides was reported in the publication relating the synthesis of the first three- and four coordinate lanthanide aryloxides.²⁴⁹ However, the first structural elucidation of a complex obtained from the silylamide route was the 3-coordinate Ce aryloxide Ce[O-2,6-*t*Bu₂-C₆H₃]₃ complex, which showed a pyramidal structure unlike the near-planar scandium analog reported by Lappert and like LnN₃.²⁵⁷ When the less sterically crowded 2,6-diisopropylphenol reacts with LnN₃, tris (aryloxides) Ln₂(OAr)₆ (Ln = Nd, Sm, Er) are obtained in good yield. The addition of a Lewis base such as THF to benzene solutions of these aryloxides results in the cleavage of the dimeric unit and formation of THF bis-adducts Ln(OAr)₃(THF)₂ as observed for the yttrium aryloxide Y₂(O-2,6-Me₂-C₆H₃)₆(THF)₂.²⁵⁰ Again, the steric effect of the 2,6-substituents of the phenyl ring affects directly the nuclearity of the complexes as previously noticed.

Divalent lanthanide aryloxides were also prepared efficiently using this route. Reaction of THF- or ether-adducts LnN₂(THF)₂ and LnN₂(OEt₂)₂ with 2 equivalents of substituted phenol in hexane at room temperature allows the synthesis of complexes of formula Ln(OAr)₂(THF)₃ (Ln = Sm, Yb). The crystal structures of the corresponding complexes with OAr = O-2,6-*t*Bu₂-4-Me-C₆H₂ exhibit a square-pyramidal structure²⁶¹ while the europium analog, prepared by salt metathesis,²⁵¹ possesses a distorted trigonal-bipyramidal conformation.

7.4.1.3. Lanthanide silyloxides

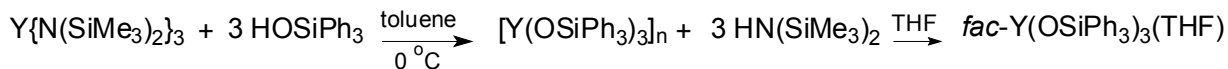
In the same way, some research was devoted to the use of bulky silanols as ligands in lanthanide chemistry. This investigation was motivated by the thermal instability observed with the tris(*tert*-butyl)methanol ligand. The strong silicon-oxygen, kinetically stable with respect to heterolytic Si-O cleavage, was assumed to avoid such problems. In addition, the lower basicity of silyoxide ligands discourages the bridging tendency. It was initially shown that the reaction of YN₃ with 3 equivalents of tris(phenyl)silanol in toluene produces a feather-like solid which was not suitable for X-ray diffraction.²⁶² Consequently, efforts were focused on the preparation of Lewis base adducts in order to increase the crystallinity (Scheme 23). Thus, in the presence of THF, the hexacoordinate complex [Y(OSi(Ph)₃)₃(THF)₃]•THF was formed, revealing a monomeric structure with approximate octahedral geometry at the yttrium^(III) core.

Scheme 23. Synthetic route to mononuclear silyoxide.²⁶²

²⁶⁰ (a) Barnhart, D. M.; Clark, D. L.; Huffman, J. C.; Vincent, R. L.; Watkin, J. G. *Inorg. Chem.* **1993**, *32*, 4077-4083. (b) Barnhart, D. M.; Clark, D. L.; Gordon, J. C.; Huffman, J. C.; Watkin, J. G.; Zwick, B. D. *J. Am. Chem. Soc.* **1993**, *115*, 8461-8462.

²⁶¹ (a) Deacon, G. B.; Hitchcock, P. B.; Holmes, S. A.; Lappert, M. F.; MacKinnon, P.; Newnham, R. H. *J. Am. Chem. Soc., Chem. Commun.* **1989**, 935-937. (b) Evans, W. J.; Anwander, R.; Ansari, M. A.; Ziller, J. W. *Inorg. Chem.* **1995**, *34*, 5-6.

²⁶² (a) McGahey, M. J.; Coan, P. S.; Folting, K.; Streib, W. E.; Caulton, K. G. *Inorg. Chem.* **1989**, *28*, 3284-3285. (b) McGahey, M. J.; Coan, P. S.; Folting, K.; Streib, W. E.; Caulton, K. G. *Inorg. Chem.* **1991**, *30*, 1723-1735.



Evans and co-workers reported an interesting comparative synthetic and structural study of triphenylmethoxide and triphenylsilyloxide complexes of the early lanthanides.²⁶³ This study shows that the OCPH_3 and OSiPh_3 ligands can form analogous solvated and unsolvated lanthanide complexes. The differences between these ligands may arise primarily from the differing O-C and O-Si distances. Thus, it was proposed that the highest solubility met with OSiPh_3 complexes may result from the longer O-Si bond that allows solvents to displace the metal-arene interaction and form solvated complexes.

7.4.1.4. Functionalized lanthanide alkoxides, aryloxides and silyloxides

As mentioned previously, the alcoholysis method allows the preparation of lanthanide alkoxides with more advanced ligand structure. Polyfunctional alkoxy-based ligands were initially designed to prepare highly volatile, soluble homoleptic alkoxide complexes. The objective is not to give here an exhaustive list of the existing complexes, but just some typical examples for alkoxide-, aryloxide and silyloxide-based ligands.

7.4.1.4.1. Alkoxide-based ligands

β -Functionalized alcohols ($\text{HOCH}(t\text{Bu})\text{CH}_2\text{OEt}$, $\text{HOCH}(t\text{Bu})\text{CH}_2\text{NEt}_2$, $\text{HOC}(t\text{Bu})_2\text{CH}_2\text{OEt}$ and $\text{HOC}(\text{CHMe}_2)_2\text{CH}_2\text{OEt}$) react with NdN_3 to form $\text{Nd}(\text{OR})_3$ complexes assumed to be monomeric. However, due to the pronounced solubility of these alkoxide complexes even in nonpolar solvents, their mononuclear composition could not be proved by X-ray structure analysis.²⁶⁴ Reduction of the steric bulk in α -position is known to increase the nuclearity of the complexes. For example, when a methylene group is in α -position, the cyclic decamer $[\text{Y}(\text{OCH}_2\text{CH}_2\text{OMe})_3]_{10}$ is obtained,²⁶⁵ while a $-\text{C}(\text{Me})_2$ group in α -position led to a dimeric complex with lutetium.²⁶⁶ Mononuclearity was made possible using 3 equivalents of a readily accessible tertiary γ -difunctionalized alcohol with two pyridine units (Figure 43).²⁶⁷ Importantly, when the reaction is conducted with two equivalents of alcohol, a mixed $\text{Ln}(\text{OR})_2\text{NR}_2$ is obtained, providing a real synthetic tool since the remaining amido group can be further substituted.

7.4.1.4.2. Aryloxide-based ligands

Well-known aryloxide-based functionalized ligands are the Schiff-base and salicylaldiminato ligands. Besides the numerous synthesis conducted in aqueous medium, Orvig *et al.* have reported lanthanide derivatives of the fully saturated amino-phenol ligands N

²⁶³ Evans, W. J.; Golden, R. E.; Ziller, J. W. *Inorg. Chem.* **1991**, *30*, 4963-4968.

²⁶⁴ Herrmann, W. A.; Anwander, R.; Denk, M. *Chem. Ber.* **1992**, *125*, 2399-2405.

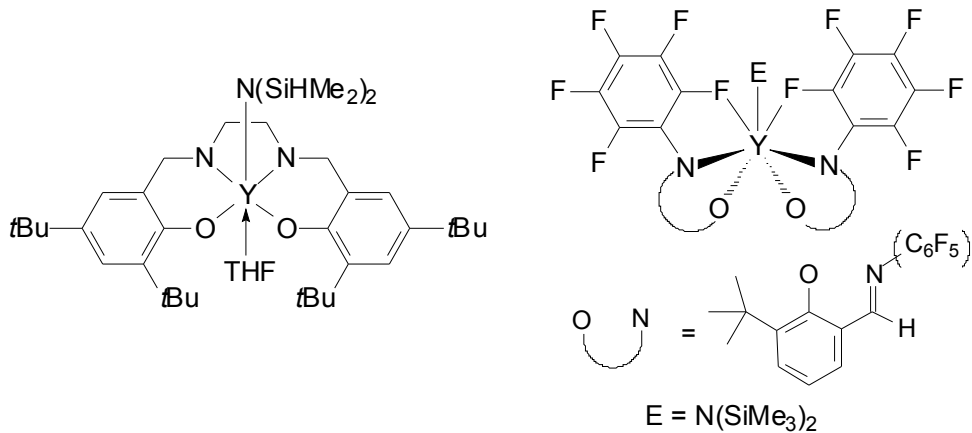
²⁶⁵ Poncelet, O.; Hubert-Pfalzgraf, L. G.; Daran, J. C.; Astier, R. *J. Chem. Soc., Chem. Commun.* **1989**, 1846-1848. The alkoxide was obtained by alcoholysis of $\text{Y}_5\text{O}(\text{OCHMe}_2)_{13}$ with the corresponding functionalized alcohol.

²⁶⁶ Anwander, R.; Munck, F. C.; Priermeier, T.; Scherer, W.; Runte, O.; Herrmann, W. A. *Inorg. Chem.* **1997**, *36*, 3545-3552.

²⁶⁷ Evans, W. J.; Anwander, R.; Berlekamp, U. H.; Ziller, J. W. *Inorg. Chem.* **1995**, *34*, 3583-3588.

$[\text{CH}_2\text{CH}_2\text{NHCH}_2(2\text{-OH-3-}R^1\text{-5-}R^2\text{-C}_6\text{H}_2)]_3$ ($R^1 = \text{H}, \text{OMe}$; $R^2 = \text{H}, \text{Cl}, \text{Br}$) in organic solvents.²⁶⁸ More recently, LnN_3 ($\text{Ln} = \text{Sm}, \text{Nd}$) was shown to react with one equivalent of the bulky heptadentate Schiff-base ligand $\text{N}[\text{CH}_2\text{CH}_2\text{N}=\text{CH}(2\text{-OH-3,5-}t\text{Bu}_2\text{-C}_6\text{H}_2)]_3$ resulting in the formation of seven-coordinate complexes with a slightly distorted capped octahedral geometry. The reaction of pentafluorophenyl substituted ligand HL^3 with YN_3 in benzene or toluene solution gave a variety of products including a seven-coordinate complex in which the two phenolate-oxygen atoms are ca. *trans* to the amido ligand.²⁶⁹ Two bonds to two of the *ortho*-fluorine atoms complete the coordination geometry (Figure 42). However, YN_3 proved to be an inefficient precursor for the synthesis of salicyladiminato yttrium complex in a THF-hexane mixture, leading to an oligomeric insoluble product. On the other hand, a monomeric yttrium complex could be isolated using the sterically less demanding $\text{Y}((\text{N}(\text{SiHMe}_2)_3)(\text{THF})_2$ (Figure 42).²⁷⁰

Figure 42. Examples of salicyladiminato-yttrium complexes synthesized using the silylamine pathway.^{269,270}



²⁶⁸ (a) Liu, S.; Yang, L.-W.; Rettig, S. J.; Orvig, C. *Inorg. Chem.* **1993**, *32*, 2773-2778. (b) Caravan, P.; Hedlund, S.; Liu, S.; Sjöberg, S.; Orvig, C. *J. Am. Chem. Soc.* **1995**, *117*, 11230-11238.

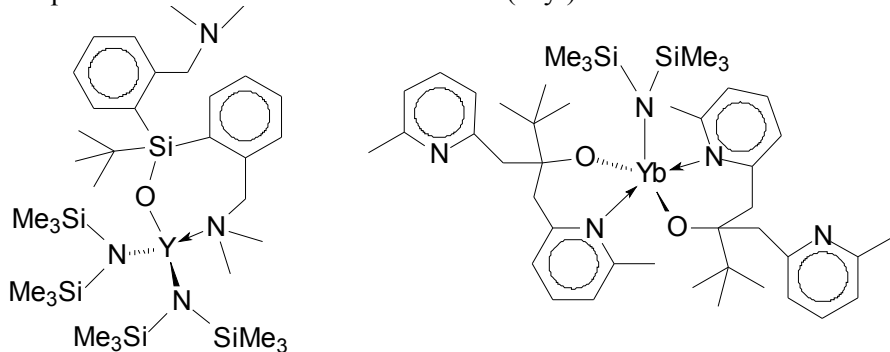
²⁶⁹ Lara-Sánchez, A.; Rodriguez, A.; Hughes, D. L.; Schormann, M.; Bochmann, M. *J. Organomet. Chem.* **2002**, *663*, 63-69.

²⁷⁰ Runte, O.; Priermeier, T.; Anwander, R. *Chem. Commun.*, **1996**, *11*, 1385-1386.

7.4.1.4.3. Silyl oxide-based ligand

Examples in this area are not so frequent, but we can however cite the work of Berg *et al.*²⁷¹ The reaction of the δ-amino-functionalized silanols ($\text{HOSi}(t\text{Bu})_{3-n}[(\text{CH}_2)_3\text{NMe}_2]_n$ ($n = 1$ or 2) (3 equiv.) with LnN_3 in toluene at room temperature produces the monomeric $\text{Y}[\text{OSi}(t\text{Bu})((\text{CH}_2)_3\text{NMe}_2)_2]_3$, $\text{Y}[(\text{OSi}(t\text{Bu})_2(\text{CH}_2)_3\text{NMe}_2]_3$, and $\text{Ce}[(\text{OSi}(t\text{Bu})_2(\text{CH}_2)_3\text{NMe}_2]_3$. The single-crystal X-ray diffraction study of $\text{Y}[(\text{OSi}(t\text{Bu})_2(\text{CH}_2)_3\text{NMe}_2]_3$ revealed a trigonal bipyramidal geometry with the equatorial sites occupied by the three silyloxides and the axial sites occupied by two NMe_2 groups, the third dimethylaminopropyl arm is not coordinated. The non-coordination of an amino-type ligand was also observed when 1 equivalent of $\text{HOSi}t\text{BuAr}$ ($\text{Ar} = \text{o-C}_6\text{H}_4(\text{CH}_2\text{NMe}_2)$) reacts with YN_3 , yielding the monosilyl oxide complex $\text{Y}[\text{OSi}t\text{BuAr}_2][\text{N}(\text{SiMe}_3)_2]_2$ without any sign of ligand redistribution (Figure 43).

Figure 43. Examples of well-defined functionalized alk(silyl)oxides.^{267,271}



7.4.2. Protonolysis of tris(alkyl) complex

The preparation of lanthanide alkoxides via protonolysis of the tris(alkyl) precursor $\text{Ln}(\text{CH}(\text{TMS})_2)_3$ (Scheme 24) proved to be an elegant and efficient method for the introduction of bulky, polyfunctionalized aryloxy-based ligands (Figure 44).^{224,272}

Scheme 24. General reaction scheme for the protonolysis of $\text{Ln}\{\text{CH}_2(\text{SiMe}_3)\}_3$.



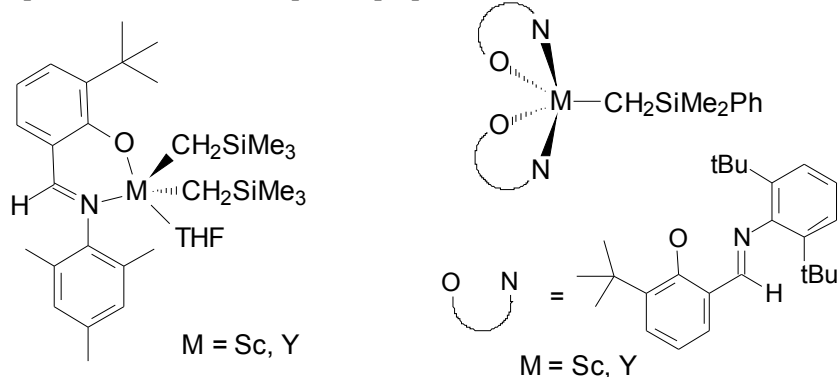
However this synthetic route was never applied to the preparation of simple alkoxides. It may suffer from the limited availability of the starting precursor, obtained by ionic exchange reaction between Ln(OAr)_3 and 3 equiv. of $\text{LiCH}(\text{TMS})_2$,²⁷³ and/or from the low thermal stability of the tris(alkyl) complex.

²⁷¹ (a) Shao, P.; Berg, D. J.; Bushnell, G. W. *Inorg. Chem.* **1994**, *33*, 3452-3458. (b) Shao, P.; Berg, D. J.; Bushnell, G. W. *Inorg. Chem.* **1994**, *33*, 6334-6339.

²⁷² Emslie, D. J. H.; Piers, W. E.; McDonald, R. *J. Chem. Soc., Dalton Trans.* **2002**, 293-294.

²⁷³ Lappert, M. F.; Pearce, R. *J. Chem. Soc., Chem. Commun.* **1973**, 126.

Figure 44. Examples of lanthanide complexes prepared via alkane elimination.²⁷²



7.4.3. Transalkoxylation

Several examples of transalkoxylation or alcohol exchange reactions were reported in the literature. The synthesis of the cyclic decamer with a β -functionalized alcohol was already mentioned above.²⁶⁵ The formation of heavier aliphatic alkoxides is also possible by reaction of $\text{LnO}(i\text{Pr})_{13}$ with the corresponding alcohol ($\text{ROH} = t\text{BuOH}; \text{CH}_3(\text{CH}_2)_n\text{CH}(\text{CH}_3)\text{CHOH}$ with $n = 1, 2, 3; \text{C}_6\text{H}_5\text{OH}$).²²⁹ The same method was also applied to the synthesis of the tri(phenyl)siloxide $\text{Y}[(\text{OSiPh}_3)_3(\text{THF})_3](\text{THF})$.²⁶² Finally, $\text{Ce}^{(\text{IV})}$ siloxide $\text{Ce}(\text{OSiPh}_3)_4(\text{DME})$ was prepared by reaction of "Ce(O*i*Pr)₄" with 4 equiv. of HOSiPh₃ in DME.²⁷⁴

7.4.4. Carboxylates

In the quest of chlorine-free metal alkoxides for the preparation of high purity metal oxides, another synthetic method was patented in the 1980's.²⁷⁵ It is claimed that the reaction of an anhydrous lanthanide carboxylate with an alkali-metal alkoxide in aromatic solvents gives high purity lanthanide alkoxides ($\text{Ln} = \text{Sc}$ to Lu) in high yields ($> 90\%$). The starting carboxylates are chosen among the formate, acetate, propionate, benzoate and oxalate and the alkali-metal alkoxides are aliphatic monofunctional compounds. No structural data were provided in the patent. A similar synthetic method was previously reported but limited to the use of the trichloroacetate derivatives.²⁷⁶

7.5. Ce^(IV) alkoxides: a special case

Hard ligands such as alkoxides are supposed to stabilize the high oxidation state of Ce^(IV). Despite this encouraging feature, Ce^(IV) alkoxide chemistry suffers from synthetic problems. Indeed, a convenient route comparable to the silylamine route has not yet been found. We have just mentioned the possibility of alcohol exchange reaction, but this method is more unusual. An alternative method of preparation utilizes cerium ammonium nitrate ((NH₄)Ce(NO₃)₆, CAN) as starting compound.²⁷⁷ Complexes with the less bulky O*i*Pr ligand document

²⁷⁴ Gradeff, P. S.; Yunlu, K.; Gleizes, A.; Galy, J. *Polyhedron* **1989**, *8*, 1001-1005.

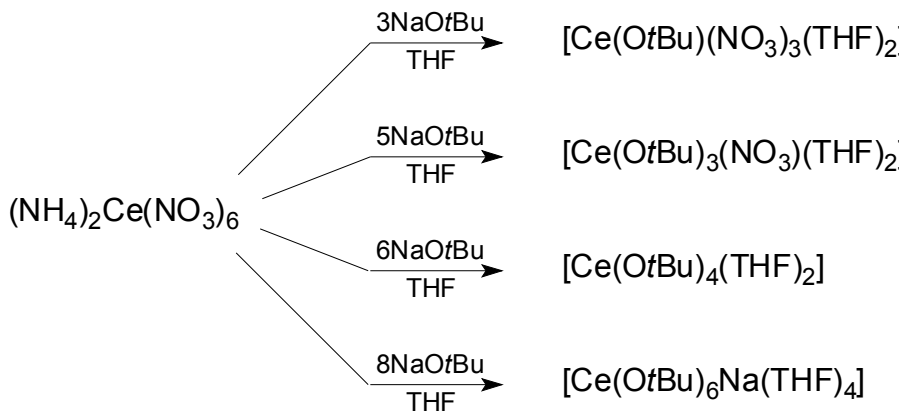
²⁷⁵ Ozaki, Y.; Kaneko, K.; Mitachi, S., WO 2529884 (Hokko Chemical Industry Co., Ltd, JP.), **1983**.

²⁷⁶ Singh, M; Misra, S. N. *J. Indian. Chem. Soc.* **1978**, *55*, 643.

²⁷⁷ Evans, W. J.; Deming, T. J.; Olofson, J. M.; Ziller, J. W. *Inorg. Chem.* **1989**, *28*, 4027-4034.

the change in steric and electronic requirements yielding the dinuclear $\text{Ce}_2(\text{O}i\text{Pr})_8(\text{HO}i\text{Pr})_2$ vs. the tetrานuclear $\text{Nd}_4(\text{O}i\text{Pr})_{12}(\text{HO}i\text{Pr})_4$. Use of the OtBu ligand even affords monomeric complexes as structurally evidenced by $\text{Ce}(\text{OtBu})_2(\text{NO}_3)_2(\text{HO}t\text{Bu})_2$ and $\text{Ce}(\mu_3\text{-}\text{OtBu})_2(\mu_2\text{-}\text{OtBu})_2(\text{OtBu})_4\text{Na}_2(\text{DME})$. Stepwise exchange of the bidentate nitrate ligand through OtBu ligands in the CAN/NaOtBu system can be controlled by varying the stoichiometry and the insolubility of NaNO_3 in THF (Scheme 25). It can also be noted that the homoleptic $\text{Ce}(\text{OtBu})_4(\text{THF})_2$ converts to $\text{Ce}_3\text{O}(\text{OtBu})_{10}$ in toluene within a few days at room temperature, a behavior comparable to the conversion of $\text{La}_3(\text{OtBu})_9(\text{HO}t\text{Bu})_2$ to $\text{La}_5\text{O}(\text{OtBu})_{13}$.²³³

Scheme 25. Structure of cerium^(IV) *tert*-butoxide as a function of the ratio CAN/NaOtBu.²⁷⁷



7.6. Conclusion

The synthetic chemistry of lanthanide alkoxides is really rich and the resulting complexes reveal surprising structure chemistry and a great diversity through the easy tuning of the ligand. In our will to use lanthanide alkoxides as precursors in polymerization catalysis, we prepared a set of neodymium alkoxide complexes to study structural, steric and electronic effects on polymerization activity. Thus, in addition to known mononuclear homoleptic complexes, i.e. $\text{Nd}(\text{O}-2,6\text{-}t\text{Bu}_2\text{-}4\text{-Me-C}_6\text{H}_2)_3(\text{THF})$,²⁴⁹ $\text{Nd}(\text{O}-2,6\text{-}t\text{Bu}_2\text{-}4\text{-Me-C}_6\text{H}_2)_3$ ²⁴⁹ and $\text{Nd}(\text{OC}t\text{Bu}_3)_3(\text{THF})$,²⁵⁶ several new complexes were synthesized by varying two parameters which have proven essential: (i) the nature of the alkoxide ligand and (ii) the synthetic route.

8. Synthesis of neodymium alkoxides

8.1. Neodymium *tert*-butoxides

Among the various neodymium alkoxides that we synthetized, neodymium *tert*-butoxide was the most widely studied. With this derivative, two synthetic routes have been evaluated: salt metathesis and alcoholysis of $\text{Nd}\{\text{N}(\text{SiMe}_3)_2\}_3$ (NdN3). Salt metathesis was conducted varying the neodymium precursor, the alkali-metal alkoxide, the solvent but also the reaction time and concentrations. The alcoholysis reaction was just performed in different solvents. The different alkoxides that have been prepared, were characterized by elemental analysis and

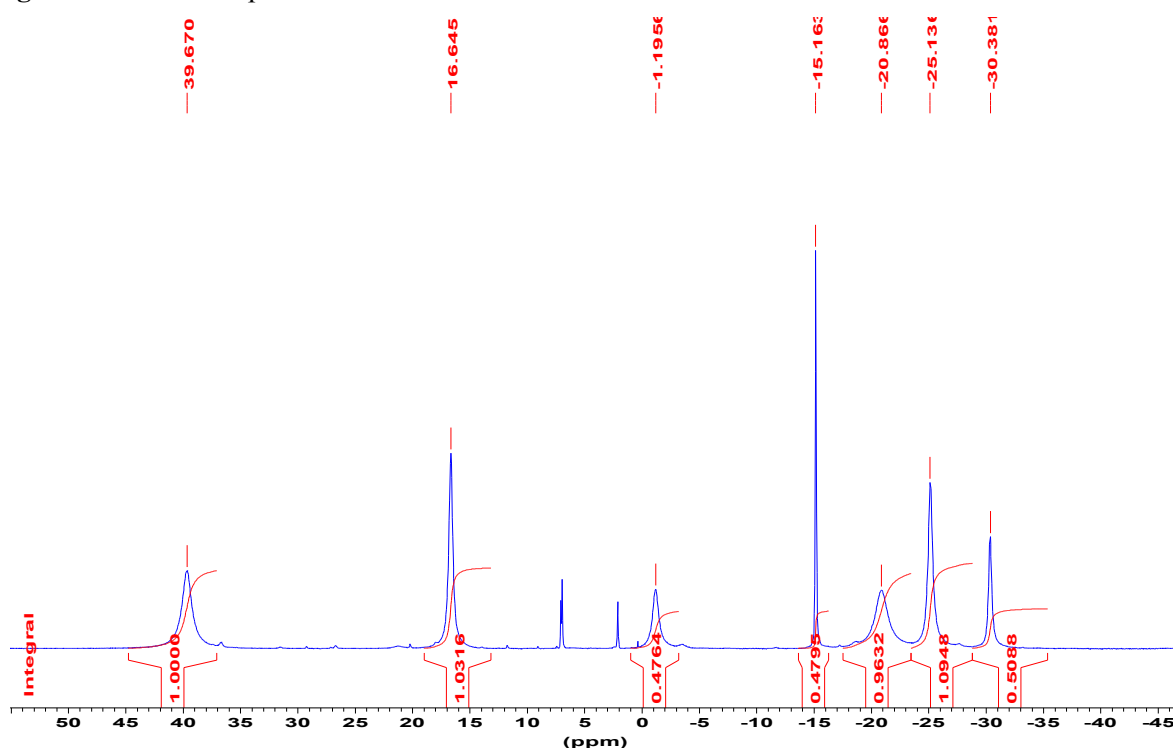
when possible by X-ray crystal structure determination and ^1H NMR spectroscopy. As it will be shown, the experimental procedure as well as the nature of precursors is critical for the final structure of the neodymium alkoxide.

8.1.1. Salt metathesis reactions

8.1.1.1. From anhydrous NdCl_3 and NaOtBu

Initially, we employed the experimental procedure described by Evans *et al.* for the preparation of lanthanum *tert*-butoxide.²³⁹ Thus, the reaction of anhydrous NdCl_3 with 3 equiv. of NaOtBu in THF at 20 °C for 3 days gives a single primary product (**1** = $\text{Nd}_3(\mu_3\text{-OtBu})_2(\mu_2\text{-OtBu})_3(\text{OtBu})_4(\text{THF})_2$) that can be routinely isolated in 80-90% yield as a pale blue solid. Elemental analysis of the bulk materials was consistent with the composition $\text{Nd}_3(\text{OtBu})_9(\text{THF})_2$ (Nd = 35 wt% and Cl < 0.1 wt%). This complex dissolves easily in benzene, toluene and hexane. Rather simple ^1H NMR spectra were expected for **1** because of the single resonance per type of *tert*-butoxide ligand and the splitting of the resonances due to the presence of paramagnetic neodymium metal centers. Variable temperature ^1H NMR spectra in toluene- d_8 of crude samples were, however, complex with broad resonances. The spectra of samples recrystallized from concentrated toluene solution proved much more informative, featuring at 5 °C seven well-resolved peaks in the region ranging from δ 45 to –30 ppm (Figure 45).

Figure 45. ^1H NMR spectrum of **1** at 5 °C in toluene- d_8 .

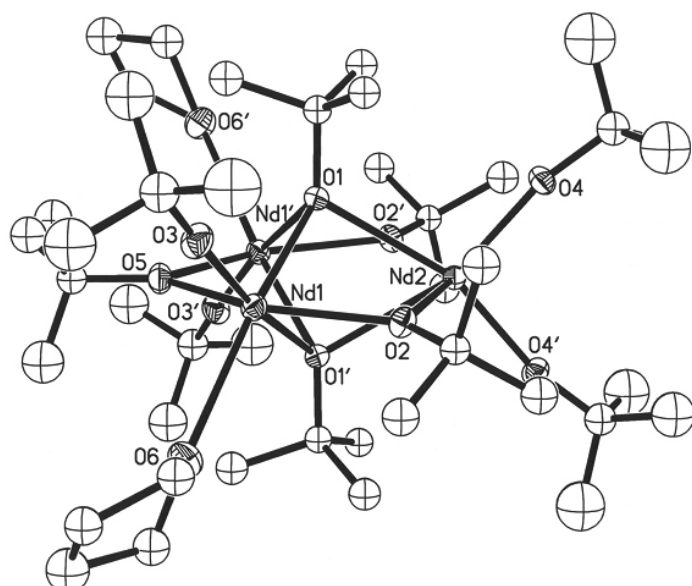


The ^1H NMR spectra of **1** proved to be highly temperature sensitive due to the paramagnetism of the Nd centers and optimal resolution (minimal resonances overlapping, line shape) was observed at 5 °C (see Appendix 1 for ^1H NMR spectra of **1** at various temperatures). Correlation between chemical shift and coordination mode of the alkoxide

groups has been previously noted in yttrium and lanthanum complexes of this type; i.e., increased bridging is associated with lower field shifts.^{239–240,243} This could not be applied, however, to determine unambiguously the geometry of **1** in solution, due to the effects of the paramagnetic neodymium centers. A crystallography study was therefore undertaken.

X-ray quality crystals of **1** were grown at –5 °C from a concentrated toluene solution of a sample prepared from NaOtBu. **1** is a trimetallic compound in which the three-neodymium atoms comprise a triangle with doubly bridging alkoxide groups along the edges of the Nd₃ triangle and triply bridging groups above and below the Nd₃ plane (Figure 46). One neodymium atom has two terminal *tert*-butoxy ligands, and one terminal *tert*-butoxy ligand and a THF molecule ligate each of the two other neodymium atoms. Thus, each neodymium atom in **1** is 6-coordinated. The same structure framework has been observed previously in heteroleptic complexes Y₃(μ₃-OtBu)(μ₃-Cl)(μ₂-OtBu)₃(OtBu)₄(THF)₂²³⁹ and Y₃(μ₃-OtBu)(μ₃-Cl)(μ₂-OtBu)₃(OtBu)₃Cl(THF)₂²⁴⁰ and in the homoleptic complex La₃(OtBu)₉(tBuOH)₂.²⁵⁴ The exact location of the *tert*-butyl alcohol molecules in the latter lanthanum complex could not be formally established because of disorder problems. In addition, **1** should be isostructural to La₃(OtBu)₉(THF)₂ prepared by salt metathesis from anhydrous LaCl₃ and NaOtBu in THF, the structure of this complex was suggested from NMR data.²³⁹ However, this would not be surprising since Nd-alkoxide chemistry proved much more related to La than Y chemistry. In both of the aforementioned yttrium complexes, the THF molecules were found to be located on the same side of the Y₃ plane, as the chloride ligands.^{239,240} In contrast, **1** has one THF molecule on each side of the trimetallic plane.

Figure 46. ORTEP plot of **1** with probability ellipsoids at 30% (hydrogen atoms omitted for clarity).



The terminal Nd–O distances of the alkoxide ligands (Nd(1)–O(3), 2.147(4); Nd(2)–O(4), 2.163(3) Å) compare well with those found in related complexes, e.g. Nd₄(OCH₂tBu)₁₂ (2.138(8) Å),^{260b} Nd₂(OCH*i*Pr₂)₆(L)₂ (L = THF, 2.146(4)–2.160(4) Å; L = Py,

2.133(4)–2.158(4) Å,^{260a} Nd(OC*t*Bu₃)₃(CH₃CN)₂ (2.149(5)–2.171(5) Å),²⁷⁸ and Nd(OC*t*Bu₃)₃(μ-Cl)Li(THF)₃ (2.150(3)–2.171(3) Å).²⁷⁹ Doubly bridging Nd–O distances are, as expected, somewhat longer than those of the terminal alkoxide ligands, one μ₂-O*t*Bu ligand forming a symmetric bridge to the two equivalent Nd atoms (Nd(1)–O(5), 2.399(3) Å), while the two other μ₂-O*t*Bu ligands form a disymmetric bridge (Nd(1)–O(2), 2.333(3); Nd(2)–O(2), 2.458(3) Å) and average 2.396 Å. The latter values are comparable to μ₂-bridging Nd–O distances of 2.383(4)–2.394(4) Å found in Nd₂(OCH*i*Pr₂)₆(L)₂ (L = THF, Py, DME),^{260a} and of 2.320(12)–2.381(12) Å in Nd₄(OCH₂*t*Bu)₁₂.^{260b} The same comments apply to the triply bridging Nd–O bond distances (Nd(1)–O(1), 2.409(3); Nd(2)–O(1), 2.624(3) Å). Due to the steric demands in the bridges, all of the three Nd atoms are highly distorted from the ideal octahedral geometry. The Nd(1)–O(3)–C(9) angle of 177.8(4)° is nearly linear, showing that the THF ligand does not bring significant steric hindrance. On the other hand, because of the replacement of the THF by a terminal bulky O*t*Bu ligand, the Nd(2)–O(4)–C(13) angle is bent to 167.3(4)°. The elongated Nd(1)–O(6)(THF) distance of 2.661(4) Å, compared to the 2.50–2.58 Å distances found in NdCl₃(THF)₄,²⁸⁰ Nd₂(OCH*i*Pr₂)₆(THF)₂,^{260b} (η⁵-C₅H₅)₃Nd(THF),²⁸¹ and [(η-C₈H₈)₃Nd(THF)₂][Nd(η-C₈H₈)₂],²⁸² gives another evidence for steric crowding in this molecule.

Table 12. Selected bond lengths [Å] and angles [°] for complex **1**.

Nd(1)–O(3)	2.147(4)	Nd(1)–O(1)–C(1)	123.1(3)
Nd(1)–O(2)	2.333(3)	Nd(2)–O(1)–C(1)	120.0(3)
Nd(1)–O(5)	2.399(3)	Nd(1)–O(2)–C(5)	131.9(3)
Nd(1)–O(1)	2.409(3)	Nd(2)–O(2)–C(5)	126.4(3)
Nd(1)–O(6)	2.661(4)	Nd(1)–O(5)–C(17)	130.82(9)
Nd(2)–O(4)	2.163(3)	Nd(1)–O(3)–C(9)	177.8(4)
Nd(2)–O(2)	2.458(3)	Nd(2)–O(4)–C(13)	167.3(4)
Nd(2)–O(1)	2.624(3)	Nd(1)–O(1)–Nd(1')	94.92(11)
Nd(1)–Nd(1')	3.6318(6)	Nd(1)–O(1)–Nd(2)	95.11(11)
Nd(1)–Nd(2)	3.7161(4)	Nd(1')–O(1)–Nd(2)	92.51(11)
Nd(2)–Nd(1')	3.7161(4)	Nd(1)–O(2)–Nd(2)	101.68(12)

Retrospectively, the pattern of seven resonances with an integrated ratio of ca. 2.2:1:1:2:2:1 in the ¹H NMR spectrum at 5 °C (Figure 45) correlates well with the structure of **1** which contains nine O*t*Bu groups in five distinct environments and two equivalent THF molecules (the THF resonances could not be distinguished unambiguously from those of O*t*Bu groups considering the similar integral ratio and the experimental uncertainty due to the variable line

²⁷⁸ Herrmann, W. A.; Anwander, R.; Kleine, M.; Scherer, W. *Chem. Ber.* **1992**, *125*, 1971–1979.

²⁷⁹ Edelmann, F. T.; Steiner, A.; Stalke, D.; Gilje, J. W.; Jagner, S.; Hakansson, M. *Polyhedron* **1994**, *13*, 539–546.

²⁸⁰ Wenqi, C.; Zhongsheng, J.; Yan, X.; Yuguo, F.; Guangdi, Y. *Inorg. Chem. Acta* **1987**, *130*, 125–129.

²⁸¹ Benetollo, F.; Bombieri, G.; Bisi Castellani, C.; Jahn, W.; Fischer, R. D. *Inorg. Chim. Acta* **1984**, *95*, L7–L10.

²⁸² Decock, C. W.; Ely, S. R.; Hopkins, T. E.; Brault, M. A. *Inorg. Chem.* **1978**, *17*, 625–631.

shape). This suggests that the solid-state structure of **1** is retained in hydrocarbon solutions; in particular, this may indicate that there is no transformation at this temperature between the two possible isomers differing in the location of the THF ligands.

The salt metathesis reaction was also performed in various solvents. As expected, the reaction conducted in toluene was not successful due to the limited solubility of the starting reagents; this ionic reaction most probably needs charge dissociation, i.e. polar solvent, to occur. Diethyl ether affords the preparation of a pale blue powder (**10***) with 65% yield, but the latter exhibits a low solubility in hexanes and toluene indicating a different solid structure. The possibility of an oligomeric structure may be considered, given the crystal structure of the *tert*-amylate derivative (**10**) prepared under the same conditions (*vide infra*). A higher yield was obtained when the reaction was performed with the cyclic ether tetrahydropyran **2**. In this case, we can rightfully consider that the final crude product has a comparable structure to **1**.

This reaction is very sensitive to the origin/purity of the neodymium precursor. Experiments performed under rigorously similar conditions with neodymium chloride coming from two different commercial sources yielded two different products as confirmed by Nd and Cl contents (Table 13). In addition, the compound with the lowest Nd content is slightly soluble in non-polar solvent whereas the other one, characterized as **1**, is highly soluble in such solvents. This suggests definitely a difference in the complex structure, the lower solubility may be ascribed to a more aggregated structure.

Table 13. Synthesis of neodymium *tert*-butoxides by salt metathesis with various Nd precursors.

Nd precursor (mmol)	reaction time (h)	[Nd] (M)	yield (%)	% Nd _{th}	% Nd _{exp}	% Cl _{th}	% Cl _{exp}
anhydrous NdCl ₃ , (Strem) (10)	72	0.1	58	38.1	31.4	0	0.75(5)
anhydrous NdCl ₃ , (Aldrich) (10)	72	0.1	81	24.3	31.4	0	0.09(5)

Reactions carried out at RT with NaOtBu (30 mmol) in THF. Theoretical values based on **1** structure.

To conclude, this experimental procedure was also applied to prepare yttrium, lanthanum, cerium^(III) and samarium *tert*-butoxides. As expected, crystals of lanthanum and yttrium *tert*-butoxides grown from toluene solutions exhibit comparable ¹H NMR spectra to La₃(OtBu)₉(THF)₂ and Y₃(OtBu)₈Cl(THF)₂ respectively.²³⁹

8.1.1.2. From anhydrous NdCl₃ and MOtBu (M = Li and K) in THF

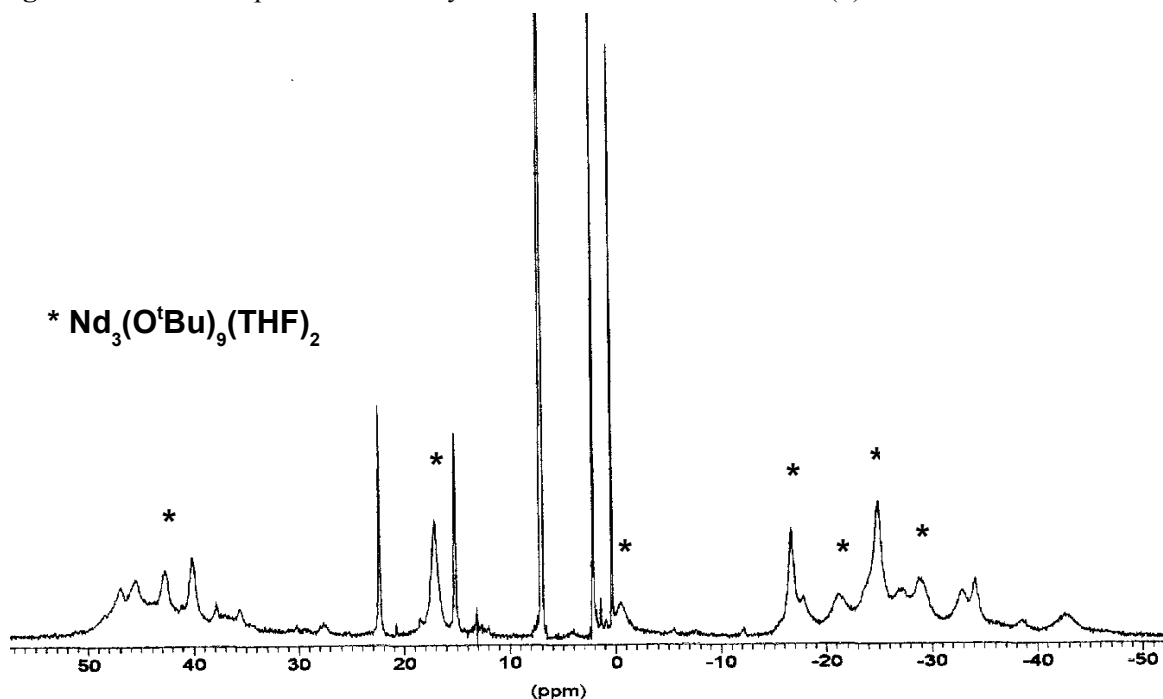
As observed in the chemistry of yttrium *tert*-butoxides or aryloxides with low steric hindrance 2,6-substituants,^{239,242,249} the nature of the metal of the alkali-metal alkoxide is crucial for the structure of the final complex. The incorporation of alkali metal atoms and of chloride in the yttrium *tert*-butoxide systems has been suggested to result from steric considerations.²³⁹ Consequently, the effect of the alkali metal on the neodymium *tert*-

butoxide structure was studied. We performed the salt metathesis reaction with LiOtBu and KOtBu in THF solution as previously described.

With LiOtBu, the final compound can not be retrieved by simple filtration. However, evaporation of the solvent and treatment with Et₂O allows the separation of the neodymium *tert*-butoxide from LiCl, resulting in a pale blue powder **3** in moderate yield (50%). The low solubility in non-polar solvents may indicate the presence of lithium in the crude product, as reported for Li₅Sm(OtBu)₈.²⁸³ Unfortunately, no indication regarding the alkoxide structure could be obtained from crystals grown from a toluene solution.

Changing the alkali-metal alkoxide from NaOtBu to KOtBu gives **4** without affecting the yield of the reaction. In the same time, the elemental analysis is comparable to that obtained for **1**. Recrystallized samples showed invariably complex ¹H NMR spectra. These spectra (toluene-*d*₈, 5 °C) featured reproducibly as the major (ca. 70%) peaks the seven resonances observed for samples of **1** prepared from NaOtBu along with additional (ca. 30%) rather broad resonances (Figure 47).

Figure 47. ¹H NMR spectrum of neodymium *tert*-butoxide ex-KOtBu (**4**).



Given our interest in the development of such alkoxides, we thought essential to continue our investigation of the synthesis of these compounds. For this purpose, we employed the newly available precursor NdCl₃(THF)₂. Indeed, the bis(THF)-adduct of NdCl₃ can be now produced in large scale by Rhodia and thus becomes readily accessible.²⁸⁴ In a view of a potential industrialization of our catalytic systems, it was necessary to check if this precursor would lead to the similar results to those observed previously with commercial anhydrous neodymium chloride.

²⁸³ Schumann, H.; Kociok-Koehn, G.; Dietrich, A.; Goerlitz, F. H. Z. Naturforsch. B: Chem. Sci. **1991**, *46*, 896-900.

²⁸⁴ Mathivet, T. WO 0228776 (Rhodia Electronics and Catalysis), **2002**.

When the reaction is carried out under the same conditions as described in §8.1.1.1, a pale blue solid was obtained in good yield (90%). The neodymium content in the crude product is consistent with the formula of **1** and residual chloride content is as low as 0.7%. However, it was not possible to characterize this complex by neither X-ray diffraction nor ^1H NMR. This results did not taint our will to fully investigate the synthesis of neodymium *tert*-butoxide from $\text{NdCl}_3(\text{THF})_2$. All the results described below in this paragraph are based only on the yield of synthesis, Nd and Cl contents in the crude product and ^1H NMR analysis of crystals.

8.1.1.3.1. Effect of the reaction time

The typical reaction time we used for salt metathesis reactions was 72 h. This reaction time is definitely too long for its industrial preparation. So we studied the effect of the reaction time on both the yield of the synthesis and the nature of the product (Table 14). Decreasing the reaction time from 72 h to 24 h does not modify the yield of the reaction and Nd and Cl contents remain unchanged. A reaction time of 4 h affords a lower yield (71%) with no change in the elemental analysis of the crude product. The highest yield of the reaction can be obtained within 24 h, Nd and Cl contents in the resulting complex being unaffected by the reaction time. However, a possible evolution of the structure complex throughout the reaction course can not be discarded.

This result can only be attributed to reactions performed with $\text{NdCl}_3(\text{THF})_2$ and not to those with commercially available anhydrous NdCl_3 . Indeed, $\text{NdCl}_3(\text{THF})_2$ proved to be more reactive than NdCl_3 towards alkali-metal alkoxides. This behavior can be ascribed to the slow *in situ* formation of the THF-adduct with NdCl_3 , adduct that might be the reactive species in this reaction process. It can be noticed that a similar observation was made during the preparation of NdN_3 .

8.1.1.3.2. Influence of the neodymium concentration

Increasing the concentration of the starting reagents was a prime objective in the study. Indeed, in the initial experimental conditions, the concentration of Nd is rather low (0.1 M). When the concentration is increased to 0.5 M, the stirring stops before completion of the addition of the NaOtBu solution because of an increase of viscosity (Table 14). After complete addition of the sodium salt, a blue gummy solid is obtained. This solid was not analyzed. Thus, the synthesis of neodymium *tert*-butoxides in THF with high Nd concentrations seems quite delicate. On that account, we studied the reaction in a non-polar solvent in which the separation of the neodymium alkoxide and the resulting chloride salt might be favored.

Table 14. Synthesis of neodymium *tert*-butoxides by salt metathesis with various Nd precursors.

Nd precursor (mmol)	reaction time (h)	[Nd] (M)	yield (%)	% Nd	% Cl
------------------------	----------------------	----------	-----------	------	------

anhydrous NdCl ₃ , (Strem) (10)	72	0.1	58	38.1	0.75(5)
NdCl ₃ (THF) ₂ (10)	25	0.1	88	34.3	0.72(5)
NdCl ₃ (THF) ₂ (10)	4	0.1	71	36.7	0.84(5)
NdCl ₃ (THF) ₂ (10)	4	0.5	nd	nd	nd

Reactions carried out at RT with NaOtBu (30 mmol) in THF.

8.1.1.4. From NdCl₃(THF)₂ in hexanes

8.1.1.4.1. Reaction time

Contrary to anhydrous NdCl₃, NdCl₃(THF)₂ allows the reaction to be carried out in hexanes (Table 15). This might be ascribed to the higher solubility of NdCl₃(THF)₂ in hexanes due to the coordinated THF molecules. Thus, under the typical experimental conditions, similar conversion (85-90%), and Nd and Cl contents (Nd = 35% and Cl ≈ 1%) were obtained for reaction times between 20 and 96 h as it was observed in THF. Decreasing the reaction time results in lower yields. However, a rather high chloride content is observed. This can be accounted for the incomplete transfer of the alkali-metal alkoxide solution onto the neodymium solution, resulting in an excess of NdCl₃(THF)₂, quite soluble in hexanes. Consequently, the reaction was performed in one pot meaning that NdCl₃(THF)₂ and NaOtBu were placed together in the same flask before addition of the solvent of reaction (see Experimental section). In this case, the reaction needs a thermoregulation (exothermic reaction); the residual chloride content falls to 0.07% and the neodymium content is in agreement with the formation of a trinuclear complex, always with a very good yield (93%).

8.1.1.4.2. Neodymium concentration

When the neodymium concentration is increased to [Nd] = 0.5 M, similar results are obtained after 20 h in larger scale reactions for both NaOtBu and KOtBu (Table 15). Complexes **5** and **6** are respectively obtained. So, it is now possible to prepare quantitatively, rapidly and cleanly (no chloride contamination) neodymium *tert*-butoxide from NdCl₃(THF)₃ in concentrated hexanes solution. In addition, the reaction time was not optimized and the results after 4 h already show a quantitative reaction.

Table 15. Synthesis of neodymium *tert*-butoxides by salt metathesis in hexanes.

Nd precursor (mmol)	alkali-metal alkoxide (mmol)	reaction time (h)	[Nd] (M)	yield (%)	% Nd	% Cl
NdCl ₃ (THF) ₂ (10)	NaOtBu (30)	96	0.1	84	37.1	0.72(5)
NdCl ₃ (THF) ₂ (10)	NaOtBu (30)	27	0.5	81	37.3	1.29(0)
NdCl ₃ (THF) ₂ (10)*	NaOtBu (30))	24	0.5	93	35.1	0.07(5)

$\text{NdCl}_3(\text{THF})_2$ (10)	NaOtBu (30)	4	0.5	91	34.3	1.10(5)
$\text{NdCl}_3(\text{THF})_2$ (100)*	NaOtBu (300)	24	0.5	85	35.4	0.15(5)
$\text{NdCl}_3(\text{THF})_2$ (100)*	KOtBu (30)	24	0.5	71	32.4	0.22(5)

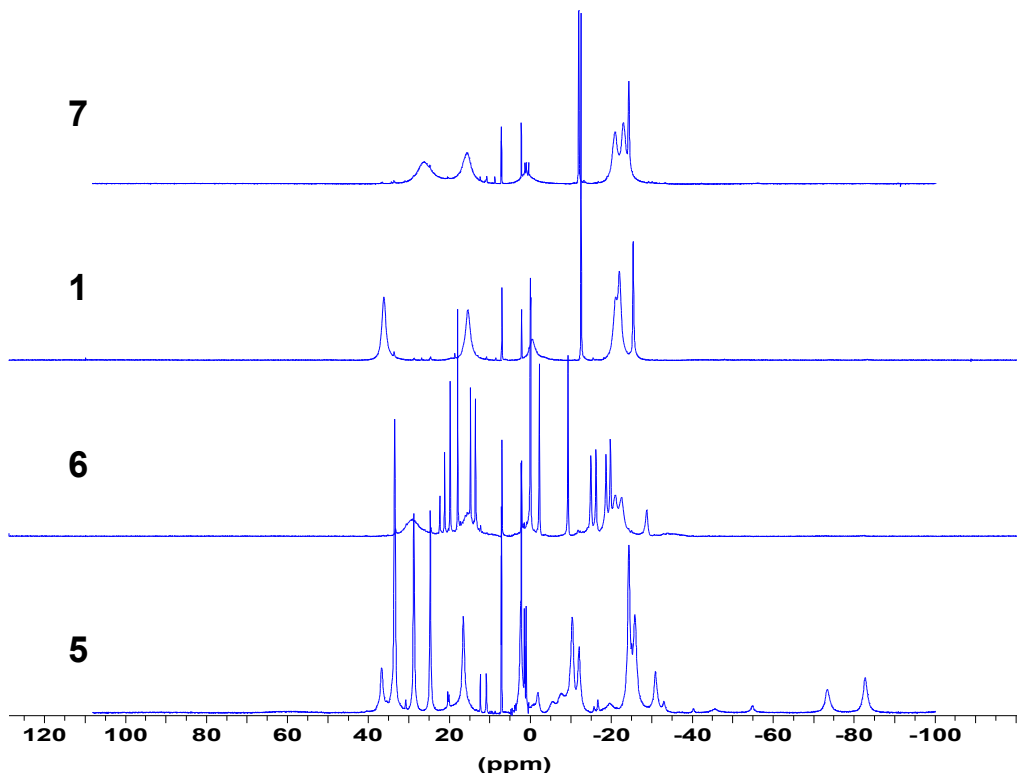
Reactions carried out in hexanes at RT. * one-pot reaction.

8.1.1.5. Conclusions

In conclusion, we were able to fully characterize the product of salt metathesis between anhydrous neodymium chloride and sodium *tert*-butoxide prepared in THF. But the structure of the neodymium of *tert*-butoxides seems strongly dependent on the nature and purity of the alkali-metal alkoxide. Even if we were not able to obtain X-ray crystal structures for the different crystals grown from synthesis carried out with MOtBu ($\text{M} = \text{Li}$ and K) and NdCl_3 and $\text{NaOtBu}/\text{NdCl}_3$ in different solvents, we have evidenced the existence of different structures (isomers?) by ^1H NMR analysis.

Furthermore, in spite of the very promising and interesting results obtained with $\text{NdCl}_3(\text{THF})_2$, we must be again very careful in our conclusions. Indeed, without any structural data, we can just relate the quantitative transformation of neodymium chloride into neodymium alkoxide in a reaction time within a range of 4 to 96 h, yielding products with equivalent elemental analyses. ^1H NMR spectra obtained for single crystals from the different syntheses are quite dissimilar (Figure 48). Since the solid-state structure of **1** is retained in toluene solution, this indicates the likely existence of different structures in the solid state. Various complexes might be obtained because of modified experimental conditions or different conditions of crystallization. Unfortunately, the exact structure of these alkoxides could not be established by X-ray crystal structure determination because of disorder problems and instability of the neodymium complexes. However, by modifying the analysis conditions, this technique might be really helpfull in the near future.

Figure 48. ^1H NMR spectra of neodymium *tert*-butoxides obtained from different synthetic routes.



8.1.2. Alcoholysis reaction

This synthetic route is documented for the preparation of lanthanum *tert*-butoxide in non polar solvents yielding $\text{La}_3(\text{OtBu})_9(\text{HOtBu})_2$.²⁵⁴ We thought interesting to check if this structure is also obtained with Nd and if the replacement of a non-coordinating solvent by the strongly coordinative THF could lead to the fully characterized **1**.

8.1.2.1. Reaction in THF

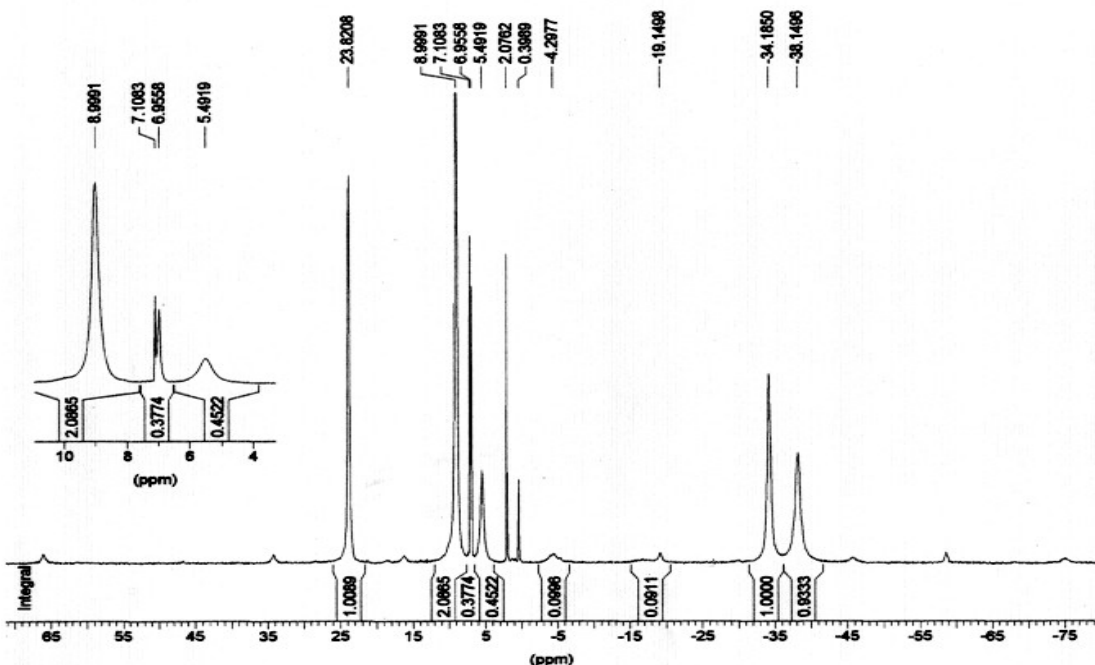
First, we will begin with the reaction performed in THF. Indeed, the treatment of $\text{Nd}[\text{N}(\text{SiMe}_3)_2]_3$ with an excess (15 equiv.) of *tert*-butanol in THF at 20 °C for 3 days yields **1** in 90% crude yield. The structure of the complex was confirmed by elemental analysis and variable temperature ^1H NMR spectroscopy.

8.1.2.2. Reaction in non polar solvents

The reaction of $\text{Nd}[\text{N}(\text{SiMe}_3)_2]_3$ with 8 equiv. (vs. Nd) of *tert*-butanol in *n*-hexane at 20 °C gives a single primary product in 90% yield. Crystallization from toluene yielded violet-blue crystals that analyzed for $\text{Nd}_3(\mu_3\text{-OtBu})_2(\mu_2\text{-OtBu})_3(\text{OtBu})_4(\text{HOtBu})_2$ (**7**). Variable temperature ^1H NMR studies were carried out to derive structural information on this alkoxide in solution. The room temperature 200 MHz ^1H NMR spectrum of **7** in toluene- d_8 showed very broad resonances characteristic of a fluxional behavior and temperatures below 5 °C were required to slow down the exchange process. Due to effects of the paramagnetic neodymium centers, important variations in the chemical shifts were observed in the

temperature range of -75 to 5 °C, causing incidental, potentially misleading, overlapping of some resonances, e.g. at -15 and -65 °C. The ^1H NMR spectrum of **7** at -45 °C showed a major series, accounting for $96 \pm 2\%$ of total OtBu groups, of six well-resolved, relatively sharp resonances with intensities in the ratio $18:36:9:2:18:18$, from lower to higher field (Figure 49).

Figure 49. ^1H NMR spectrum of **7** at -45 °C in toluene- d_8 .



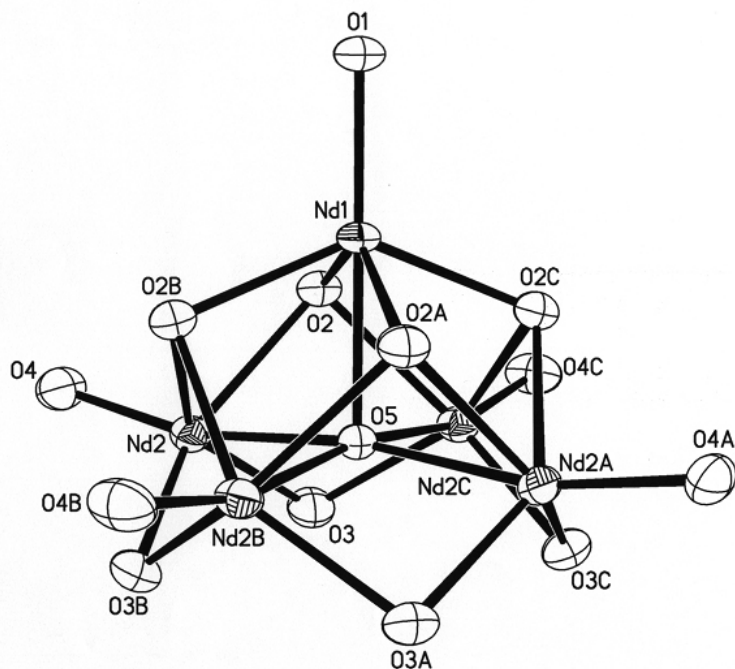
This pattern is fully consistent with the trinuclear geometry established for the equivalent yttrium and lanthanum compounds,²⁵⁴ isostructural to **1**, that contains two capping $\mu_3\text{-OtBu}$ groups magnetically equivalent (singlet of relative intensity 2), three bridging $\mu_2\text{-OtBu}$ groups in two different environments ($2 + 1$), and two terminal ligands for each metal of which two out of six are the coordinated $t\text{BuOH}$ ($2 + 4$). Beside this major set of resonances, a significant minor series of six peaks was also observed in the variable temperature NMR spectra; its relative intensity vs. the major series ($4 \pm 2\%$) did not vary within uncertainty in the temperature range of -75 to 5 °C. This suggests, as in the case of **1**, the existence of two isomeric structures differing in the relative location of the coordinated alcohols, i.e. either both on the same side or on opposite sides of the Nd_3 plane.

8.1.2.3. Evolution of $\text{Nd}_3(\mu_3\text{-OtBu})_2(\mu_2\text{-OtBu})_3(\text{OtBu})_4(\text{HOtBu})_2$

Interestingly, stirring a toluene solution of complex **7** for two weeks at room temperature resulted in the formation of the oxo complex $\text{Nd}_5(\mu_5\text{-O})(\mu_3\text{-OtBu})_4(\mu_2\text{-OtBu})_4(\text{OtBu})_5$ (**8**). The variable temperature ^1H NMR spectra of **8** in the range of -70 to 20 °C displayed broad, unresolved resonances and did not provide an insight into the solution structure of **8**. The identity of **8** was established by X-ray diffraction (Figure 50). The molecular structure

corresponds to a pentagonal cluster made of four basal and one apical neodymium centers having each one terminal $OtBu$ group, connected by four μ_3 - and four μ_2 -bridging $OtBu$ groups and comprising a central μ_5 -oxo ligand.

Figure 50. ORTEP plot of $Nd_5(\mu_5\text{-O})(\mu_3\text{-}OtBu)_4(\mu_2\text{-}OtBu)_4(OtBu)_5$ (**8**) with probability ellipsoids at 30% (carbon and hydrogen atoms omitted for clarity).



This corresponds to the basic square pyramidal framework observed for lanthanide oxoisopropoxides $Ln_5(\mu_5\text{-O})(OiPr)_{13}$ ^{232,285} and the lanthanum equivalent of **8**, which has been independently reported during the course of this study.²³³ The Nd_5 square pyramid in **8** is quite regular as revealed by the equivalence of the basal Nd atoms and the nearly 90° Nd–O–Nd bond angles ($Nd(2B)\text{--}O(5)\text{--}Nd(2)$, $89.60(3)^\circ$; $Nd(1)\text{--}O(5)\text{--}Nd(2)$, $94.8(2)^\circ$), with the apical/basal Nd–Nd distance longer than the basal/basal one ($3.6550(6)$ vs. $3.5139(5)$ Å). The Nd–O distances of the terminal alkoxide ligands ($Nd(1)\text{--}O(1)$, $2.146(9)$; $Nd(2)\text{--}O(4)$, $2.138(6)$ Å), the doubly bridging ligands ($Nd(2)\text{--}O(3)$, $2.351(3)$ Å) and the triply bridging ligands ($Nd(1)\text{--}O(2)$, $2.418(5)$; $Nd(2)\text{--}O(2)$, $2.523(3)$ Å) all fall within the range of values observed for the terminal Nd–O(alkoxy) bonds in complex **1** and the aforementioned neodymium alkoxy complexes. Also, the terminal ligands are associated with nearly linear Nd–O–C angles ($178.8(6)$ – $180.0(0)^\circ$), much larger than those for bridging ligands ($121.1(3)$ – $131.18(12)^\circ$). Contrary to the lanthanum equivalent of **8**,²³³ but as observed in $[Nd_5(\mu_5\text{-O})(OiPr)_{13}]$,²³⁴ the apical Nd– μ_5 -oxo bond length ($Nd(1)\text{--}O(5)$, $2.473(9)$ Å) is only slightly shorter than those involving the basal neodymium centers ($Nd(2)\text{--}O(5)$, $2.4933(8)$ Å) (Table 16).

Table 16. Selected bond lengths [Å] and angles [°] for complex **8**.

²⁸⁵ (a) Bradley, D. C.; Chudzynska, H.; Frigo, D. M.; Hursthouse, M. B.; Mazid, M. A. *J. Chem. Soc., Chem. Commun.* **1988**, 1258–1259. (b) Bradley, D. C.; Chudzynska, H.; Frigo, D. M.; Hammond, M. E.; Hursthouse, M. B.; Mazid, M. A. *Polyhedron* **1990**, 9, 719–726.

Nd(1)–O(1)	2.146(9)	Nd(1)–O(1)–C(1)	180.000(3)
Nd(1)–O(2)	2.418(5)	Nd(1)–O(2)–C(4)	126.5(5)
Nd(1)–O(5)	2.473(9)	Nd(2)–O(2)–C(4)	121.1(3)
Nd(2)–O(2)	2.523(3)	Nd(1)–O(2)–Nd(2)	95.38(15)
Nd(2)–O(3)	2.351(3)	Nd(2)–O(3)–C(7)	131.18(12)
Nd(2)–O(4)	2.138(6)	Nd(2)–O(3)–Nd(2C)	96.73(18)
Nd(2)–O(5)	2.4933(8)	Nd(2)–O(4)–C(10)	178.8(6)
O(1)–C(1)	1.402(18)	Nd(2)–O(5)–Nd(2A)	170.4(4)
O(2)–C(4)	1.458(10)	Nd(1)–O(5)–Nd(2)	94.8(2)
O(3)–C(7)	1.415(13)	Nd(2B)–O(5)–Nd(2)	89.60(3)
O(4)–C(10)	1.423(12)	Nd(1)–O(5)–Nd(2B)	94.8(2)

8.2. Other neodymium *tert*-alkoxides

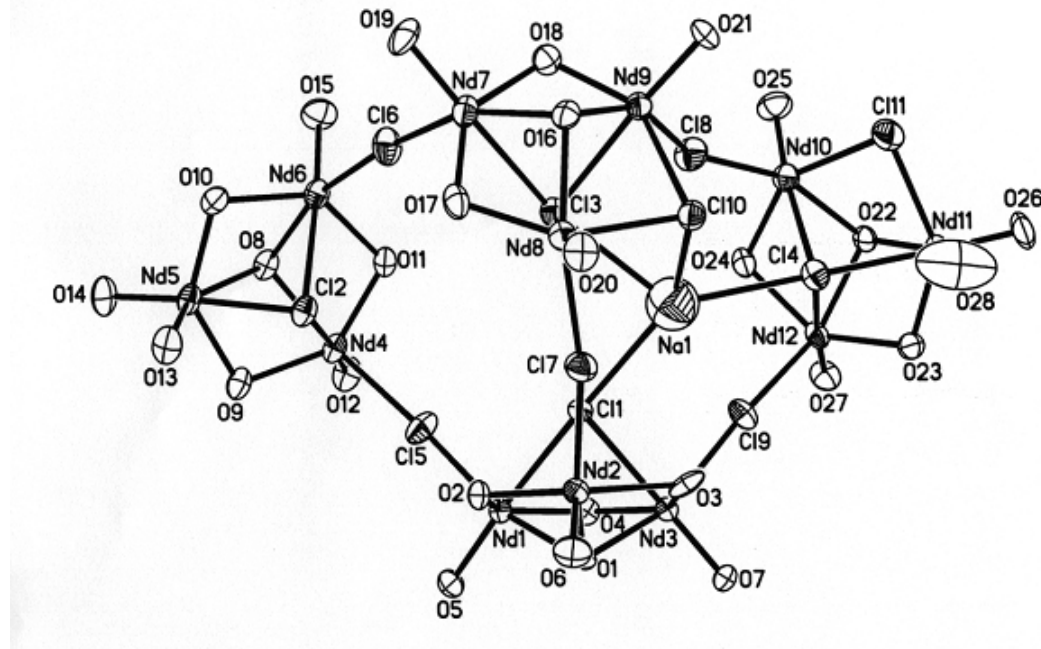
8.2.1. Synthesis of neodymium *tert*-amyloxide by salt metathesis

The preparation of neodymium *tert*-amyloxide from NdCl₃ and NaOtAm in THF at room temperature was similarly performed, giving a pale-blue solid (**9**) in 66% yield. The variable temperature ¹H NMR spectra of **9** in toluene-*d*₈ and in THF-*d*₈ are complicated. In fact, the expected multiplicity (singlets, triplets, quartets) for the different types of hydrogen was hampered by the paramagnetic neodymium centers and the spectra featured many singlet-like resonances that turned out uninformative. Previous reports have shown that the *tert*-butoxide and the *tert*-amyloxide groups enforce similar structures in group 3 (Y, La, Pr) alkoxide chemistry.²⁵⁴⁻²⁸⁶ It is therefore reasonable to assume that **9** has the same structure as **1**. This hypothesis is comforted by the nearly identical reactivity of **1** and **9** in ethylene polymerization chemistry (*vide infra*). In addition, the reaction performed with KO*t*Bu proceeds similarly (yield, product aspect,...). However, the catalytic data in ethylene polymerization prove again that, as proposed for neodymium *tert*-butoxide, the potassium alkoxide affords likely a different complex.

When the above salt metathesis reactions between NdCl₃ and 3 equiv. of NaOtAm was carried out in diethyl ether in place of THF as solvent, the reaction took a different course. The crude product recovered after usual workup was slightly soluble in hexane and toluene, as observed for the corresponding *tert*-butoxide (see §8.1.1.1), and its ¹H NMR spectrum was complex, featuring many resonances with variable line shape. Recrystallization of the crude product from toluene gave a crystalline product (**10**) in low yield; however, the latter was no longer soluble in toluene nor in THF. X-ray quality crystals allowed to establish its geometry in the solid state (Figure 51).

²⁸⁶ Hubert-Pfalzgraf, L. G.; Daniele, S.; Bennaceur, A.; Daran, J. C.; Vaissermann, J. *Polyhedron* **1997**, *16*, 1223-1234.

Figure 51. ORTEP plot of $\text{Nd}_{12}(\text{OtAm})_{26}(\text{HOtAm})_2\text{Cl}_{11}\text{Na} \cdot (\text{OEt}_2)_2$ (**10**) with probability ellipsoids at 30% (carbon and hydrogen atoms omitted for clarity).



$\text{Nd}_{12}(\text{OtAm})_{26}(\text{HOtAm})_2\text{Cl}_{11}\text{Na} \cdot (\text{OEt}_2)_2$ (**10**) has an unprecedented complex aggregate structure basically formed of four independent trinuclear Nd_3 units that are linked by sharing μ_2 -chloro ligands (Figure 51). In addition, the sodium atom is coordinated by four chlorine atoms related to three Nd_3 units and that enforces no symmetry in the molecular structure.²⁴¹ Schematically, it is possible to divide the structure of **10** in four trimetallic fragments **A–D** and one NaCl molecule (Figure 51):

- A:** $\text{Nd}(1)-\text{Nd}(3), \text{Nd}_3(\mu_3-\text{OtAm})(\mu_3-\text{Cl})(\mu_2-\text{OtAm})_3(\text{OtAm})_3\text{Cl}$
- B:** $\text{Nd}(4)-\text{Nd}(6), \text{Nd}_3(\mu_3-\text{OtAm})(\mu_3-\text{Cl})(\mu_2-\text{OtAm})_3(\text{OtAm})_3\text{Cl}(\text{HOtAm})$
- C:** $\text{Nd}(7)-\text{Nd}(9) \text{Nd}_3(\mu_3-\text{OtAm})(\mu_3-\text{Cl})(\mu_2-\text{OtAm})_3(\mu_2-\text{Cl})(\text{OtAm})_3\text{Cl}$
- D:** $\text{Nd}(10)-\text{Nd}(12), \text{Nd}_3(\mu_3-\text{OtAm})(\mu_3-\text{Cl})(\mu_2-\text{OtAm})_3(\mu_2-\text{Cl})(\text{OtAm})_3\text{Cl}(\text{HOtAm})$

The formulas for **A–D** do not describe the bridging between the fragments but show structural relationships between them and heteroleptic trinuclear complexes reported in the literature. Thus, fragments **A** and **B** have a formula unit related to $\text{Y}_3(\mu_3-\text{OtBu})(\mu_3-\text{Cl})(\mu_2-\text{OtBu})_3(\text{OtBu})_3\text{Cl}(\text{THF})_{2240}$ and, structurally, these units are nearly identical. Fragments **C** and **D** feature also a similar structure and a formula unit related to **A** and **B** except that a μ_2 -Cl ligand has replaced a μ_2 -OtAm ligand. The bond distances observed for the terminal alkoxide (2.090(8)–2.113(7) Å in **A** and **B**; 2.070(7)–2.100(7) Å in **C** and **D**), the bridging Nd–O(μ_2 -OR) (2.347(7)–2.497(7) Å in **A** and **B**; 2.314(7)–2.380(7) Å in **C** and **D**) and Nd–O(μ_3 -OR) (2.442(7)–2.521(6) Å in **A** and **B**; 2.452(7)–2.555(7) Å in **C** and **D**) are similar to those found in **1** (Table 17). The presence of two coordinated molecules of HOtAm, one in fragment **B** and one in **D**, is clearly revealed by the longer Nd–O bond distances (Nd(5)–O(13), 2.545(7) Å; Nd(11)–O(28), 2.435(12) Å) compared with the adjacent and other terminal Nd–OtAm groups (Nd(5)–O(14), 2.109(7) Å; Nd(11)–O(26), 2.089(8) Å). This is also reflected in the smaller La–O–C bond angles (Nd(5)–O(13)–C(61), 147.0(6)°; Nd(11)–O(28)–C(136), 158.2(18)°) for

the coordinated alcohols, which have only one lone pair for π -donation to vacant metal orbitals, vs. the angles of the adjacent covalently bound *tert*-amyloxy groups which have two lone pairs and therefore approach a limiting angle of 180° ($\text{Nd}(5)\text{--O}(14)\text{--C}(66)$, $176.7(9)^\circ$; $\text{Nd}(11)\text{--O}(26)\text{--C}(126)$, $174.0(10)^\circ$). Each of the four Nd_3 units has one $\mu_3\text{-Cl}$ ligand with $\text{Nd}\text{--Cl}$ bond distances in the range of $2.945(3)\text{--}3.022(3)$ Å, values that compare well with that observed in $\text{Nd}_6(\text{O}i\text{Pr})_{17}\text{Cl}$ ($3.05(1)$ Å)²³⁸ where the chlorine atom is equidistant from the six Nd atoms in a trigonal prism. All fragments **A****–****D**, as defined with the above formula units, have coordinative vacancies which are filled by linking **A****–****B**, **B****–****C**, **C****–****D**, **D****–****A** and **A****–****C** via symmetrically bridging chlorine ligands with normal $\text{Nd}\text{--}(\mu_2\text{-Cl})$ distances ($2.792(3)\text{--}2.848(3)$ Å). The $\text{Nd}\text{--Cl--Nd}$ bond angles for the links between the fragments are all similar (four in the range $169.11(12)\text{--}173.00(14)^\circ$), except the one linking fragments **C** and **D** ($151.97(13)^\circ$). This narrow angle likely results from the constraint induced by the coordination of the Na atom. Indeed, the latter is 4-coordinated by one $\mu_3\text{-Cl}$, two internal $\mu_2\text{-Cl}$ and one $\mu_2\text{-Cl}$ bridging two Nd_3 units, with $\text{Na}\text{--Cl}$ distances in the range $3.222(11)\text{--}3.339(11)$ Å. These $\text{Na}\text{--Cl}$ distances are far longer than those observed in $\text{LnNa}_8(\text{OtBu})_{10}\text{Cl}$ complexes ($\text{Ln} = \text{Y, Eu}$; $2.642(5)\text{--}3.032(5)$ Å; average $\text{Na}\text{--Cl}$, $2.82(13)$ Å).²⁴¹

Table 17. Selected bond lengths [Å] and angles [°] for complex **10**.

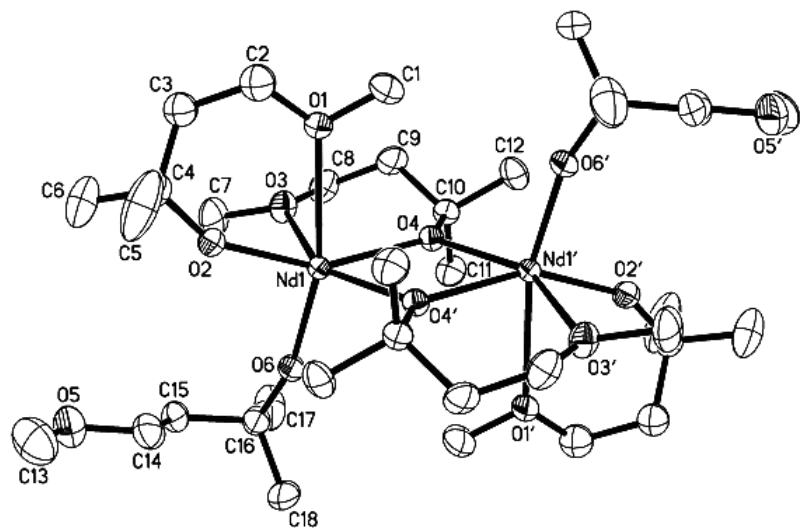
Nd(1)–O(5)	2.100(7)	Nd(1)–O(5)–C(21)	163.7(8)
Nd(1)–O(2)	2.348(7)	Nd(1)–O(2)–C(6)	127.4(7)
Nd(1)–O(1)	2.521(6)	Nd(1)–O(1)–C(1)	118.9(5)
Nd(1)–Cl(5)	2.842(3)	Nd(1)–Cl(5)–Nd(4)	169.49(13)
Nd(1)–Cl(1)	2.992(2)	Nd(1)–Cl(1)–Na(1)	177.4(2)
Nd(2)–Cl(7)	2.834(3)	Nd(8)–Cl(7)–Nd(2)	169.11(12)
Nd(2)–Cl(1)	3.009(2)	Nd(2)–Cl(1)–Na(1)	100.1(2)
Nd(3)–O(3)	2.483(7)	Nd(3)–O(3)–Nd(2)	98.0(3)
Nd(4)–Cl(5)	2.848(3)	O(12)–Nd(4)–Cl(5)	91.9(2)
Nd(4)–Cl(2)	3.010(3)	Cl(5)–Nd(4)–Cl(2)	90.87(8)
Nd(5)–O(14)	2.109(7)	Nd(5)–O(14)–C(66)	176.7(9)
Nd(5)–O(10)	2.374(7)	Nd(5)–O(10)–Nd(6)	103.2(3)
Nd(5)–O(9)	2.380(7)	Nd(5)–O(9)–Nd(4)	103.3(3)
Nd(5)–O(8)	2.442(7)	Nd(5)–O(8)–Nd(6)	98.2(2)
Nd(5)–O(13)	2.545(7)	Nd(5)–O(13)–C(61)	147.0(6)
Nd(7)–O(19)	2.090(7)	Nd(7)–O(19)–C(91)	171.1(9)
Nd(7)–O(17)	2.370(8)	Nd(8)–O(17)–Nd(7)	105.9(3)
Nd(7)–O(16)	2.555(7)	Nd(8)–O(16)–Nd(7)	96.3(2)
Nd(7)–Cl(6)	2.792(3)	Nd(7)–Cl(6)–Nd(6)	173.00(14)
Nd(7)–Cl(3)	2.991(3)	Nd(7)–Cl(3)–Na(1)	165.2(2)
Nd(8)–Cl(7)	2.808(3)	O(20)–Nd(8)–Cl(7)	95.3(2)
Nd(8)–Cl(10)	2.870(3)	Nd(9)–Cl(10)–Nd(8)	85.72(7)
Nd(8)–Cl(3)	2.945(3)	O(20)–Nd(8)–Cl(3)	173.6(2)
Nd(10)–Cl(4)	2.961(3)	Nd(10)–Cl(4)–Nd(12)	77.39(6)
Nd(12)–Cl(9)	2.799(3)	Nd(12)–Cl(9)–Nd(3)	170.39(12)

8.2.2. Synthesis of difunctional *tert*-alkoxides by alcoholysis reaction

The foregoing examples have shown that neodymium centers expand readily their coordination sphere by additional adduct formation despite the presence of the relatively bulky *tert*-butoxy and *tert*-amyloxy ligands. To enforce a lower degree of agglomeration we investigated the use of a γ -donor-functionalized alcohol. The alcoholysis reaction of Nd[N(SiMe₃)₂]₃ with 3 equiv. of the monoclinching alcohol 4-methoxy-2-methylbutan-2-ol in benzene at 20 °C gives, after recrystallization from toluene, blue crystals of Nd₂(μ_2 , η^2 -OR)₂(η^2 -OR)₂(η^1 -OR)₂ (OR = OCMe₂CH₂CH₂OMe) **11** (Figure 52). When the alcoholysis reaction was performed in THF, an oily residue was recovered after removal of the volatiles under

vacuum. Attempts to extract or to recrystallize this residue were unsuccessful. Again, the variable temperature ^1H NMR spectra in toluene- d_8 of this compound showed broad, unresolved resonances and proved uninformative with regard to its solution structure.

Figure 52. ORTEP plot of $\text{Nd}_2(\mu_2,\eta^2\text{-OR})_2(\eta^2\text{-OR})_2(\eta^1\text{-OR})_2$ (**11**) with probability ellipsoids at 30% (carbon and hydrogen atoms omitted for clarity).



An X-ray diffraction study revealed that complex **11** adopts in the solid-state a symmetric dinuclear structure in which the ether-alkoxide ligand is found in three different ligation modes (Figure 52, Table 18).

Table 18. Selected bond lengths [\AA] and angles [$^\circ$] for complex **11**.

Nd(1)–O(6)	2.1526(13)	O(4)–Nd(1)–O(3)	78.26(4)
Nd(1)–O(2)	2.1759(13)	O(4')–Nd(1)–O(3)	150.45(4)
Nd(1)–O(4)	2.3977(12)	O(2)–Nd(1)–O(1)	70.70(5)
Nd(1)–O(4')	2.3992(12)	O(4)–Nd(1)–O(1)	84.40(4)
Nd(1)–O(3)	2.5198(13)	O(4')–Nd(1)–O(1)	92.17(5)
Nd(1)–O(1)	2.6629(14)	O(3)–Nd(1)–O(1)	79.13(5)
Nd(1)–Nd(1')	3.8615(2)	C(1)–O(1)–C(2)	106.6(2)
		Nd(1)–O(1)–C(1)	119.98(13)
O(6)–Nd(1)–O(1)	163.73(5)	Nd(1)–O(1)–C(2)	126.82(16)
O(2)–Nd(1)–O(4)	154.46(5)	Nd(1)–O(2)–C(4)	151.88(12)
O(2)–Nd(1)–O(4')	112.67(5)	Nd(1)–O(3)–C(8)	129.22(12)
O(6)–Nd(1)–O(2)	98.62(5)	Nd(1)–O(3)–C(7)	115.49(14)
O(6)–Nd(1)–O(3)	89.12(5)	Nd(1)–O(4)–C(10)	132.30(11)
O(6)–Nd(1)–O(4)	104.34(5)	Nd(1')–O(4)–C(10)	120.41(10)
O(6)–Nd(1)–O(4')	103.46(5)	Nd(1)–O(4)–Nd(1')	107.22(4)
O(4)–Nd(1)–O(4')	72.78(4)	Nd(1)–O(6)–C(16)	163.57(13)
O(2)–Nd(1)–O(3)	91.21(5)	C(13)–O(5)–C(14)	112.0(2)

^[a] Only the major site-occupancy for C(2) and C(3) are listed.

The neodymium centers are symmetrically bridged by two μ_2,η^2 -ligands via the O (alkoxide) atoms (Nd(1)–O(4) bond lengths, 2.3977(12) and 2.3992(12) \AA ; O(4)–Nd(1)–O(3) bite angle, 78.26(4) $^\circ$). Each neodymium center possesses one terminal η^2 -ether-alkoxide ligand (O(2)–Nd(1)–O(1) bite angle, 70.70(5) $^\circ$) and one terminal η^1 -alkoxide ligand, and is thus 6-coordinated. The axial O(1)–Nd(1)–O(6) angle of 163.73(5) $^\circ$ is distorted from the idealized 180 $^\circ$, likely because of steric demands in the bridge and in the 6-membered chelate ring. This steric crowding is further documented by the bending of the terminal *OtBu* ligand (Nd(1)–O(6)–C(16) angle, 163.57(13) $^\circ$), as discussed for **1**. The Nd–O(alkoxide) bond lengths in **11** lie within the range of values observed for the different structural types of *OtBu* ligands in complexes **1**, **8** and **10** and the other aforementioned neodymium alkoxy complexes. The terminal Nd–O(alkoxide) bond distance in the η^2 -ligand (Nd(1)–O(2), 2.1759(13) \AA) is only slightly elongated compared to that in the η^1 -ligand (Nd(1)–O(6), 2.1526(13) \AA), indicating rather weak ring strain in the terminal η^2 -ligand. The Nd–O(ether) contact within this chelate ring (Nd(1)–O(1), 2.6629(14) \AA) compares well with the long Nd–O(THF) distance of 2.661

(4) Å observed in **1**, ascribed to steric crowding. On the other hand, the Nd–O(ether) distance in the μ_2,η^2 -ligand (Nd(1)–O(3), 2.5198(13) Å) is comparable to values found in much less crowded complexes, e.g. NdCl₃(THF)₃ (average 2.50 Å).²⁸⁰

The solid-state structure of **11** differs significantly from that observed in the homoleptic dinuclear complex Lu₂(OCMe₂CH₂OMe)₆, synthesized according to the silylamine route from the corresponding β-donor-functionalized alcohol.²⁶⁶ Lu₂(OCMe₂CH₂OMe)₆ features an asymmetric structure with three μ_2,η^2 -bridging ligands, resulting in a completely different alkoxide environment for the two lutetium centers that are, respectively, 6-coordinated and 7-coordinated. Enhanced steric flexibility of our β-functionalized alkoxy ligand and a large difference in the effective ionic radii of the 6-coordinated metal centers (Lu³⁺, 1.00 Å; Nd³⁺, 1.12 Å) presumably account for these structural changes.

9. Neodymium aryloxides: a contribution to the reported work

Our work on the synthesis of neodymium aryloxides was limited to the preparation of the (O-2,6-*t*Bu-4-Me-C₆H₂) derivatives. The synthesis of this neodymium aryloxide was well studied because of its mononuclear structure²⁴⁶ and its application for the preparation of the tris(alkyl) neodymium Nd[CH(SiMe₃)₂]₃.²²¹ For us, this complex will exhibit a great potential as catalytic precursor for butadiene (co)-polymerization (*vide infra*).

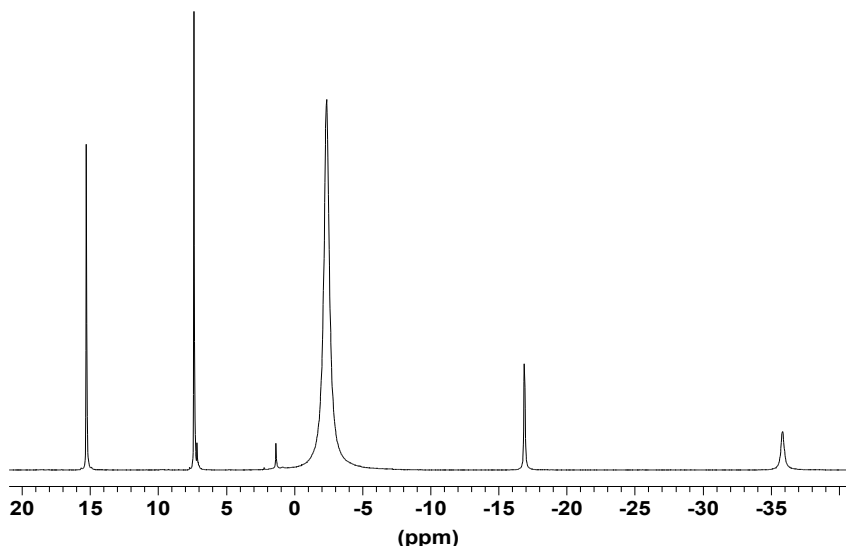
9.1. Salt metathesis

The reaction of salt metathesis as described by Lappert *et al.* affords the mononuclear complex Nd(OAr)₃(THF) in good yield.²⁴⁹ The mononuclear structure was verified by X-ray crystal determination, showing exactly the same structure as the one previously described.²⁴⁶ However, there is no available data on the characterization of this compound by ¹H NMR spectroscopy. Of course, this analytical method is not always well suited for these paramagnetic complexes,²⁸⁷ but in this case, simple spectra are obtained. Thus, the proton NMR spectrum of Nd(O-2,6-*t*Bu-4-Me-C₆H₂)₃(THF) (**12**) (prepared according to reference 249) revealed the presence of five singlets at δ 15.28, 7.36, -2.38, -16.89 and -35.81 ppm which can be attributed on the basis of the integral values respectively to the aromatic protons, methyl group, *tert*-butyl groups and THF (Figure 53). However, the two signals assigned to the THF molecules can not be unambiguously attributed. The ¹³C NMR spectrum is also quite simple, consisting of nine peaks ranging from δ 251 to 0.85 ppm (Appendix 2). The paramagnetism of the neodymium center does not affect dramatically the chemical shift of the carbons atoms of the aryloxide ligands. On the other hand, δ values of the THF molecules carbon atoms are significantly shifted downfield with a low intensity attributed to a fast intermolecular exchange on the NMR time-scale (δ 31.1 and 0.85 ppm).

²⁸⁷ (a) Bertini, L.; Luchinat, C.; *NMR of Paramagnetic molecules in biological systems*, Menlo Park, **1986**. (b) Bertini, L.; Luchinat, C. *Coord. Chem. Rev.* **1996**, *150*, 1-292.

On a synthetic aspect, we can also mention that we were able to prepare **12** by salt metathesis in hexanes using $\text{NdCl}_3(\text{THF})_2$ as Nd precursor. At room temperature with $[\text{Nd}] = 0.5 \text{ M}$, the reaction proceeds rather rapidly and quantitatively. The elemental analysis is consistent with the structure $\text{Nd}(\text{OAr})_3(\text{THF})$, structure correlated by the ^1H and ^{13}C NMR spectra (see Figure 53 and Appendix 2).

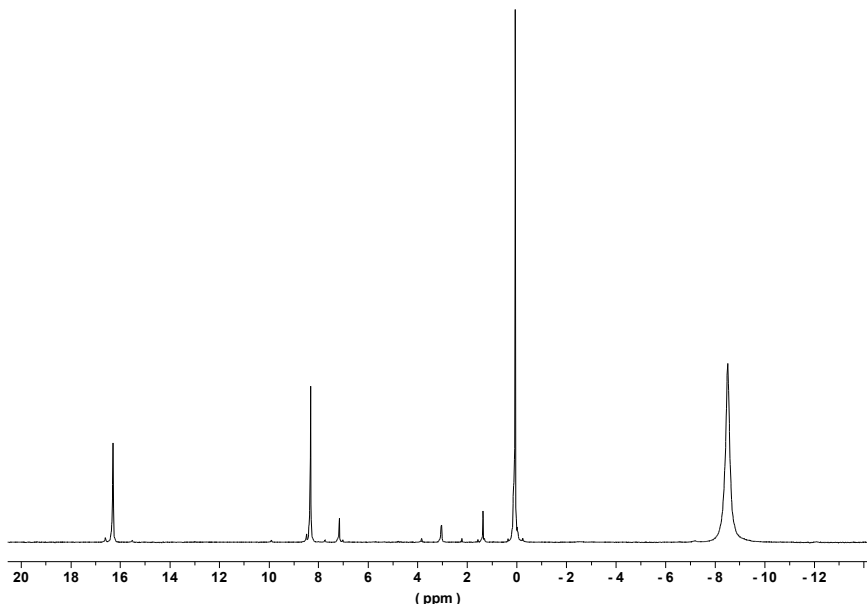
Figure 53. ^1H NMR spectrum of $\text{Nd}(\text{O}-2,6-t\text{Bu}-4-\text{Me-C}_6\text{H}_2)_3(\text{THF})$ (**12**) in C_6D_6 at 23°C .



9.2. Alcoholsysis reaction

Alcoholsysis reactions conducted in pentane or deuterated benzene yield invariably the homoleptic complex $\text{Nd}(\text{O}-2,6-t\text{Bu}-4-\text{Me-C}_6\text{H}_2)_3$ (**13**), which can be also obtained by sublimation of the THF-adduct **12** (i.e. $\text{Nd}(\text{O}-2,6-t\text{Bu}-4-\text{Me-C}_6\text{H}_2)_3(\text{THF})$) at 210°C and 10^{-3} mmHg. Again this compound was analyzed by ^1H NMR spectroscopy giving an even simpler spectrum than the corresponding THF-adduct (Figure 54). Monitoring the reaction between NdN_3 and 3 equiv. of $\text{HO}-2,6-t\text{Bu}-4-\text{Me-C}_6\text{H}_2$ gives after few minutes a clean ^1H NMR spectrum. This spectrum is composed of three signals at δ 16.32, 8.32, -8.53 ppm, corresponding respectively to the aromatic protons, methyl group and *tert*-butyl groups. It can be noticed that, in the absence of coordinated THF, the aromatic protons and the methyl group resonate at higher field whereas those of the *tert*-butyl groups are shielded along with a broadening of the signal, indicating a change in the spatial arrangement of the complex.

Figure 54. *In situ* formation of Nd(O-2,6-*t*Bu-4-Me-C₆H₂)₃ (**13**) in C₆D₆ at 23 °C monitored by ¹H NMR.

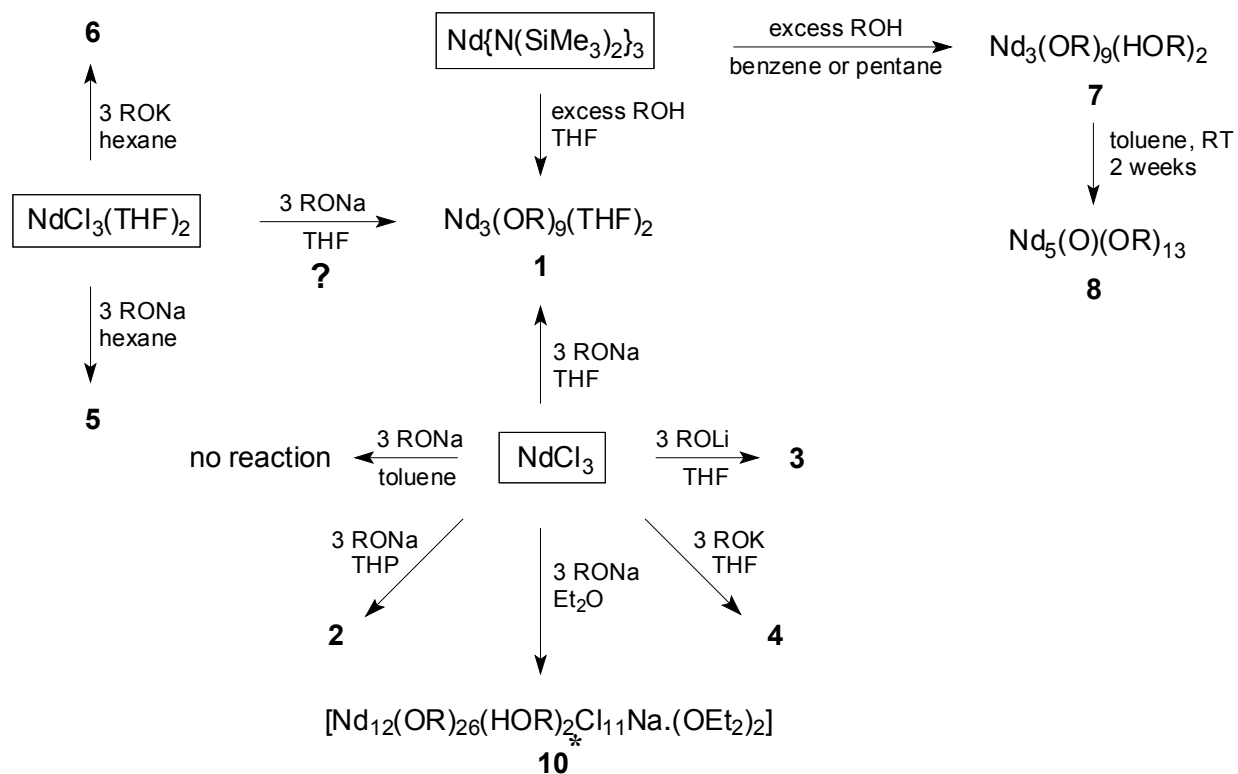


10. Conclusions

A set of polynuclear neodymium alkoxides, featuring a remarkable structural diversity and complexity, has been obtained from simple monometallic precursors. Although the detailed intermediates and interconversion processes involved in the construction of these polymetallic alkoxides remain to be clarified, the results described above give clear evidence how specific factors substantially influence the outcome of the syntheses.

Particularly striking is the importance of the reaction details, i.e. the choice of alkali metal counteraction and ether solvent, during simple salt metathesis reactions between NdCl₃ and alkali metal alkoxides. Given the numerous examples in group 3 organometallic chemistry in which the presence and specific nature of the cation strongly influences the chemistry,^{73,226} it is not unreasonable to see somewhat different results in the NaOR vs. KOR (R = *t*Bu, *t*Am) reactions. Wider variety of products and, in particular, the presence of several alkali metal atoms in yttrium alkoxides has been often associated with LiO*t*Bu (vs. NaO*t*Bu) since lithium appears to be more readily carried along in these systems.^{239,240,243} The formation with the early lanthanide Nd³⁺ of homoleptic alkoxides **1**, **9** and heteroleptic complex aggregate **10**, upon replacing THF by Et₂O, suggests that factors other than steric considerations should be also taken into account. The discrepancy noticed between ethers could be due to the different solubility of metal alkali chlorides and/or LnCl₃ in these solvents. In addition, the ability of LnCl₃ to form THF adducts (LnCl₃•OEt₂ adducts are not reported in the literature) can also be a likely reason for such differences. The various synthetic routes to neodymium *tert*-butoxides are summarized on Scheme 26.

Scheme 26. Various synthetic routes to neodymium *tert*-butoxides.



Finally, a new synthetic route was developed for the synthesis of Nd(O-2,6-*t*Bu-4-Me-C₆H₂)₃(THF) (**12**). This neodymium aryloxide as well as the homoleptic Nd(O-2,6-*t*Bu-4-Me-C₆H₂)₃ (**13**) complex were easily characterized using ¹H NMR, an analytical method often neglected for these paramagnetic species.

Chapter 3

Methyl methacrylate polymerization

11.

12. Methyl methacrylate polymerization: preliminary screening

As stated in the presentation of the research project, our objective is the development of new catalyst systems based on the use of group 3 alkoxides and a dialkylmagnesium reagent. So in this study, we focused mainly on the use of $\text{Ln}_3(\text{OtBu})_9(\text{THF})_2$ ($\text{Ln} = \text{La, Nd}$) and $\text{Y}_3(\text{OtBu})_8\text{Cl}(\text{THF})_2$, all readily prepared by salt metathesis between MCl_3 ($\text{M} = \text{Y, La, Nd}$) and NaOtBu in THF (see Chapter 2 §8.1.1.1), combined with di-*n*-hexylmagnesium (DHM) as catalyst system. We have shown that few examples were reported regarding the use of lanthanide alkoxides in MMA polymerization, systems based on lanthanide isopropoxides.¹⁵⁴⁻¹⁵⁸ As far as we know, none of these systems allowed syndiotactic and/or controlled polymerizations.

The experimental procedure we have employed in this study derived from preliminary results that we obtained with $\text{MOtBu}/\text{MgR}_2$ ($\text{M} = \text{Li, Na, K}$) as catalyst systems in MMA polymerization. Comparatively to the sole dialkylmagnesium as initiating system, its association with an alkali-metal *tert*-butoxide allowed quantitative polymerizations and lower polydispersities to be obtained (yield > 90% and $M_w/M_n < 1.5$). When DHM is combined with LiOtBu , a highly isotactic PMMA can be prepared ($\text{mm} = 84\%$).²⁸⁸ The possible *in situ* formation of magnesiates²⁸⁹ species was proposed to explain this change of catalytic behavior.

Consequently, the reactions were performed as follows: the lanthanide alkoxide and DHM are mixed for 1 h at the desired temperature, then this catalytic solution is transferred into the reaction flask followed by the monomer. The polymerization is conducted for 1 h at the desired temperature, typically 0 °C.

Under these experimental conditions, none of the above alkoxides initiates as such MMA polymerization. But, when combined with one mol equivalent (vs. Ln) of DHM, they all allowed complete conversion of MMA within 1 h to yield syndiotactic-rich PMMA ($\text{rr} = 74\text{-}80\%$). The polymers recovered under these conditions have a broad molecular weight distribution (Table 19).

Table 19. Lanthanide *tert*-butoxide/DHM catalyst systems in MMA polymerization.

Ln	Ln/Mg	yield (%)	$M_n(10^{-3})$	M_w/M_n	tacticity (%)		
					rr	mr	mm
Y	1	100	40	2.7	80	15	5
La	1	100	22	5.9	74	19	7
Nd	1	100	16	8.2	76	16	8

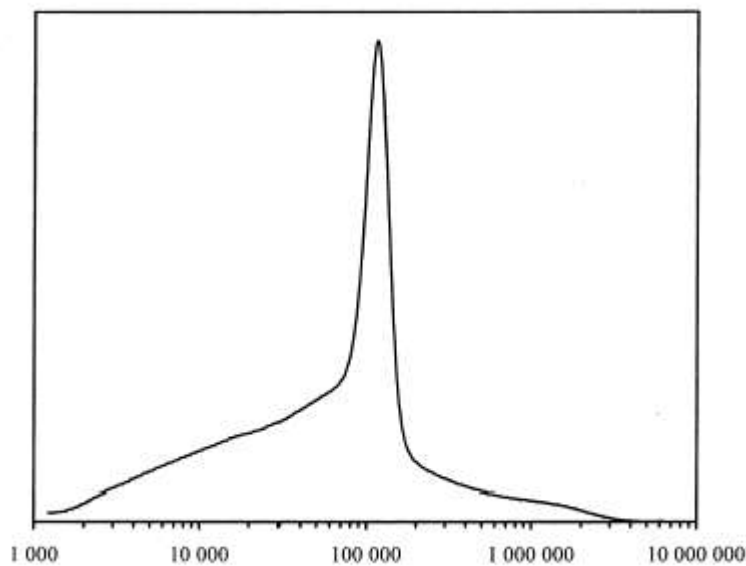
Conditions: a solution of DHM (1 mmol) and lanthanide alkoxide in toluene (100 mL) was stirred for 1 h at RT; MMA (50 mmol) was then added via syringe and the reaction mixture was stirred for 1 h at 0 °C.

²⁸⁸ Gromada, J.; Fouga, C.; Chenal, T.; Mortreux, A.; Carpentier, J.-F. *Macromol. Chem. Phys.* **2002**, *203*, 550-555.

²⁸⁹ (a) Screttas, C. G.; Micha-Screttas, M. *J. Organomet. Chem.* **1985**, *290*, 1-13. (b) Screttas, C. G.; Micha-Screttas, M. *J. Organomet. Chem.* **1986**, *316*, 1-13. (c) Hanawalt, E. M.; Richey, H. G. *J. Am. Chem. Soc.* **1990**, *112*, 4983-4984. (d) Richey, H. G.; DeStephano, J. P. *J. Org. Chem.* **1990**, *55*, 3281-3286.

The size exclusion chromatograph for the PMMA produced from the La-based system (Figure 55) showed, however, the emergence of a sharp signal ($M_w/M_n = 1.03$; $M_n = 112,000$) out of the broad envelope, indicating that part of the polymer (28 wt%) was efficiently initiated. The same observation was made for the Nd-based initiator system though the molecular weight for this fraction of PMMA was about one order of magnitude lower, indicating presumably a higher efficiency of initiation ($M_w/M_n = 1.03$; $M_n = 13,000$; 25 wt%). The formation of such well-defined grade of PMMA was not distinctly observed in the polymer samples obtained upon using the yttrium *tert*-butoxide; this possibly results from the different chemical structure of this precatalyst compared to the La and Nd alkoxides, in particular by the presence of a bridging chlorine atom.²³⁹

Figure 55. SEC trace of PMMA produced from $\text{La}_3(\text{OtBu})_9(\text{THF})_2/\text{DHM}$ combination ($\text{La}/\text{Mg} = 1:1$)



These preliminary results suggest that the Nd precatalyst affords higher efficiency of initiation in MMA polymerization. Since we have fully characterized this Nd alkoxide and a higher catalytic activity is generally observed with neodymium-based catalyst, we have decided to optimize the catalyst system composed of $\text{Nd}_3(\text{OtBu})_9(\text{THF})_2$ (**1**) and DHM. Many parameters have been studied such as the Nd/Mg ratio as well as the temperatures for *in situ* activation of the system components and for polymerization. Also, other alkylating agents or cocatalysts have been evaluated in association with $\text{Nd}_3(\text{OtBu})_9(\text{THF})_2$, and the nature of the neodymium precursor was also varied.

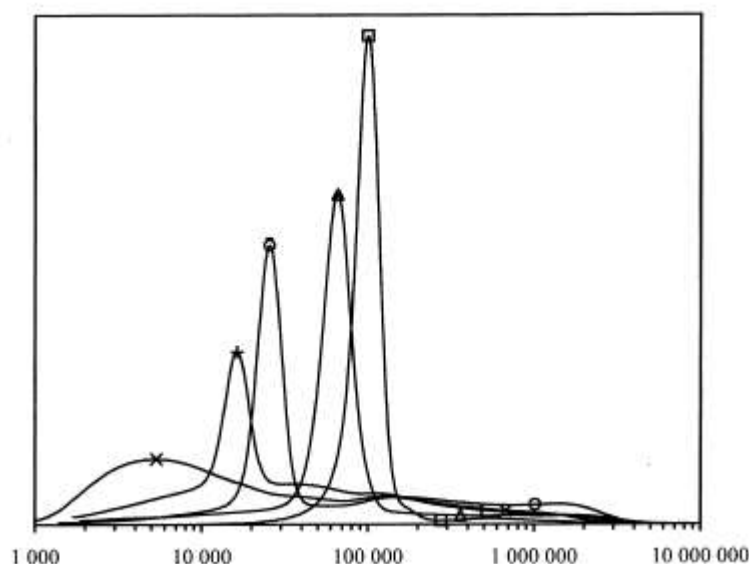
13. Optimization of the $\text{Nd}_3(\text{OtBu})_9(\text{THF})_2/\text{Mg}(n\text{-Hex})_2$ catalyst system

13.1. Influence of Nd/Mg ratio

The ratio Nd/Mg was varied from 0.33 to 10. The SEC traces (Figure 56) clearly show that an increase of the Nd/Mg ratio leads to an enrichment of the narrow polydispersity PMMA

fraction ($M_w/M_n \leq 1.2$) in the crude final polymer recovered after 1 h reaction while a decrease of Nd/Mg leads to lower yield and syndiotacticity (Table 20).

Figure 56. SEC traces of PMMAs produced from 1/DHM combinations. (conditions see Table 20) (X) Nd/Mg = 0.33; (+) Nd/Mg = 1.0; (o) Nd/Mg = 3.3; (Δ) Nd/Mg = 5.0 and () Nd/Mg = 10.



At $Nd/Mg \geq 5$, from 80%-enriched to virtually unimodal PMMA with relatively low molecular weight ($M_n = 20\text{-}90,000$) and narrow MWD was obtained after 1 h reaction. At this ratio the narrow polydispersity fraction becomes significant: the whole polymer product contained 88 wt% of a narrow polydispersity fraction with $M_n = 51,000$ and $M_w/M_n = 1.10$, and 12 wt% of PMMA with $M_n = 252,000$ and $M_w/M_n = 1.76$. The formation of PMMA with high polydispersity can be ascribed, at least for low Nd/Mg ratio, to the anionic uncontrolled polymerization initiated by a dialkylmagnesium residue. For $Nd/Mg = 10$, the undesired PMMA fraction with broad molecular weight distribution becomes negligible (< 3 wt%). Excess of $Nd_3(OtBu)_9(THF)_2$ vs. DHM above this limit, induced however, a significant decrease in the polymer yield. This behavior can be attributed to the lower concentration of active species yielding either a very slow polymerization or a fast deactivation due to important side reactions. However, extension of the reaction time to 2 h does not allow a significant increase of the yield, confirming a deactivation of the active species during the reaction course. In addition, a broadening of the molecular weight distribution is also observed. The SEC trace shows a shoulder in the region of the low molecular weight polymer accounting for termination and/or transfer reactions, or a secondary slow initiation process (Table 20).

Table 20. Influence of Nd/Mg ratio in $\text{Nd}_3(\text{OtBu})_9(\text{THF})_2/\text{Mg}(n\text{-Hex})_2$ systems.

Nd/Mg	yield (%)	$M_n(10^{-3})$	M_w/M_n	tacticity (%)		
				rr	mr	mm
0.33	85	9.4	2.5	59	18	23
1.0	100	16	8.2	76	16	8
3.3	100	150	3.1	77	16	7
5.0	100	70 ^a	1.80 ^a	77	20	3
10	40	86	1.06	76	22	2
10 ^b	50	104	1.79	75	21	4

Conditions: a solution of DHM and **1** (0.33 mmol, 1.0 mmol Nd) in toluene (100 mL) was stirred for 1 h at RT; MMA (50 mmol) was then added via syringe and the reaction mixture was stirred for 1 h at 0 °C. ^a average values for the entire polymer sample (see text for details). ^b reaction time: 2 h.

The dependence of polymerization on time was also investigated. The SEC traces showed the rapid formation of a finite amount (ca. 10% of initial monomer) of high molecular mass PMMA (polymer B, $M_n \geq 150,000$) in the early stage of polymerization and a gradual, comparatively slow conversion of the monomer to relatively low molecular weight PMMA (polymer A) with very narrow MWD (Figure 56 and Table 21). Despite the low M_w/M_n ratios, plots of M_n vs. yield of the low molecular weight polymers did not exhibit a linear relationship; this indicates that polymerization with these dialkylmagnesium/rare earth *tert*-butoxide systems does not proceed in living, although controlled manner (Table 21). The initiation efficiency ranges from 3 to 9% assuming initiation of one PMMA chain per alkylated Nd atom. For all of these experiments, the syndiotacticity was in the range 76–81% (rr triads), suggesting a syndio-rich content of the uncontrolled PMMA (see Appendix 3 for typical ^1H NMR spectrum of PMMA obtained with **1**/DHM). Given the low syndiotacticity (rr = 42%) and yield (< 5%) observed with DHM under the same conditions, the initiation of the polymer B by the latter might be ruled out (see §13.1) to the detriment of a new uncontrolled initiating species, arising from the combination of $\text{Nd}_3(\text{OtBu})_9(\text{THF})_2$ with DHM.

Table 21. Variation of the polymerization time for Nd/Mg = 5.0.

t_{polym} (h)	yield (%)	polymer A			polymer B		
		$M_n(10^{-3})$	M_w/M_n	wt%	$M_n(10^{-3})$	M_w/M_n	wt%
0.25	27	27	1.10	56	166	1.88	44
0.50	54	37	1.09	69	237	2.3	31
1.0	100	51	1.10	88	252	1.76	12

Conditions: a solution of DHM and **1** (0.33 mmol, 1.0 mmol Nd) in toluene (100 mL) was stirred for 1 h at RT; MMA (50 mmol) was then added via syringe and the reaction mixture was stirred for a desired time at 0 °C.

13.2. Activation temperature

Assuming that the active species formed by the combination $\text{Nd}_3(\text{OtBu})_9(\text{THF})_2/\text{DHM}$ are alkyl-lanthanide species (*vide infra*), we can consider that the latter might be rather unstable given the absence of stabilizing ancillary ligand on the neodymium center. So, in order to increase their stability, the activation temperature was modified. Thus, an increase of the activity, i.e., an increase of the initiation efficiency is expected.

Decreasing the activation temperature (T_{act}) of the precursors from 0 to -20 °C resulted in a slight increase of the rr triads and a narrower MWD, especially noticeable at low Nd/Mg ratios (Table 22). The increase in the initiation efficiency is apparent for Nd/Mg = 10 since the number-average molecular weight decreases with a yield increase. In this case, the initiation efficiency goes from 3 to 6% (from 25 to 50% if we consider the formation of one polymer chain per DHM), indicating a higher concentration of active species for the controlled polymerization of MMA ($\times 2$), i.e. a low thermal stability of the active species. In addition, the polymerization really appeared to be best conducted at 0 °C or below, since at 20 °C a significant broadening of molecular weight distributions was noticed (Table 22).

Table 22. Effect of activation temperature in MMA polymerization.

Nd/Mg	T_{act} (°C)	yield (%)	$M_n(10^{-3})$	M_w/M_n	tacticity (%)		
					rr	mr	mm
3.3	20	100	150	3.1	77	16	7
3.3 ^a	0	100	130	1.78	78	19	3
5.0	20	100	51 ^b	1.10 ^b	77	20	3
5.0 ^a	0	100	54	1.26	78	19	3
5.0 ^c	20	100	59	3.1	77	21	2
10	20	40	80	1.06	76	22	2
10 ^a	0	63	60	1.12	79	19	2

Conditions: a solution of DHM and **1** (0.33 mmol, 1.0 mmol Nd) in toluene (100 mL) was stirred for 1 h at RT or 0 °C^a; MMA (50 mmol) was then added via syringe and the reaction mixture was stirred for 1 h at 0 °C or RT^c. ^b 88 wt% of the whole polymer.

13.3. Polymerization temperature

Based on the optimized Nd/Mg = 5.0 ratio, we performed the polymerizations at different temperatures. A quantitative polymerization is observed for a reaction temperature ranging from -20 to 20 °C (Table 23). Decreasing the reaction temperature from 20 to 0 °C allows a significant narrowing of the molecular weight distribution while the syndiotacticity remains unchanged. However, a further lowering of the polymerization temperature leads to higher polydispersities concomitantly with a slight increase of the syndio-content of the PMMA. The increase of the syndiotacticity with the lowering of the temperature is consistent with the observation made with most of lanthanide-based catalyst systems.¹¹⁷ The broadening of the molecular weight distribution can be explained by a slow formation of the active species, i.e. a

slow initiation process, concurrently with a competition between propagation and termination/transfer reactions.

Table 23. Effect of polymerization temperature in MMA polymerization.

T _{polym} (°C)	yield (%)	M _n (10 ⁻³)	M _w /M _n	tacticity (%)		
				rr	mr	mm
-20	100	89	4.8	80	15	5
0	100	54	1.26	76	21	3
20	100	59	3.1	77	21	2

Conditions: a solution of DHM (0.2 mmol) and **1** (0.33 mmol, 1.0 mmol Nd) in toluene (100 mL) was stirred for 1 h at -20 °C; MMA (50 mmol) was then added via syringe and the reaction mixture was stirred for 1 h at desired temperature.

Given these results, the best compromise between monomer conversion, molecular weight distribution and syndiotacticity was obtained by carrying out activation/polymerization at 0 °C with Nd/Mg = 5.

14. Alkylating agent

Most of the experiments were carried out with DHM as cocatalyst in association with Nd₃(OtBu)₉(THF)₂. However, based on the hypothetical formation of an alkyl-neodymium species as initiator, we studied the effect of other potential alkylating agents. Indeed, the formation of alkyllanthanide species by transmetallation with alkyllithium or alkylaluminum species has precedent in related lanthanide alkoxide chemistry.^{218-220,222,290} One equiv. of *n*-BuLi (vs. Nd) gives isotactic PMMA (mm = 74%) in 13% yield with M_n = 19,000 and M_w/M_n = 3.6 (Table 24). The yield is dependent of the alkyl lithium concentration, keeping the same level of isotacticity. These results are consistent with an anionic polymerization initiated by *n*-BuLi.¹⁰² The effect of the rare earth compound in this system seems negligible; the neodymium-based active species that may be formed here might be much more unstable than those formed with DHM. The more reactive *t*-BuLi allows similar results although the polymerization proceeds quantitatively. The use of organoaluminum reagents does not afford better results: trimethylaluminum and trioctylaluminum lead to atactic PMMA in 6-12% yields. Finally, potassium hydride and triethyl boron give completely inert species in MMA polymerization.

²⁹⁰ Schumann, H.; Genthe, W.; Bruncks, N.; Pickardt, J. *Organometallics* **1982**, *1*, 1194-1200.

Table 24. Influence of the alkylating agent on $\text{Nd}_3(\text{OtBu})_9(\text{THF})_2/\text{MR}$ catalyst systems.

alkylating agent	Nd/M	yield (%)	tacticity (%)			$M_n(10^{-3})$	M_w/M_n
			rr	mr	mm		
<i>n</i> -BuLi	0.3	7	6	20	74	nd	nd
<i>n</i> -BuLi	1.0	13	6	21	73	18.7	3.6
<i>n</i> -BuLi	2.0	20	10	16	74	14.2	4.6
<i>t</i> -BuLi	2.0	100	15	15	70	25.0	4.7
AlMe ₃	1.0	6	37	33	30	nd	nd
AlOct ₃	0.33	12	35	35	30	nd	nd
BEt ₃	1.0	0	-	-	-	-	-
KH	1.0	0	-	-	-	-	-

Conditions: a solution of alkylating agent and **1** (0.33 mmol, 1.0 mmol Nd) in toluene (100 mL) was stirred for 1 h at RT; MMA (50 mmol) was then added via syringe and the mixture was stirred for 1 h at 0 °C.

Consequently, it seems that only alkylmagnesium reagents allow the synthesis of highly syndiotactic PMMA, in high yield, with low polydispersity. Consequently, various dialkylmagnesium and Grignard reagents were also tested in MMA polymerization (Table 25). *n*-BuEtMg affords similar results to DHM. Surprisingly, no polymerization takes place when Mg(CH₂SiMe₃)₂•Et₂O is employed. A likely explanation could be a lower reactivity of either the dialkylmagnesium reagent towards the neodymium alkoxide or the active species formed *in situ* from the combination Nd₃(OtBu)₉(THF)₂/Mg(CH₂SiMe₃)₂•Et₂O towards MMA. EtMgBr gives at -20 °C syndiotactic PMMA (rr = 80%) in 92% yield with $M_n = 124,000$ and $M_w/M_n = 3.0$, while PhMgBr gives still higher syndiotacticity (rr = 82%) but in a lower yield (60%) and a broader molecular weight distribution. A real difference exists between dialkylmagnesium and Grignard reagents in this binary system and dialkylmagnesium derivatives with straight alkyl chains are preferred.

Table 25. Influence of the alkyl magnesium reagent.

MgR_2/RMgX	yield (%)	$M_n(10^{-3})$	M_w/M_n	tacticity (%)		
				rr	mr	mm
BEM ^a	25	110	1.12 ^c	80	15	5
Mg(<i>n</i> -Hex) ₂ ^a	20	130	1.08 ^d	80	18	2
Mg(CH ₂ SiMe ₃) ₂ •Et ₂ O ^b	0	-	-	-	-	-
EtMgBr ^b	92	124	3	80	17	3
PhMgBr ^b	60	38	9	82	14	4

Conditions: ^a a solution of magnesium reagent (0.02 mmol) and **1** (0.033 mmol, 0.1 mmol Nd) in toluene (100 mL) was stirred for 1 h at -20 °C; MMA (50 mmol) was then added via syringe and the reaction mixture was stirred for 1 h at -20 °C. ^b same except magnesium reagent (0.5 mmol).

15. Neodymium precursor

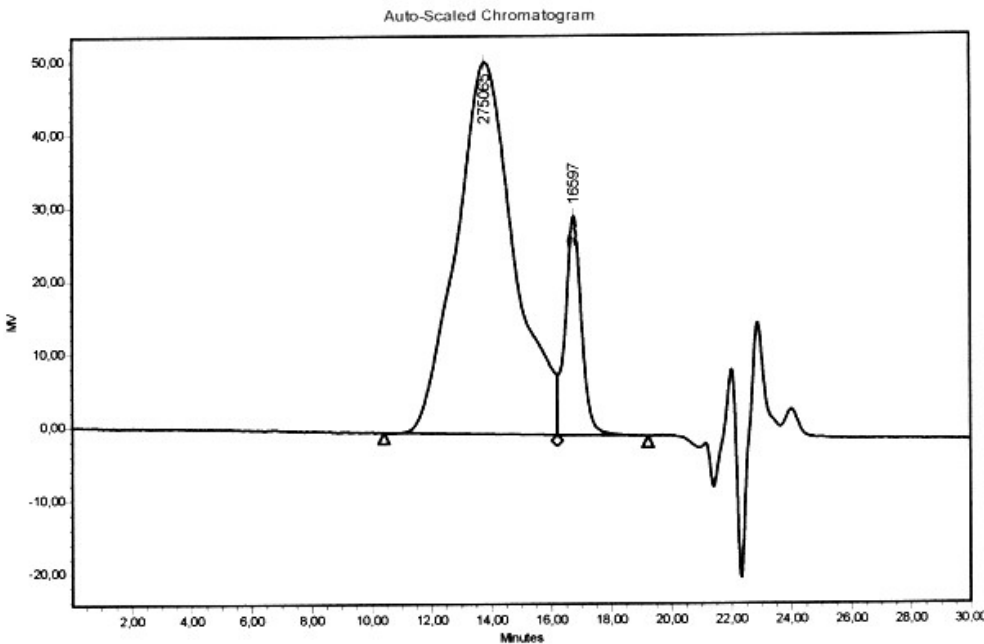
For the first time, it is possible to control the syndiotactic MMA polymerization under quite attractive experimental conditions with a simple binary system based on a Cp-free lanthanide precursor. However, it was interesting to extend this system to other neodymium salts. Thus, different neodymium alk(aryl)oxides were evaluated in MMA polymerization in combination with DHM as cocatalyst (Table 26).

Table 26. Neodymium precursors in binary Nd/Mg(*n*-Hex)₂ catalyst systems.

Nd precursor	Nd/Mg	yield (wt%)	tacticity (%)			$M_n(10^{-3})$	M_w/M_n
			rr	mr	mm		
"Nd(O <i>t</i> Bu) ₃ " (1)	5.0	100	77	20	3	70	1.8
"Nd(O <i>t</i> Bu) ₃ " ^a (4)	5.0	79	80	15	5	360	2-3
"Nd(O <i>t</i> Am) ₃ " (9)	5.0	5	nd	nd	nd	nd	nd
Nd(OAr) ₃ (THF) (12)	1.0	11	35	32	33	nd	nd
Nd(acac) ₃	1.0	100	69	21	10	61.5	8.7
Nd{N(SiMe ₃) ₂ } ₃	1.0	16	20	18	62	16.3	27
Nd{N(SiMe ₃) ₂ } ₃ ^b	1.0	100	42	21	35	10.5	9.6

Conditions: a solution of DHM(1 mmol) and Nd precursor in toluene (100 mL) was stirred for 1 h at RT; MMA (50 mmol) was then added via syringe and the reaction mixture was stirred for 1 h at 0 °C. ^a reaction time: 15 min. ^b *n*-BuLi was used as cocatalyst.

We showed previously that the synthetic route to neodymium *tert*-butoxides has a significant effect on the final complex structure, based on ¹H NMR analyses. So, it was necessary to verify if this change of complex structure would affect the catalytic activity of the Nd precursor. We decided to carry out MMA polymerization under the optimized conditions with a neodymium *tert*-butoxide (**4**) synthesized by salt metathesis between KO*t*Bu and NdCl₃ in THF. The SEC traces shows two polymer populations. The polymer recovered under these conditions has a broad molecular weight distribution, but is syndiotactic-rich (rr = 80%). The whole polymer product contained 90 wt% of a broad molecular weight distribution polymer fraction with $M_n = 360,000$ and $M_w/M_n = 2-3$, and 10 wt% of PMMA with $M_n = 16,000$ and $M_w/M_n = 1.10$. Only this narrow polydispersity fraction polymer may be attributed to the small part of Nd₃(O*t*Bu)₉(THF)₂ in the Nd precursor. This result shows the high sensitivity of this binary system to the structure of the Nd complex.

Figure 57. SEC trace of PMMA produced by **4/DHM** ($\text{Nd}/\text{Mg} = 5.0$) at 0°C .

With the Nd *tert*-amyloxide (**9**) (assumed to be isostructural to $\text{Nd}_3(\text{O}_t\text{Bu})_9(\text{THF})_2$, see Chapter 2 §8.1.1.1), a low monomer conversion is observed, yielding a PMMA with a very low solubility in THF. These conversion and solubility are typically observed with DHM as initiating system under the same conditions. So, it seems that the highly syndiotacticity as well as the controlled character of the polymerization are strongly dependent of the structure of the Nd complex but also of the bulkiness of the ligand. Indeed, a slight change in the ligand structure affects dramatically the catalytic activity.

With the mononuclear complex $\text{Nd}(\text{O}-2,6-t\text{Bu}-4-\text{Me}-\text{C}_6\text{H}_2)(\text{THF})$ (**12**), similar results to (**9**) were obtained. In this case, the tacticity showed the atactic nature of the PMMA.

Commercially available $\text{Nd}(\text{acac})_3$ proved less efficient than $\text{Nd}_3(\text{O}_t\text{Bu})_9(\text{THF})_2$: combined with 5 equiv. (vs. Nd) of DHM, it allowed total conversion of MMA at -20°C to give syndiotactic ($\text{rr} = 69\%$) PMMA with $M_n = 61,500$ and $M_w/M_n = 8.7$ (Table 26). This result is in direct line with the work reported by Sun *et al.* using lanthanide carboxylates in combination with Grignard reagents.¹⁶⁰

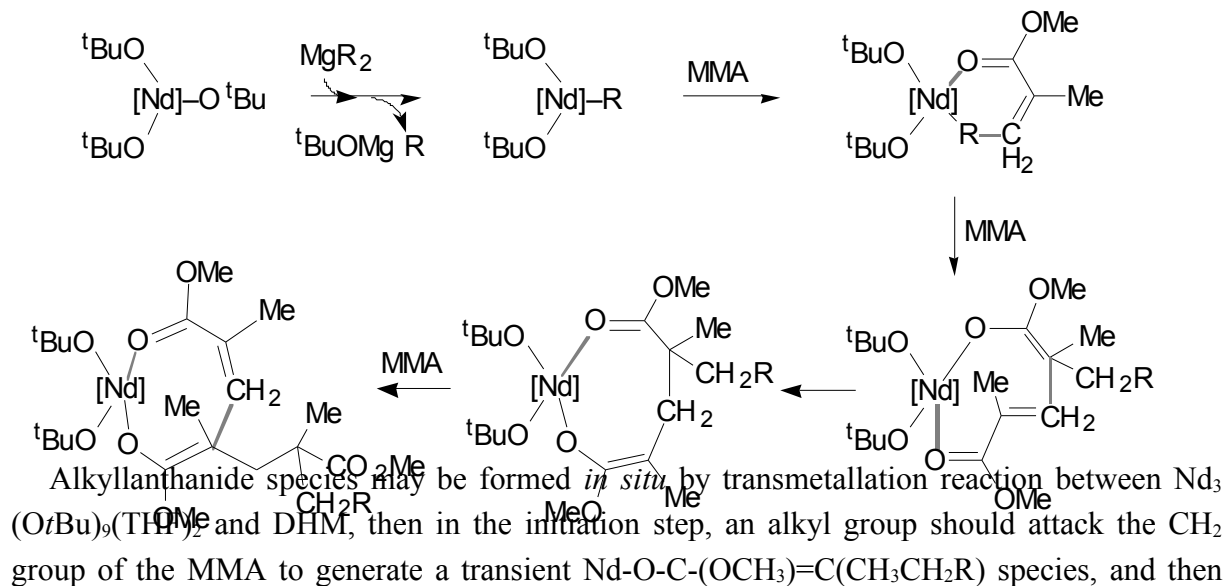
Even if the purpose of the study is not the polymerization of MMA initiated by $\text{Nd}\{\text{N}(\text{SiMe}_3)_2\}_3$, the results that we obtained with this precursor are quite informative. In association with DHM, an iso-rich PMMA in low yield was produced. However, combined with *n*-BuLi, a quantitative polymerization occurred. The molecular weight distribution remains broad and the PMMA is atactic. When the $\text{Nd}/n\text{-BuLi}$ ratio is increased to 5.0, the emergence of a sharp signal ($M_w/M_n = 1.23$, $M_n = 9700$) out of the broad envelope, accounting for 58 wt% of the polymer was observed. This result shows again that each binary system is really particular and predicting the activity or the stereospecificity of the polymerization based on one single experiment is very difficult.

16. Proposed mechanism

The above results indicate that the combination of DHM with $\text{Nd}_3(\text{OtBu})_9(\text{THF})_2$ (**1**) in toluene generates an initiator species responsible for the syndiotactic and controlled polymerization of MMA, that coexists with one (or several) inefficient initiator(s) present in variable amount(s) according to the Nd/Mg ratio. The prerequisite to use a deficiency of the dialkylmagnesium reagent for optimal performances, in combination with the rapid formation of high molecular weight PMMA chains in the early stage of the reaction, suggests that undesirable polymers originate from either this initial co-reagent or a new very reactive species (see §13.1).

On the other side, the formation of very low dispersity and highly syndiotactic PMMA for $\text{Nd}/\text{Mg} \geq 5$ strongly supports formation of an initiator neodymium species analogous to alkyllanthanocenes. Indeed, trivalent organolanthanide complexes $[(\text{Cp}^*)_2\text{LnR}]_n$ ($\text{Ln} = \text{Sm}, \text{Y}, \text{Lu}; \text{R} = \text{H, alkyl}; n = 1, 2$) have been shown by Yasuda *et al.* to be extremely efficient initiators for the highly syndiotactic, living polymerization of alkyl methacrylates.^{116,117} For instance, PMMA with similar characteristics to ours ($M_n = 58,000$, $M_w/M_n = 1.02$, $rr = 82\%$) was obtained quantitatively by reacting $[(\text{Cp}^*)_2\text{SmH}]_2$ with 500 equiv. of monomer at 0 °C in toluene.¹¹⁷ The formation of homoleptic alkyllanthanide and mixed alkyl-alkoxy lanthanide species by alkyl-tert-butoxide metathesis reactions using alkali (Li, K) and aluminum alkyls has been reported.^{215-223,290} However, the most striking evidence for supporting the generation of an alkyllanthanide species from the **1**/DHM combination is the possibility to achieve with this system efficient ethylene polymerization *and* ethylene-MMA block copolymerization through initial homopolymerization of ethylene and sequential addition of MMA (see Chapter 4). Organolanthanide complexes $[(\text{Cp}^*)_2\text{LnR}]_n$ displays the same unique capabilities.²⁹¹ Degradation of PMMA characteristics (increased MWD) when polymerization is carried above 0 °C is consistent with the high sensitivity of alkyllanthanides. A schematic plausible generation and initiation mechanism is depicted in Scheme 27.

Scheme 27. Assumed mechanism for the initiation of MMA polymerization using **1**/DHM.



²⁹¹ Yasuda, H.; Furo, M.; Yamamoto, H.; Nakamura, A.; Miyake, S.; Kibino, N. *Macromolecules* **1992**, *25*, 5115-5116.

the incoming MMA molecule may participate in a 1,4-addition to afford the eight-membered ring intermediate as previously reported for lanthanocene-mediated MMA polymerizations.

17. Conclusion

In conclusion we have developed a new catalyst system consisting of the combination of DHM with $\text{Nd}_3(\text{OtBu})_9(\text{THF})_2$. In toluene and at moderately low temperature ($T \leq 0^\circ\text{C}$), this association generates an initiator species responsible for the highly syndiotactic and controlled polymerization of MMA. The main advantage of this new *in situ* combination of a rare earth alkoxide and a dialkylmagnesium compound lies in its simplicity and its readily availability. It thus provides an efficient alternative to sophisticated alkyllanthanocenes for the controlled syndiotactic polymerization of MMA under attractive conditions of solvent and temperature. Further investigations aiming at understanding the mechanism of formation of the active species will be described in Chapter 6.

Chapter 4

Ethylene polymerization

and diblock copolymerization

ethylene-MMA

18.

19. Ethylene polymerization

19.1. Introduction

As highlighted in Chapter 3, the development of new catalytic binary systems based on lanthanide alkoxides have proved complicated and rather unpredictable in MMA polymerization. However, the potential *in situ* formation of an alkyllanthanide species have prompted us to explore the ability of the lanthanide alkoxides to serve as Cp-free precursors for olefin polymerization, even if moderate results have been previously obtained with well defined alkyl-alkoxy complexes in olefin polymerization (see Presentation of the research project). So, we have decided to focus on the use of *in situ* combinations of lanthanide alkoxides with alkylating agents MR in ethylene polymerization by varying the nature of the lanthanide alkoxide, of the alkylating agent but also both alkyl/alkoxide metathesis and polymerization conditions, i.e., Ln/MRz ratio, reaction and activation time, and temperature.

It was initially verified that, correspondingly to thermodynamics studies, none of these alkoxides could initiate as such ethylene polymerization. Indeed, calorimetric studies showed that ethylene insertion into an Ln-O bond is enthalpically unfavorable.¹⁵⁷ Consequently, we can consider that the reactivity observed with these *in situ* combinations would result from the formation of (an) alkyllanthanide species as suggested in MMA polymerization. The most striking result of this preliminary screening is that only dialkylmagnesium reagents lead to active systems under 1 atm of ethylene in toluene solution; no polymerization activity was detected upon using *n*-BuLi, *t*-BuLi, LiCH₂TMS, AlMe₃, Al(*n*-Oct)₃, AlH(*i*-Bu)₂, [*n*-BuAlH(*i*-Bu)₂][Li], BEt₃, ZnEt₂ or even Grignard reagents (PhMgBr, EtMgBr), under various reaction conditions.* It is noteworthy that this does not necessarily imply the absence of alkyl/alkoxide metathesis processes between some of these reagents and the neodymium alkoxides (see Chapter 6). However, using one equiv. of di-*n*-hexylmagnesium (DHM) vs. Ln as co-reagent and toluene or hexane as solvent, several neodymium alkoxides proved to be effective polymerization catalyst precursors.

So we would like to describe here the development of these catalyst systems. We will show that with the appropriate catalyst, under mild conditions, a pseudo-living ethylene polymerization could be observed, producing highly linear and crystalline polyethylenes with high molecular weights. In addition, under those reaction conditions, a polymer-like precipitate forms during the reaction course. More interestingly, this solid proved to be an equivalent catalyst to the initial *in situ* system for the slurry ethylene polymerization. Finally, by taking advantage of this pseudo-livingness, high molecular weights diblock poly(ethylene-*b*-methyl methacrylate) copolymers have been successfully prepared, using both *in situ* and solid initiating systems.

* Other inorganic Nd precursors such as Nd{N(SiMe₃)₂}₃, Nd(acac)₃ and Nd(versatate)₃ revealed to be completely inactive for ethylene polymerization upon addition of dialkylmagnesium under our experimental conditions.

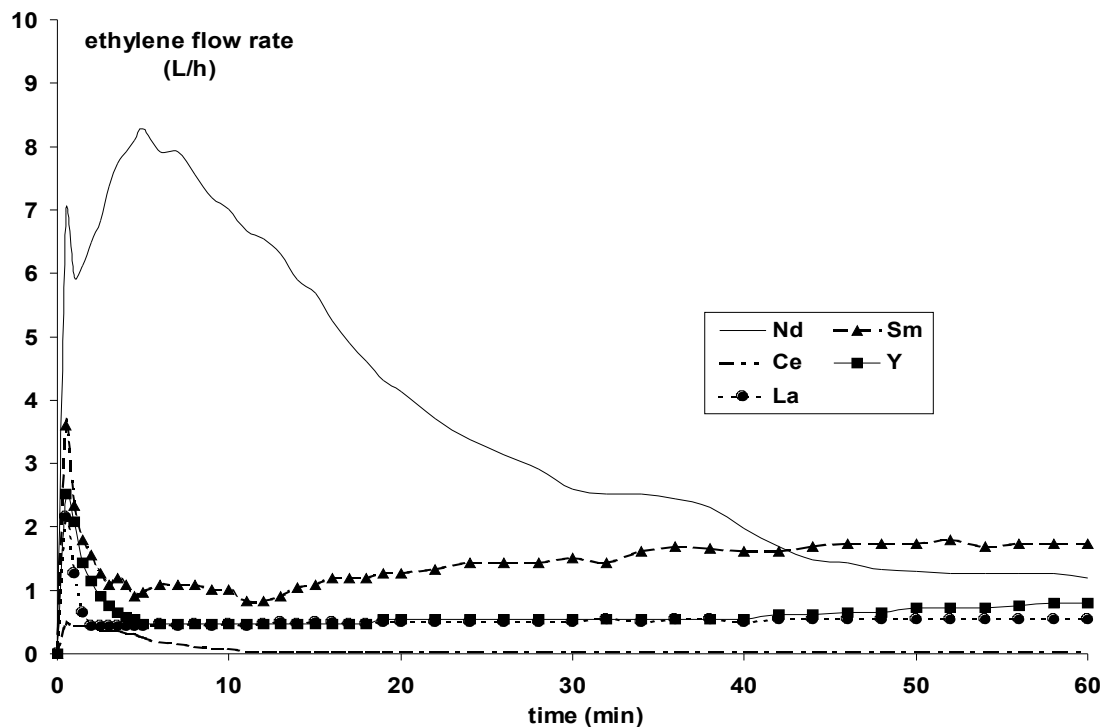
19.2.Preliminary screening

19.2.1. Influence of the rare earth metal

Based on the previous results in MMA polymerization, we have firstly investigated the use of various lanthanide *tert*-butoxides using the optimized experimental conditions i.e., activation temperature 0 °C for 1 h, polymerization temperature 0 °C for 1 h with Ln/Mg = 1.0, under 1 bar ethylene pressure in toluene. It must be mentioned that the replacement of toluene by pentane or hexane does not affect the polymerization activity as it was observed in butadiene polymerizations.¹⁸⁷ In this case, the excess of free dialkylmagnesium will not be responsible for side reactions, although dialkylmagnesium reagents are known to be excellent transfer agents in chlorolanthanocene-mediated ethylene polymerization.⁵²

For this purpose, we prepared Y, La, Ce, Nd and Sm *tert*-butoxides (symbolized by "Ln(O*t*Bu)₃") by salt metathesis between the anhydrous LnCl₃ and NaO*t*Bu in THF. The evolution of the ethylene flow rates with time observed under these conditions is reported in Figure 58.

Figure 58. Ethylene flow rates observed with various "Ln(O*t*Bu)₃"/DHM systems (Ln/DHM = 1.0; 1 atm; activation 1 h at 0 °C then polymerization 1 h at 0 °C).



Mainly two kinds of consumption curves can be distinguished. For Y, La, Ce and Sm, the ethylene flow rate increases slowly with time and the activity is rather low ($A = 0.02\text{-}1.60 \text{ kgPE/molLn/atm/h}$). This increase of activity with time may be ascribed to a slow initiation process. SEC traces of the resulting polymers show a bimodal polymer distribution. Beside a polymer fraction with high molecular weight and broad molecular distribution, an important polymer fraction (60-80 wt%) has a low molecular weight with quite low polydispersity ($M_n = 700\text{-}2500$ and $M_w/M_n = 1.5\text{-}1.7$). The highest molecular weight was obtained with the samarium precursor. It is also interesting to note that Y and La *tert*-butoxides exhibit the same

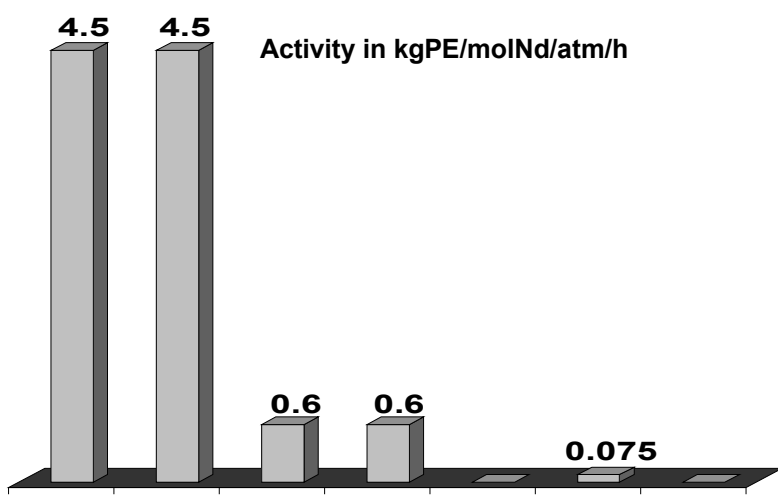
catalytic behavior while these precursors are known to have different molecular structures.²³⁹ On the other hand, the isostructural La and Nd *tert*-butoxides behave differently. The strongest Ln-O bond energy of La vs. Nd (La-O = 799 ± 4 kJ/mol; Nd-O = 703 ± 13 kJ/mol) may be accounted for the highest stability of the La alkoxide, i.e. its lowest activity in polymerization.²⁹²

For the neodymium *tert*-butoxide, the activity reaches its maximum within a few minutes (7-8 min) and then decreases, concomitantly with the appearance of an insoluble polymer-like material, to attain a plateau after 60 min, at ca. 1/10 of the maximal activity ($A = 4\text{-}5 \text{ kgPE/molNd/atm/h}$). This activity corresponds to a moderate value on absolute Gibson's activity scale,²⁹ but remains ca. two orders of magnitude lower than for an equivalent lanthanocene system, e.g., $\text{Cp}^*_2\text{SmCl}_2\text{Li(OEt}_2)_2/n\text{-BuEtMg}$ (1:1) gave 340 kgP/mol/atm/h under the same reaction conditions.⁵² SEC analysis of the final polymer was not possible due to its insolubility under the analysis conditions (135 °C in 1,2,4-trichlobenzene) suggesting high molecular weights. However, a five minutes experiment gave a PE with $M_n = 301,000$ and $M_w/M_n = 2.3$, the latter indicating the existence of only one type of active sites.²⁴ The formation of a single site catalyst as well as the highest activity encourages the development of neodymium-based precursors.

19.2.2. Ethylene polymerization with various Nd alkoxides

Many neodymium alk(aryl)oxides ("Nd(OR)₃") were prepared by either salt metathesis between NdCl₃ and the corresponding sodium alkoxide in THF (NaOR with OR = O*t*Bu, O*t*Am, OCMe₂Ph, O*i*Bu, O*i*Pr, OAr (OAr = O-2,6-*t*Bu₂-4-Me-C₆H₂)) or by the silylamine route (HO*C**t*Bu₃). The overall activity calculated over 1 h polymerization time is reported in Figure 59.

Figure 59. Activity in ethylene polymerization with various "Nd(OR)₃"/DHM systems (Nd/DHM = 1.0; 1 atm; activation 1 h at 0 °C then polymerization 1 h at 0 °C, except *, see text).



R-*t*-butoxide and *R*-*t*-amyloxide ligands exhibit the highest activities ($A = 4\text{-}5 \text{ kgPE/molNd/atm/h}$). Contrary to MMA polymerization, a slight modification of the steric

²⁹² Kerr, J. A. in *CRC Handbook of Chemistry and Physics*, Lide D. R. Ed.; CRP Press, Boca Raton, Florida, USA, 81st Edition, 2000.

hindrance around the Nd center, for instance by replacing the *tert*-butoxide by a *tert*-amyloxide ligand, does not affect the catalytic activity. In this case, the approach of the monomer to the metal center may be unchanged. With OCMe₂Ph, the absence of activity may result from an increased stability of the neodymium center due to intramolecular π -interactions, as already reported in some lanthanide aryloxide complexes.²⁹³ The very bulky and mononuclear Nd(O-2,6-*t*Bu₂-4-Me-C₆H₂)₃(THF) and Nd(OctBu₃)₃(THF) complexes are inactive at 0 °C but exhibit a low activity when heated up at respectively 40 and 80 °C. The requirement of higher polymerization temperature may be ascribed to the steric hindrance of the ligand or the slow formation of the active species. Surprisingly, the trinuclear neodymium *tert*-butoxide and amyloxide complexes appeared to be more reactive. The use of the secondary alkoxides does not allow the formation of active initiators. The resulting activity with "Nd(O*i*Bu)₃" is very low, and "Nd(O*i*Pr)₃", assumed to be Nd₇(O*i*Pr)₁₇Cl₂₃₈ is completely inactive even at higher temperatures.

19.2.3. Influence of the synthetic route of neodymium *tert*-butoxide

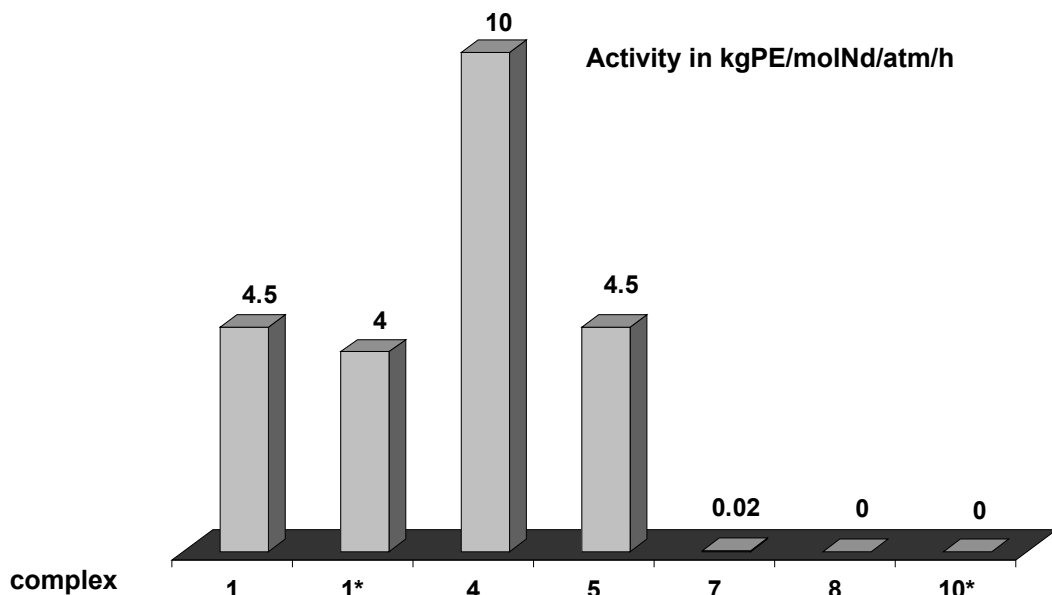
We have shown in Chapter 2 that the mode of preparation of the neodymium *tert*-butoxide affects directly its structure. In MMA polymerization, the products obtained from salt metathesis between NdCl₃ and NaOtBu, and NdCl₃ and KOtBu exhibit completely different behaviors. The former allows highly syndiotactic PMMA with narrow polydispersity to be synthesized while the latter produces also syndiotactic PMMA but with a broad molecular weight distribution. Consequently, it was interesting to investigate how the activity in ethylene polymerization would be affected by the synthetic route of the neodymium alkoxide, i.e., how the molecular structure of the neodymium *tert*-butoxide would affect the polymerization activity. The results are depicted in Figure 60. Nevertheless, aware of the importance of minor details on the outcome of the reactions in this area, special attention has been paid in this study to the reproducibility of the syntheses. So, before going further, it has been checked that isolated crystals of Nd₃(OtBu)₉(THF)₂ and initial bulk materials feature comparable catalytic behavior for olefin polymerization.

As expected, the activity varies with the origin of the neodymium *tert*-butoxide. The alkoxides synthesized by salt metathesis (between NdCl₃ and NaOtBu in THF (**1**) or NdCl₃(THF)₂ and NaOtBu in hexanes (**5**)) and alcoholysis reaction in THF (**1***) give the same overall activity ca 4-5 kgPE/molNd/atm/h. However, they exhibit quite different evolution of ethylene flow rate with time. When **1** is used as precursor, the polymerization proceeds as described in §19.2.1. Complex **1***, which crystallized as **1**, and complex **5** need to be activated at room temperature (typically 10 min) to allow ethylene polymerization. After this activation step, **5** shows a similar consumption profile to **1** while **1*** leads to a progressive increase of activity throughout the reaction course. Complex **4**, from salt metathesis between NdCl₃ and KOtBu in THF shows an activity twice higher than **1**.* In this case, the overall consumption profiles are quite similar. The final polymer is also insoluble in SEC analysis conditions, however, a

²⁹³ (a) Deacon, G. B.; Nickel, S.; MacKinnon, P.; Tiekkink, E. R. T. *Aust. J. Chem.* **1990**, *43*, 1245. (b) Barnhart, D. M.; Clark, D. L.; Gordon, J. C.; Huffman, J. C.; Vincent, R. L.; Watkin, J. G.; Zwick, B. D. *Inorg. Chem.* **1994**, *33*, 3487-3497.

polymerization carried out for 5 minutes gives a polyethylene with $M_n = 118,000$ and $M_w/M_n = 3.02$. The M_n value is 3 times lower than with **1**, at the same time the increase of activity in this short time reaction is only 25% (21.6 vs. 28.8 kgPE/molNd/atm/h). This indicates a higher efficiency of initiation, i.e., a higher concentration of active species. This change in the catalytic activity can be correlated to our ^1H NMR analyses that suggest their different complex structures (see Chapter 2 §8.1.1.5).

Figure 60. Activity in ethylene polymerization with various Nd *tert*-butoxides: effect of the synthetic route (Nd/DHM = 1.0; 1 atm; activation 1 h at 0 °C then polymerization 1 h at 0 °C).



The *in situ* system based on the *tert*-butoxy complex **7**, prepared by alcoholysis of the tris(amido) precursor, showed an activity ca. two orders of magnitude lower under similar conditions ($A = 0.08 \text{ kgPE/mol/atm/h}$). The quasi-absence of activity may be attributed to the reaction of the dialkylmagnesium reagent with the coordinated *tert*-butyl alcohol molecules, hampering the formation of the polymerization active species. However, addition of an excess of DHM did not afford higher activity.

The alkoxide **10*** formed by salt metathesis in Et_2O does not exhibit any activity, even when activated at higher temperature. Most likely, its aggregated complex structure does not allow the formation of active species suitable for ethylene polymerization, as it was observed with $\text{Nd}_7(\text{O}i\text{Pr})_{17}\text{Cl}$.

Finally, the pentanuclear complex **8** and the dinuclear complex **11** with a γ -donor-functionalized alkoxy ligand proved also completely inactive in ethylene polymerization when activated by one equiv. of DHM.

* A similar increase of activity was observed with Sm *tert*-butoxide. More surprisingly, neodymium *tert*-amyloxide prepared from salt metathesis between NdCl_3 and $\text{KO}t\text{Bu}$ is an inactive precursor.

In conclusion, we have to be extremely careful on the origin/structure/composition of the neodymium *tert*-butoxide as precursor in ethylene polymerization since the formation of the active species seems extremely sensitive to the structure of the Nd alkoxide. Because of the pseudo-living polymerization observed in MMA polymerization with **1**, we have chosen to continue our investigation with this Nd precursor. Indeed, the possibility of copolymerization between ethylene and MMA may be a very interesting target.

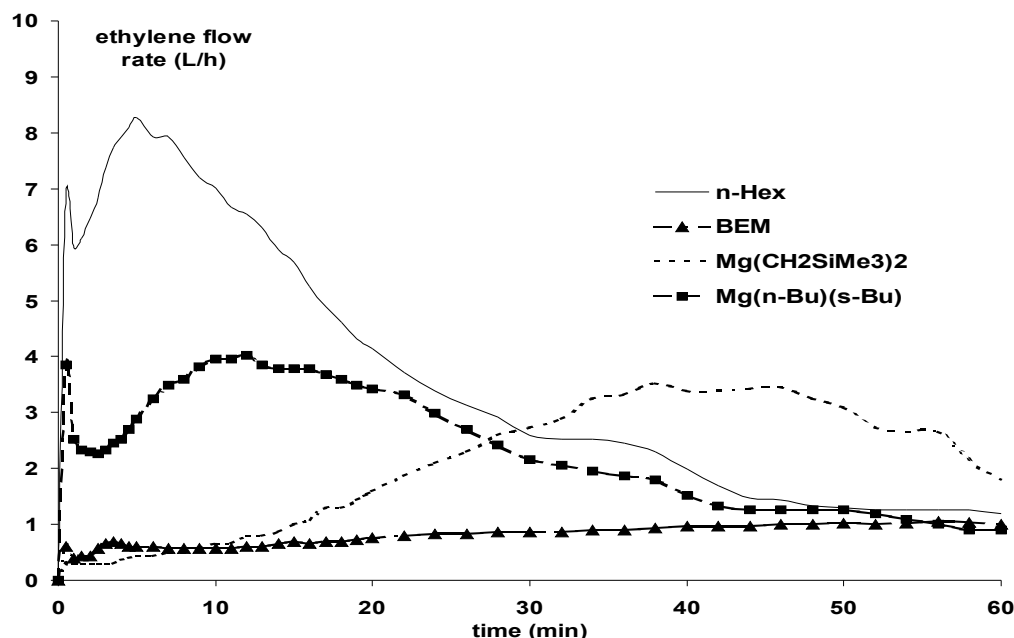
19.3. Ethylene polymerization with $\text{Nd}_3(\text{OtBu})_9(\text{THF})_2$ in slurry

We will now focus strictly on the use of **1/MgRR'** as catalyst systems. Originally, the polymerizations were conducted with various dialkylmagnesium reagents.

19.3.1. Influence of the nature of the dialkylmagnesium reagent

As shown in Figure 61, the nature of the dialkylmagnesium reagent affects the activity of the system as judged by the amount of polyethylene recovered after 1 h and also by the ethylene flow rates. Compared to *n*-butylethylmagnesium (BEM) and bis(trimethylsilyl-methyl)magnesium, di-*n*-hexylmagnesium gives the most productive catalyst. DHM and Mg (*n*-Bu)(*s*-Bu) give comparable consumption profile. However, the latter yields a polyethylene with a rather low molecular weight ($M_n = 56,000$) and a broad molecular weight distribution ($M_w/M_n = 7.8$), indicating the existence of multiple active sites. The presence of two different kinds of alkyl chains on the magnesium compound may be responsible for the formation of two active species with different energy of activation (rate of initiation), and thus lead to a broadening of the MWD. The other mixed dialkylmagnesium (BEM) exhibit a singular behavior. The system is poorly active but the activity increases slowly with time. This behavior can be tentatively ascribed to the more aggregated structure of BEM compared to DHM, leading to a slower formation of active species. With the silylated derivative, a more usual consumption plot is observed but the maximum of activity is reached within 40 min and not within 7-8 min as noticed with DHM. The initial low activity might be ascribed again to a slow initiation process due to the bulkiness of the CH_2SiMe_3 group. Because of its high productivity, DHM will be preferred for the rest of the study.

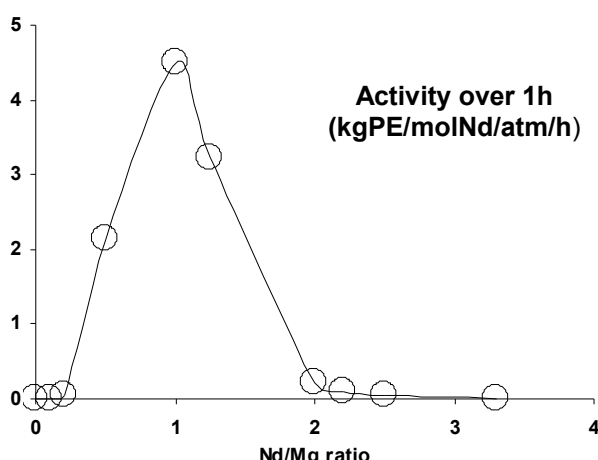
Figure 61. Ethylene flow rates observed with **1/MgRR'** systems ($\text{Nd}/\text{Mg} = 1.0$; 1 atm; activation 1 h at 0°C then polymerization 1 h at 0°C).



19.3.2. Influence of the Nd/Mg ratio

It was shown in MMA polymerization that a precise Nd/Mg ratio was essential to observe the pseudo-living character of the polymerization. Indeed, an excess of dialkylmagnesium initiated uncontrolled MMA polymerization or formed some other uncontrolled anionic initiating species. This behavior is of course not expected in ethylene polymerization. However, as displayed in Figure 62 the maximum of productivity is observed only for a definite Nd to Mg ratio of 1.0, a deviation from this value results in a rapid drop of the activity. This contrasts markedly with chlorolanthanocene/dialkylmagnesium systems that proved to accommodate up to 1000 equiv. of MgR_2 vs. Ln with still high ethylene polymerization activity.⁵² Consequently, it will be necessary to perform the polymerization with a precise measurement of the Nd/Mg ratio, ratio equal to 1.0 for an optimal productivity.

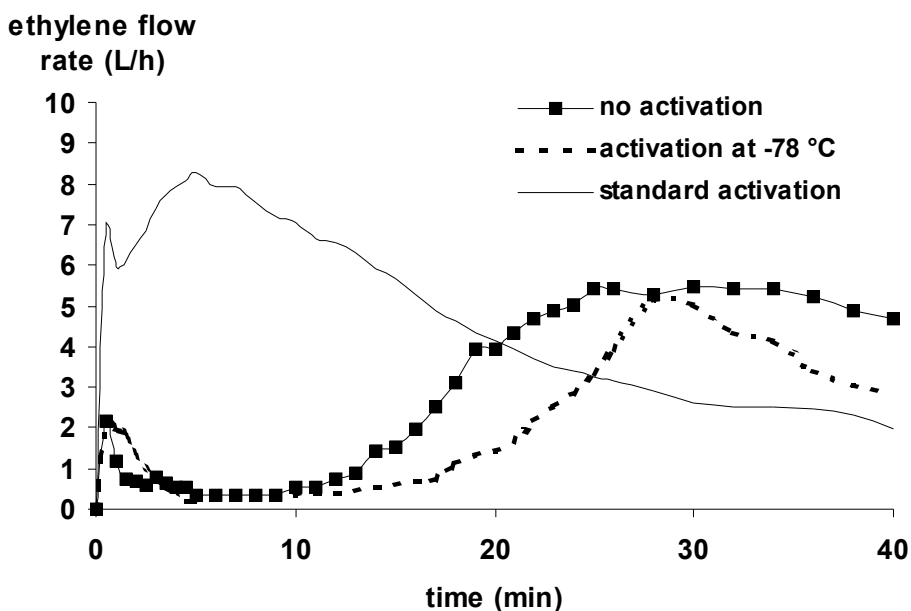
Figure 62. Influence of the Nd/Mg ratio on the polymerization activity of **1/DHM** system (1 atm; activation 1 h at 0°C then polymerization 1 h at 0°C).



19.3.3. Influence of activation conditions

The activation is a key step since it leads to the formation of the active species. We have seen that the bulky $\text{Nd}(\text{OAr})_3(\text{THF})$ and $\text{Nd}(\text{OC}t\text{Bu}_3)_3(\text{THF})$ complexes need to be activated at least at room temperature to initiate ethylene polymerization. With **1**, the reactions carried out at 0 °C allowed moderate activities. Increasing the activation time or the activation temperature leads to lower productivities for both DHM and BEM (Table 27). This result is consistent with the supposed low thermal stability of the active species in the absence of monomer. However, decreasing the activation temperature to -78 °C results in a 5 min induction period. The polymerization starts slowly, reaching its maximum of activity after 30 min (Figure 63). This indicates that temperatures above -78 °C are required to form actives species from **1**/DHM combinations. A slow polymerization can be ruled out since fast ethylene polymerization was observed at -50 °C (*vide infra*).

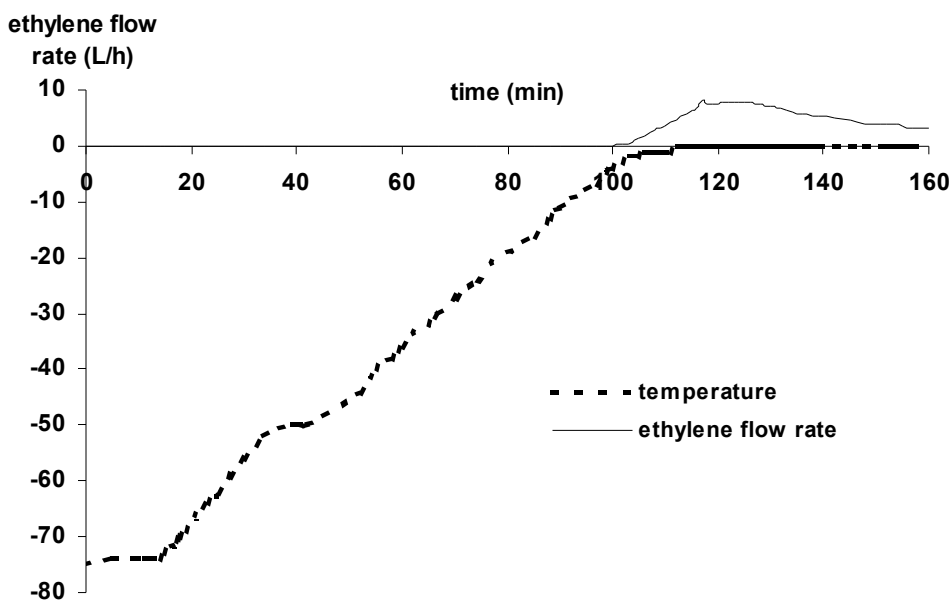
Figure 63. Effect of activation on ethylene flow rates with **1**/DHM system (Nd/Mg = 1.0; 1 atm; activation 1 h at 0 °C then polymerization 1 h at 0 °C).



A similar behavior was observed in complete absence of activation at 0 °C. In order to get a better insight in the kinetics of formation of the active species, we carried out an experiment in which the temperature of the polymerization mixture containing **1**/DHM from -78 to 0 °C was raised progressively with a simultaneous monitoring of the temperature and ethylene flow rate (Figure 64). This experiment confirmed the aforementioned results since a standard ethylene polymerization took place when the temperature reached -5 °C. Consequently a minimal temperature is required to observe a sufficiently rapid formation of the active species, e.g. between -10 and 0 °C. The same reaction performed in the presence of *n*-BuLi (1 equiv. vs. Nd) gave a slightly higher productivity ($A = 5.7 \text{ kgPE/molNd/atm/h}$) but with a similar consumption profile. It seems that the formation of active species is not disrupted by the presence of *n*-BuLi, although *n*-BuLi may react with **1** (*vide infra*), indicating

the stabilization of the neodymium alkoxide by the presence of DHM and the role of scavenger of *n*-BuLi in this experiment.

Figure 64. Evolution of the ethylene flow rate with temperature ($1/\text{DHM} = 1.0$; 1 atm; activation 1 h at 0°C then polymerization 1 h at 0°C).



Finally, raising the activation temperature to 20°C with $\text{Mg}(\text{CH}_2\text{SiMe}_3)_2$ is beneficial in terms of productivity (from 1.8 to 2.5 kgPE/molNd/atm/h). This result may be attributed to the increase of the propagation rate constant but also to a higher stability of the active species, a faster formation of the latter or a higher efficiency of initiation (Table 27).

Table 27. Influence of the alkylation conditions on the polymer yield with **1/MgRR'** systems.

MgRR'	T_{alkyl} (°C)	t_{alkyl} (min)	T_{polym} (°C)	PE (g)
R, R' = CH_2SiMe_3	0	60	0	1.80
CH_2SiMe_3	20	60	20	2.50
<i>n</i> -Bu, Et	0	60	0	1.19
<i>n</i> -Bu, Et	0	180	0	0.53
<i>n</i> -Hex*	-78	60	0	1.60
<i>n</i> -Hex	0	60	0	4.70
<i>n</i> -Hex	0	180	0	1.69
<i>n</i> -Hex	20	60	0	1.09
<i>n</i> -Hex	20	60	20	0.92

Conditions: $\text{Nd}/\text{Mg} = 1.0$; 1 atm ethylene pressure, polymerization time 1 h except * 40 min.

19.3.4. Effect of the polymerization temperature

The effects of the polymerization and activation temperatures are comparable. At temperatures below 0 °C, the productivity increases significantly while raising the temperature over 20 °C leads to a severe decrease in the polymer yield as well as in the molecular weight, e.g. at 80 °C: $M_n = 1700$; $M_w/M_n = 1.55$; 29 % vinyl chain-ends (Table 28). This is tentatively ascribed to a process involving β-H elimination and subsequent deactivation of the resulting neodymium-hydride species (*vide infra*).

Table 28. Effect of the polymerization temperature on the activity with 1/DHM system.

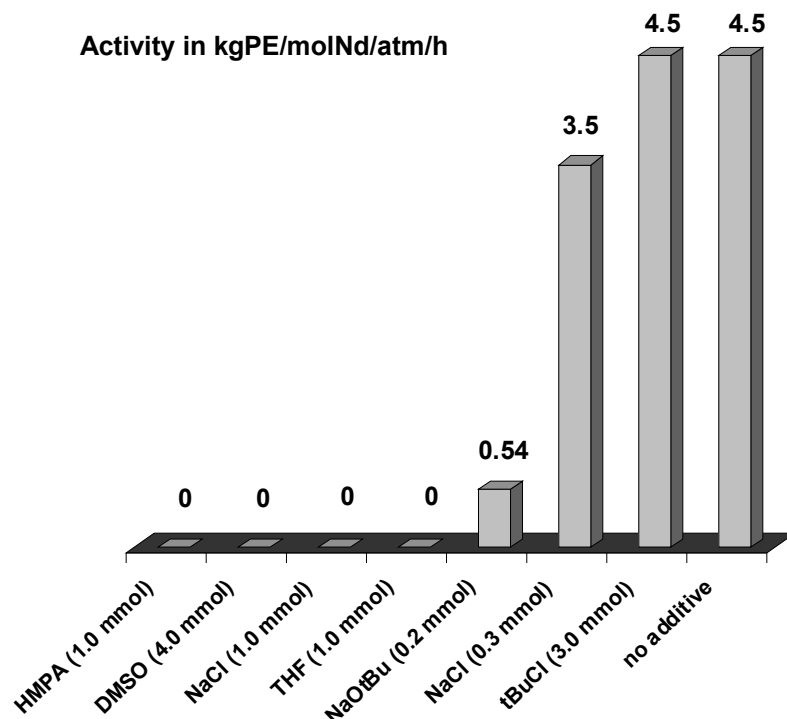
temperature (°C)	polymerization time (min)	M_n	M_w/M_n	activity (kgPE/molNd/atm/h)
-50	30	not soluble	-	9.0
-20	15	not soluble	-	6.0
0	60	not soluble	-	4.5
40	90	6900	32	1.8
80	35	1720	1.55	1.0

Conditions: Nd/DHM = 1.0; 1 atm; activation 1 h at 0 °C then polymerization 1 h at various temperatures.

19.3.5. Effect of various additives on the polymerization activity

Some additives were added to the polymerization solution in order to stabilize the active species and/or desaggregates the dialkylmagnesium reagent. The overall activities noticed over 1 h are reported in Figure 65. First, it is noteworthy that, although trinuclear complex **1** contains two coordinated THF molecules, the addition of 1 mol equiv. of THF vs. Nd (i.e. 0.3 equiv. vs. 1) proved sufficient to inhibit all polymerization activity. Evans *et al.* observed a similar phenomenon with $\text{Y}(\text{OtBu})_3\text{Cl}_2/\text{Al}(\text{Me})_3$ systems.²¹⁹ He imputed this lack of reactivity to the formation of the unreactive $\text{Al}(\text{Me})_3(\text{THF})$. Inhibition was also observed when 1 equiv. of NaCl (or KCl) vs. Nd was added to the 1/DHM (1:1) system while 0.3 equiv. just reduced the activity. However, addition of an excess of *t*-BuCl (3 equiv. vs. Nd) organic halide usually employed as chlorinated agent in lanthanide-mediated polymerization¹⁸⁹ has no effect on the polymerization. Because the dialkylmagnesium reagents are known to have aggregated structures, some other additives such as hexamethylphosphoramide (HMPA), dimethyl sulfoxide (DMSO) and sodium *tert*-butoxide were added to the catalytic in order to increase the efficiency of initiation. Unfortunately, these attempts ended in a failure. These results show the extreme sensitivity of the active species generated from this combination towards Lewis bases. This may also account for the inefficiency of the systems based on Grignard reagents since these potential activators are only available as ether solutions, and those based on complexes **7** and **11** since they each contain "poisoning" moieties within their structure.

Figure 65. Influence of various additives on the polymerization activity with **1/DHM** system ($\text{Nd/Mg} = 1.0$; 1 atm; activation 1 h at 0°C then polymerization 1 h at 0°C).



19.3.6. Polymerization in the presence of transfer agent

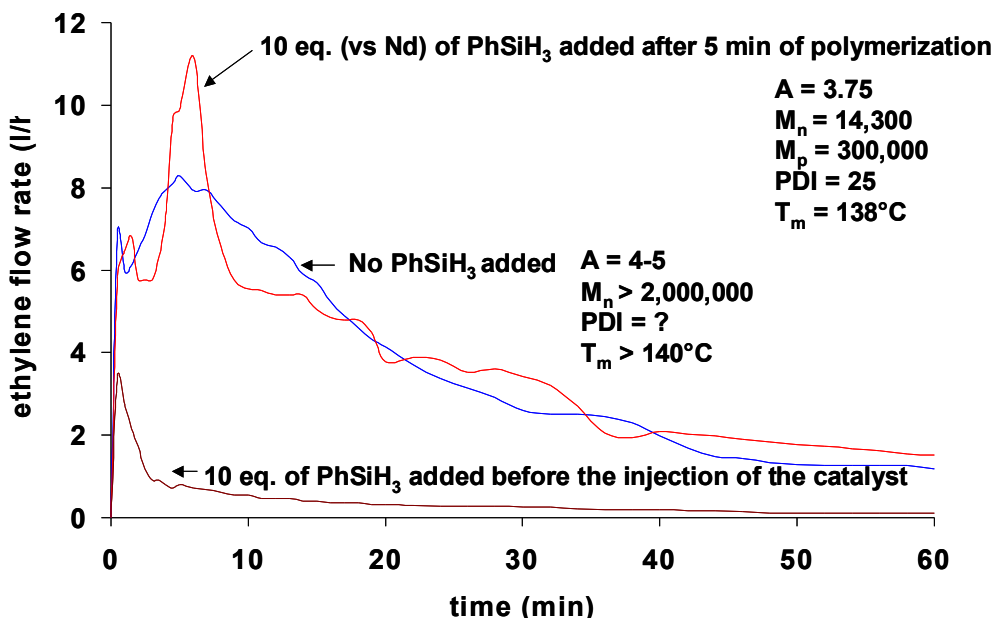
After methanol quenching, workup and drying, the polyethylenes recovered under the optimized conditions ($\text{Nd/Mg} = 1.0$; activation at 0°C for 1 h then polymerization at 0°C) are highly crystalline (85–90 % according to DSC and XRD) with consistent high melting temperatures in the range 139 – 143°C , $M_n = 200,000$ – $400,000$ and $M_w/M_n = 2.3$ – 2.5 . We showed that the polyethylene characteristics do not vary significantly; in particular, high molecular weight polyethylene ($M_n = 301,000$, $M_w/M_n = 2.30$) is already present after 5 min. No low molecular weight chains with vinyl end groups were detected in the final polymer produced under these conditions, indicating that at 0°C , β -H elimination and transfer reactions to the monomer are almost absent, if any (see Appendix 4 & 5 for typical ^1H NMR spectrum of PE and DSC chromatogram). In order to obtain analyzable lower molecular weight polyethylenes, we have investigated the reactivity of our catalyst system towards two well-known transfer agents in lanthanide-mediated olefin polymerization: phenylsilane and dihydrogen.

19.3.6.1. Phenylsilane

The reactivity of the **1/DHM** combination towards transfer agents was briefly evaluated using phenylsilane as transfer agent. The introduction of 10 equiv. of PhSiH_3 (vs. Nd) after 5 min of polymerization did not affect the ethylene flow rate shown in Figure 66 and the related productivity at 0°C . The analysis of the polymer recovered after 1 h revealed, however, that a transfer reaction had occurred, as the M_n decreased to 14,300 with $M_w/M_n = 25$. Addition of

phenylsilane after 2.5 min of polymerization or before injection of the catalytic solution yielded even lower molecular weights respectively, 11,900 and 2400, however, accompanied by a significant drop of the activity ($A = 0.4\text{--}0.8 \text{ kgPE/molNd/atm/h}$). The efficiency of transfer reaction was proved by the ^1H and ^{13}C NMR analysis of the polymer that clearly showed the formation of end-capped PhSiH₂-polyethylenes ($\delta ^1\text{H}$ ($\text{C}_2\text{D}_2\text{Cl}_4$, 130 °C): 4.33 (PhSiH₂), 0.19 (CH_2Si) ppm, see Appendix 6).

Figure 66. Ethylene flow rates in the presence of phenylsilane with **1/DHM** system ($\text{Nd/Mg} = 1.0$; 1 atm; activation 1 h at 0 °C then polymerization 1 h at 0 °C).



19.3.6.2. Molecular dihydrogen

Dihydrogen proved an even better transfer agent. Compared to the reaction carried out with pure ethylene, using 2% (v/v) of H₂ in ethylene led to a similar activity profile but with almost doubled productivity (9–10 kgPE/molNd/atm/h) (Figure 67).*

Analysis of 6 aliquots sampled every 10 min over the polymerization course under those conditions indicated a constant M_n value of 17,000 (± 500) and a molecular weight distribution M_w/M_n of 5.8, showing that an efficient transfer has also occurred. It must be noticed that mechanical stirring allows lower M_n to be obtain with the same H₂ concentration, however, with a slight decrease of activity (Table 29). Effective response of the catalyst system to H₂ was observed in the range 1–10% (v/v). Nevertheless, this could not be used to prevent catalyst decay at temperatures above 0 °C; e.g. the productivity of the **1/DHM** combination at 20 °C in the presence of 2% (v/v) of H₂ decreased to 4.4 kgPE/molNd/atm/h ($M_n = 7800$; $M_w/M_n = 37$).

Figure 67. Typical ethylene consumption plots observed with the **1/DHM** system with pure C₂H₄ and a 98:2 v/v C₂H₄/H₂ mixture ($\text{Nd/Mg} = 1.0$; 1 atm; activation 1 h at 0 °C, polymerization 1 h at 0 °C).

* A doubled activity was also observed with Mg(CH₂SiMe₃)₂ (5.7 kgPE/molNd/atm/h, activation 1 h at 20 °C then polymerization 1 h at 20 °C), and with Sm *tert*-butoxide/DHM combination (2.7 kgPE/molSm/atm/h, activation 1 h at 0 °C then polymerization 1 h at 0 °C).

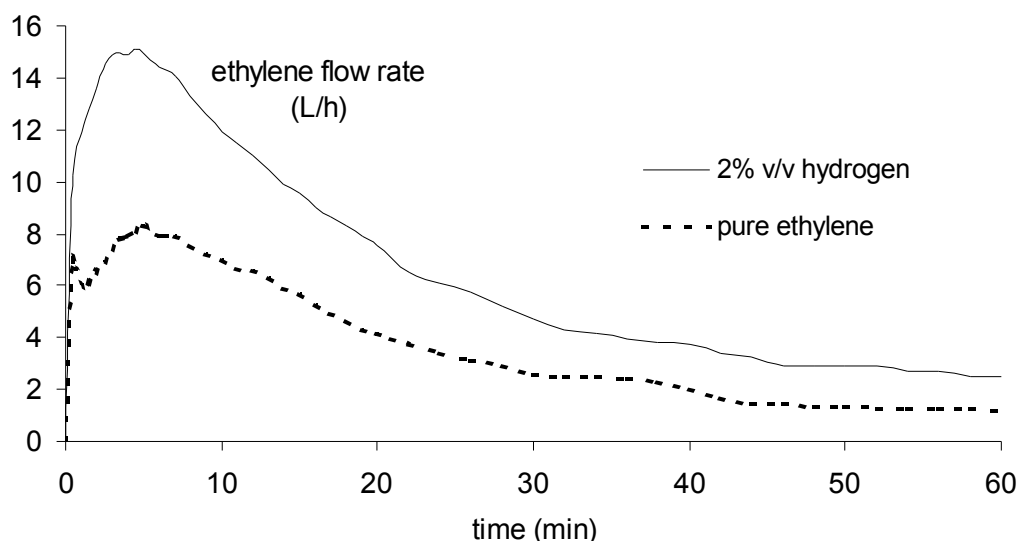


Table 29. Polymer characteristics and activites for different H₂ concentrations.

H ₂ (%)	M _n (10 ⁻³)	M _w /M _n	T _m (°C)	Activity (kgPE/molNd/atm/h)
0	not soluble	-	140-143	4.5
1	not soluble		140	10
2	310	2.4	139	9.6
2 ^a	17	5.8	nd	7.0
2 ^b	7.8	37	134.8	4.4
10	27	10.6	137.5	8.8

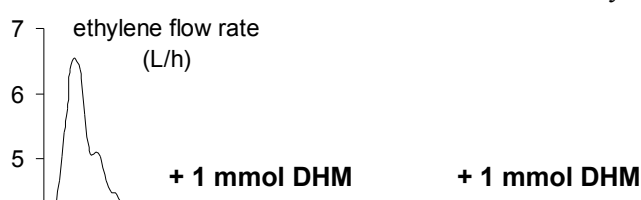
Conditions: Nd/Mg = 1.0; 1 atm; activation 1 h at 0 °C then polymerization 1 h at 0 °C. ^a mechanical stirring.

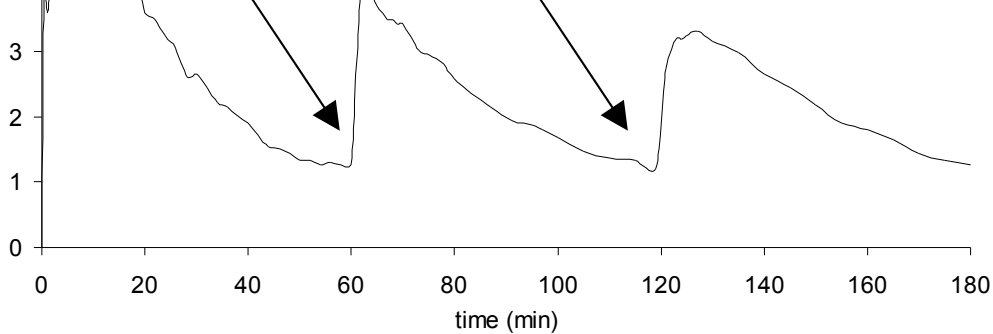
^b polymerization temperature: 20 °C.

19.3.7. Effect of further additions of dialkylmagnesium

The apparent polymerization activity (ethylene flow rate) of the **1**/DHM combination decreases after a few minutes to reach a plateau after 60 min, at ca. 1/10 of the maximal activity (Figure 58). We observed that the latter could be rapidly, although partially restored upon adding 1.0 equiv. of DHM vs. Nd to the reaction mixture; then, polymerization proceeded as in the initial batch (Figure 68). Similar restoration of activity was achieved three times consecutively from the same initial *in situ* combination. It should be noted that addition of **1** (1 mmol) after 1 h of polymerization did not affect the polymerization at all, indicating the absence of free dialkylmagnesium reagent for subsequent formation of active species. Consequently, this shows that the decrease in the ethylene flow rate does not stem from an irreversible deactivation process but suggests rather a gradual "drowsiness" of the active species, that may be associated to the concomitant accumulation of insoluble, high molecular weight materials over the reaction course.

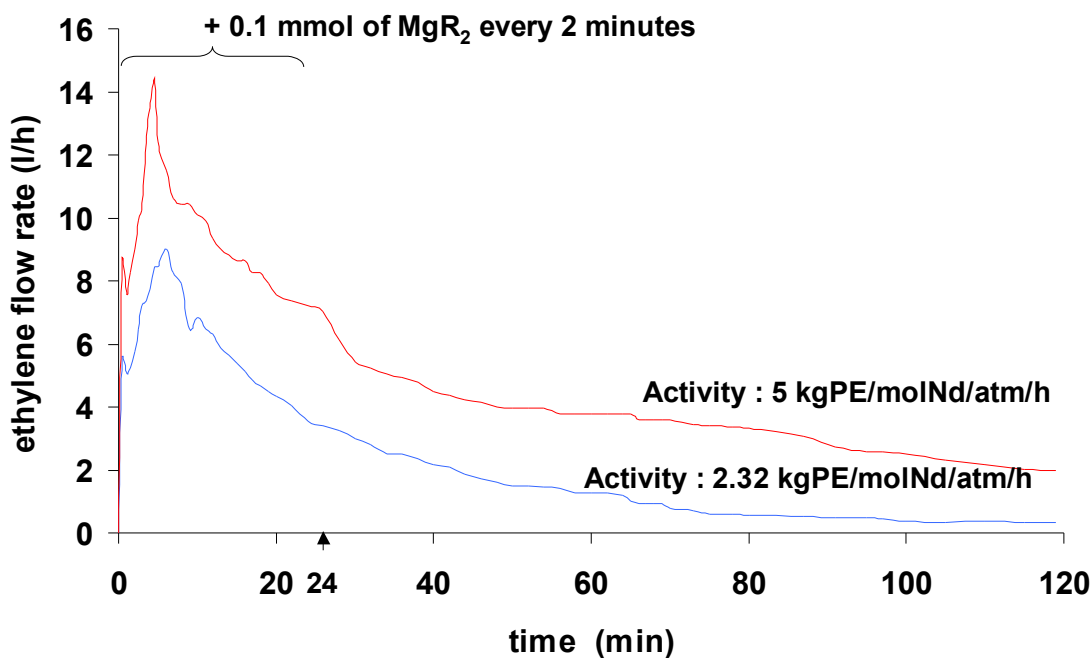
Figure 68. Consecutive reactivations of the *in situ* **1**/DHM system by addition of DHM.





Repeated additions of 0.1 mmol of DHM every 2 min during the first 25 min of polymerization proved to be another possible way to increase the activity of the catalyst system. The overall activity jumps from 4.5 to 7.6 kgPE/molNd/atm/h over 1 h of polymerization and doubled after 2 h (Figure 69). A significant increase of the molecular weight throughout the polymerization is consistent with the SEC analyses. Indeed, the polymer obtained after 30 min of polymerization presents $M_n = 222,000$ with $M_w/M_n = 3.6$ while the resulting polymers recovered after 1 and 2 hours are insoluble under the conditions of analysis. Nevertheless, this result is quite surprising since with an initial ratio Nd/Mg = 2.0, the catalytic system is poorly active (see §19.3.2). The dialkylmagnesium may act as a scavenger or creates new initiating species.

Figure 69. Effect of sequential additions of DHM during the early stage of the polymerization.

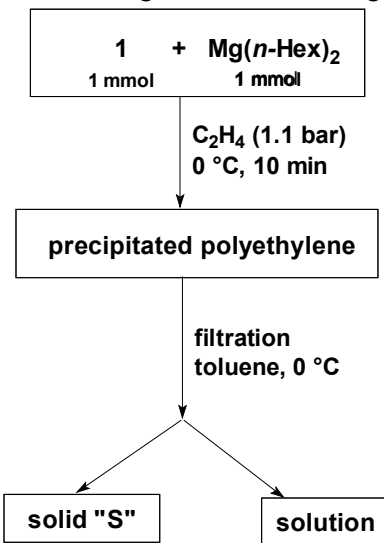


19.4. Ethylene polymerization with the precipitated polymer

19.4.1. Principle

In order to determine the distribution of total and active Nd in solution (homogeneous) and in the polymeric material precipitated (heterogeneous) during the reaction course, the latter was isolated from the reaction mixture by filtration and subsequently washed with toluene under rigorous exclusion of oxygen and water at 0 °C, as schematically represented in Figure 70. The beige solid (**S**) recovered was subjected to microanalyses which revealed, over three different samples, that $15 \pm 2\%$ of initial Nd (and $20 \pm 4\%$ of Mg) is present in the precipitate. The Nd/Mg ratio in **S** is 1.2 ± 0.4 and approaches therefore that introduced for the *in situ* system ($\text{Nd/Mg} = 1.0$). Interestingly, similar distribution of the lanthanide metal between the toluene solution and the solid precipitated was observed from the " $\text{Sm}(\text{OtBu})_3$ "/ $\text{Mg}(n\text{-hex})_2$ /ethylene system.

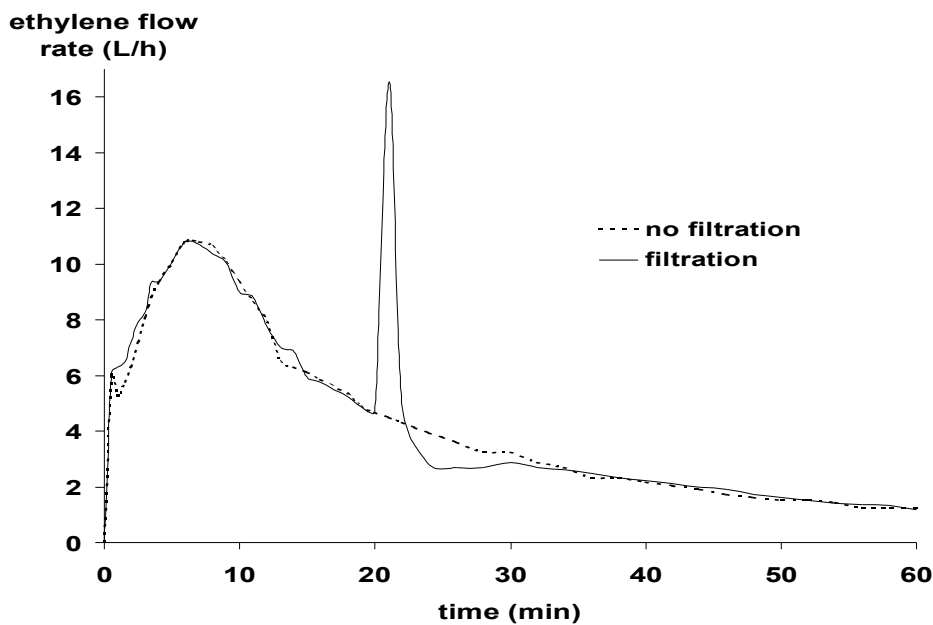
Figure 70. Principle of separation of homogeneous and heterogeneous species.



19.4.2. Activity of the separated phases

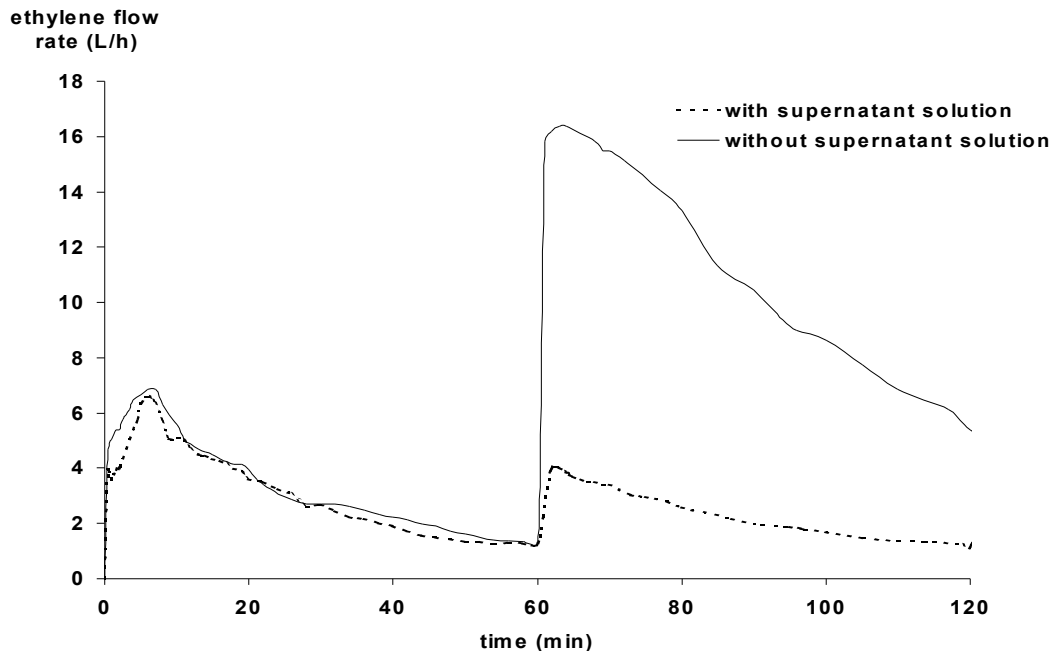
More interestingly, when **S** was contacted with ethylene in a fresh toluene slurry (1 atm, 0 °C), polymerization took place with the same activity as in the corresponding *in situ* experiment, just before its isolation (Figure 71). On the other hand, the clear filtrate that contains $85 \pm 2\%$ of initial Nd proved completely inactive towards ethylene, even upon reactivation with fresh DHM. These results establish that all of the active species generated from the *in situ* combination of **1** with DHM (1:1) are contained in solid **S**. As a matter of fact, it turned out that **S** polymerizes ethylene under solid-gas conditions with significant activity (6 kgPE/molNd/atm/h over 30 min at 0 °C).

Figure 71. Influence of solution removal on the ethylene flow rate ($\text{Nd}/\text{DHM} = 1.0$; 1 atm; activation 1 h at 0°C then polymerization 1 h at 0°C).



Noteworthy, when a fresh toluene suspension of **S** was treated with 1.0 equiv. of DHM (vs. Nd used in the *in situ* combination to prepare **S**), the ethylene polymerization activity could be strongly enhanced as compared to the initial polymerization reaction (up to 100 kgPE/molNd/atm/h) (Figure 72).

Figure 72. Effect of the addition of 1.0 equiv. of DHM (vs. $[\text{Nd}]_0$) to the reaction mixtures with and without supernatant on the ethylene flow rates ($\text{Nd}/\text{DHM} = 1.0$; 1 atm; activation 1 h at 0°C then polymerization 1 h at 0°C).



To clarify this phenomenon, which is in direct line with the aforementioned restoration of the catalytic activity upon addition of dialkylmagnesium to the *in situ* system, separate experiments were conducted. No redistribution of Nd metal between the solid and the supernatant toluene solution (Induced Conductively Plasma elemental analysis) was observed upon treatment of a toluene suspension of **S** with excess of DHM. These results rule out the hypothesis of a simple transmetallation process between the dialkylmagnesium reagent and insoluble (slowly active) Nd-polyethylenyl species contained in **S** to form soluble (highly active) Nd-alkyl species. Two other hypotheses that remain to be supported are: a scavenging action of MgR₂ comparable to the well-documented effect of trialkylaluminums in group 4-promoted polymerization and/or more likely the formation of new active sites.

20. Diblock copolymerizations

Given the high interest in the preparation of polar-non polar diblock copolymer and the possibility to achieve pseudo-living polymerizations of ethylene and MMA with the same catalyst system, we have decided to investigate the diblock copolymerization of ethylene with various polar monomers, focusing on MMA.

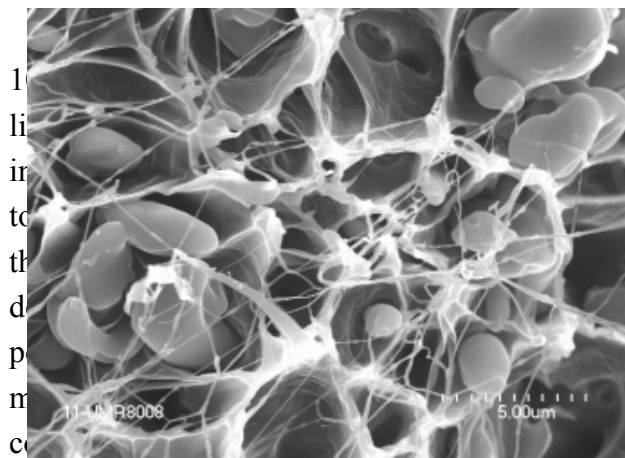
20.1. Synthesis of olefin-MMA diblock copolymers in the literature

The ability to produce controlled polyolefin-based functional materials containing functional groups into polyolefin main chain is the ultimate goal in the macromolecular engineering.⁴ The incorporation of polar groups may exercise control over important properties such as toughness, adhesion, barrier properties, surface properties (paintability, printability...), solvent resistance (or its inverse), miscibility with other polymers, and rheological properties.²⁹⁴ An important feature of successful copolymerization of two monomers is the ability to control the amount and distribution of comonomer in the final polymer. So we would like to give a brief overview of the different techniques and catalysts used for the preparation of ethylene-polar monomer diblock copolymers, focusing almost exclusively on ethylene-MMA diblock copolymerization.

20.1.1. With lanthanide-based catalysts

The first example of well-controlled block copolymerizations was allowed by the dual catalytic function of Cp*₂LnR (Ln = Sm, Yb, Lu; R = H, Me) towards both polar and nonpolar olefins.¹²¹ Thus, the desired copolymerization of ethylene with MMA was achieved by a two-step procedure: the homopolymerization of ethylene under mild conditions (1 bar ethylene pressure, 20 °C in toluene) is followed by a sequential addition of MMA. Reversed addition of the respective monomers (MMA then ethylene) did not perform the block copolymerization. Only homo-polymerization of the methacrylate occurred.

²⁹⁴ For a recent review on compatibilization of polymer blends, see: Koning, C.; Van Duin, M.; Pagnoulle, C.; Jerome, R. *Prog. Polym. Sci.* **1998**, 23, 707–757.

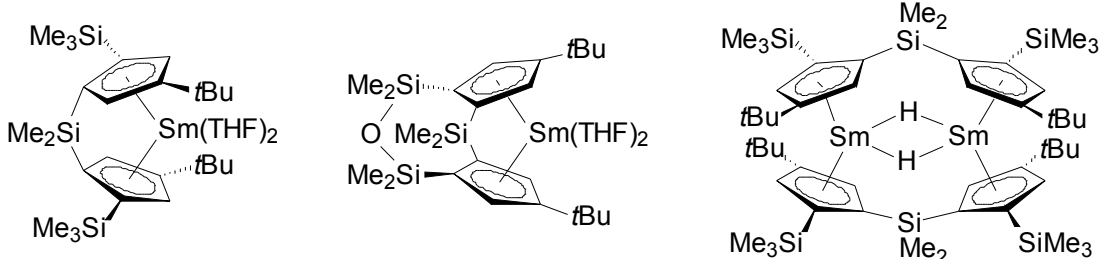


ichlorobenzene and 1,2,4-trichlorobenzene at 100 °C. The reaction yields quantitative conversion into the desired block copolymers from hot THF display molecular weights up to 1,900. The relative molar ratio of polyethylene in the range of 100:1 to 100:103 when M_n of the PE block is increased. Increasing M_n value of the PE block results in a decrease in the molecular weight especially when $M_n > 12,000$, i.e. when the PE blocks are too long to be active sites by the crystalline polyethylene sites and hence causes suppression of further polyethylene diblock copolymerization with ethyl or methyl acrylate, and δ -valerolactone or ϵ -caprolactone.

The resulting molecular weights observed with Cp^*_2LnR are too low to provide excellent physical properties. Thus, higher molecular weight copolymers were prepared using $[Me_2Si(C_5H_3-3-SiMe_3)_2SmH]_2$ as catalyst.²⁹⁵ In this case, molecular weights up to 70,000 were obtained with $M_w/M_n = 1.67-1.69$; PMMA content remained relatively high (19 mol%). Even higher molecular weights were obtained with the monocyclopentadienyl complex $Cp^*La(CTMS)_2$ but as expected the incorporation of MMA is low. The PMMA content is lower than 1 mol% for $M_n = 136,500$.¹³⁷

Block copolymerizations of higher olefins such as 1-pentene or 1-hexene with polar monomers like MMA or ϵ -caprolactone were first obtained using dinuclear trivalent lanthanide complexes (Figure 73).

Figure 73. Efficient lanthanide complexes in olefin-MMA diblock copolymerization.



Again, the order of addition should respect the following order: first addition of the olefin and then of the polar monomer. The crude product is composed of two kinds of polymers as evidenced by SEC analysis. The extraction products using hot hexane gives rise to the remaining block copolymers, which show a unimodal pattern. The ratio of olefin to polar monomer unit can be varied from 5:1 to 1:5 by adjustment of the feed ratios of the two monomers.²⁹⁶ The molecular weights are still quite low since $M_n = 53,000$ is the highest M_n value obtained.

²⁹⁵ Desurmont, G.; Li, Y.; Yasuda, H.; Maruo, T.; Kanehisa, N.; Kai, Y. *Organometallics* **2000**, *19*, 1811-1813.

²⁹⁶ (a) Desurmont, G.; Tokimitsu, T.; Yasuda, H. *Macromolecules* **2000**, *22*, 7679-7681. (b) Desurmont, G.; Tanaka, M.; Li, Y.; Yasuda, H.; Tokimitsu, T.; Tone, S.; Yanagase, A. *J. Polym. Sci., Part A: Polym. Chem.* **2000**, *38*, 4095-4109. (c) Yasuda, H. *J. Organomet. Chem.* **2002**, *647*, 128-138.

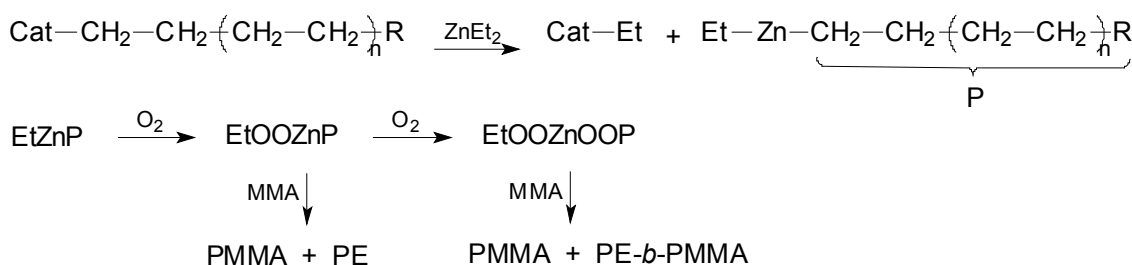
Finally, it can be noticed that ABA-type triblock copolymers were also prepared using bridged divalent rare-earth metal complexes such as the *meso* Me₂Si(Me₂SiOSiMe₂)-(C₅H₂-3-*t*Bu)₂Sm(THF), the *racemic* Me₂Si(2-SiMe₃-4-*t*BuMe₂SiC₅H₂)Sm(THF)₂ (Figure 73).¹¹⁷

20.1.2. With Group 4 catalysts

20.1.2.1. Multistep procedures

Initially, traditional Ziegler-Natta catalysts have been employed for the preparation of diblock copolymers. The first developed method consisted of converting the "living" chains into free radicals in the presence of peroxides to allow the formation of the blocks.²⁹⁷ This method yielded few percents of block copolymer since the number of living chains is extremely low (ca. 10⁻³ mol per mol of TiCl₃). On the other hand, it has been found in the 1970's, that the incorporation of a suitable chain transfer agent such as diethyl zinc during the olefin polymerization provides a new way to increase considerably the number of active sites, which are capable to initiate, in the presence of a radical initiator, the polymerization of polar monomers (Scheme 28).²⁹⁸ This method gave good yields of ethylene-MMA block copolymers containing variable amounts of MMA (up to 63 wt%), even if the formation of homo-PMMA was ineluctable. The molecular weights of the copolymers are not given, however, the molecular weight of the polyethylene block is in the range M_v = 46,000-68,000.

Scheme 28. Ethylene-MMA diblock copolymerization using ZnEt₂ as transfer agent with Ziegler-Natta catalysts.²⁹⁸



The approach consisting of using transfer agent was more recently reported with homogeneous metallocene catalysts.²⁹⁹ A new borane (9-borabicyclo[3.3.1]nonane dimer or 9-BBN) was shown to be effective as *in situ* chain transfer agent in metallocene-catalyzed olefin polymerization. This chemistry provides a convenient route to the synthesis of borane-terminated polyolefins that are very valuable intermediates for preparing functionalized polyolefins with a polar end group or diblock copolymers with a polar polymer segment. Indeed, the oxidation of the borane group by NaOH/H₂O₂ leads to the hydroxy-terminated polymer while its oxidation by O₂ in the presence of MMA leads to the desired diblock copolymer. Under these conditions, only 10% of the crude product is removed by Soxhlet

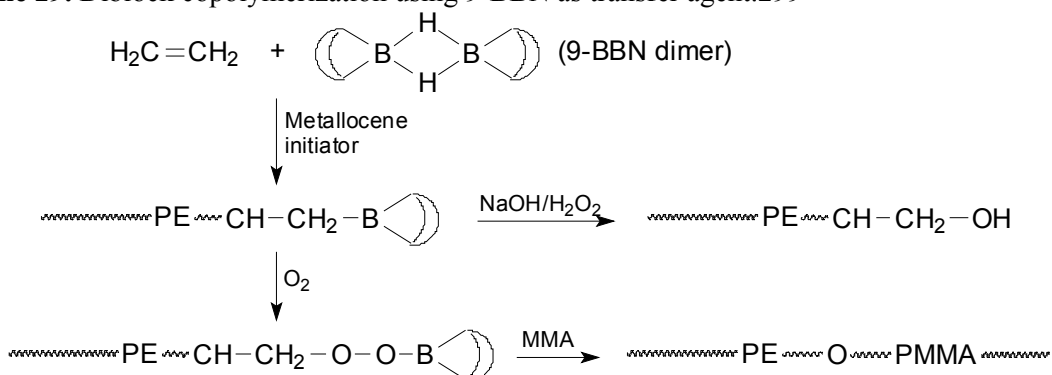
²⁹⁷ Jezl, J. L.; Chu, N. S.; Khelghatian, H. M. *ACS meeting, San Francisco, 1968*.

²⁹⁸ Agouri, E.; Parlant, C.; Mornet, P.; Rideau, J.; Teitgen, F. F. *Makromol. Chem.* **1970**, *137*, 229-243.

²⁹⁹ (a) Chung, T. C.; Lu, H. L.; Janvikul, W. *Polymer* **1997**, *38*, 1495-1502. (b) Xu, G.; Chung, T. C. *J. Am. Chem. Soc.* **1999**, *121*, 6763-6764.

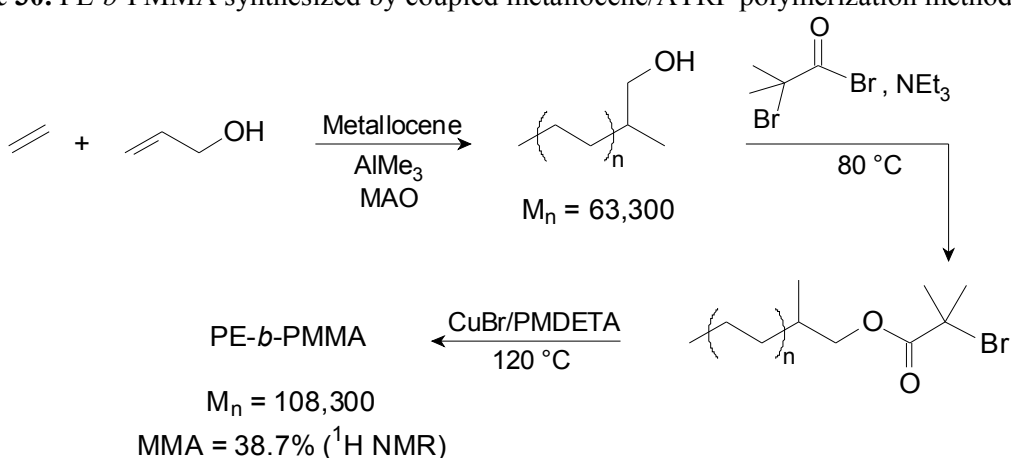
extraction using boiling THF. The insoluble part shows a rather high molecular weight ($M_n = 90,300$) with a 1:1 PE/PMMA molar ratio.

Scheme 29. Diblock copolymerization using 9-BBN as transfer agent.²⁹⁹



The preparation of hydroxy-terminated PE was also reported via the copolymerization of ethylene and allylic alcohol using a specific metallocene catalyst.³⁰⁰ The modification of this hydroxy-terminated PE leads a bromo-terminated polyolefin which can be employed as macroinitiator in ATRP. Subsequent polymerization of MMA initiated by this macroinitiator yields a high molecular weight PE-*b*-PMMA ($M_n = 108,300$) (Scheme 30).³⁰¹ It is worth noting that hydroxy-terminated polyolefins were also used as macroinitiators for the synthesis of polyolefin-*b*-polycaprolactone diblock copolymers.³⁰²

Scheme 30. PE-*b*-PMMA synthesized by coupled metallocene/ATRP polymerization methods.³⁰¹



Finally, isotactic poly(propylene)-*b*-poly(methyl methacrylate) copolymers were reported using magnesium bromide-terminated poly(propylene) as an anionic initiator for MMA polymerization.³⁰³ This macro-Grignard reagents were prepared by hydroboration of the

³⁰⁰ Imuta, J.-I.; Kashiwa, N.; Toda, Y. *J. Am. Chem. Soc.* **2002**, *124*, 1176-1177.

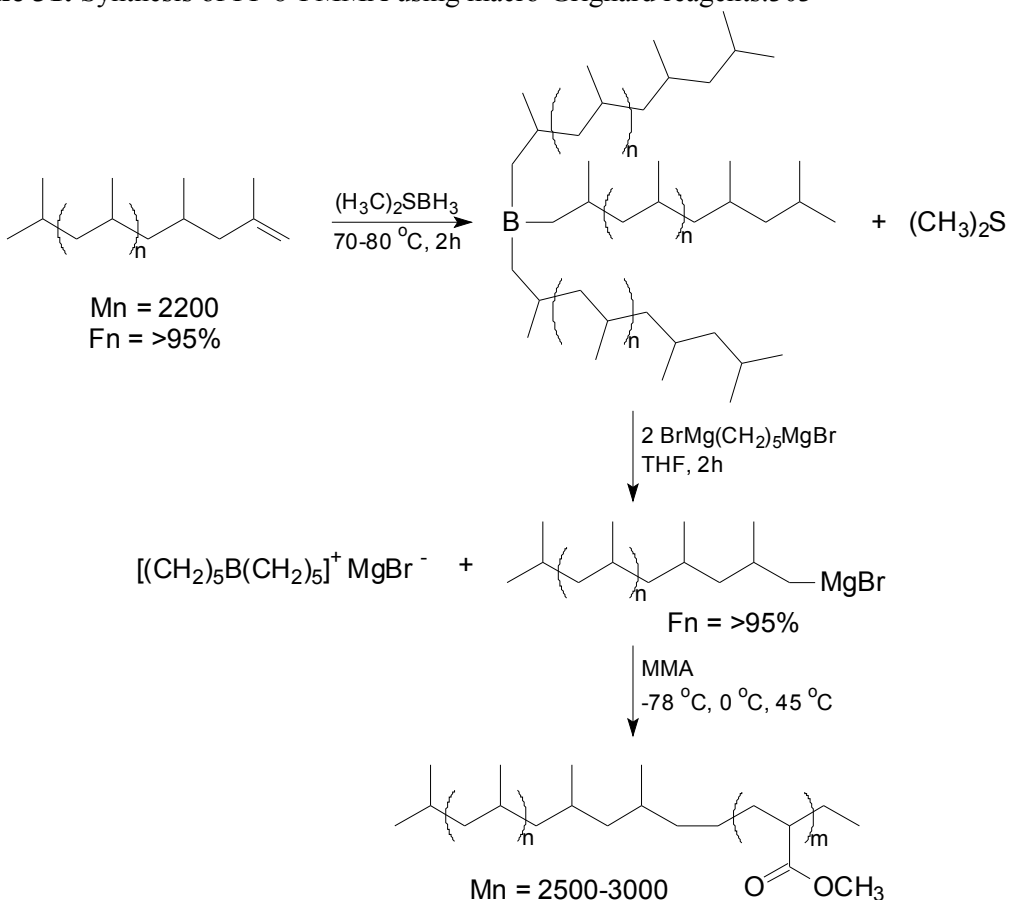
³⁰¹ Kojoh, S.; Matsugi, T.; Kaneko, H.; Matsuo, S.; Kawahara, N.; Imuta, J.; Kashiwa, N. (Mitsui Chemicals); *EUPOC 2003*, Milano.

³⁰² (a) Sosnowski, S.; Slomkowski, S; Penczak, S.; Florjanczyk, Z. *Makrom. Chem.* **1991**, *192*, 1457-1465. (b) Mulhaupt, R.; Duschek, T.; Rosch, J. *Polym. Adv. Technol.* **1993**, *4*, 439. (c) Han, C. J.; Lee, M. S.; Byun, D.-J.; Kim, S. Y. *Macromolecules* **2002**, *35*, 8923-8925.

³⁰³ Shiono, T.; Akino, Y.; Soga, K. *Macromolecules* **1994**, *27*, 6229-6231.

terminal vinylidene unsaturation by a borane dimethylsulphide complex followed by a reaction with pentane-1,5-di(magnesiumbromide) as depicted in Scheme 31.

Scheme 31. Synthesis of PP-*b*-PMMA using macro-Grignard reagents.³⁰³



The different methods of synthesis of olefin-MMA diblock and graft copolymers based on borane have been recently reviewed.³⁰⁴

20.1.2.2. Two-step procedures

The first two-step procedure using a zirconocene-based catalyst system for the ethylene-MMA diblock copolymerization was reported 10 years after Yasuda's work with lanthanocene complexes.³⁰⁵ The catalyst was generated *in situ* from Me₂C(Cp)(Ind)ZrMe₂ and B(C₆F₅)₃ in toluene. Block polymerization is achieved via the sequential addition of the monomers, starting with ethylene, as previously reported for lanthanocene-mediated copolymerizations. SEC copolymers analysis shows a broad but unimodal molecular weight distribution ($M_w/M_n = 2.4\text{-}2.6$) and limited molecular weights ($M_n = 12,000\text{-}17,000$). The PMMA segments are highly isotactic as expected from MMA homopolymerization with [Me₂C(Cp)(Ind)Zr-Me(THF)][B(Ph)₄].¹⁶⁹ At the same time, Chen and co-workers have presented the diblock

³⁰⁴ Chung, T. C. *Prog. Polym. Sci.* **2002**, 27, 39-85.

³⁰⁵ Frauenrath, H.; Balk, S.; Keul, H.; Höcker, H. *Macromol. Rapid Commun.* **2001**, 22, 1147-1151.

copolymerization of propylene and MMA using a constrained geometry catalyst.³⁰⁶ Using $[\text{Me}_2\text{Si}(\eta^5\text{-Me}_4\text{Cp})(t\text{BuN})\text{TiMe}][\text{MeB}(\text{C}_6\text{F}_5)_3]$, it is possible to synthesize stereo-diblock copolymers with an atactic poly(propylene) block and a syndiotactic PMMA segment. The resulting copolymers exhibit the narrowest molecular weight distributions ever obtained for such diblock copolymer ($M_w/M_n = 1.08\text{-}1.14$), if we do not take into account the copolymers prepared by the indirect way which consists in the hydrogenation of butadiene copolymers (*vide infra*). However, the molecular weights are again low and do not exceed 21,100 g/mol. The MMA units content is high (up to 70 mol%) depending on the reaction conditions. Interestingly, isotactic-PP-*b*-isotactic-PMMA can be produced with the C_2 -symmetric *rac*-(EBI)ZrMe₂ (EBI = ethylene bis(indenyl)) activated by B(C₆F₅)₃. With this catalyst, the living behavior of the polymerization is not observed ($M_w/M_n = 1.66\text{-}2.20$) and the molecular weights are even lower ($M_n = 11,000\text{-}13,000$). Finally, it must be noted that the choice of the activator is crucial in these systems, determining the relative amount of the copolymer vs. homopolymers.

20.1.3. Indirect method: hydrogenation of polybutadiene

Selective hydrogenation of the polybutadiene segment of polybutadiene-*b*-poly(methyl methacrylate) copolymers is another attractive method for the preparation of ethylene-polar monomer diblock copolymers.³⁰⁷ The advantage of this method relies on the precise control of the molecular weight of the copolymer since they can be prepared by either living anionic or controlled/"living" radical polymerizations.³⁰⁸ However, the resulting polyethylene block usually presents many short chain-branchings due to the initial 1,2-polymerization of the butadiene, providing inferior mechanical properties.

20.2. Ethylene-MMA

20.2.1. Preparation of the copolymers

A major interest of alkyl-lanthanides in polymerization relies on their unique propensity to induce both polymerization of ethylene and polar monomers.¹¹⁷ We investigated therefore the ability of the new *in situ* catalyst combination **1**/DHM and that of isolated compound **S** (solid recovered from slurry ethylene polymerization) to initiate the diblock copolymerization of ethylene and MMA.

³⁰⁶ (a) Bolig, A. D.; Jin, J.; Xu, J. Chen, E. Y.-X. 223rd National ACS meeting, **2001**. (b) Jin, J.; Chen, E. Y.-X. *Macromol. Chem. Phys.* **2002**, *203*, 2329-2333.

³⁰⁷ For examples: (a) Yokota, K.; Hirabayashi, T. *Polym. J.* **1981**, *13*, 813. (b) Auschra, C.; Stadler, R. *Polym. Bull.* **1993**, *30*, 257. (c) Ren, Q.; Zhang, H. J.; Zhang, X. K.; Huang, B. T. *J. Polym. Sci., Part A; Polym. Chem.* **1993**, *31*, 847-851. (d) Yu, J. M.; Yu, Y.; Dubois, P.; Teyssie, P. Jerome, R. *Polymer* **1997**, *38*, 3091-3101.

³⁰⁸ For the synthesis of well-defined butadiene copolymers see: (a) Hadjichristidis, N.; Pitsikalis, M.; Pispas, S.; Iatrou, H. *Chem. Rev.* **2001**, *101*, 3747-3792. (b) Patten, T. E.; Matyjaszewski, K. *Adv. Mater.* **1998**, *10*, 901-915.

20.2.1.1. *In situ* system

The copolymerization was carried out by sequential addition of MMA after a prepolymerization of ethylene for 10–15 min under the standard conditions described in §19.2.2. Reverse order of addition of the monomers results as observed with lanthanocene and zirconocene catalysts in the formation of homo-PMMA.^{121,305} The crude polymer, obtained via initial polymerization of ethylene with the *in situ* system and subsequent addition of MMA to the reaction mixture at 0 °C, was shown to contain 15–20% of atactic homo-PMMA (Soxhlet extraction with THF for 3 days). This suggests that the *in situ* combination **1/DHM** generates more than one active species for the polymerization of MMA, of which only one is able to initiate the polymerization of ethylene. Indeed, we checked that the solution recovered after filtration of precipitate **S** from the reaction mixture that contains 80–85% of Nd and Mg initially introduced but proved inactive towards ethylene, does initiate the polymerization of MMA to give atactic PMMA in moderate activity.

20.2.1.2. Solid **S** as initiator

On the other hand, the crude polymer recovered from the reaction of MMA with a slurry of solid **S** in fresh toluene at 0 °C contained only 3% of extractable products; ¹H NMR analysis showed that the latter are low molecular weight MMA-rich block copolymers (MMA/ethylene ~ 3). The MMA molar fraction in the THF-insoluble material obtained under typical conditions (see Experimental section) is 7 ± 2% according to the weight increase, ¹H NMR and SEC analyses. The DSC analysis revealed the T_g of the PMMA block at 122 °C and the T_m of the PE block as a narrow peak at 142 °C. The SEC analyses of the polyethylene obtained from the hydrolysis of an aliquot of **S** (before addition of MMA) and of the final THF-insoluble material showed an increase of the molecular weight from M_n = 200,000 to M_n = 250,000 with a M_w/M_n of 4.0 (monomodal) in both cases (see Appendix 7 & 8 for ¹H NMR and IR spectra of PE-*b*-PMMA). All of these results confirm the true diblock nature of the polymer and, in turns, that ethylene polymerization using the **1/DHM** combination proceeds in a "pseudo-living" fashion to give the Nd-polyethylenyl intermediate **S**. In addition to the monomer efficiency of the diblock polymerization process, the possibility to attain block lengths as high as 200,000 for the PE block and ca. 50,000 for the PMMA block is especially interesting. As far as we are aware, these values are significantly higher than those realized with lanthanocene initiators,^{295,296} and allow to consider these materials as valuable compatibilizers.

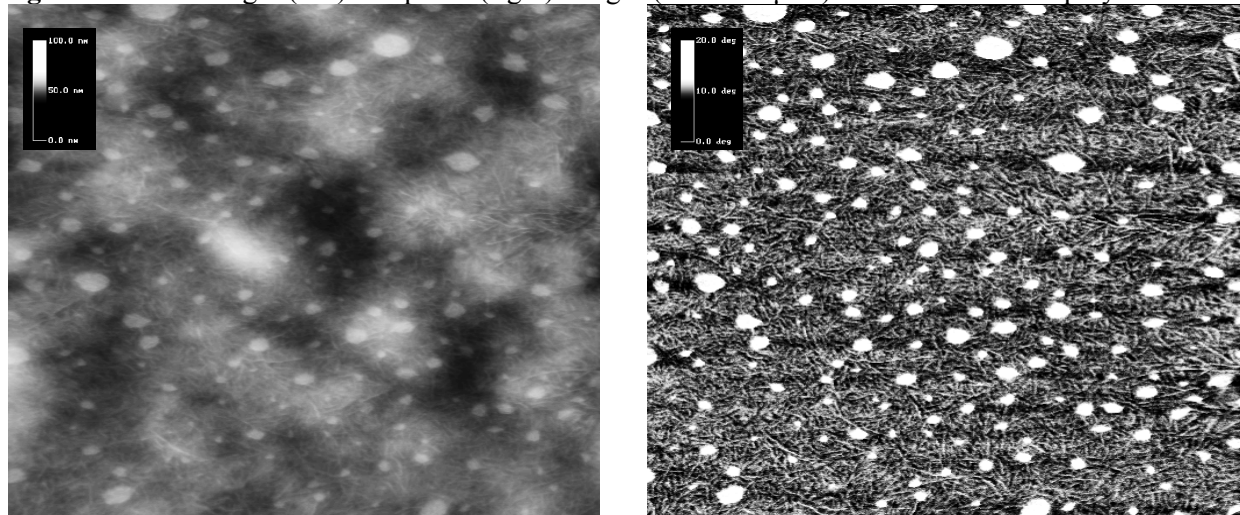
20.2.2. Morphological characterization

Beside the usual characterization by ¹H NMR and SEC analyses, we carried out a morphological investigation of our poly(ethylene-*b*-methyl methacrylate) diblock copolymers. Two different but complementary microscopy techniques could be employed: the atomic force microscopy (AFM) and the transmission electron microscopy (TEM). The "material contrast" between the different components is achieved in TEM by selective staining methods with

reactive heavy metal compounds, and is generated in AFM with phase contrast imaging in tapping mode. We will describe here the preliminary results obtained by AFM using a copolymer with $M_n = 420,000$. $M_w/M_n = 4.5$ and a moderate MMA units content (11 mol %).

The AFM measurements were performed on thin polymer films obtained by solvent casting on a freshly cleaved mica substrate. Film deposition was carried out as follows: a copolymer solution (1 mg/mL) in $C_2H_2Cl_4$ was deposited on the substrate with a microsyringe and left to evaporate for up to 96 h at room temperature in a dessicator. Then, the polymer sample was annealed (160 °C) in vacuum overnight in order to improve the phase separation process. Both topographic (height) and phase imaged were recorded simultaneously. The phase signal is most sensitive to difference in tip-surface interactions; it enables to distinguish between domains with different mechanical or adhesion properties and gives a sharp response over the edges between the domains. It is therefore complementary to height cartography. The images obtained with a scan size of 3 μm are shown in Figure 74.

Figure 74. AFM height (left) and phase (right) images ($3.0 \times 3.0 \mu\text{m}^2$) of PE-*b*-PMMA copolymer.



On these AFM images, we can see a clear phase-separation contrary to the observations made by Yasuda *et al.*²⁹⁶ The higher molecular weight as well as the lowest PMMA content of our sample may be responsible for such difference. The material is composed of a crystalline matrix that can be attributed to the PE, in which we can find some amorphous spherical domains of 75-300 nm diameters. The presence of highly crystalline PE is consistent with DSC and XRD measurements that suggest 80-90% of crystallinity in homopolyethylene samples, indicating that the presence of PMMA does not affect the crystallinity of the PE block. It is worth noting that structural changes in block copolymers containing a crystallizable component, in particular chain-folding, resulting from crystallization compete with those occurring due to microphase separation. Experiments suggest that the final morphology after crystallization depends on whether the sample is cooled from a microphase-separated melt or crystallizes from a homogeneous melt or solution.³⁰⁹

³⁰⁹ Hamley, I. W. *Adv. Polym. Sci.* **1999**, 148, 113-137.

The spherical domains that may be attributed to the PMMA or to an amorphous PE-PMMA mixture are well distributed over the entire surface of the sample. However, the sizes of these domains are quite heterogeneous and can be correlated to the broad molecular weight distribution of the copolymer sample. Indeed, the polymer chains may have a wide range of PMMA content. The phase image is complementary of the height image regarding the heterogeneity of the sample surface. In addition, it allows for measuring the distance between the folded PE, which form the lamellae of the crystalline matrix (15-30 nm). Attempts to get complementary data by transmission electron microscopy are under way.

20.2.3. Application as compatibilizing agent

As aforementioned, PE-PMMA diblock copolymers with such a high molecular weight may be excellent compatibilizing agents.^{301,310} Consequently, we have prepared some polymer blends of various compositions with or without addition of copolymer using a conical double-screw extruder.

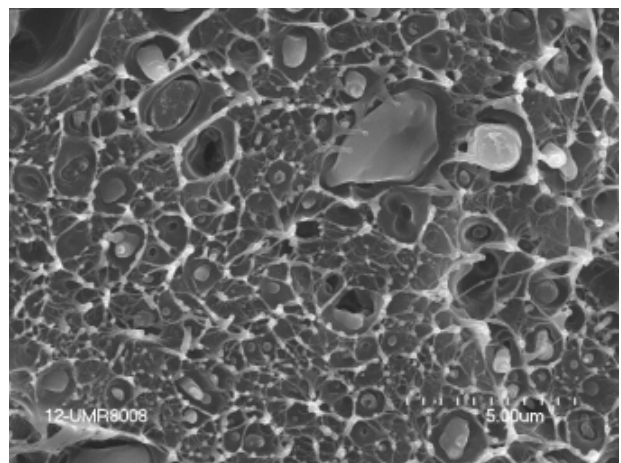
Thus, high density polyethylene (Du Pont, $M_n = 90,000$, $M_w/M_n = 3.5$), poly(methyl methacrylate) (Atochem, $M_n = 41,000$; $M_w/M_n = 2.1$), and poly(ethylene-*b*-methyl methacrylate) ($M_n = 420,000$; $M_w/M_n = 4.5$ with PMMA = 11 mol%) were mixed together at 190 °C for 5 min at 50 rpm. Under these conditions, the samples were assumed to be "homogeneous" given the stabilization of the monitored internal torque. PE/PMMA (80/20 wt%), and PE/PMMA/copolymer (73/18/9) blends were analyzed by scanning electron microscopy (SEM) to study the compatibilizing effect of the copolymer.

The samples were prepared by cryo-cut in liquid nitrogen of polymer plates. The micrographs shown in Figure 75 are consistent with compatibilizing effect of the diblock copolymer. Indeed, in the presence of the copolymer, the sample exhibits an enhanced homogeneity; PMMA particles are well dispersed in the PE matrix yielding most probably a blend with enhanced mechanical properties. This will be explored in a near future as well as the study of these polymer blends by transmission electronic microscopy.

The catalytic system composed of **1** and DHM proves to be an efficient catalyst for ethylene-MMA block copolymerization. This feature allows once again for direct comparison with lanthanocene catalysts. The prepared copolymers were characterized using different techniques including SEC analysis, NMR spectroscopy, differential scanning calorimetry and atomic force microscopy, corroborating the true nature of the diblock copolymer. In addition, used as a compatibilizer, this copolymers seems to have a real effect in PE/PMMA blends. However, further microscopic investigation of these materials and blends as well as the evaluation of the mechanical properties needs to be performed.

Figure 75. SEM micrographs ($20 \times 15 \mu\text{m}^2$) of a neat PE/PMMA blend (left) and a PE/PMMA blend in the presence of PE-*b*-PMMA (9 wt%).

³¹⁰ Kobori, Y.; Yasumitsu, R.; Akiyama, S.; Akiba, I.; Sano, H. *Polymer*, **2002**, *43*, 6065-6067.



20.3. Other diblock copolymerizations

In addition to the diblock copolymerization ethylene-MMA, we performed also the diblock copolymerization of ethylene with methyl acrylate (MA) and ϵ -caprolactone. The successful preparation of these diblock copolymers was previously reported using lanthanocene-based systems.¹¹⁷

20.3.1. Ethylene-methyl acrylate diblock copolymerization

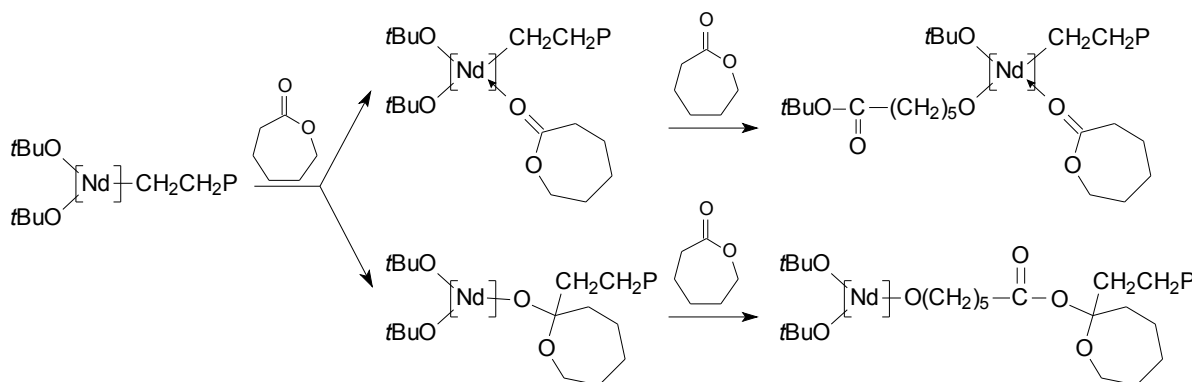
The copolymerization was carried out as reported for MMA using the solid **S** as macroinitiator. Methyl acrylate conversion calculated from the gravimetrically determined polymer yield is consistent with the preparation of a copolymer containing 30 wt% of MA. Extraction of the crude polymer in boiling THF for 3 days, results in the solubilization of 5 wt% of the polymer. The THF-insoluble fraction was characterized by ^1H NMR, SEC and IR-FT analyses. Integral values of the ^1H NMR spectrum are not in agreement with a copolymer containing 25 wt% of MA but rather with a much lower MA content (< 5 wt%). However, the IR spectrum shows unambiguously the presence of acrylate comonomer. The SEC chromatogramm of the purified copolymer displays a broad monomodal pattern with $M_n = 51,500$ and $M_w/M_n = 6.6$.

20.3.2. Ethylene- ϵ -caprolactone diblock copolymerization

Unfortunately, we were not able to achieve successfully the diblock copolymerization of ethylene with ϵ -caprolactone using **S** as macroinitiator. Addition of lactone to the solid **S** in suspension in fresh toluene results in a fast and quantitative lactone polymerization (complete conversion within 5-10 min). Extraction of the crude polymer in hot THF gives a high soluble fraction (62 wt%) accounting for 98% of the initial charge of lactone. ^1H NMR analysis shows the homopolymer nature of the extracted polymer, and SEC analysis gives $M_n = 7000$ and $M_w/M_n = 2.5$. However, ^1H NMR spectrum of the insoluble fraction shows the presence of lactone units with a ratio ethylene/lactone $\gg 100$, indicating a slow initiation or propagation process with the Nd-polyethylenyl species (see Appendix 9). This result is not surprising and can be explained using 2 scenarios. Firstly, we can suggest that the solid **S** possesses 2 initiating species for lactone polymerization: a very reactive Ln-O bond that can convert

quantitatively the monomer in a short period of time and a less reactive Nd-C bond from the Nd-(polyethylenyl) part that can just insert few monomer units at the same time. This would be in direct line with the observations made with lanthanocene-based systems, i.e. alkoxylanthanide species proved much more efficient initiators than alkylanthanides,¹¹⁷ and consistent with the alkoxo-alkyl nature of the initiating species in our system. Or, second hypothesis, the lactone polymerization may proceed by an anionic mechanism in which the magnesium species may intervene.* The proposed mechanism is summarized in Scheme 32.

Scheme 32. Proposed mechanism for lactone (co)-polymerization using the solid **S** as macroinitiator.

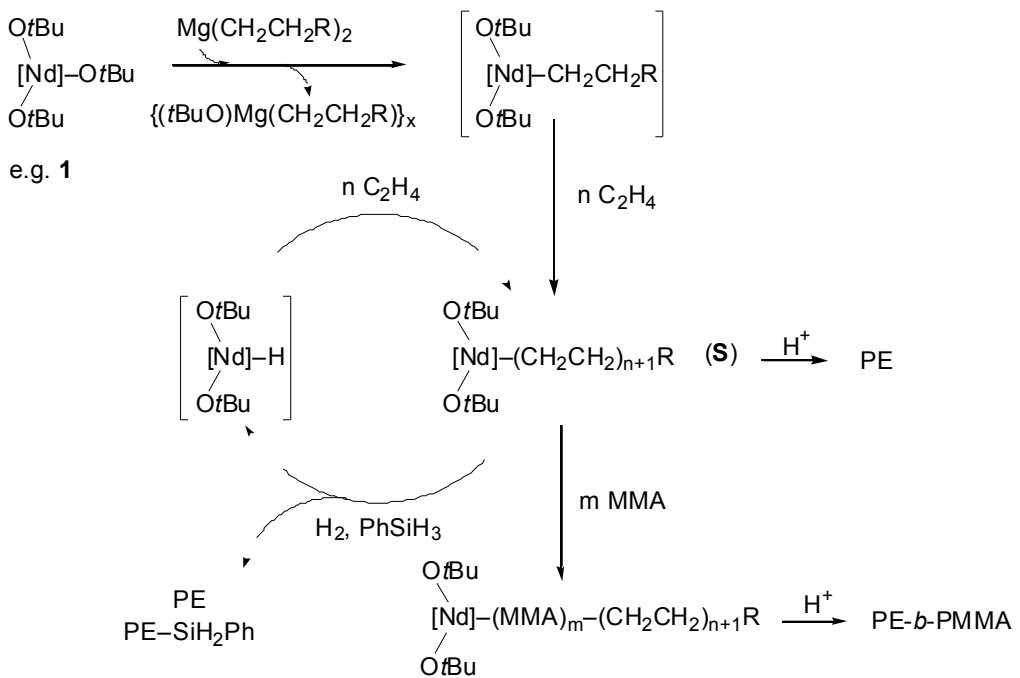


21. Proposed mechanism

The above results, particularly the effective transfer reactions using PhSiH₃ and H₂ and the possibility to achieve ethylene-MMA block-copolymerization, are in direct line with reactivity trends observed for lanthanocene initiators. This is consistent with a coordination-insertion mechanism starting from a neodymium-alkyl species produced by alkylation of **1** with the dialkylmagnesium co-reagent. The scheme below describes both the aforementioned putative mechanism for the production of the [Nd]-{n-hex} and [Nd]-H species, and their use as either initiator in the case of ethylene polymerization, followed by MMA copolymerization, or as catalysts (cycle) for the hydride in the case of polymerization using PhSiH₃ or H₂ as a transfer reagent. In Chapter 6, we will try to prove this proposed polymerization mechanism based on NMR investigations of **1**/MgRR' combinations and X-ray crystal structure determination of active species or intermediates of reaction.

Figure 76. Proposed mechanism for ethylene (co)-polymerization with **1**/DHM system.

* Homopolymerization of ε-caprolactone with **1**/DHM system (1/0.3) was carried out in toluene at 0 °C as described for MMA polymerization. Under these conditions, only 20% conversion was reached within one hour. It is worth noting that **1** polymerizes as such ε-caprolactone in CH₂Cl₂ at RT. After 12 h, the conversion reached 97% and the final polymer had a high molecular weight ($M_n = 61,000$) with rather narrow MWD ($M_w/M_n = 1.40$). In this case, the efficiency of initiation is close to 50%.



22. Conclusion

These results confirm the ability of some alkoxy/aryloxy residues to act as valuable ancillary ligands for lanthanide metals in the field of polymerization. Thus, the association of an alkoxy neodymium complex with a dialkylmagnesium co-reagent can generate significantly active species for ethylene polymerization. Under optimized experimental conditions, activity up to 100 kgPE/molNd/atm/h can be observed with **1/DHM** as catalyst system, yielding highly crystalline linear polyethylenes. In addition, this system exhibits alkylanthanocene-like properties such as effective transfer reactions using $PhSiH_3$ and H_2 , but more interestingly the possibility to achieve efficient ethylene-MMA block-copolymerization. These copolymers have the highest molecular weight ever shown for such diblock copolymers. They were characterized by various methods including microscopy techniques. Their application as compatibilizer was also investigated but remains still unclear. The polymerization results suggest a polymerization mechanism via coordination-insertion of the monomer onto an alkyl-neodymium species that would be produced by alkyl/alkoxide metathesis between the alkoxy-lanthanide precursor and the dialkylmagnesium co-reagent.

Unfortunately, this catalyst system appeared to be completely inactive towards higher olefins (propene, 1-hexene, 1-octene) under these standard polymerization conditions. Indeed, ethylene polymerization carried out in 1-octene with **1/DHM** (1:1) under the standard conditions, showed a standard activity of ca. 4-5 kgPE/molNd/atm/h. However, the formation of stable allyl derivatives as observed with lanthanocene catalysts⁴³ can not be ruled out, at least in the presence of propene.

Chapter 5

Butadiene polymerization

and diblock copolymerization

butadiene-glycidyl methacrylate

23.

24. Introduction

Synthesis of highly stereospecific polybutadiene (PBD) is a major goal for elastomer industry since the resulting polymers can find wide applications as synthetic rubbers.^{171a} Among the variety of organometallic or metalorganic complexes used for this purpose, rare earth metal-based compounds are most effective and attractive candidates.^{171c} As shown in Chapter 1, in binary or ternary systems, associated with aluminum alkyls and/or alkyl halides, these precursors enable the synthesis of *cis*-1,4-PBD with high selectivity (> 98%).¹⁸⁷ *Trans*-1,4-PBD has been obtained with rare earth allyl compounds¹⁹⁵⁻¹⁹⁹ or by replacing alkylaluminum with dialkylmagnesium reagents.^{205a} Oxygen-based ligands have been largely combined with rare earth metals for BD polymerization. The most common catalyst precursors are long-chain, hindered carboxylates ($\text{Ln}(\text{carboxylate})_3/\text{AlR}_3/\text{AlR}_{3-n}\text{X}_n$).³¹¹ Alcohols proved also to be efficient ligands when associated with the binary system $\text{LnCl}_3/\text{AlR}_3$.¹⁷⁹ It has been reported that lanthanide alkoxides " $\text{Ln}(\text{OR})_3$ ", especially those with linear alkoxy radicals rather than corresponding branched isomers, led to active triple component systems due to the higher degree of covalency of the $\text{Ln}-\text{O}$ bonds.¹⁸⁷

Despite the high activity and stereoregularity so far achieved in BD polymerization, in particular with neodymium-based systems,²⁰⁸ development of new catalysts is still under way to improve control over the polymerization.³¹² Indeed, it is of interest to prepare new materials based on stereoregular PBD, such as block copolymers. In this respect, highly stereospecific living polymerizations of BD and isoprene have been achieved recently with lanthanocene-based systems, enabling their block copolymerizations with styrene²¹³ and ϵ -caprolactone,³¹³ respectively.

We would like to describe now the use of neodymium alk(aryl) oxide/dialkylmagnesium systems for BD polymerization, but also its statistical copolymerization with styrene (St) and block copolymerization with glycidyl methacrylate (GMA). As neodymium precursors, we employed the well-defined trinuclear complex $\text{Nd}_3(\text{OtBu})_9(\text{THF})_2$ (**1**) and mononuclear complexes $\text{Nd}(\text{O}-2,6-t\text{Bu}_2-4-\text{Me-C}_6\text{H}_2)_3(\text{THF})$ (**12**) and $\text{Nd}(\text{O}-2,6-t\text{Bu}_2-4-\text{Me-C}_6\text{H}_2)_3$ (**13**).

25. Butadiene homopolymerization

25.1. With $\text{Nd}_3(\text{OtBu})_9(\text{THF})_2$

25.1.1. Preliminary results

In light of literature (*vide supra*), we did not expect a high polymerization activity from the system formed by **1** and DHM. The reaction was first performed at room temperature in

³¹¹ (a) Zhiqan, S.; Jun, O.; Fusong, W.; Zhenya, H.; Baogong, J. *J. Polym. Sci., Polym. Chem. Ed.* **1980**, *18*, 3345-3357. (b) Pross, A.; Marquardt, P.; Reichert, K. H.; Nentwig, W.; Knauf, T. *Angew. Makromol. Chem.* **1993**, *211*, 89-101.

³¹² Miyazawa, A.; Kase, T.; Soga, K. *J. Polym. Sci., Part A: Polym. Chem.* **1999**, *37*, 695-697.

³¹³ (a) Barbier-Baudry, D.; Bonnet, F.; Dormont, A.; Finot, E.; Visseaux, M. *Macromol. Chem. Phys.* **2002**, *203*, 1194-1200. (b) Bonnet, F.; Barbier-Baudry, D.; Dormond, A.; Visseaux, M. *Polym. Int.* **2002**, *51*, 986-993.

hexane solution with $[Nd]_0 = [Mg]_0 = 3.0 \times 10^{-2}$ M and $[BD]_0 = 3.0$ M for 17 h (run 1), after a 1 h activation period at room temperature. The results are reported in Table 30.

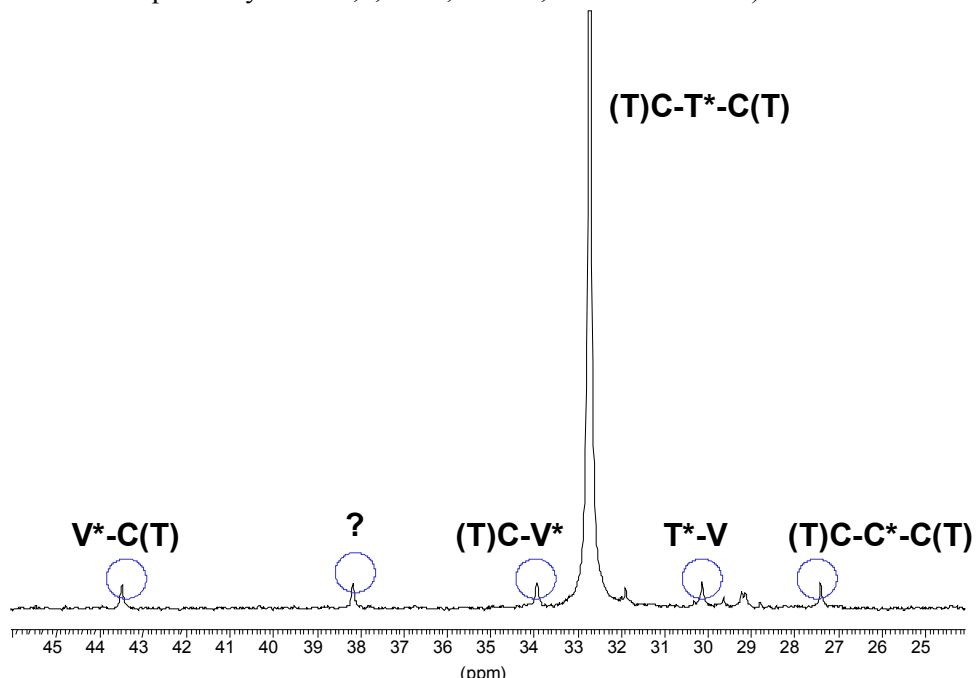
Table 30. Butadiene polymerizations promoted by **1/DHM**.

run	Nd/Mg	BD/Mg	t-BuCl/Nd	t (h)	yield (%)	M_n (g/mol)	$M_{n,th}$ (g/mol)	M_w/M_n
1 ^a	1.0	100	-	17	5	1900	135	1.77
2	1.0	100	-	17	22	2700	595	2.40
3	1.0 ^b	100	-	17	24	950	650	2.90
4	0.2	20	-	17	95	1700	370	4.40
5	1.0	100	3.0	17	68	3050	1840	4.20
6	0.2	200	-	17	47	10,300	2540	5.10
7	0.2	200	3.0	17	91	6100	4920	24

Polymerizations were carried out with $[BD]_0 = 3.0$ M in hexane at 60 °C except ^a at 20 °C; $M_{n,th} = (([BD]_0/2[Mg])_0) \times (\text{yield}/100) \times M_0$; ^bBEM was used.

Indeed, both the conversion and initiation efficiency (based on the formation of two polymer chains per MgR₂) are very low, leading to a low molecular weight PBD ($M_n = 1900$ g/mol) with a quite broad molecular weight distribution ($M_w/M_n = 1.77$). The stereospecificity of the polymerization under those conditions was checked by ¹³C and ¹H NMR (Figure 77 and Appendix 10). The latter reveals a high *trans*-1,4 content (ca. 95 %) along with small amounts of 1,2-PBD.

Figure 77. ¹³C NMR spectrum (CDCl₃) of homo-polybutadiene synthesized from **1/DHM** (run 2); (T, C and V stand for respectively *trans*-1,4, *cis*-1,4 and 1,2-butadiene units).



When the reaction was performed at higher temperature (60 °C), the rate of polymerization increased because of the concurrent increase of the propagation rate constant and initiation efficiency (from 7 to 22 %) (run 2-7).

The effect of the nature of the dialkylmagnesium was studied. DHM was replaced by BEM, resulting in a lower molecular weight PBD, which corresponds to an increase in the initiation efficiency from 25 to 70%. The same decrease in the polymer molecular weight on using BEM instead of DHM was noticed previously in ethylene polymerization.

The effect of an alkyl halide in the polymerization medium was evaluated using *tert*-butyl chloride ($[Nd]_0 = 3.0 \times 10^{-2}$ M; $[Nd]_0/[Cl]_0 = 0.33$). The addition of halide donors in Ziegler-Natta type catalytic systems is known to be essential for the synthesis of *cis*-1,4-rich PBD.¹⁸² Also, the synthesis of *cis*-1,4-PBD was reported with the ternary system Nd(P_{507})₃/Mg(*n*-Bu)₂/CHCl₃.²¹¹ With our system, a higher initiation efficiency along with a broad MWD were observed (run 5) while the latter had no influence on ethylene polymerization, however, under milder conditions. *t*-BuCl probably favored the formation of supplementary active sites through the creation of Ln-X bonds. However, the presence of *t*-BuCl had no influence on the *trans*-1,4 content of the polymer (*trans*-1,4 = 96%) while a *cis*-1,4-rich PBD was prepared with di(isobutyl)aluminumhydride (DIBAL-H) instead of DHM (*cis*-1,4 = 97%).

25.1.2. Influence of the Nd/Mg ratio

The variation of the Nd/Mg ratio was also investigated. With $[Nd]_0/[Mg]_0 = 0.2$, the monomer conversion after 17 h was nearly complete (run 4). Despite a high polydispersity, the molecular weight was in agreement with the calculated one, considering the initial ratio of monomer to magnesium concentrations, the monomer conversion and the initiation efficiency of run 2. This shows clearly that one can control the molecular weight of PBD by adjusting the ratio $[BD]_0/[Mg]_0$ as it can be done in "living"/controlled polymerizations. Here, the dialkylmagnesium acts as a preliminary alkylating reagent and then as a reversible transfer agent, while the rare earth metal acts as a catalyst. In ethylene and MMA polymerizations, the latter played a role of initiator and an excess of Mg led respectively to a loss of activity or of the living character. Definitely, we can not ascribe a living nature to BD polymerizations promoted by **1**/DHM given the high polydispersity values ($M_w/M_n = 1.80\text{-}4.40$). Slow initiation and significant transfer and/or termination reactions might be the causes of such values. Decreasing the catalyst concentration to 3.0×10^{-3} M had no particular influence on the polymerization (run 6). The experimental molecular weight matched with the calculated one and the percentage of *trans*-1,4 units was not modified. Thus, the **1**/DHM system exhibits a moderate activity for stereospecific *trans*-1,4 BD polymerization with control over the molecular weight. Unfortunately, the efficiency of initiation remains low (Eff. < 25 %) but can be improved by addition of an alkyl halide or with other magnesium reagents as shown in §25.1.1.

25.2. With neodymium aryloxides

25.2.1. *Nd(O-2,6-tBu₂-4-Me-Ph)₃(THF) as precursor*

The precursor Nd(O-2,6-*t*Bu₂-4-Me-Ph)₃(THF) (**12**), prepared by ionic metathesis and that contains one THF-coordinated molecule, was evaluated under similar conditions to **1** (Table 31, run 8). This precursor showed a much more interesting activity compared to the trinuclear **1** complex.

Table 31. Butadiene polymerizations promoted by **12**/DHM.

run	Nd/Mg	BD/Mg	t (h)	yield (%)	M _n (g/mol)	M _{n,th} (g/mol)	M _w /M _n
2	1.0	100	17	5	1900	135	1.77
8	1.0	100	17	99	5800	2700	1.26
9	0.2	20	17	98	1100	540	1.15
10	1.0	200	2	60	6300	3250	1.18
11	1.0	1000	17	99	49,900	26,800	1.86
12*	1.0	100	17	99	2700	2680	1.53
13*	1.0	1000	17	99	28,700	26,800	2.07

Polymerizations were carried out with [BD]₀ = 3 M in hexane at 20 °C; M_{n,th} = (([BD]₀/2[Mg]₀)×(yield/100) ×M₀); * Nd(O-2,6-*t*Bu₂-4-Me-Ph)₃ was used.

Complete monomer conversion was reached at room temperature within 17 h, although it must be noticed that the reaction times were not optimized. The main feature of the PBD produced under those conditions is its quite low polydispersity (M_w/M_n = 1.26). The initiation efficiency is now close to 50%. This increase could be explained by the mononuclearity of the complex, enabling a better interaction between the dialkylmagnesium reagent and the coordination sphere of the lanthanide, and/or to the higher acidity of the ligands conferring to the metal center a higher intrinsic activity. But still, this result is opposite to the observations made in ethylene polymerization.

The stereospecificity of the polymerization was unchanged, suggesting that BD polymerization using **1** and **12** proceeds via the same mechanism despite a different precursor structure. The molecular weight is roughly determined by the [BD]₀/[Mg]₀ ratio as suggested by the results obtained in run 9. Modification of this ratio showed that the higher the magnesium concentration, the lower the polydispersity (compare runs 9 and 11). For low M_n values (M_n < 10,000 g/mol), the polymerization can be considered as "living"/controlled since we have both control over the molecular weights and low polydispersities. When higher molecular weights were targeted, a deviation from these living characteristics was noticed. As observed for *tert*-butoxide complex, the molecular weights are well-controlled (up to 50,000 g/mol) whereas the polydispersities remained below 2.0.

The activity of **12** associated with other alkylating agents was evaluated. Usual aluminum derivatives, i.e. Al(*n*-Oct)₃, DIBAL-H, DIBAL-H/AlEt₂Cl as well as BEt₃ were found to lead to inactive systems for BD polymerization. On the other hand, two equivalents of *n*-HexMgBr or *n*-BuLi vs. Nd enabled the synthesis, with low yield (< 20%), of *trans*-1,4-PBD with respectively M_n = 1600 and M_w/M_n = 1.40, and M_n = 5300 and M_w/M_n = 1.35 when the reaction was performed for 2 h at room temperature. Diene polymerization appears thus less sensitive to the nature of the alkylating agent as it was noticed for ethylene polymerization.

25.2.2. Nd(O-2,6-*t*Bu₂-4-Me-Ph)₃ as precursor

It was also interesting to carry out BD polymerizations with the THF-free analog precursor Nd(O-2,6-*t*Bu₂-4-Me-Ph)₃ (**13**). It is known that the addition of a small amount of THF in Nd (versatate)₃/MgR₂ systems enhances the *trans* content of PBD205^a and the presence of an additional vacancy on the metal could modify the stereospecificity of the polymerization.¹⁷⁸ A set of experiments was performed with [Nd]₀/[Mg]₀ = 1.0 (runs 12 and 13) and can be directly compared to runs 8 and 11. For a similar monomer conversion, the molecular weights are twice lower (2700 vs. 5800 and 28,700 vs. 49,900) with a minor broadening of the MWD. The efficiency of initiation is now over 95%. Also, the ¹³C NMR spectrum showed that the PBD microstructure is not affected. Consequently, the absence of coordinated THF did not lead to the bidentate coordination of the monomer, suggested to be a key factor for producing *cis*-1,4-PBD with rare earth-based catalysts. The steric hindrance of the aryloxy groups and the possible presence of the magnesium derivative in the coordination sphere of the Nd, which may be correlated to the higher efficiency of initiation, might prevent such coordination (*vide infra*).

26. Butadiene copolymerizations

26.1. Butadiene-styrene statistical copolymerization

Styrene-butadiene copolymers (SBR) have a great importance in the elastomer industry. Prepared by anionic or radical polymerizations, the polymers do not exhibit the perfect SBR profile, i.e, high *cis*-1,4 content, high molecular weight, and more than 20% of incorporation of styrene. To fulfill these requirements, many catalysts based on Ni, Co, Ti and lanthanides have been developed.²⁰⁷ Even if "Nd(OR)₃"/MgR₂ systems did not produce rich *cis*-1,4-polybutadiene, we judged interesting to consider the statistical copolymerization of butadiene and styrene.

A preliminary experiment was carried out with pure styrene and complex **12** as catalyst precursor (Table 32, run 14). Under the typical polymerization conditions, 30% conversion and a low molecular weight polystyrene was obtained. SEC analysis showed a monomodal chromatogram with M_w/M_n = 1.45. As revealed by ¹³C NMR, the polymerization did not show any kind of stereospecificity.

The BD-St copolymerizations were performed in bulk. At room temperature, for 2 h, an overall monomer conversion of 45% was reached (run 15). This value corresponds to

complete BD conversion and 13% conversion of St, which is in agreement with the estimation made from the integrals ratio in the ^1H NMR spectrum of the polymer recovered. The molecular weight distribution is quite large and bimodal.

Table 32. Styrene-butadiene statistical copolymerization promoted by **12/DHM**.

run	Nd/Mg	BD or St	t (h)	yield (%)	M_n (g/mol)	M_w/M_n	St. (mol%)
14 ^a	1/1	100	17	30	2400	1.45	-
15	1/2	200	2	45	5200	2.42	13
16	1/2	1000	2	21	20,200	1.72	3.5
17	1/2	1000	20	41	25,200	2.13	13.5
18	1/1	1000	20	41	42,800	2.25	8.5
19 ^b	1/1	1000	1	39	35,100	1.90	10

Polymerizations were carried out with $[\text{BD}]_0 = [\text{St}]_0 = 4.9 \text{ M}$ in hexane at 20°C . ^a Styrene homopolymerization.

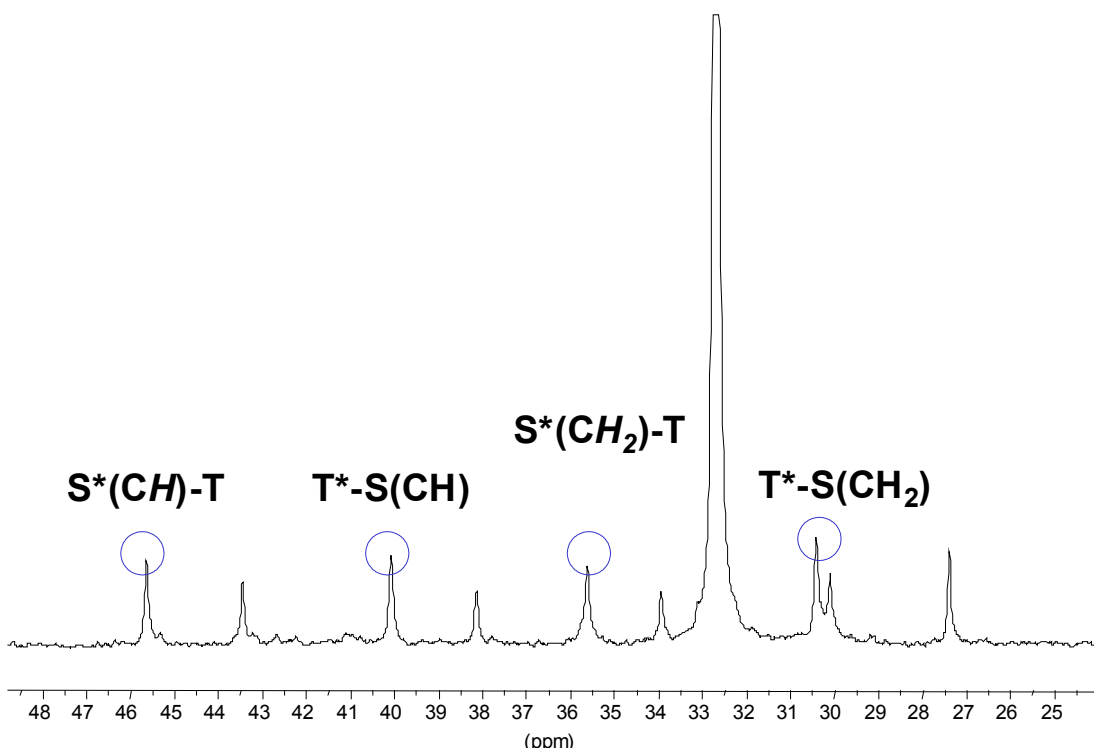
^b Polymerization carried out in toluene solution at 50°C : $[\text{BD}]_0 = [\text{St}]_0 = 3 \text{ M}$; $[\text{Nd}]_0 = 3 \times 10^{-3} \text{ M}$.

To establish the true nature of the copolymer, the microstructure was studied by ^{13}C NMR spectroscopy (Figure 78). In addition to the signals observed for homo-PBD (Figure 77), a new set of peaks was noticed, with resonances at δ 45.68 and 35.61 ppm corresponding to the St units of a *trans*-1,4-BD-St diad, and at δ 40.08 and 30.41 ppm corresponding to the BD units of the same sequence.³¹⁴ The *trans*-1,4 content of the polymer remained unchanged since only *trans*-1,4-BD-styrene sequences were observed. That behavior differs from *cis*-1,4 stereospecific BD polymerizations. In these cases, the insertion of styrene induced a decrease of the *cis*-1,4 content attributed to the back-biting reaction, i.e. the coordination of the penultimate monomer unit onto the catalyst.²⁰⁹ Thus, each styrene unit is immediately followed by a *trans* BD. However, the possibility of a long range coordination effect was also suggested.²⁰⁹

When the catalyst concentration was reduced to $[\text{Nd}]_0 = 3.0 \times 10^{-3} \text{ M}$, the monomer conversion after 2 h dropped to 20% and the amount of St incorporated was low (3.5%) (run 16). Again, the molecular weight was roughly determined by the $[\text{BD}]_0/[\text{MgR}_2]_0$ ratio. Prolonging the reaction from 2 to 20 h enabled a higher monomer conversion and the styrene content jumped from 3.5 to 13.5% (run 17). Unfortunately, the molecular weight did not increase proportionally with the latter. The late formation of a low molecular weight copolymer with high styrene content can not be discarded.

Figure 78. ^{13}C NMR spectrum (CDCl_3) of poly(butadiene-*co*-styrene) obtained from **12/DHM** (run 8); (circled peaks refer to resonances specific to BD-St diads; non-circled peaks refer to resonances for PBD).

³¹⁴ (a) Kobayashi, E.; Furukawa, J.; Ochiai, M.; Tsujimoto, T. *Eur. Polym. J.* **1983**, *19*, 871-875. (b) Conti, F.; Delfini, M.; Segre, A. L. *Polymer* **1977**, *18*, 310-311. (c) Walsh, N. G.; Hardy, J. K.; Rinaldi, P. L. *Appl. Spectrosc.* **1997**, *51*, 889-897. (d) Caprio, M.; Serra, M. C.; Bowen, D. E.; Grassi, A. *Macromolecules* **2002**, *35*, 9315-9322.



The effect of temperature was evaluated in order to increase the styrene content into the copolymer. In bulk conditions, above 50 °C, the polymers obtained after purification were insoluble in toluene, THF or CHCl₃. When the polymerization was conducted at 50 °C in toluene solution, comparable results to those observed at room temperature in bulk were obtained but in a reduced reaction time (1 h). The styrene content remained low for all the experimental conditions. This can be ascribed to its strong coordination to the metal due to the nature of the ligand as it has been already reported.²⁰⁸ None of the copolymerizations presented a living character. However, ¹³C NMR spectra showed, for all the conditions, the sole presence of BD-St sequences and no signals characteristic of homo-polystyrene.

26.2. Butadiene-glycidyl methacrylate diblock copolymerization

As stated in the introduction part, the synthesis of new materials based on stereospecific PBDs is of high interest, especially block copolymers with polar monomers.³¹³ We were particularly focused on glycidyl methacrylate (GMA) as a co-monomer given its reactive epoxide function. It can react with both electrophiles and nucleophiles providing versatility in compatibilization. Thus, GMA has been used as a grafting monomer onto polyolefins but also more recently onto St-BD-St rubbers.³¹⁵ In tire industry, these materials can be applied as reinforcement agent with mineral charges (SiO₂). Poly(GMA-*b*-BD-*b*-GMA) triblock copolymer was synthesized by living anionic polymerization facing drastic experimental conditions.³¹⁶ Grubbs and co-workers used nitroxide-mediated polymerization to prepare related copolymers.³¹⁷ Both techniques led to well-defined block copolymers but without any

³¹⁵ (a) Lu, M.; Keskkula, H.; Paul, D. R. *J. Appl. Polym. Sci.* **1995**, *58*, 1175-1188. (b) Cordella, C. D.; Cardozo, N. S. M.; Baumhardt Neto, R.; Mauler, R. S. *J. Appl. Polym. Sci.* **2003**, *87*, 2074-2079.

³¹⁶ Ming, J.; Dubois, P.; Jerome, R. *J. Polym. Sci., Part A: Polym. Chem.* **1997**, *35*, 3507-3515.

³¹⁷ Grubbs, R. B.; Dean, J. M.; Broz, M. E.; Bates, F. S. *Macromolecules* **2000**, *33*, 9522-9534.

stereospecificity of the PBD block. To our knowledge, no report mentioned so far the use of rare earth catalyst for this application. Given the ability of our catalytic systems to polymerize stereospecifically butadiene and methacrylates in a "living"/controlled fashion, we investigated the synthesis of poly(BD-*b*-GMA) diblock copolymers.

26.2.1. Initial results: copolymer characterization

The block copolymers were obtained by pre-polymerization of BD followed by sequential addition of GMA. Both precursors **1** and **12** associated with various alkylating reagents were tested. The results are reported in Table 33.

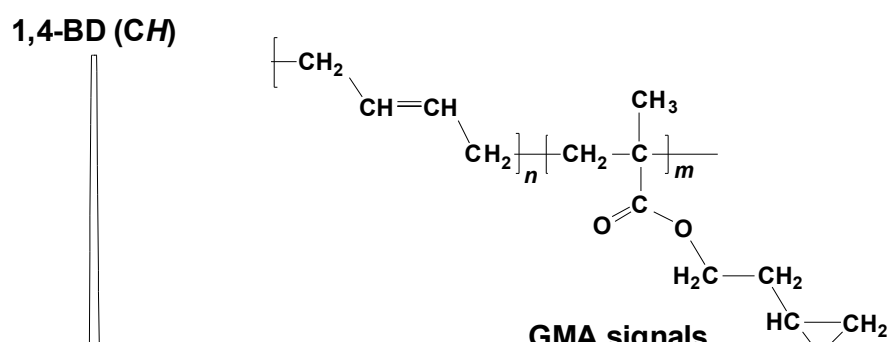
Table 33. Results of the sequential diblock copolymerization of butadiene and glycidyl methacrylate.

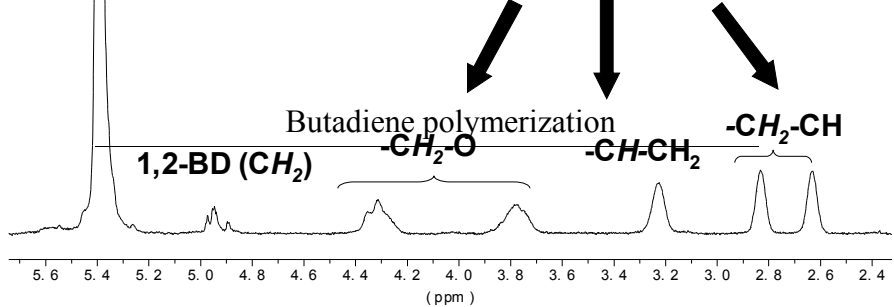
run	"Nd(OR) ₃ " (equiv.)	Alkyl reag. (equiv. vs. Nd)	BD t (h) T (°C)	GMA t (h) T (°C)	Yield (%)	M _n (g/mol)	M _w /M _n	BD/GMA
20	1 (0.5)	DHM (1)	18; 60	1.5, 25	43	23,800	1.84	1.9
21	12 (0.5)	DHM (1)	2; 25	3, 25	60	11,900	1.40	10
22	12 (0.5)	DHM (1)	2; 25	18, 25	60	11,600	1.40	10
23	12 (0.5)	DHM (1)	2; 25	3, 0	43	7100	2.0	12
24	1 + 12 (0.5/0.5)	DHM (1)	2; 25	3, 25	47	9500	1.92	4.4
25	12 (0.5)	<i>n</i> -BuLi (2)	2; 25	3, 25	20	10,000	2.67	7
26	12 (0.5)	<i>n</i> -HexMgBr (2)	2; 25	3, 25	23	3900	2.10	n c
27	12 (0.5)	Al(<i>n</i> -Oct) ₃ (1)	2; 25	3, 25	0	-	-	-
28	12 (0.5)	DIBAL-H/ <i>n</i> -BuLi (0.5/0.5)	2; 25	3, 25	63	11,900	1.40	PBD
29	versatate (0.5)	DHM (1)	2; 25	3, 25	27	22,800	4.8	0.25

[BD]₀ = 3 M in hexane; BD = 100 equiv.; GMA = 15 equiv.

The resulting polymers were analyzed by NMR and IR spectroscopies. Figure 79 shows the ¹H NMR spectrum of a copolymer synthesized using **12**/DHM as catalyst. Resonances at δ 5.40 and 4.95 ppm correspond to the 1,4-BD and 1,2-BD units, respectively. The characteristic signals of PGMA were found at δ 4.32, 3.78, 3.23, 2.84, and 2.63 ppm, indicating that the oxirane functionality was not affected during the polymerization. Integration of the different signals provides the BD/GMA ratio, which is ca. 8 in this case.

Figure 79. Detail of the ¹H NMR spectrum (CDCl₃) of poly(butadiene)-*b*-poly(glycidyl methacrylate) diblock copolymer (run 21).





IR spectroscopy confirmed these results with bands at 967 (very strong, 1,4-*trans*-PBD) and 910 cm⁻¹ (weak, 1,2-PBD), consistent with a *trans*-1,4-rich content,^{179c} and PGMA was characterized with bands at 1733, 1260, 1150, 849 and 760 cm⁻¹ (see Appendix 11).³¹⁸ Still, these results were insufficient to confirm the true nature of the block copolymer. ¹³C NMR proved uninformative as linking carbons of BD-GMA sequences, estimated to be at δ 29-30 ppm and 32-35 ppm, could not be unambiguously detected, which was not unexpected considering their low concentration. SEC analyses with UV detection were more enlightening. For this purpose, the selective incorporation of a typical phenyl chromophore by ring-opening of the pending oxirane functions with PhSH was performed.³¹⁹ The UV spectra of the modified copolymer, recorded at characteristic wavelengths (254 and 219 nm), showed the presence of GMA and BD, respectively, on the entire range of molar mass. In addition to SEC data (*vide infra*), this proves that PGMA blocks are linked to PBD blocks, and so the diblock nature of the copolymer.

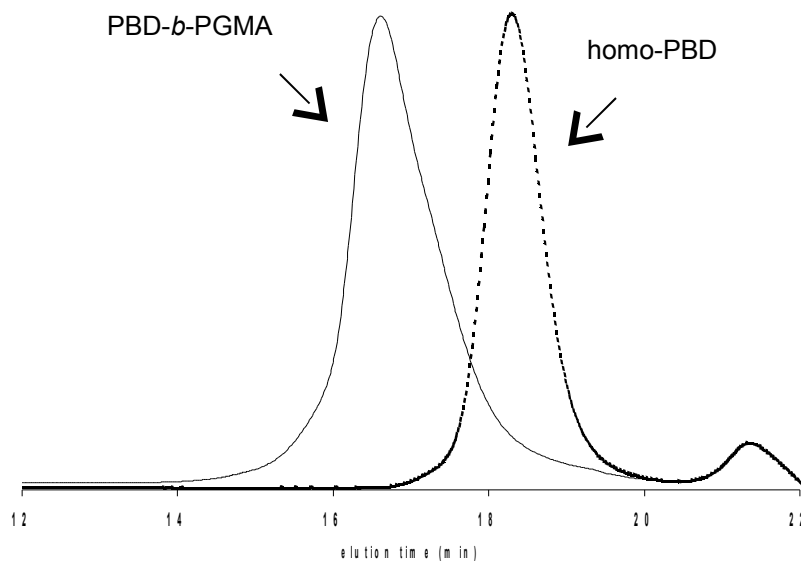
26.2.2. Copolymerization results

With **1**/DHM, a polymer with quite high M_n and polydispersity was recovered (Table 33, run 20). A broad MWD was already observed for BD homopolymerization with this system. The GMA content (BD/GMA > 2) is in agreement with the high reactivity towards methacrylates of initiating systems based on neodymium *tert*-butoxide (see Chapter 3). The use of the **12**/DHM combination was next investigated (run 21-23). The SEC traces display the evolution of the molecular weight after addition of the GMA to the "living" PBD chains obtained with this system (Figure 80). As expected for a diblock copolymer, the initial symmetrical trace of the homo-PBD block moved to higher molecular weights to give a monomodal trace, still with a tailing on low molecular masses. This tailing can be ascribed to a slow initiation and/or termination reactions, although the MWD remained narrow.

³¹⁸ Swaraj, P.; Rânby, B. *Analytical Chem.* **1975**, 47, 1428-1429.

³¹⁹ Node, M.; Nishide, K.; Shigeta, Y.; Obata, K.; Shiraki, H.; Kunishige, H. *Tetrahedron* **1997**, 53, 12883-12894.

Figure 80. SEC traces of homopolybutadiene and diblock copolymer PBD-*b*-PGMA (run 21).



The BD/GMA ratio obtained with this system is rather low ($\text{BD}/\text{GMA} = 10$) and likely accounts for the lower activity of neodymium aryloxide/ MgR_2 systems towards methacrylates (see Chapter 3 §5.4). Longer reaction times did not allow higher monomer conversion, neither a higher GMA content in the copolymer. When GMA polymerization was carried out at 0°C , the molecular weight decreased while the polydispersity increased due to the slower initiation of the methacrylate polymerization. The GMA content could be improved on using simultaneously a mixture of *tert*-butoxide and aryloxide complexes as catalyst precursors (run 24). The difference of activity of the two distinct catalysts resulted in a large MWD due to the mixture of copolymers with different GMA contents.

The use of alternative alkylating agents was investigated with precursor **12** (run 25-28). *n*-BuLi was found to be somewhat effective for $\text{Li/Nd} = 2.0$; lower ratios led only to BD homopolymerization. With *n*-hexylmagnesium bromide, the copolymerization took place only with a low activity. In both cases, the *trans*-1,4 stereospecificity of the diene polymerization and a significant broadening of the MWD were noticed. Alkylaluminum and aluminate (formed *in situ* by reaction of DIBAL-H and *n*-BuLi) were inefficient. The former did not polymerize butadiene and side reactions (ring-opening) occurred with GMA. The latter did not incorporate GMA, leaving pure PBD. It is noteworthy that diblock copolymers with a rich GMA content could be prepared with $\text{Nd}(\text{versatate})_3/\text{DHM}$, though this system induced a large MWD (run 29).

27. Mechanistic considerations

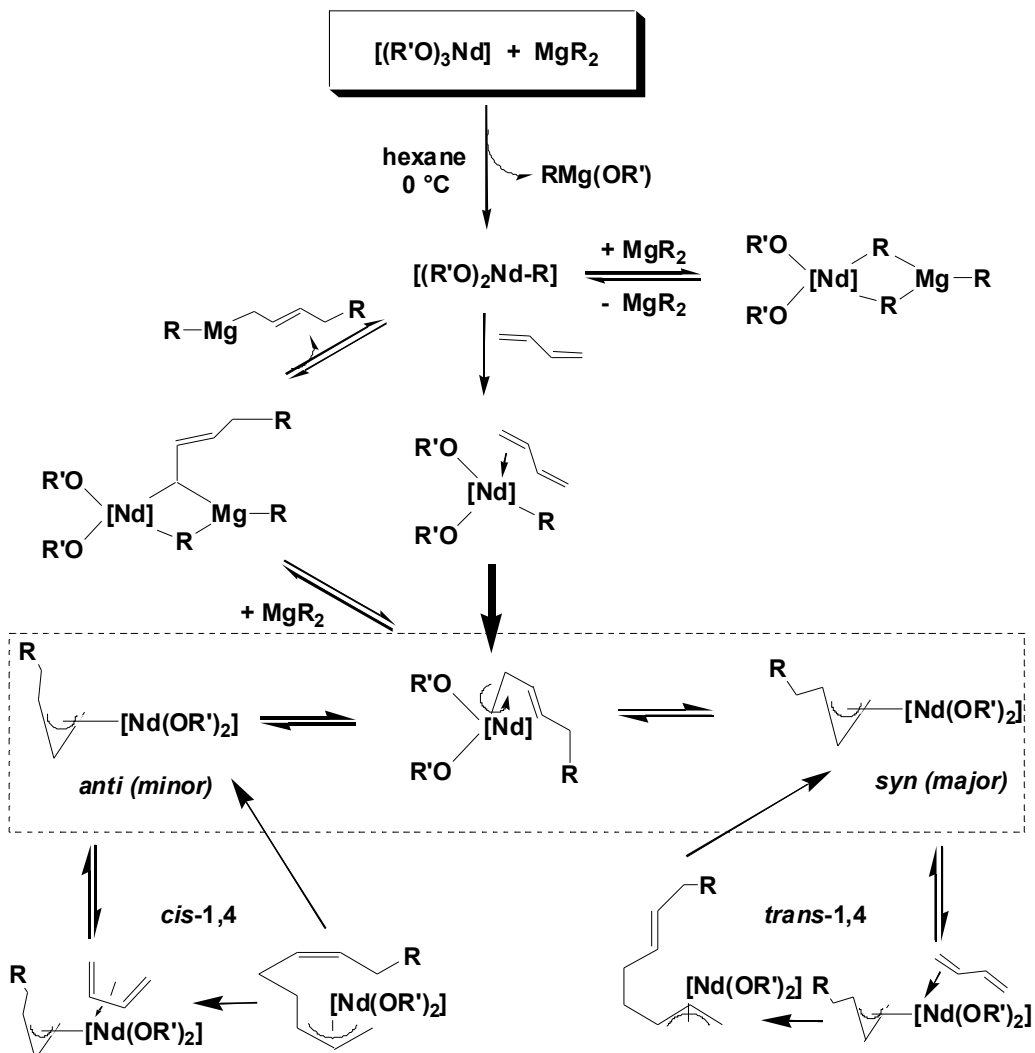
Because of the unique transfer reactions to the magnesium observed in BD polymerization, we would like to end this part with the proposition of a polymerization mechanism essentially based on polymerization results, independently to the mechanistic study that we will describe in the next chapter.

The assumed mechanism for *trans*-1,4 stereospecific polymerization of dienes was previously described (see Chapter 1 §5.2). In " $\text{Nd}(\text{OR})_3/\text{MgR}_2$ " systems, the *in situ* formation

of alkyl-lanthanide species has been suggested for MMA and ethylene polymerizations. However, interaction of the resulting alkyl-lanthanide species with the magnesium derivative, e.g. via alkyl μ -bridging, to form a bimetallic Nd-Mg species active in polymerization can not be discarded. Existence of μ -alkyl(allyl)-bridged bimetallic Nd-Mg species, in fast dissociation equilibrium with mononuclear alkyl(allyl)-Nd species and with fast reversible transfer of alkyl(allyl) chains between the Nd and Mg centers, is the most likely hypothesis to account for the pseudo-living character of BD polymerization, as it has been shown earlier for olefin polymerization with chlorolanthanocene-dialkylmagnesium systems.⁵² Based on the existing literature, *trans*-selective BD polymerization with the present systems is assumed to proceed through initial BD insertion into a Nd-R bond and then monodentate monomer coordination followed by 1,3-insertion into the *syn*- π -allyl bond, the bulkiness of the ligands shifting the equilibrium between *anti* and *syn* configurations towards the *syn* structure (Scheme 33). Since *cis*-1,4 polymers are usually observed with weakly coordinating ligands, it is coherent to have *trans*-1,4 stereospecificity with such strongly coordinated ligands as alkoxides and THF.

The difference of reactivity noticed between the systems based on $\text{Nd}_3(\text{OtBu})_9(\text{THF})_2$ and $\text{Nd}(\text{O}-2,6-t\text{Bu}_2-4-\text{Me-Ph})_3(\text{THF})$ or its THF-free analog can arise from their different intrinsic activity but also their difference in stability. Since aryloxides are more acidic ligands than *tert*-butoxide, the Nd center in systems based on **12** or **13** is expected to be more electrophilic and thus more active than those based on **1**. Also the bulkiness of the aryloxy ligand as well as the monomer coordination might stabilize and prevent decomposition of the corresponding alkyl (allyl)-Nd species and further contributes to the overall higher reactivity of those systems. Consistent with those trends, the formation of mononuclear alkyl complexes $(\text{ArO})_2\text{NdR}$ isolated from *in situ* **12**/MgR₂ combinations and easier β -H elimination for *tert*-butoxide than aryloxide systems will be discussed in Chapter 6. The pseudo-living nature of diene polymerization, evidenced by the true nature of poly(BD-*b*-GMA) block copolymers and their low polydispersities, is another indicator of the robustness of the alkyl/allyl-Nd species generated from $\text{Nd}(\text{OAr})_3(\text{THF})$. We can reasonably assume that the polymerization mechanism of GMA is identical to the coordinative-anionic mechanism reported by Yasuda and co-workers for MMA polymerization initiated by alkyl-lanthanocenes.¹¹⁶

Scheme 33. Assumed mechanism of diene polymerization catalyzed by "Nd(OR)₃"/MgR₂ systems.



28. Conclusion

Binary combinations of neodymium alkoxide/aryloxide precursors with dialkylmagnesium reagents led to the formation of active systems for the controlled stereospecific *trans*-1,4 polymerization of 1,3-butadiene in hexane solution. The exact nature of the active species was not established but experimental results agreed with the formation *in situ* of a bis(alkoxy) monoalkyl neodymium species. These species might be the active species by themselves but they may also require the presence of a magnesium derivative to generate the catalyst. Best results were observed with neodymium aryloxides. Under specific conditions, they allow a precise control of the polymer molecular weight along with a low polydispersity. Experimental M_n values approach the ones calculated by $([BD]_0 \times \text{Eff.})/[Mg]_0$, irrespective of the Nd/Mg ratio, which is consistent with a dynamic equilibrium between growing polymer chains on Nd and dormant chains on Mg centers, i.e. fast reversible transfer. It was taken advantage of the livingness of the system and its reactivity towards methacrylates to achieve efficiently the original stereospecific diblock copolymerization of butadiene with glycidyl methacrylate. In addition, the statistical copolymerization of butadiene and styrene was successfully conducted. Copolymers with controlled molecular weight and moderate styrene content were obtained. ^{13}C NMR spectra revealed that styrene incorporation did not modify

the stereoregularity of the polybutadiene unlike the observation made in *cis*-1,4 polymerizations. Binary combinations "Nd(OR)₃"/MgR₂ appear as versatile systems. They were already shown to be efficient for syndiotactic pseudo-living MMA polymerization, ethylene polymerization and its copolymerizations with MMA, they are also active for butadiene co-polymerization with styrene and GMA.

Chapter 6

Mechanistic study

The syndiotactic pseudo-living MMA polymerization, the ethylene polymerization with effective transfer reactions using PhSiH₃ and H₂, and the possibility to achieve efficient ethylene-MMA block-copolymerization, are in direct line with reactivity trends observed for alkylanthanocene initiators. This suggests that the polymerization mechanism with Nd₃(OtBu)₉(THF)₂ (**1**)/DHM as initiating system proceeds via coordination-insertion of the monomer onto an alkyl-neodymium species that would be produced by alkyl/alkoxide metathesis between the alkoxy-lanthanide precursor and the dialkylmagnesium co-reagent. In order to prove the formation of these suggested alkyl/alkoxylanthanide species, two methods were employed: the NMR monitoring of the reaction between the lanthanide catalytic precursor and alkylating agent, and the isolation of active species or intermediates. We would like to show that despite the high reactivity and instability of these systems, we were able to obtain tangible proofs for the existence of alkyl/alkoxylanthanide species.

1. NMR investigations

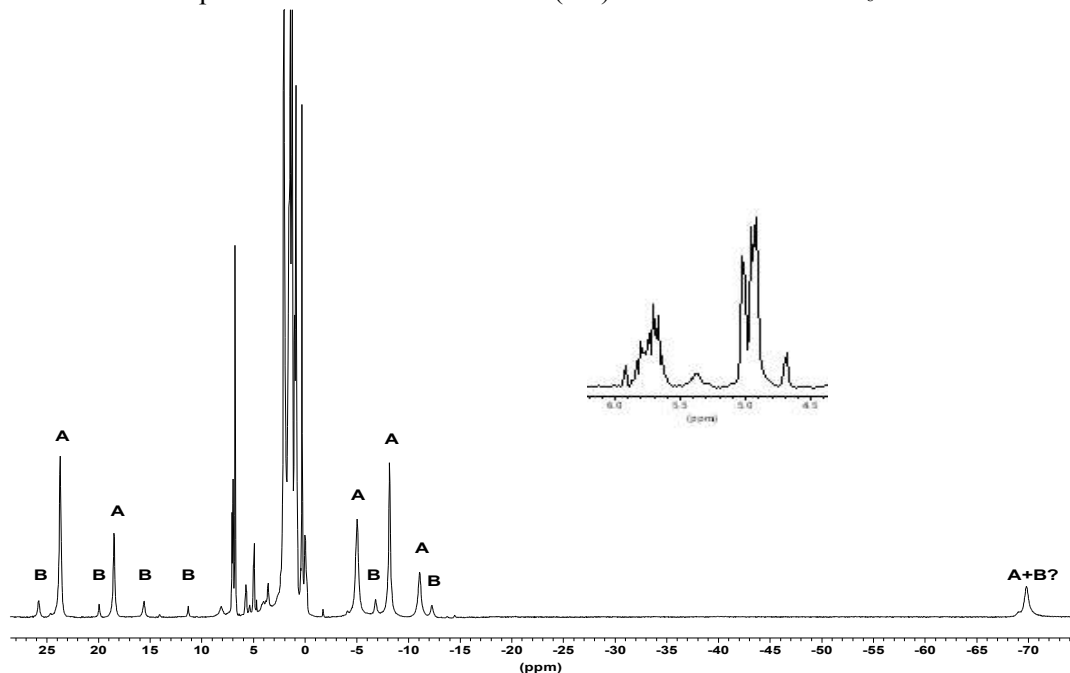
Despite paramagnetism of neodymium and because isostructural diamagnetic lanthanum complexes proved to be, to a great extent, less efficient catalytic precursors, the study was performed mostly with neodymium complexes

28.1.NMR monitoring of **1/RM**

28.1.1. ***1/DHM***

The reaction of **1** with various alkylating reagents was monitored by variable temperature ¹H NMR. First, the ¹H NMR spectrum of a 1:1 mixture of **1** and DHM in toluene-d₈ at -80 °C showed signals for the unreacted reagents, explaining the induction period observed when the activation step was carried out at -78 °C (see Chapter 4 §19.3.3). On raising the temperature, the latter signals progressively decreased to the profit of at least two sets of resonances attributed to tBuO ligands of new neodymium species. Formation of 1-hexene was observed from -20 °C. No further evolution of the system was noticed after 15 h at 5 °C: 40% of Mg(*n*-hex)₂ was transformed into 1-hexene and **1** was completely converted to two new species present in a ca. 10 to 1 ratio according to ¹H NMR (Figure 81). Six resonances in the range of -70 to 26 ppm with an integrated ratio of 2:1:2:2:1:1 were unambiguously attributed to the major species (A), suggesting a polynuclear structure with tBuO ligands in variable (terminal, bridging) environment. Reacting a 1:1 mixture of **1** and DHM in toluene-d₈ directly at 20 °C for 30 min led to the same mixture of products.

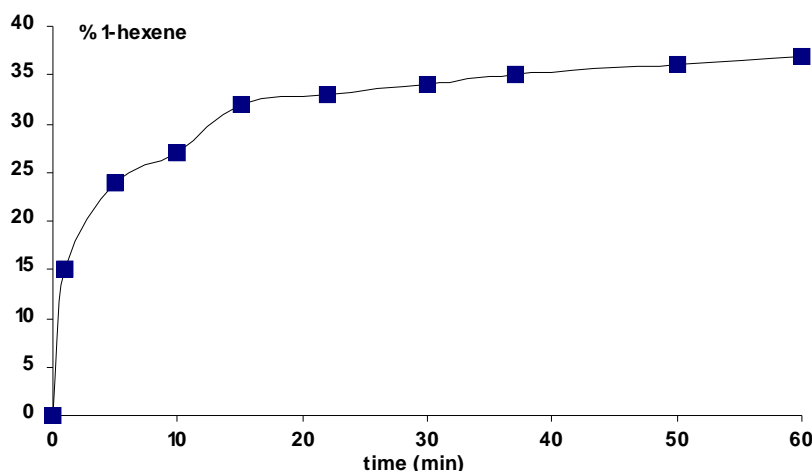
Figure 81. ^1H NMR spectrum of a **1**/DHM mixture (1:1) after 1 h in toluene- d_8 at RT.



The release of 1-hexene is the first indirect evidence for the *in situ* formation of an alkyllanthanide species. Indeed, the formation of 1-hexene can only reasonably be ascribed to the initial formation of a [Nd]-Hex species, followed by a β -H elimination reaction. The maximum amount of 1-hexene released in this reaction (40% vs. Nd) indicates also that only a limited amount of Nd undergoes the ligand exchange reaction. The latter may produce the active species and thus explain the low efficiency of initiation met in ethylene but also MMA polymerizations. However, we must be careful in our conclusions. Even if the polymerization is not affected by the presence of 1-alkene (see Chapter 4, §21), it is worth noting that the ^1H NMR spectra show only free 1-hexene (chemical shift and coupling constant identical to neat 1-hexene). Coordinated alkene, if any, can not be identified due to the paramagnetism of Nd. For the same reason, we are not able to characterize neodymium alkyl, allyl and/or hydride species.

The formation of 1-hexene with time was monitored at 0 °C for 1 h, i.e., under the standard conditions of activation, and the results are reported in Figure 82. This plot clearly shows an initial fast release of 1-hexene, especially during the first 5 minutes (25% vs. Nd), and then the formation slows down to reach a plateau at approximately 35%. Consequently, under standard conditions, ethylene polymerization takes place with a catalytic solution containing 35% vs. Nd of 1-hexene. It is worth noting that in the absence of activation, the polymerization starts only after 8-10 min, i.e. when 25% of 1-hexene is formed. These results would indicate that the active species in ethylene polymerization are or arise from neodymium hydride species. However, since the polymerization does not start before reaching these 25% of 1-alkene in the absence of activation, the subsequent formation of active species from further metathesis reactions or complex re-arrangement may be suggested.

Figure 82. Evolution of 1-hexene formation with time at 0 °C with **1**/DHM system (Nd/Mg = 1:1).



28.1.2. I/MgRR'

When *n*-BuMgEt was reacted with **1** under similar conditions, the formation of 1-butene was observed from -30 °C and reached a maximum of 14% vs. Nd after 15 min at 20 °C. The parallel release of ethylene (δ 5.26 ppm) was detected at temperatures as low as -60 °C but the amount of this monomer in the reaction medium started to decrease from -20 °C and no ethylene was detected at 0 °C; simultaneously, the formation of polyethylene in the NMR tube was observed (see Appendix 12). This phenomenon is simply rationalized considering the polymerization activity of the **1**/MgR₂ systems towards ethylene and its inactivity towards α -olefins (1-hexene, 1-butene). It shows also that the nature of the alkyl radical is important in the rate of formation/decomposition of the alkyllanthanide species, thus the decomposition of [Nd]-Et is faster than that of [Nd]-hex. And contrary to our previous hypothesis, the alkylation process is not slower with BEM than with DHM. Furthermore, this reaction confirms the minimal temperature of activation for ethylene polymerization (-20 °C) since the ethylene was not polymerized below this temperature. If one assumes that [Nd]-Bu and [Nd]-Hex species have similar rates of decomposition via β -H elimination, we can propose that the initiating species in our system would be the resulting neodymium hydride species or species arising from their formation. These results are in direct line with those obtained with DHM.

The 1:1 combination of **1** with Mg(CH₂SiMe₃)₂, an alkylating reagent having no H on the β -position, proved more thermally stable (although not more active for polymerization) but release of isobutene was observed from 0 °C and amounted 40% vs. Nd after 24 h at 20 °C (signal at δ 4.7 ppm). In fact, DHM and BEM led also to isobutene when combined with **1** but in lower amounts (Table 34), possibly because they undergo previous β -H elimination to some extent and that the hydride further evolves in a different way.

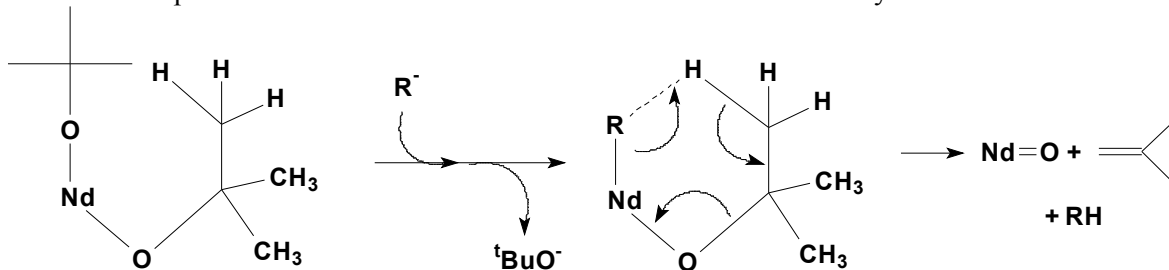
Table 34. Influence of the dialkylmagnesium reagent on the formation of isobutene.

MgRR'	% max isobutene/Nd
Mg(<i>n</i> -Hex) ₂	2-5
Mg(CH ₂ SiMe ₃) ₂	40
BuMgEt	2

Nd/RM = 1.0, toluene-*d*₈, 20 °C, 48 h.

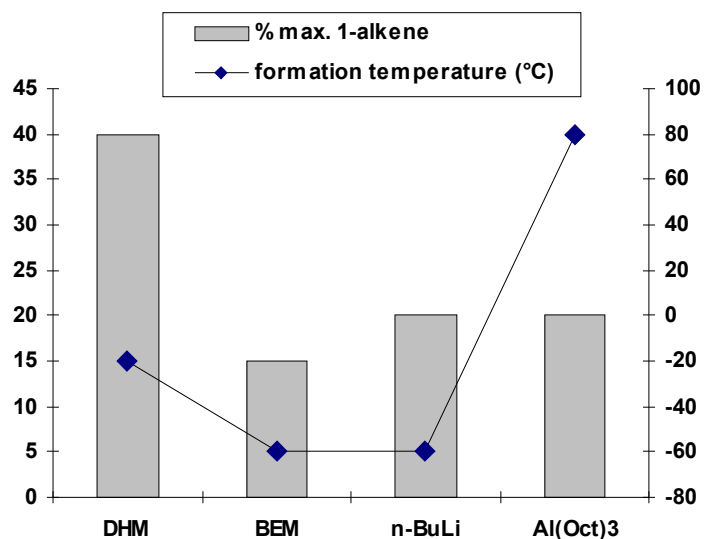
Formation of isobutene (alkene) has been reported in some cases to occur via simple thermolysis of *tert*-butoxy (alkoxy) lanthanide complexes, without any assistance from the alkylating reagent.⁸³ Nonetheless, the smooth conditions under which the release of isobutene proceeds (0 °C) and the nearly 1:1 concomitant formation of isobutene and SiMe₄ (identified by ¹H and ¹³C NMR) upon using Mg(CH₂SiMe₃)₂ suggest that the loss of isobutene proceeds in this case via concerted dealkylation of a O*t*Bu group by an adjacent alkyl (hydride) group rather than by another O*t*Bu group. In this case, the expected inorganic co-product is an oxo species, such as **8**, but it could not be identified so far.

Scheme 34. Proposed mechanism of formation of isobutene from **1**/DHM system.



28.1.3. *I/RM systems*

Fast release of 1-butene was also observed from the **1**/*n*-BuLi combination since -60 °C (up to 20% vs. Nd after 15 min) (Figure 83). This suggests rapid alkyl/alkoxy metathesis and subsequent β-H elimination from the resulting [Nd]-Bu species. The high instability of the latter likely accounts for the impossibility to achieve ethylene polymerization from neodymium alkoxide/alkyllithium systems; it indicates also that dialkylmagnesiums may serve not only as alkylating reagents of the alkoxy precursor but also as stabilizers of the resulting alkyl-[Nd] species, as they do in chlorolanthanocene/MgR₂ systems via μ-alkyl bridging.⁵² These bridgings may be also responsible for the high stability observed with Al(*n*-Oct)₃ as alkylating agent. Such bridged Al-Nd complexes were previously reported.²²⁰ Indeed, the presence of 1-octene could not be detected after 1 h at 20 °C; heating up the mixture to 80 °C for 1 h yielded 20% of 1-octene vs. Nd. Nevertheless, the detection of 1-octene, synonymous of formation of Nd-H species, does not allow ethylene polymerization.

Figure 83. Formation of 1-alkene with various **1/RM** systems ($Nd/M = 1.0$).

28.2."Ln(O*t*Bu)₃"/DHM

This qualitative study was also carried out with various lanthanide *tert*-butoxides. Thus, we have examined metathesis reactions between dialkylmagnesium reagents and La₃(O*t*Bu)₉(THF)₂ (**III**₂) and Y₃(O*t*Bu)₈Cl(THF)₂ (**III**₁) but also with the "uncharacterized" Ce and Sm derivatives. Although combinations of these alkoxides with DHM were found to be significantly less efficient than those based on **1** for ethylene polymerization, one might expect due to their structural relation to **1** some common reactivity features. In addition, alkyl derivatives of diamagnetic lanthanide centres can be easily detected by their intrinsic alkyl chemical shifts. Thus, to get additional clues for the probable formation of alkyl-lanthanide species in the systems studied, La and Y alkoxides may be very informative.

28.2.1. Formation of alkenes

The release of 1-hexene and isobutene were quantified after 30 min and 24 h at room temperature, no evolution could be further observed for longer reaction times (Table 35). After 30 min at RT, the amount of 1-hexene is below 10% vs. Nd and increases slowly during the monitoring time to reach a maximum value within 24 h, except for the neodymium alkoxide that exhibits similar 1-hexene formation after 30 min and 24 h. The maximum release of hexene and isobutene vary with the nature of the rare earth metal, and the sum of the released alkenes is in the range 45-50% vs. Ln except for Sm. These disparities may be attributed to the intrinsic properties of the metal or to the structural differences of the alkoxide complexes.

Table 35. Influence of the rare earth metal on the formation of 1-hexene and isobutene with "Ln(O*t*Bu)₃"/DHM systems.

"Ln(O <i>t</i> Bu) ₃ "	% 1-hexene/Ln after 30 min	% max 1-hexene/Ln	% max isobutene/Ln
Nd ₃ (O <i>t</i> Bu) ₉ (THF) ₂ (1)	40	40	2-5
La ₃ (O <i>t</i> Bu) ₉ (THF) ₂ (III₂)	6	30	12
"Ce(O <i>t</i> Bu) ₃ "	8	30	27
"Sm(O <i>t</i> Bu) ₃ "	8	16	14
Y ₃ (O <i>t</i> Bu) ₈ Cl(THF) ₂ (III₁)	1	22	23

Ln/DHM = 1.0, toluene-*d*₈, 20 °C, 48 h.

From these results it is difficult to establish a direct relation between the rate of formation and the amount of 1-alkene formed, and the activity observed in polymerization. However, the highest propensity of the neodymium precursor to undergo β-H elimination may probably explain its higher and singular reactivity in ethylene polymerization.

28.2.2. Evidences for alkyllanthanide species

As expected, the reactions performed with the diamagnetic centers revealed to be quite informative. When the reaction of a 1:1 mixture of La₃(O*t*Bu)₉(THF)₂ (**III₂**) and DHM in toluene-*d*₈ was monitored by variable temperature ¹H NMR, a new multiplet signal at δ -0.90 ppm, characteristic of a La–CH₂ moiety,²²³ appeared from -10 °C and was observed till 20 °C (see Appendix 13). However, its relative intensity remained small with respect to other resonances (*t*BuO, CH₂ from MgR₂) and the progressive formation of 1-hexene was observed. When the same experiment was carried out using Mg(CH₂SiMe₃)₂, the methylene singlet resonance for this reagent (δ -1.37 ppm) disappeared to the benefit of three new singlet resonances in a ca. 1:4:2 ratio (δ -1.13, -1.23, -1.99 ppm, respectively).

Another informative observation was made upon monitoring the reaction of a 1:1 mixture of Y₃(O*t*Bu)₇Cl₂(THF)₂ (**III₁**) and DHM in toluene-*d*₈ at 20 °C. The ¹H NMR spectra showed the formation of a new multiplet signal at δ -0.13 ppm, with couplings of 4 Hz, consistent with ²J(⁸⁹Y,¹H) splitting^{95,215,218-220} and products of general formula Y(O*t*Bu)_xCl_y(*n*-hex)_z were indicated; release of 1-hexene was observed at the same time (Appendix 14). These experiments provide therefore clues supporting alkyl/*tert*-butoxide metathetic exchange between lanthanide and magnesium metal centers. It can be noticed that a similar example of metathetic exchange involving a dialkylmagnesium reagent describing the preparation of [Cp₃Ce(O*i*Pr)] by reaction of Ce(O*i*Pr)₄•(iPrOH) with two equiv. of MgCp₂, have been previously reported.³²⁰ In addition, some reports on lanthanide-alkoxy/alkyl metathesis reactions involving alkylating agents other than dialkylmagnesium reagents were also published (*vide infra*).^{290,321}

³²⁰ Greco, A.; Cesca, S.; Bertolini, G. *J. Organomet. Chem.* **1976**, *113*, 321-330.

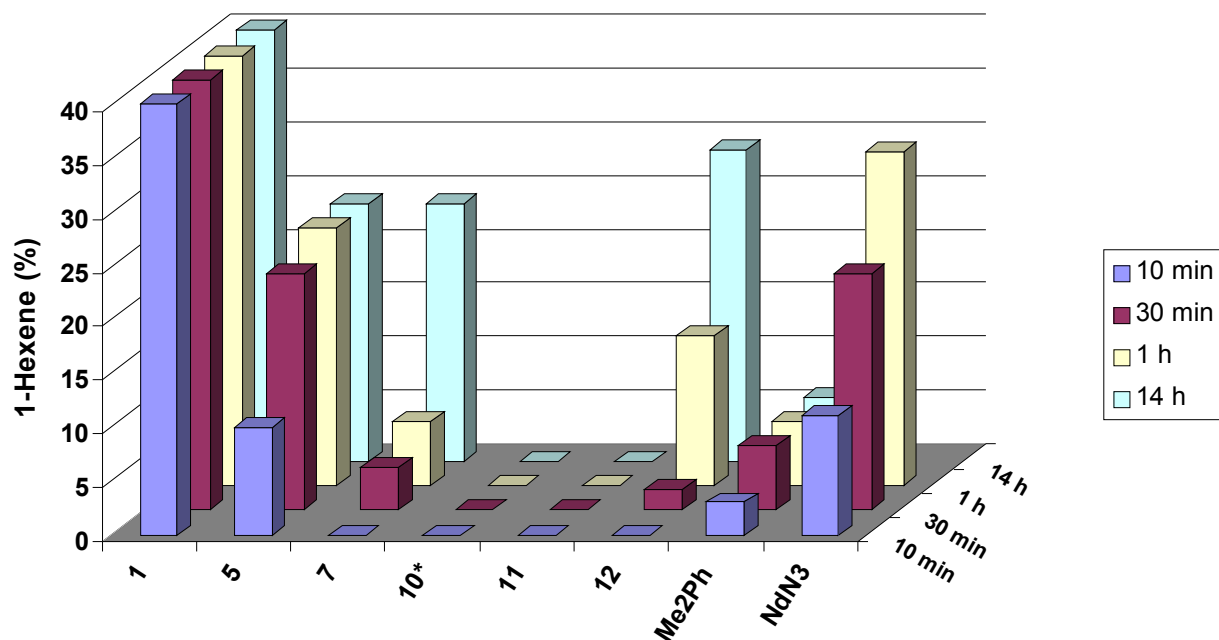
28.3."Nd(OR)₃"/DHM systems

Even if we were not able to establish a direct correlation between the formation of alkene and activity in ethylene polymerization with various lanthanide *tert*-butoxides, we thought interesting to study the association of DHM with some neodymium complexes we have tested in polymerization.

The evolution of the amount of 1-hexene released with time at 20 °C is reported in Figure 84. Again, **1** exhibits the fastest rate of formation of 1-hexene. In these cases, the nature of the metal can not be considered. As a matter of fact, the discrepancy lies only on the different structure of the complex. A slow formation of 1-hexene was noticed with Nd₃(OtBu)₉(HOtBu)₂ (**7**) while no alkene could be observed with Nd₁₂(OtAm)₂₆(HOtAm)₂Cl₁₁Na•(OEt₂)₂ (**10**) and Nd₂(μ₂,η²-OR)₂(η²-OR)₂(η¹-OR)₂ (**11**). A difficult alkylation process or an absence of alkylation may explain the absence of activity in ethylene polymerization of **10** and **11**. More surprisingly, complex **5**, that was initially supposed to be **1**, shows a progressive increase of the released amount of 1-hexene, and the maximum value tends to be 24%, i.e. a value twice lower than that observed with **1**. This indicates, as suggested by ¹H NMR (see Chapter 2 §8.1.1.3), that **1** and **5** have different structures. The maximum 1-hexene formation is similar to the one noted with **7**. However, **5** revealed to be an efficient precursor in ethylene polymerization only when activated at room temperature while **7** did not. Consequently, the release of alkene is not sufficient to allow the formation of polymerization active species even if the precursor is a *tert*-butoxide derivative. This conclusion can also be applied to the OC(Me)₂Ph derivative (**Me2Ph**) which shows a low formation of alkene but no polymerization activity, and also to the tris(amido) Nd{N(SiMe₃)₂}₃ (**NdN3**) complex that interestingly undergoes ligand exchange reaction quite rapidly, however without leading to an efficient ethylene polymerization catalyst. The metathesis reaction between DHM and the mononuclear complex Nd(OAr)₃(THF) (**12**) displayed also a slow and regular release of 1-hexene over 14 h, indicating either a higher stability of the alkyl neodymium species or a slower reaction between DHM and the aryloxide. The bulkiness and the basicity of the OR group as well as the change of nuclearity of the complex may be factors that could considerably affect this ligand exchange.

³²¹ (a) Shreider, V. A.; Turevskaya, E. P.; Kozlova, N. L.; Turova, N. Y. *Inorg. Chim. Acta* **1981**, *53*, L73-L76.
(b) Gulino, A.; Casarin, N.; Conticello, V. P.; Gaudiello, J. G.; Marks, T. J. *Organometallics* **1988**, *7*, 2360-2364.

Figure 84. Evolution of 1-hexene formation with time with various Nd precursor/DHM systems at 20 °C (Nd/Mg = 1.0).



28.4. Conclusion

In conclusion, variable temperature ¹H NMR monitoring of the metathesis exchange reaction between a lanthanide alkoxide and a dialkylmagnesium reagent provided quite informative results. With diamagnetic metal centers, we have evidenced the presence of alkyllanthanide species in our catalytic systems. Their decomposition via β-H elimination was observed and quantified for all the precursors. Unfortunately, we were not able to characterize or to get evidences for the resulting putative hydrido species. In addition to the 1-alkene formed by β-H elimination, the release of isobutene was also noticed with lanthanide *tert*-butoxides; isobutene arising from the decomposition of the *tert*-butoxy ligand. However, it is impossible to draw a direct and simple relation between alkene formation and polymerization activity. We can only note that the highest activity in ethylene polymerization is obtained with **1**, which provides the fastest and largest 1-hexene release.

29. Isolation of active species or intermediates

Preliminary NMR experiments at variable temperature of **1** or **III₂** with DHM showed that a fast exchange of ligands or "alkylation" takes place in this reaction, leading to the formation of transient unstable alkyl-lanthanide species. However, no valuable information concerning the mechanism of this reaction or the nature of these active species or intermediates could be obtained. In order to get a better understanding of these systems, we placed much effort on the characterization of the intermediates and active species of this reaction. The crystallization of the latter seemed to be the most promising method. Consequently, we carried out crystallization tests in toluene solution at low temperature (-30 °C). The crystallization solutions were composed of a neodymium alk(aryl)oxide precursor (**1** and **12**) associated with

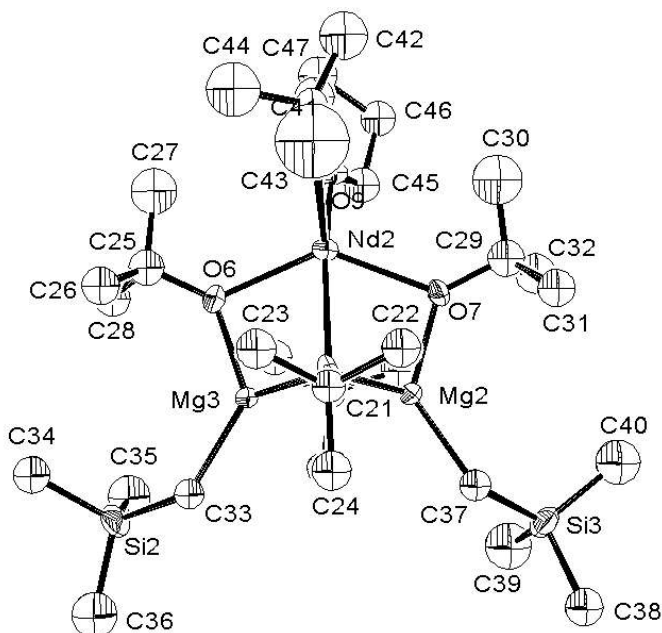
$\text{Mg}(\text{CH}_2\text{SiMe}_3)_2\bullet\text{Et}_2\text{O}$ in various ratios in the presence of coordinative species such as THF, dimethoxyethane or monomers (MMA, isoprene...). The typical $\text{Mg}(n\text{-Hex})_2$ used for polymerization experiments was replaced by $\text{Mg}(\text{CH}_2\text{SiMe}_3)_2\bullet\text{Et}_2\text{O}$ to avoid β -H elimination reaction in order to stabilize alkyl-lanthanide species. Nevertheless, it must be borne in mind that β -H elimination is not the only decomposition process in *tert*-butoxide/ MgR_2 systems since the *tert*-butoxy ligand can also decompose into isobutene to give the corresponding neodymium oxide. Another advantage of $\text{Mg}(\text{CH}_2\text{SiMe}_3)_2\bullet\text{Et}_2\text{O}$ over DHM and higher long-chain dialkylmagnesium reagents relies on its higher propensity to crystallize.

29.1. Isolation of metathesis products from " $\text{Nd}(\text{OR})_3$ "/ MgR_2 systems

When the reaction was performed with **1/TMSM** ($\text{Nd}/\text{Mg} = 1.0$) in the absence of co-reagent, it was not possible to isolate any species from the resulting dark brown solution. On the other hand, in the presence of THF (10 equiv. vs. Nd) the solution remained blue. Blue crystals were grown from this solution. ^1H NMR spectrum of these crystals was identical to the starting trinuclear alkoxide meaning that an excess of THF impedes the alkylation reaction to take place. Such behavior explains the inactivity of **1/DHM** in the presence of THF for the polymerization of ethylene (see Chapter 4 §19.3.5).

Given the successful results of Yasuda and co-workers in their effort to isolate a lanthanocene-based intermediate in MMA polymerization¹¹⁶ and the efficient controlled syndiotactic polymerization of this monomer achieved with **1/DHM** (see Chapter 3), MMA was added to some of our crystallization solutions. Pale blue crystals suitable for X-ray analysis appeared after few weeks. Surprisingly, our attempts conducted to the formation of a new heterobimetallic complex $\text{Nd}(\text{THF})(\mu_3\text{-O}t\text{Bu})_2(\mu_2\text{-O}t\text{Bu})_2(\text{O}t\text{Bu})\text{Mg}_2(\text{CH}_2\text{TMS})_2$ (**14**), which obviously has no MMA moiety (Figure 85). The initial stoichiometry between Nd and Mg was not recovered in the final complex. The latter has still a trinuclear structure where two neodymium atoms were replaced by magnesium. The neodymium center is hexa-coordinated with one terminal *tert*-butoxy ligand in dynamic exchange with a THF molecule. Doubly and triply bridged *t*BuO link the neodymium to tetra-coordinate magnesium atoms. The structure is completed with the presence of two alkyl groups on the magnesium. This complex shows the highest oxophilicity of Nd vs. Mg ($\text{Nd}-\text{O} = 703 \pm 13 \text{ kJ/mol}$ and $\text{Mg}-\text{O} = 363 \pm 13 \text{ kJ/mol}$) keeping six oxygen atoms in its environment, the alkyl chains being borne by the magnesium atom.²⁹²

Figure 85. ORTEP plot of $\text{Nd}(\text{THF})(\mu_3\text{-O}t\text{Bu})_2(\mu_2\text{-O}t\text{Bu})_2(\text{O}t\text{Bu})\text{Mg}_2(\text{CH}_2\text{TMS})_2$ (**14**) with probability ellipsoids at 30%. (Hydrogen atoms omitted for clarity)



Many examples of well-characterized mixed-metal lanthanide alkoxides complexes have been previously described, however, these complexes result from the interaction of lanthanide alkoxide and aryloxides with trialkylaluminum. Thus, $(t\text{BuO})(\text{THF})\text{Y}[(\mu_2\text{-O}t\text{Bu})(\mu_2\text{-Me})\text{AlMe}_2]_2$,²¹⁹ $(t\text{BuO})(\text{Cl})(\text{THF})_2\text{Y}(\mu_2\text{-O}t\text{Bu})_2\text{AlMe}_2$,²¹⁹ $[\text{Ln}(\mu_2\text{-O}t\text{Bu})_3(\mu_2\text{-Me})_3(\text{AlMe}_2)_3]$ ($\text{Ln} = \text{Y}, \text{Pr}, \text{Nd}$),²²⁰ $(\text{ArO})\text{Sm}[(\mu_2\text{-OAr})(\mu_2\text{-R})\text{AlR}_2]_2$ ($\text{Ar} = 2,6\text{-}i\text{Pr}_2\text{-C}_6\text{H}_3, \text{R} = \text{Me}, \text{Et}$),³²² $(\text{ArO})\text{Y}[(\mu_2\text{-OAr})(\mu_2\text{-Me})\text{AlMe}_2]_2$ ($\text{Ar} = 2,6\text{-}i\text{Pr}_2\text{-C}_6\text{H}_3$),³²³ $(\text{ArO})_2\text{Ln}[(\mu_2\text{-Me})_2\text{AlMe}_2]$ ($\text{Ln} = \text{Y}, \text{Lu}; \text{Ar} = 2,6\text{-}t\text{Bu}_2\text{-C}_6\text{H}_3$),³²³ $(\text{ArO})\text{La}[(\mu\text{-OAr})\text{AlMe}_2]_2$,^{322b} $(\text{ArO})_2(\text{THF})_2\text{Ln}[(\mu_2\text{-OAr})_2\text{AlMe}_2]$ ($\text{Ln} = \text{Nd}, \text{Yb}, \text{Ar} = 2,6\text{-Me}_2\text{-C}_6\text{H}_3, \text{R} = \text{Me}, \text{Et}$),³²⁴ and $\text{Nd}[(\mu_2\text{-OAr})_2\text{AlMe}_2]_3$ ($\text{Ar} = 4\text{-Me-C}_6\text{H}_4$),³²⁵ have been reported. In addition, we can also mention the heterobimetallic complexes $\{[(i\text{PrO})(i\text{Bu})\text{Al}(\mu_2\text{-O}i\text{Pr})_2\text{Sm}(Oi\text{Pr})(HOi\text{Pr})](\mu_2\text{-O}i\text{Pr})\}_2$ and $[(\text{THF})_2\text{Sm}(\text{O}t\text{Bu})_2(\mu_2\text{-O}t\text{Bu})\text{Al}(i\text{Bu})_2]$ obtained by reaction of $\text{Sm}\{\text{N}(\text{SiMe}_3)_2\}_3$ and AlR_3 in the presence of alcohol as well as $(\text{ArO})_3\text{Sm}[(\mu_2\text{-O}t\text{Bu})_2\text{Al}_2(\text{O}t\text{Bu})_4]$ ($\text{Ar} = 2,6\text{-}i\text{Pr}_2\text{-C}_6\text{H}_3$) prepared by reaction of $[\text{Sm}(\text{OAr})_3]_2$ with $\text{Al}_2(\text{O}t\text{Bu})_6$.³²⁶ Interestingly, the formation of "peralkylated" $\text{Ln}(\mu\text{-R})_x\text{Al}(\mu\text{-R})_y$ ($x + y = 4$) fragments has not yet been fully identified in such systems. To conclude with the reported complexes, examples of heterobimetallic organometallic Ln-Mg complexes are rather rare and none of them contain alk(aryl)oxide ligands.³²⁷

³²² (a) Gordon, J. C.; Giesbrecht, G. R.; Brady, J. T.; Clark, D. L.; Keogh, D. W.; Scott, B. L.; Watkin, J. G. *Organometallics*, **2002**, *21*, 127-131. (b) Giesbrecht, G. R.; Gordon, J. C.; Brady, J. T.; Clark, D. L.; Keogh, D. W.; Michalczyk, R.; Scott, B. L.; Watkin, J. G. *Eur. J. Inorg. Chem.* **2002**, 723-731.

³²³ Fischbach, A.; Herdtweck, E.; Anwander, R.; Eickerling, G.; Scherer, W. *Organometallics* **2003**, *22*, 499-509.

³²⁴ Evans, W. J.; Ansari, M. A.; Ziller, J. W. *Inorg. Chem.* **1995**, *34*, 3079-3082.

³²⁵ Evans, W. J.; Ansari, M. A.; Ziller, J. W. *Polyhedron* **1997**, *16*, 3429-3434.

³²⁶ Giesbrecht, G. R.; Gordon, J. C.; Clark, D. L.; Scott, B. L.; R.; Watkin, J. G.; Young, K. J. *Inorg. Chem.* **2002**, *41*, 6372-6379.

³²⁷ (a) Wu, W. L.; Chen, M. W.; Zhou, P. *Organometallics* **1991**, *10*, 98-104. (b) Lin, J.; Wang, Z. J. *Organomet. Chem.* **1999**, *589*, 127-132.

In $\text{Nd}(\text{THF})(\mu_3\text{-O}t\text{Bu})_2(\mu_2\text{-O}t\text{Bu})_2(\text{O}t\text{Bu})\text{Mg}_2(\text{CH}_2\text{TMS})_2$, the neodymium atom is 6-coordinated as it can be observed for most of the *tert*-butoxy derivatives (see Chapter 3 §8.1). The same structure framework as the starting alkoxide is observed where the $[\text{Nd}(\text{THF})(\text{O}t\text{Bu})]$ and $[\text{Nd}(\text{O}t\text{Bu})_2]$ moieties have been replaced by $\text{MgCH}_2\text{SiMe}_3$. Consequently, it is interesting to compare directly both structures. The terminal Nd–O distance of the alkoxide ligand ($\text{Nd}(2)\text{-O}(8)$, 2.246(8) Å) is quite longer than those found in **1**. However, this value may be correlated to the shortest Nd(2)-O(THF) distance (2.353(8) Å vs. 2.661(4) Å). Indeed, the dynamic exchange of THF and *O*tBu ligands leads probably to the measurement of an average bond length. Doubly bridging Nd–O distances are slightly longer than those of the terminal alkoxide ligands ($\text{Nd}(2)\text{-O}(7)$, 2.301(5) and $\text{Nd}(2)\text{-O}(6)$, 2.312(5) Å), and comparable to those measured in **1** (average value, 2.396 Å). Finally, the unequivalent triply bridging Nd–O bond distances ($\text{Nd}(2)\text{-O}(4)$, 2.763(5); $\text{Nd}(2)\text{-O}(5)$, 2.611(6) Å) show that the Nd atom is highly distorted from the ideal octahedral geometry. Angles around the neodymium center are quite similar to those observed in **1** except for the $\text{O}(\mu_3)\text{-Nd}\text{-O}(\mu_3)$ angle, which is smaller in the heterobimetallic complex (55.74(15) vs. 65.96(13)°). This difference may be ascribed to the asymmetry in the complex caused by the shortest Mg–O bonds compared to the Nd–O ones.

The magnesium atoms are four-coordinated, showing a distorted tetrahedron geometry. This geometry was found in some mixed alkoxy-amido complexes such as $(\text{CMeNC}_6\text{H}_3\text{-2,6-}i\text{Pr}_2)\text{Mg}(\mu_2\text{-O}t\text{Bu})(\text{THF})$ and $(\text{CMeNC}_6\text{H}_3\text{-2,6-}i\text{Pr}_2)\text{Mg}(\mu_2\text{-OC}_6\text{H}_9)$.³²⁸ The doubly bridging Mg–O distances ($\text{Mg}(2)\text{-O}(7)$, 1.987(6) and $\text{Mg}(3)\text{-O}(6)$, 1.972(6) Å) and Mg–O–Nd angles ($\text{Mg}(2)\text{-O}(7)\text{-Nd}(2)$, 95.45(19) and $\text{Mg}(3)\text{-O}(6)\text{-Nd}(2)$, 95.50(19)°) compare well with the values observed in $(\text{CMeNC}_6\text{H}_3\text{-2,6-}i\text{Pr}_2)\text{Mg}(\mu_2\text{-O}t\text{Bu})(\text{THF})$ (Mg-O , 1.997(2) and 1.994(2) Å, and Mg-O-Mg , 98.56(6)°).

Table 36. Selected bond lengths [Å] and angles [°] for **14**.

³²⁸ Chisholm, M. H.; Gallucci, J.; Phomphrai, K. *Inorg. Chem.* **2002**, *41*, 2785-2794.

Nd(2)-O(8)	2.246(8)	O(8)-Nd(2)-O(7)	109.8(2)
Nd(2)-O(7)	2.301(5)	O(8)-Nd(2)-O(6)	104.7(2)
Nd(2)-O(6)	2.312(5)	O(7)-Nd(2)-O(6)	135.08(19)
Nd(2)-O(9)	2.353(8)	O(8)-Nd(2)-O(9)	93.4(3)
Nd(2)-O(5)	2.611(6)	O(7)-Nd(2)-O(9)	99.8(2)
Nd(2)-O(4)	2.763(5)	O(8)-Nd(2)-O(5)	107.1(2)
Nd(2)-Mg(3)	3.180(2)	O(7)-Nd(2)-O(5)	71.21(17)
Nd(2)-Mg(2)	3.180(2)	O(8)-Nd(2)-O(4)	162.6(2)
Si(2)-C(33)	1.827(7)	O(5)-Nd(2)-O(4)	55.74(15)
Si(2)-C(36)	1.830(14)	O(7)-Mg(2)-O(4)	93.1(2)
Si(2)-C(34)	1.873(9)	O(4)-Mg(2)-O(5)	76.3(2)
Si(2)-C(35)	1.937(12)	O(6)-Mg(3)-C(33)	131.0(3)
Si(3)-C(37)	1.821(8)	O(4)-Mg(3)-C(33)	127.7(3)
Si(3)-C(38)	1.865(10)	O(5)-Mg(3)-C(33)	121.4(3)
Si(3)-C(40)	1.874(12)	Mg(2)-O(4)-Mg(3)	100.4(2)
Si(3)-C(39)	1.919(12)	Mg(2)-O(4)-Nd(2)	81.66(18)
Mg(2)-O(7)	1.987(6)	Mg(2)-O(5)-Mg(3)	98.8(2)
Mg(2)-O(4)	2.025(5)	Mg(2)-O(5)-Nd(2)	85.1(2)
Mg(2)-O(5)	2.050(5)	Mg(3)-O(5)-Nd(2)	84.9(2)
Mg(2)-C(37)	2.116(8)	Mg(2)-O(7)-Nd(2)	95.45(19)
Mg(2)-Mg(3)	3.121(3)	C(37)-Si(3)-C(38)	114.0(4)
Mg(3)-O(6)	1.972(6)	C(37)-Si(3)-C(40)	114.7(5)
Mg(3)-O(4)	2.036(5)	C(37)-Si(3)-C(39)	111.0(4)
Mg(3)-O(5)	2.060(6)	O(6)-Mg(3)-C(33)	131.0(3)
Mg(3)-C(33)	2.121(8)	O(4)-Mg(3)-C(33)	127.7(3)
C(33)-Si(2)-C(36)	116.8(5)	O(5)-Mg(3)-C(33)	121.4(3)
C(33)-Si(2)-C(34)	111.4(4)		
C(33)-Si(2)-C(35)	112.6(4)		
O(7)-Mg(2)-C(37)	129.4(3)		
O(4)-Mg(2)-C(37)	129.8(3)		
O(5)-Mg(2)-C(37)	121.1(3)		

The solution structure of this complex was studied by ^1H NMR in toluene- d_8 . At room temperature, the spectrum revealed a set of seven resonances with relative integrations 1:0.8:2:1.5:0.4:0.8:0.4. As shown in Figure 86, the spectrum was composed of both narrow and broad signals. This result does not match with the expected spectrum of the isolated structure. The latter might change in solution or ligand exchanges might occur.

In order to slow down these potential dynamic exchanges, a variable ^1H NMR experiment was conducted from 20 to -80 °C. Going from room temperature to -30 °C yielded a refinement of the signals initially at δ 15.04 (B), -15.87 (E), -30.70 (F) and -33.77 (G) ppm, as indicating the $\Delta\nu_{1/2}$ values, and a broadening of the analysis window (Table 37, Figure 86). In addition, integration values for the peaks B and F increased from 0.8 to 1.0 along with a slight

broadening of the peak base at δ 1.33 ppm (D). An enlargement of the signals is again observed from -40 °C.

Figure 86. ^1H NMR spectra of **14** in toluene- d_8 at various temperatures.

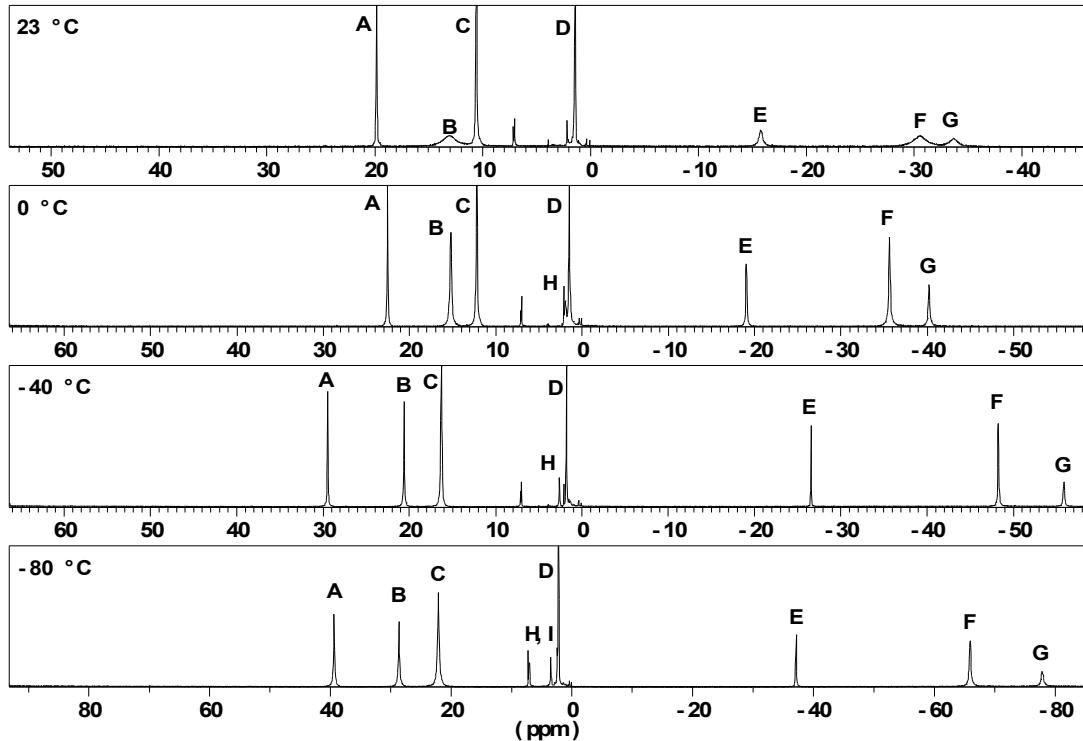


Table 37. Evolution of $\Delta\nu_{1/2}$ (Hz) with the temperature.

Peak	23 °C	10 °C	0 °C	-30 °C	-40 °C
B	260.17	92.86	41.83	18.21	19.57
E	100.06	65.04	27.42	11.01	12.35
F	284.18	91.46	43.03	21.01	24.44
G	180.12	79.25	41.03	32.42	34.48

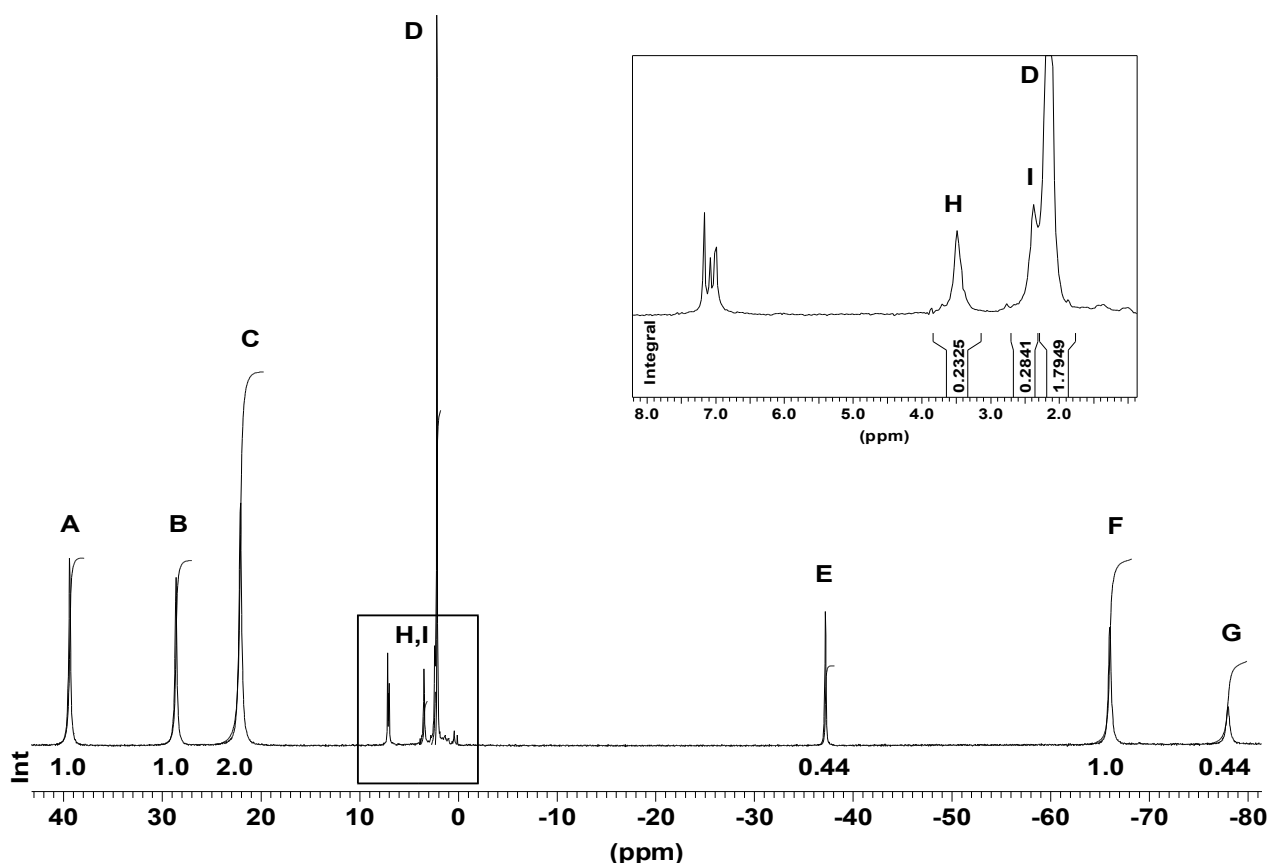
From 0 to -80 °C, the integral values of A, B, C, E, F, and G remained constant with the following relative ratio 1:1:2:0.44:1:0.44. At -10 °C, the appearance of a signal coming out from D at -10 °C with an integral value of 0.22-0.24 (peak H) was noticed. This can be interpreted by separation of the CH_2 signals of the $\text{CH}_2\text{-SiMe}_3$ groups. A coupling constant $^1J = 9.16$ Hz was measured from -20 to -40 °C. Below this temperature, this signal appears as a singlet. At -80 °C, a new signal appears from the basis of D, again integrated for 0.2-0.3 (peak I) (Figure 87). This signal can be attributed to the second methylene group of $\text{CH}_2\text{-SiMe}_3$ fragments. This observation is important for the attribution of the signals since it indicates that the -SiMe_3 groups are magnetically inequivalent. It also correlates well with the ^1H NMR spectrum recorded at -80 °C. Thus, the two signals integrated for 18H must be attributed to the $\mu_3\text{-OtBu}$ or $\mu_2\text{-OtBu}$ groups, which is consistent with their propensity to exchange rapidly, even at low temperatures.

Consequently, at this low temperature, the ^1H NMR spectrum is in agreement with the solid-state structure determined by X-ray analysis. Number of signals and integral values are

consistent with the structure $\text{Nd}(\mu_3\text{-O}t\text{Bu})_2(\mu_2\text{-O}t\text{Bu})_2(\text{O}t\text{Bu})\text{Mg}_2(\text{CH}_2\text{TMS})_2(\text{THF})$. Based on the relative intensities, we can propose the following assignment: A: $\text{O}t\text{Bu}$, B: $\text{CH}_2\text{-Si}(\text{CH}_3)_3$, C: $\mu_3\text{-O}t\text{Bu}$ or $\mu_2\text{-O}t\text{Bu}$, H: $\text{CH}_2\text{-Si}(\text{CH}_3)_3$, I: $\text{CH}_2\text{-Si}(\text{CH}_3)_3$, D: $\mu_3\text{-O}t\text{Bu}$ or $\mu_2\text{-O}t\text{Bu}$, E: THF, F: $\text{CH}_2\text{-Si}(\text{CH}_3)_3$, and G: THF.

Unfortunately, contrary to diamagnetic complexes, it is not possible to predict the chemical shift of the *tert*-butoxy ligand in paramagnetic complexes based on its degree of coordination, hence creating an uncertainty on C and D assignment. In addition, we can not explain the quite surprising magnetic inequivalence of the $\text{CH}_2\text{-Si}(\text{CH}_3)_3$ groups in solution, even if they are inequivalent in the solid-state structure.

Figure 87. ^1H NMR spectra of **14** in toluene- d_8 at -80 °C.



This new heterobimetallic complex (**14**) was exposed to ethylene (1 bar) and the monomer consumption was monitored by ^1H NMR. At room temperature, even after a long contact time (48 h), the formation of polyethylene could not be observed. However, addition of excess of TMSM on **14** under ethylene atmosphere led to a slow polymerization. Unfortunately, we were not able to compare this polymerization activity with the ones obtained with the *in situ* system. Given this result, we can assume that **14** might be an intermediate in the formation of the real active species in **1/MgR₂** systems for ethylene polymerization. However, we can not discard the potential catalytic activity of other products that would be formed in this reaction. Indeed, based on the stoichiometry of the reaction, the formation of $[(t\text{BuO})_2\text{Nd-R}]_n$ species is possible.

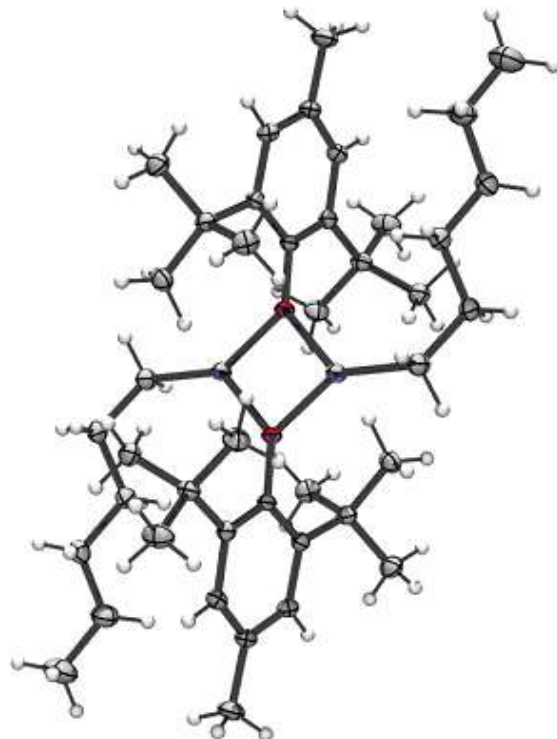
Finally, the addition of another monomer in the crystallization solution afforded the characterization and the isolation of an other metathesis product from $\text{Nd}_3(\text{OtBu})_9\text{THF}_2/\text{Mg}(\text{CH}_2\text{SiMe}_3)_2\bullet\text{Et}_2\text{O}$ systems. Indeed, in the presence of isoprene, large colorless square crystals were isolated from the dark brown solution. ^1H and ^{13}C NMR spectra agreed with the structure $[(t\text{BuO})\text{Mg}(\text{CH}_2\text{SiMe}_3)](\text{THF})$ (**15**) (see Appendix 15 & 16 for ^1H and ^{13}C NMR spectra).

29.2. Isolation of metathesis products from $\text{Nd(OAr)}_3(\text{THF})/\text{MRz}$ systems

Since no other crystals suitable for X-ray analysis could be prepared from our tests with $\text{Nd}_3(\text{OtBu})_9\text{THF}_2$, we focused then on the use of $\text{Nd}(\text{O}-2,6-t\text{Bu}_2-4-\text{Me-Ph})_3(\text{THF})$ (**12**). This neodymium precursor might yield more stable complexes and might induce products easier to crystallize.

Valuable information was initially obtained with the **12**/DHM system; the reaction of these precursors in a 1:1 ratio at room temperature in toluene gives a mixed alkyl/aryloxide magnesium compound $[(n\text{-hex})\text{Mg}(\text{O}-2,6-t\text{Bu}_2-4-\text{Me-C}_6\text{H}_2)]_2$ (**16**), that was isolated in 90% yield as colourless crystals and fully characterized by NMR and X-ray diffraction study (Figure 88 and Appendix 17 & 18 for ^1H and ^{13}C NMR spectra).

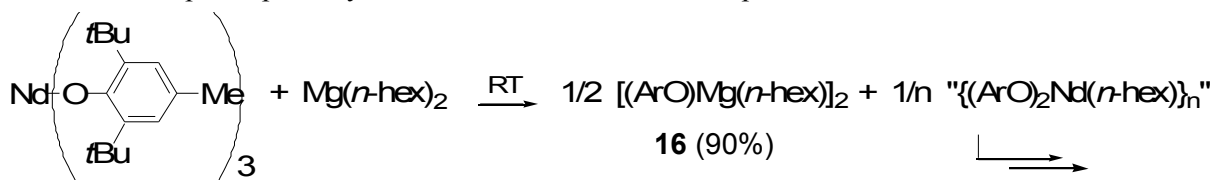
Figure 88. ORTEP plot of **16** with probability ellipsoids at 50% (Hydrogen atoms omitted for clarity).



Unfortunately, the neodymium co-product of this metathesis reaction could not be isolated nor identified in solution due to the paramagnetic Nd centers. One may reasonably propose, however, a stoichiometry of the process as outlined in Scheme 35. We have shown previously by monitoring the reaction at 20 °C by ^1H NMR the gradual formation of uncoordinated 1-hexene (up to 30% vs. Nd after 17 h), suggesting that the expected primary product,

"[(*n*-hex)Nd(O-2,6-*t*Bu₂-4-Me-C₆H₂)₂]_n", is not stable under these conditions and rapidly undergoes β-H elimination to form so far unidentified lanthanide products.

Scheme 35. Proposed pathway for the formation of metathesis product **16**.



Consequently, we carried on our investigation using $Mg(CH_2SiMe_3)_2 \cdot Et_2O$ as alkylating agent, in order to avoid decomposition via β-H elimination reaction. Again, the expected alkyllanthanide "[(Me_3SiCH_2)Nd(O-2,6-*t*Bu₂-4-Me-C₆H₂)₂]_n" species could not be isolated. On the other hand, the addition of THF (10 equiv. vs. Nd) to **12**/TMSM (1:1) enabled the crystallizations of $Nd(O-2,6-*t*Bu₂-4-Me-Ph)_2(CH_2SiMe_3)(THF)_2$ (**17**) along with $(Ar^*\text{OMgCH}_2\text{SiMe}_3)_2$ (**18**) from toluene solutions at -30 °C (see Appendix 19 & 20 for ¹H and ¹³C NMR spectra of **18**).

The overall molecular structure of **17** in the solid state consists of a lanthanide metal center coordinated in a distorted trigonal bipyramidal fashion by two aryloxy and one methylene trimethylsilyl groups in the equatorial positions and two axial THF ligands as shown in Figure 89. Trigonal bipyramidal coordination has been observed previously in structurally characterized $Ln(OR)_3L_2$ complexes such as $Nd(OOctBu_3)_3(CH_3CN)$ ²²⁵⁹ and $Ce(O-2,6-*t*Bu₂-C₆H₃)_3(CN-*t*Bu)_2$,²⁵⁷ although the latter complex features one axial and one equatorial isocyanide ligand, but also in some mixed halogen-aryloxide complexes such as $Ln(O-2,6-*t*Bu₂-4-Me-C₆H₂)_2Cl(THF)$,²²⁴⁵ ($Ln = Er$ and Yb) and $Sm(OAr)_2I(THF)_2$,³²⁹ and in the mixed alkyl-halogen complex (2,6-dimesitylphenyl)YbCl₂(THF)₂.³³⁰ In the latter, the chlorine atoms occupy the axial positions. The (THF)-O-Nd-O(THF) angle is lower than in theory, probably because of the bulkiness of the aryloxide ligands. It is also interesting to compare the coordination geometries of complex **17** and trisaryloxide precursor **12**, which is a four-coordinated Nd atom forming a distorted tetrahedron. The increase in coordination number from **12** to **17** may be attributed to the decreasing steric requirement of CH₂TMS compared to the very bulky aryloxide. This can also explain why it was not possible to isolate this alkyl complex in the absence of THF. The necessary addition of a Lewis base for crystallisation was also observed for the crystallization of $[Nd(\mu_2-OAr)(OAr)_2(py)_2]_2$.³²⁶

The Nd-O(Ar) distances of 2.23 Å are identical for both ligand units and are somewhat longer than those in **12**, but comparable to those in $[Nd(Odpp)_3(DME)]$ (2.191 Å),³³¹ $[Nd(Odpp)_3(THF)_2]$ (2.190 Å), $[Nd(Odpp)_3(THF)]$ (2.193 Å)³³² ($Odpp = O-2,6-Ph_2-C_6H_3$) and K

³²⁹ Hou, Z. M.; Fujita, A.; Yoshimura, T.; Jesorka, A.; Zhang, Y. G.; Yamazaki, H.; Wakatsuki, Y. *Inorg. Chem.* **1996**, *35*, 7190-7195.

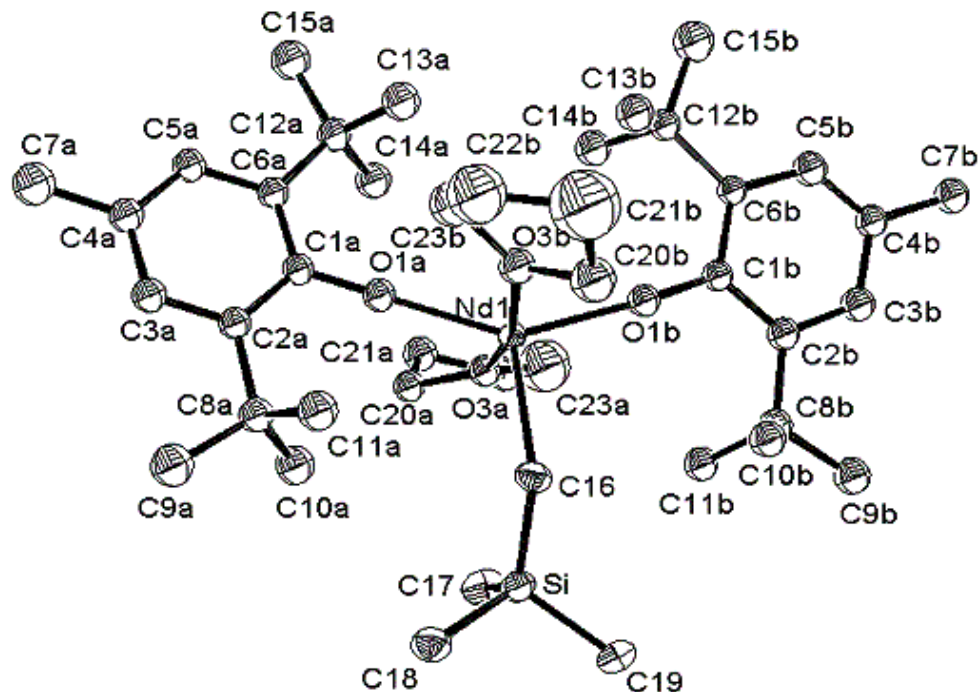
³³⁰ Rabe, G. W.; Berube, C. D.; Yap, G. P. A.; Lam, K.-C.; Concolino, T. E.; Rheingold, A. L. *Inorg. Chem.* **2002**, *41*, 1446-1453.

³³¹ Deacon, G. B.; Feng, T.; Junk, P. C.; Skelton, B. W.; White, A. H. *Chem. Ber.* **1997**, *130*, 851-857.

³³² Deacon, G. B.; Feng, T.; Skelton, B. W.; White, A. H. *Aust. J. Chem.* **1995**, *48*, 741-756.

$[\text{Nd}(\text{O}-2,6-\text{iPr}_2-\text{C}_6\text{H}_3)_4]$ (2.211 Å).²⁴⁷ The Nd-O(THF) distances (2.49–2.50 Å) are within the range of values noticed with $\text{NdCl}_3(\text{THF})_4$,²⁸⁰ $\text{Nd}_2(\text{OCHiPr}_2)_6(\text{THF})_2$,^{260b} ($\eta^5\text{-C}_5\text{H}_5$)₃ Nd (THF)²⁸³. The neodymium-carbon distance can be compared to the terminal Sm-C distance in $[\text{Li}(\text{THF})]_2[\text{Sm}(\text{OAr})_3(\text{CH}_2\text{SiMe}_3)_2]$ (Ar = 2,6-*i*Pr₂-C₆H₃).²²² These bond lengths are within the same range (2.497(6) Å for Nd-C and 2.451(10) Å for Sm-C) of values but much lower than that in $[\text{La}\{\text{CH}(\text{SiMe}_3)_2\}\{1,1'-(2-\text{OC}_6\text{H}_2t\text{Bu}-3,5)_2\}(\text{THF})_3]$ (La-C, 2.676(13) Å) where the larger ionic radius, hexa-coordination and the bulkiness of both aryloxide and alkyl groups may explain such a long Ln-C distance.²²³

Figure 89. ORTEP plot of **17** with probability ellipsoids at 50% (Hydrogen atoms omitted for clarity).



The characterization of these complexes by ¹H NMR was successful even if it was not possible to obtain neat analytical solutions. However, assignment of all the signals was unambiguous. Complex (**17**) exhibits the usual patterns of $\text{Nd}(\text{O}-2,6-t\text{Bu}_2-4\text{-Me-Ph})_3(\text{THF})$ spectrum i.e. narrow signals for aromatic and Me protons, and broad singlet for *tert*-butyl groups, but at a higher field (see Experimental section). The signals assigned to the alkyl group were found at δ –1.25 and –7.15 ppm respectively for the methylene and trimethylsilyl groups. And broad resonances for the two coordinated THF molecules were located at δ -6.90 and -9.66 ppm.

Table 38. Selected bond lengths [Å] and angles [°] for **17**.

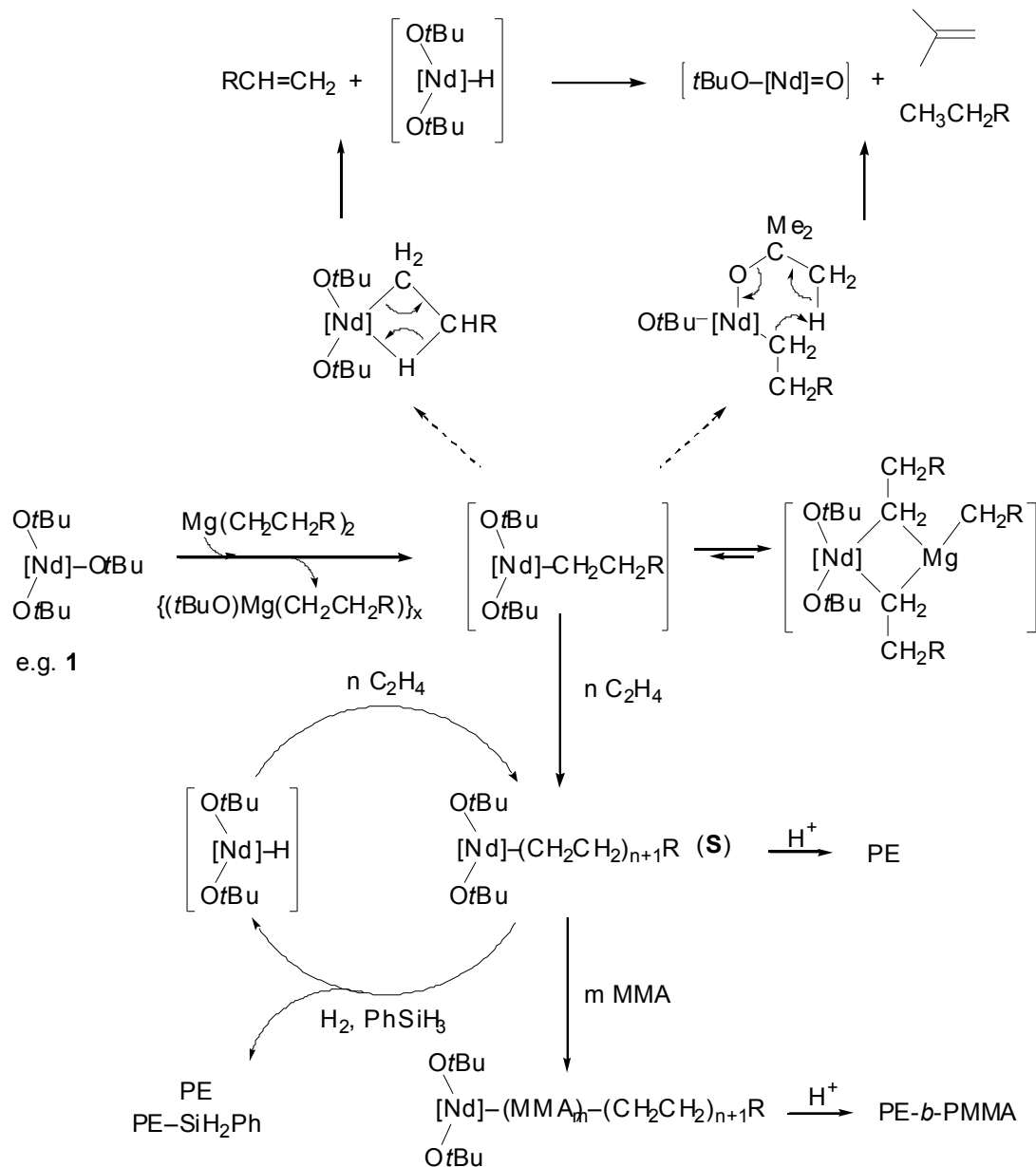
Nd(1)-O(1A)	2.230(4)	O(1A)-Nd(1)-O(1B)	146.69(15)
Nd(1)-O(1B)	2.235(4)	O(1A)-Nd(1)-O(3B)	83.65(15)
Nd(1)-O(3B)	2.491(4)	O(1B)-Nd(1)-O(3B)	91.51(15)
Nd(1)-C(16)	2.497(6)	O(1A)-Nd(1)-C(16)	112.50(19)
Nd(1)-O(3A)	2.506(4)	O(1B)-Nd(1)-C(16)	100.23(19)
O(1A)-C(1A)	1.359(7)	O(3B)-Nd(1)-C(16)	88.37(18)
O(1B)-C(1B)	1.344(7)	O(1A)-Nd(1)-O(3A)	84.50(14)
C(16)-Si	1.838(7)	O(1B)-Nd(1)-O(3A)	93.75(14)
Si-C(18)	1.879(7)	O(3B)-Nd(1)-O(3A)	165.42(14)
Si-C(17)	1.899(7)	C(16)-Nd(1)-O(3A)	104.03(18)
Si-C(19)	1.907(7)	Si-C(16)-Nd(1)	134.5(3)

30. Conclusion

Based on the polymerizations observations, the NMR monitoring of **1**/DHM mixtures and the characterization of **17**, we can now give a more complete and justified mechanism for the production of the active [Nd]-{*n*-hex} species from Mg(*n*-hex)₂ and neodymium *tert*-butoxide, but also its decomposition pathways and its use as either initiator or catalyst for polymerization (Scheme 36).

Our results demonstrate that the association of an homoleptic alkoxy-neodymium complex with a dialkylmagnesium co-reagent can generate significantly active species for MMA, ethylene and butadiene (co)-polymerizations. Nevertheless, the most striking results are the ethylene polymerization and its efficient diblock copolymerization with MMA. As expected from parallel work in group 4 chemistry,^{24,29} these Cp-free systems show similar (and sometimes superior) polymerization performance to the corresponding metallocene systems. It confirms thus the ability of some alkoxy/aryloxy residues to act as valuable ancillary ligands for lanthanide metals in the field of polymerization. Several questions arise however, concerning the difficulties to produce *and* stabilize such active species. Our results highlight the narrow window in which effective polymerization can be achieved with regards to the nature of the alkoxy-lanthanide precursor and alkylating co-reagent.

Scheme 36. Proposed general mechanism for activation and deactivation pathways of *tert*-butoxy-neodymium/dialkylmagnesium polymerization systems.



In fact, to find an adequate balance between the thermal stability of alkyl-alkoxy-lanthanide species and their reactivity towards olefin monomers appears as the major issue of this chemistry. NMR investigations indicate a relative easiness of the alkyl/alkoxy metathesis reaction to proceed and the tendency of the resulting alkyl-alkoxy-lanthanide species to undergo rapid β -H elimination and ligand (*tert*-butoxy) thermolysis. In this regard, the exact influence of alkoxy ancillary ligands on the reactivity of alkyl-lanthanide remains a quite controversial issue. On one hand, one may argue that electron-withdrawing alkoxide ligands, compared to good σ -donor Cp-type ligands, increase the electrophilicity of the metal center and, therefore, facilitate β -H elimination from alkyl-alkoxy-lanthanide species. This simple view may allow for the easy release of α -olefins observed from combinations of lanthanide alkoxides with alkylating agents in the absence of ethylene. On the other hand, the relative thermodynamics of $\text{Ln}-\text{C}$ vs. $\text{Ln}-\text{H}$ bond dissociation energies suggests that chain termination

(β -H elimination, chain transfer) reactions should be further inhibited or slow, in comparison with the rate of propagation by replacement of Cp^* ligands by hard, electronegative *tert*-butoxide ligands.¹⁵⁷ Such arguments have been used to account for the stability of the bridging alkyl groups in $[Y(C_5Me_5)(O-2,6-tBu_2C_6H_3)]_2(\mu\text{-H})(\mu\text{-CH}_2CH_2R)$ towards β -H elimination⁶⁵ and fit well with the formation of high molecular weight polymer observed with the $Nd_3(OtBu)_9(THF)_2/MgR_2$ /ethylene systems.

The high sensitivity of the active species generated from **1**/ MgR_2 combinations towards Lewis bases suggests that usual strategies, based on the introduction of additional donor atoms within the ligand framework (e.g. in **11**),⁷³ may be inappropriate to stabilize alkyl-alkoxy-lanthanide species aimed at ethylene polymerization. We suspect that the adequate (although not ultimate) balance between stability and activity found in **1**/ MgR_2 combinations may originate from the degree of aggregation (nuclearity) of the active species and specificities of dialkylmagnesiums (e.g. the electronegativity of Mg which is equivalent to that of the lanthanides).

Formation of dimers and higher polymetallic species has been often related to decreased polymerization activity in group 4 chemistry.²⁴⁻²⁹ In this regard, it is remarkable that we have detected only sluggish polymerization systems derived from mononuclear lanthanide precursors such as $Nd(O-2,6-tBu_2-4-Me-C_6H_2)_3(THF)$ and $Nd(OCtBu_3)_3(THF)$ that induce the formation of monolanthanide alkyl-alkoxy(aryloxy) species as described in Chapter 4 §29.2. Much more active polymerization systems derive from trinuclear precursor **1** based on the *tert*-butoxy ligand, which often leads to polynuclear structures due to its relative moderate bulkiness. Therefore, it is not unreasonable to think that aggregation to some extent of " $[(tBuO)_2LnR]$ " moieties may contribute to stabilize an active polymerization site. A considerable difficulty usually associated to the chemistry of lanthanide alkoxides relies in their high tendency to form a variety of cluster aggregates, which hampers their isolation in pure form and their characterization. This may prove, however, to be also a key issue for the successful development of new alkoxy-based lanthanide catalysts.

Concluding remarks

We have described in this manuscript the discovery, the applications and the characterization of a new lanthanide-based initiating system for olefin polymerization. This system, based on lanthanide alk(aryl)oxide/MgR₂ combinations, is the first example of post-lanthanocene catalyst with such high versatility and efficiency. Indeed, the use of the trinuclear **1** in association with DHM allows the pseudo-living syndiotactic polymerization of MMA, ethylene polymerization and the ethylene-MMA diblock copolymerization. This system also allows the pseudo-living stereospecific butadiene polymerization and its diblock copolymerization with GMA. In addition, mechanistic investigations showed the formation of alkyllanthanide species, which may act as active species, as suggested by the polymerization results.

However, this work must not be considered as over, but just as the early beginning of the development of a new generation of catalysts for olefin polymerization. Indeed, many questions remain unanswered. We still do not know how to explain the discrepancy of activity in ethylene polymerization between the different neodymium *tert*-butoxides, different neodymium alkoxides or different lanthanide alkoxides. In fact, a complete understanding of these binary systems includes the full characterization of neodymium precursors (X-ray crystal structure determination and correlation with ¹H NMR spectroscopy), isolation and characterization of the active species or intermediates, followed by their test in polymerization. A deeper NMR investigation based on isostructural diamagnetic complexes should be a mine of information regarding the mechanism of formation of the active species. Once a general mechanism determined, a rational development of new catalysts may be expected.

Besides the development of new catalyst systems, we prepared new materials that were previously inaccessible. Given their unique composition, their mechanical and morphological properties as well as their application as compatibilizer or reinforcement agent may be thoroughly evaluated and should be one of the driving forces for further developments in that area.

Experimental section

31.

32. Solvents and reagents

Given oxygen- and moisture-sensitivities of lanthanide salts and dialkylmagnesium reagents, all operations were performed under dry argon using standard Schlenk techniques or in a dry glove box under nitrogen. All the glassware was dried at 140 °C and cooled down under vacuo prior to use.

All solvents and deuterated solvents were freshly distilled from sodium-potassium amalgam under argon and degassed prior to use.

Anhydrous NdCl₃ (99.9%) was purchased from Strem and used as received, while analytically pure NdCl₃(THF)₂ was provided by Rhodia. *Tert*-butyl, *tert*-amyl, isopropyl, and isobutyl alcohols and dimethylphenylmethanol were dried over and distilled from CaH₂. NaOtBu (97%, Aldrich), LiOtBu (97%, Aldrich) and KOtBu (95%, Aldrich) were dried at 130 °C under 10⁻³ Torr prior to use. Sodium and potassium alkoxides were prepared from sodium or potassium metal and the corresponding alcohol at 25 °C; excess alcohol was removed by evaporation and NaOR were dried at 130 °C under high vacuum. Na(O-2,6-*t*Bu₂-4-Me-Ph) (THF) was prepared by reaction of the corresponding phenol (purified by sublimation) with metallic sodium in THF solution at room temperature for 24 h.

Ethylene (Air Liquide, N35) was purified by passage through a moisture filter (Chrompack, n° 7971); butadiene (Air Liquide, N25) was used without purification.

Methyl methacrylate (99%, Aldrich), methyl acrylate (99%, Aldrich), ϵ -caprolactone (99%, Aldrich), glycidyl methacrylate (99%, Aldrich) and styrene (99%, Aldrich) were vacuum distilled over CaH₂ and stored at -20 °C under argon.

Alkylating agents AlMe₃, Al(*n*-Oct)₃, AlH(*i*Bu)₂ (Schering), *n*-BuEtMg (20 wt% solution in heptane, Texas Alkyl), Mg(*n*-Hex)₂ (1.33 M solution in heptane, Akzo Nobel), (*n*-Bu)(*s*-Bu)Mg (1.0 M in heptane), PhMgBr (1.0 M solution in THF), EtMgBr (3.0 M solution in THF), BEt₃ (1.0 M solution in hexanes), *n*-BuLi (1.6 M solution in hexanes) and *t*-BuLi (1.7 M solution in pentane) (all Aldrich) were used as received. Mg(CH₂SiMe₃)₂•OEt₂ was prepared according to literature.³³³ [*n*-BuAlH(*i*-Bu)₂][Li] was prepared prior to use from equimolar amounts of AlH(*i*-Bu)₂ and *n*-BuLi.

Complexes Nd[N(SiMe₃)₂]₃•252³³⁴ Nd(OC*t*Bu₃)₃(THF)•256^a and Nd(O-2,6-*t*Bu₂-4-Me-C₆H₂)₃(THF)•249 and Nd(O-2,6-*t*Bu₂-4-Me-C₆H₂)₃³²⁴⁹ were prepared according to the reported procedures and sublimed prior to use, or using a modified procedure (*vide infra*).

³³³ Andersen, R. A.; Wilkinson, G. J. *J. Chem. Soc. Dalton Trans.* **1977**, 809-811.

³³⁴ Dash, A.; Razavi, A.; Mortreux, A.; Lehmann, C. W.; Carpentier, J.-F. *Organometallics* **2002**, *21*, 3238-3249.

33. Analyses

NMR spectra were recorded on Bruker AC-200, AC-300 or AM-400 spectrometers. ^1H (200, 300 and 400 MHz) and ^{13}C (50, 75 and 100 MHz) chemical shifts are expressed in ppm, reported vs. SiMe₄ and were determined by reference to the residual solvent peaks. NMR spectra of lanthanide alkoxides were recorded in Teflon-valved NMR tubes at variable temperature. ^1H and ^{13}C NMR spectra of polyethylenes and polyethylene-*b*-poly(methyl methacrylate) copolymers were recorded at 130 °C in C₂D₂Cl₄. Polymers microstructure and/or composition of PMMA and butadiene (co)-polymers were measured by NMR at 23 °C in CDCl₃.

IR spectra were recorded on a Nicolet 510 FTIR spectrophotometer in KBr pellets and are expressed by wave number (cm⁻¹).

Elemental analyses were performed by Pascher Laboratories, Erlagen, Germany and at Rhodia Research Center, Aubervilliers, France.

Molecular weights of polyethylenes and polyethylene-*b*-poly(methyl methacrylate) copolymers were determined by size exclusion chromatography (SEC) using polystyrene gel columns at 135-155 °C and *o*-dichlorobenzene as the solvent, with either a PL220 (Polymer Laboratories) apparatus or a Waters apparatus equipped with coupled refractometer and viscosity detectors. The number-average molecular weight (M_n) and polydispersity ratio (M_w/M_n) were calculated by universal calibration in reference to polystyrene standards.

Molecular weights of methacrylates and butadiene (co)-polymers were determined by size exclusion chromatography in THF at 20 °C using a Waters SIS HPLC-pump, a Waters 410 refractometer, a DAD-UV detector and Waters styragel columns (HR2, HR3, HR4, HR5E) or PL-GEL Mixte B and 100A columns. The number-average molecular masses and polydispersity ratio of the resultant polymers were calculated with reference to a polystyrene calibration without using the corresponding correction factors.

Melting points (T_m), glass transition temperature (T_g), and crystallinity of polymers were determined by DSC (Setaram DSC 141 apparatus, 10 °C/min, under nitrogen) and X-ray diffraction (XRD, Siemens D5000 spectrometer, CuK $\alpha_{1,2}$, 5° < 2θ < 55°) analysis.

X-ray crystal structure determinations of lanthanide alkoxides were made using a Bruker SMART CCD area-detector diffractometer.

Scanning Electronic Microscopy (SEM) analyses were performed using a Hitachi S4700 microscope and Atomic Force Microscopy (AFM) analysis was carried out using the nanoscope-III multimode system (Digital Instruments, Santa Barbara, CA).

34. Preparation of lanthanide alkoxides

34.1. Synthesis of neodymium *tert*-butoxides

34.1.1. $Nd_3(\mu_3-OtBu)_2(\mu_2-OtBu)_3(OtBu)_4(THF)_2$ (**1**)

Salt metathesis route: In a glove box, NaOtBu (2.88 g, 30.0 mmol) was dissolved in THF (50 mL) and transferred to a flask containing a suspension of anhydrous NdCl₃ (2.51 g, 10.0 mmol) in THF (50 mL). The mixture was stirred with a magnetic stir bar for 3 days at 25 °C. The solution was decanted overnight and filtered, leaving behind a pasty solid that was discarded. Removal of solvents from the solution at 20 °C and drying the residue under 10⁻³ torr for 6 h offered a pale blue solid (3.36 g, 82%). ¹H NMR (400 MHz, toluene-*d*₈): δ (5 °C) = 41.0 (s, 18H), 17.2 (s, 18H), -1.5 (s, 9H), -14.7 (s, 9H), -21.7 (s, 18H), -25.8 (s, 18H), -29.5 (s, 9H); δ (27 °C) = 34.2 (brs, 18H), 14.8 (brs, 18H), -0.5 (brs, 9H), -9.9 (s, 9H), -20.2 (brs, 27H), -22.8 (s, 18H); elemental analysis calculated (%) for **1**, C₄₄H₉₇O₁₁Nd₃ (1234.97): C 42.79, H 7.92; found C 41.32, H 7.74; crude samples of **1** prepared by salt metathesis and worked-up as described above were shown to contain less than 0.5% of Cl.

Amide alcoholysis route: In a Schlenk tube, *t*BuOH (3.0 mL, 31.0 mmol) was added dropwise to a stirred solution of Nd{N(SiMe₃)₂}₃ (1.25 g, 2.0 mmol) in THF (20 mL). The resulting clear light-blue solution was stirred for 3 days at room temperature. Removal of volatiles under high vacuum for 10 h at room temperature gave a light blue solid that was subsequently recrystallized from toluene (0.48 g, 57%). The ¹H NMR spectra (toluene-*d*₈, 5 °C) of the crystals featured reproducibly as the major (ca. 70%) peaks the seven resonances observed for samples of **1** prepared from NaOtBu along with additional (ca. 30%) rather broad resonances at δ 46.8, 45.5, 40.0, 22.3, 15.1, -27.3, -33.0, -34.1, -42.6.

X-ray crystal structure determination of **1•THF:** Crystals of **1**•THF were grown from a concentrated toluene solution of the crude product obtained from NaOtBu at -5 °C. A pale blue crystal of approximate dimensions 0.19 × 0.20 × 0.21 mm was mounted on a glass fiber. X-ray measurements were made using a Bruker SMART CCD area-detector diffractometer with MoKα (λ = 0.71073 Å) at T = 158(2) K.

Crystal data: orthorhombic *Pbcn*: *a* = 17.0538(10), *b* = 20.0343(12), *c* = 17.7400(11) Å; *V* = 6061.1(6) Å³; formula unit: C₄₄H₉₇O₁₁Nd₃•C₄H₈O with *Z* = 4; formula weight: 1307.04; calculated density = 1.432 g.cm⁻³; *F*(000) = 2676; μ (MoKα) = 2.581 mm⁻¹. 38059 reflections were collected (1.57°>θ>28.27°). The structure was solved by direct methods.³³⁵ The *tert*-butoxide ligand located on the two-fold axis and the THF ligands were disordered. The carbon atoms associated with these ligands were included using multiple components with partial site-occupancy-factors. There was also one disordered THF solvent molecule present per formula unit. Hydrogen atoms associated with the disordered *tert*-butoxide ligand and with the

³³⁵ (a) SMART Software Users Guide, Version 5.0, Bruker Analytical X-Ray Systems, Inc.; Madison, WI 1999; (b) SAINT Software Users Guide, Version 6.0, Bruker Analytical X-Ray Systems, Inc.; Madison, WI 1999; (c) Sheldrick, G. M. SADABS, Bruker Analytical X-Ray Systems, Inc.; Madison, WI 1999; (d) Sheldrick, G. M. SHELXTL Version 5.10, Bruker Analytical X-Ray Systems, Inc.; Madison, WI 1999.

solvent molecule were not included in the refinement. Full-matrix least-squares refinement on F^2 based on 7315 independent reflections converged with 213 variable parameters and 30 restraints. $R1 = 0.0410$ (for those 5589 data with $I > 2\sigma(I)$); $wR2 = 0.1044$; GoF (F^2) = 1.059.³³⁶ $\Delta\rho_{\max} = 1.505$ and -1.027 e. \AA^{-3} .

34.1.2. $Nd_3(\mu_3\text{-}OtBu)_2(\mu_2\text{-}OtBu)_3(OtBu)_4(HOtBu)_2$ (7)

In a Schlenk tube, *t*BuOH (7.0 mL, 73.0 mmol) was slowly added over ca. 5 min to a stirred solution of Nd{N(SiMe₃)₂}₃ (3.85 g, 6.15 mmol) in *n*-hexane (60 mL). The resulting clear light-blue solution was stirred for 3 days at room temperature. Volatiles were then removed by evaporation in vacuum for 12 h at room temperature to give a light blue solid (2.30 g, 90% based on Nd). Crystallization from toluene offered analytically pure blue crystals (1.55 g, 61%). ¹H NMR (200 MHz, toluene-*d*₈, -15 °C): δ = 19.5 (s, 18H), 6.4 (s, 45H), -13.5 (s, 2H; OH), -25.2 (s, 18H), -32.0 (s, 18H); (-45 °C): δ = 23.8 (s, 18H), 9.0 (s, 36H), 5.5 (s, 9H; 1 μ_2 -OtBu), -4.3 (s, 2H; OH), -34.2 (s, 18H), -38.1 (s, 18H). (-65 °C): δ = 27.3 (s, 18H), 10.9 (s, 36H), 2.7 (s, 9H; 1 μ_2 -OtBu), -6.0 (s, 2H; OH), -42.4 (s, 36H); elemental analysis calculated (%) for C₄₄H₁₀₁O₁₁Nd₃ (1239.00): C 42.65, H 8.22; found C 41.8, H 7.92.

34.1.3. $Nd_5(\mu_5\text{-}O)(\mu_3\text{-}OtBu)_4(\mu_2\text{-}OtBu)_4(OtBu)_5$ (8)

In a glove box, 7 (0.720 g, 1.74 mmol Nd) was dissolved in toluene (ca. 5 mL) and the clear blue solution was allowed to stand at room temperature for 2 weeks. After concentration to ca. 2 mL under vacuum, the solution was placed at -5 °C, leaving X-ray quality crystals of **8·2(toluene)** (that lost toluene in vacuo) (0.310 g, 53%); elemental analysis calculated (%) for the toluene-free complex C₅₂H₁₁₇O₁₄Nd₅ (1687.7): C 37.00, H 6.99; found C 36.2, H 7.56.

X-ray crystal structure determination of **8·2(toluene):** A pale purple crystal of approximate dimensions 0.33 × 0.41 × 0.52 mm was mounted on a glass fiber. X-ray measurements were made using a Bruker SMART CCD area-detector diffractometer with MoK α ($\lambda = 0.71073 \text{ \AA}$) at T = 163(2) K.

Crystal data: tetragonal *P*4/*nmm*: $a = 16.6902(6)$, $b = 16.6902(6)$, $c = 14.0266(7) \text{ \AA}$; $V = 3907.3(3) \text{ \AA}^3$; formula unit: C₅₂H₁₁₇Nd₅O₁₄•2(C₇H₈) with $Z = 2$; formula weight: 1871.92; calculated density = 1.591 g.cm⁻³; $F(000) = 1882$; $\mu(\text{MoK}\alpha) = 3.317 \text{ mm}^{-1}$. 40230 reflections were collected (1.45°>θ>28.29°). The structure was solved by direct methods.³³⁵ There were two molecules of toluene solvent present per formula unit. Two of the *tert*-butoxide ligands were disordered. Carbon atoms C(2), C(3), C(11), C(12) and C(13) were included using partial site-occupancy-factors. The toluene methyl carbon C(17) was also disordered and included as above. Hydrogen atoms were not included in the refinement. Full-matrix least-squares refinement on F^2 based on 2710 independent reflections converged with 90 variable parameters and no restraints. $R1 = 0.0452$ (for those 2410 data with $I > 2\sigma(I)$); $wR2 = 0.1266$; GoF (F^2) = 1.086.³³⁶ $\Delta\rho_{\max} = 2.561$ and -1.211 e. \AA^{-3} .

³³⁶ $R1 = ||F_0| - |F_c|| / |F_0|$; $wR2 = [[w(F_0^2 - F_c^2)^2] / [w(F_0^2)^2]]^{1/2}$; GoF = [[w(F₀² - F_c²)²] / (n-p)]^{1/2} where n is the number of reflections and p is the total number of parameters refined.

34.1.4. Synthesis of neodymium *tert*-butoxide in hexanes (**5**) & (**6**)

In a glove box, MOtBu (M = Na, K; 30.0 mmol) and NdCl₃(THF)₂ (3.90 g, 10.0 mmol) were weighed and placed in the same Schlenk flask. Hexane (20 mL) was added to the mixture and the suspension was stirred for 24 h at room temperature. The mixture was filtered over celite, resulting in a limpid blue solution. After removal of the solvent under vacuum at 25 °C, a blue powder was obtained (3.84 g, 93%). Analytical data for Nd and Cl gave Nd = 35.1 wt% and Cl = 0.07(5) wt%. X-ray structure determination and ¹H NMR analysis were unsuccessful.

34.1.5. Various neodymium *tert*-butoxides prepared by salt metathesis

Many variations on the experimental procedure described in Chapter 2 §34.1.1 have been performed using various MOtBu and solvents. Unfortunately, NMR and X-ray analyses were not informative. Consequently, only the yields of reaction are reported in Table 39.

Table 39. Various neodymium *tert*-butoxides prepared by salt metathesis.

MOtBu	solvent	product	yield (%)
NaOtBu	Et ₂ O	10*	65
NaOtBu	THP	2	85
NaOtBu	toluene	-	0
LiOtBu	THF	3	50
KOtBu	THF	4	85

34.2. Other characterized neodymium alk(aryl)oxides

34.2.1. Nd₃(μ₃-OtAm)₂(μ₂-OtAm)₃(OtAm)₄(THF)₂ (**9**)

Compound **9** was prepared by salt metathesis in a similar way to that described above for **1**, starting from anhydrous NdCl₃ (2.51 g, 10.0 mmol) and NaOtAm (3.31 g, 30.0 mmol) in THF (100 mL). Workup left compound **9** as a pale blue solid (3.1 g, 66%). This crude material was directly used for polymerization experiments.

34.2.2. Nd₁₂(OtAm)₂₆Cl₁₁Na•2(Et₂O) (**10**)

In a glove box, NaOtAm (1.67 g, 15.1 mmol) was dissolved in Et₂O (25 mL) and transferred to a flask containing a suspension of anhydrous NdCl₃ (1.25 g, 5.0 mmol) in Et₂O (25 mL). The mixture was stirred with a magnetic stir bar for 3 days at 25 °C. The solution was decanted overnight and filtered, leaving behind a pasty solid that was discarded. Removal of solvents from the solution at 20 °C and drying the residue under 10⁻³ torr for 6 h left a blue solid (1.52 g). X-ray quality crystals of **10** were isolated in low yield from a concentrated solution of this material in toluene at -5 °C. The crystals, once isolated, were insoluble even in THF.

X-ray crystal structure determination of 3•2Et₂O: A pale blue crystal of approximate dimensions $0.40 \times 0.42 \times 0.51$ mm was mounted on a glass fiber. X-ray measurements were made using a Bruker SMART CCD area-detector diffractometer with MoK α ($\lambda = 0.71073$ Å) at T = 163(2) K.

Crystal data: monoclinic $P21/c$: $a = 30.7931(14)$, $b = 19.9495(9)$, $c = 34.4764(15)$ Å, $\beta = 105.3890(10)^\circ$; $V = 20419.7(16)$ Å³; formula unit: C₁₄₀H₃₁₀Cl₁₁NaNd₁₂O₂₈•2(C₄H₁₀O) with Z = 4; formula weight: 4733.94; calculated density = 1.540 g.cm⁻³; $F(000) = 9504$; $\mu(\text{MoK}\alpha) = 3.190$ mm⁻¹. 153104 reflections were collected ($0.69^\circ > \Theta > 23.26^\circ$). The structure was solved by direct methods.³³⁵ There were two molecules of diethylether solvent present per formula unit. Two of the *tert*-butoxide ligands were disordered. It was necessary to employ geometric and thermal parameter restraints (2815 total) to all carbon atoms and the solvent molecules via the SHELXTL using the SAME, EADP and PART commands. Disordered atoms were included using multiple components with partial site-occupancy-factors. Hydrogen atoms were not included in the refinement. Full-matrix least-squares refinement on F^2 based on 29327 independent reflections converged with 959 variable parameters and 2815 restraints. $R1 = 0.0544$ (for those 24067 data with $I > 2\sigma(I)$); $wR2 = 0.1645$; GoF (F^2) = 1.053.336 $\Delta\rho_{\max} = 2.469$ and -2.199 e.Å⁻³.

34.2.3. Nd₂(OCMe₂CH₂CH₂OMe)₆ (11)

In a Schlenk tube, 4-methoxy-2-methylbutan-2-ol (0.718 g, 6.06 mmol) dissolved in benzene (10 mL) was added dropwise via canula to a stirred solution of Nd[N(SiMe₃)₂]₃ (1.266 g, 2.02 mmol) in benzene (10 mL). The resulting clear light-blue solution was stirred for 36 h at room temperature. Evaporation of volatiles, followed by drying under high vacuum for 6 h at 50 °C, gave a blue pasty solid in quantitative yield. Crystallization from toluene at -5 °C offered pure blue crystals suitable for X-ray diffraction (0.58 g, 58%); elemental analysis calculated (%) for C₃₆H₇₈Nd₂O₁₂ (991.46): C 43.61, H 7.93; found C 43.2, H 7.81.

X-ray crystal structure determination of 11: A pale purple crystal of approximate dimensions $0.28 \times 0.48 \times 0.48$ mm was mounted on a glass fiber. X-ray measurements were made using a Bruker SMART CCD area-detector diffractometer with MoK α ($\lambda = 0.71073$ Å) at T = 163(2) K.

Crystal data: triclinic P : $a = 9.4496(3)$, $b = 10.7702(4)$, $c = 12.8522(5)$ Å; $\alpha = 96.7120(10)$, $\beta = 96.5560(10)$, $\gamma = 115.7290(10)^\circ$; $V = 1150.21(7)$ Å³; formula unit: C₃₆H₇₈Nd₂O₁₂ with Z = 1; formula weight: 991.46; calculated density = 1.431 g.cm⁻³; $F(000) = 510$; $\mu(\text{MoK}\alpha) = 2.282$ mm⁻¹. 12462 reflections were collected ($1.62^\circ > \Theta > 28.30^\circ$). The structure was solved by direct methods.³³⁵ Carbon atoms C(2) and C(3) were disordered and included using multiple components with partial site-occupancy-factors (major 0.70; minor 0.30). Full-matrix least-squares refinement on F^2 based on 5448 independent reflections converged with 341 variable parameters and no restraints. $R1 = 0.0178$ (for those 5286 data with $I > 2\sigma(I)$); $wR2 = 0.0449$; GoF (F^2) = 1.033.336 $\Delta\rho_{\max} = 0.801$ and -0.610 e.Å⁻³.

4-Methoxy-2-methylbutan-2-ol: A diethyl ether solution of MeMgI (100 mL of a 3.0 M solution, 0.3 mol) in a 250 mL round-bottom flask fitted with an addition funnel under nitrogen was cooled to 0 °C. Methyl 3-methoxypropionate (14.2 g, 0.12 mol) in diethyl ether (90 mL) was added dropwise over 40 min at 0 °C and the reaction mixture was allowed to stir for 18 h at room temperature. The reaction mixture was poured in ice (50 g) and treated with a saturated aqueous solution of NH₄Cl till clear separation of the two phases occurred. The aqueous layer was extracted with Et₂O (15 mL). The ether layers were combined, washed first with a cold saturated aqueous solution of NaHCO₃ (30 mL) and then cold water (2 × 30 mL), and dried over MgSO₄. Removal of the solvent and distillation of the residue (Eb = 85 °C under 95 Torr) gave a colorless liquid (8.4 g, 59%). ¹H NMR (300 MHz, CDCl₃): δ = 1.21 (s, 6H; CH₃), 1.73 (t, J = 5.9 Hz, 2H; CH₂), 3.17 (s, 1H; OH), 3.33 (s, 3H; OCH₃), 3.60 (t, J = 5.9 Hz, 2H; OCH₂). ¹³C NMR (75 MHz, CDCl₃): δ = 29.3 (CMe₂), 41.4 (CH₂), 58.9 (MeO), 70.2 (OCH₂), 70.8 (COH).

34.2.4. Modified synthesis of Nd(O-2,6-tBu₂-4-Me-Ph)₃(THF) (**12**) and Nd(O-2,6-tBu₂-4-Me-Ph)₃ (**13**)

Na(O-2,6-tBu₂-4-Me-Ph)(THF) (24.15 g, 77.0 mmol) and NdCl₃(THF)₂ (10.11 g, 25.6 mmol) were weighed and placed in the same Schlenk flask in a glove box. Hexane (125 mL) was added to the mixture and the suspension was stirred for 20 h at room temperature. The mixture was filtered over celite, resulting in a limpid violet solution. After removal of the solvent under vacuum at 25 °C, a deep blue powder was obtained (18.50 g, 90%). Analytical data for Nd and Cl and ¹H NMR spectroscopy agreed with the formation of Nd(O-2,6-tBu₂-4-Me-Ph)₃(THF) (**12**). Analytical data for Nd and Cl and ¹H NMR spectroscopy agreed with the formation of Nd(O-2,6-tBu₂-4-Me-Ph)₃(THF) (**12**). ¹H NMR (200 MHz, C₆D₆): δ (23 °C) = 15.29 (s, 2H, Ar), 7.37 (s, 3H, Me), -2.36 (brs, 18 H, tBu), -16.88 (s, 4H, THF), -35.84 (s, 4H, THF). Sublimation of **12** at 220 °C under 10⁻³ mmHg yielded Nd(O-2,6-tBu₂-4-Me-Ph)₃ (**13**). ¹H NMR (200 MHz, C₆D₆): δ (23 °C) = 16.32 (s, 2H, Ar), 8.32 (s, 3H, Me), -8.53 (brs, 18 H, tBu).

34.3. Miscellaneous lanthanide alkoxides

Yttrium and lanthanide alkoxides were prepared by salt metathesis from LnCl₃ (Ln = Y, La, Nd, Sm, Ce) and MOR (R = tBu, iPr, iBu, and PhMe₂C and M = Li, Na and K) in THF, using the experimental procedure described in Chapter 2 §34.1.1.

Table 40. Lanthanide alkoxides prepared by salt metathesis.

LnCl ₃	MOR	yield (%)
La239	NaOtBu	70
La	KOtBu	47
Y239	NaOtBu	78
Y	KOtBu	77
Ce	NaOtBu	49
Sm	NaOtBu	48
Sm	KOtBu	55
Nd	NaO <i>i</i> Pr	70
Nd	NaO <i>i</i> Bu	63
Nd	NaOCMe ₂ Ph	37

35. MMA polymerization

35.1.Preparation of the initiator

The lanthanide *tert*-butoxide and the dialkylmagnesium derivative were weighted in a glove box and placed in two separate Schlenk tubes. The latter were each filled in on the Schlenk line with toluene (10 mL) (cooled to 0 °C if necessary); the *tert*-butoxide solution was then transferred via canula on the alkylmagnesium solution and the mixture was stirred for 1 h at desired temperature.

35.2.MMA polymerization

Toluene (80 mL) and the solution (20 mL) of the *in situ* prepared initiator were transferred into a 500-mL Schlenk tube via canula. The resulting solution was cooled at the required temperature and MMA (5.0 mL, 50 mmol) was introduced by means of a glass syringe. Polymerization was carried for 1 h under stirring and then stopped by adding methanol (ca. 2 mL). The polymers were recovered by precipitation into methanol and dried at 60 °C for 24 h. PMMA chain tacticity was measured using ¹H NMR spectroscopy by integration of Me resonances (mm 1.19, mr 1.00, rr 0.84 ppm). ¹H NMR (300 MHz, CDCl₃): δ (23 °C) = 3.58 (COCH₃), 2.0-1.5 (CH₂), 1.20-0.70 (CH₃). ¹³C NMR (100 MHz, CDCl₃): δ (23 °C) = 178.64, 178.37, 177.57, 54.69, 52.52, 45.38, 45.04, 19.39, 17.21.

Preliminary experiments aimed at evaluating the ability of other lanthanide alkoxide/alkylating reagent combinations, were conducted using a similar procedure.

36. Ethylene homo-polymerization

36.1.With *in situ* "Nd(OR)₃"/MR_z combinations

In a typical experiment, a solution of complex **1** (0.37 g, 0.30 mmol) in toluene (10 mL) was added to a solution of Mg(*n*-hex)₂ (0.98 g, 1.0 mmol) in toluene (10 mL) and the reaction

mixture was stirred for 1 h at 0 °C. The resulting brown solution was injected via syringe into a 500-mL Schlenk tube containing toluene (80 mL) kept at 0 °C under 1 atm of ethylene (previously saturated solution). Magnetic stirring was started (1100 rpm) and the ethylene consumption was monitored by a mass flowmeter (Aalborg, GFM17) connected to a totalling controller (KEP), which acts as a flow rate integrator. The reaction was quenched by addition of a 5% HCl methanol solution (200 mL) to the reaction mixture and the polymer was recovered by filtration and dried under vacuum.

¹H NMR (400 MHz, C₂D₂Cl₄): δ (135 °C) = 1.29 (CH₂), 1.05-0.82 (CH₃). ¹³C NMR (100 MHz, C₂D₂Cl₄): δ (135 °C) = 39.84, 33.08, 30.90, 27.70, 25.31, 23.75, 15.10. The intensity of the peaks attributed to short branches is very low compared to the main signal centered at δ 30.90 ppm.

Experiments conducted at different temperatures, Nd/Mg ratios or in the presence of a transfer agent (feed with a preformed C₂H₄/H₂ mixture or introduction of PhSiH₃ via syringe in the reaction mixture after 5 min), and preliminary experiments aimed at evaluating the ability of other lanthanide alkoxide/alkylating reagent combinations, were conducted using a similar procedure.

36.2. With the isolated solid catalyst **S**

36.2.1. Isolation of solid catalyst **S**

A typical ethylene polymerization experiment was conducted as described above over 30 min. The resulting reaction mixture was placed under argon and filtrated over a sintering glass funnel while keeping temperature at 0 °C. The clear filtrate was collected under argon at 0 °C for analytical purposes and polymerization catalysis assays. The solid recovered was washed with cold toluene (2 × 50 mL) at 0 °C, to give **S** as a beige gummy solid, which was rapidly used for further polymerization. ICP (Inductively-Coupled Plasma) microanalyses of three different batches of **S** prepared under the above conditions showed that it contains 15 ± 2% of Nd and 20 ± 4% of Mg initially introduced (as **1** and Mg(*n*-hex)₂, respectively), and the balance for these metals was found in the filtrate. Chlorine content in **S** was below detection level of elemental analysis.

36.2.2. Gas phase ethylene polymerization

The polymerization was carried out directly in the sintering glass funnel by contacting isolated solid **S** with 1 atm of ethylene at 0 °C. In a typical experiment, upon using a solution of **1** (0.37 g, 0.30 mmol) activated by Mg(*n*-hex)₂ (0.98 g, 1.0 mmol) in toluene (100 mL) for 1 h at 0 °C allowed to collect, after 10 min of reaction with 1 atm of ethylene at 0 °C, 3.4 g of **S** as a beige precipitate. The latter was filtered-off at 0 °C and washed twice with cold toluene (2 × 50 mL). Ethylene (1 atm) was then contacted onto the beige solid, resulting in the rapid growth of white efflorescence of polyethylene and a consumption of 0.5 g of ethylene over 90 min. Upon stirring with a magnetic stir bar in the bottom of the sintering funnel, 1.4 g of

ethylene were additionally polymerized over 30 min. Quenching and workup as described above afforded 5.4 g of polyethylene.

36.2.3. Slurry phase ethylene polymerization:

In a glove box, freshly prepared solid **S** (typically 4–5 g) was introduced into a 500 mL-Schlenk. Cold toluene (100 mL) was introduced and the resulting mixture was placed at 0 °C. After purging with 1 atm of ethylene, magnetic stirring was rapidly started (1100 rpm). Ethylene consumption monitoring and final quenching were performed as described above.

37. Diblock ethylene-MMA copolymerization

Diblock ethylene-MMA copolymerization was achieved using the standard *in situ* system or by reacting a suspension of solid **S** in toluene with MMA at 0 °C.

37.1. With the *in situ* system

A solution of complex **1** (0.37 g, 0.30 mmol) in toluene (10 mL) was added to a solution of Mg(*n*-hex)₂ (0.98 g, 1.0 mmol) in toluene (10 mL) and the reaction mixture was stirred for 1 h at 0 °C. The resulting brown solution was injected via syringe into a 500 mL-Schlenk tube containing toluene (80 mL) kept at 0 °C under 1 atm of ethylene (previously saturated solution). After a desired time (typically between 10-30 min), freshly distilled MMA (9.0 mL, 90 mmol) was introduced rapidly (ca. 5 s) via syringe and the reaction mixture was stirred magnetically (1100 rpm) for 1 h at 0 °C. After addition of a 5% HCl methanol solution (200 mL), 4.8 g of crude polymer was obtained by filtration. Soxhlet extraction with boiling THF for 72 h led to the solubilization of only 15% of the crude material. Most of analytical data for the final copolymer are provided in Chapter 4 §20.2.1; ¹H NMR (400 MHz, C₂D₂Cl₄): δ (135 °C) = 3.72 (MMA, COCH₃), 1.96 (MMA, CH₂), 1.40 (ethylene, CH₂), 1.18-0.94 (MMA, CH₃). ¹³C NMR (100 MHz, C₂D₂Cl₄): δ (135 °C) = 16, 176.49, 176, 22, 54.05, 52.32, 51.22, 46.03, 45.54, 45.29, 29.60, 22.31, 19.56, 17.89. IR (KBr): ν = 1729, 1194 and 1148 cm⁻¹.

37.2. With the solid **S**

A typical experiment is as follows: Upon using a solution of **1** (0.37 g, 0.30 mmol) activated by Mg(*n*-hex)₂ (0.98 g, 1.0 mmol) in toluene (100 mL) for 1 h at 0 °C allowed to collect, after 10 min of reaction with 1 atm of ethylene at 0 °C, 3.3 g of **S** as a beige precipitate. The latter was filtered-off at 0 °C, washed twice with cold toluene (2 × 50 mL) and introduced into a Schlenk-tube with toluene (100 mL) at 0 °C. Freshly distilled MMA (9.0 mL, 90 mmol) was then introduced rapidly (ca. 5 s) via syringe and the reaction mixture was stirred magnetically (1100 rpm) for 1 h at 0 °C. After addition of a 5% HCl methanol solution (200 mL), 4.8 g of crude polymer was obtained by filtration. Soxhlet extraction with boiling THF for 72 h led to the solubilization of only 3% of the crude material.

38. Butadiene (co)-polymerization

38.1. Butadiene homo-polymerization

The initiator was prepared by reacting a neodymium alkoxide (**1**, **12**, **13**) and a dialkylmagnesium reagent (typically 1.0 mmol of each) in hexane or toluene for 1 h under magnetic stirring at 0 °C. The neodymium salt and dialkylmagnesium derivative were weighed in a glove box and placed in two separate Schlenk tubes. The latter were each filled in on the Schlenk line with hexane or toluene (12.5 mL) and the solutions were cooled to 0 °C; the neodymium solution was then transferred via canula onto the dialkylmagnesium solution and the mixture was stirred for 1 h. The catalytic solution was placed at -30 °C and butadiene (8.5 mL, 100 mmol) added via canula. Polymerization was carried out for 1 to 17 h under stirring at the desired temperature and then stopped by adding methanol (ca. 2 mL). The polymer was recovered by extraction with chloroform and dried at 60 °C until constant weight. ¹H NMR (200 MHz, CDCl₃): δ (23 °C) = 5.40 (1,4-PBD, =CH), 4.95 (1,2-PBD, =CH₂), 2.02 (1,4-PBD, CH₂), 1.51 (1,2-PBD, CH₂); ¹³C NMR (50 MHz, CDCl₃): δ (23 °C) = 151.49, 142.68, 137.80, 135.70, 131.24, 130.42, 129.99, 129.82, 129.41, 129.01, 128.33, 128.20, 125.49, 125.25, 114.23, 43.40, 38.09, 33.88, 32.66, 31.82, 30.05, 29.58, 29.14, 29.06, 27.35, 22.62, 17.86, 14.05.

38.2. Butadiene-styrene statistical copolymerization

The neodymium salt and dialkylmagnesium derivative were weighed in a glove box and placed in two separate Schlenk tubes. The latter were each filled in on the Schlenk line with styrene (6.0 mL, 50 mmol) and the solutions were cooled to -30 °C. The neodymium solution was transferred via canula onto the dialkylmagnesium solution and butadiene (typically 8.5 mL, 100 mmol) was added via canula. Polymerization was carried out for 1 to 17 h under magnetic stirring at the desired temperature and then stopped by adding methanol (ca. 2 mL). The polymer was recovered by extraction with chloroform and dried at 60 °C until constant weight. ¹H NMR (200 MHz, CDCl₃): δ (23 °C) = 7.4-6.9 (styrene, Ar), 5.40 (1,4-PBD, =CH), 4.95 (1,2-PBD, =CH₂), 2.02 (1,4-PBD, CH₂), 1.51 (1,2-PBD, CH₂); ¹³C NMR (50 MHz, CDCl₃): δ (23 °C) = homoPBD signals plus : 145.36, 136.80, 131.35, 130.70, 130.25, 128.45, 128.11, 127.95, 127.75, 126.17, 125.82, 133.73, 45.63, 42.69, 42.33, 40.07, 35.62, 34.20, 30.32, 21.19.

38.3. Butadiene-GMA diblock copolymerization

Butadiene homopolymerization was performed as described above. Before quenching, at a desired reaction time, the reaction mixture was vented, refilled with argon and cooled down at 0 °C. GMA (2.0 mL, 15 mmol) was added dropwise and the resulting solution was warmed up to room temperature for additional 2 h. The polymerization was quenched by addition of aqueous THF (1% water). Volatile solvents were removed under reduced pressure at room temperature and the resultant polymer was dissolved in dry THF, and then filtered over celite. Removal of the solvent yielded the block copolymer as a white powder. ¹H NMR (200 MHz,

CDCl_3): δ (23 °C) = 5.40 (1,4-PBD, $=\text{CH}$), 4.95 (1,2-PBD, $=\text{CH}_2$), 4.32 (PGMA, $\text{CH}_2\text{-O}$), 3.78 (PGMA, $\text{CH}_2\text{-O}$), 3.23 (PGMA, $\text{CH}\text{-CH}_2$), 2.84 (PGMA, $\text{CH}_2\text{-CH}$), 2.63 (PGMA, $\text{CH}_2\text{-CH}$), 2.02 (1,4-PBD, CH_2), 1.90 (PGMA, CH_2), 1.51 (1,2-PBD, CH_2), 1.26 (PGMA, CH_3), 1.10 (PGMA, CH_3), 0.92 (PGMA, CH_3). ^{13}C NMR (50 MHz, CDCl_3) restricted to 0-70 ppm: δ (23 °C) = homoPBD signals plus : 67.90, 65.88, 65.65, 54.27, 51.64, 49.08, 49.94, 48.76, 45.60, 45.09, 44.76, 44.53, 34.64, 34.17, 30.28, 25.55, 21.13, 19.61.

39. Mechanism section

39.1.NMR monitoring of 1/MgR₂ combinations

In a typical experiment, in a glove box, a Teflon valve NMR tube was charged with **1** (33.6 mg, 0.027 mmol), $\text{Mg}(n\text{-hex})_2\bullet 0.5(\text{heptane})$ (20.0 mg, 0.080 mmol) and 1,2,4,5-tetramethylbenzene (10.6 mg, 0.079 mmol; NMR internal standard). Toluene- d_8 was then vacuum transferred at -80 °C, the solution was made homogeneous at this temperature and the tube was introduced in the pre-cooled NMR probe. The progress of the reaction was monitored on 200 MHz spectrometer upon raising the temperature by 10 °C intervals. The formation of 1-hexene (δ ^1H = 4.98 (m, 2H), 5.72 (m, 1H); δ ^{13}C = 108.2, 132.9; confirmed by GC/MS) was observed from -30 °C and that of isobutene (δ ^1H = 4.70 (s); δ ^{13}C = 111.0, 141.7) from 0 °C. After 14 h at 20 °C, the amounts of 1-hexene and isobutene were 40 and 2%, respectively. Resonances for two new Nd species were observed at δ = 23.7 (relative intensity, 20), 18.5 (10), -5.0 (20), -8.2 (20), -11.1 (10), -69.8 (10) and δ = 25.7 (2), 19.9 (1), 15.6 (2), 11.3 (1), -6.8 (2), -12.3 (2); other resonances attributable to these species possibly overlapped with signals of diamagnetic species in the range of 4 to -1 ppm.

Reactions performed with other lanthanide alkoxides or alkylating reagents were conducted using a similar protocol.

39.2.Synthesis of active species or intermediates

39.2.1. $\text{Nd}(\mu_3\text{-}OtBu)_2(\mu_2\text{-}OtBu)_2(OtBu)\text{Mg}_2(\text{CH}_2\text{SiMe}_3)_2(\text{THF})$ (**14**)

In a glove box, **1** (124 mg, 0.10 mmol) was dissolved in a minimal amount of toluene (250 mg, 0.29 mL). To the resulting deep blue solution, methyl methacrylate (10 μL , 0.01 mmol), then $\text{Mg}(\text{CH}_2\text{SiMe}_3)_2\bullet \text{Et}_2\text{O}$ (84 mg, 0.33 mmol) were added at room temperature. The solution turned green after addition of the magnesium reagent and was immediately placed at -30 °C. After several days (typically 10 days), pale blue crystals of **14** were grown from the dark green solution (27 mg, 37 %), which proved suitable for X-ray analysis. ^1H NMR (200 MHz, C_6D_6): δ (23 °C) = 19.56 (s, 1H), 12.82 (brs, 0.6H), 10.40 (s, 2H), 1.37 (s, 2H), -15.87 (s, 0.4H), -30.11 (brs, 0.7H), -33.43 (brs, 0.4H); ^1H NMR (200 MHz, C_6D_6): δ (-35 °C) = 27.54 (s, 1H), 19.09 (s, 1H), 15.16 (s, 2H), 2.25 (s, 0.2H), 2.10 (s, 0.1 H), 1.69 (s, 1.5H), -24.53 (s, 0.4H), -44.86 (s, 1H), -51.62 (s, 0.4H); ^1H NMR (200 MHz, C_6D_6): δ (-80 °C) = 39.38 (s, 1H), 28.60 (s, 1H), 22.06 (s, 2H), 3.48 (s, 0.25H), 2.37 (s, 0.25H), 2.15 (s, 1.85H), -37.21 (s, 0.4H), -66.03 (s, 1H), -78.01 (s, 0.4H).

X-ray crystal structure determination of 14: A pale blue crystal of approximate dimensions $0.50 \times 0.20 \times 0.15$ mm was mounted on a glass fiber. X-ray measurements were made using a Bruker SMART CCD area-detector diffractometer with MoKa ($\lambda = 0.71073$ Å) at T = 100(2) K.

Crystal data: monoclinic C2: $a = 26.312(5)$, $b = 11.595(2)$, $c = 22.887(5)$ Å; $\alpha = 90.00$, $\beta = 109.127(3)$, $\gamma = 90.00^\circ$; $V = 6597(2)$ Å³; formula unit: C₃₂H₇₅O₆Mg₂Nd with Z = 6; formula weight: 729.36; calculated density = 1.102 g.cm⁻³; F(000) = 2112; $\mu(\text{MoK}\alpha) = 1.293$ mm⁻¹. 22487 reflections were collected ($2.27^\circ > \Theta > 25^\circ$). The structure was solved by direct methods. The molecule was located about an inversion center. Hydrogen atoms were located from a difference-Fourier map and refined (x, y, z and U_{iso}). Full-matrix least-squares refinement on F² based on 11197 independent reflections converged with 393 variable parameters and 1 restraint. R1 = 0.053 (for those 10265 data with I > 2σ(I)); wR2 = 0.1490; GoF (F²) = 1.071. Δρ_{max} = 1.78 and -0.966 e.Å⁻³.

39.2.2. [(Me₃SiCH₂)Mg(OtBu)(THF)] (15)

In a glove box, **1** (124 mg, 0.10 mmol) was dissolved in a minimal amount of toluene (250 mg; 0.29 mL). To the resulting deep blue solution, isoprene (10 μL, 0.01 mmol), then Mg(CH₂SiMe₃)₂•Et₂O (84 mg, 0.33 mmol) were added at room temperature. The solution turned green after addition of the magnesium reagent and was immediately placed at -30 °C. After several days (typically 10 days), pale blue crystals of **15** were grown from the dark green solution (27 mg, 37 %). ¹H NMR (200 MHz, C₆D₆): δ (23 °C) = 3.68 (t, 4H, THF), 1.29 (s, 9H, tBu), 1.24 (t, 4H, THF), 0.41 (s, 9H, SiMe₃), -1.33 (s, 2H, CH₂). ¹³C NMR (50 MHz, C₆D₆): δ (23 °C) = 69.74 (CH₂-O, THF), 67.85 (C_q, tBu), 35.32 (CH₃, tBu), 25.51 (CH₂, THF), 5.60 (Si(CH₃)), -5.98 (CH₂-Mg).

39.2.3. [(n-hex)Mg(O-2,6-tBu₂-4-Me-C₆H₂)]₂ (16)

In the glove box, a solution of **12** (0.42 g, 0.52 mmol) in a minimum of toluene was added to a solution of dry Mg(n-hex)₂ (1.01 g, 0.52 mmol) in toluene. The mixture was allowed to stand at -40 °C for three days, resulting in the formation of colourless crystals of **16** that were separated out from the supernatant solution (0.227 g, 90 %). ¹H NMR (300 MHz, C₆D₆): δ (23 °C) = 0.04 (dd, $J \sim 8$ Hz, 2H, CH₂Mg), 0.85 (t, $J = 7.0$ Hz, 3H, CH₃ hex), 1.24 (m, 6H, CH₂CH₂CH₂), 1.54 (s, 6H; tBu), 1.63 (m, 2H; CH₂), 2.25 (s, 3H; CH₃ Ar), 7.15 (s, 2H; H_{aro}). ¹³C NMR (75 MHz, C₆D₆): δ (23 °C) = 7.6, 14.6, 21.4, 23.3, 29.1, 32.5, 32.9 (CMe₃), 35.1, 38.2, 127.1, 129.0, 139.4, 154.3. Elemental analysis calculated (%) for C₄₂H₇₂O₂Mg₂ (657.62): C 76.71, H 11.04; found C 76.9, H 10.91.

X-ray crystal structure determination of 16: A colorless crystal of approximate dimensions $0.29 \times 0.32 \times 0.46$ mm was mounted on a glass fiber. X-ray measurements were made using a Bruker SMART CCD area-detector diffractometer with MoKa ($\lambda = 0.71073$ Å) at T = 163(2) K.

Crystal data: triclinic P : $a = 9.3991(4)$, $b = 9.8064(4)$, $c = 11.5627(5)$ Å; $\alpha = 92.2830(10)$, $\beta = 106.1100(10)$, $\gamma = 97.9190(10)^\circ$; $V = 1010.72(7)$ Å³; formula unit: C₄₂H₇₂O₂Mg₂ with $Z = 1$; formula weight: 657.62; calculated density = 1.080 g.cm⁻³; $F(000) = 364$; $\mu(\text{MoK}\alpha) = 0.091$ mm⁻¹. 10924 reflections were collected ($1.84^\circ > \Theta > 28.29^\circ$). The structure was solved by direct methods.³³⁵ The molecule was located about an inversion center. Hydrogen atoms were located from a difference-Fourier map and refined (x, y, z and U_{iso}). Full-matrix least-squares refinement on F^2 based on 4783 independent reflections converged with 352 variable parameters and no restraints. $R1 = 0.0381$ (for those 3952 data with $I > 2\sigma(I)$); $wR2 = 0.1006$; GoF (F^2) = 1.027.336 $\Delta\rho_{\max} = 0.365$ and -0.189 e.Å⁻³.

39.2.4. Nd(O-2,6-tBu₂-4-Me-Ph)₂(CH₂SiMe₃)(THF)₂ (17)

In a glove box, Nd(O-2,6-tBu₂-4-Me-Ph)₃THF (87.4 mg, 0.1 mmol) was dissolved in a mixture of toluene (140 mg, 0.16 mL) and THF (50 mg, 0.55 mL, 0.70 mmol). To the resulting violet solution, Mg(CH₂SiMe₃)₂•Et₂O (27.2 mg, 0.1 mmol) was added at room temperature and the mixture was immediately placed at -30 °C. After few days, colorless crystals* were removed from the solution and blue crystals suitable for X-ray analysis were obtained from the blue solution after a month (25.2 mg, 34%). ¹H NMR (200 MHz, C₆D₆): δ (23 °C) = 21.36 (s, 2H, Ar), 10.47 (s, 3H, Me), 7.99 (brs, 18H, tBu), -1.25 (s, 2H, CH₂), -6.90 (brs, THF), -7.15 (s, SiMe₃), -9.66 (brs, THF)

X-ray crystal structure determination of 17: A pale blue crystal of approximate dimensions 0.45 × 0.25 × 0.12 mm was mounted on a glass fiber. X-ray measurements were made using a Bruker SMART CCD area-detector diffractometer with MoK α ($\lambda = 0.71073$ Å) at T = 100(2) K.

Crystal data: orthorhombic $Pca2$: $a = 23.732(5)$, $b = 9.799(2)$, $c = 18.902(4)$ Å; $\alpha = 90.00$, $\beta = 90.00$, $\gamma = 90.00^\circ$; $V = 4395.7(16)$ Å³; formula unit: C₄₂H₇₃O₄Si₂Nd with $Z = 4$; formula weight: 740.75; calculated density = 1.119 g.cm⁻³; $F(000) = 1432$; $\mu(\text{MoK}\alpha) = 1.240$ mm⁻¹. 30722 reflections were collected ($2.15^\circ > \Theta > 28.04^\circ$). The structure was solved by direct methods.^[66] The molecule was located about an inversion center. Hydrogen atoms were located from a difference-Fourier map and refined (x, y, z and U_{iso}). Full-matrix least-squares refinement on F^2 based on 9437 independent reflections converged with 433 variable parameters and one restraint. $R1 = 0.0436$ (for those 7321 data with $I > 2\sigma(I)$); $wR2 = 0.1163$; GoF (F^2) = 1.049.^[67] $\Delta\rho_{\max} = 1.903$ and -0.799 e.Å⁻³.

39.2.5. [(Me₃SiCH₂)Mg(O-2,6-tBu₂-4-Me-Ph)]₂ (18)

This compound was obtained as colorless crystals from a Nd(O-2,6-tBu₂-4-Me-Ph)₃THF/Mg(CH₂SiMe₃)₂•Et₂O mixture in toluene/THF (see §39.2.4). (13 mg, 39%) These crystals were analyzed by NMR spectroscopy. ¹H NMR (200 MHz, C₆D₆): δ (23 °C) = 7.19 (s, 2H, Ar), 2.29 (s, 3H, Me), 1.59 (s, 18H, tBu), 0.06 (s, 9H, SiMe₃), -1.16 (s, 2H, CH₂). ¹³C NMR (50 MHz, C₆D₆): δ (23 °C) = 159.46 (C_{Ar}), 139.83 (C_{Ar}), 128.91 (C_{Ar}), 127.60 (C_{Ar}), 35.70 (C_q, tBu), 33.96 (CH₃, tBu), 21.89 (CH₃), 4.13 (Si(CH₃)), -6.23 (CH₂-Mg).

* Crystals characterized by NMR as [(Me₃SiCH₂)Mg(O-2,6-tBu₂-4-Me-Ph)]₂ (18).

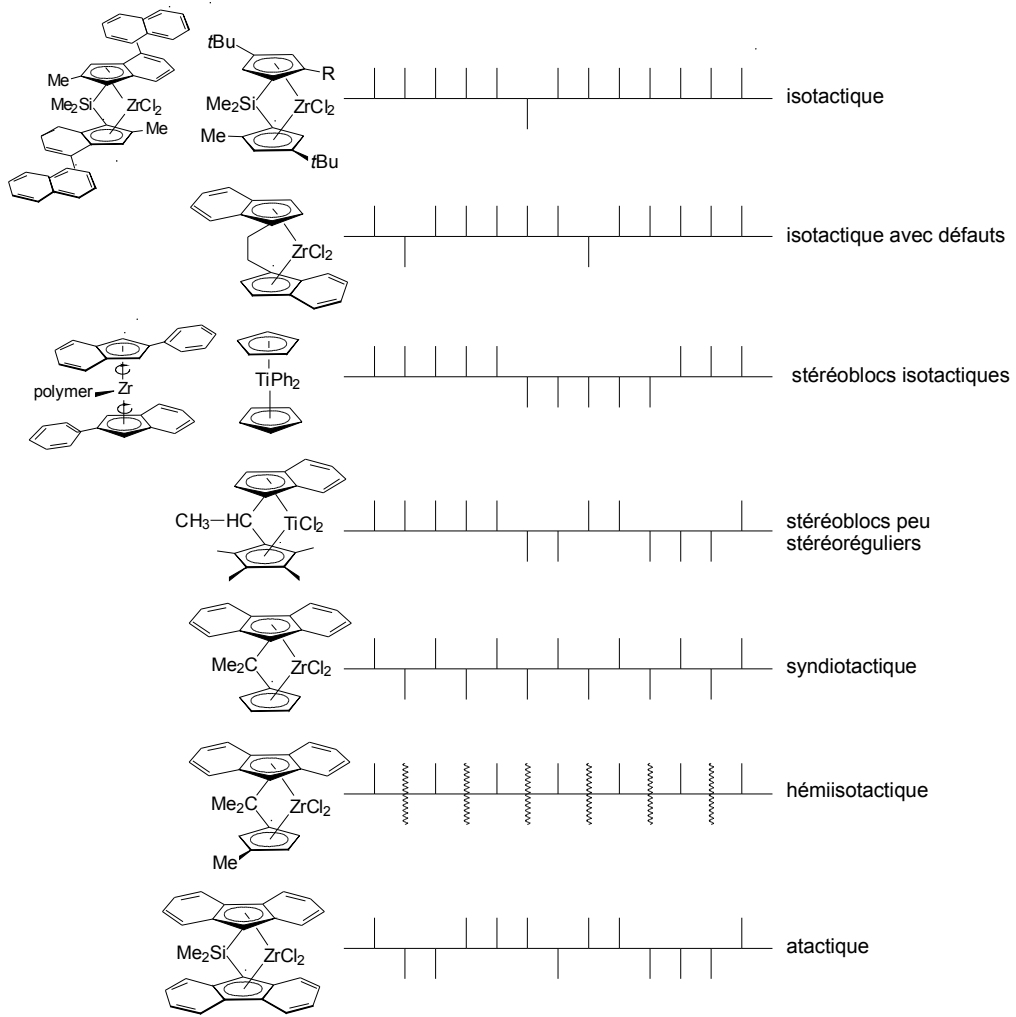
French summary

1. Introduction

La découverte de la catalyse de polymérisation par les métaux de transition par Karl Ziegler dans les années 50,¹⁰ a sans nul doute été le véritable point de départ du développement des polyoléfines. Ces systèmes catalytiques initialement composés du couple $\text{TiCl}_4/\text{AlR}_3$ sont maintenant, à l'échelle industrielle, composés d'un halogénure de titane supporté sur chlorure de magnésium, d'un activateur (dérivé organoaluminique) et d'un additif (diéther, alkoxy silane).^{13,15} Ils permettent de hautes activités catalytiques ($\geq 10^5 \text{ kg/molTi}$) et une importante isospécificité en polymérisation du propylène. Ils sont responsables de 97% de la production mondiale de polyoléfines qui s'élève aujourd'hui à environ 80 millions de tonnes par an. Le reste de la production est obtenu par le biais de catalyseurs homogènes communément appelés métallocènes.

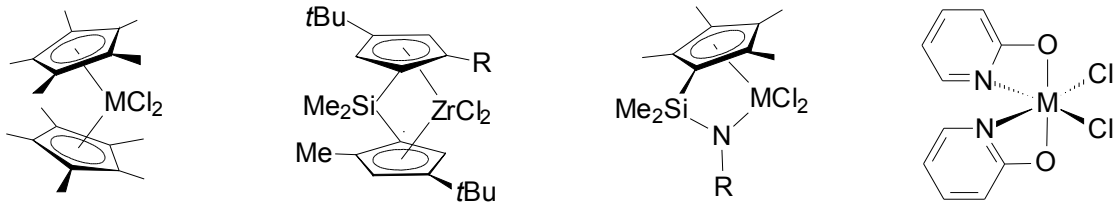
Ces systèmes homogènes ont à l'origine été synthétisés afin d'étudier le mécanisme de polymérisation des oléfines.¹⁷ Mais c'est grâce à l'utilisation du méthylaluminoxane (MAO) que ces catalyseurs homogènes ont réellement été utilisés pour la synthèse de polyoléfines.¹⁹ En effet, cet activateur a rendu ces catalyseurs très productifs (jusqu'à 10^6 kg/molTi) et pour la première fois il était possible d'établir une corrélation directe entre la structure du catalyseur, son activité et la microstructure du polymère formé (Figure 1).²⁸

Figure 1. Corrélation entre la microstructure du polypropylène et la structure du catalyseur.



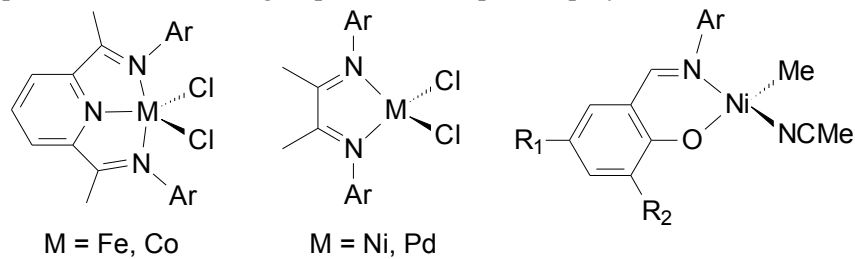
Ainsi, la recherche de nouveaux catalyseurs homogènes toujours plus actifs, plus stéréosélectifs et stéréospécifiques a été et reste l'objet de nombreuses études, permettant la préparation de nombreux (co)-polymères jusque-là inaccessibles. Ces catalyseurs homogènes peuvent être classés en fonction de la nature de leur(s) ligand(s). Ils peuvent être métallocéniques,²⁴ *ansa*-métallocéniques,²⁴ à géométrie contrainte²⁷ ou post-métallocéniques²⁹ comme le montre la Figure 2.

Figure 2. Evolution de la structure des ligands des complexes de métaux du groupe 4 ($M = Ti, Zr$).



Plus récemment, la catalyse de polymérisation a été étudiée avec les métaux des groupes 5 à 10.²⁹ Les métaux de fin de transition ont particulièrement attiré l'attention étant donné leurs bonnes activités catalytiques³⁸ et la possibilité de copolymériser des monomères polaires et apolaires (Figure 3).³⁹ En effet, la synthèse de tels copolymères diblocs suscite un vif intérêt puisqu'elle conduit à des matériaux possédant de nouvelles structures et propriétés.⁴ Dans ce domaine, les catalyseurs lanthanocéniques se sont révélés jusqu'à présent les plus efficaces,⁵ même si certains complexes à base de métaux du groupe 4 semblent prometteurs.

Figure 3. Complexes de métaux des groupes 8, 9 et 10 pour la polymérisation d'oléfines.³⁷⁻³⁹



Dans ce contexte, nous nous sommes focalisés sur l'utilisation de systèmes à base de lanthanide pour la catalyse de polymérisation d'oléfines et leur copolymérisation avec des monomères polaires. En premier lieu, nous montrerons l'énorme potentiel des complexes de lanthanide pour la polymérisation de l'éthylène, du méthacrylate de méthyle (MAM) et du butadiène (BD). Ensuite, nous présenterons la synthèse et la caractérisation de nouveaux alcoolates de néodyme, suivies de leur application en polymérisation lorsqu'ils sont associés à un dialkylmagnésien. Enfin, nous terminerons cette étude par quelques considérations mécanistiques.

40. Systèmes catalytiques à base de métaux du groupe 3

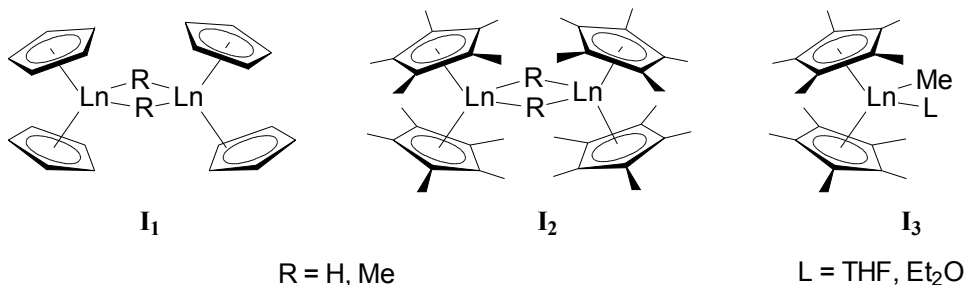
Malgré toutes les recherches menées en catalyse de polymérisation, les métaux du groupe 3 restent à ce jour une partie de la classification périodique encore relativement peu explorée. Comme pour les métaux du groupe 4, les ligands de type cyclopentadiènyle ont été largement utilisés, puis une évolution vers des ligands de types "ansa" et à géométrie contrainte a été observée, suivie du développement des complexes post-lanthanocéniques (*vide infra*). Nous allons maintenant étudier cette évolution dans le cas des complexes trivalents de lanthanide ainsi que leur application en polymérisation des α -oléfines non fonctionnalisées et du MAM. Le cas particulier de la polymérisation des diènes sera ensuite discuté.

40.1. Polymérisation des α -oléfines non fonctionnalisées

40.1.1. Catalyseurs lanthanocéniques

Les complexes trivalents de type $[Cp^{(*)}_2Ln^{(III)}R]_n$ ($\eta^5\text{-C}_5\text{H}_5 = Cp$; $\eta^5\text{-C}_5\text{Me}_5 = Cp^*$; $n = 1$ ou 2 ; $M = \text{Sc, Y, Ln}$ et $R = \text{H ou un groupe alkyle}$) sont des complexes isoélectroniques des composés alkyl-cationiques des métaux du groupe 4 ($[\text{LnMR}]^+$ avec $M = \text{Ti, Zr, Hf}$) (Figure 4) ce qui leur confère intrinsèquement une haute réactivité envers les oléfines en absence d'activateur tels que les tris(alkyl)aluminums ou le MAO.

Figure 4. Complexes lanthanocéniques pour la polymérisation des α -oléfines.

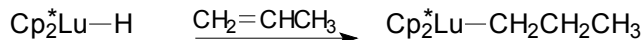
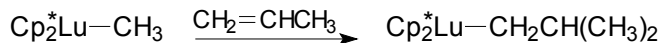


L'utilisation de catalyseurs de type " Cp_2LnR " pour la polymérisation de l'éthylène a montré que les divers substituants portés par les ligands cyclopentadiényles influençaient l'activité de polymérisation (10-100 kgPE/molLn/atm/h). Plus l'encombrement stérique est élevé, plus l'activité est élevée et plus les masses molaires des polymères obtenus sont basses.⁴¹

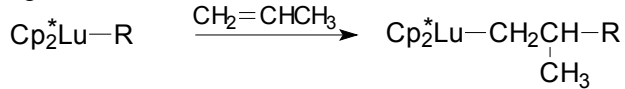
Ces catalyseurs se sont révélés très peu actifs en polymérisation du propylène, conduisant uniquement à la formation d'oligomères. Une étude spectroscopique de l'insertion du propylène dans un complexe du lutétium ($(Cp_2^*\text{LuMe})_2$) a permis de mettre en évidence la régiospécificité de l'insertion ainsi que la nature des réactions de transfert et de terminaison.⁴² La réaction de terminaison par abstraction d'hydrogène allylique, menant à la formation d'un complexe π -allyle très stable, est considérée comme la cause principale de la faible réactivité observée. Cette hypothèse a été corroborée par de récents résultats obtenus par modélisation moléculaire⁴⁵ mais aussi par une étude RMN utilisant un complexe de scandium.⁴⁸

Schéma 1. Principales étapes lors de la polymérisation du propène avec $(Cp_2^*LuMe)_2$.⁴³

Amorçage



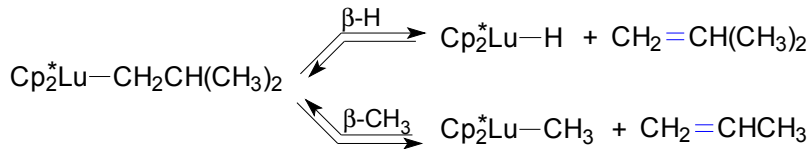
Propagation



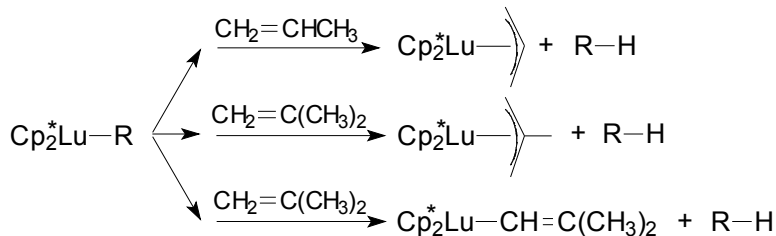
Réaction de terminaison et de transfert



Réactions de terminaison et de transfert par élimination d'oléfine



Terminaison par activation C-H



La réactivité de ces complexes lanthanocéniques et particulièrement ceux à base de néodyme a été étudiée par Marks.⁴⁹ Il a montré que la nature du groupe alkyle influençait l'activité de polymérisation. En effet, le complexe $Cp_2^*NdCH(TMS)_2$ ne réagit pas avec l'éthylène alors que le complexe correspondant obtenu après hydrogénolyse, $(Cp_2^*NdH)_2$, permet de polymériser l'éthylène avec une très grande efficacité. Toutefois, cette activité n'est observée que pendant une très courte période et l'efficacité d'amorçage reste modeste. Une absence de réaction de transfert par β -H élimination et une distribution des masses molaires relativement faible ($M_w/M_n \approx 2$) prouvent le caractère pseudo-vivant de la polymérisation et l'existence d'un seul type de site actif (Tableau 1).

Tableau 1. Polymérisations de l'éthylène catalysées par $(Cp^*_2NdH)_2$.⁴⁹

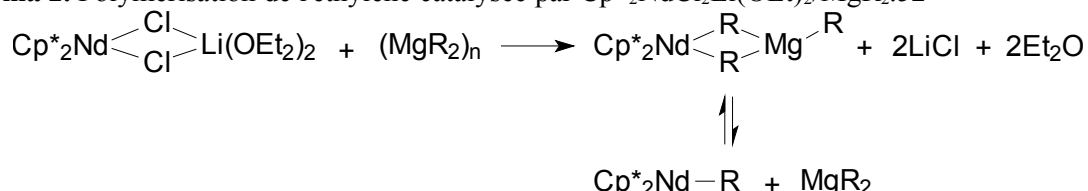
concн (μM)	temps (s)	activité (kg/molNd/atm/h)	$10^{-3} M_n$	M_w/M_n	chaînes/Nd
22	5	$1,37 \times 10^5$	590	1,81	0,32
60	10	$3,84 \times 10^4$	233	4,46	0,46
22*	600	$5,22 \times 10^2$	648	1,95	0,13

Réactions effectuées dans 140 mL de cyclohexane à 25 °C sous 1 bar d'éthylène excepté * à -78 °C.

40.1.2. Systèmes lanthanocéniques binaires

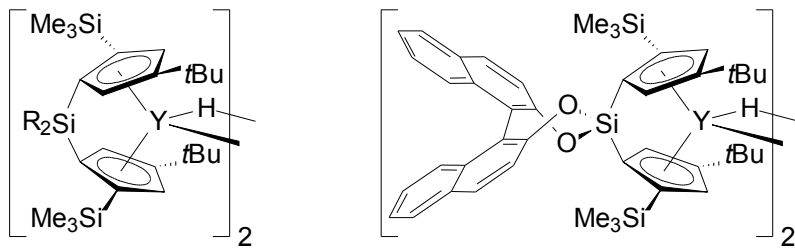
Cependant, ces systèmes lanthanocéniques présentent le désavantage d'être très sensibles à l'eau, à l'oxygène et à la chaleur. Leur synthèse s'avère de plus souvent longue et fastidieuse. De fait, l'utilisation de précurseurs chlorolanthanocéniques a été explorée pour contourner ce problème. Combiné à un dialkylmagnésien, le complexe $Cp^*_2NdCl_2Li(OEt)_2$ permet la formation *in situ* d'espèces alkyl-lanthanide et conduit à une polymérisation stable de l'éthylène. Des réactions de transfert au magnésium engendrent la formation de dialkylmagnésiens à longues chaînes avec une distribution des masses molaires relativement étroite.⁵² Il est intéressant de noter que les dérivés aluminiques ne permettent pas d'activer correctement $Cp^*_2NdCl_2Li(OEt)_2$ alors qu'ils ont été utilisés avec succès pour la (co)-polymérisation de l'éthylène avec $(\eta^5-tBuC_5H_4)_2Nd(\mu-Cl)_2Li(OEt_2)_2$.⁵⁴

Schéma 2. Polymérisation de l'éthylène catalysée par $Cp^*_2NdCl_2Li(OEt)_2/MgR_2$.⁵²

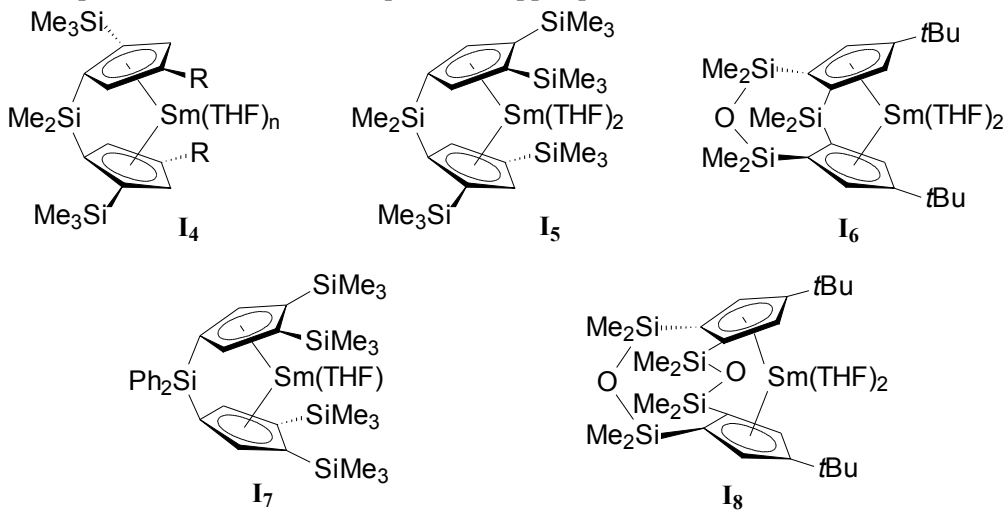


40.1.3. Catalyseurs ansa-lanthanocéniques et à géométrie contrainte

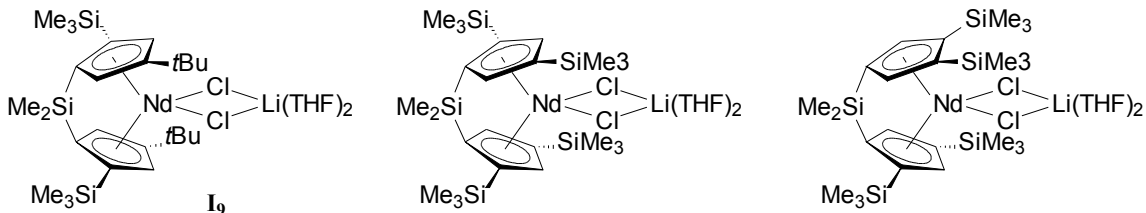
Afin de trouver de nouveaux catalyseurs efficaces pour la polymérisation du propylène, la structure des ligands a été modifiée, l'évolution étant comparable à celle notée avec les métaux du groupe 4. La structure du ligand régie incontestablement l'activité catalytique, la stéréospécificité et la possibilité de polymériser certains monomères. Par exemple, $[\text{Me}_2\text{Si}(\eta^5-\text{C}_5\text{Me}_4)_2\text{LnH}]_2$ ($\text{Ln} = \text{Nd}, \text{Sm}, \text{Lu}$) ne permet que l'oligomérisation du propène et la dimérisation de l'hexène⁵⁷ alors que $[\text{Me}_2\text{Si}(2-\text{SiMe}_3-4-t\text{BuC}_5\text{H}_2)_2\text{YH}]_2$ donne lieu à une polymérisation hautement stéréospécifique du pentène.⁵⁸ Toutefois les masses molaires restent modestes. L'obtention de hautes masses a été possible grâce au remplacement du pont SiMe_2 par un pont binaphtoxysilyle (Figure 5).⁵⁹

Figure 5. Exemples de complexes *ansa*-lanthanocéniques pour la polymérisation d' α -oléfines.⁵⁸⁻⁵⁹

D'autres complexes ont été développés par l'équipe de Yasuda.⁶⁰ Ils ont montré que l'activité dépendait de plusieurs paramètres dont la nature du métal, l'encombrement stérique du ligand ainsi que le nombre de molécules de solvant coordonnées. Ainsi, l'activité décroît dans l'ordre: **I₆** > **I₄** > **I₇** > **I₅** > **I₈** (Figure 6).

Figure 6. Complexes *ansa*-lanthanocéniques développés par Yasuda *et al.*⁶⁰

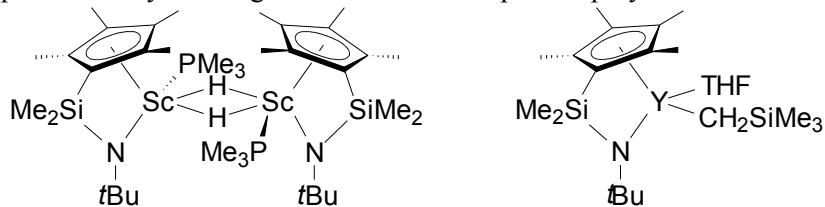
Tout comme pour les ligands Cp non pontés, des précurseurs *ansa*-chlorolanthanocènes ont été synthétisés et évalués en polymérisation de l'octène (Figure 7).⁶¹ Cependant, seule une oligomérisation de l'octène a été observée.

Figure 7. *Ansa*-chlorolanthanocènes utilisés pour l'oligomérisation de l'octène.⁶¹

Parallèlement aux complexes *ansa*-lanthanocènes, la voie des complexes à géométrie contrainte a été explorée. Le précatalyseur amido-monocyclopentadiényle de scandium décrit par Bercaw conduit à des polymérisations non stéréospécifiques et avec une faible activité.⁶³

Les complexes à base d'yttrium, $[Y(\eta^5:\eta^1\text{-C}_5\text{Me}_4\text{SiMe}_2\text{NCMe}_3)(\text{THF})(\mu\text{-H})]_2$ et $[Y(\eta^5:\eta^1\text{-C}_5\text{Me}_4\text{SiMe}_2\text{NCMe}_3)(\text{CH}_2\text{SiMe}_3)(\text{THF})]$ se sont révélés prometteurs pour la polymérisation des monomères polaires (acrylate de tertiobutyle et acrylonitrile) et non polaires (éthylène) (Figure 8).⁶⁴

Figure 8. Exemples de catalyseurs à géométrie contrainte pour la polymérisation de l'éthylène.^{63,64}



40.1.4. Réactions de transfert

Outre les réactions de transfert habituellement non sélectives rencontrées lors de la polymérisation des α -oléfines (H_2 , β -H/alkyl élimination, transfert au monomère, transfert au cocatalyseur), deux agents de transfert spécifiques ont été développés. Le premier, PhSiH_3 , réagit suivant une réaction de métathèse Si-H/Ln-C et génère des chaînes de polymère terminées par le groupement SiH_2Ph .⁶⁹ Le second, $\text{C}_4\text{H}_4\text{S}$, est efficace grâce à l'activation de la liaison C-H du thiophène.⁷²

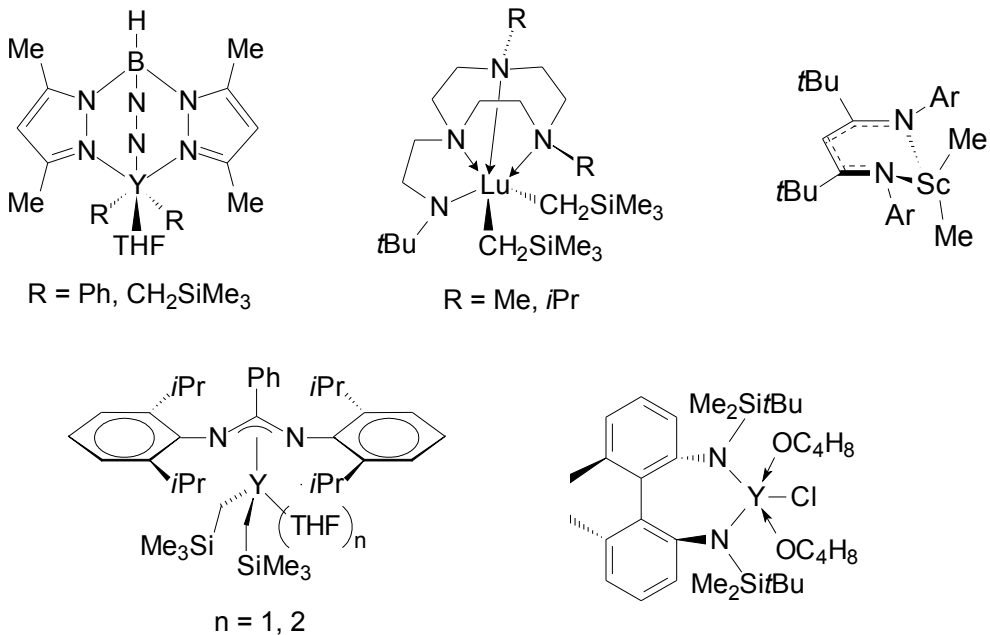
40.1.5. Catalyseurs post-lanthanocéniques

Ces catalyseurs, non porteurs de ligands de type Cp, ont vu le jour assez tardivement et font suite aux difficultés rencontrées lors de la synthèse des catalyseurs lanthanocéniques, mais aussi en raison des faibles activités/stéréospécificités obtenues jusque-là lors de la polymérisation des α -oléfines. Parmi ces nouveaux complexes, on retrouve des ligands de type alcoolate/phénate,⁷³ polypyrazolylborate,⁷⁶ amidure,⁷⁷ phosphine,⁷⁸ benzamidinate,⁸¹... Cette liste n'est en aucun cas exhaustive. Malgré le nombre impressionnant de complexes qui ont été décrits, seuls quelques uns ont montré une réelle activité en polymérisation. A ce jour, les résultats demeurent toutefois en deçà de ceux obtenus avec les complexes lanthanocéniques présentés précédemment. Parmi ces complexes, on peut distinguer ceux porteurs de ligands azotés et ceux porteurs de ligands oxygénés.

40.1.5.1. Complexes porteurs de ligands azotés

Les activités rencontrées en polymérisation de l'éthylène avec ces complexes sont généralement modestes (1-4 kgPE/molLn/atm/h)^{85,88,92} et seule l'oligomérisation des α -oléfines est possible.⁸⁸ Toutefois, de récents résultats obtenus avec des complexes cationiques semblent beaucoup plus encourageants.⁹⁰

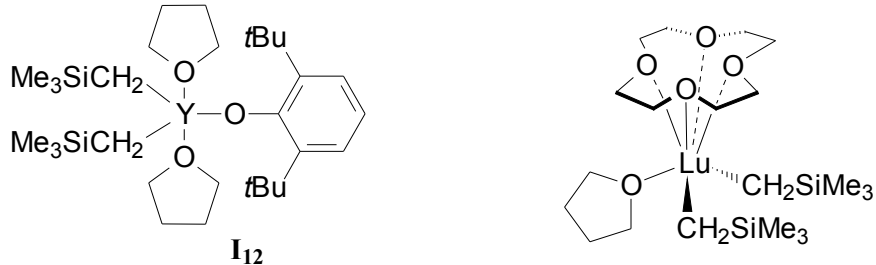
Figure 9. Complexes post-lanthocéniques porteurs de ligands azotés pour la polymérisation de l'éthylène.^{85,88,89,90,92}



40.1.5.2. Complexes porteurs de ligands oxygénés

Ces complexes sont très intéressants puisque les ligands oxygénés devraient théoriquement offrir une meilleure stabilisation du complexe grâce aux fortes liaisons Ln-O. Pourtant, parmi la dizaine de complexes alkyl-Ln bien définis et porteurs de ligands oxygénés, seul $[\text{Y}\{\text{CH}(\text{SiMe}_3)_2\}_2(\text{O}-2,6-t\text{Bu}_2\text{C}_6\text{H}_3)(\text{THF})_2]$ a montré une activité en polymérisation de l'éthylène, bien que très faible (0,009 kgPE/molY/atm/h).⁹⁵ Comme il l'a été remarqué avec les ligands azotés, une meilleure activité est obtenue avec les complexes cationiques.⁹⁶ Les systèmes binaires composés d'un complexe de lanthanide porteur d'un ligand calix[n]arène et d'un dérivé aluminique donnent également des résultats encourageants (activité = 56 kgPE/molLn/h).⁹⁷

Figure 10. Complexes porteurs de ligands oxygénés pour la polymérisation de l'éthylène.^{95,96}



40.2. Polymérisation du méthacrylate de méthyle

En dépit des innombrables progrès réalisés en polymérisation anionique⁹⁹ et radicalaire,¹¹² la recherche de nouveaux systèmes d'amorçage de polymérisation du MAM est

toujours d'actualité. Cette recherche se concentre maintenant sur de nouveaux systèmes permettant un contrôle accru de la polymérisation (contrôle des masses molaires et de leur distribution) avec une stéréospécificité encore améliorée, un PMAM syndiotactique de haute masse molaire étant la cible. Dans ce domaine, les complexes de lanthanide se sont révélés particulièrement efficaces.

40.2.1. Complexes lanthanocéniques

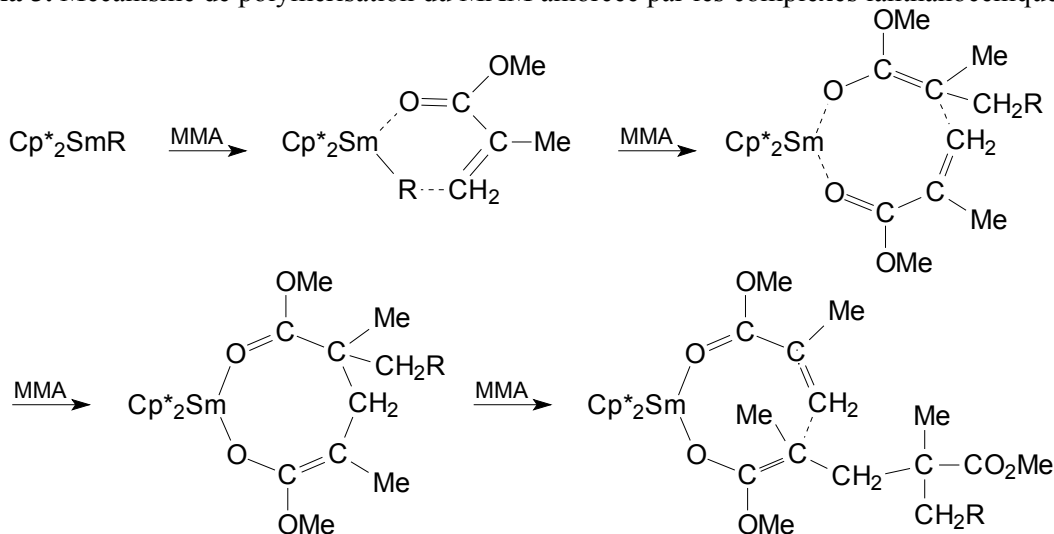
Les premiers résultats obtenus avec les complexes lanthanocéniques au début des années 80 par Yasuda et ses collaborateurs demeurent la référence en la matière.¹¹⁶⁻¹¹⁷ En effet, ces composés conduisent à la formation de PMAM hautement syndiotactique ($77\% < rr < 93\%$), de haute masse molaire ($M_n > 100\,000$) et de faible polymolécularité ($M_w/M_n = 1,05-1,10$) (Tableau 2).

Tableau 2. Polymérisation du MAM amorcée par $[\text{Cp}^*_2\text{SmH}]_2$.¹¹⁶

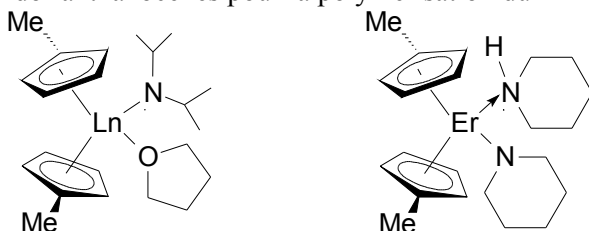
température. (°C)	MAM/amorceur (mol/mol)	$10^{-3} M_n$	M_w/M_n	rr (%)	conversion (%) (temps de réaction, h)
40	500	55	1,03	77,3	99 (1)
25	500	57	1,02	79,9	99 (1)
0	500	58	1,02	82,4	99 (1)
0	1500	215	1,03	82,6	93 (2)
-78	500	82	1,04	93,1	97 (17)

^a Conditions : solvant, toluène; solvant/[M₀] = 10 vol/vol.

Le caractère vivant de la polymérisation a été étudié par addition séquentielle de monomère, et il a été montré que 60% des chaînes étaient encore vivantes après 10 h à 0 °C. Le suivi de réactions de deutéroylse ainsi que la caractérisation d'un adduit entre le complexe amorceur et 2 molécules de MAM ont permis d'élucider le mécanisme de polymérisation. Il a ainsi été prouvé que le mécanisme est de type coordinatif-anionique, dans lequel c'est une espèce énolate qui est l'espèce active (Schéma 3). L'évolution vers des complexes cyclopentadiényles substitués par des groupements triméthylsilyles n'a pas permis d'améliorer les résultats acquis avec les Cp non substitués.¹²⁴

Schéma 3. Mécanisme de polymérisation du MAM amorcée par les complexes lanthanocéniques.¹¹⁶

Contrairement à l'éthylène, la polymérisation du MAM peut également être amorcée par un complexe ne possédant pas de liaison Ln-C. Ainsi, des complexes amido-lanthanocènes se sont montrés très réactifs vis-à-vis du MAM.¹²⁵

Figure 11. Complexes amido-lanthanocènes pour la polymérisation du MAM.¹²⁵

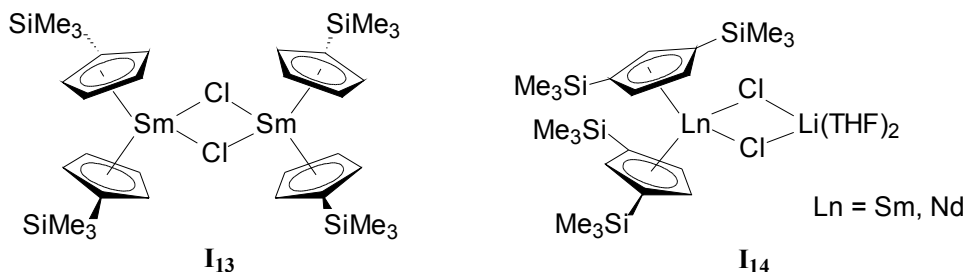
Enfin, il faut signaler que les réactions de polymérisation du MAM peuvent être menées en présence d'un agent de transfert choisi parmi la méthylisobutylcétone, l'acétophénone et le tertiobutylthiol.^{142,143} Dans ces conditions, la quantité d'amorceur organométallique peut être réduite et une diminution de la coloration du PMAM fondu (due aux résidus catalytiques) est observée.

40.2.2. Systèmes lanthanocéniques binaires

Alors que les meilleurs résultats en polymérisation de l'éthylène sont obtenus avec un dialkylmagnésien comme agent alkylant, c'est le *n*-butyllithium qui s'avère le plus efficace pour la polymérisation du MAM lorsqu'il est combiné au précurseur chloré $\text{Cp}^*_2\text{NdCl}_2\text{Li(OEt)}_2$.¹³⁹ Toutefois, les résultats sont décevants par rapport à ceux obtenus avec les complexes alkyl-lanthanocéniques bien définis. La syndiotacticité est certes élevée ($\text{rr} = 86\%$), mais le contrôle de la polymérisation reste faible ($M_w/M_n = 1,75$). Cependant, le contrôle peut être

amélioré en utilisant des complexes chlorolanthanocènes substitués; dans ce cas, la distribution des masses molaires peut être inférieure à 1,35.124

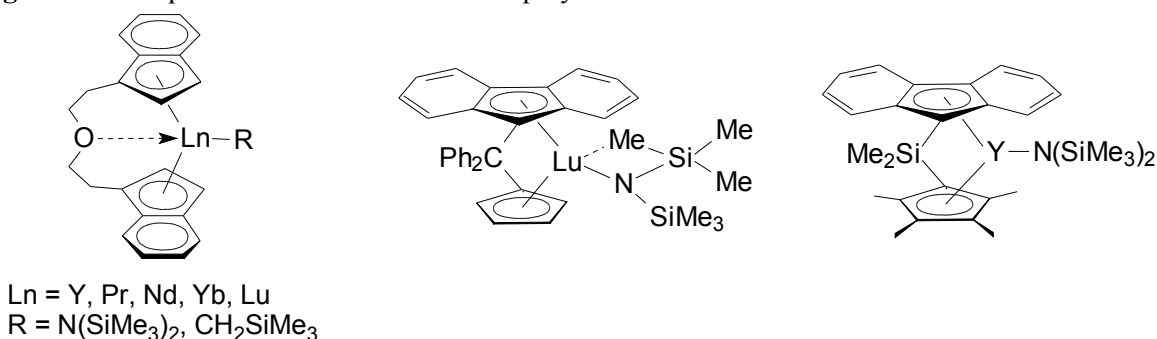
Figure 12. Complexes chlorolanthanocéniques en polymérisation du MAM.124



40.2.3. Complexes *ansa*-lanthanocéniques

De nombreux exemples de complexes *ansa*-lanthanocéniques ont été publiés. Principalement basés sur des ligands de type indényle¹²⁷ ou fluorényle,^{128,130} ces complexes se sont révélés moins actifs et moins stéréospécifiques que les systèmes initiaux de Yasuda. En effet, les polymérisations ne sont pas quantitatives, la syndiotacticité ne dépasse pas les 70% et les masses molaires ainsi que leur distribution ne sont pas contrôlées.

Figure 13. Complexes *ansa*-lanthanocènes en polymérisation du MAM.127^{128,130}

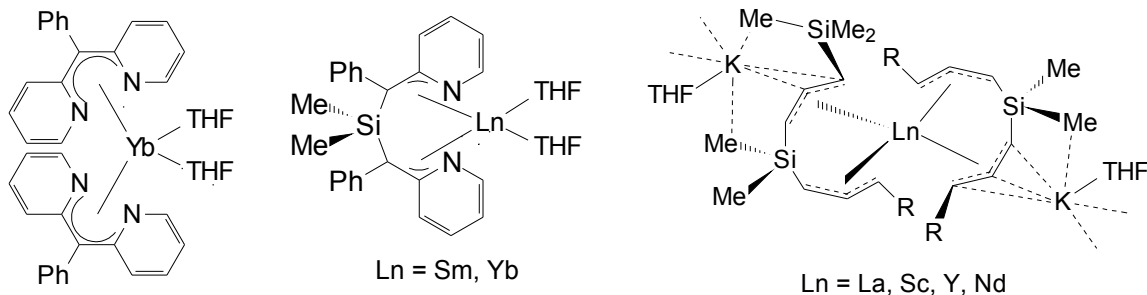


40.2.4. Amorceurs post-lanthanocéniques

Parmi les différents types de complexes post-lanthanocéniques, nous avons choisi de ne développer que ceux permettant une polymérisation contrôlée et/ou stéréospécifique.

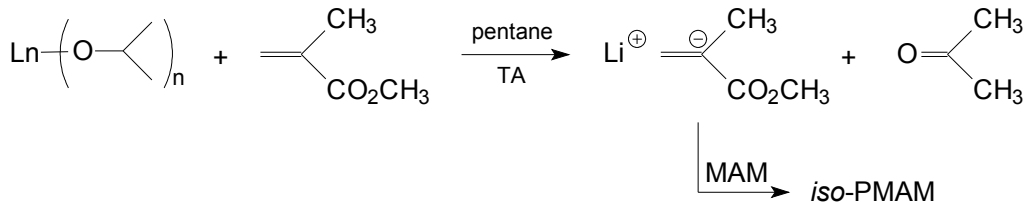
40.2.4.1. Complexes allyliques

Les résultats obtenus avec cette famille de complexes sont variables. Une polymérisation non contrôlée est observée avec le complexe bis(allyl)samarium décrit par Ihara.¹⁴⁴ Par contre, les nouveaux complexes ioniques synthétisés par Bochman *et al.* montrent une très grande activité ($> 80\,000 \text{ molMAM/molLn/h}$) et un certain contrôle de la polymérisation ($M_w/M_n < 1,5$), le PMAM obtenu étant atactique.¹⁴⁵

Figure 14. Complexes allyliques en polymérisation du MAM.^{144,145}

40.2.4.2. Alcoolates de lanthanide

Parmi les alcoolates de lanthanide, seul l'isopropylate permet d'amorcer la polymérisation du MAM.¹⁵⁴ Un mécanisme de réduction de type Meerwein-Ponndorf-Verley a été mis en évidence grâce à une étude en MALDI-TOF des différents produits formés lors de l'oligomérisation du MAM. Cet amorceur de polymérisation conduit à un PMAM isotactique ($mm = 80\%$).

Schéma 4. Polymérisation du MAM amorçée par "Ln(O*i*Pr)₃".¹⁵⁴

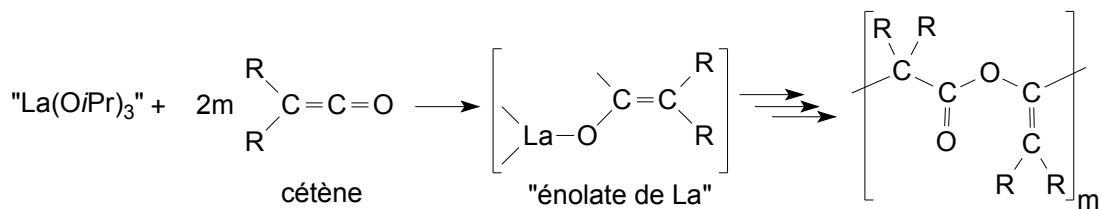
40.2.4.3. Thiolates de lanthanide

L'utilisation d'arènethiolates de lanthanide s'est montrée particulièrement efficace en polymérisation du MAM.¹⁵⁶ Un PMAM syndiotactique ($rr = 82\%$) et de plutôt faible polymolécularité ($M_w/M_n = 1,33$) est ainsi obtenu. Il a été prouvé que la polymérisation s'effectuait par insertion du MAM dans la liaison Ln-S, générant une espèce énolate similaire à celle observée avec les complexes lanthanocéniques.

40.2.5. Systèmes post-lanthanocéniques binaires

Associé à un cétène, l'isopropylate de lanthane génère une espèce active, de type énolate, pour la polymérisation du MAM (Schéma 5).^{158,159} La polymérisation est relativement contrôlée mais peu stéréospécifique. Le caractère vivant de la polymérisation est observé en présence d'un excès de cétène, puisqu'un copolymère dibloc poly(cétène-*b*-MAM) est obtenu. L'alcoolate "Ln(O*i*Pr)₃" ici utilisé a été préparé par une voie de synthèse différente de celle décrite dans le §40.2.4.2. Ceci a très probablement pour effet de modifier la structure du complexe et donc sa réactivité comme nous le montrerons un peu plus tard.

Schéma 5. Polymérisation du MAM amorcée par le système "La(O*i*Pr)₃"/cétène.¹⁵⁸



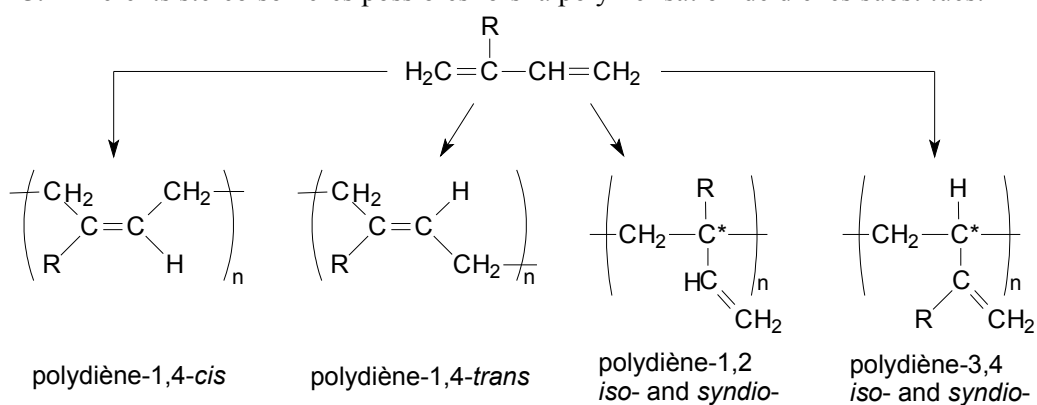
Afin d'être complet, il nous faut citer le travail réalisé par Sun et ses collaborateurs. Ces derniers ont étudié l'association de composés oxygénés de lanthanide (phosphonate, acetylacetonate, naphténate) et de triisobutylaluminium pour la polymérisation du MAM.¹⁶⁰ Ces systèmes se sont avérés actifs mais aucune information concernant la tacticité ou la distribution des masses molaires n'est donnée.¹⁶¹ L'association de ces précurseurs au dibutylmagnésium a également été décrite mais de manière identique très peu d'informations sur le PMAM obtenu ont été publiées.¹⁶²

40.3. Polymérisation du butadiène

40.3.1. Généralités

La polymérisation des diènes conjugués est d'un intérêt considérable, tant du point de vue scientifique qu'industriel. En effet, une polymérisation non stéréospécifique des diènes peut conduire à la présence de nombreux stéréoisomères au sein de la chaîne macromoléculaire (Figure 15).

Figure 15. Différents stéréoisomères possibles lors la polymérisation de diènes substitués.



Parmi ces différentes formes isomères, le polybutadiène 1,4-*cis* est de loin le plus important étant donné ses propriétés proches de celles du caoutchouc naturel; propriétés qui sont nécessaires dans des applications telles que les pneumatiques.¹⁷¹ Les principaux systèmes catalytiques utilisés industriellement se trouvent dans le tableau ci-dessous.

Tableau 3. Systèmes catalytiques industriellement utilisés pour la polymérisation du butadiène.¹⁷¹

système catalytique	M (mg/L)	PBD (kg/gM)	<i>cis</i> (%)
TiCl ₄ /I ₂ /Al(<i>i</i> Bu) ₃ (1/1,5/8)	50	4-10	93
Co(OCOR) ₂ /H ₂ O/AlEt ₂ Cl (1/10/200)	1-2	40-160	96
Ni(OCOR) ₂ /BF ₃ .OEt ₂ /AlEt ₃ (1/7,5/8)	5	30-90	97
Nd(OCOR) ₃ /AlEt ₂ Cl/Al(<i>i</i> Bu) ₂ H	10	7-15	98

M = métal de transition; PBD = polybutadiène

Bien que le système à base de cobalt soit le plus répandu, celui à base de néodyme demeure très intéressant puisqu'il possède une meilleure stéréospécificité ce qui améliore les propriétés mécaniques du polymère. De plus, le caractère vivant de la polymérisation permet l'introduction de groupes fonctionnels. Les systèmes catalytiques à base de lanthanide qui permettent la polymérisation 1,4-*cis* du butadiène (BD) peuvent se classer en 3 catégories. La première est composée de systèmes binaires où le sel de lanthanide est un halogénure, complexé ou non, par un ligand électrodonneur.¹⁷⁹⁻¹⁸⁰ La seconde comporte des systèmes ternaires. Dans ce cas, le complexe de lanthanide est un carboxylate, un alcoolate, un phosphonate auquel sont associés un dérivé aluminique et une molécule organique/organométallique source d'halogène.^{181-182,183} Enfin, un troisième groupe est formé par l'association de complexes de lanthanide comprenant des ligands mixtes (halogène et ligand oxygéné) et un tris(alkyl)aluminium.¹⁸⁶ En plus de ces trois grandes familles, quelques systèmes catalytiques particuliers permettent la polymérisation 1,4-*cis* du butadiène. Ceux-ci seront discutés ultérieurement.

40.3.2. Caractéristiques générales de la polymérisation 1,4-*cis* du butadiène 187

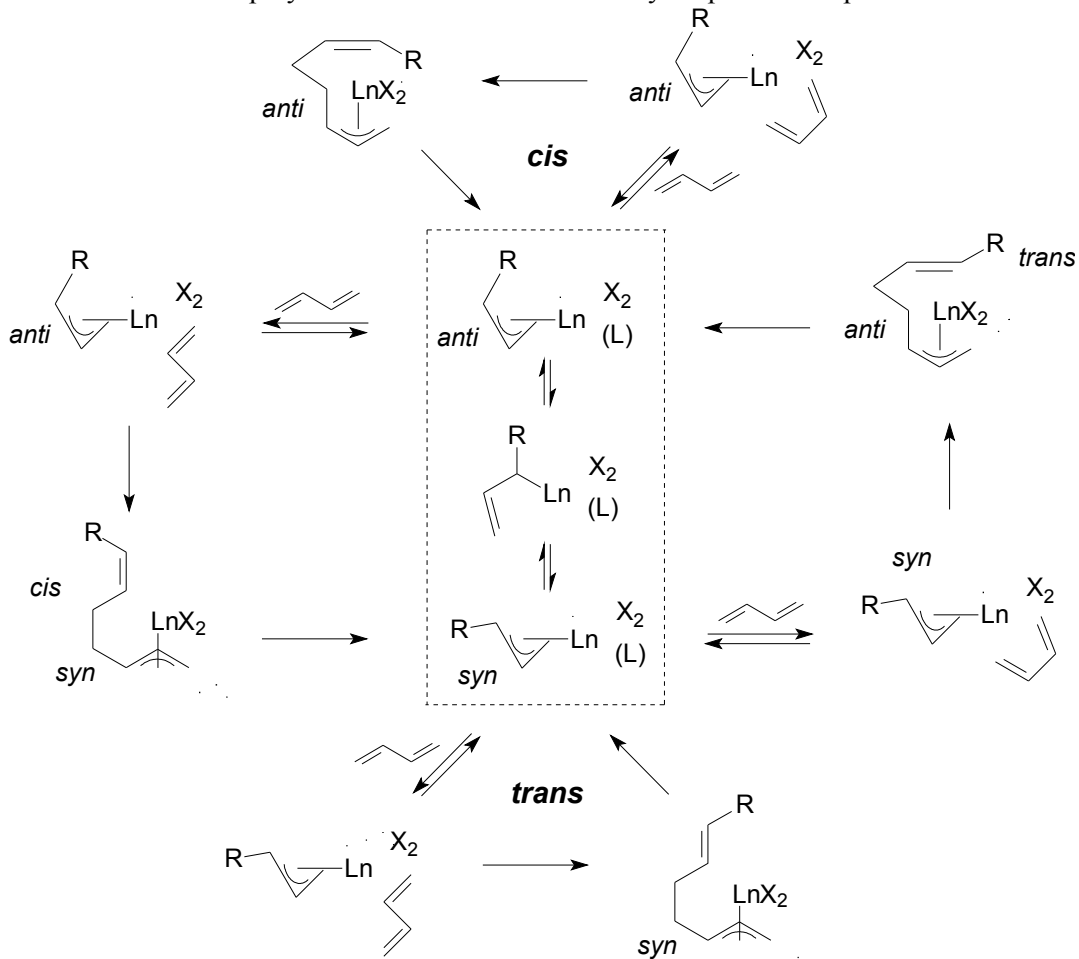
Ces caractéristiques ne sont valables que pour les système catalytiques entrant dans les 3 catégories définies ci-dessus.

Les polymérisations sont généralement effectuées dans des solvants aliphatiques à une température variant entre 20 et 60 °C. La nature du solvant n'affecte pas la stéréospécificité de la polymérisation, par contre les solvants aromatiques diminuent l'activité. De même, la température n'influe pas sur la stéréospécificité, par contre les masses molaires diminuent avec la température. Les polymères obtenus possèdent de hautes masses molaires ($M_n = 10^5-2.10^6$) et leur distribution est large, voire bimodale, suggérant l'existence de plusieurs espèces actives. La microstructure du polymère ne dépend pas de la composition du système catalytique ni des conditions de polymérisation comme nous venons de le montrer. Toutefois, l'activité est fonction de la nature de l'halogène présent dans le système catalytique. Les chlorures sont préférés aux bromures et aux iodures. Elle dépend aussi de la nature de l'agent alkylant (AlR₃ ou AlR₂Cl), qui affecte également les masses molaires en jouant le rôle d'agent de transfert.¹⁹³

40.3.3. Mécanisme de polymérisation

La polymérisation des diènes s'effectue selon un mécanisme d'insertion allylique.¹⁷⁸ Ce mécanisme prouvé par RMN est généralement accepté (Schéma 6).¹⁷⁶

Schéma 6. Mécanisme de polymérisation du butadiène catalysée par les complexes de lanthanide.¹⁷¹



40.3.4. Autres systèmes de stéréospécificité 1,4-*cis*

La contribution de Taube dans ce domaine est très importante. En effet, il a réalisé une étude très approfondie de l'utilisation de nombreux complexes π -allyliques de néodyme en polymérisation du butadiène. Il a montré que la stéréospécificité intrinsèque 1,4-*trans* des complexes $\text{LiNd}(\text{allyl})_4$, $[\{\text{La}(\eta^3\text{-allyl})_3(\eta^1\text{-C}_4\text{H}_8\text{O}_2)\}_2(\mu\text{-C}_4\text{H}_8\text{O}_2)]$, et $[\text{Nd}(\eta^3\text{-allyl})_3(\mu\text{-C}_4\text{H}_8\text{O}_2)]_n$ ($\text{C}_4\text{H}_8\text{O}_2 = 1,4\text{-dioxane}$) pouvait être modifiée en présence d'alkylaluminium.¹⁹⁵ Ainsi des polybutadiènes possédant une stéréospécificité 1,4-*cis* supérieure à 90% ont été obtenus. Les complexes chlorés $\text{Nd}(\eta^3\text{-allyl})\text{Cl}_2\bullet(\text{THF})_2$ et $\text{Nd}(\eta^3\text{-allyl})_2\text{Cl}\bullet(\text{THF})_{1,5}$ combinés au MAO offrent quant à eux une sélectivité 1,4-*cis* supérieure à 95%.¹⁹⁹

Récemment, d'excellents résultats ont été obtenus avec le système catalytique $\text{Nd}(\text{N}(\text{SiMe}_3)_2)_3/\text{Al}(i\text{Bu})_3/\text{AlEt}_2\text{Cl}$. L'activité et la sélectivité sont aussi élevées qu'avec un système à base de carboxylate.

Les systèmes catalytiques lanthanocéniques n'ont fait leur apparition en polymérisation du butadiène que très tardivement. En effet, les complexes tels que $(\text{Cp}^*_2\text{LnR})$ ($\text{R} = \text{Me}, \text{H}$) ou $\text{Cp}^*_2\text{Sm}(\text{THF})_2$ sont totalement inactifs en polymérisation du butadiène à cause de la formation de complexes η^3 -allyl trop stables. Néanmoins, combiné au MMAO (méthylaluminoxane modifié), $\text{Cp}^*_2\text{Sm}(\text{THF})_2$ polymérise efficacement le butadiène.²⁰² Outre la très bonne sélectivité 1,4-*cis* (98,8%), le polybutadiène présente une polymolécularité plutôt faible ($M_w/M_n = 1,8$). Des résultats encore plus intéressants ont été obtenus avec le complexe bimétallique $(\text{C}_5\text{Me}_5)_2\text{Sm}[(\mu\text{-Me})\text{AlMe}_2(\mu\text{-Me})]_2\text{Sm}(\text{C}_5\text{Me}_5)_2$ activé par $[\text{Ph}_3\text{C}][\text{B}(\text{C}_6\text{F}_5)_4]$ et un léger excès de triméthylaluminium. Enfin, un complexe cationique $[(\text{C}_5\text{Me}_5)_2\text{Gd}][\text{B}(\text{C}_6\text{F}_5)_4]$ a permis la préparation d'un polybutadiène de haute masse molaire ($M_n = 100\ 000$ -400 000) et de microstructure quasi-parfaite (1,4-*cis* = 99,9%).²⁰⁴

40.3.5. Polymérisation 1,4-*trans*

Même si le polybutadiène 1,4-*trans* est peu recherché, il serait impossible de terminer cette partie sans traiter des catalyseurs ayant une haute sélectivité 1,4-*trans*. Les premiers résultats obtenus par Mazzei avec le complexe $\text{Li}(\text{Nd}(\eta^3\text{-allyl})_4)(\text{dioxane})_{1,5}$ en absence de cocatalyseur, montrent une sélectivité relativement élevée (1,4-*trans* = 70-90%).¹⁹⁴ Le complexe neutre $\text{Nd}(\eta^3\text{-allyl})_3$ catalyse aussi la polymérisation 1,4-*trans* du butadiène¹⁹⁶ (80-85%) tout comme le système catalytique composé de versatate de néodyme et de di-*n*-butylmagnésium (1,4-*trans* = 97%).²⁰⁵

40.4. Copolymérisation butadiène-styrène

Les copolymères statistiques butadiene-styrène sont très largement utilisés commercialement sous le nom de SBR (styrene-butadiene-rubbers). Le copolymère idéal devrait avoir une masse molaire élevée, une teneur en butadiène 1,4-*cis* élevée et un taux d'incorporation de styrène (St) proche de 25%. Or, l'obtention de ces caractéristiques est impossible dans les conditions de production actuelles (polymérisation radicalaire ou anionique).²⁰⁶ Par conséquent, la synthèse de SBR par catalyse organométallique a été et fait encore l'objet de nombreuses recherches.

40.4.1. Systèmes ternaires

Les meilleurs résultats ont été obtenus avec les systèmes catalytiques à base d'un carboxylate de lanthanide. L'utilisation d'autres ligands oxygénés a conduit à une teneur en styrène trop faible.²⁰⁸ Le système le plus étudié, tout comme en homopolymérisation du butadiène, est du type $\text{Ln}(\text{OCOR})_3/\text{AlEt}_2\text{Cl}/\text{Al}(i\text{Bu})_3$ (où $\text{Ln} = \text{Pr}, \text{Nd}, \text{Gd}, \text{Dy}, \text{Yb}$ and $\text{R} = \text{CF}_3, \text{CCl}_3, \text{CHCl}_2, \text{CH}_3$).²⁰⁹ L'étude de ce système a montré que les meilleures activités

étaient observées avec les complexes de néodyme et particulièrement avec Nd(OCOCCl₃)₃. Il a aussi été observé que l'activité, les masses molaires, et la sélectivité 1,4-*cis* diminuaient lorsque la teneur en styrène augmentait. Les résultats sont regroupés dans le Tableau 4.

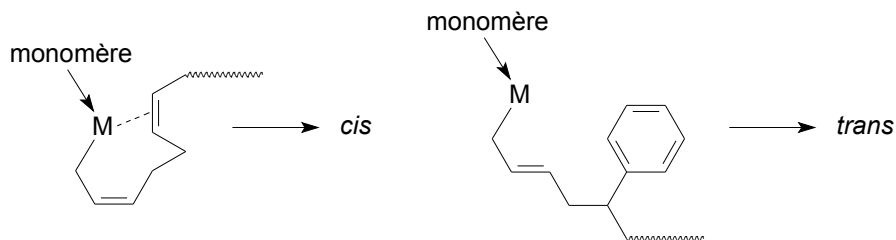
Tableau 4. Copolymérisation BD-St avec Nd(OCOCCl₃)₃/AlEt₂Cl/Al(*i*Bu)₃ dans l'hexane.²⁰⁹

St (mol %)	tps polymn (min)	conv. (%)	1,4- <i>cis</i> (%)	teneur St (%)	M _w (g/mol)
10	5	8,6	94,4	2,3	81 000
20	10	5,8	85,9	4,7	53 000
50	30	7,2	75,1	27,9	32 000
80	45	8,2	63,8	69,8	10 000
90	45	8,3	55,4	71,1	2000

Conditions: T = 50 °C; [BD]₀ + [St]₀ = 4 M; [Nd]₀ = 10⁻³ M et Nd(OCOCCl₃)₃/AlEt₂Cl/Al(*i*Bu)₃ (1/2/25).

La diminution de la stéréospécificité avec l'augmentation de la teneur en styrène a été expliquée par le modèle de "back-biting" proposé par Kobayashi *et al.*, dans lequel la coordination de l'avant-dernière unité de la chaîne en croissance régule la stéréospécificité. Lorsque cette avant-dernière unité est le styrène, la forte coordination au centre métallique force la dernière unité butadiène à changer sa configuration de 1,4-*cis* en 1,4-*trans*.²⁰⁹

Figure 16. Modèle de "back-biting" en copolymérisation BD-St.²⁰⁹



40.4.2. Systèmes lanthanocéniques

Wakatsuki *et al.* ont étudié la copolymérisation BS-St avec le système composé du complexe bimétallique (C₅Me₅)₂Sm[(μ-Me)AlMe₂(μ-Me)]₂Sm(C₅Me₅)₂ activé par [Ph₃C][B(C₆F₅)₄]/AlMe₃.²¹³ La stéréospécificité et la teneur en styrène sont proches des valeurs observées avec les systèmes ternaires. Toutefois, les masses molaires sont un peu plus élevées (Tableau 5).

Tableau 5. Copolymérisation BD-St catalysée par $(C_5Me_5)_2Sm[(\mu\text{-}Me)AlMe_2(\mu\text{-}Me)]_2Sm(C_5Me_5)_2$ activé par $[Ph_3C][B(C_6F_5)_4]/Al(iBu)_3$.213

St (mol %)	tps polymn (h)	conv. (%)	1,4-cis (%)	teneur St (%)	M _n (g/mol)	M _w /M _n
40	0,5	21	94,6	4,6	101 000	1,41
50	1	22	95,1	7,2	78 600	1,59
60	6	20	91,7	11,4	73 900	1,69
70	12	23	87,4	19,1	39 700	1,75
80	50	21	80,3	33,2	23 400	2,23

Conditions: $[BD]_0 + [St]_0 = 6 \text{ M}$; $[Nd]_0 = 3 \times 10^{-5} \text{ M}$; $[Al(iBu)_3]_0/[Nd]_0 = 3$ et $[[Ph_3C][B(C_6F_5)_4]]_0/[Nd]_0 = 1$; dans le toluène à 50 °C.

41. Présentation du projet de recherche

Dans notre étude bibliographique, nous avons montré que les complexes trivalents de type "CpLnR" étaient très actifs en polymérisation de l'éthylène et du MAM. L'évolution vers des ligands de type Cp substitué, Cp ponté, indényle ou encore fluorényle, a permis la polymérisation stéréospécifique des α -oléfines et du MAM. Toutefois, la recherche permanente de nouvelles générations de catalyseurs a aussi permis le développement de nouveaux ligands ancillaires autres que les cyclopentadiènyles. L'utilisation de ligands alcoolate/phénate est particulièrement attrayante puisque ces ligands "durs" et électronégatifs devraient stabiliser, grâce aux fortes liaisons Ln-O, les complexes électropositifs de lanthanide. Parmi la dizaine de complexes alkyl-alcoxylanthanide caractérisés, $[(2,6-tBu-C_6H_3-O)Y(CH(SiMe_3)_2)_2](THF)$ est le seul complexe actif en polymérisation de l'éthylène, activité au demeurant très faible. Ceci est très surprenant puisque ces ligands électroattracteurs sont supposés rendre le centre métallique encore plus déficient en électrons et donc encore plus réactif vis-à-vis des oléfines.

Ainsi, dans l'esprit de la recherche menée sur l'alkylation *in situ* de précurseurs chlorolanthanocéniques pour la polymérisation de l'éthylène et du MAM, nous avons entrepris une nouvelle étude qui vise à remplacer ces chlorolanthanocènes par des alcoolates de néodyme. Etant donné la complexité de la chimie des alcoolates de terres rares, nous nous sommes attachés à caractériser au préalable la série d'alcoolates que nous avons synthétisée. Ces composés ont ensuite été utilisés comme précurseur catalytique, en combinaison avec un dialkylmagnésien, pour la polymérisation de l'éthylène, du MAM, du butadiène et leur copolymérisation. Enfin, une étude mécanistique a permis de mettre en évidence la formation *in situ* d'espèces alkyl-Ln à partir de ces nouveaux systèmes binaires.

42. Synthèse d'alcoolates/phénates de lanthanide

42.1. Etude bibliographique

Nous allons maintenant présenter rapidement les principales voies de synthèse des alcoolates de lanthanide décrites dans la littérature.

42.1.1. Réaction de métathèse ionique

La réaction de métathèse ionique correspond à la réaction entre un halogénure de lanthanide et un alcoolate de métal alcalin comme le montre le Schéma 7. Cette méthode fait partie des méthodes les plus couramment utilisées.

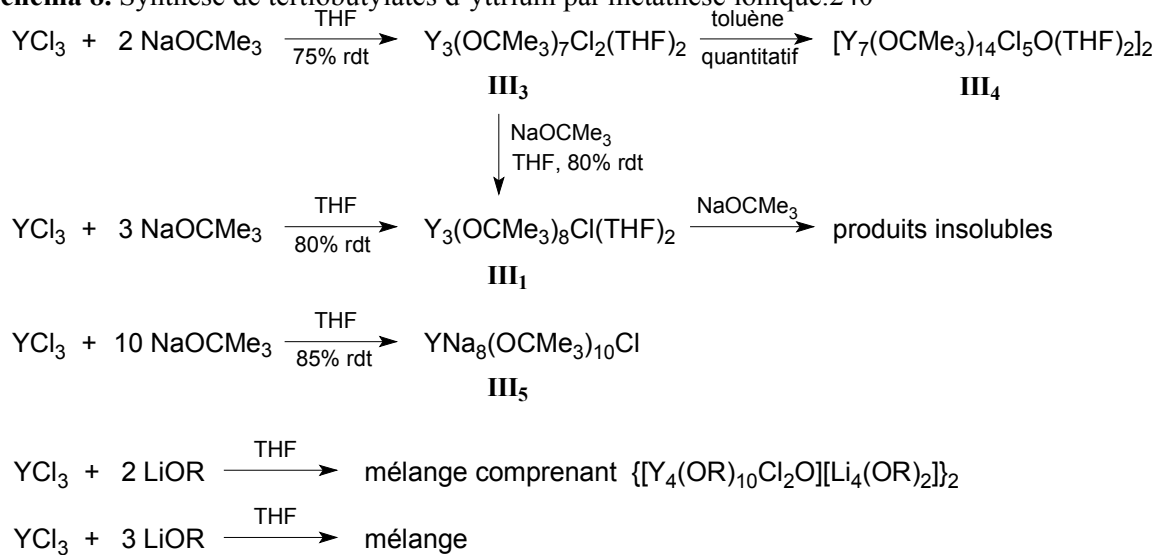
Schéma 7. Schéma général de métathèse ionique.



Elle peut être effectuée en présence d'alcool comme l'a montré l'équipe de Mehrotra.²³⁵
²³⁶ Cependant, ces conditions ne permettent pas d'obtenir de bons rendements et la purification du produit de réaction est délicate. La caractérisation de l'isopropylate de néodyme par diffraction des rayons-X montre une structure polynucléaire et la présence de chlore au sein du complexe ($\text{Nd}_6(\text{OCH}(\text{CH}_3)_2)_{17}\text{Cl}$).²³⁸

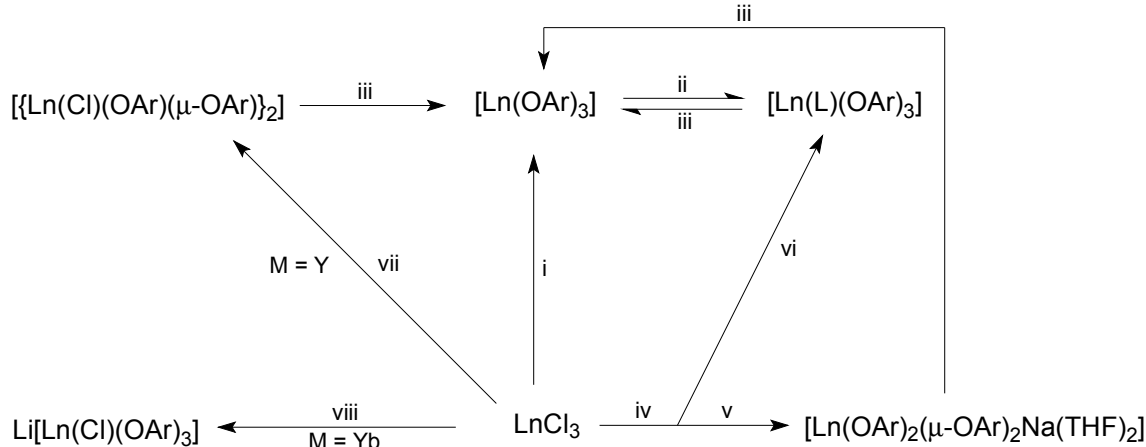
Ces conditions expérimentales ont rapidement été abandonnées et les réactions ont été effectuées en absence d'alcool dans des solvants tels que le THF ou le toluène. L'étude très complète d'Evans *et al.* des systèmes $\text{YCl}_3/\text{NaOtBu}$ et $\text{YCl}_3/\text{LiOtBu}$ a contribué au développement de la chimie des tertiobutylates de lanthanide suivant cette méthode. Ils ont montré comment les conditions expérimentales et la nature des réactifs influaient sur la structure des composés obtenus. Ainsi, lorsque YCl_3 réagit avec 3 équiv. de NaOtBu dans le THF, le complexe trinucléaire $\text{Y}_3(\mu_3\text{-OtBu})(\mu_3\text{-Cl})(\mu_2\text{-OtBu})_3(\text{OtBu})_4(\text{THF})_2$ (**III₁**) est obtenu alors que le dérivé du lanthane possède la structure $\text{La}_3(\mu_3\text{-OtBu})_2(\mu_2\text{-OtBu})_3(\text{OtBu})_4(\text{THF})_2$ (**III₂**).^{239,240,241} Cette structure trimétallique s'avère être la base structurale dans la chimie des tertiobutylates de lanthanide. Toutefois, des structures beaucoup plus complexes sont observées lorsque NaOtBu est remplacé par LiOtBu (Schéma 8).

Schéma 8. Synthèse de tertiobutylates d'yttrium par métathèse ionique.240



La synthèse de phénates de lanthanide de structure non polymérique a été développée par métathèse ionique. L'utilisation stoechiométrique de précurseurs lithiés conduit à la formation de composés de type "ate" tels que $[\text{Ln}(\text{Cl})(\text{OAr})(\mu_2\text{-Cl})_2\text{Li}(\text{THF})_2]$ lorsque la synthèse est effectuée dans le THF et $[\text{Ln}(\text{Cl})(\text{OAr})(\mu_2\text{-OAr})_2]$ quand elle l'est dans le toluène ($\text{OAr} = \text{O}-2,4,6-(t\text{Bu})_3\text{-C}_6\text{H}_2$).²⁴² Ce type de complexes est obtenu avec NaOtBu lorsque la stoechiométrie entre LnCl_3 et NaOtBu n'est pas respectée.²⁴⁵⁻²⁴⁶ Par contre, lorsque LnCl_3 réagit avec 3 equiv. de $\text{NaO}-2,6-t\text{Bu}_2-4\text{-Me-C}_6\text{H}_2$, le complexe homoleptique $\text{Ln}(\text{OAr})_3\text{THF}$ est formé.²⁴⁹ Ce dernier, peut être transformé en $\text{Ln}(\text{OAr})_3$ par sublimation. Les différentes voies de synthèse conduisant à la formation de phénates de lanthanide sont représentées sur le Schéma 9.

Schéma 9. Synthèse de phénates de lanthanide dérivés de $\text{HO}-2,6-t\text{Bu}_2-4\text{-Me-C}_6\text{H}_2$.²⁴⁹

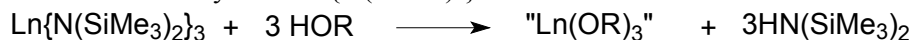


i, 3 $\text{NaOAr}(\text{OEt}_2)$, THF, reflux, > 36 h; ii, $\text{L} = \text{THF}$ ou $\text{P}(\text{O})\text{Ph}_3$, benzène, 20 °C, 18 h; iii, sublimation sous vide; iv, 3 $\text{NaOAr}(\text{OEt}_2)$, THF, 20 °C, 16 h, puis reflux, 24 h, évaporation du solvant sous vide, pentane et filtration; v, précipitation à partir de iv; vi, filtration à partir de iv; vii, 3 $[\text{Li}(\mu\text{-OAr})(\text{OEt}_2)]_2$, toluène, 20 °C, 72 h puis reflux, 24 h, évaporation du solvant sous vide; viii, 3 $[\text{Li}(\mu\text{-OAr})(\text{OEt}_2)]_2$, toluène, 20 °C, 48 h puis reflux, 36 h, évaporation du solvant sous vide.

42.1.2. Alcoolyse de complexes tris(amidure)

Cette réaction consiste en l'addition d'alcool/phénol à un complexe tris(amidure) de lanthanide (Schéma 10). L'utilisation du précurseur $\text{Ln}[\text{N}(\text{SiMe}_3)_2]_3$ (LnN3) (facilement synthétisé)²⁵² rend cette méthode très simple de part la volatilité de l'amine libérée, évitant ainsi tous les problèmes de filtration ou de centrifugation rencontrés lors de la réaction par métathèse ionique.

Schéma 10. Réaction d'alcoolyse de $\text{Ln}[\text{N}(\text{SiMe}_3)_2]_3$.



Cette méthode est adaptée à la synthèse de tous types d'alcoolates de lanthanide. De fait, on retrouve dans la littérature la préparation d'alcoolates simples aliphatiques comme le

tertiobutylate de lanthane.²⁵⁴ Le composé obtenu dans le benzène $(La(\mu_3-OtBu)_2(\mu_2-OtBu)_3(OtBu)_4(tBuOH)_2$ complex (**III₆**) présente une structure trimétallique similaire à **III₂**. Le chauffage à reflux de **III₆** dans le THF permet la substitution des 2 molécules de *t*BuOH par 2 molécules de THF conduisant à **III₂**. Une structure similaire a été proposée avec l'alcool tertioamylique alors que des structures dimériques ont été suggérées avec les alcools tertiaires $HOCMe_2*i*Pr$, $HOCMeEt*i*Pr$ et $HOCEt_3$.

Des complexes dérivés du tris(*tert*-butyl)méthanol n'ont pu être obtenus à partir de LnN_3 pour les métaux de petit rayon ionique. Ce problème a été résolu en utilisant $Ln[N(SiHMe_2)_2]_3$ qui offre un encombrement stérique plus faible.^{255,256} Le complexe à base de cérium $Ce[OC(tBu)_3]_3$ a montré une faible résistance à la chaleur, se décomposant en $[Ce(O)(OCH*t*Bu_2)_3]_2$ et en isobutylène.²⁵⁸

De nombreux phénates ont également été synthétisés selon cette méthode. Celle-ci permet de synthétiser des complexes non porteurs de solvant coordonné²⁵⁷ (diminution du nombre de coordination) et des phénates substitués en position 2 et 6 par des groupements méthyle et isopropyle sous la forme $Ln(OAr)_3(THF)_2$.²⁵⁰

Cependant, l'avantage majeur de cette méthode est la possibilité de synthétiser des alcoolates de lanthanide à partir d'alcool fonctionnalisés. Parmi les différents exemples décrits, nous pouvons citer ceux issus d'alcools β -fonctionnalisés ($HOCH(tBu)CH_2OEt$, $HOCH(tBu)CH_2NET_2$, $HOC(tBu)_2CH_2OEt$, $HOC(CHMe_2)_2CH_2OEt$).²⁶⁴ Une structure monomérique est suggérée pour tous ces complexes sur la base de leur forte solubilité dans les solvants non polaires. La réduction de l'encombrement stérique sur la position α conduit à la formation de complexes polynucléaires. Ainsi, un groupement méthylène en position α conduit au composé polynucléaire $[Y(OCH_2CH_2OMe)_3]_{10}$.²⁶⁵ Enfin, des phénates fonctionnalisés (base de Schiff et salicylaldimine) ont également été utilisés avec succès.

42.1.3. Protonolyse de complexes tris(alkyl)lanthanide

L'utilisation de composés tris(alkyl)- Ln ($Ln(CH(TMS)_2)_3$ et $Ln(CH(CH_2SiMe_2Ph)_2)_3$) comme précurseur pour la synthèse d'alcoolates fonctionnalisés a également été décrite.²⁷² Cette voie de synthèse s'est montrée tout aussi élégante et efficace que l'alcoolyse du tris (amidure). Cependant, aucun rapport ne mentionne l'utilisation de cette méthode avec des alcools aliphatiques non fonctionnalisés. La synthèse difficile de ces précurseurs et leur faible stabilité sont autant de facteurs qui limitent l'utilisation de cette méthode.

42.1.4. Conclusion

La chimie des alcoolates de lanthanide est très riche et les complexes obtenus offrent une très grande diversité grâce à la modification du ligand. Etant donné notre volonté d'utiliser les alcoolates de lanthanide comme précurseur catalytique en polymérisation des oléfines, nous

avons préparé et caractérisé une série d'alcoolates et étudié l'effet des modifications structurales, stériques et électroniques sur l'activité de polymérisation.

42.2.Synthèse d'alcoolates de néodyme

42.2.1. *Tertiobutylates de néodyme*

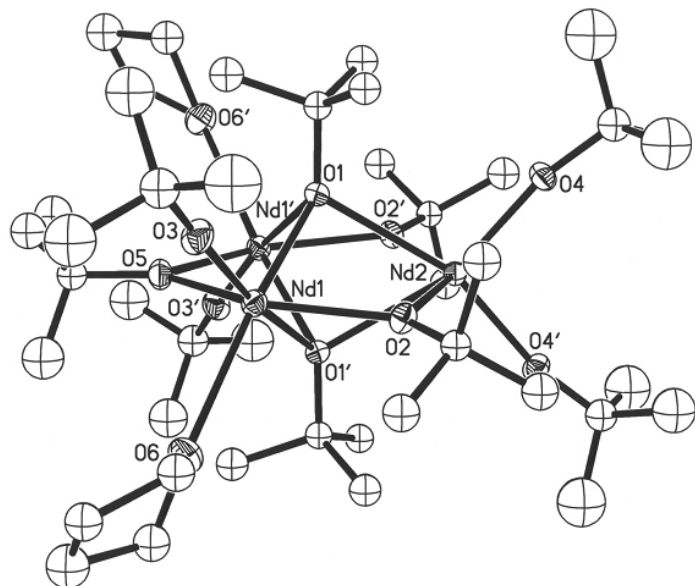
Parmi les différents alcoolates que nous avons préparés, le tertiobutylate de néodyme a été celui que nous avons le plus étudié. En effet, nous avons effectué sa synthèse par métathèse ionique en faisant varier différents paramètres tels que la nature des réactifs, le solvant, le temps de réaction...et par alcoolysé de NdN₃ dans différents solvants.

42.2.1.1. Réactions de métathèse ionique

42.2.1.1.1. *A partir de NdCl₃/NaOtBu dans divers solvants*

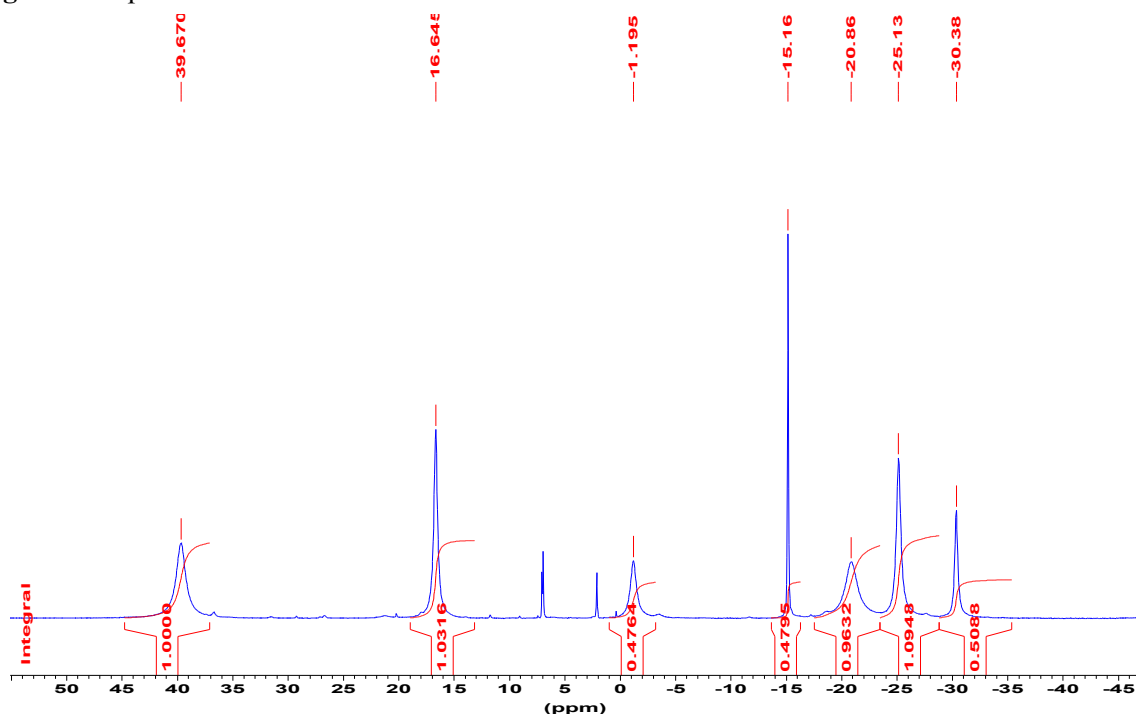
Lorsque NdCl₃ réagit avec 3 équiv. de NaOtBu dans le THF à température ambiante pendant 72 h suivant les conditions décrite par Evans *et al.*,²³⁹ un produit unique est isolé avec un rendement de 80 à 90% (**1** = Nd₃(μ₃-OtBu)₂(μ₂-OtBu)₃(OtBu)₄(THF)₂). L'analyse élémentaire du produit brut est en accord avec la structure Nd₃(OtBu)₉(THF)₂. Ce complexe a été caractérisé par diffraction RX et RMN du proton à température variable. L'étude par diffraction des rayons-X montre que **1** est un composé trimétallique dans lequel les 3 atomes de néodyme forment un triangle; les différents atomes de Nd sont reliés entre eux par des ponts (μ₂-OtBu) le long du triangle et par des ligands OtBu triplement pontés au-dessus et en-dessous du plan formé par les atomes de Nd. Enfin, un atome de néodyme possède 2 ligands OtBu terminaux alors que les 2 autres portent un ligand OtBu terminal et une molécule de THF, ces 2 molécules de THF se trouvant de part et d'autre du plan trimétallique. Cette structure avait déjà été observée dans de nombreux autres tertiobutylates de lanthanide tels que (La₃(OtBu)₉(tBuOH)₂,²⁵⁴ Y₃(μ₃-OtBu)(μ₃-Cl)(μ₂-OtBu)₃(OtBu)₄(THF)₂²²³⁹ et Y₃(μ₃-OtBu)(μ₃-Cl)(μ₂-OtBu)₃(OtBu)₃Cl(THF)₂²²⁴⁰.

Figure 17. Figure ORTEP de Nd₃(μ₃-OtBu)₂(μ₂-OtBu)₃(OtBu)₄(THF)₂ (**1**).



Le paramagnét ux ainsi que leur dispersion sur l'échelle spectrale en RMN. Toutefois, les spectres obtenus à 5 °C semblent optimisés (superposition des signaux minimale). Ainsi, le spectre RMN ^1H montre une série de 7 résonances ayant pour intégration relative 2:2:1:1:2:2:1 (Figure 18). Ceci est en accord avec la structure de **1** où l'on retrouve neuf groupements $\text{O}t\text{Bu}$ dans 5 environnements différents et 2 molécules de THF suggérant que les structures de **1** à l'état solide et en solution sont strictement identiques. Cependant, il est impossible d'attribuer sans ambiguïté ces signaux. Contrairement aux complexes à base d'yttrium, la corrélation entre déplacement chimique et degré de coordination des ligands ne peut s'appliquer.

Figure 18. Spectre RMN ^1H de **1** dans le toluène- d_8 à 5 °C.

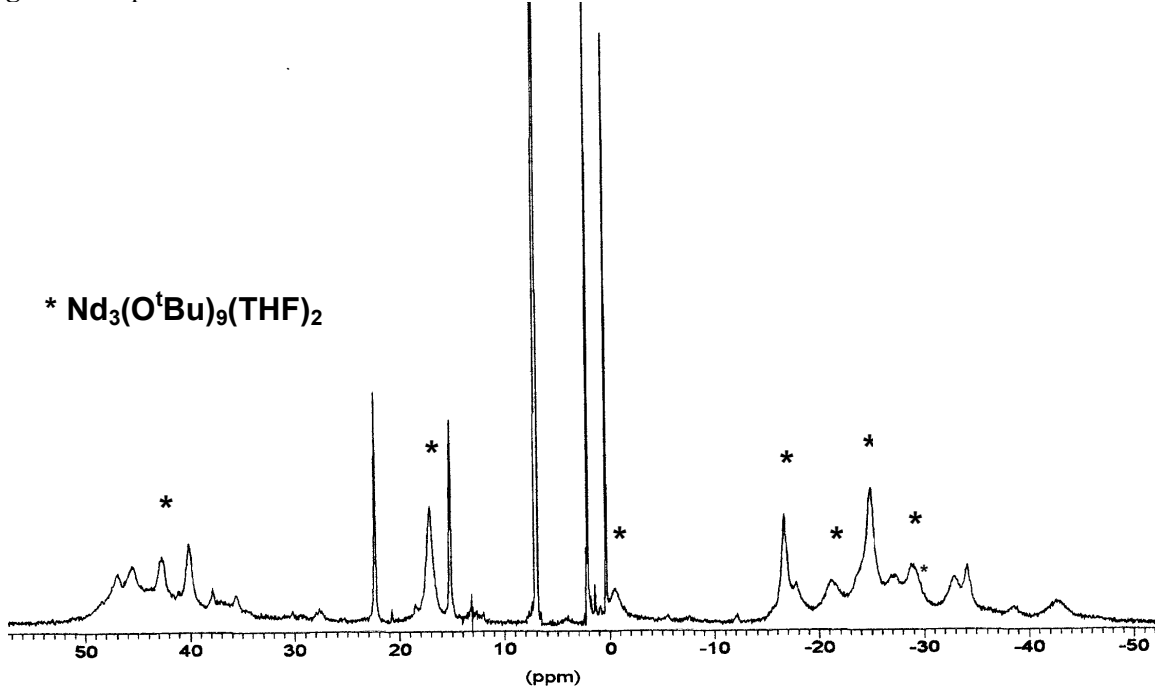


Cette réaction a également été effectuée dans divers solvants. Aucune réaction n'a eu lieu dans le toluène (aucune dissociation des charges); par contre la synthèse dans l'éther diéthylique a conduit à la formation d'un composé (**10***) peu soluble dans les hydrocarbures. L'éventualité d'une structure oligomérique est tout à fait possible, surtout au vue des résultats obtenus avec l'alcool tertioamylique dans les mêmes conditions (*vide infra*). La réaction effectuée dans le tétrahydropyrane conduit à un complexe **2** dont la structure doit très probablement être comparable à **1**.

42.2.1.1.2. A partir de $NdCl_3/MOtBu$ ($M = Li, K$) dans le THF

Comme il l'a été observé avec les alcoolates/phénates d'yttrium,^{239,242,249} la nature du métal associé au précurseur MOR(Ph) a un rôle déterminant sur la structure du complexe final. Par conséquent, nous avons étudié cet effet pour la synthèse du tertiobutylate de Nd dans le THF. Lorsque la synthèse est effectuée avec LiOtBu, le produit final ne peut être isolé par simple filtration. Toutefois, un produit peu soluble dans les hydrocarbures est isolé après évaporation et traitement à l'éther diéthylique (**3**). La faible solubilité pourrait résulter de la présence de Li au sein de la structure du complexe. L'utilisation de KOtBu ne modifie pas le rendement de la réaction. L'analyse élémentaire de ce complexe donne des valeurs comparables à celles obtenues pour **1**. Par contre, le spectre RMN 1H observé à 5 °C indique la présence des signaux caractéristiques de **1** à 70% et de larges signaux attribués à un produit **4** (Figure 19).

Figure 19. Spectre RMN 1H de **4** dans le toluène- d_8 à 5 °C.



42.2.1.1.3. A partir de $NdCl_3(THF)_2$ dans le THF

Etant donné notre intérêt pour le développement de ces alcoolates, nous avons continué nos recherches en utilisant le nouveau précurseur chloré $\text{NdCl}_3(\text{THF})_2$ préparé par Rhodia.²⁸⁴ En effet, dans l'optique d'une future industrialisation de ces complexes, il est impératif de vérifier que ces précurseurs mènent aux même résultats que les précurseurs anhydres commerciaux.

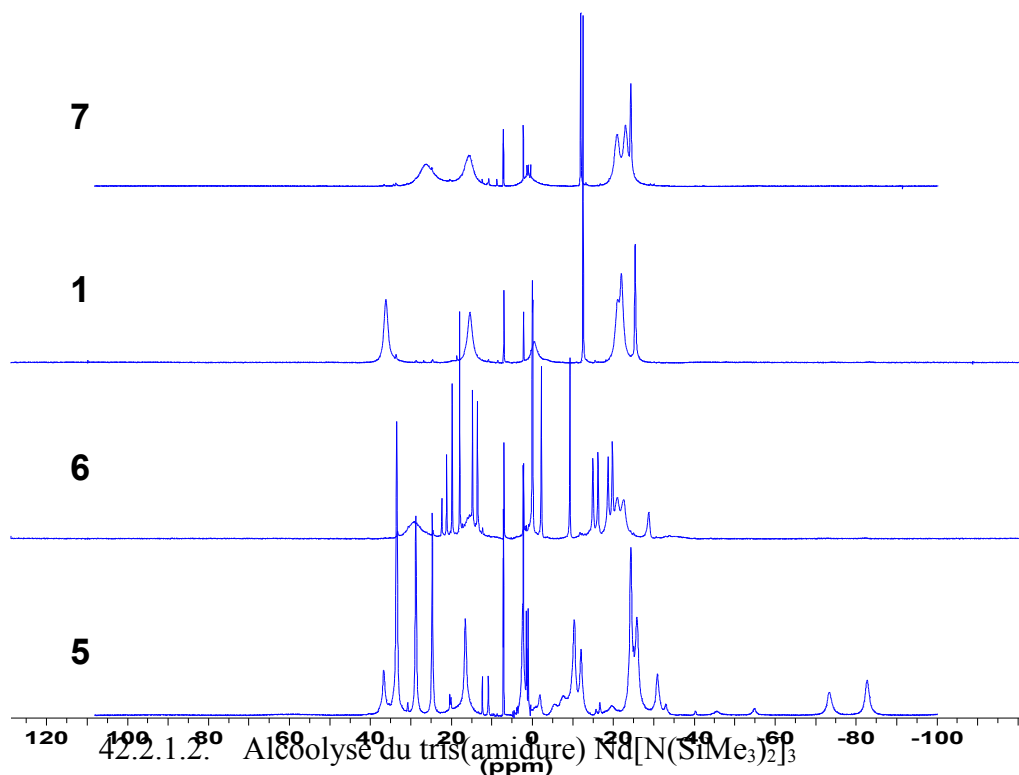
Lorsque la réaction est menée dans les conditions décrites au paragraphe 42.2.1.1.1, une poudre bleue est obtenue quantitativement. Son analyse élémentaire est similaire à celle du composé **1**. Cependant, il n'a pas été possible d'analyser ce complexe par diffraction RX ce qui n'a en rien altéré notre volonté d'étudier la synthèse de tertiobutylate de néodyme avec ce nouveau précurseur. Plusieurs paramètres de réactions ont donc été évalués.

Diminuer le temps de réaction de 72 à 4 h n'affecte pas les teneurs en Nd et en Cl du produit brut, seule une légère baisse de la conversion (de 90 à 70 %) est notée. Il semble donc que le temps de réaction soit un facteur n'ayant qu'une légère influence sur le cours de la réaction. Cependant, nous ne pouvons pas écarter une évolution de la structure au cours du temps. De plus, ces résultats ne s'appliquent en aucun cas aux chlorures de néodyme anhydres commerciaux, le complexe $\text{NdCl}_3(\text{THF})_2$ possédant une plus grande réactivité. Cette réactivité se retrouve lors des essais effectués avec une concentration en Nd plus élevée. En effet, augmenter la concentration en néodyme de $[\text{Nd}] = 0,1 \text{ M}$ à $[\text{Nd}] = 0,5 \text{ M}$ conduit à des réactions très rapides (5 min), stoppées par l'apparition d'une pâte très visqueuse de laquelle il est quasiment impossible d'extraire l'alcoolate de lanthanide. Etant donné ces résultats, nous avons décidé d'effectuer ces réactions en milieu concentré dans un solvant apolaire (hexane) afin de diminuer la réactivité.

Après s'être heurté à quelques problèmes de mise en suspension des réactifs dans l'hexane, nous avons choisi d'utiliser une technique "one-pot" c'est à dire que $\text{NdCl}_3(\text{THF})_2$ et MOtBu ($\text{M} = \text{Na, K}$) sont placés dans un même réacteur avant l'addition du solvant. Dans ces conditions, la réaction est quantitative (conv. > 80%) et rapide (4-24 h); le produit obtenu possède toujours les teneurs en Nd et Cl attendues pour un complexe de structure identique à **1**. Les composés synthétisés dans ces conditions à partir de NaOtBu et KOtBu sont appelés respectivement **5** et **6**.

Malgré l'intérêt des résultats obtenus à partir de $\text{NdCl}_3(\text{THF})_2$, nous devons rester prudents. En effet, sans informations structurales, seules des indications quantitatives peuvent être données. Ceci est d'autant plus vrai que les spectres RMN ^1H des différents composés obtenus sont assez dissemblables (Figure 20). Etant donné que **1** conserve sa structure en solution, nous pouvons raisonnablement penser que **5** et **6** possèdent des structures différentes. Malheureusement, la structure exacte de ces complexes n'a pu être déterminée par diffraction RX (instabilité des complexes, désordre moléculaire).

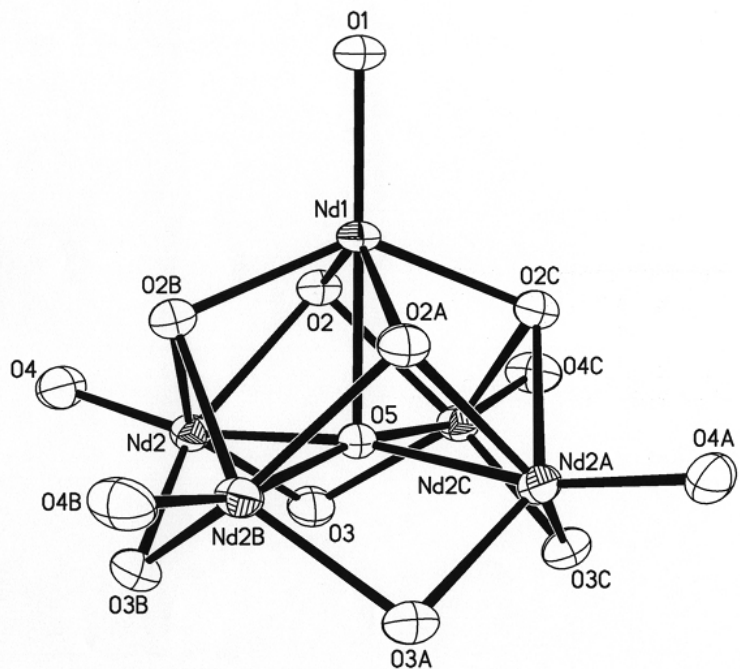
Figure 20. Spectre RMN ^1H de tertiobutylates de néodyme obtenus par différentes voies de synthèse.



L'analyse élémentaire et le spectre RMN ^1H du produit obtenu après 72 h de réaction dans le THF (15 équiv. *t*BuOH vs. Nd) sont en accord avec la structure $\text{Nd}_3(\mu_3\text{-OtBu})_2(\mu_2\text{-OtBu})_3(\text{OtBu})_4(\text{THF})_2$ (**1**). Par contre, lorsque $\text{Nd}[\text{N}(\text{SiMe}_3)_2]_3$ réagit avec 8 équiv. (vs. Nd) de *t*BuOH dans l'hexane à 20 °C, le composé $\text{Nd}_3(\mu_3\text{-OtBu})_2(\mu_2\text{-OtBu})_3(\text{OtBu})_4(\text{HOtBu})_2$ (**7**) est obtenu quantitativement (conv. = 90%). Ce dernier possède une géométrie structurale identique à **1** dans laquelle les 2 molécules de THF de **1** ont été remplacées par 2 molécules de tertiobutanol. Ceci a été corroboré par l'analyse RMN ^1H . Cette géométrie est de plus comparable à celles publiées pour les complexes correspondant de lanthane et d'yttrium.²⁵⁴

La formation du complexe oxo pentanucléaire $\text{Nd}_5(\mu_5\text{-O})(\mu_3\text{-OtBu})_4(\mu_2\text{-OtBu})_4(\text{OtBu})_5$ (**8**) est observée après agitation d'une solution toluénique du complexe **7** à 20 °C pendant deux semaines. Ce complexe a été caractérisé par diffraction RX, l'analyse RMN s'étant révélée peu informative. La structure moléculaire correspond à un ensemble pentagonal constitué d'une base formée par quatre atomes de Nd et un atome de Nd en position apical. Tous les atomes de néodyme possède un groupe OtBu terminal, et sont connectés entre eux par quatre groupes $\mu_3\text{-OtBu}$ et quatre groupes $\mu_2\text{-OtBu}$ pontants ainsi que par un atome d'oxygène central (Figure 21).

Figure 21. Figure ORTEP de $\text{Nd}_5(\mu_5\text{-O})(\mu_3\text{-OtBu})_4(\mu_2\text{-OtBu})_4(\text{OtBu})_5$ (**8**).



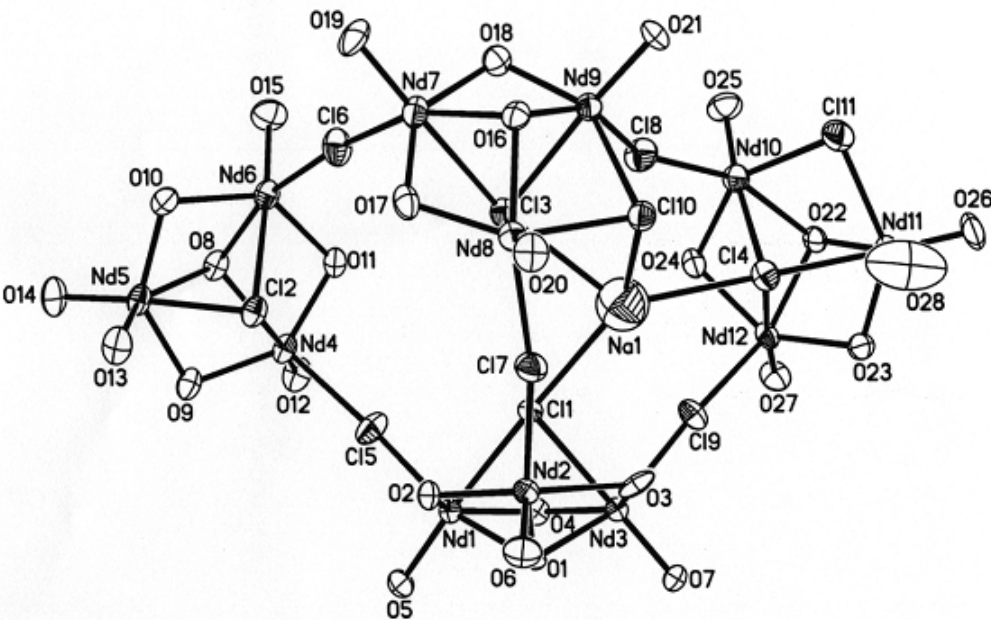
42.2.2. Autres alcoolates de néodyme

42.2.2.1. Synthèse du tertioamylate de néodyme par métathèse ionique

La préparation de tertioamylate de néodyme a été effectuée suivant le mode opératoire décrit au paragraphe 42.2.1.1.1. L'analyse par RMN de ce complexe **9** n'a pas permis d'élucider sa structure. Cependant, nous pouvons raisonnablement supposer que **9** et **1** possèdent la même structure puisqu'il a été montré que les ligands -OtBu et -OtAm donnent des structures similaires avec les métaux du groupe 3.254²⁸⁶

Lorsque le THF est remplacé par l'éther diéthylique, un produit peu soluble dans les hydrocarbures est obtenu. La recristallisation de ce complexe dans le toluène a permis d'isoler le complexe (**10**) (Figure 22).

Figure 22. Figure ORTEP de Nd₁₂(OtAm)₂₆(HOtAm)₂Cl₁₁Na•(OEt₂)₂ (**10**).



$\text{Nd}_{12}(\text{OtAm})_{26}(\text{HOtAm})_2\text{Cl}_{11}\text{Na} \cdot (\text{OEt}_2)_2$ (**10**) possède une structure très complexe composée de quatre unités trinucléaires indépendantes reliées par des ponts $\mu_2\text{-Cl}$, un atome de sodium coordonné à quatre atomes de chlore venant terminer la structure.

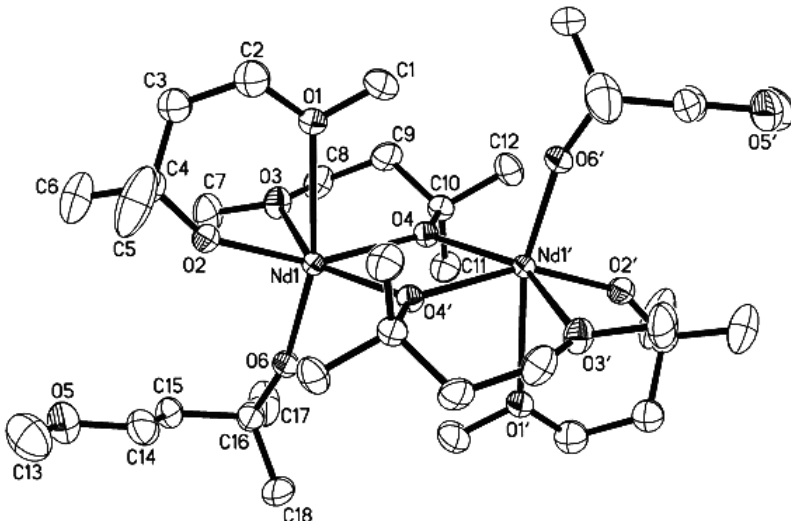
$\text{Nd}_{12}(\text{OtAm})_{26}(\text{HOtAm})_2\text{Cl}_{11}\text{Na} \cdot (\text{OEt}_2)_2$ peut être décomposé schématiquement en quatre fragments **A–D** et une molécule de NaCl :

- A:** $\text{Nd}(1)\text{-Nd}(3), \text{Nd}_3(\mu_3\text{-OtAm})(\mu_3\text{-Cl})(\mu_2\text{-OtAm})_3(\text{OtAm})_3\text{Cl}$
- B:** $\text{Nd}(4)\text{-Nd}(6), \text{Nd}_3(\mu_3\text{-OtAm})(\mu_3\text{-Cl})(\mu_2\text{-OtAm})_3(\text{OtAm})_3\text{Cl}(\text{HOtAm})$
- C:** $\text{Nd}(7)\text{-Nd}(9) \text{Nd}_3(\mu_3\text{-OtAm})(\mu_3\text{-Cl})(\mu_2\text{-OtAm})_3(\mu_2\text{-Cl})(\text{OtAm})_3\text{Cl}$
- D:** $\text{Nd}(10)\text{-Nd}(12), \text{Nd}_3(\mu_3\text{-OtAm})(\mu_3\text{-Cl})(\mu_2\text{-OtAm})_3(\mu_2\text{-Cl})(\text{OtAm})_3\text{Cl}(\text{HOtAm})$

42.2.2.2. Synthèse d'alcoolate tertiaire fonctionnalisé par alcoolysé de $\text{Nd}[\text{N}(\text{SiMe}_3)_2]_3$

Afin d'obtenir des complexes de nucléarité plus faible, nous avons utilisé un alcool γ -fonctionnalisé. La réaction d'alcoolysé de $\text{Nd}[\text{N}(\text{SiMe}_3)_2]_3$ par 3 équiv. de 4-méthoxy-2-méthylbutan-2-ol dans le benzène à 20 °C donne après recristallisation le complexe $\text{Nd}_2(\mu_2,\eta^2\text{-OR})_2(\eta^2\text{-OR})_2(\eta^1\text{-OR})_2$ (**11**) (Figure 23). Un produit huileux est obtenu quand la réaction est conduite dans le THF. Le complexe **11** adopte une structure dimérique symétrique dans laquelle les ligands alcoxy-éther se coordonnent au métal de trois manières différentes.

Figure 23. Figure ORTEP de $\text{Nd}_2(\mu_2,\eta^2\text{-OR})_2(\eta^2\text{-OR})_2(\eta^1\text{-OR})_2$ (**11**).

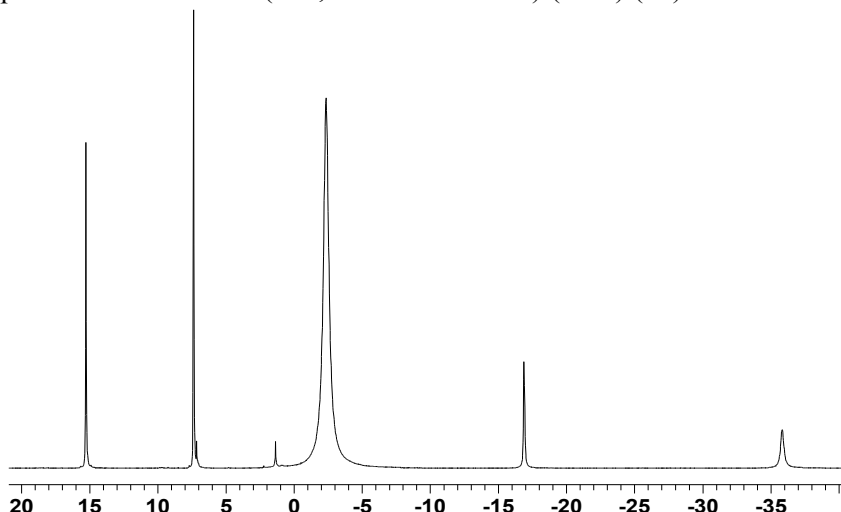


42.2.3. Synthèse de phénates de néodyme

Notre travail a consisté en l'optimisation de la synthèse de phénates par métathèse ionique et par alcoolysse de $\text{Nd}[\text{N}(\text{SiMe}_3)_2]_3$. Notre étude a porté plus particulièrement sur l'utilisation du ligand -O-2,6-*t*Bu-4-Me-C₆H₂ et la caractérisation par RMN ¹H et ¹³C des complexes correspondants, méthode très souvent négligée pour ces complexes paramagnétiques.

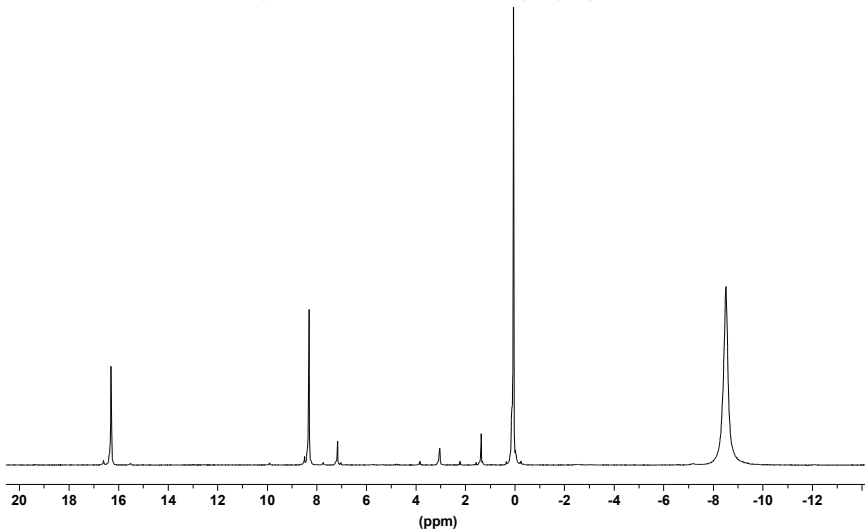
Ainsi, le complexe Nd(O-2,6-*t*Bu-4-Me-C₆H₂)₃(THF) (**12**), déjà décrit par Lappert *et al.*,²⁴⁹ a été synthétisé par métathèse ionique utilisant les précurseurs NdCl₃ dans le THF et NdCl₃(THF)₂ dans l'hexane et par alcoolysse du tris(amidure) dans le THF. Les 3 voies de synthèse se sont révélées quantitatives et mènent à une structure similaire comme le montre l'obtention de spectres RMN ¹H identiques (Figure 24).

Figure 24. Spectre RMN ¹H de Nd(O-2,6-*t*Bu-4-Me-C₆H₂)₃(THF) (**12**) dans C₆D₆ à 23 °C.



La réaction d'alcoolysse effectuée dans le benzène deutérié ou le pentane mène invariablement au même complexe Nd(O-2,6-*t*Bu-4-Me-C₆H₂)₃ (**13**), qui peut être aussi obtenu par sublimation du complexe **12** à 210 °C et 10⁻³ mmHg. Le spectre RMN ¹H de ce complexe est reporté ci-dessous (Figure 25).

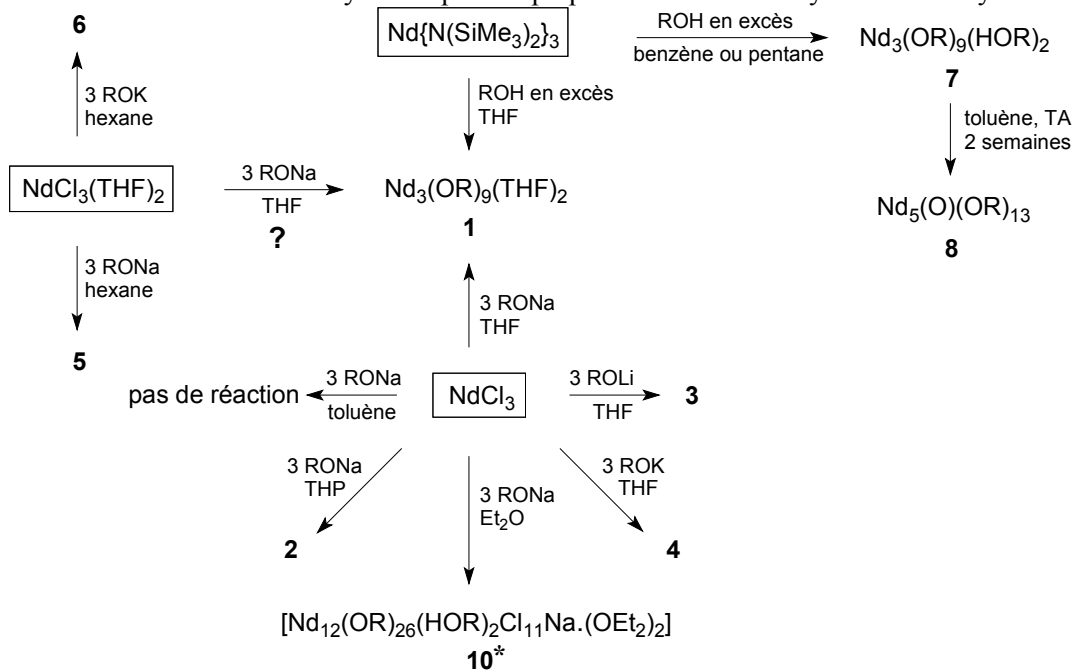
Figure 25. Spectre RMN ^1H de $\text{Nd}(\text{O}-2,6-t\text{Bu}-4-\text{Me-C}_6\text{H}_2)_3$ (**13**) dans C_6D_6 à 23°C .



42.3. Conclusion

Nous avons synthétisé une série d'alcoolates de néodyme montrant une remarquable diversité structurale et une grande complexité. Notre étude a montré que de nombreux paramètres tels que la nature des réactifs, leur pureté ou le solvant de synthèse influaient fortement sur la structure du produit final. Les différentes voies de synthèse que nous avons explorées sont résumées sur le Schéma 11.

Schéma 11. Différentes voies de synthèse pour la préparation de tertiobutylates de néodyme.

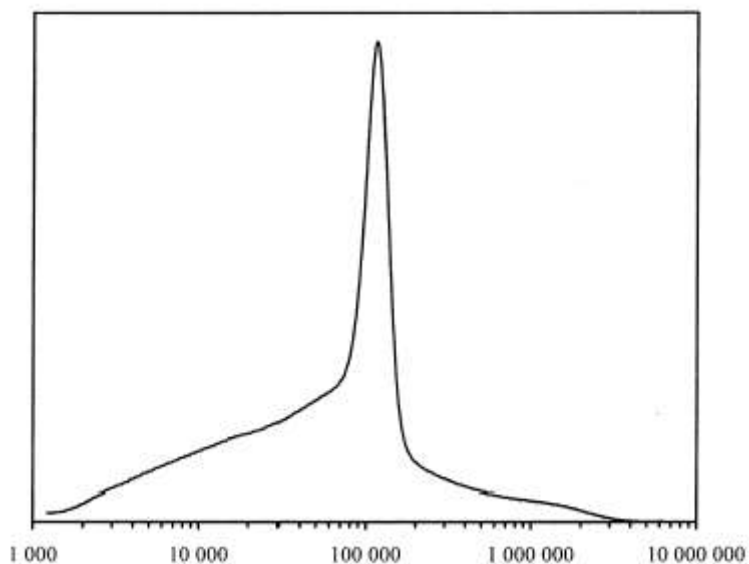


43. Polymérisation du méthacrylate de méthyle

43.1. Résultats préliminaires

Comme il a été mentionné dans la présentation du projet de recherche, notre objectif est l'utilisation, en polymérisation, d'alcoolates de lanthanide associés à un dialkylmagnésien. Dans cette partie, nous nous sommes plus particulièrement intéressés aux systèmes $\text{Ln}_3(\text{OtBu})_9(\text{THF})_9/\text{DHM}$ ($\text{Ln} = \text{La, Nd}$) et $\text{Y}_3(\text{OtBu})_8\text{Cl}(\text{THF})_2/\text{DHM}$ où DHM est le di-*n*-hexylmagnésium. Avant de commencer cette étude, nous avons vérifié que ces alcoolates n'amorçaient pas en tant que tels la polymérisation du MAM dans nos conditions opératoires (polymérisation dans le toluène à 0 °C). Cette vérification faite, nous avons associé ces différents alcoolates au DHM. Cette combinaison a permis la polymérisation rapide, quantitative et syndiotactique du MAM ($\text{rr} = 74\text{-}80\%$), mais avec une large distribution des masses molaires. Toutefois, les chromatogrammes GPC des PMAM obtenus avec les complexes à base de lanthane et de néodyme présentent un pic étroit de polymolécularité très faible ($M_w/M_n = 1,03$; $M_n = 112\,000 \text{ g/mol}$), correspondant à 28% en poids du polymère (Figure 26). Cette observation suggère que la combinaison $\text{Ln}_3(\text{OtBu})_9(\text{THF})_9/\text{DHM}$ ($\text{Ln} = \text{La, Nd}$) génère plusieurs amorceurs de polymérisation dont un s'avère très efficace.

Figure 26. Chromatogramme GPC du PMAM obtenu avec la combinaison $\text{La}_3(\text{OtBu})_9(\text{THF})_9/\text{DHM}$ ($\text{La}/\text{Mg} = 1:1$).



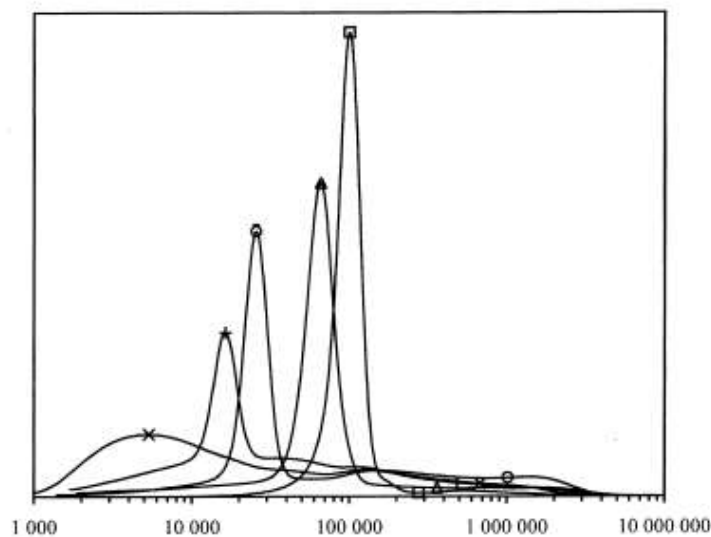
43.2.Optimisation du système catalytique $\text{Nd}_3(\text{OtBu})_9(\text{THF})_9/\text{DHM}$

Etant donné que nous avons complètement caractérisé $\text{Nd}_3(\text{OtBu})_9(\text{THF})_9$ et que les complexes à base de néodyme sont régulièrement les plus actifs en catalyse de polymérisation, nous avons choisi de nous focaliser sur le système d'amorçage $\text{Nd}_3(\text{OtBu})_9(\text{THF})_9/\text{DHM}$.

43.2.1. Influence du rapport Nd/Mg

Des rapports Nd/Mg de 0,33 à 10 ont été étudiés. Les chromatogrammes montrent clairement que les rapports Nd/Mg élevés conduisent à un enrichissement en PMAM de faible polymolécularité ($M_w/M_n < 1,20$) (Figure 27) tout en gardant le même niveau de syndiotacticité. Les résultats sont reportés dans le Tableau 6.

Figure 27. Chromatogrammes GPC de PMAM obtenus avec la combinaison 1/DHM (X) Nd/Mg = 0,33; (+) Nd/Mg = 1,0; (o) Nd/Mg = 3,3; (Δ) Nd/Mg = 5,0 and () Nd/Mg = 10.



La rapide formation de PMAM de haute masse, comparativement à la formation relativement lente et continue de PMAM de faible polymolécularité, est prépondérante à faibles rapports Nd/Mg. Ce phénomène pourrait être attribué à une polymérisation anionique incontrôlée amorcée par le DHM résiduel. Toutefois, les tacticités obtenues sont en désaccord avec cette hypothèse et la formation d'une seconde espèce active "non contrôlée" est envisagée.

Tableau 6. Influence du rapport Nd/Mg en polymérisation du MAM.

Nd/Mg	conv. (%)			tacticité (%)		
		$M_n(10^{-3})$	M_w/M_n	rr	mr	mm
(wt%)						
0,33	85	9,4	2,5	59	18	23
1,0	100	16	8,2	76	16	8
3,3	100	150	3,1	77	16	7
5,0	100	70 ^a	1,80 ^a	77	20	3
10	40	86	1,06	76	22	2

Conditions: une solution de DHM et de **1** (0,33 mmol; 1,0 mmol Nd) est agitée pendant 1 h dans le toluène à température ambiante; le MAM est ensuite additionné par seringue et le mélange réactionnel est agité pendant 1 h à 0 °C. ^a valeur moyenne sur l'ensemble du polymère.

43.2.2. Températures d'activation et de polymérisation

Etant donné que les espèces actives sont censées être des composés instables de type alkyl-Nd, nous pouvons considérer que diminuer la température d'activation et/ou de polymérisation devrait conduire à une meilleure efficacité d'amorçage et donc à une meilleure activité. Les résultats obtenus en menant l'activation (prémélange **1**/DHM) à -20 °C sont en accord avec cette supposition puisque l'efficacité d'amorçage est doublée, la polymolécularité plus faible et la syndiotacticité encore plus élevée (Tableau 7).

Tableau 7. Effet de la température d'activation en polymérisation du MAM.

Nd/Mg	conv. (%)	$M_n(10^{-3})$	M_w/M_n	tacticité (%)		
				rr	mr	mm
3,3	100	150	3,1	77	16	7
3,3	100	130	1,78	78	19	3
5,0	100	54	1,26	78	19	3
10	40	80	1,06	76	22	2

Conditions: une solution de DHM et **1** (0,33 mmol; 1,0 mmol Nd) est agitée pendant 1 h dans le toluène à -20 °C; le MAM est ensuite additionné par seringue et le mélange réactionnel est agité pendant 1 h à 0 °C.

Diminuer la température de polymérisation permet d'augmenter la syndiotacticité. Par contre, il semble qu'une température de polymérisation de 0 °C soit optimale pour obtenir de faibles polymolécularités (Tableau 8).

Tableau 8. Effet de la température de polymérisation.

$T_{\text{polym}} (\text{°C})$	conv. (%)	$M_n(10^{-3})$	M_w/M_n	tacticité (%)		
				rr	mr	mm
-20	100	89	4,8	80	15	5
0	100	54	1,26	76	21	3
20	100	59	3,1	77	21	2

Conditions: une solution de DHM et **1** (0,33 mmol; 1,0 mmol Nd) est agitée pendant 1 h dans le toluène à 0 °C; le MAM est ensuite additionné par seringue et le mélange réactionnel est agité pendant 1 h à différentes températures.

43.3.Nature de l'agent alkylant

La formation hypothétique d'une espèce active de type alkyl-Ln nous a incité à étudier d'autres agents alkylants; des réactions de transmétallation avec des alcoolates de lanthanide ont déjà été décrites avec des dérivés lithiés et aluminiques.^{218-220,222,290} L'utilisation d'un équivalent de *n*-BuLi (vs. Nd) donne un PMAM isotactique (mm = 74%) avec un faible

rendement. Des résultats similaires en termes de tacticité et polymolécularité ont été obtenus avec le *t*-BuLi mais avec une conversion totale du monomère. L'utilisation de tris(alkyl) aluminium a mené à la préparation de PMAM atactique alors que BEt₃ et KH se sont avérés inefficaces (Tableau 9).

Tableau 9. Influence de la nature de l'agent alkylant.

agent alkylant	Nd/M	conv. (%)	tacticité (%)			M _n (10 ⁻³)	M _w /M _n
			rr	mr	mm		
<i>n</i> -BuLi	1,0	13	6	21	73	18,7	3,6
<i>t</i> -BuLi	2,0	100	15	15	70	25,0	4,7
AlMe ₃	1,0	6	37	33	30	nd	nd
BEt ₃	1,0	0	-	-	-	-	-
KH	1,0	0	-	-	-	-	-

Conditions: une solution de RM et **1** (0,33 mmol; 1,0 mmol Nd) est agitée pendant 1 h dans le toluène à 0 °C; le MAM est ensuite additionné par seringue et le mélange réactionnel est agité pendant 1 h à 0 °C.

Il semble donc que seuls les dialkylmagnésiens génèrent, lorsqu'ils sont associés à **1**, des espèces actives pour la polymérisation pseudo-vivante et syndiotactique du PMAM. Nous avons vérifié cette hypothèse en utilisant d'autres dérivés du magnésium. Tous conduisent effectivement à un PMAM syndiotactique mais le contrôle de la polymérisation n'est observé qu'avec les dialkylmagnésiens (Tableau 10).

Tableau 10. Influence de la nature du dérivé de magnésium.

MgR ₂ /RMgX	conv. (%)	M _n (10 ⁻³)	M _w /M _n	tacticité (%)		
				rr	mr	mm
BEM	25	110	1,12	80	15	5
Mg(<i>n</i> -Hex) ₂	20	130	1,08	80	18	2
Mg(CH ₂ SiMe ₃) ₂ •Et ₂ O ^a	100	0	-	-	-	-
EtMgBr ^a	92	124	3	80	17	3
PhMgBr ^a	60	38	9	82	14	4

Conditions: une solution de RM (0,02 mmol Mg) et **1** (0,33 mmol Nd) est agitée pendant 1 h dans le toluène à 0 °C; le MAM est ensuite additionné par seringue et le mélange réactionnel est agité pendant 1 h à 0 °C.

^a 0,5 mmol Mg.

43.4. Nature du précurseur de néodyme

Les résultats très intéressants obtenus avec le complexe **1** nous ont encouragé à étendre notre recherche à d'autres précurseurs inorganiques de néodyme. Les composés évalués dans nos conditions standards de polymérisation sont "Nd(O*t*Bu)₃" (**4**), "Nd(O*t*Am)₃" (**9**), Nd(OAr)₃ (THF) (**12**) et Nd[N(SiMe₃)₂]₃ (Tableau 11).

Tableau 11. Précurseurs inorganiques de Nd associés au DHM pour la polymérisation du MAM.

précurseur Nd	Nd/Mg	conv. (%)	tacticité (%)			$M_n(10^{-3})$	M_w/M_n
			rr	mr	mm		
"Nd(O <i>t</i> Bu) ₃ " (1)	5,0	100	77	20	3	70	1,8
"Nd(O <i>t</i> Bu) ₃ " (4)	5,0	79	80	15	5	360	2-3
"Nd(O <i>t</i> Am) ₃ " (9)	5,0	5	nd	nd	nd	nd	nd
Nd(OAr) ₃ (THF) (12)	1,0	11	35	32	33	nd	nd
Nd{N(SiMe ₃) ₂ } ₃	1,0	16	20	18	62	16,3	27

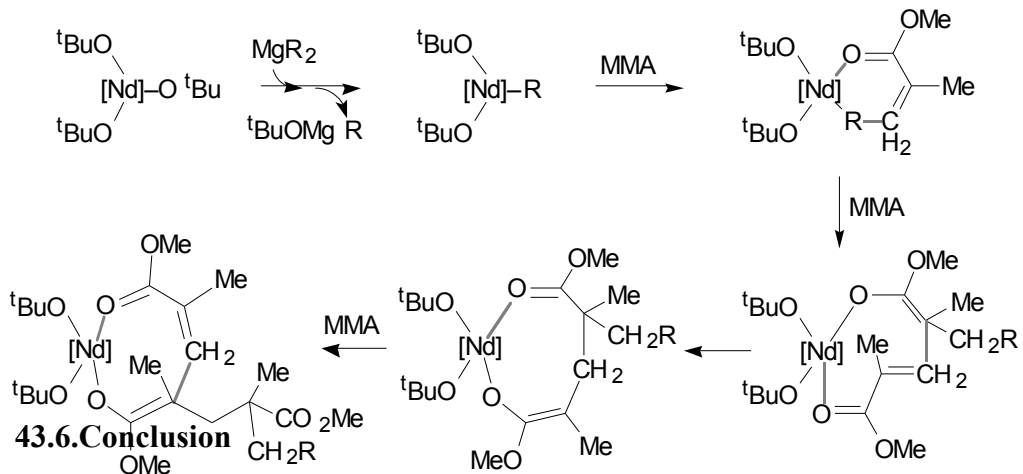
Conditions: une solution de RM et **1** (1,0 mmol) est agitée pendant une heure dans le toluène à 0 °C; le MAM est ensuite additionné par seringue et le mélange réactionnel est agité pendant 1 h à 0 °C.

La voie de synthèse du tertiobutylate de néodyme semble très importante puisque **1** et **4** ne conduisent pas aux mêmes résultats. Cette différence est en accord avec la différence de structure des complexes **1** et **4** (§42.2.1.1.2) et montre la très grande sensibilité du système catalytique à la structure du précurseur de Nd. De même, le tertioamylate **9**, censé posséder une structure identique à **1**, ne permet qu'une très faible conversion du monomère. Le phénate encombré **12** ne se montre pas beaucoup plus actif et donne un PMAM atactique. Enfin, on peut noter que Nd{N(SiMe₃)₂}₃ conduit à un PMAM isotactique, ce qui montre une fois encore que prévoir l'activité et la stéréospécificité de ces systèmes binaires est délicate.

43.5. Mécanisme proposé

Ces résultats montrent que l'association du DHM à **1** conduit à la formation d'une espèce responsable de la polymérisation pseudo-vivante et syndiotactique du MAM. Les caractéristiques de la polymérisation sont en accord avec ceux obtenus avec les systèmes lanthanocéniques et renforce l'hypothèse de la formation *in situ* d'une espèce alkylalcooxy-lanthanide.^{116,117} De plus, les résultats médiocres obtenus à des températures supérieures à 20 °C sont en accord avec la grande instabilité d'une espèce alkyl-lanthanide. Un mécanisme pour la formation de l'espèce active et son utilisation en polymérisation du MAM est proposé.

Schéma 12. Mécanisme de polymérisation amorcée par Nd₃(O*t*Bu)₉(THF)₂/DHM.



En conclusion, un nouveau système d'amorçage composé de Nd₃(OtBu)₉(THF)₂ et de di-*n*-hexylmagnésium a été développé pour la polymérisation pseudo-vivante et hautement syndiotactique du MAM. L'avantage majeur de ce système réside dans sa simplicité. Il procure ainsi une intéressante alternative aux systèmes lanthanocéniques pour la polymérisation du MAM dans des conditions opératoires attrayantes.

44. Homopolymérisation de l'éthylène et copolymérisation dibloc éthylène-MAM

La formation *in situ* d'une espèce alkyl-Ln à partir du système 1/DHM nous a encouragés à étudier ce type de système pour la polymérisation de l'éthylène. Une étude préliminaire a montré que les alcoolates de lanthanide ne polymérisent pas l'éthylène. L'insertion de l'éthylène dans la liaison Ln-O est en effet défavorisée, une étude thermodynamique l'ayant d'ailleurs montré.¹⁵⁷ Ainsi, diverses associations alcoolates de lanthanide/agent alkylant ont été testées en variant les conditions opératoires (rapport Ln/RM, température et temps de réaction...). Le screening des différents agents alkylants s'est avéré surprenant puisque seuls les dialkylmagnésiens ont conduit à une polymérisation de l'éthylène. Lithiens, aluminiques, réactifs de Grignard se sont avérés inefficaces. Par conséquent, nous avons concentré notre étude sur les systèmes "Ln(OR)₃"/MgR₂.

44.1. Etude préliminaire des systèmes "Ln(OR)₃"/MgR₂

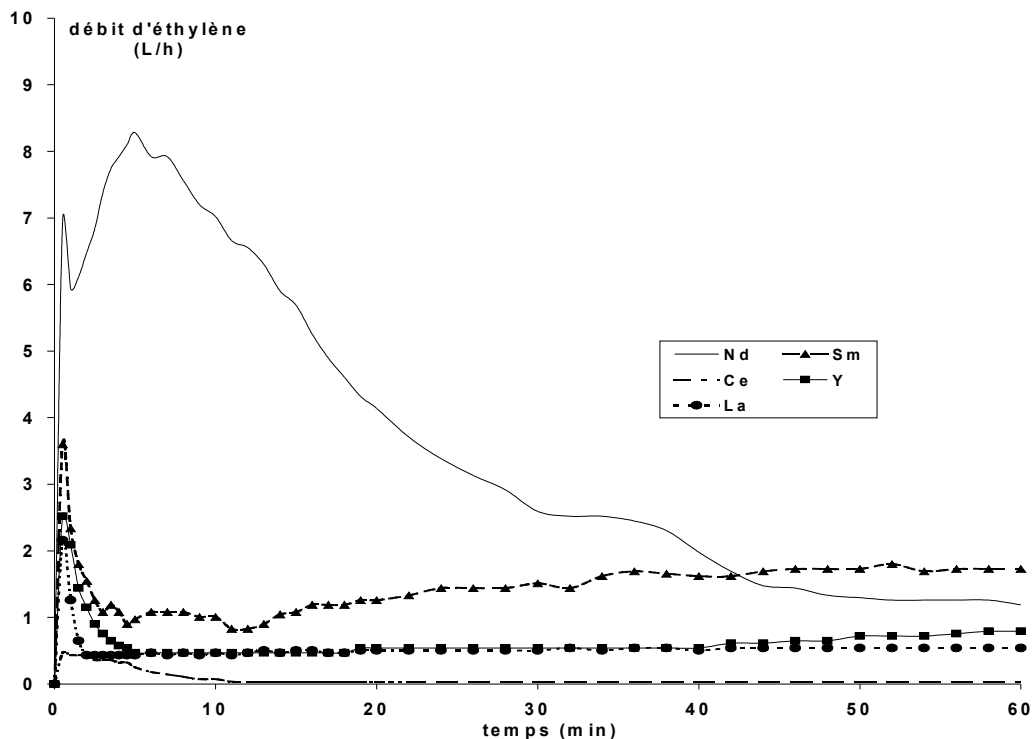
Les principaux paramètres qui ont été étudiés sont la nature du lanthanide, la nature de l'alcoolate et enfin la voie de synthèse des complexes. Les conditions de polymérisation sont identiques aux conditions standards de polymérisation du MAM définies précédemment à une exception près: le rapport Ln/Mg est fixé à 1,0.

La nature du métal a été modifiée avec le ligand tertiobutylate. Ainsi, les tertiobutylates de lanthane, d'yttrium, de cérium^(III), de samarium^(III) et de néodyme ont été préparés par réaction de LnCl₃ et de 3 équivalents de NaOtBu dans le THF (voir §42.2.1.1.1). Les courbes de

consommation d'éthylène pour différents systèmes "Ln(O*t*Bu)₃"/DHM sont reportées sur le graphique suivant (Figure 28).

De faibles activités (0,02-1,60 kgPE/molLn/atm/h) ont été observées avec tous ces complexes, sauf avec le complexe à base de néodyme qui présente en plus d'une meilleure activité (4-5 kgPE/molLn/atm/h), un profil de consommation différent. En effet, dans ce cas, l'activité initiale est très élevée et décroît avec la précipitation du polymère. Ce polymère est insoluble dans les conditions d'analyse de la GPC (135 °C dans le 1,2,4-trichlorobenzène) suggérant une masse molaire élevée. Le polyéthylène recueilli après 5 min de polymérisation offre une polymolécularité relativement faible pour ce type de catalyse ($M_w/M_n = 2,3$), indiquant l'existence d'une seule espèce active. Etant donné ces derniers résultats, nous nous sommes focalisés sur l'utilisation de complexes de néodyme.

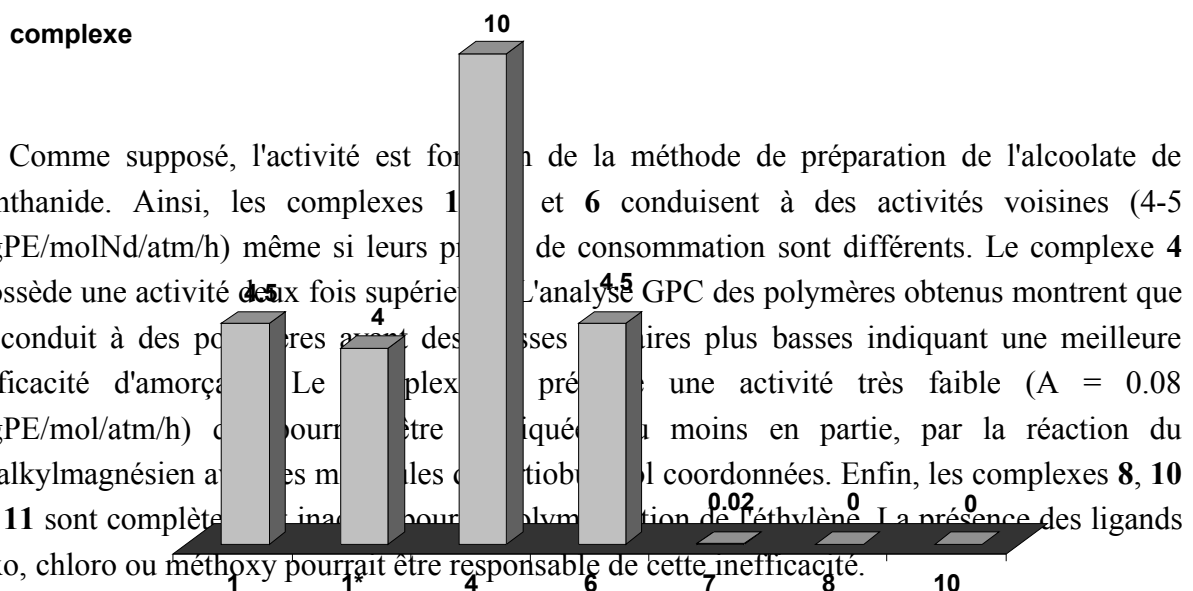
Figure 28. Consommation d'éthylène observée avec divers systèmes "Ln(O*t*Bu)₃"/DHM (Ln/DHM = 1.0; 1 atm; activation 1 h à 0 °C puis polymérisation 1 h à 0 °C).



De nombreux alcoolates de néodyme "Nd(OR)₃" ont été synthétisés, soit par métathèse ionique (OR = O*t*Bu (**1**), O*t*Am (**9**), OCMe₂Ph, O*i*Bu, O*i*Pr, O-2,6-*t*Bu-4-Me-C₆H₂ (**12**))), soit par alcoolyse de NdN₃ (OR = OC*t*Bu₃). Les meilleures activités sont rencontrées avec les tertiobutylate et tertioamylate. Contrairement à la polymérisation du MAM, ces deux complexes supposés isostructuraux, possèdent des activités similaires, suggérant un accès du monomère au centre métallique comparable. Les complexes plus encombrés que sont Nd(O-2,6-*t*Bu-4-Me-C₆H₂)₃(THF) (**12**) et Nd(OC*t*Bu)₃(THF) montrent une certaine activité lorsqu'ils sont activés à température ambiante alors que les autres complexes sont quasiment inactifs.

Etant donné les différents résultats obtenus par **1** et **4** en polymérisation du MAM (voir §43.4), il était important d'étudier l'influence de la voie de synthèse des tertiobutylates de néodyme sur l'activité de polymérisation (voir §42.3 pour un résumé des différentes voies de synthèse). Les résultats sont reportés sur la Figure 29.

Figure 29. Activité en polymérisation de l'éthylène amorcée par différents "Nd(O*t*Bu)₃": influence de la voie de synthèse (Ln/DHM = 1.0; 1 atm; activation 1 h à 0 °C puis polymérisation 1 h à 0 °C).



En conclusion, nous devons être extrêmement attentifs à l'origine, à la structure, et à la composition du tertiobutylate de néodyme utilisé comme précurseur de polymérisation de l'éthylène. En effet, la formation des espèces actives est fortement dépendante de ces paramètres. Nous avons donc décidé de poursuivre notre étude en utilisant uniquement le complexe Nd₃(OtBu)₉(THF)₂ (**1**) puisqu'il permet aussi la polymérisation pseudo-vivante du MAM. La possibilité d'une copolymérisation dibloc éthylène-MAM étant une perspective très attrayante.

44.2. Polymérisation de l'éthylène en slurry amorcée par Nd₃(OtBu)₉(THF)₂

En vue de l'optimisation du système catalytique formé par Nd₃(OtBu)₉(THF)₂ associé à un dérivé dialkylmagnésien, nous avons étudié les différents paramètres qui pourraient affecter l'activité de polymérisation.

D'abord, la nature du dialkylmagnésien a été modifiée. Les meilleurs résultats ont été obtenus avec les dialkylmagnésiens porteurs de longues chaînes aliphatiques tels que le DHM et le Mg(*n*-Bu)(*s*-Bu). L'utilisation de BEM ou de (bistriméthylsilyl)magnésium ne permet pas d'accroître l'activité, bien au contraire. La structure polymérique du premier et l'encombrement stérique des groupes alkyles du second pourraient expliquer ce résultat. Par conséquent, seul le di-*n*-hexylmagnésium sera utilisé dans le reste de l'étude.

Le rapport Nd/Mg a aussi été étudié, même si contrairement au MAM, aucune polymérisation anionique secondaire n'est possible. Cette étude s'est avérée pertinente puisque le maximum d'activité est obtenu pour un rapport Nd/Mg = 1,0. Modifier légèrement ce rapport s'accompagne d'une baisse d'activité. Ceci contraste fortement avec les systèmes chlorolanthanocéniques qui s'accommode généralement d'un excès de magnésien.⁵² C'est donc un rapport Nd/Mg = 1,0 qui sera utilisé pour le reste de l'étude.

L'activation ou alkylation du précurseur est une étape primordiale puisqu'elle génère les espèces actives. En conséquence, en fonction de la cinétique de formation de ces espèces et de leur stabilité, modifier la température et le temps d'activation pourrait conduire à la formation d'un plus grand nombre d'espèces et donc à de meilleures activités. Les résultats consignés dans le Tableau 12 montrent qu'augmenter la température ou le temps d'activation conduit à de plus faibles activités. Ceci est cohérent avec la supposée instabilité des espèces alkyl-Ln en absence de monomère (*vide infra*). De plus, une température d'activation trop basse ou une absence d'activation conduit au même résultat.

Tableau 12. Influence des conditions d'activation sur l'activité de polymérisation avec **1/DHM**.

T _{alkyl} (°C)	t _{alkyl} (min)	T _{polym} (°C)	PE (g)
-78	60	0	1,60
0	0	0	2,50
0	60	0	4,70
0	180	0	1,69
20	60	0	1,09

Ln/DHM = 1.0; 1 atm; activation 1 h puis polymérisation 1 h à 0 °C.

Les températures d'activation et de polymérisation affectent la polymérisation de la même manière (Tableau 13). Ainsi, une meilleure activité est observée à -50 °C alors que celle-ci décroît lorsque la température dépasse 20 °C. A 80 °C, un PE de basse masse, riche en doubles liaisons terminales, est obtenu.

Tableau 13. Influence de la température de polymérisation avec **1**/DHM system (Nd/Mg = 1,0).

température (°C)	t. polymn (min)	M _n	M _w /M _n	activité (kgPE/molNd/atm/h)
-50	30	non soluble	-	9,0
0	60	non soluble	-	4,5
80	35	1720	1,55	1,0

Ln/DHM = 1.0; 1 atm; activation 1 h à 0 °C puis polymérisation 1 h.

44.2.1. Effet de certains additifs sur l'activité de polymérisation

De nombreux additifs ont été testés en polymérisation de l'éthylène afin de stabiliser les espèces actives et/ou de désagréger le dialkylmagnésien. Bien que le complexe **1** comprenne deux molécules de THF coordonnées, l'addition d'un équivalent supplémentaire par Nd inhibe totalement la polymérisation. L'addition d'un équivalent de NaCl (ou KCl) vs. Nd a le même effet, tout comme l'addition d'un équivalent d'hexaméthylphosphoramide ou de diméthylsulfoxyde. Ces résultats sont en relation directe avec l'inefficacité des réactifs de Grignard comme agent alkylant et celle des complexes **7** and **11** puisque tous possèdent une base de Lewis dans leur structure.

44.2.2. Polymérisation en présence d'agent de transfert

Comme nous l'avons indiqué précédemment, le système catalytique **1**/DHM mène à la préparation de PE de très haute masse molaire, le polymère étant insoluble dans les conditions normales d'analyse des polyoléfines. Par conséquent, nous avons étudié l'utilisation d'agents de transfert. D'abord, en présence de phénylsilane, des polyéthylènes de basses masses, terminés par un groupement PhSiH₂, sont obtenus (11 900 et 2400 g/mol) comme il l'a été observé avec les catalyseurs lanthanocéniques.⁶⁹ L'hydrogène (2 vol.%) se révèle être un meilleur agent de transfert. En plus d'une diminution des masses molaires, masses constantes au cours de la réaction, une augmentation d'activité est notée (9–10 kgPE/molNd/atm/h).

Tableau 14. Polymérisation en présence d'hydrogène (Nd/Mg = 1,0).

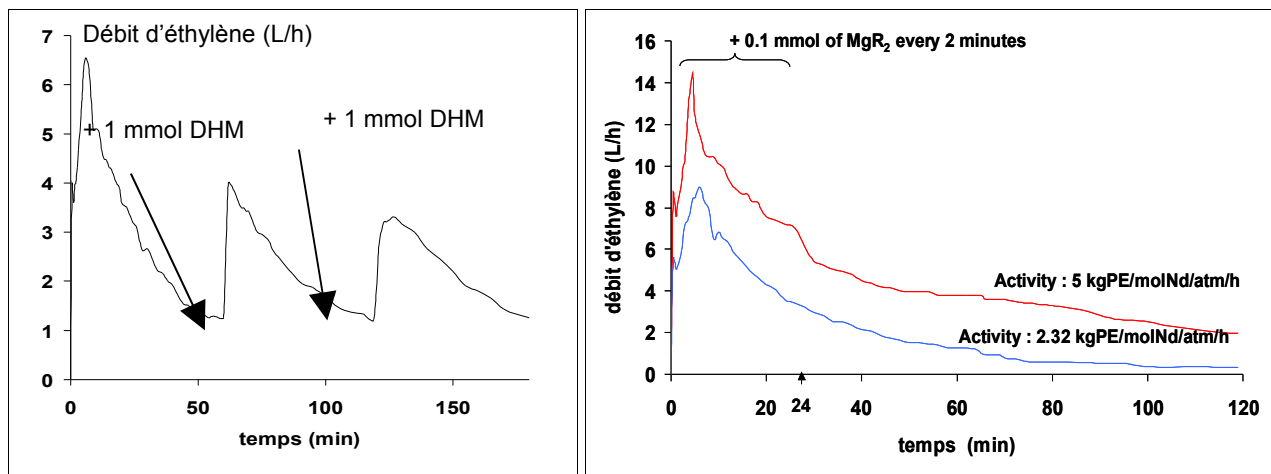
H ₂ (%)	M _n (10 ⁻³)	M _w /M _n	T _f (°C)	Activité (kgPE/molNd/atm/h)
0	non soluble	-	140-143	4-5
1	non soluble		140	10
2	310	2,4	139	9,6
10	27	10,6	137,5	8,8

Ln/DHM = 1.0; 1 atm; activation 1 h à 0 °C puis polymérisation 1 h à 0 °C.

44.2.3. Addition de dialkylmagnésium en cours de polymérisation

Il a été observé que l'addition de dialkylmagnésium en cours de polymérisation permet aussi un gain d'activité. L'ajout de ce dernier (1 équiv. vs. Nd) après une heure de réaction résulte en une restauration partielle (70%) de l'activité initiale, restauration qui a pu être notée 3 fois consécutivement. L'addition répétée de 0,1 mmol de DHM toutes les 2 minutes pendant 25 minutes permet quant à elle de doubler l'activité sur 2 heures de polymérisation. Ces résultats pourraient être justifiés par le rôle de piège à impuretés joué par le DHM ou par la création de nouvelles espèces actives. De plus, ils confirment que la perte d'activité observée au cours de la polymérisation provient probablement de l'hétérogénéisation du système catalytique.

Figure 30. Réactivation du système 1/DHM par addition de DHM.



44.3. Polymérisation de l'éthylène avec le polymère précipité (S)

44.3.1. Principe

Après 10-15 minutes de polymérisation, le mélange réactionnel peut être filtré et divisé en 2 parties: une partie solide constituée du polymère précipité **S** et une phase liquide **Liq**. L'analyse du polymère précipité **S** a permis de montrer la présence de $15 \pm 2\%$ du Nd initial et de $20 \pm 4\%$ du Mg, correspondant à un rapport Nd/Mg dans **S** de $1,2 \pm 0,4$, valeur proche du rapport initial ($\text{Nd/Mg} = 1,0$). Le précipité **S** placé dans du toluène permet de polymériser l'éthylène avec une activité similaire à celle observée avant l'isolation de **S** alors que la solution résultante **Liq** est complètement inerte vis-à-vis de l'éthylène. L'addition de 1,0 équiv. de DHM vs. Nd à **S** conduit à une importante augmentation de l'activité de polymérisation (100 kgPE/molNd/atm/h). L'analyse du polymère résultant montre qu'il n'y a pas de redistribution du Nd entre les phases solide et liquide, éliminant toute possibilité de réaction de transmétallation entre le DHM et l'espèce active. Il semble donc que le DHM agit comme supposé précédemment en tant que "scavenger" ou plus probablement comme générateur d'espèces actives.

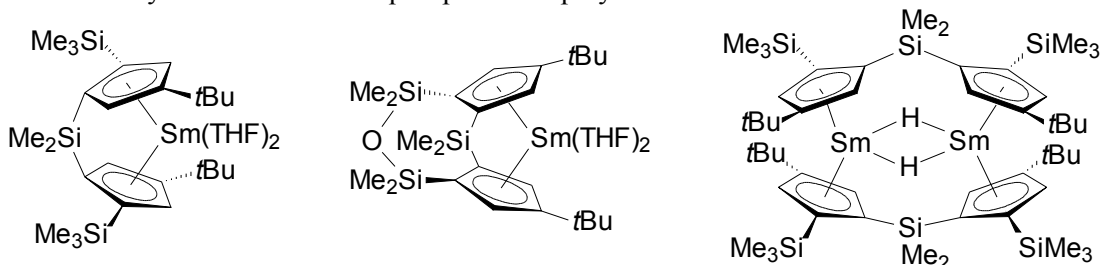
44.4.Copolymérisation dibloc PE-*b*-PMAM

44.4.1. Synthèse de copolymères diblocs oléfine-MAM

La possibilité de produire des polyoléfines fonctionnalisées est un véritable challenge puisque ces matériaux permettent d'améliorer certaines propriétés telles que la rigidité, l'adhésion, les propriétés de surface, la miscibilité de polymères... Différentes techniques ont été décrites dans la littérature pour la préparation de ces matériaux.

Ainsi, les premières copolymérisations diblocs contrôlées de l'éthylène et du MAM ont été obtenues avec des catalyseurs lanthanocéniques de type Cp^*LnR ($\text{Ln} = \text{Sm}, \text{Yb}, \text{Lu}; \text{R} = \text{H}, \text{Me}$).¹²¹ La réaction s'effectue en 2 étapes. Une prépolymérisation de l'éthylène est suivie d'une polymérisation du MAM, l'ordre inverse de polymérisation ne menant qu'à la formation d'homo-PMAM. Cette méthode permet la synthèse de copolymères de masses molaires relativement basses ($M_n < 25\,000 \text{ g/mol}$) comportant jusqu'à 50 mol% de MAM. De plus hautes masses ont pu être obtenues avec $[\text{Me}_2\text{Si}(\text{C}_5\text{H}_3\text{-SiMe}_3)_2\text{SmH}]_2$ avec toujours une teneur en MAM conséquente (20 mol%)²⁹⁵ et de bons résultats ont été obtenus avec le complexe *meso* $\text{Me}_2\text{Si}(\text{Me}_2\text{SiOSiMe}_2)\text{-}(\text{C}_5\text{H}_2\text{-3-}t\text{Bu})_2\text{Sm}(\text{THF})$ et le racémique $\text{Me}_2\text{Si}(2\text{-SiMe}_3\text{-4-}t\text{BuMe}_2\text{SiC}_5\text{H}_2)\text{Sm}(\text{THF})_2$.¹¹⁷

Figure 31. Catalyseurs lanthanocéniques pour la copolymérisation dibloc PE-*b*-PMAM.²⁹⁵



L'utilisation de catalyseurs à base de métaux du groupe 4 pour la préparation de copolymères diblocs PE-PMAM ou PP-PMAM a aussi été décrite. Les résultats peuvent être regroupés en 2 catégories. Dans la première, la polymérisation de l'oléfine par catalyse organométallique est suivie par une polymérisation radicalaire ou anionique du méthacrylate. Ainsi, des copolymères PE-PMAM ont été préparés en utilisant un catalyseur Ziegler-Natta traditionnel associé à un agent de transfert tel que ZnEt_2 , suivie de la polymérisation radicalaire du MAM.²⁹⁸ L'utilisation d'un agent de transfert a aussi été appliquée aux systèmes métallocéniques. Ainsi, l'addition d'un dérivé du bore (9-BBN) conduit à la préparation d'un polymère fonctionnalisé qui après oxydation sous oxygène en présence de MAM mène à la formation d'un copolymères PE-PMAM.²⁹⁹ La copolymérisation éthylène-alcool allylique permet la synthèse d'un PE hydroxylé, qui après fonctionnalisation, génère un macroamorceur actif en ATRP du MAM.³⁰¹ Enfin un copolymère poly(propylène)-*b*-poly(méthacrylate de méthyle) a été préparé en utilisant un PP terminé par une fonction MgBr , amorceur de la polymérisation anionique du MAM.³⁰³ Dans la seconde catégorie, le catalyseur organométallique joue le rôle de catalyseur/amorceur pour les polymérisations de

l' α -oléfine et du MAM, comme le font les catalyseurs lanthanocéniques. Les premiers résultats ont été obtenus avec le complexe $\text{Me}_2\text{C}(\text{Cp})(\text{Ind})\text{ZrMe}_2$ activé par $\text{B}(\text{C}_6\text{F}_5)_3$.³⁰⁵ L'ordre d'addition éthylène puis MAM est fondamental comme il a été observé avec les complexes de lanthanide. Dans ce cas, les masses molaires sont plutôt faibles ($M_n = 12\,000$ - $17\,000$) et le PMAM est hautement isotactique. L'obtention d'un copolymère dibloc possédant un bloc PMAM syndiotactique est possible avec $[\text{Me}_2\text{Si}(\eta^5\text{-Me}_4\text{Cp})(t\text{BuN})\text{TiMe}][\text{MeB}(\text{C}_6\text{F}_5)_3]$, conduisant à un copolymère de très faible polymolécularité ($M_w/M_n = 1,08$ - $1,14$).³⁰⁶ Il a aussi été remarqué que le type d'activateur régissait le rapport entre copolymère et homopolymère.

Enfin, une dernière technique a aussi été développée pour la préparation de copolymères diblocs PE-PMAM: l'hydrogénéation sélective du bloc polybutadiène d'un copolymère polybutadiène-*b*-poly(méthacrylate de méthyle) préparé par polymérisation anionique.³⁰⁷

44.4.2. Copolymérisation dibloc éthylène-MAM

*44.4.2.1. Système *in situ**

Etant donné la possibilité d'amorcer/catalyser les polymérisations du MAM et de l'éthylène en utilisant le système **1**/DHM, il était impératif de tester notre système en copolymérisation dibloc éthylène-MAM. La réaction a d'abord été réalisée en slurry par addition de MAM après 15 min de prépolymérisation de l'éthylène, l'ordre inverse d'addition conduisant à la formation unique de PMAM. L'extraction au THF du polymère final montre la formation de 15% en poids de PMAM atactique. Ceci peut être aisément expliqué par la présence d'espèces actives pour la polymérisation anionique du MAM dans la solution de polymérisation (**Liq**).

*44.4.2.2. Utilisation du solide **S** comme amorceur de copolymérisation*

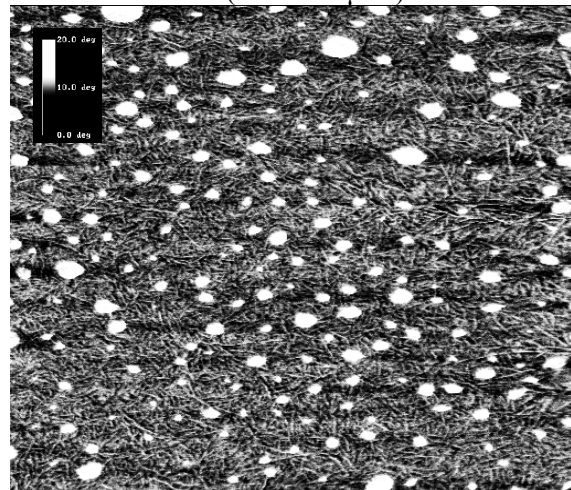
Par contre, l'utilisation de **S** comme macroamorceur permet de ne retirer que 3% en poids du copolymère synthétisé, 3 % attribuables à un copolymère éthylène-MAM de basse masse molaire et riche en MAM. La teneur en MAM de ces copolymères varie typiquement entre 5 et 11 mol%. De plus, toutes les techniques analytiques (GPC, RMN, DSC) sont en accord avec la structure dibloc du copolymère. A notre connaissance, ces copolymères possèdent les masses molaires les plus élevées jusque-là obtenues pour ce type de matériaux ($M_n = 250\,000$).

44.4.2.3. Etude morphologique

En plus des techniques habituelles de caractérisation (RMN, GPC), nous avons décidé d'étudier la morphologie de nos copolymères par deux techniques microscopiques complémentaires : la microscopie par force atomique (AFM) et la microscopie à transmission électronique. Nous ne décrirons ici que les résultats préliminaires obtenus en AFM sur un copolymère dont les caractéristiques sont $M_n = 420\,000$, $M_w/M_n = 4,5$ et une teneur en MAM de 11 mol%.

Les clichés obtenus montrent nettement une séparation de phase entre les parties polaires et apolaires contrairement à ce qui a été observé par Yasuda *et al.*²⁹⁶ Les masses molaires plus élevées ainsi qu'une teneur en MAM plus faible pourraient expliquer ce phénomène. Le matériau constitué d'une matrice PE cristalline contient une multitude de domaines amorphes sphériques de diamètre compris entre 75 et 300 nm. Ces domaines amorphes, attribués au PMAM ou à un mélange PE-PMAM, sont régulièrement distribués mais leur taille reste hétérogène, ce qui pourrait être imputé à la distribution des masses molaires relativement large.

Figure 32. Cliché AFM (mode phase) d'un copolymère of PE-*b*-PMMA ($3.0 \times 3.0 \mu\text{m}^2$).

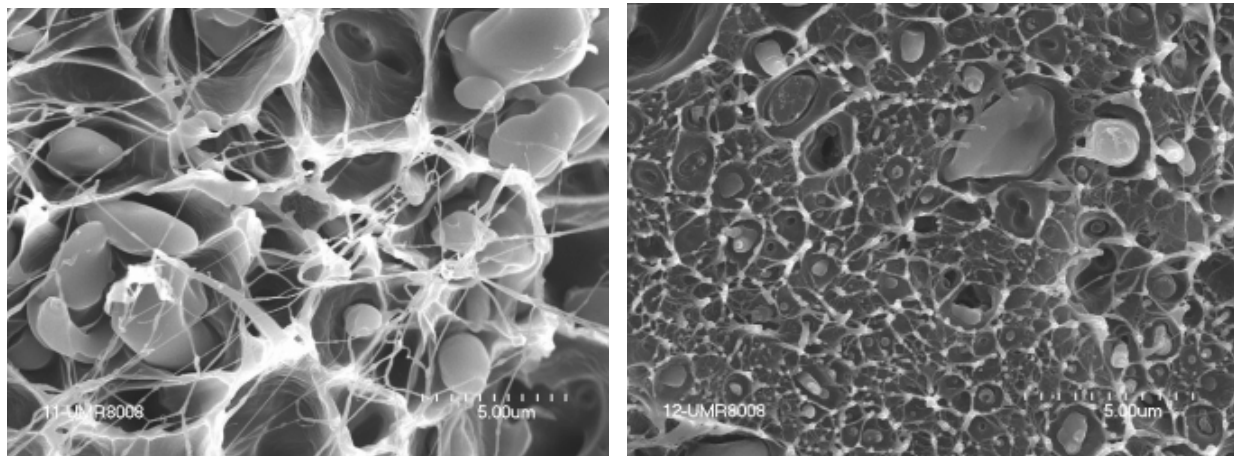


44.4.2.4. Application comme agent compatibilisant

Afin de vérifier l'application potentielle de nos copolymères comme agent compatibilisant de mélanges PE/PMAM, deux polymères immiscibles, nous avons préparé différents mélanges PE/PMMA (80/20 wt%) et PE/PMMA/copolymère (73/18/9 wt%) à l'aide d'une extrudeuse à double vis. Ces mélanges ont ensuite été étudiés par microscopie électronique à balayage. Les clichés obtenus sont en accord avec un effet compatibilisant puisqu'une homogénéité accrue de l'échantillon est observée. Ces premiers résultats sont encourageants et donneront suite à une étude plus poussée par microscopie électronique à transmission.

Tout comme les systèmes lanthanocéniques, le système catalytique composé de **1** associé au DHM permet la copolymérisation dibloc éthylène-MAM. La nature dibloc de ces copolymères a été prouvée par GPC, RMN et AFM, et leur application en tant qu'agent compatibilisant de mélanges PE/PMAM a été évaluée par microscopie électronique à balayage. Toutefois, une étude morphologique plus approfondie de ces nouveaux matériaux ainsi qu'une évaluation des propriétés mécaniques des mélanges PE/PMAM/copolymères doivent encore être effectuées.

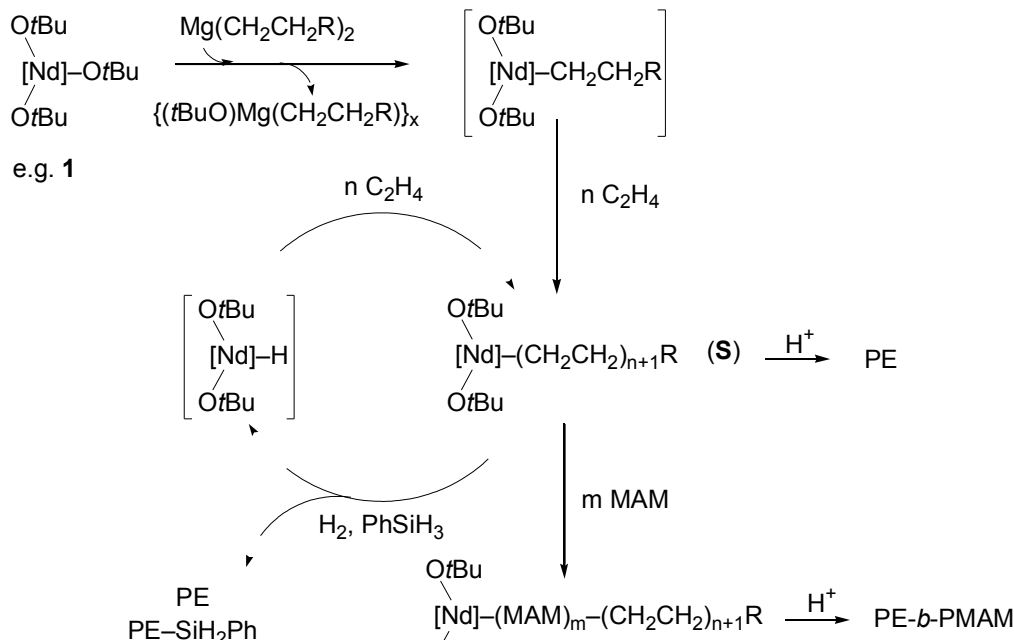
Figure 33. Clichés obtenus par microscopie électronique à balayage de mélanges PE/PMMA (gauche) et PE/PMMA/copolymère ($20 \times 15 \mu\text{m}^2$).



44.4.3. Mécanisme

Les résultats ci-dessus, en particulier les réactions de transfert au phénylsilane et à l'hydrogène, la polymérisation pseudo-vivante et syndiotactique du MAM, et la copolymérisation dibloc éthylène-MAM sont en relation directe avec la réactivité observée avec les catalyseurs lanthanocéniques. Ceci est cohérent avec un mécanisme de polymérisation par coordination-insertion dans lequel l'espèce active alkyl-Nd est formée *in situ* par alkylation de **1** par le DHM. Le Schéma 13 décrit le mécanisme proposé pour la formation de l'espèce Nd-Hex et son utilisation comme amorceur de polymérisation.

Schéma 13. Proposition de mécanisme pour la (co)-polymérisation de l'éthylène amorcée/catalysée par **1**/DHM.



Cependant, ce système catalytique est complètement inert vis-à-vis des α -oléfines longues (hex-1-ène et oct-1-ène) dans les conditions standards de polymérisation. En effet, une polymérisation de l'éthylène effectuée dans l'octène ou dans le toluène conduit à une activité

identique. Toutefois, la formation de complexes π -allyliques stables ne peut être exclue en présence de propène.

45. (Co)-Polymérisation du butadiène

La préparation de polybutadiène hautement stéréospécifique est très importante pour des applications industrielles.^{171a} Parmi les différents systèmes catalytiques utilisés, les systèmes à base de lanthanide ont montré un potentiel très intéressant grâce à leurs hautes activités et stéréospécificités.^{171c} Toutefois, un meilleur contrôle de la polymérisation est actuellement recherché afin de préparer de nouveaux matériaux par copolymérisation.³¹²

Nous allons maintenant décrire l'utilisation d'alcoolates/phénates de néodyme ($\text{Nd}_3(\text{OtBu})_9$)₂ (1), $\text{Nd}(\text{O}-2,6-t\text{Bu}_2-4-\text{Me}-\text{C}_6\text{H}_2)_3$ (THF) (12), et $\text{Nd}(\text{O}-2,6-t\text{Bu}_2-4-\text{Me}-\text{C}_6\text{H}_2)_3$ (13)) associé à un dialkylmagnésien pour la polymérisation du butadiène (BD) et ses copolymérisations statistique avec le styrène (St) et dibloc avec le méthacrylate de glycidyle (GMA).

45.1. Homopolymérisation

45.1.1. Avec $\text{Nd}_3(\text{OtBu})_9(\text{THF})_2$

Comme indiqué dans la littérature, ce système à base d'alcoolate tertiaire ne présente pas une grande réactivité. En effet, lorsque les réactions sont effectuées en solution dans l'hexane à 60 °C, la conversion et l'efficacité d'amorçage sont médiocres. De plus, les masses molaires sont faibles et les polymolécularités élevées (Tableau 15).

Tableau 15. Polymérisations du butadiène catalysées par 1/DHM.

entrée	Nd/Mg	BD/Mg	<i>t</i> -BuCl/Nd	conv. (%)	M_n (g/mol)	$M_{n,\text{th}}$ (g/mol)	M_w/M_n
1	1,0	100	-	22	2700	595	2,40
2	1,0 ^a	100	-	24	950	650	2,90
3	0,2	20	-	95	1700	370	4,40
4	1,0	100	3,0	68	3050	1840	4,20
5	0,2	200	-	47	10 300	2540	5,10
6	0,2	200	3,0	91	6100	4920	24

$[\text{BD}]_0 = 3.0 \text{ M}$ dans l'hexane à 60 °C pendant 17 h; $M_{n,\text{th}} = (([\text{BD}]_0/2[\text{Mg}]_0) \times (\text{conv.}/100) \times M_0)$;

^a Mg = BEM.

L'analyse des spectres RMN ¹H et ¹³C montre une stéréospécificité 1,4-*trans* supérieure à 95%. L'utilisation de BEM à la place du DHM conduit à une meilleure efficacité d'amorçage comme cela avait déjà été remarqué en polymérisation de l'éthylène (entrée 2/1). L'ajout de chlorure de tertiobutyle au système 1/DHM ($[\text{Nd}]_0/[\text{Cl}]_0 = 0,33$) permet d'augmenter

davantage cette efficacité probablement grâce à la formation de nouveaux sites actifs de type Nd-Cl. Par contre, l'influence sur la stéréospécificité est nulle (*1,4-trans* = 96%) (entrée 6).

L'étude de l'effet du rapport Nd/Mg montre que diminuer ce rapport permet de rendre la polymérisation quantitative (entrée 3/1). De plus, il apparaît que la masse molaire du polymère est directement proportionnelle à la quantité de dialkylmagnésien utilisée et donc qu'il est possible de contrôler la masse molaire du polybutadiène en modifiant simplement le rapport $[BD]_0/[Mg]_0$. Ici, le dialkylmagnésien agit d'abord comme agent alkylant puis comme agent de transfert (réversible), alors que le néodyme est un catalyseur et non un amorceur comme pour les polymérisations du MAM et de l'éthylène.

*45.1.2. Avec les phénates de néodyme **12** et **13***

Le précurseur monométallique $Nd(O-2,6-tBu_2-4-Me-Ph)_3(THF)$ (**12**) se révèle être beaucoup plus actif que le tertiobutylate précédemment testé. En effet, une conversion complète du monomère est observée après 17 h (temps de réaction non optimisé) à température ambiante contre 60 °C précédemment. Ce précurseur présente en outre une meilleure efficacité d'amorçage (Eff = 50%) et un indice de polymolécularité plus faible ($M_w/M_n < 1,30$) (entrée 8/9). Ceci peut être attribué à la mononucléarité du complexe qui permet une meilleure interaction avec le dialkylmagnésien ou à une plus grande réactivité intrinsèque du complexe due à l'acidité du ligand.

Tableau 16. Polymérisations du butadiène catalysées par **12/DHM**.

entrée	Nd/Mg	BD/Mg	t (h)	conv. (%)	M_n (g/mol)	$M_{n,th}$ (g/mol)	M_w/M_n
7	1,0	100	17	5	1900	135	1,77
8	1,0	100	17	99	5800	2700	1,26
9	0,2	20	17	98	1100	540	1,15
10	1,0	200	2	60	6300	3250	1,18
11	1,0	1000	17	99	49 900	26 800	1,86
12*	1,0	100	17	99	2700	2680	1,53
13*	1,0	1000	17	99	28 700	26 800	2,07

$[BD]_0 = 3 \text{ M}$ dans l'hexane à 20 °C; $M_{n,th} = (([BD]_0/2[Mg]_0) \times (\text{yield}/100) \times M_0)$; * Nd = $Nd(O-2,6-tBu_2-4-Me-Ph)_3$ (**13**).

La stéréospécificité de la polymérisation est comparable à celle observée avec **1** ce qui implique un mécanisme similaire. Les masses molaires sont également déterminées par le rapport $[BD]_0/[Mg]_0$. Augmenter la quantité de magnésien résulte en une baisse des masses

molaires et de l'indice de polymolécularité. Ainsi, pour des masses molaires inférieures à 10 000 g/mol, la polymérisation peut être considérée comme vivante.

Le précurseur $\text{Nd}(\text{O}-2,6-t\text{Bu}_2-4-\text{Me-Ph})_3$ (**13**) a été évalué dans des conditions identiques à **12**. Les masses molaires sont 2 fois plus basses que celles obtenues avec **12** (2700 vs. 5800 et 28 700 vs. 49 900; entrée 8/12 et 11/13) indiquant une efficacité d'amorçage maintenant proche de 100%. L'analyse RMN ^{13}C du polybutadiène montre une microstructure 1,4-*trans* (> 95%). Par conséquent, l'absence de THF coordonné ne permet pas la coordination bidentate du butadiène, type de coordination supposé mener à un polybutadiène 1,4-*cis*. L'encombrement stérique des ligands phénoxy et/ou la présence de dialkylmagnésium dans la sphère de coordination du néodyme pourrait expliquer ce comportement.

45.2.Copolymérisation du butadiène

45.2.1. Copolymérisation statistique butadiène-styrène

Les copolymères butadiène-styrène ont une grande importance dans l'industrie des élastomères. Toutefois, leur synthèse actuelle ne permet pas d'obtenir le copolymère idéal c'est à dire un copolymère ayant une teneur élevée en polybutadiène 1,4-*cis*, de haute masse molaire et présentant un taux d'incorporation de styrène supérieur à 20%. C'est dans ce but que de nombreux systèmes catalytiques ont été développés.²⁰⁷ Même si notre système catalytique **12/DHM** ne produit pas de polybutadiène 1,4-*cis*, nous l'avons brièvement évalué en copolymérisation statistique butadiène-styrène.

A température ambiante pendant 2 h, une conversion globale de 45% et une teneur en styrène dans le copolymère de 13% sont obtenues (entrée 15).

Tableau 17. Copolymérisations statistiques butadiène-styrène catalysées par **12/DHM**.

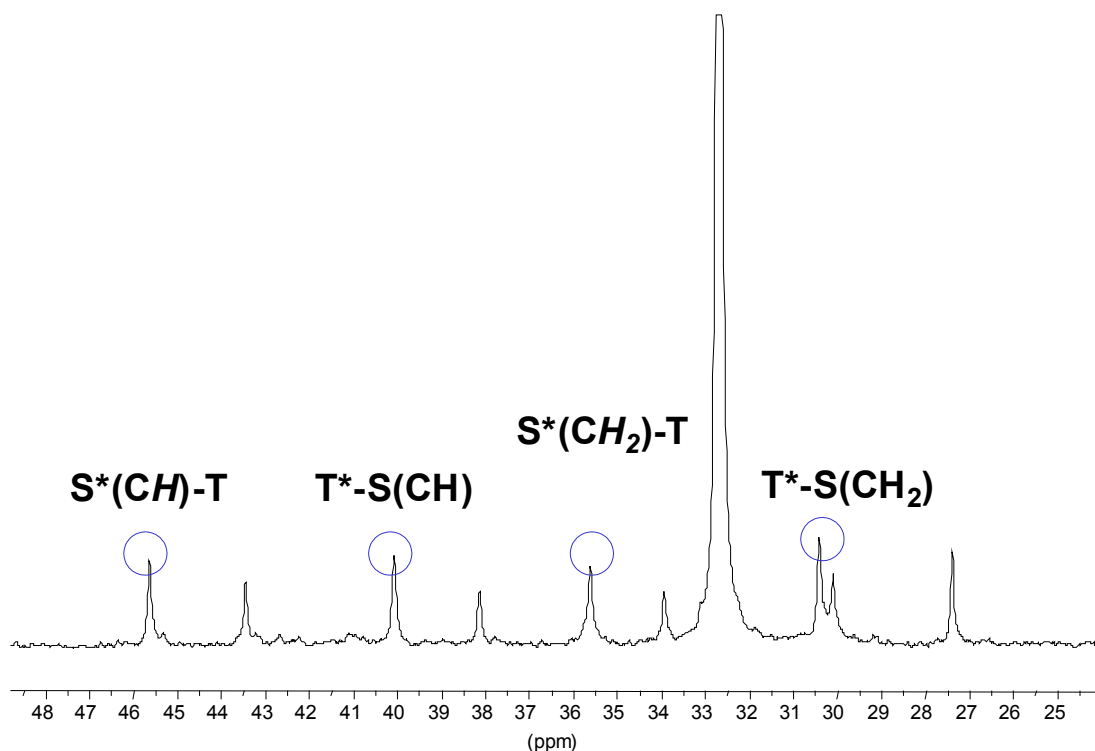
entrée	Nd/Mg	BD or St	t (h)	conv. (%)	M_n (g/mol)	M_w/M_n	St. (mol%)
14 ^a	1/1	100	17	30	2400	1,45	-
15	1/2	200	2	45	5200	2,42	13
16	1/2	1000	2	21	20 200	1,72	3,5
17	1/2	1000	20	41	25 200	2,13	13,5
18	1/1	1000	20	41	42 800	2,25	8,5
19 ^b	1/1	1000	1	39	35 100	1,90	10

$[\text{BD}]_0 = [\text{St}]_0 = 4,9 \text{ M}$ dans l'hexane à 20 °C. ^a homopolymérisation du styrène. ^b Polymérisation dans le toluène à 50 °C: $[\text{BD}]_0 = [\text{St}]_0 = 3 \text{ M}$; $[\text{Nd}]_0 = 3 \times 10^{-3} \text{ M}$.

Afin d'établir la véritable nature du copolymère, sa microstructure a été étudiée par RMN ^{13}C (Figure 34). En plus des pics attribués à l'homopolybutadiène, le spectre présente une nouvelle série de signaux spécifiques des diades 1,4-*trans*-BD-St.

Diminuer la quantité de catalyseur conduit à une conversion globale plus basse ainsi qu'à un faible taux d'incorporation du styrène (3,5%) (entrée 16). De nouveau, la masse molaire du polymère est régie par le rapport $[BD]_0/[MgR_2]_0$. Augmenter le temps de polymérisation permet d'augmenter la conversion et la teneur en styrène, toutefois, la masse molaire du copolymère reste constante suggérant la formation de nouvelles espèces actives en cours de polymérisation (entrée 17). Le paramètre température de polymérisation a également été étudié sans pouvoir améliorer les résultats précédemment obtenus, les polymères préparés à une température supérieure à 50 °C étant insolubles dans les solvants tels que le THF et le chloroforme (entrée 18).

Figure 34. Spectre RMN ^{13}C (CDCl_3 , 23 °C) de poly(butadiène-*co*-styrène) obtenu avec **12**/DHM (entrée 8); (les signaux encerclés réfèrent aux résonances spécifiques des diades BD-St; les signaux non encerclés réfèrent aux résonances spécifiques du PBD).



45.2.2. Copolymérisation dibloc butadiène-méthacrylate de glycidyle

La synthèse de nouveaux matériaux, et particulièrement de copolymères diblocs butadiène-monomère polaire est très recherchée.³¹³ Etant donné la possibilité de polymériser le butadiène et le MAM grâce aux systèmes alcoolate de lanthanide/dialkylmagnésien, nous nous sommes attardés sur la copolymérisation dibloc butadiène-méthacrylate en se focalisant sur l'utilisation du méthacrylate de glycidyle, comonomère très intéressant de part sa fonction époxy réactive.³¹⁵ Dans l'industrie des pneumatiques, ces copolymères pourraient être utilisés comme agent de renforcement associé à des charges minérales (SiO_2). A notre connaissance, aucun système catalytique à base de lanthanide n'a été décrit pour une telle application.

Les copolymères diblocs ont été préparés par prépolymérisation du butadiène suivie de l'ajout de GMA. Les résultats sont consignés dans le tableau suivant.

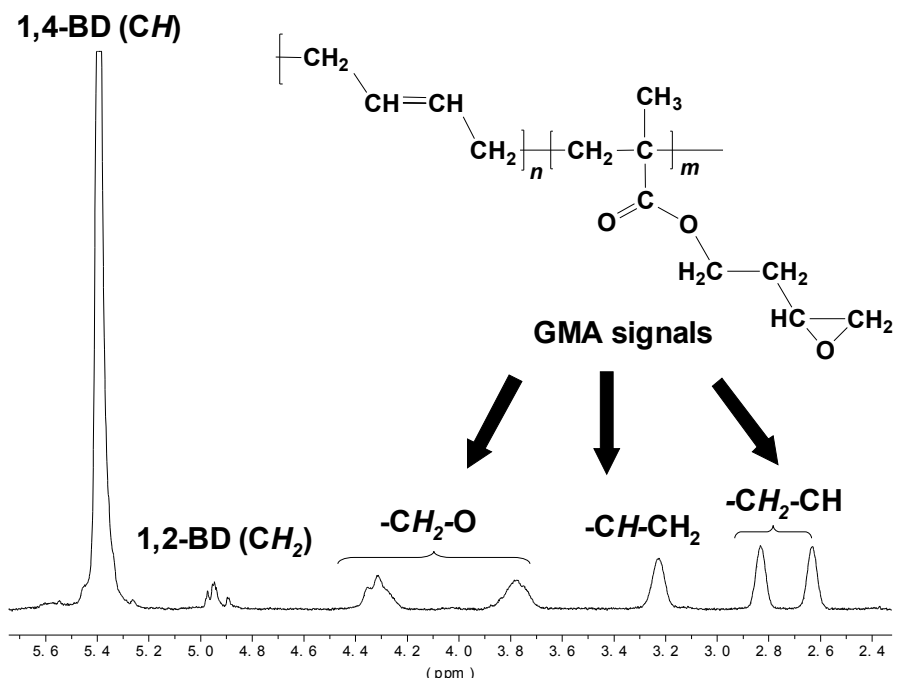
Tableau 18. Résultats obtenus en copolymérisation dibloc butadiène-méthacrylate de glycidyle.

entrée	"Nd(OR) ₃ "	BD t (h) T (°C)	MAG t (h) T (°C)	conv (%)	M _n (g/mol)	M _w /M _n	BD/GMA
20	1	<i>18; 60</i>	<i>1,5, 25</i>	43	23 800	1,84	1,9
21	12	<i>2; 25</i>	<i>3, 25</i>	60	11 900	1,40	10
22	12	<i>2; 25</i>	<i>18, 25</i>	60	11 600	1,40	10
23	12	<i>2; 25</i>	<i>3, 0</i>	43	7100	2,0	12

[BD]₀ = 3 M dans l'hexane; BD = 100 équiv.; GMA = 15 équiv.; Nd = 0,5 équiv.; Nd/DHM = 1.

Les copolymères synthétisés ont été caractérisés par différentes techniques analytiques. Les analyses RMN et IR ont permis de quantifier la teneur en méthacrylate dans le copolymère. La nature dibloc des copolymères a quant à elle été vérifiée par GPC à l'aide d'un détecteur UV après l'introduction sélective d'un groupe chromophore phényle.

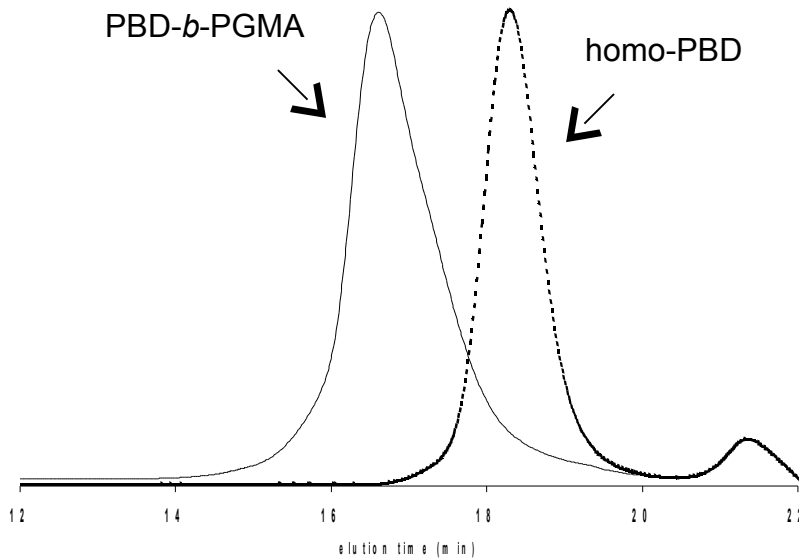
Figure 35. Spectre RMN ¹H (CDCl₃, 23 °C) de PBD-*b*-PGMA (entrée 21).



Un copolymère de haute masse molaire ayant une large distribution des masses est obtenu avec 1/DHM (entrée 20). La teneur en GMA est relativement élevée (30-35%) et en accord avec la forte réactivité de ce système vis-à-vis des méthacrylate (cf. §43) L'utilisation du

système **12**/DHM permet d'obtenir un copolymère de polymolécularité plus faible comme le montre le chromatogramme GPC (Figure 36) (entrée 21/23). De plus, l'évolution des masses molaires montre que la majorité des chaînes de polybutadiène sont vivantes et prolongées par des motifs méthacryliques.

Figure 36. Chromatogrammes GPC de l'homopolybutadiène et du copolymère dibloc PBD-*b*-PGMA obtenus avec **12**/DHM (entrée 21).



Toutefois, la teneur en GMA est plus faible qu'avec le système à base de tertiobutylate (5-10%). Un temps de polymérisation plus long ne permet ni d'augmenter la conversion ni d'accroître le rapport BD/GMA (entrée 22).

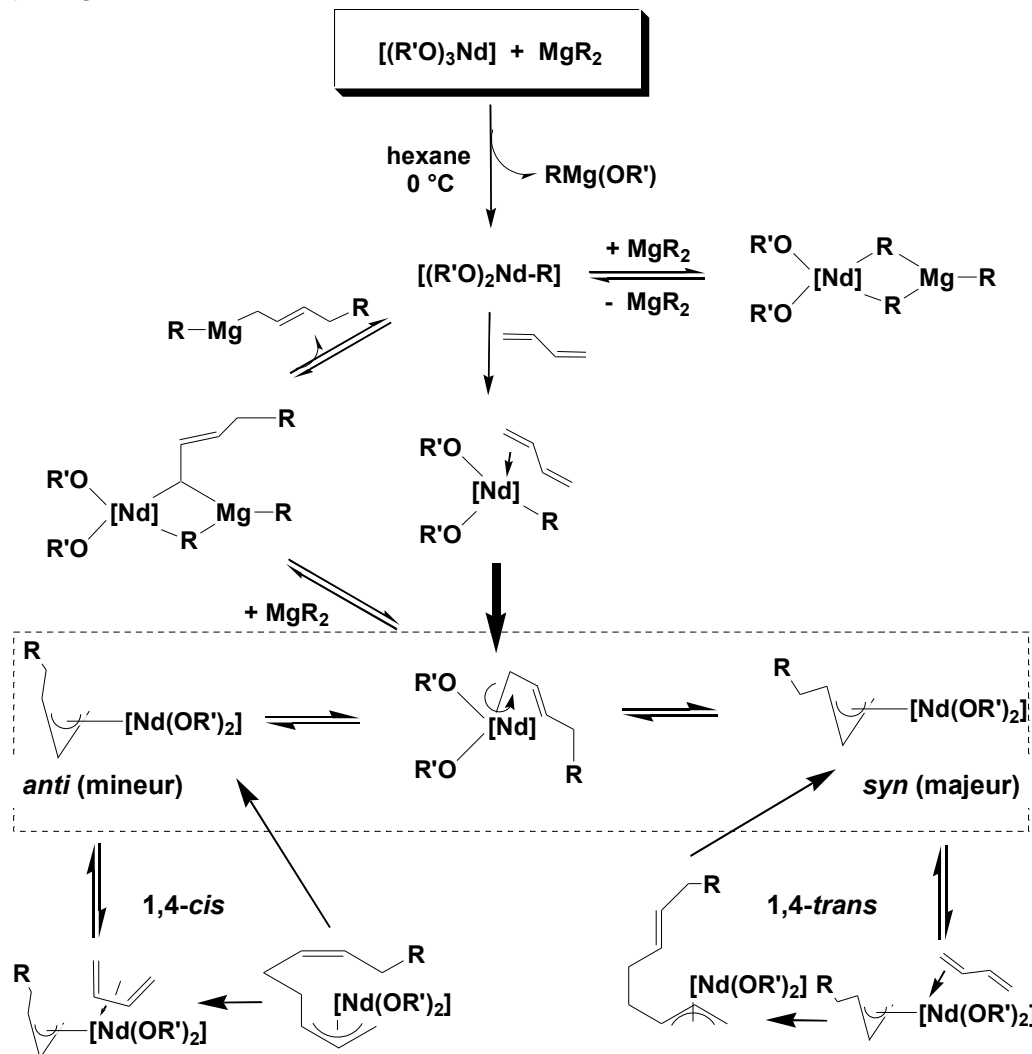
45.3. Mécanisme

Etant donné les réactions de transfert au magnésium observées lors de la polymérisation du butadiène, il nous semble nécessaire de terminer cette partie sur quelques considérations mécanistiques, et cela indépendamment du paragraphe suivant qui sera dédié à l'étude du mécanisme de polymérisation pour les formations de PMAM et de PE.

Avec les systèmes " $\text{Nd}(\text{OR})_3$ "/ MgR_2 , la formation *in situ* d'espèces alkyl-lanthanide a été précédemment suggérée. Toutefois, l'interaction de cette espèce avec le dialkylmagnésien, par exemple par la création de ponts μ -alkyle, générant un complexe bimétallique Nd-Mg actif en polymérisation ne peut être écartée. L'existence de ce complexe bimétallique ponté, en équilibre rapide de dissociation avec l'espèce mononucléaire alkyl(allyl)-Nd et avec un transfert de chaînes alkyles rapide et réversible entre les centres Nd et Mg, est l'hypothèse la plus plausible pour expliquer le caractère pseudo-vivant observé lors de la polymérisation du butadiène. Ce mécanisme a été proposé auparavant pour la polymérisation de l'éthylène avec des précurseurs lanthanocéniques.⁵² Ainsi, la polymérisation s'effectue par une insertion

initiale du butadiène dans la liaison Nd-R et ensuite le monomère mono-coordonné effectue une insertion-1,3 dans la liaison *syn*- π -allyle, l'encombrement stérique des ligands alcoxy/phénoxy déplaçant l'équilibre entre les configurations *syn* et *anti* vers la structure *syn* (Schéma 14). Puisque les polybutadiènes 1,4-*cis* sont généralement obtenus avec des ligands faiblement coordonnants, il est cohérent d'observer une stéréospécificité 1,4-*trans* avec des ligands aussi fortement coordonnés que sont les alcoolates et phénates.

Schéma 14. Proposition de mécanisme pour la polymérisation des diènes catalysée par les systèmes "Nd(OR)₃"/MgR₂.



La réactivité supérieure des phénates par rapport au tertiobutylate peut être attribuée à leur plus grande activité intrinsèque et/ou à leur meilleure stabilité. En effet, les ligands phénates étant plus acides que le tertiobutylate, le centre métallique se trouve déficient en électrons et donc plus réactif vis-à-vis des oléfines. L'encombrement stérique des ligands phénoxy et la coordination du monomère sont deux paramètres qui pourraient stabiliser et donc prévenir la décomposition des alkyl(allyl)-Nd. Le caractère pseudo-vivant des polymérisations catalysées par le complexe **12** est un autre indice montrant la robustesse des espèces alkyl/allyl-Nd.

générées à partir de **12**/DHM. Enfin, nous pouvons raisonnablement penser que la polymérisation du méthacrylate de glycidyle s'effectue suivant le mécanisme de type coordinatif-anionique proposé par Yasuda *et al.* pour la polymérisation du MAM amorcée par les complexes lanthanocéniques.¹¹⁶

46. Etude mécanistique

La polymérisation pseudo-vivante et syndiotactique du MAM, la polymérisation de l'éthylène et ses réactions de transfert en présence de PhSiH₃ et d'hydrogène, la possibilité de préparer des copolymères diblocs PE-*b*-PMAM sont autant d'indices en faveur d'une polymérisation amorcée par une espèce de type alkyl-Nd, obtenue par échange de ligand alcoxy-alkyle entre le précurseur de lanthanide et le dialkylmagnésien. Afin de vérifier cette hypothèse, nous avons étudié ces mélanges catalytiques par RMN et avons tenté d'isoler par cristallisation les espèces actives en polymérisation.

46.1. Etude RMN

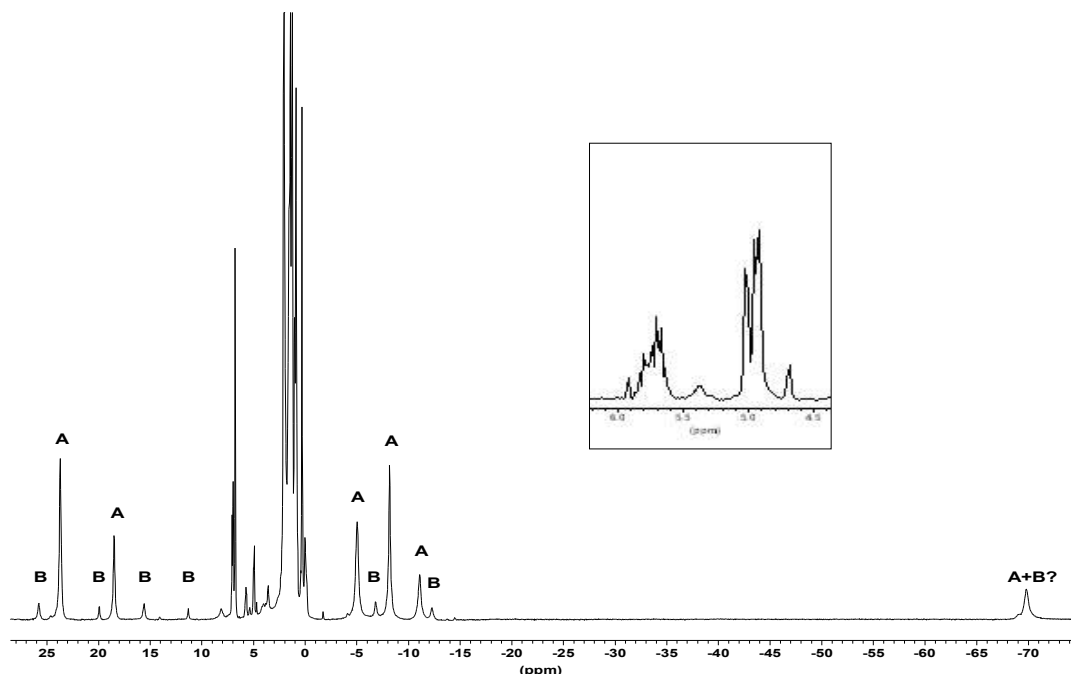
Malgré le paramagnétisme du métal, la majeure partie de l'étude a porté sur les complexes de néodyme puisque ces derniers se sont révélés être de loin les plus actifs en polymérisation.

46.1.1. Evolution des systèmes "Ln(OR)₃"/DHM (Ln/Mg = 1,0)

D'abord, la réaction entre **1** et le DHM a été suivie à température variable. A partir de -50 °C, une modification du spectre est observée, laissant apparaître progressivement une nouvelle série de signaux attribuables aux ligands O*t*Bu d'une nouvelle espèce à base de Nd. La formation d'hex-1-ène est notée vers -20 °C. Après 15 h à 5 °C (ou 1 h à 23 °C), le système n'évolue plus. **1** est complètement converti en 2 espèces dans un rapport 10:1 et 40% du DHM est transformé en hex-1-ène (Figure 37).

La formation d'hexène est la première preuve indirecte pour la formation *in situ* d'une espèce alkyl-Ln. En effet, ce phénomène peut raisonnablement être attribué à la formation initiale d'une espèce Nd-Hex suivie de sa décomposition par β-H élimination. Le pourcentage maximum d'hexène formé (40%) indique que tout le DHM ne participe pas à "l'alkylation" du précurseur de Nd et par conséquent explique les faibles taux d'efficacité d'amorçage observés. L'étude de ce mélange à 0 °C dans nos conditions d'activation montre une formation initiale d'hexène très rapide (25% vs. Nd en 5 min) suivie d'une lente progression avant d'atteindre un plateau après 30 min. Il semble donc que l'espèce active pour la polymérisation de l'éthylène est (ou provient) de l'espèce Nd-H. Etant donné qu'en absence d'activation, la polymérisation de l'éthylène ne démarre qu'après une période d'induction de 8-10 min, le réarrangement de cette espèce peut être suggéré.

Figure 37. Spectre RMN ¹H d'un mélange 1/DHM après 1 h à température ambiante.



La formation d'hexène a aussi été quantifiée à partir de tertiobutylate d'yttrium (**III₁**), de lanthane (**III₂**), de cérium^(III) et de samarium^(III). Comme le montre le tableau suivant, la vitesse de formation d'hexène ainsi que son pourcentage maximum de formation sont fonction de la nature du métal. Ceci est en accord avec la différence de réactivité de tous ces composés observée en polymérisation de l'éthylène. L'étude RMN ¹H des composés diamagnétiques (Y et La) a surtout permis de mettre en évidence sans ambiguïté la présence d'espèces [Ln]-Hex.

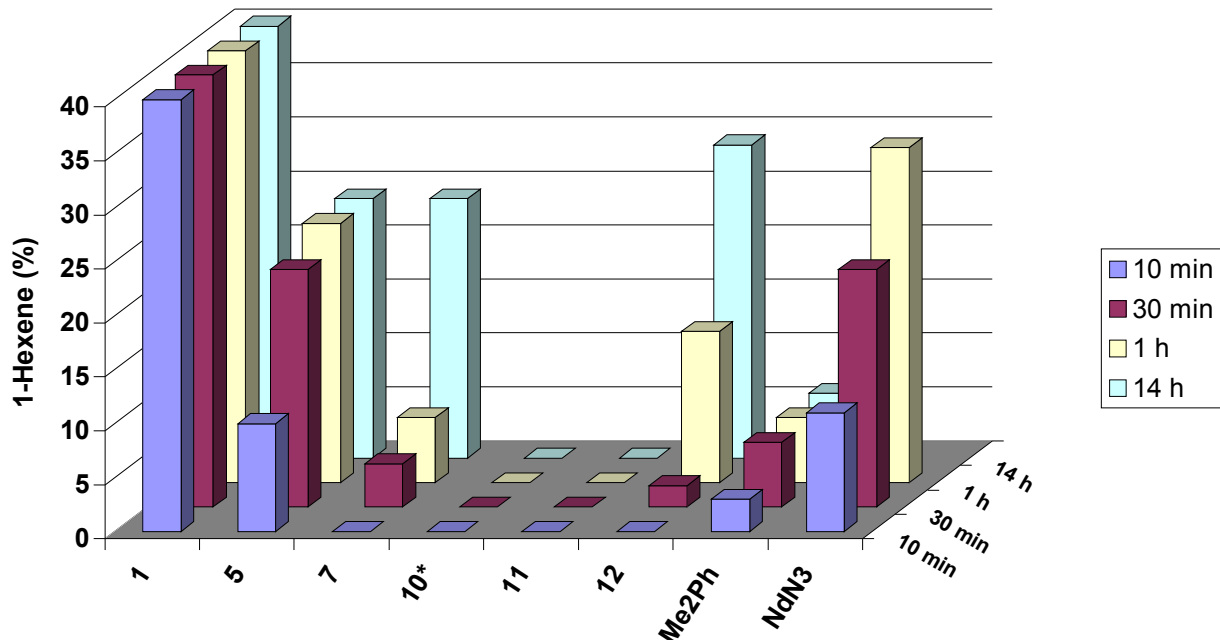
Tableau 19. Influence de la nature du métal sur la formation d'hex-1-ène.

"Ln(OtBu) ₃ "	% hexène/Ln après 30 min	% max hexène/Ln	% max isobutène/Ln
Nd ₃ (OtBu) ₉ (THF) ₂ (1)	40	40	2-5
La ₃ (OtBu) ₉ (THF) ₂ (III₂)	6	30	12
"Ce(OtBu) ₃ "	8	30	27
"Sm(OtBu) ₃ "	8	16	14
Y ₃ (OtBu) ₈ Cl(THF) ₂ (III₁)	1	22	23

Ln/DHM = 1,0; toluène-*d*₈; 20 °C; 48 h.

Enfin, d'autres alcoolates de néodymes associés au DHM et testés en polymérisation de l'éthylène, ont également été utilisés pour cette étude. Ici, la nature du métal ne peut intervenir, c'est donc la variation de la structure du ligand et/ou du complexe qui régit la réactivité. L'évolution de la quantité d'hexène formée à température ambiante pour les différents systèmes est représentée sur la Figure 38.

Figure 38. Formation d'hexène observée avec différents précurseurs de Nd associés au DHM à 20 °C.



De manière générale, il est possible de relier l'activité catalytique en polymérisation de l'éthylène et la formation d'hexène pour les systèmes "Nd(OR)₃"/DHM. Ainsi, l'absence de formation d'alcène avec les complexes **10*** et **11** correspond à l'inactivité de ces complexes en polymérisation de l'éthylène. Sa lente formation avec les complexes **5** et **7** est en accord avec une température d'activation plus élevée et/ou un profil de consommation différent. Le faible pourcentage d'hexène formé avec OC(Me)₂Ph concorde avec son inactivité en polymérisation. La plus grande stabilité du phénate (**12**) par rapport aux tertiobutylates peut être visualisée à l'aide d'une formation d'hexène lente et progressive. Enfin, l'exemple du complexe tris (amidure) NdN₃ montre de nouveau que la formation d'hexène ne conduit pas nécessairement à une espèce active en polymérisation.

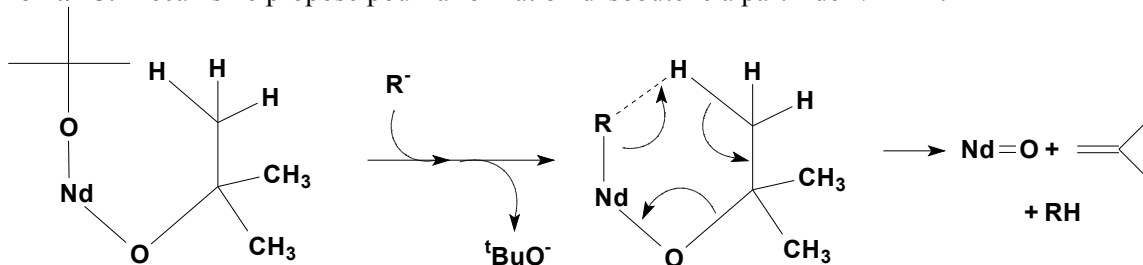
46.1.2. Evolution des systèmes **1/RM** ($Ln/M = 1,0$)

Nous avons ensuite étudié l'influence de la nature de l'agent alkylant sur cette réaction. D'abord, l'importance de la structure du dialkylmagnésien a été évaluée. En présence de BEM, la formation de butène est observée à -30 °C et atteint un maximum de 14% vs. Nd après 15 min à 20 °C. Parallèlement, la formation d'éthylène est constatée dès -60 °C mais ce dernier disparaît progressivement à partir de -20 °C et aucune trace ne peut être détectée à 0 °C. Ce phénomène est simplement rationalisé par la polymérisation *in situ* de l'éthylène formé. Ceci montre que la vitesse de formation-décomposition de l'espèce Nd-R dépend fortement de la nature du radical alkyle. Ainsi, la décomposition de [Nd]-Et est plus rapide que celle de [Nd]-Hex. Cette réaction montre aussi que la température minimale d'activation est de -20 °C avec le système **1/BEM**, et que si les vitesses de décomposition des espèces [Nd]-Bu et

[Nd]-Hex sont comparables, alors l'espèce active est un hydrure de néodyme (ou provient de sa formation), comme nous l'avons suggéré pour **1/DHM**.

Contrairement aux systèmes précédents, le système **1/Mg(CH₂SiMe₃)₂** ne possédant pas d'atome d'hydrogène en position β se montre thermiquement plus stable. Cependant, la formation d'isobutène est observée à partir de 0 °C. Le pourcentage maximum de formation d'isobutène est égal à 40% vs. Nd après 24 h à 20 °C. En fait, la présence d'isobutène avait aussi été détectée avec le DHM et le BEM mais en moindre quantité (2%). Les formations d'isobutène et de SiMe₄ étant simultanées, un mécanisme concerté à 6 centres peut être avancé afin d'expliquer cette réaction (Schéma 15).

Schéma 15. Mécanisme proposé pour la formation d'isobutène à partir de **1/DHM**.



La formation d'hexène a également été notée avec d'autres agents alkylants tels que le *n*-BuLi et le tri(octyl)aluminium. La réaction est rapide et a lieu à basse température (-60 °C) pour le dérivé lithié alors qu'il est nécessaire de chauffer le mélange à 80 °C pour observer la formation d'alcène avec Al(Oct)₃. L'absence de réactivité des systèmes **1/n**-BuLi et **1/Al(Oct)₃** vis-à-vis de l'éthylène peut être expliquée respectivement par son instabilité et sa trop grande stabilité (due à la présence d'espèces pontées). Ces résultats montrent que les dialkylmagnésiens servent d'agent alkylant mais aussi d'agent stabilisant comme ils le font dans les systèmes chlorolanthanocène/MgR₂ grâce à la présence de ponts μ -alkyle.⁵²

46.2.Cristallisation des espèces actives

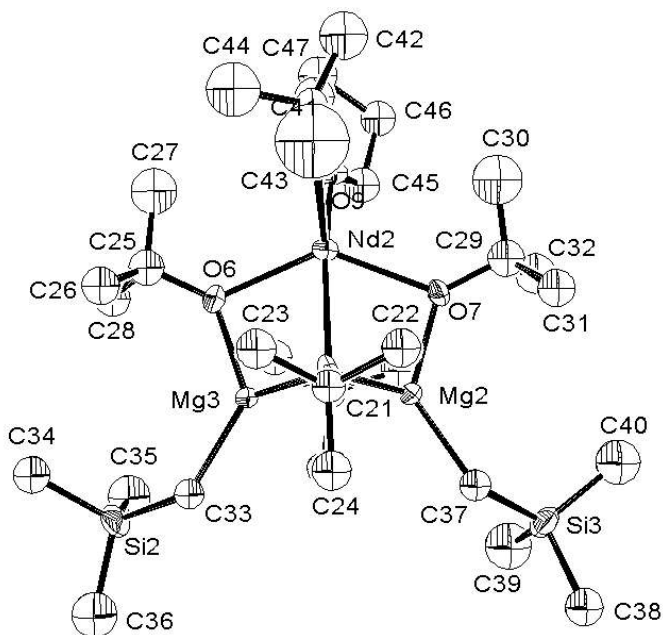
Malgré les nombreuses informations recueillies lors de l'étude RMN des systèmes "Ln(OR)₃"/DHM, aucune indication n'a pu être obtenue concernant le mécanisme de formation et la nature exacte des espèces actives. De fait, nous nous sommes attachés à isoler les espèces intermédiaires ou espèces actives par cristallisation dans le toluène à -20 °C.

46.2.1. Cristallisation de Nd(THF)(μ₃-OtBu)₂(μ₂-OtBu)₂(OtBu)Mg₂(CH₂TMS)₂ (**14**)

La réaction de **1** avec Mg(CH₂SiMe₃)₂ (Nd/Mg = 1,0) en absence d'additif n'a conduit à la formation d'aucun cristal. L'addition de THF (10 équiv. vs. Nd) engendre l'apparition de cristaux identifiés par RMN comme étant le complexe trinucléaire de départ, indiquant que l'excès de THF empêche la réaction d'alkylation. Ceci est en accord avec l'inhibition de la polymérisation observée en présence de THF (cf. §45.1.1). L'obtention d'un intermédiaire de

polymérisation obtenu par Yasuda en présence de MAM nous a poussé à utiliser la même méthode.¹¹⁶ L'ajout de MAM s'est avérée efficace. Ainsi, des cristaux bleus sont apparus après plusieurs semaines. Toutefois, de manière assez surprenante, ces derniers ne comportent pas de MAM au sein de leur structure (Figure 39). Le complexe formé ne possède pas la stoechiométrie initiale puisque c'est un complexe trinucléaire qui est obtenu où deux atomes de Nd ont été remplacés par des atomes de Mg. L'atome de Nd est hexacoordonné avec un ligand *OtBu* terminal en équilibre dynamique avec une molécule de THF. Des ligands de type μ_2 -*OtBu* et μ_3 -*OtBu* relient les atomes de néodyme aux atomes de magnésium tétracoordonnés. La structure est complétée par deux groupes CH_2SiMe_3 portés par les atomes de magnésium. Ce complexe montre l'oxophilie plus importante du Nd par rapport au Mg ($\text{Nd}-\text{O} = 703 \pm 13 \text{ kJ/mol}$ et $\text{Mg}-\text{O} = 363 \pm 13 \text{ kJ/mol}$) puisque les chaînes alkyles sont portées par les atomes de Mg, le néodyme étant entouré de six atomes d'oxygène.²⁹² De nombreux exemples de complexes bimétalliques basés sur des complexes de type alcoxylanthanide ont déjà été décrits, tous obtenus à partir de AlR_3 .^{219,220,322-326} Les seuls complexes bimétalliques Ln/Mg isolés ne comportent pas de ligands alcoxy/phénoxy.³²⁷

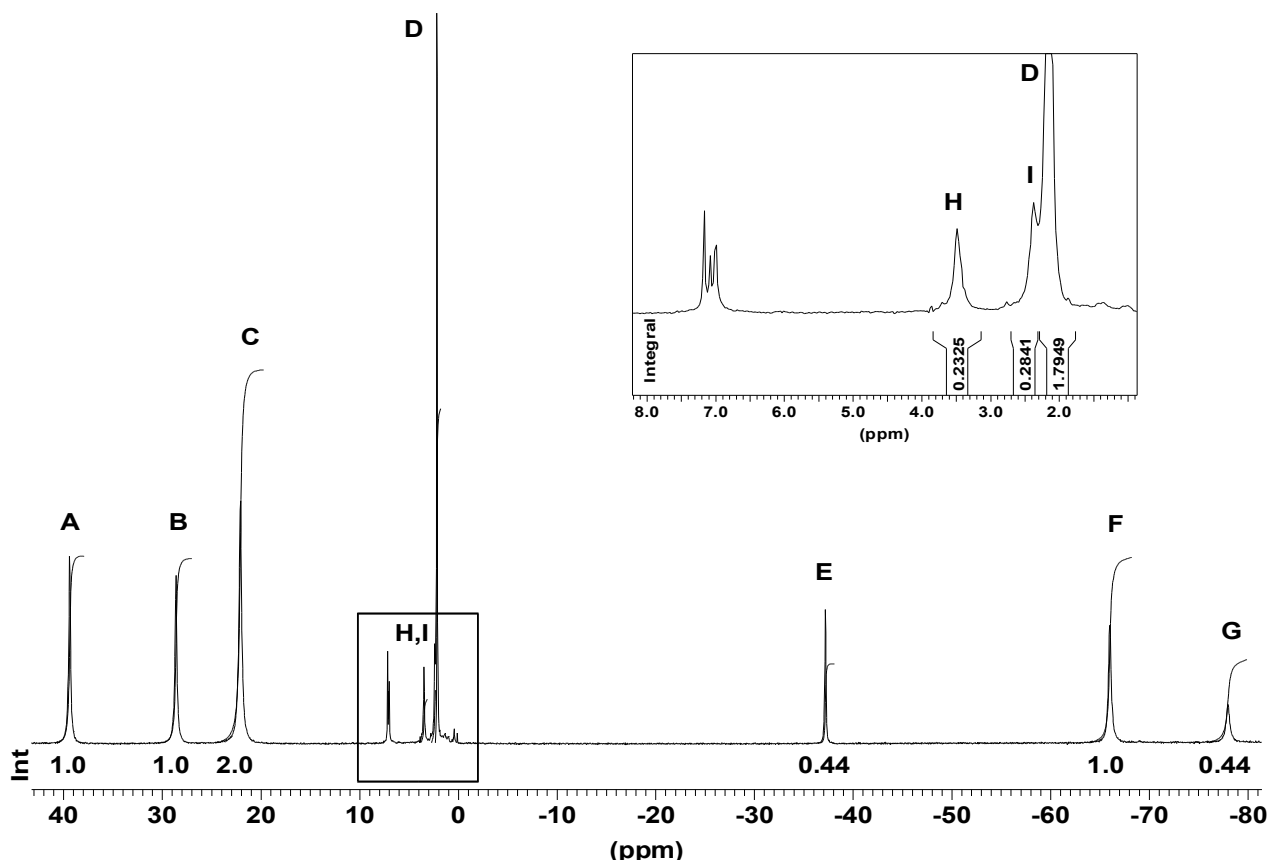
Figure 39. Figure ORTEP de $\text{Nd}(\text{THF})(\mu_2\text{-OtBu})_2(\mu_3\text{-OtBu})_2(\text{OtBu})\text{Mo}_2(\text{CH}_2\text{TMS})_2$ (**14**)



La structure de ce nouveau complexe a été étudiée par RMN ¹H. A température ambiante, le spectre obtenu montre sept signaux d'intégration relative 1:0,8:2:1,5:0,4:0,8:0,4, valeurs en désaccord avec la structure à l'état solide. Ce résultat étant attribué à des équilibres dynamiques, nous avons choisi d'effectuer la mesure à plus basse température afin de ralentir ces équilibres. A -80 °C, le spectre est en accord avec la structure déterminée par diffraction RX (Figure 40). En fonction des différentes intensités, l'attribution des signaux pourrait être la suivante : A: *OtBu*, B: $\text{CH}_2\text{-Si}(\text{CH}_3)_3$, C: $\mu_3\text{-OtBu}$ or $\mu_2\text{-OtBu}$, H: $\text{CH}_2\text{-Si}(\text{CH}_3)_3$, I: $\text{CH}_2\text{-Si}$

$(CH_3)_3$, D: μ_3 -OtBu or μ_2 -OtBu, E: THF, F: $CH_2\text{-Si}(CH_3)_3$, and G: THF. Cependant, il demeure toujours une incertitude quant à l'attribution des signaux C et D. Contrairement aux composés diamagnétiques, il est impossible de relier degré de coordination du ligand et déplacement chimique. De plus l'inéquivalence des groupes $CH_2\text{-Si}(CH_3)_3$ en solution est difficilement explicable, même si ces groupes sont inéquivalents à l'état solide.

Figure 40. Spectre RMN 1H de **14** dans le toluène- d_8 à -80 °C.



Ce nouveau complexe a enfin été placé sous éthylène (1 bar) afin de vérifier son activité en tant qu'amorceur de polymérisation. Après 48 h à 20 °C, aucune consommation d'éthylène n'est notée. Par contre, l'ajout de $Mg(CH_2SiMe_3)_2$ à **14** sous éthylène conduit à une lente polymérisation dont l'activité n'a pu être mesurée. Etant donné ces résultats, nous pouvons penser que **14** est bien un intermédiaire dans la formation de l'espèce active en polymérisation des systèmes **1/MgR₂**. Toutefois, nous ne pouvons écarter l'hypothèse selon laquelle l'activité catalytique serait due à d'autres espèces formées lors de cette réaction. En effet, en tenant compte de la stoechiométrie de la réaction, la formation d'espèces de type $[(tBuO)_2Nd\text{-R}]_n$ est également possible.

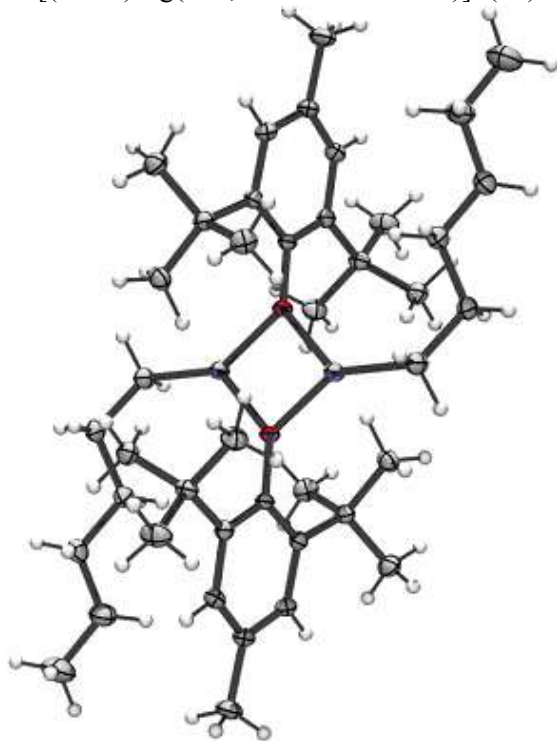
Finalement, lorsque le mélange **1/Mg(CH₂SiMe₃)₂** est effectué en présence d'isoprène, un autre produit de réaction est isolé. Ainsi, de larges cristaux incolores correspondant au composé de formule $[(tBuO)Mg(CH_2SiMe_3)](THF)$ (**15**) ont été caractérisés par RMN.

46.2.2. Cristallisation de composés issus de systèmes $Nd(OAr)_3(THF)/RM$

Etant donné qu'aucun autre monocrystal analysable par diffraction RX n'a pu être obtenu à partir de $Nd_3(OtBu)_9THF_2$, nous nous sommes focalisés sur l'utilisation de $Nd(O-2,6-tBu_2-4-Me-Ph)_3(THF)$ (**12**), ce précurseur devant conduire à des complexes plus stables et plus facilement cristallisables.

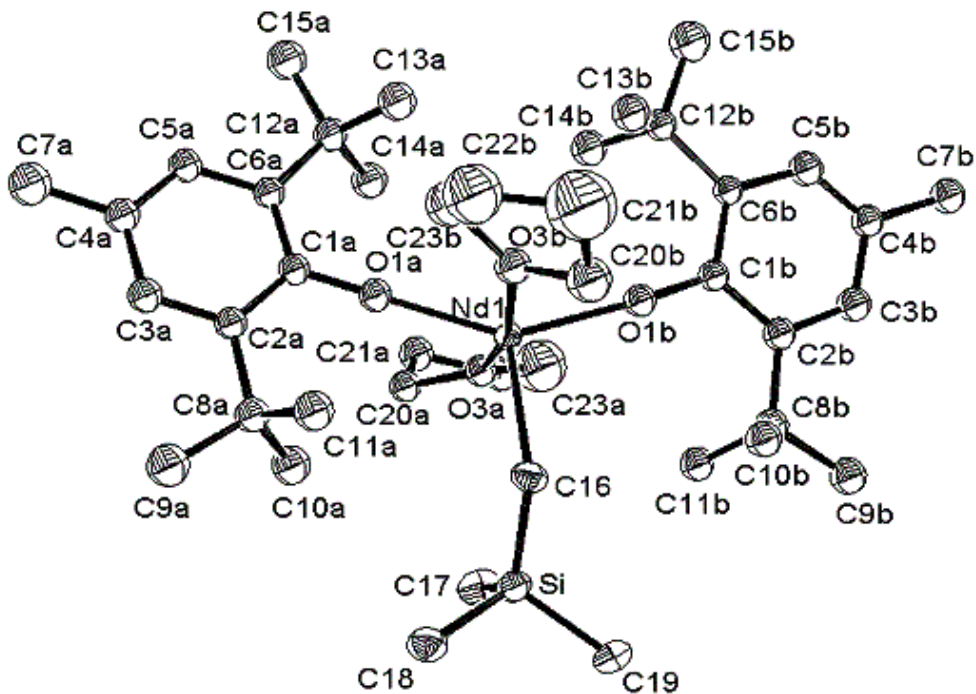
Un complexe mixte alkyl/phénate de magnésium $[(n\text{-hex})Mg(O-2,6-tBu_2-4-Me-C_6H_2)]_2$ (**16**) a été isolé à partir d'un mélange **12**/DHM. Ce complexe a été caractérisé par RMN et diffraction RX (Figure 41). Le co-produit de cette réaction portant l'atome de néodyme n'a pu être isolé, ni identifié. La structure de ce dernier devrait être " $[(n\text{-hex})Nd(O-2,6-tBu_2-4-Me-C_6H_2)_2]_n$ " si la stoechiométrie de la réaction est respectée. Ce composé est probablement instable et doit se décomposer par β -H élimination pour former des produits non identifiés.

Figure 41. Figure ORTEP de $[(n\text{-hex})Mg(O-2,6-tBu_2-4-Me-C_6H_2)]_2$ (**16**).



Par conséquent, nous avons utilisé $Mg(CH_2SiMe_3)_2$ à la place du DHM afin d'éviter cette supposée décomposition par β -H élimination. De nouveau l'espèce alkyl-Nd n'a pu être isolée. Par contre, l'addition de THF (10 équiv. vs. Nd) au mélange **12**/ $Mg(CH_2SiMe_3)_2$ (1:1) a permis la cristallisation du complexe alkyl-néodyme $Nd(O-2,6-tBu_2-4-Me-Ph)_2$ ($CH_2SiMe_3)(THF)_2$ (**17**) et du complexe mixte $(Ar^*OMgCH_2SiMe_3)_2$ (**18**). Les complexes **17** et **18** ont été caractérisés par RMN. L'étude par diffraction RX du complexe **17** montre une structure consistant en un atome de néodyme pentacoordonné par 2 groupes phénolys et un groupe CH_2SiMe_3 en position équatoriale, et 2 molécules de THF en position axiale (Figure 42).

Figure 42. Figure ORTEP de $\text{Nd}(\text{O}-2,6-t\text{Bu}_2-4-\text{Me-Ph})_2(\text{CH}_2\text{SiMe}_3)(\text{THF})_2$ (**17**).

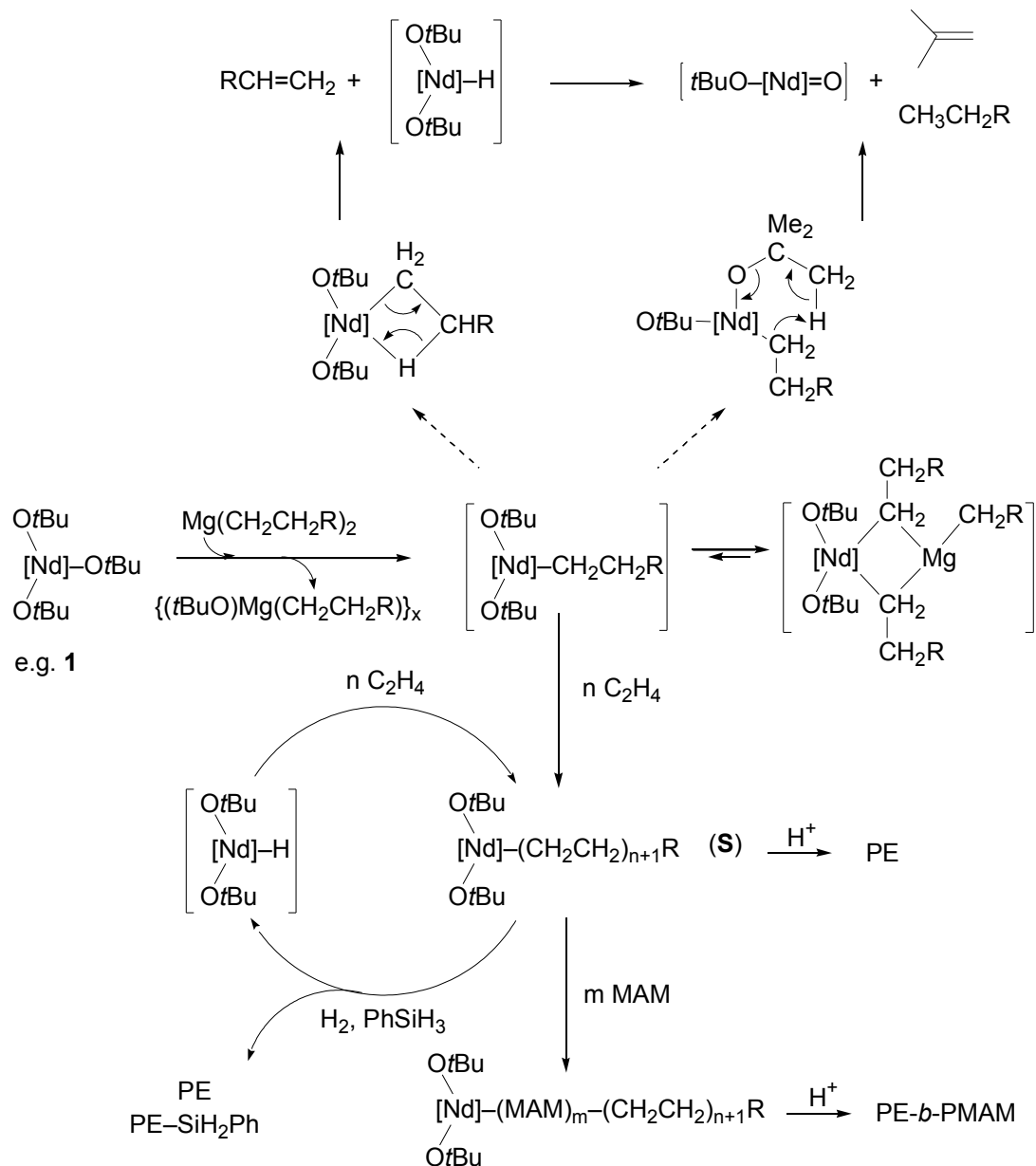


46.3. Conclusion

Les résultats de polymérisation, le suivi par RMN des mélanges **1**/DHM et la caractérisation de **17** (complexe issu de la réaction entre un phénate de néodyme et un dialkylmagnésien) permettent maintenant de proposer un mécanisme complet et justifié de la formation et de la décomposition d'une espèce active de type [Nd]-Hex à partir de **1**/DHM et son utilisation en polymérisation (Schéma 16).

Nos résultats montrent que l'association d'un complexe homoleptique alcoxy-lanthanide avec un dialkylmagnésien peut générer une espèce active pour la (co)-polymérisation du MAM, de l'éthylène et du butadiène. Cependant, le résultat le plus surprenant demeure la copolymérisation dibloc éthylène-MAM. Ces précurseurs inorganiques présentent une réactivité similaire aux composés lanthanocéniques, ce qui valide ainsi la possibilité d'utiliser des ligands de type alcoxy/phénoxy comme ligand ancillaire. Toutefois, de nombreuses questions restent sans réponse concernant la formation et la stabilisation de ces espèces actives. Nos résultats illustrent la difficulté de trouver un couple "Ln(OR)₃"/agent alkylant efficace en polymérisation. En fait, l'objectif majeur dans cette chimie est de trouver une balance adéquate entre la stabilité du complexe alkyl-alcoxy-lanthanide et sa réactivité vis-à-vis des oléfines.

Schéma 16. Mécanisme global d'activation et de désactivation des systèmes " $\text{Nd}(\text{OtBu})_3/\text{MgR}_2$ ".



Les études RMN ont montré la relative facilité avec laquelle s'effectue la réaction de métathèse entre l'alcoolate/phénate de lanthanide et l'agent alkylant ainsi que la tendance qu'ont les complexes alkyl-alcoxy-lanthanide à se décomposer (β -H élimination et thermolyse du ligand tertiobutoxy). L'influence exacte des ligands alkoxy sur la réactivité des complexes alkyl-lanthanide reste un sujet très controversé. D'une part, on peut considérer que les ligands alkoxy électroattracteurs, comparés au ligands Cp donneurs σ , augmentent l'électrophilie du centre métallique et ainsi facilitent la réaction de β -H élimination des espèces alkyl-alcoxy-lanthanide. Ceci expliquerait la formation aisée d'alcène à partir des combinaisons "Ln(OR)₃"/agent alkylant en absence de monomère. Par contre, des considérations thermodynamiques, basées sur les énergies de liaisons Ln-C vs. Ln-H, suggèrent que le remplacement des ligands Cp* par des ligands "durs" et électronégatifs de type *tert*-butoxy devraient inhiber ou ralentir les réactions de transfert par rapport à la propagation.¹⁵⁷ Cet argument a été avancé pour expliquer l'absence de β -H élimination avec $[Y(C_5Me_5)(O-2,6-tBu_2C_6H_3)]_2(\mu-H)(\mu-CH_2CH_2R)$

65 et est en accord avec l'obtention de polyéthylènes de haute masse molaire avec $\text{Nd}_3(\text{O}t\text{Bu})_9$ ($\text{THF})_2/\text{MgR}_2$.

La faible tolérance des espèces actives générées à partir **1/MgR₂** envers les bases de Lewis montrent que la stratégie habituelle qui consiste à introduire des groupements électrodonneurs dans la structure du ligand (e.g. complexe **11**),⁷³ est inappropriée pour stabiliser les espèces alkyl-alcoxy-lanthanide destinées à la polymérisation de l'éthylène. Nous pouvons penser que le rapport adéquat entre stabilité et réactivité du système **1/MgR₂** provient du degré d'association (nucléarité) de ces espèces actives et de la spécificité des dialkylmagnésiens (par exemple, l'électronégativité du Mg est équivalente à celle des lanthanides). Les très faibles activités rencontrées avec les complexes mononucléaires $\text{Nd}(\text{O}-2,6-t\text{Bu}_2-4-\text{Me-C}_6\text{H}_2)_3(\text{THF})$ et $\text{Nd}(\text{OC}t\text{Bu}_3)_3(\text{THF})$ illustrent parfaitement cette hypothèse. Par conséquent, la formation d'agrégats souvent associée à la chimie des alcoolates de lanthanide, pourrait être le paramètre clé pour le développement de nouveaux systèmes actifs en catalyse de polymérisation.

47. Conclusion générale

Nous avons décrit dans ce manuscrit la découverte, les applications et la caractérisation d'un nouveau système catalytique pour la polymérisation des oléfines. Ce système composé d'un alcoolate/phénate de lanthanide associé à un dialkylmagnésien est le premier exemple de catalyseur post-lanthanocénique possédant cette efficacité et cette polyvalence. En effet, l'utilisation du complexe trinucléaire $\text{Nd}_3(\text{O}t\text{Bu})_9(\text{THF})_2$ (**1**) combiné au di-*n*-hexylmagnésium (DHM) permet la polymérisation pseudo-vivante et syndiotactique du MAM, la polymérisation de l'éthylène et la copolymérisation dibloc éthylène-MAM. La polymérisation pseudo-vivante et stéréospécifique du butadiène et les copolymérisations statistique avec le styrène et dibloc avec le méthacrylate de glycidyle ont également été observées. Dans ce dernier cas, le complexe mononucléaire $\text{Nd}(\text{O}-2,6-t\text{Bu}_2-4-\text{Me-C}_6\text{H}_2)_3(\text{THF})$ (**12**) s'est avéré plus adapté.

Toutefois, ce travail ne doit pas être considéré comme achevé mais plutôt comme le point de départ d'une nouvelle génération de catalyseurs pour la polymérisation des oléfines. En effet, de nombreuses questions restent sans réponse. Par exemple, la différence de réactivité des tertiobutylates de néodyme issus de différentes voies de synthèse reste inexpliquée. Une compréhension totale de ces systèmes binaires est donc nécessaire, ce qui signifie une caractérisation complète des précurseurs, des intermédiaires et des espèces actives. Dès que le mécanisme de formation de ces espèces actives sera déterminé, le développement rationnel de nouveaux systèmes catalytiques pourra être envisagé.

Enfin, outre le développement de nouveaux systèmes catalytiques, nous avons aussi préparé de nouveaux matériaux qui étaient auparavant inaccessibles. Etant donné leur unique composition, leurs propriétés mécaniques et morphologiques ainsi que leur application en tant

qu'agent compatibilisant devront être évaluées et devraient être le principal moteur pour le développement de nouveaux systèmes catalytiques à base de terres rares.

Bibliographical references

1. Staudinger, H. *Helv. Chim. Acta* **1922**, *5*, 785.
2. Ulbrich, D.; Vollmer, M. S. *Macromol. Mater. Eng.* **2002**, *287*, 435-441.
3. Sinclair, K. B. *Macromol. Symp.* **2001**, *173*, 237-261.
4. (a) Lodge, T. P. *Macromol. Chem. Phys.* **2003**, *204*, 265-273. (b) Yanjarappa, M. J.; Sivaram, S. *Prog. Polym. Sci.* **2002**, *27*, 1347-1398. (c) Boffa, L. S.; Novak, B. M. *Chem. Rev.* **2000**, *100*, 1479-1493.
5. (a) Yasuda, H. *J. Organomet. Chem.* **2002**, *647*, 128-138. (b) Hou, Z.; Wakatsuki, Y. *Coord. Chem. Rev.* **2002**, *231*, 1-22.
6. Von Pechmann, H. *Ber. Dtsch. Chem. Ges.* **1898**, *31*, 2643.
7. Fawcett, E. W.; Gibson, R. O.; Perrin, M. W.; Paton, J. G.; Williams, E. G., GB 471590 (Imperial Chemical Industries Ltd.), **1937**.
8. (a) Brown, D. W.; Wall, L. A. *J. Phys. Chem.* **1963**, *67*, 1016-1019. (b) Mortimer, G. A.; Arnold, L. C. *J. Polym. Sci.* **1964**, *A2*, 4247-4253.
9. (a) Meerwein, H.; Burnelet, W. *Ber. Dtsch. Chem. Ges.* **1928**, *618*, 1845. (b) Hanford, W. E., US 2,377,779 (Du Pont), **1942**. (c) Roedel, M. J., US 2,475,520 (Du Pont), **1944**.
10. (a) Ziegler, K., US 3579493, **1955**. (b) Ziegler, K.; Holzkamp, E.; Breil, H.; Martin, H. *Angew. Chem.* **1955**, *67*, 426. (c) Ziegler, K.; Martin, H. *Angew. Chem.* **1955**, *67*, 541.
11. Banks, J. P.; Banks, R. L., US 2,825,721 (Phillips), **1953**.
12. (a) Natta, G.; Pino, P.; Corradini, P.; Danusso, F.; Mantica, E.; Mazzanti, G.; Moraglio, G. *J. Am. Chem. Soc.* **1955**, *77*, 1708-1710. (b) Natta, G. *Angew. Chem.* **1956**, *68*, 393.
13. (a) Jeong, T.; Lee, D. H. *Makromol. Chem.* **1990**, *191*, 1487-1496. (b) Albizzati, E.; Giannini, U.; Collina, G.; Noristi, L.; Resconi, L. in "Polypropylene Handbook", E. P. Moore Jr., Ed., Hanser Publishers, Munich **1996**, p11.
14. Chadwick, J. C. *Macromol. Symp.* **2001**, *173*, 21-36.
15. Moore, E. P. Jr., "The rebirth of Polypropylene: Supported Catalysts" Ed., Hanser Publishers, Munich, **1998**.
16. (a) Pino, P.; Mülhaupt, R. in "Transition Metal Catalyzed Polymerizations – Part A", Vol. 4, R. P. Quirk, Ed., MMI Press Symposium Series, Harwood Academic Publishers, New York **1981**, p1. (b) Fink, G.; Rottler, R.; *Angew. Makromol. Chem.* **1981**, *94*, 25-47.
17. (a) Cossee, P. *J. Catal.* **1964**, *3*, 80. (b) Arlman, E. J.; Cossee, P. *J. Catal.* **1966**, *5*, 178.
18. Jordan, R. F. *Adv. Organomet. Chem.* **1991**, *32*, 325.
19. (a) Sinn, H.; Mottweiler, R.; Andresen, A.; Cordes, H.-G.; Herwig, J.; Kaminsky, W.; Merck, A.; Vollmer, H.-J.; Pein, J., DE 2608863 (BASG AG), **1976**. (b) Sinn, H.; Mottweiler, R.; Andresen, A.; Cordes, H.-G.; Herwig, J.; Kaminsky, W.; Merck, A.; Vollmer, H.-J.; Pein, J., DE 2608933 (BASF AG), **1976**.
20. (a) Sinn, H.; Kaminsky, W.; Vollmer, H.-J.; Woldt, R. *Angew. Chem.* **1980**, *92*, 396. (b) Sinn, H.; Kaminsky, W. *Adv. Organomet. Chem.* **1980**, *18*, 99-149.
21. Wild, F. R. W. P.; Zsolnai, L.; Huttner, G.; Brintzinger, H.-H. *J. Organomet. Chem.* **1982**, *232*, 233-247.
22. Ewen, J. A. *J. Am. Chem. Soc.* **1984**, *106*, 6355-6364.
23. Kaminsky, W.; Kuelper, K.; Brintzinger, H.-H.; Wild, F. R. W. P. *Angew. Chem.* **1985**, *97*, 507-508.
24. (a) Brintzinger, H.-H.; Fischer, D.; Mülhaupt, R.; Rieger, B.; Waymouth, R. M. *Angew. Chem. Int. Ed. Engl.* **1995**, *34*, 1143-1170. (b) Bochmann, M. *J. Chem. Soc., Dalton Trans.* **1996**, 255-270. (c) Resconi, L.; Cavallo, L.; Fait, A.; Piemontesi, F. *Chem. Rev.* **2000**, *100*, 1253-1345. (d) Angermund, K.; Fink, G.; Jensen, V. R.; Kleinschmidt, R. *Chem. Rev.* **2000**, *100*, 1457-1470. (e) Coates, G. W. *Chem. Rev.* **2000**, *100*, 1223-1252. (f) Coates, G. W. *J. Chem. Soc., Dalton Trans.* **2002**, 467-475.
25. Ewen, J. A.; Jones, R. L.; Razavi, A.; Ferrara, J. D. *J. Am. Chem. Soc.* **1988**, *110*, 6255-6256.
26. Coates, G. W.; Waymouth, R. M. *Science* **1995**, *267*, 217-219.
27. McKnight, A. L.; Waymouth, R. M. *Chem. Rev.* **1998**, *98*, 2587-2598.
28. Mülhaupt, R. *Macromol. Chem. Phys.* **2003**, *204*, 289-327.
29. (a) Britovsek, G. J. P.; Gibson, V. C.; Wass, D. F. *Angew. Chem. Int. Ed. Engl.* **1999**, *38*, 428-447. (b) Gibson, V. C.; Spitzmesser, S. K. *Chem. Rev.* **2003**, *103*, 283-315.
30. (a) Scollard, J. D.; McConville, D. H. *J. Am. Chem. Soc.* **1996**, *118*, 10008-10009. (b) Scollard, J. D.; McConville, D. H. *Organometallics* **1997**, *16*, 1810-1812. (c) Baumann, R.; Davis, W. M.; Schrock, R. R. *J. Am. Chem. Soc.* **1997**, *119*, 3830-3831. (d) Mehrkhodavandi, P.; Schrock, R. R. *J. Am. Chem. Soc.* **2001**, *123*, 10746-10747.
31. Bourget-Merle, L.; Lappert, M. F.; Severn, J. R. *Chem. Rev.* **2002**, *102*, 3031-3066.
32. (a) Yoshida, Y.; Matsui, S.; Takagi, Y.; Mitani, M.; Nitabaru, M.; Nakano, T.; Fujita, T.; Kashiwa, T. *Chem. Lett.* **2000**, 1270-1271. (b) Yoshida, Y.; Matsui, S.; Takagi, Y.; Mitani, M.; Nakano, T.; Tanaka, H.; Kashiwa, T.; Fujita, T. *Organometallics* **2001**, *20*, 4793-4799. (c) Dawson, D. M.; Walker, D. A.; Thornton-Pett, M.; Bochmann, M. *J. Chem. Soc., Dalton Trans.* **2000**, 459-466.
33. Richter, J.; Edelmann, F. T.; Noltemeyer, M.; Schmidt, H. G.; Shmulinson, M.; Eisen, M. S. *J. Mol. Catal. A: Chem.* **1998**, *130*, 149-162.

34. (a) Matsui, S.; Mitani, M.; Saito, J.; Tohi, Y.; Makio, H.; Matsukawa, N.; Tagaki, Y.; Tsuru, K.; Nitaburu, M.; Nakano, T.; Fujita, T. *J. Am. Chem. Soc.* **2001**, *123*, 6847-6856. (b) Mitani, M.; Mohri, J.; Yoshida, Y.; Saito, J.; Ishii, S.; Tsuru, K.; Matsui, S.; Furuyama, R.; Nakano, T.; Tanaka, H.; Kojoh, S.-I.; Matsugi, T.; Kashiba, N.; Fujita, T. *J. Am. Chem. Soc.* **2002**, *124*, 3327-3336. (c) Tian, J.; Coates, G. W. *Angew. Chem. Int. Ed. Engl.* **2000**, *39*, 3626-3629. (d) Hustad, P. D.; Tian, J.; Coates, G. W. *J. Am. Chem. Soc.* **2002**, *124*, 3614-3621.
35. (a) Tshuva, E. Y.; Goldberg, I.; Kol, M.; Weitman, H.; Goldschmidt, Z. *Chem. Commun.* **2000**, 379-380. (b) Tshuva, E. Y.; Groysman, S.; Goldberg, I.; Kol, M.; Weitman, H.; Goldschmidt, Z. *Organometallics* **2002**, *21*, 662-670.
36. Swarc, M. *Nature* **1956**, *178*, 1168.
37. Johnson, L. K.; Killian, C. M.; Brookhart, M. *J. Am. Chem. Soc.* **1995**, *117*, 6414-6415.
38. (a) Small, B. L.; Brookhart, M. *J. Am. Chem. Soc.* **1998**, *120*, 7143-7144. (b) Britovsek, G. J. P.; Gibson, V. C; Kimberly, B. S.; Maddox, P. J.; McTavish, S. J.; Solan, G. A.; White, A. J. P.; Williams, D. *J. Chem. Commun.* **1998**, 849-850.
39. Younkin, T. R.; Connor, E. F.; Henderson, J. I.; Friedich, S. K.; Grubbs, R. H.; Bansleben, D. A. *Science* **2000**, *287*, 460-462.
40. Drent, E.; Van Dijk, R.; Van Ginkel, R.; Van Oort, B.; Pugh, R. I. *Chem. Commun.* **2002**, 744-745.
41. Ballard, D. G. H.; Courtis, A.; Holton, J.; McMeeking, J.; Pearce, R. *J. Chem. Soc., Chem. Commun.* **1978**, 994-995.
42. (a) Watson, P. L. *J. Am. Chem. Soc.* **1982**, *104*, 337-339. (b) Watson, P. L.; Herskovitz, T. *ACS Symp. Ser.* **1983**, *212*, 459.
43. (a) Watson, P. L.; Roe, D. C. *J. Am. Chem. Soc.* **1982**, *104*, 6471-6473. (b) Watson, P. L.; Parshall, G. W. *Acc. Chem. Res.* **1985**, *18*, 51-56.
44. Den Haan, K. H.; Wielstra, Y.; Eshuis, J. J. W.; Teuben, J. H. *J. Organomet. Chem.* **1987**, *323*, 181-192.
45. (a) Casey, P. C.; Tunge, J. A.; Fagan M. A. *J. Organomet. Chem.*, **2002**, *663*, 91-97. (b) Casey, P. C.; Tunge, J. A.; Lee, T.-Y.; Carpenetti II, D. W. *Organometallics*, **2002**, *21*, 389-396. (c) Casey, P. C.; Tunge, J. A.; Lee, T.-Y.; Fagan, M. A. *J. Am. Chem. Soc.* **2003**, *125*, 2641-2651.
46. (a) Sändig, N.; Dargel, T. K.; Koch, W. *Z. Anorg. Allg. Chem.* **2000**, *626*, 392-399. (b) Sändig, N.; Koch, W. *Organometallics* **2002**, *21*, 1861-1869.
47. Thompson, M. E.; Bercaw, J. E. *Pure & Appl. Chem.* **1984**, *56*, 1-11.
48. Burger, B. J.; Thompson, M. E.; Cotter, W. D.; Bercaw, J. E. *J. Am. Chem. Soc.* **1990**, *112*, 1566-1577.
49. Jeske, G.; Lauke, H.; Mauermann, H.; Swepton, P. N.; Schumann, H.; Marks, T. J. *J. Am. Chem. Soc.* **1985**, *107*, 8091-8103.
50. Radu, N. S.; Don Tilley, T.; Rheingold, A. L. *J. Am. Chem. Soc.* **1992**, *114*, 8293-8295.
51. (a) Evans, W. J.; Forrestal, K. J.; Ziller, J. W. *Angew. Chem., Int. Ed. Engl.* **1997**, *36*, 774-776. (b) Evans, W. J.; Forrestal, K. J.; Ansari, M. A.; Ziller, J. W. *J. Am. Chem. Soc.* **1998**, *120*, 2180-2181. (c) Evans, W. J.; Forrestal, K. J.; Ziller, J. W. *J. Am. Chem. Soc.* **1998**, *120*, 9273-9282.
52. (a) Olonde, X.; Bujadoux, K.; Mortreux, A.; Petit, F., FR 9307180 (ECP Enichem Polymeres France S.A.), **1994**. (b) Pelletier, J.-F.; Bujadoux, K.; Olonde, X.; Adisson, E.; Mortreux, A.; Chenal, T., EP 736536 (Enichem S.P.A., Italy; Université Des Sciences et Technologies De Lille), **1996**. (c) Olonde, X.; Mortreux, A. Petit, F.; Bujadoux, K. *J. Mol. Catal.* **1993**, *82*, 75-82. (d) Pelletier, J.-F.; Mortreux, A.; Petit, F.; Olonde, X.; Bujadoux, K. In *Catalyst Design for Tailor made Polyolefins*, Soga, K. and Terano, M., Eds, Elsevier, Amsterdam, **1994**, p249. (e) Pelletier, J.-F.; Mortreux, A.; Olonde, X.; Bujadoux, K. *Angew. Chem. Int. Ed. Engl.* **1996**, *35*, 1854-1856. (f) Bujadoux, K.; Chenal, T.; Fouga, C.; Olonde, X.; Pelletier, J.-F.; Mortreux, A. In *Metalorganic Catalysts for Synthesis and Polymerization*, Kaminsky, W., Ed, Springer-Verlag, Berlin, **1999**, p590. (g) Bogaert, S.; Carpentier, J.-F.; Chenal, T.; Mortreux, A.; Ricart, G. *Macromol. Chem. Phys.* **2000**, *201*, 1813-1822.
53. Pettijohn, T. M.; Hsieh, H. L., US 5,109,085 (Phillips Petroleum Co., USA). **1992**.
54. (a) Barbotin, F.; Boisson, C.; Spitz, R., FR 2,799,468 (Michelin Recherche et Technique S.A.), **1999**. (b) Boisson, C.; Barbotin, F.; Spitz, R.; Congress Organometallic Catalysts and Olefin Polymerization, Oslo, Norway, June **2002**.
55. Evans, W. J.; Bloom, I.; Hunter, W. E.; Atwood, J. L. *J. Am. Chem. Soc.* **1981**, *103*, 6507-6508.
56. Evans, W. J.; DeCoster, D. M.; Greaves, J. *Macromolecules* **1995**, *28*, 7929-7936.
57. (a) Jeske, G.; Laurel, E.; Schock, P.; Swepton, P. N.; Schumann, H.; Marks, T. J. *J. Am. Chem. Soc.* **1985**, *107*, 8103-8110. (b) Mauermann, H.; Swepton, P. N.; Marks, T. J. *Organometallics* **1985**, *4*, 200-202. (c) Marks, T. J.; Mauermann, H., WO 8605788 (Northwestern University, USA) **1986**.
58. (a) Wiesenfeldt, H.; Reimnuth, A.; Barsties, E., Evertz, K; Brintzinger, H.-H. *J. Organomet. Chem.* **1989**, *369*, 359-370. (b) Roll, W.; Brintzinger, H.-H.; Riegler, B.; Zolk, R. *Angew. Chem. Int. Ed. Engl.* **1990**, *29*, 279.

59. (a) Mitchell, J. P.; Hajela, S.; Brookhart, K.; Hardcasble, K. I.; Henling, L. M.; Bercaw, J. E. *J. Am. Chem. Soc.* **1996**, *118*, 1045-1053. (b) Gilchrist, J. H.; Bercaw, J. E. *J. Am. Chem. Soc.* **1996**, *118*, 12021-12028.
60. (a) Ihara, E.; Nodono, M.; Yasuda, H. *Macromol. Chem. Phys.* **1996**, *197*, 1909-1917. (b) Ihara, E.; Nodono, M.; Katsura, K.; Adachi, Y.; Yasuda, H.; Yamagashira, M.; Hashimoto, H.; Kanehisa, N.; Kai, Y. *Organometallics* **1998**, *17*, 3945-3956. (c) Yasuda, H.; Ihara, E.; Nitto, Y.; Kakehi, T.; Morimot, M.; Nodono, M. *ACS Symp. Ser.* **1998**, *704*, 149-162. (d) Yasuda, H. *Prog. Polym. Sci.* **2000**, *25*, 573-626. (e) Ihara, E.; Yoshioka, S.; Furo, M.; Katsura, K.; Yasuda, H.; Mohri, S.; Kanehisa, N.; Kai, Y. *Organometallics* **2001**, *20*, 1752-1761.
61. Bogaert, S.; Chenal, T.; Mortreux, A.; Nowogrocki, G.; Lehmann, C. W.; Carpentier, J.-F. *Organometallics* **2001**, *20*, 199-205.
62. Arndt, S.; Okuda, J. *Chem. Rev.* **2002**, *102*, 1953-1976.
63. (a) Coughlin, E. B.; Shapiro, P. J.; Bercaw, J. E. *Polym. Prepr. (ACS, Div. Polym. Chem.)* **1992**, *33*, 1226-1227. (b) Piers, W. E.; Shapiro, P. J.; Bunel, E. E.; Bercaw, J. E. *Synlett* **1990**, 74-84. (c) Bercaw, J. E. *Polym. Prepr. (ACS, Div. Polym. Chem.)* **1991**, *32*, 459-460. (d) Shapiro, P. J.; Bunel, E.; Schaefer, W. P.; Bercaw, J. E. *Organometallics* **1990**, *9*, 867-869. (e) Shapiro, P. J.; Schaefer, W. P.; Labinger, J. A.; Bercaw, J. E.; Cotter, W. D. *J. Am. Chem. Soc.* **1994**, *116*, 4623-4640.
64. (a) Arndt, S.; Beckerle, K.; Hultsch, K. C.; Sinnema, P.-J.; Voth, P.; Spaniol, T. P.; Okuda, J. *J. Mol. Catal. A: Chem.* **2002**, *190*, 215-223. (b) Okuda, J.; Arndt, S.; Beckerle, K.; Hultsch, K. C.; Voth, P.; Spaniol, T. P. *Organometallic Catalysts and Olefin Polymerization* **2001**, 156-165, and references therein.
65. (a) Schaverien, C. J. *Adv. Organomet. Chem.* **1994**, *36*, 283-362. (b) Schaverien, C. J. *J. Mol. Catal.* **1994**, *90*, 177-183. (c) Schaverien, C. J. *Organometallics* **1994**, *13*, 69-82.
66. (a) Miotti, R. D.; de Souza Maia, A.; Paulino, I. S.; Schuchardt, U.; de Oliveira, W. *Journal of Alloys and Compounds* **2002**, *344*, 92-95. (b) Lavini, V.; Maia, A. S.; Paulino, I. S.; Schuchardt, U.; Oliveira, W. *Inorg. Chem. Commun.* **2001**, *4*, 582-584.
67. (a) Hou, Z.; Zhang, Y.; Tezuka, H.; Xie, P.; Tardif, O.; Koizumi, T.; Yamazaki, H.; Wakatsuki, Y. *J. Am. Chem. Soc.* **2000**, *122*, 10533-10543. (b) Hou, Z.; Koizumi, T.-A.; Nishiura, M.; Wakatsuki, Y. *Organometallics* **2001**, *20*, 3323-3328. (c) Tardif, O.; Hou, Z.; Nishiura, M.; Koizumi, T.-A.; Wakatsuki, Y. *Organometallics* **2001**, *20*, 4565-4573. (d) Kaita, S.; Wakatsuki, Y. *Pure Appl. Chem.* **2001**, *73*, 291-294. (e) Hou, Z.; Zhang, Y.; Nishiura, M.; Wakatsuki, Y. *Organometallics* **2003**, *22*, 129-135.
68. Trifonov, A. A.; Kirillov, E. N.; Fisher, A.; Edelmann, F. T.; Bochkarev, M. N. *Chem. Commun.* **1999**, 2203-2204.
69. (a) Fu, P.-F.; Marks, T. J. *J. Am. Chem. Soc.* **1995**, *117*, 10747-10748. (b) Koo, K.; Fu, P.-F.; Marks, T. J. *Macromolecules* **1999**, *32*, 981-988.
70. (a) Watson, P. L. *J. Chem. Soc., Chem. Commun.* **1983**, 276-277. (b) Evans, W. J.; Ulibarri, T. A.; Ziller, J. W. *Organometallics* **1991**, *10*, 134-142. (c) Booij, M.; Meetsma, A.; Teuben, J. H. *Organometallics* **1991**, *10*, 3246-3252. (d) Booij, M.; Deelman, B. J.; Duchateau, R.; Postma, D. S.; Meetsma, A.; Teuben, J. H. *Organometallics* **1993**, *12*, 3531-3540.
71. Deelman, B.-J.; Stevels, W. M.; Teuben, J. H.; Lakin, M. T.; Spek, A. L. *Organometallics* **1994**, *13*, 3881-3891.
72. (a) Hessen, B.; Ringelberg, S. N.; Meppelder, G.-J.; Teuben, J. H. *Polym. Prep. (ACS, Div. Polym. Chem.)* **2000**, *41*, 397-398. (b) Sinnema, P.-J.; Hessen, B.; Teuben, J. H. *Macromol. Rapid Comm.* **2000**, *21*, 562-566.
73. Anwander, R.; *Top. Curr. Chem.* **1996**, *179*, 151-245, and references therein.
74. Edelmann, F. T. *New. J. Chem.* **1995**, *19*, 535-550, and references therein.
75. Reger, D. L.; Knox, S. J.; Lindeman, J. A.; Lebodia, L. *Inorg. Chem.* **1990**, *29*, 416-419.
76. (a) Reger, D. L.; Lindeman, J. A.; Lebodia, L. *Inorg. Chem.* **1988**, *27*, 1890-1896. (b) Hasinoff, L.; Takats, J.; Zhang, X.; Bond, A. H.; Rogers, R. D. *J. Am. Chem. Soc.* **1994**, *116*, 8833-8834.
77. Anwander, R.; *Top. Curr. Chem.* **1996**, *179*, 33-110, and references therein.
78. Rabe, G. W.; Riede, J.; Schier, A. *Inorg. Chem.* **1996**, *35*, 40-45.
79. Schaverien, C. J.; Orpen, A. G. *Inorg. Chem.* **1991**, *30*, 4968-4978.
80. Lee, L.; Berg, D. J.; Einstein, F. W. *Organometallics* **1997**, *16*, 1819-1831.
81. (a) Duchateau, R.; van Wee, C. T.; Meetsma, A.; Teuben, J. H. *J. Am. Chem. Soc.* **1993**, *115*, 4931-4932. (b) Duchateau, R.; Meetsma, A.; Teuben, J. H. *Organometallics* **1996**, *15*, 1656-1661. (c) Duchateau, R.; van Wee, C. T.; Meetsma, A.; van Duijnen, P. T.; Teuben, J. H. *Organometallics* **1996**, *15*, 2279-2290. (d) Duchateau, R.; van Wee, C. T.; Teuben, J. H. *Organometallics* **1996**, *15*, 2291-2302.
82. (a) Lee, L. W. M.; Piers, W. E.; Elsegood, M. R. J.; Clegg, W.; Parvez, M. *Organometallics* **1999**, *18*, 2947-2949. (b) Hayes, P. G.; Piers, W. E.; Lee, L. W. M.; Knight, L. K.; Parvez, M.; Elsegood, M. R. J.; Clegg, W. *Organometallics* **2001**, *20*, 2533-2544.

83. Duchateau, R.; Tuinstra, T.; Brussee, E. A. C.; Meetsma, A.; van Duijnen, P. T.; Teuben, J. H. *Organometallics* **1997**, *16*, 3511-3522.
84. Hillier, A. C.; Liu, S. Y.; Sella, A.; Elsegood, M. R. J. *Journal of Alloys and Compounds* **2000**, *303-304*, 83-93.
85. (a) Bianconi, P. A. *Book of Abstracts, 211th ACS National Meeting, New Orleans, LA, March 24-28 1996*, (b) Long, D. P.; Bianconi, P. A. *J. Am. Chem. Soc.* **1996**, *118*, 12453-12454.
86. Domingo, A.; Elsegood, M. R. J.; Hillier, A. C.; Lin, G.; Liu, S. Y.; Lopes, I.; Marques, N.; Maunder, G. H.; McDonald, R.; Sella, A.; Steed, J. W.; Takats, J. *Inorg. Chem.* **2002**, *41*, 6761-6768.
87. Hajela, S.; Schaefer, W. P.; Bercaw, J. E. *J. Organomet. Chem.* **1997**, *532*, 45-53.
88. (a) Bambirra, S.; Van Leusen, D.; Meetsma, A.; Hessen, B.; Teuben, J. H. *Abstracts of Papers, 222nd ACS National Meeting, Chicago, IL, United States, August 26-30, 2001*. (b) Bambirra, S.; van Leusen, D.; Meetsma, A.; Hessen, B.; Teuben, J. H. *Chem. Commun.* **2001**, 637-638.
89. Hayes, P. G.; Piers, W. E.; McDonald, R. *J. Am. Chem. Soc.* **2002**, *124*, 2132-2133.
90. Bambirra, S.; Van Leusen, D.; Meetsma, A.; Hessen, B.; Teuben, J. H. *Chem. Commun.* **2003**, 522-523.
91. Fryzuk, M. D.; Giesbrecht, G.; Rettig, S. J. *Organometallics* **1996**, *15*, 3329-3336.
92. Gountchev, T. I.; Don Tilley, T. *Organometallics* **1999**, *18*, 2896-2905.
93. Graf, D. D.; Davis, W. M.; Schrock, R. R. *Organometallics* **1998**, *17*, 5820-5824.
94. Baumann, R.; Davis, W. M.; Schrock, R. R. *J. Am. Chem. Soc.* **1997**, *119*, 3830-3831.
95. Evans, W. J.; Broomhall-Dillard, R. N. R.; Ziller, J. W. *J. Organomet. Chem.* **1998**, *569*, 89-97.
96. Arndt, S.; Spaniol, T. P.; Okuda, J. *Chem. Commun.* **2002**, 896-897.
97. Chen, Y.; Zhang, Y.; Shen, Z.; Kou, R.; Chen, L. *Eur. Polym. J.* **2001**, *37*, 1181-1184.
98. Yang, M.; Zhang, X.; Li, J.; Shen, Z. *J. Polym. Sci., Part A: Polym. Chem.* **1992**, *30*, 63-69.
99. (a) Lochmann, L.; Rodova, M.; Trekoval, J. *J. Polym. Sci (Chem. Ed.)* **1974**, *12*, 2091-2094. (b) Lochmann, L.; Pokorny, J.; Trekoval, J.; Alder, H. J.; Berger, W. *Makromol. Chem.* **1983**, *184*, 2021-2031. (c) Lochmann, L.; Müller, A. H. E. *Makromol. Chem.* **1990**, *191*, 1657-1664. (d) Janata, M.; Lochmann, L.; Vlcek, P.; Dybal, J.; Müller, A. H. E. *Makromol. Chem.* **1992**, *193*, 101-112. (e) Janata, M.; Lochmann, L.; Müller, A. H. E. *Makromol. Chem.* **1993**, *194*, 625.
100. (a) Wang, J. S.; Jérôme, R.; Bayard, P.; Patin, M.; Teyssié, P. *Macromolecules* **1994**, *27*, 4635-4638. (b) Maurer, A.; Marcarian, X.; Müller, A. H. E.; Navarro, C.; Vuillemin, B. *Polym. Prepr. (ACS, Div. Polym. Chem.)* **1997**, *38*, 467-468.
101. (a) Fayt, R.; Forte, R.; Jacobs, C.; Jérôme, R.; Ouhadi, T.; Teyssié, P.; Varshney, S. K. *Macromolecules* **1987**, *20*, 1442-1444. (b) Baskaran, D.; Sivaram, S. *Macromolecules* **1997**, *30*, 1869-1874. (c) Baskaran, D.; Müller, A. H. E.; Sivaram, S. *Macromolecules* **1999**, *32*, 1356-1361.
102. (a) Zundel, T.; Teyssié, P.; Jérôme, R. *Macromolecules* **1998**, *31*, 2433-2439. (b) Zundel, T.; Zune, C.; Teyssié, P.; Jérôme, R. *Macromolecules* **1998**, *31*, 4089-4092.
103. (a) Hatada, K.; Ute, K.; Tanaka, K.; Okamoto, Y.; Kitayama, T. *Polym. J.* **1986**, *18*, 1037. (b) Hatada, K.; Kitayama, T.; Ute, K.; Masuda, E.; Shinozaki, T.; Yamamoto, M. *Polym. Prepr. (ACS, Div. Polym. Chem.)* **1988**, *29*, 54-55. (c) Ballard, D. G. H.; Bowles, R. J.; Haddleton, D. M.; Richards, S. N.; Sellens, R.; Twose, D. L. *Macromolecules* **1992**, *25*, 5907-5913. (d) Haddleton, D. M.; Muir, A. V. G.; O'Donnell, J. P.; Richards, S. N.; Twose, D. L. *Macromol. Symp.* **1995**, *91*, 91. (e) Seebach, D.; Pietzonka, T. *Angew. Chem.* **1993**, *105*, 741. (f) Wang, J. S.; Teyssié, P.; Heim, P.; Vuillemin, B., EP 95400861.1, **1995**. (g) Schlaad, H.; Schmitt, B.; Müller, A. H. E.; Jüngling, S.; Weiss, H. *Macromolecules* **1998**, *31*, 573-577. (h) Schlaad, H.; Schmitt, B.; Müller, A. H. E *Angew. Chem., Int. Ed.* **1998**, *37*, 1389-1391.
104. (a) Reetz, M. T.; Ostarek, R. *Chem. Commun.* **1988**, 213-214. (b) Raj, D. J. A.; Wadgaonkar, P. P.; Sivaram, S. *Macromolecules* **1992**, *25*, 2774-2776. (c) Zagala, A. P.; Hogen-Esch, T. E. *Macromolecules* **1996**, *29*, 3038-3039. (d) Baskaran, D.; Müller, A. H. E. *Macromolecules* **1997**, *30*, 1869-1874.
105. (a) Müller, A. H. E. In *Comprehensive Polymer Science*; G. Allen, J. C. Bevington Eds.; Pergamon, Oxford, U.K., **1988**; p 387. (b) Warmkessel, J.; Kim, J.; Quirk, R.; Brittain, W. *Polym. Prepr. (ACS, Div. Polym. Chem.)* **1994**, *35*, 589-590.
106. (a) Hatada, K.; Ute, K.; Tanaka, K.; Kitayama, T.; Okamoto, Y. *Polym. J.* **1985**, *17*, 977. (b) Hatada, K.; Ute, K.; Tanaka, K.; Okamoto, Y.; Kitayama, T. *Polym. J.* **1986**, *18*, 1037. (c) Nakano, N.; Ute, K.; Okamoto, Y.; Matsuura, Y.; Hatada, K. *Polym. J.* **1989**, *21*, 935. (d) Hatada, K. *J. Polym. Sci., Part A: Chem.* **1999**, *37*, 245-260.
107. Yasuda, H.; Yamamoto, H.; Yamashita, M.; Yokota, K.; Nakamura, A.; Miyake, S.; Kai, Y.; Kanehisa, N. *Macromolecules* **1993**, *26*, 7134-7143.
108. Cao, Z. K.; Okamoto, Y.; Hatada, K. *Kobunshi Ronbunshu* **1986**, *43*, 857.
109. Abe, H.; Imai, K.; Matsumoto, M. *J. Polym. Sci., Part C*, **1968**, C23, 469.
110. Hatada, K.; Nakanishi, H.; Ute, K.; Kitayama, T.; Okamoto, Y. *Polym. J.* **1986**, *18*, 581. For related studies with Grignard and dialkylmagnesium reagents, see: (a) Allen, P. E. M.; Bateup, B. O. *Eur. Polym. J.* **1978**, *14*, 1001-1010. (b) Allen, P. E. M.; Mair, C. *Eur. Polym. J.* **1983**, *20*, 697-705. (c) Matsuzaki,

- K.; Tanaka, H.; Kanai, T. *Makromol. Chem.* **1981**, *182*, 2905-2918. (d) Soum, A.; D'Accorso, N.; Fontanile, M. *Makromol. Chem., Rapid Commun.* **1983**, *4*, 471-477.
111. (a) Webster, O. W.; Hertler, W. R.; Sogah, D. Y.; Farnham, W.; Rajanbabu, T. V. *J. Am. Chem. Soc.* **1983**, *105*, 5706-5708. (b) Sogah, D. Y.; Hertler, W. R.; Webster, O. W.; Cohen, G. M. *Macromolecules* **1987**, *20*, 1473-1488. (c) Webster, O. W. *Science* **1991**, *251*, 887.
112. (a) "Controlled Radical Polymerization"; Matyjaszewski, K., Ed.; American Chemical Society: Washington, DC **1998**; Vol.685. (b) "Controlled/living Radical Polymerization: Progress in ATRP, NMP, and RAFT"; Matyjaszewski, K., Ed.; American Chemical Society: Washington, DC **2000**; Vol.685. (c) Matyjaszewski, K.; Davis, T. P. *Handbook of Radical Polymerization*; John Wiley and Sons, Inc., Hoboken, **2002**.
113. (a) Matyjaszewski, K.; Xia, J. *Chem. Rev.* **2001**, *101*, 2921-2990. (b) Kamigaito, M.; Ando, T.; Sawamoto, M. *Chem. Rev.* **2001**, *101*, 3689-3746.
114. Hawker, C. J.; Bosman, A. W.; Harth, E. *Chem Rev.* **2001**, *101*, 3661-3688.
115. Matsumoto, A. In *Handbook of Radical Polymerization*; Matyjaszewski, K.; Davis, T. P. Ed. ; John Wiley and Sons, Inc., Hoboken, **2002**, 691-774.
116. Yasuda, H.; Yamamoto, H.; Yokota, K.; Miyake, S.; Nakamura, A. *J. Am. Chem. Soc.* **1992**, *114*, 4908-4910.
117. (a) Yasuda, H.; Tamai, H. *Prog. Polym. Sci.* **1993**, *18*, 1097-1139. (b) Yasuda, H.; Ihara, E. *Macromol. Chem. Phys.* **1995**, *196*, 2417-2441. (c) Yasuda, H.; Ihara, E.; Hayakawa, T.; Kakehi, T. *J. Macromol. Sci., Pure Appl. Chem.* **1997**, *A34*, 1929-1944. (d) Yasuda, H.; Ihara, E. *Adv. Polym. Sci.* **1997**, *133*, 53-101. (e) Yasuda, H.; Ihara, E. *Bull. Chem. Soc. Jpn.* **1997**, *70*, 1745-1767. (f) Yasuda, H.; Ihara, E.; Nitto, Y.; Kakehi, T.; Morimoto, M.; Nodono, M. *ACS Symp. Ser.* **1998**, *704*, 149-162. (g) Yasuda, H. *Top. Organomet. Chem.* **1999**, *2*, 255-283.
118. (a) Novak, B. M.; Boffa, L. S. *Polym. Prepr. (ACS, Div. Polym. Chem.)* **1994**, *35*, 528-529; (b) Boffa, L. S.; Novak, B. M. *Macromolecules* **1994**, *27*, 6993-6995. (c) Novak, B. M.; Boffa, L. S., WO 9521873, (University of California, USA), **1995**.
119. Yasuda, H.; Yamamoto, H.; Takemoto, Y.; Yamashita, M.; Yokota, K.; Miyake, S.; Nakamura, A. *Makromol. Chem., Macromol. Symp.* **1993**, *67*, 187-201.
120. Ihara, E.; Morimoto, M.; Yasuda, H. *Macromolecules* **1995**, *28*, 7886-7892.
121. Yasuda, H.; Furo, M.; Yamamoto, H.; Nakamura, A.; Miyake, S.; Kibino, N. *Macromolecules* **1992**, *25*, 5115-5116.
122. Giardello, M. A.; Yamamoto, Y.; Brard, L.; Marks, T. J. *J. Am. Chem. Soc.* **1995**, *117*, 3276-3277.
123. Giardello, M. A.; Conticello, V. P.; Brard, L.; Gagne, M. R.; Marks, T. J. *J. Am. Chem. Soc.* **1994**, *116*, 10241-10254.
124. Satoh, Y.; Ititake, N.; Nakayama, Y.; Okuno, S.; Yasuda, H. *J. Organomet. Chem.* **2003**, *667*, 42-52.
125. (a) Mao, L.; Shen, Q.; Sun, J. *J. Organomet. Chem.* **1998**, *566*, 9-14. (b) Mao, L.; Shen, Q. J.; *J. Polym. Sci., Part A: Polym. Chem.* **1998**, *36*, 1593-1597.
126. Sun, J.; Pan, Z.; Zhong, Y.; Hu, W.; Yang, S. *Eur. Polym. J.* **2000**, *36*, 2375-2380.
127. Qian, C.; Zou, G.; Chen, Y.; Sun, J. *Organometallics* **2001**, *20*, 3106-3112.
128. Lee, M. H.; Hwang, J.-W.; Kim, Y.; Kim, J.; Han, Y.; Do, Y. *Organometallics* **1999**, *18*, 5124-5129.
129. Nie, W.; Qian, C.; Chen, Y.; Jie, S. *J. Organomet. Chem.* **2002**, *647*, 114-122.
130. Qian, C.; Nie, W.; Chen, Y.; Jie, S. *J. Organomet. Chem.* **2002**, *645*, 82-86.
131. Knjazhanski, S. Y.; Elizalde, L.; Cadenas, G.; Bulychev, B. M. *J. Polym. Sci., Part A: Polym. Chem.* **1998**, *36*, 1599-1606.
132. Maciejewski, P. J. L.; Agoston, T.; Lal, T. K.; Waymouth, R. M. *J. Am. Chem. Soc.* **1998**, *120*, 11316-11322.
133. Knjazhanski, S. Y.; Lopez-Gonzalez, H. R.; Larios-Lopez, L.; Cadenas, G. *Polym. Prepr. (ACS, Div. Polym. Chem.)* **2000**, *41*, 1294-1295.
134. Sheng, E.; Wang, S.; Yang, G.; Zhou, S.; Cheng, L.; Zhang, K.; Huang, Z. *Organometallics* **2003**, *22*, 684-692.
135. Knjazhanski, S. Y.; Elizalde, L.; Cadenas, G.; Bulychev, B. M. *J. Organomet. Chem.* **1998**, *568*, 33-40.
136. Bolig, A. D.; Chen, E. Y.-X. *J. Am. Chem. Soc.* **2001**, *123*, 7943-7944.
137. Tanaka, K.; Furo, M.; Ihara, E.; Yasuda, H. *J. Polym. Sci., Part A: Polym. Chem.* **2001**, *39*, 1382-1390.
138. Zi, G.; Li, H.-W.; Xie, Z. *Organometallics* **2002**, *21*, 1136-1145.
139. Ph.D. Thesis, Fouga, C., Université de Lille, **1997**.
140. Sun, J.; Pan, Z.; Yang, S. *J. Appl. Polym. Sci.* **2001**, *79*, 2245-2250.
141. Bala, M. D.; Huang, J.; Zhang, H.; Qian, Y.; Sun, J.; Liang, C. J. *Organomet. Chem.* **2002**, *647*, 105-113.
142. Yanagase, A.; Tone, S.; Tokimitsu, T.; Nodono, M. WO 9804595 (Mitsubishi Rayon Co., LTD) **1999**.
143. Nodono, M.; Tokimitsu, T.; Makino, T.; Yanagase, A. *Macromol. Chem. Phys.* **2000**, *201*, 2282-2288.
144. Ihara, E.; Koyama, K.; Yasuda, H.; Kanehisa, N.; Kai, Y. *J. Organomet. Chem.* **1999**, *574*, 40-49.
145. Woodman, T. J.; Schormann, M.; Bochmann, M. *Organometallics* **2003**, *22*, 2938-2943.

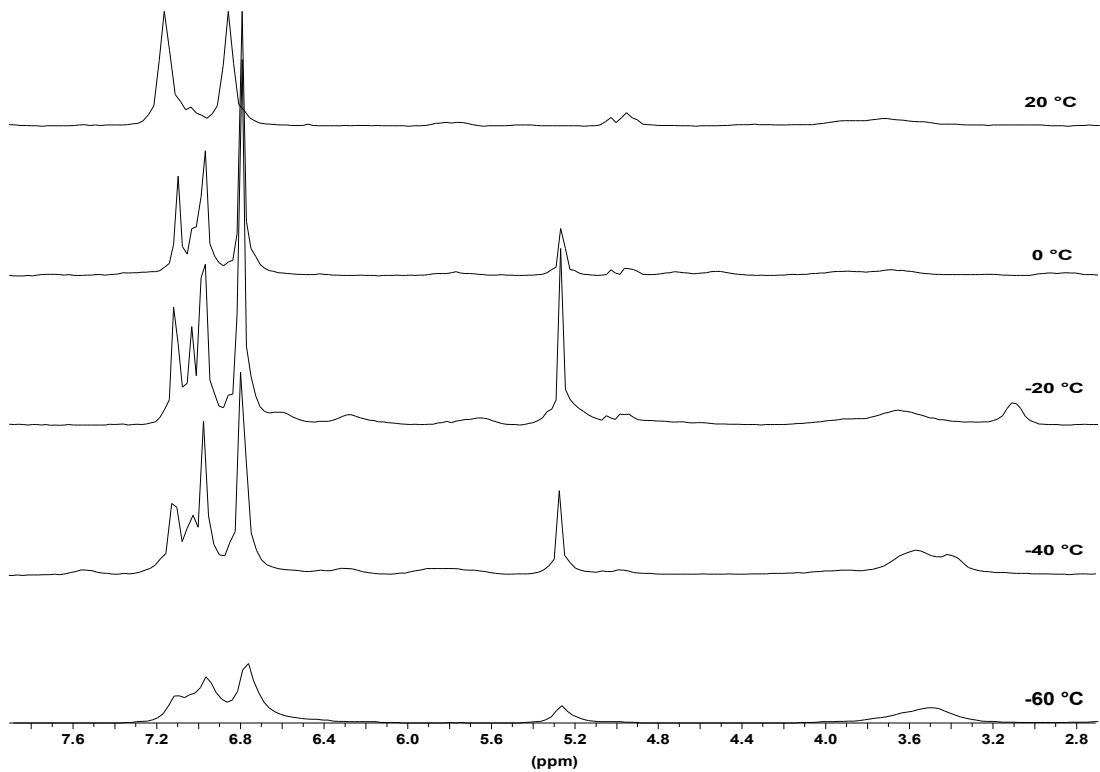
146. Woodman, T. J.; Schormann, M.; Hughes, D. L.; Bochmann, M. *Organometallics* **2003**, *22*, 3028-3030.
147. Yasuda, H.; Ihara, E.; Nitto, Y.; Kakehi, T.; Morimoto, M.; Nodono, M. *ACS Symp. Ser.* **1998**, *704*, 149-162.
148. Ihara, E.; Adachi, Y.; Yasuda, H.; Hashimoto, H.; Kanehisa, N.; Kai, Y. *J. Organomet. Chem.* **1998**, *569*, 147-157.
149. Estler, F.; Eickerling, G.; Herdtweck, E.; Anwander, R. *Organometallics* **2003**, *22*, 1212-1222.
150. Luo, Y.; Yao, Y.; Shen, Q.; Yu, K.; Weng, L. *Eur. J. Inorg. Chem.* **2003**, *318*-323.
151. Zhou, S.-L.; Wang, S.-W.; Yang, G.-S.; Liu, X.-Y.; Sheng, E.-H.; Zhang, K.-H.; Cheng, L.; Huang, Z.-X. *Polyhedron* **2003**, *22*, 1019-1024.
152. Karl, M.; Seybert, G.; Massa, W.; Harms, K.; Agarwal, S.; Maleika, R.; Stelter, W.; Greiner, A.; Heitz, W.; Neumüller, B.; Dehnische, K. *Z. Anorg. Allg. Chem.* **1999**, *625*, 1301-1309.
153. Yao, Y.; Zhang, Y.; Zhang, Z.; Shen, Q.; Yu, K. *Organometallics* **2003**, *22*, 2876-2882.
154. Habaue, S.; Yoshikawa, M.; Okamoto, Y. *Polym. J.* **1995**, *27*, 986-992.
155. Lebrun, A.; Namy, J.-L.; Kagan, H. B. *Tetrahedron Lett.* **1991**, *32*, 2355-2358.
156. Nakayama, Y.; Shibahara, T.; Fukumoto, H.; Nakamura, A. *Macromolecules* **1996**, *29*, 8014-8016.
157. Nolan, S. P.; Stern, D.; Marks, T. J. *J. Am. Chem. Soc.* **1989**, *111*, 7844-7853.
158. Sugimoto, H.; Inoue, S. *Polym. Prepr. (ACS, Div. Polym. Chem.)* **2000**, *41*(1), 424-425.
159. Sugimoto, H.; Kato, M.; Inoue, S. *Macromol. Chem. Phys* **1997**, *198*, 1605-1610.
160. (a) Sun, J. Q.; Wang, G. M.; Shen, Z. Q. *Chin. J. Appl. Chem.* **1993**, *10*(4), 1-5. (b) Liu, J. F.; Sun, J. Q., Shen, Z. Q. *Chem. Res. Chin. Univ.* **1993**, *9*(2), 148-152. (c) Sun, J. Q. *Chem. Res. Chin. Univ.* **1997**, *13*(4), 344-349. (d) Sun, J. Q. Pan, Z. D. *Chin. J. Appl. Chem.* **1997**, *14*(2), 1-4.
161. Liu, J.; Shen, Z. Q.; Sun, J. Q. *Eur. Polym. J.* **1996**, *32*, 883-886.
162. Jiang, L.; Shen, Z. Q.; Zhang, Y. *Eur. Polym. J.* **2000**, *36*, 2513-2516.
163. Collins, S.; Ward, D. G. *J. Am. Chem. Soc.* **1992**, *114*, 5460-5462.
164. (a) Collins, S.; Ward, D. G.; Suddaby, K. H. *Macromolecules* **1994**, *27*, 7222-7224. (b) Li, Y.; Ward, D. G.; Reddy, S. S.; Collins, S. *Macromolecules* **1997**, *30*, 1875-1883.
165. (a) Soga, K.; Deng, D.; Yano, T.; Shiono, T. *Macromolecules* **1994**, *27*, 7938-7940. (b) Shiono, T.; Saito, T.; Saegusa, N.; Hagihara, H.; Ikeda, T.; Deng, H.; Soga, K. *Macromol. Chem. Phys.* **1998**, *199*, 1573-1579.
166. Deng, D.; Shiono, T.; Soga, K. *Macromolecules* **1995**, *28*, 3067-3073.
167. Cameron, P. A.; Gibson, V. C.; Graham, A. J. *Macromolecules* **2000**, *33*, 4329-4335.
168. Nguyen, H.; Jarvis, A. P.; Lesley, M. J. G.; Kelly, W. M.; Reddy, S. S.; Taylor, N. J.; Collins, S. *Macromolecules* **2000**, *33*, 1508-1510.
169. Frauenrath, H.; Keul, H.; Höcker, H. *Macromolecules* **2001**, *34*, 14-19.
170. Jin, J.; Wilson, D. R.; Chen, E. Y.-X. *Chem. Commun.* **2002**, *708*-709.
171. (a) "Ullmann's Encyclopedia of Industrial Chemistry", 5th edition, vol. A4, VCH, Weinheim (**1993**) p22. (b) L. Porri, A. Giarrusso, In *Comprehensive Polymer Science*: G.C. Eastmond, A. Ledwith, S. Russo, P. Sigwalt, Eds. Pergamon Press: Oxford, U.K. 4 (**1989**) p53. (c) R. Taube, G. Sylvester, "Stereospecific Polymerization of Butadiene or Isoprene", in "Applied Homogeneous Catalysis with Organometallic compounds", B. Cornils, W.A. Herrmann, Eds., 2nd Ed., vol. 1, VCH, Weinheim-New York-Basel-Cambridge-Tokyo, **2002**, pp. 285-315. (d) Porri, L.; Ricci, G.; Shubin, N. *Macromol. Symp.* **1998**, *128*, 53-61. (e) Porri, L.; Ricci, G.; Giarrusso, A.; Shubin, N.; Lu, Z. *ACS Symp. Ser.* **2000**, No 749, 15-30.
172. Witte, J. *Angew. Makromol. Chem.* **1981**, *94*, 119-146.
173. (a) Robinson, I. M.; Schreyer, R. C., US 3,118,864 (Du Pont), **1964**. (b) Shen, T.-C.; Gung, C.-Y.; Chung, C.-C.; Ouyang, J. *Sci. Sin.* **1964**, *13*, 1339.
174. (a) Natta, G.; Porri, L.; Carbonaro, A. *Makromolek. Chem.* **1964**, *77*, 126-138. (b) Soga, K.; Shiono, T.; Sano, T.; Yamamoto, K. *Polym. Prepr., Jpn.* **1982**, *31*, 1445.
175. (a) Wilke, G.; Bogdanovic, B.; Hardt, P.; Heimbach, P.; Keim, W.; Kröner, M.; Oberkirch, W.; Tanaka, K.; Steinrucke, E.; Wlater, D.; Zimmermann, H. *Angew. Chem. Int. Ed. Engl.* **1966**, *5*, 151. (b) Porri, L.; Natta, G.; Gallazzi, M. C. *J. Polym. Sci. C* **1967**, *16*, 2525.
176. Warin, R.; Teyssié, P.; Bourdaudurq, P.; Dawans, F. *J. Polym. Sci., Polym. Lett.* **1973**, *11*, 177-183.
177. Dolgoplosk, B.A.; Beilin, S.I.; Korshak, Y.V.; Makovetsky, K.L.; Tinyakova, E.I. *J. Polym. Sci., Part A-1* **1973**, *11*, 2569-2590.
178. Taube, R.; Windisch, H.; Maiwald, S. *Macromol. Symp.* **1995**, *89*, 393-409.
179. (a) Shen, Z.; Ouyang, J.; Wang, F.; Hu, Z.; Yu, F.; Qian, N. J. *Polym. Sci. Chem. Ed.* **1980**, *18*, 3345-3357. (b) Srinivasa Rao, G. S.; Updhyay, V. K.; Jain, R. C. *Angew. Makromol. Chem.* **1997**, *251*, 193-205. (c) Srinivasa Rao, G. S.; Updhyay, V. K.; Jain, R. C. *J. Appl. Polym. Sci.* **1999**, *71*, 595-602.
180. Yang, J. H.; Tsutsui, M.; Shen, Z.; Bergbreiter, D. E. *Macromolecules* **1982**, *15*, 230-233.
181. Wang, F.; Bolognesi, A.; Immirzi, A.; Porri, L. *Makromolek. Chem.* **1981**, *182*, 3617-3623.
182. Wilson, D. J. *Polym. Int.* **1996**, *39*, 235-242.
183. Ricci, G.; Italia, S.; Cabassi, F.; Porri, L. *Polym. Commun.* **1987**, *28*, 223.

184. Sigaeva, N. N.; Usmanov, T. S.; Budtov, V. P.; Spivak, S. I.; Zaikov, G. E.; Monakov, Y. B. *J. Appl. Polym. Sci.* **2002**, *87*, 358-368.
185. Dong, W.; Masuda, T. J. *Polym. Sci., Part A: Polym. Chem.* **2002**, *40*, 1838-1844.
186. Jin, Y.-T.; Sun, Y.-F.; Ouyang, J. *Chem. Abstr.* **1980**, *93*, 150747h.
187. (a) Marina, N.G.; Monakov, Y. B.; Rafikov, S. R.; Gadaleva, K. K. *Polym. Sci. U.S.S.R.* **1984**, *26*, 1251.
(b) Wilson, D. J. *Makromol. Chem. Macromol. Symp.* **1993**, *66*, 273-288.
188. Kwag, G. *Macromolecules* **2002**, *35*, 4875-4879.
189. Wilson, D. J.; Jenkins, D. K. *Polymer* **1992**, *27*, 407-411.
190. Evans, W. J.; Giarikos, D. G.; Ziller, J. W. *Organometallics* **2001**, *20*, 5751-5758.
191. Kwag, G.; Lee, H.; Kim, S. *Macromolecules* **2001**, *34*, 5367-5369.
192. Shan, C.; Lin, Y.; Ouyang, J.; Fan, Y.; Yang, G. *Makromol. Chem.* **1987**, *188*, 629-635.
193. (a) Friebe, L.; Nuyken, O.; Windisch, H.; Obrecht, W. *Macromol. Chem. Phys.* **2002**, *203*, 1055-1064. (b) Quirk, R. P.; Kells, A. M.; Yunlu, K.; Cuif, J.-P. *Polymer*, **2000**, *41*, 5903-5908.
194. Mazzei, A. *Makromol. Chem. Suppl.* **1981**, *4*, 61-72.
195. Taube, R.; Maiwald, S.; Sieler, J. *J. Organomet. Chem.* **1996**, *513*, 37-47.
196. Maiwald, S.; Weißenborn, H.; Sommer, C.; Müller, G.; Taube, R. *J. Organomet. Chem.* **2001**, *640*, 1-9.
197. Maiwald, S.; Weißenborn, H.; Windisch, H.; Sommer, C.; Müller, G.; Taube, R. *Macromol. Chem. Phys.* **1997**, *198*, 3305-3315.
198. Maiwald, S.; Sommer, C.; Müller, G.; Taube, R. *Macromol. Chem. Phys.* **2002**, *203*, 1029-1039.
199. Maiwald, S.; Sommer, C.; Müller, G.; Taube, R. *Macromol. Chem. Phys.* **2001**, *202*, 1446-1456.
200. Boisson, C.; Barbotin, F.; Spitz, R. *Macromol. Chem. Phys.* **1999**, *200*, 1163-1166.
201. Evans, W. J.; Ulibarri, T. A.; Ziller, J. W. *J. Am. Chem. Soc.* **1990**, *112*, 2314-2324.
202. Kaita, S.; Hou, Z.; Wakatsuki, Y. *Macromolecules* **1999**, *32*, 9078-9079.
203. Barbotin, F.; Spitz, R.; Boisson, C. *Macromol. Rapid Commun.* **2001**, *22*, 1411-1414.
204. Kaita, S.; Hou, Z.; Nishiura, M.; Doi, Y.; Kurazumi, J.; Wakatsuki, Y. *Macromol. Rapid Commun.* **2003**, *24*, 179-184.
205. (a) Jenkins, D.K. *Polymer* **1985**, *26*, 147-151. (b) Chigir, N. N.; Sharaev, O. K.; Tinyakova, E. I.; Dolgoplosk, B. A. *Chem. Abstr.* **1983**, *98*, 126695x. (c) Chigir, N. N.; Guzman, I. S.; Sharaev, O. K.; Tinyakova, E. I.; Dolgoplosk, B. A. *Chem. Abstr.* **1982**, *97*, 56281n. (d) Maiwald, S.; Weißenborn, H.; Sommer, C.; Müller, G.; Taube, R. *J. Organomet. Chem.* **2001**, *640*, 1-9.
206. Tate, P.; Bethea, T. W. In *Encyclopedia of Polymer Science and Engineering*, Vol. 7, 2nd Edition, Wiley Interscience Publication, John Wiley & Sons, Inc.: New York, **1985**, p537.
207. (a) Gehrke, K.; Harwart, M. *Plast. Kautsch.* **1993**, *40*, 356. (b) Oehme, A.; Gebauer, U.; Gehrke, K. *Macromol. Rapid Commun.* **1995**, *16*, 563-569. (c) Zambelli, A.; Proto, A.; Longo, P.; Oliva, P. *Macromol. Chem. Phys.* **1994**, *195*, 2623-2631.
208. Kobayashi, E.; Kaita, S.; Aoshima, S.; Furukawa, J. *J. Polym. Sci., Part A: Polym. Chem.* **1995**, *33*, 2175-2182.
209. (a) Kobayashi, E.; Kaita, S.; Aoshima, S.; Furukawa, J. *J. Polym. Sci., Part A: Polym. Chem.* **1994**, *32*, 1195-1198. (b) Kobayashi, E.; Kaita, S.; Aoshima, S.; Sakakibara, S.; Furukawa, J. *J. Polym. Sci., Part A: Polym. Chem.* **1996**, *34*, 3431-3434. (c) Kobayashi, E.; Hayashi, N.; Aoshima, S.; Furukawa, J. *J. Polym. Sci., Part A: Polym. Chem.* **1998**, *36*, 241-247.
210. Zhang, Q.; Li, W.; Shen, Z. *Eur. Polym. J.* **2002**, *38*, 869-873.
211. Zhang, Q.; Ni, X.; Shen, Z. *Polym. Int.* **2002**, *51*, 208-212.
212. Windisch, H.; Sylvester, G.; Taube, R.; Maiwald, S.; Giesemann, J.; Rosenstock, T., WO 0185814 (Bayer Aktiengesellschaft, Germany), **2001**.
213. Kaita, S.; Hou, Z.; Wakatsuki, Y. *Macromolecules* **2001**, *34*, 1539-1541.
214. (a) Steel, P. G. *J. Chem. Soc., Perkin Trans.* **2001**, *1*, 2727-2751. (b) *Lanthanides: Chemistry and Uses in Organic Synthesis*, Ed. S. Kobayashi, Springer-Verlag, Berlin, **1999**.
215. Evans, W. J.; Broomhall-Dillard, N. R.; Ziller, J. W. *Organometallics* **1996**, *15*, 1351-1355.
216. Evans, W. J.; Shreeve, J. L.; Broomhall-Dillard, N. R.; Ziller, J. W. *J. Organomet. Chem.* **1995**, *501*, 7-11.
217. Evans, W. J.; Broomhall-Dillard, N. R.; Ziller, J. W. *J. Organomet. Chem.* **1998**, *569*, 89-97.
218. Evans, W. J.; Boyle, T. J.; Ziller, J. W. *J. Organomet. Chem.* **1993**, *462*, 141-148.
219. Evans, W. J.; Boyle, T. J.; Ziller, J. W. *J. Am. Chem. Soc.* **1993**, *115*, 5084-5092.
220. Biagini, P.; Lugli, G.; Abis, L.; Millini, R. *J. Organomet. Chem.* **1994**, *474*, C16-C18.
221. Hitchcock, P. B.; Lappert, M. F.; Smith, R. G.; Bartlett, R. A.; Power, P. P. *J. Chem. Soc. Chem. Commun.* **1988**, 1007-1009.
222. Clarck, D. L.; Gordon, J. C.; Huffman, J. C.; Watkin, J. G.; Zwick, B. D. *Organometallics* **1994**, *13*, 4266-4270.
223. Schaverien, C. J.; Meijboom, N.; Orpen, A. G. *J. Chem. Soc. Chem. Commun.* **1992**, 124-126.
224. Cai, C.-X.; Toupet, L.; Lehmann, C. W.; Carpentier, J.-F. *J. Organomet. Chem.* **2003**, *in press*.

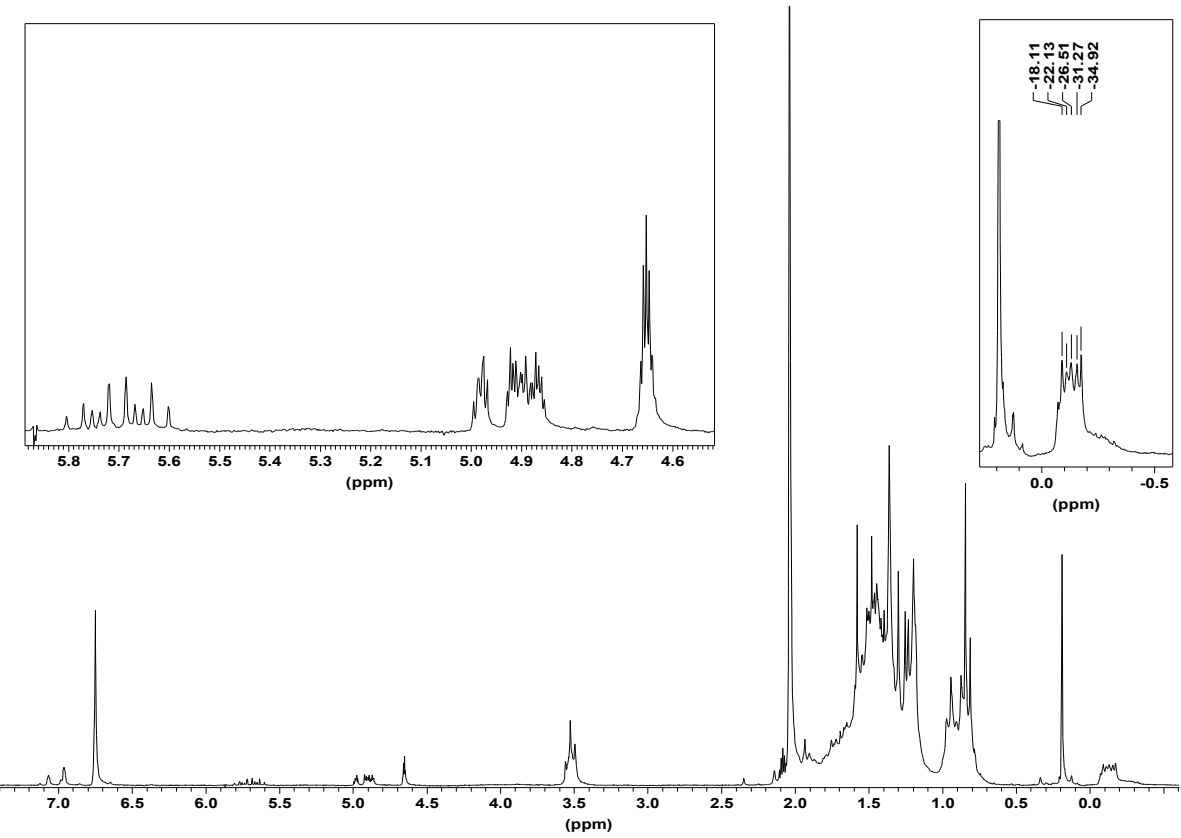
225. Chandler, C. D.; Rogers, C.; Hampden-Smith, M. J. *Chem. Rev.* **1993**, *93*, 1205-1241.
226. (a) Hubert-Pfalzgraf, L. G. *New J. Chem.* **1987**, *11*, 663-675. (b) Bradley, D. C. *Chem. Rev.* **1989**, *89*, 1317-1322. (c) Caulton, K. G.; Hubert-Pfalzgraf, L. G. *Chem. Rev.* **1990**, *90*, 969-995.
227. Bednorz, J. G.; Müller, K. A.; Takashige, M. *Science* **1987**, *236*, 73.
228. Mehrotra, R. C.; Singh, A.; Tripathi, U. M. *Chem. Rev.* **1991**, *91*, 1287-1303.
229. (a) Mazdiyasni, K. S.; Lynch, C. T.; Smith, J. S. *Inorg. Chem.* **1966**, *5*, 342-346. (b) Brown, L. M.; Mazdiyasni, K. S. *Inorg. Chem.* **1970**, *9*, 2783-2786.
230. Adkins, H.; Cox, F. W. *J. Am. Chem. Soc.* **1938**, *60*, 1151-1159.
231. Poncelet, O.; Sartain, W. J.; Hubert-Pfalzgraf, L. G.; Folting, K.; Caulton, K. G. *Inorg. Chem.* **1989**, *28*, 263-267.
232. Kritikos, M.; Wijk, M.; Moustakimov, M.; Westin, G. *J. Chem. Soc., Dalton Trans.* **2001**, 1931-1938.
233. Daniele, S.; Hubert-Pfalzgraf, L. G.; Hitchcock, P. B.; Lappert, M. F. *Inorg. Chem. Comm.* **2000**, *3*, 218-220.
234. Helgesson, G.; Jagner, S.; Poncelet, O.; Hubert-Pfalzgraf, L. G. *Polyhedron* **1991**, *10*, 1559-1564.
235. (a) Misra, S. N.; Misra, T. N.; Kapoor, R. N.; Mehrotra, R. C. *Chem. Ind.* **1963**, 120. (b) Misra, S. N.; Misra, T. N.; Mehrotra, R. C. *Aust. J. Chem.* **1968**, *21*, 797-800.
236. Misra, S. N.; Misra, T. N.; Mehrotra, R. C. *Proc. Nucl. Radiation Chem. Symp.* **1965**, 15-19.
237. Zeit. Anorg. Allg. Chem. **1963**, 325, 67-71.
238. Andersen, R. A.; Templeton, D. H.; Zalkin, A. *Inorg. Chem.* **1978**, *17*, 1962-1965.
239. Evans, W. J.; Sollberger, M. S.; Hanusa, T. P. *J. Am. Chem. Soc.* **1988**, *110*, 1841-1850.
240. Evans, W. J.; Sollberger, M. S. *Inorg. Chem.* **1988**, *27*, 4417-4423.
241. Evans, W. J.; Sollberger, M. S.; Ziller, J. W. *J. Am. Chem. Soc.* **1993**, *115*, 4120-4127.
242. Lappert, M. F.; Singh, A.; Atwood, J. L.; Hunter, W. E. *J. Chem. Soc., Chem. Commun.* **1981**, 1191-1193.
243. Evans, W. J.; Olofson, J. M.; Ziller, J. W. *J. Am. Chem. Soc.* **1990**, *112*, 2308-2314.
244. (a) Bradley, D. C.; Chudzynska, H.; Hursthouse, M. B.; Motevalli, M. *Polyhedron* **1993**, *12*, 1907-1918. (b) Bradley, D. C.; Chudzynska, H.; Hursthouse, M. B.; Motevalli, M. *Polyhedron* **1994**, *13*, 7-14.
245. Yao, Y.-M.; Shen, Q.; Zhang, Y.; Xue, M.-Q.; Sun, J. *Polyhedron* **2001**, *20*, 3201-3208.
246. Zhang, L.-L.; Yao, Y.-M.; Luo, Y.-J.; Shen, Q.; Sun, J. *Polyhedron* **2000**, *19*, 2243-2247.
247. Clark, D. L.; Watkin, J. G.; Huffman, J. C. *Inorg. Chem.* **1992**, *31*, 1556-1558.
248. Evans, W. J.; Ansari, M. A.; Ziller, J. W.; Khan, S. I. *J. Organomet. Chem.* **1998**, *553*, 141-148.
249. (a) Hitchcock, P. B.; Lappert, M. F.; Singh, A. *J. Chem. Soc., Chem. Commun.* **1983**, 1499-1501. (b) Lappert, M. F.; Singh, A.; Smith, R. G. *Inorg. Synth.* **1990**, *27*, 164-168.
250. Evans, W. J.; Olofson, J. M.; Ziller, J. W. *Inorg. Chem.* **1989**, *28*, 4309-4311.
251. Van den Hende, J. R.; Hitchcock, P. B.; Holmes, S. A.; Lappert, M. F.; Leung, W.-P.; Mak, T. C. W.; Prashar, S. *J. Chem. Soc., Dalton Trans.* **1995**, 1427-1433.
252. Bradley, D. C.; Ghotra, J. S.; Hart, F. A. *J. Chem. Soc., Dalton Trans.* **1973**, 1021-1023.
253. Wedler, M.; Gilje, J. W.; Pieper, U.; Stalke, D.; Noltemeyer, M.; Edelmann, F. T. *Chem. Ber.* **1991**, *124*, 1163-1165.
254. Bradley, D. C.; Chudzynska, H.; Hursthouse, M. B.; Motevalli, M. *Polyhedron* **1991**, *10*, 1049-1059.
255. Herrmann, W. A.; Anwander, R.; Scherer, W. *Chem. Ber.* **1993**, *126*, 1533-1539.
256. Herrmann, W. A.; Anwander, R.; Munck, F. C.; Scherer, W.; Dufaud, V.; Huber, N. W.; Artus, G. R. J. Z. *Naturforsch., B: Chem. Sci.* **1994**, *49*, 1789-1797.
257. Stecher, H. A.; Sen, A.; Rheingold, A. L. *Inorg. Chem.* **1988**, *27*, 1130-1132.
258. Stecher, H. A.; Sen, A.; Rheingold, A. L. *Inorg. Chem.* **1989**, *28*, 3280-3282.
259. Herrmann, W. A.; Anwander, R.; Kleine, M.; Scherer, W. *Chem. Ber.* **1992**, *125*, 1971-1979.
260. (a) Barnhart, D. M.; Clark, D. L.; Huffman, J. C.; Vincent, R. L.; Watkin, J. G. *Inorg. Chem.* **1993**, *32*, 4077-4083. (b) Barnhart, D. M.; Clark, D. L.; Gordon, J. C.; Huffman, J. C.; Watkin, J. G.; Zwick, B. D. *J. Am. Chem. Soc.* **1993**, *115*, 8461-8462.
261. (a) Deacon, G. B.; Hitchcock, P. B.; Holmes, S. A.; Lappert, M. F.; MacKinnon, P.; Newnham, R. H. J. *Chem. Soc., Chem. Commun.* **1989**, 935-937. (b) Evans, W. J.; Anwander, R.; Ansari, M. A.; Ziller, J. W. *Inorg. Chem.* **1995**, *34*, 5-6.
262. (a) McGahey, M. J.; Coan, P. S.; Folting, K.; Streib, W. E.; Caulton, K. G. *Inorg. Chem.* **1989**, *28*, 3284-3285. (b) McGahey, M. J.; Coan, P. S.; Folting, K.; Streib, W. E.; Caulton, K. G. *Inorg. Chem.* **1991**, *30*, 1723-1735.
263. Evans, W. J.; Golden, R. E.; Ziller, J. W. *Inorg. Chem.* **1991**, *30*, 4963-4968.
264. Herrmann, W. A.; Anwander, R.; Denk, M. *Chem. Ber.* **1992**, *125*, 2399-2405.
265. Poncelet, O.; Hubert-Pfalzgraf, L. G.; Daran, J. C.; Astier, R. *J. Chem. Soc., Chem. Commun.* **1989**, 1846-1848.
266. Anwander, R.; Munck, F. C.; Priermeier, T.; Scherer, W.; Runte, O.; Herrmann, W. A. *Inorg. Chem.* **1997**, *36*, 3545-3552.
267. Evans, W. J.; Anwander, R.; Berlekamp, U. H.; Ziller, J. W. *Inorg. Chem.* **1995**, *34*, 3583-3588.

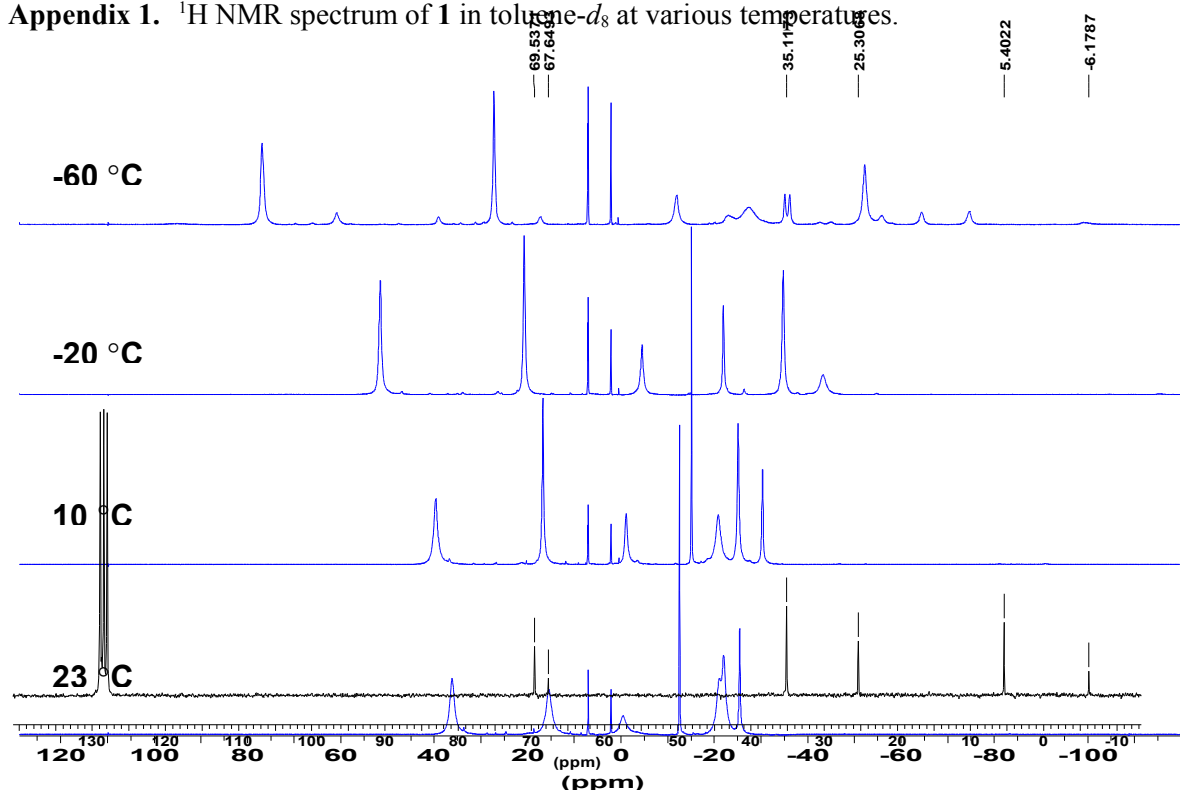
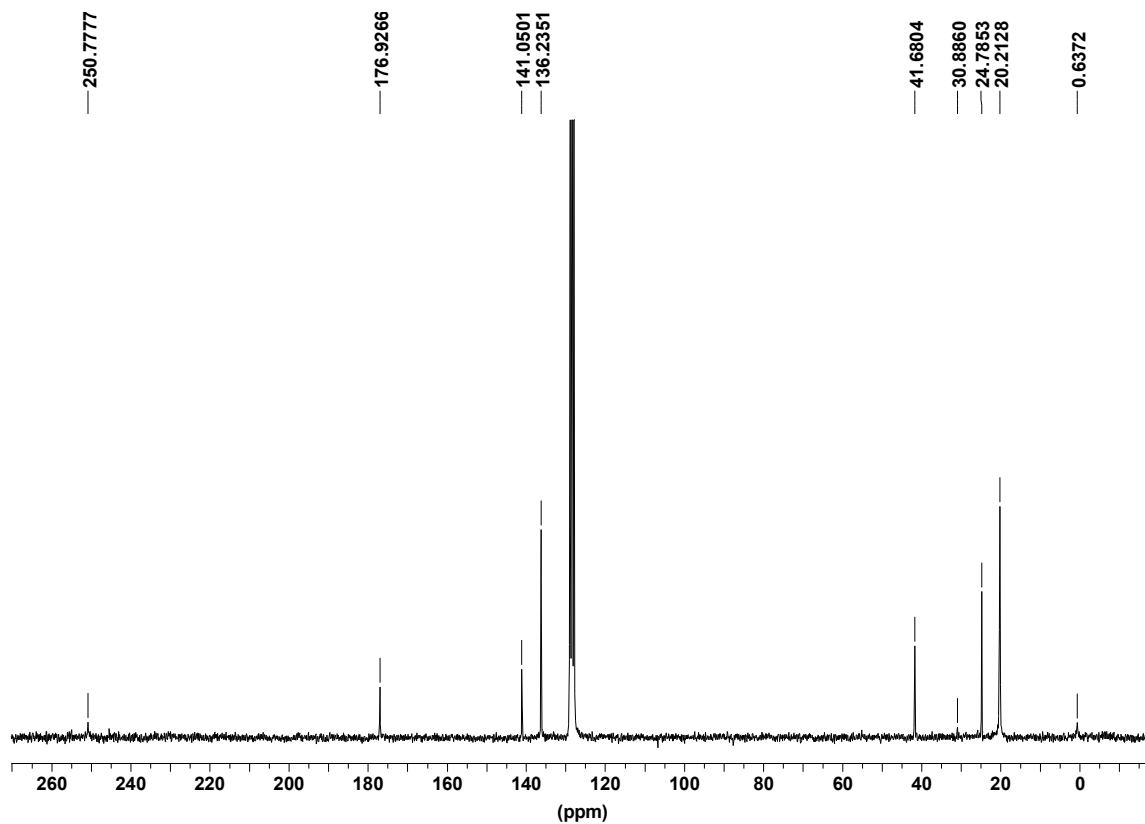
268. (a) Liu, S.; Yang, L.-W.; Rettig, S. J.; Orvig, C. *Inorg. Chem.* **1993**, *32*, 2773-2778. (b) Caravan, P.; Hedlund, S.; Liu, S.; Sjöberg, S.; Orvig, C. *J. Am. Chem. Soc.* **1995**, *117*, 11230-11238.
269. Lara-Sanchez, A.; Rodriguez, A.; Hughes, D. L.; Schormann, M.; Bochmann, M. *J. Organomet. Chem.* **2002**, *663*, 63-69.
270. Runte, O.; Priermeier, T.; Anwander, R. *Chem. Commun.*, **1996**, *11*, 1385-1386.
271. (a) Shao, P.; Berg, D. J.; Bushnell, G. W. *Inorg. Chem.* **1994**, *33*, 3452-3458. (b) Shao, P.; Berg, D. J.; Bushnell, G. W. *Inorg. Chem.* **1994**, *33*, 6334-6339.
272. Emslie, D. J. H.; Piers, W. E.; McDonald, R. *J. Chem. Soc., Dalton Trans.* **2002**, 293-294.
273. Lappert, M. F.; Pearce, R. J. *Chem. Soc., Chem. Commun.* **1973**, 126.
274. Gradeff, P. S.; Yunlu, K.; Gleizes, A.; Galy, J. *Polyhedron* **1989**, *8*, 1001-1005.
275. Ozaki, Y.; Kaneko, K.; Mitachi, S., WO 2529884 (Hokko Chemical Industry Co., Ltd, JP.), **1983**.
276. Singh, M.; Misra, S. N. *J. Indian. Chem. Soc.* **1978**, *55*, 643.
277. Evans, W. J.; Deming, T. J.; Olofson, J. M.; Ziller, J. W. *Inorg. Chem.* **1989**, *28*, 4027-4034.
278. Herrmann, W. A.; Anwander, R.; Kleine, M.; Scherer, W. *Chem. Ber.* **1992**, *125*, 1971-1979.
279. Edelmann, F. T.; Steiner, A.; Stalke, D.; Gilje, J. W.; Jagner, S.; Hakansson, M. *Polyhedron* **1994**, *13*, 539-546.
280. Wenqi, C.; Zhongsheng, J.; Yan, X.; Yuguo, F.; Guangdi, Y. *Inorg. Chem. Acta* **1987**, *130*, 125-129.
281. Benetollo, F.; Bombieri, G.; Bisi Castellani, C.; Jahn, W.; Fischer, R. D. *Inorg. Chim. Acta* **1984**, *95*, L7-L10.
282. Decock, C. W.; Ely, S. R.; Hopkins, T. E.; Brault, M. A. *Inorg. Chem.* **1978**, *17*, 625-631.
283. Schumann, H.; Kociok-Koehn, G.; Dietrich, A.; Goerlitz, F. H. *Z. Naturforsch. B: Chem. Sci.* **1991**, *46*, 896-900.
284. Mathivet, T. WO 0228776 (Rhodia Electronics and Catalysis), **2002**.
285. (a) Bradley, D. C.; Chudzynska, H.; Frigo, D. M.; Hursthouse, M. B.; Mazid, M. A. *J. Chem. Soc., Chem. Commun.* **1988**, 1258-1259. (b) Bradley, D. C.; Chudzynska, H.; Frigo, D. M.; Hammond, M. E.; Hursthouse, M. B.; Mazid, M. A. *Polyhedron* **1990**, *9*, 719-726.
286. Hubert-Pfalzgraf, L. G.; Daniele, S.; Bennaceur, A.; Daran, J. C.; Vaissermann, J. *Polyhedron* **1997**, *16*, 1223-1234.
287. (a) Bertini, L.; Luchinat, C.; *NMR of Paramagnetic molecules in biological systems*, Menlo Park, **1986**. (b) Bertini, L.; Luchinat, C. *Coord. Chem. Rev.* **1996**, *150*, 1-292.
288. Gromada, J.; Fouga, C.; Chenal, T.; Mortreux, A.; Carpentier, J.-F. *Macromol. Chem. Phys.* **2002**, *203*, 550-555.
289. (a) Screttas, C. G.; Micha-Screttas, M. *J. Organomet. Chem.* **1985**, *290*, 1-13. (b) Screttas, C. G.; Micha-Screttas, M. *J. Organomet. Chem.* **1986**, *316*, 1-13. (c) Hanawalt, E. M.; Richey, H. G. *J. Am. Chem. Soc.* **1990**, *112*, 4983-4984. (d) Richey, H. G.; DeStephano, J. P. *J. Org. Chem.* **1990**, *55*, 3281-3286.
290. Schumann, H.; Genthe, W.; Bruncks, N.; Pickardt, J. *Organometallics* **1982**, *1*, 1194-1200.
291. Yasuda, H.; Furo, M.; Yamamoto, H.; Nakamura, A.; Miyake, S.; Kibino, N. *Macromolecules* **1992**, *25*, 5115-5116.
292. Kerr, J. A. in *CRC Handbook of Chemistry and Physics*, Lide D. R. Ed.; CRP Press, Boca Raton, Florida, USA, 81st Edition, **2000**.
293. (a) Deacon, G. B.; Nickel, S.; MacKinnon, P.; Tiekkink, E. R. T. *Aust. J. Chem.* **1990**, *43*, 1245. (b) Barnhart, D. M.; Clark, D. L.; Gordon, J. C.; Huffman, J. C.; Vincent, R. L.; Watkin, J. G.; Zwick, B. D. *Inorg. Chem.* **1994**, *33*, 3487-3497.
294. Koning, C.; Van Duin, M.; Pagnoulle, C.; Jerome, R. *Prog. Polym. Sci.* **1998**, *23*, 707-757.
295. Desurmont, G.; Li, Y.; Yasuda, H.; Maruo, T.; Kanehisa, N.; Kai, Y. *Organometallics* **2000**, *19*, 1811-1813.
296. (a) Desurmont, G.; Tokimitsu, T.; Yasuda, H. *Macromolecules* **2000**, *22*, 7679-7681. (b) Desurmont, G.; Tanaka, M.; Li, Y.; Yasuda, H.; Tokimitsu, T.; Tone, S.; Yanagase, A. *J. Polym. Sci., Part A: Polym. Chem.* **2000**, *38*, 4095-4109. (c) Yasuda, H. *J. Organomet. Chem.* **2002**, *647*, 128-138.
297. Jezl, J. L.; Chu, N. S.; Khelghatian, H. M. *ACS meeting, San Francisco*, **1968**.
298. Agouri, E.; Parlant, C.; Mornet, P.; Rideau, J.; Teitgen, F. F. *Makromol. Chem.* **1970**, *137*, 229-243.
299. (a) Chung, T. C.; Lu, H. L.; Janvikul, W. *Polymer* **1997**, *38*, 1495-1502. (b) Xu, G.; Chung, T. C. *J. Am. Chem. Soc.* **1999**, *121*, 6763-6764.
300. Imuta, J.-I.; Kashiwa, N.; Toda, Y. *J. Am. Chem. Soc.* **2002**, *124*, 1176-1177.
301. Kojoh, S.; Matsugi, T.; Kaneko, H.; Matsuo, S.; Kawahara, N.; Imuta, J.; Kashiwa, N. (Mitsui Chemicals); *EUPOC* **2003**, Milano.
302. (a) Sosnowski, S.; Slomkowski, S.; Penczek, S.; Florjanczyk, Z. *Makromol. Chem.* **1991**, *192*, 1457-1465. (b) Mulhaupt, R.; Duschek, T.; Rosch, J. *Polym. Adv. Technol.* **1993**, *4*, 439. (c) Han, C. J.; Lee, M. S.; Byun, D.-J.; Kim, S. Y. *Macromolecules* **2002**, *35*, 8923-8925.
303. Shiono, T.; Akino, Y.; Soga, K. *Macromolecules* **1994**, *27*, 6229-6231.
304. Chung, T. C. *Prog. Polym. Sci.* **2002**, *27*, 39-85.

305. Frauenrath, H.; Balk, S.; Keul, H.; Höcker, H. *Macromol. Rapid Commun.* **2001**, *22*, 1147-1151.
306. (a) Bolig, A. D.; Jin, J.; Xu, J. Chen, E. Y.-X. *223rd National ACS meeting*, **2001**. (b) Jin, J.; Chen, E. Y.-X. *Macromol. Chem. Phys.* **2002**, *203*, 2329-2333.
307. (a) Yokota, K.; Hirabayashi, T. *Polym. J.* **1981**, *13*, 813. (b) Auschra, C.; Stadler, R. *Polym. Bull.* **1993**, *30*, 257. (c) Ren, Q.; Zhang, H. J.; Zhang, X. K.; Huang, B. T. *J. Polym. Sci., Part A: Polym. Chem.* **1993**, *31*, 847-851. (d) Yu, J. M.; Yu, Y.; Dubois, P.; Teyssie, P. Jerome, R. *Polymer* **1997**, *38*, 3091-3101.
308. (a) Hadjichristidis, N.; Pitsikalis, M.; Pispas, S.; Iatrou, H. *Chem. Rev.* **2001**, *101*, 3747-3792. (b) Patten, T. E.; Matyjaszewski, K. *Adv. Mater.* **1998**, *10*, 901-915.
309. Hamley, I. W. *Adv. Polym. Sci.* **1999**, *148*, 113-137.
310. Kobori, Y.; Yasumitsu, R.; Akiyama, S.; Akiba, I.; Sano, H. *Polymer* **2002**, *43*, 6065-6067.
311. (a) Zhiqian, S.; Jun, O.; Fusong, W.; Zhenya, H.; Baogong, J. *J. Polym. Sci., Polym. Chem. Ed.* **1980**, *18*, 3345-3357. (b) Pross, A.; Marquardt, P.; Reichert, K. H.; Nentwig, W.; Knauf, T. *Angew. Makromol. Chem.* **1993**, *211*, 89-101.
312. Miyazawa, A.; Kase, T.; Soga, K. *J. Polym. Sci., Part A: Polym. Chem.* **1999**, *37*, 695-697.
313. (a) Barbier-Baudry, D.; Bornet, F.; Dormont, A.; Finot, E.; Visseaux, M. *Macromol. Chem. Phys.* **2002**, *203*, 1194-1200. (b) Bonnet, F.; Barbier-Baudry, D.; Dormond, A.; Visseaux, M. *Polym. Int.* **2002**, *51*, 986-993.
314. (a) Kobayashi, E.; Furukawa, J.; Ochiai, M.; Tsujimoto, T. *Eur. Polym. J.* **1983**, *19*, 871-875. (b) Conti, F.; Delfini, M.; Segre, A. L. *Polymer* **1977**, *18*, 310-311. (c) Walsh, N. G.; Hardy, J. K.; Rinaldi, P. L. *Appl. Spectrosc.* **1997**, *51*, 889-897. (d) Caprio, M.; Serra, M. C.; Bowen, D. E.; Grassi, A. *Macromolecules* **2002**, *35*, 9315-9322.
315. (a) Lu, M.; Keskkula, H.; Paul, D. R. *J. Appl. Polym. Sci.* **1995**, *58*, 1175-1188. (b) Cordella, C. D.; Cardozo, N. S. M.; Baumhardt Neto, R.; Mauler, R. S. *J. Appl. Polym. Sci.* **2003**, *87*, 2074-2079.
316. Ming, J.; Dubois, P.; Jerome, R. *J. Polym. Sci., Part A: Polym. Chem.* **1997**, *35*, 3507-3515.
317. Grubbs, R. B.; Dean, J. M.; Broz, M. E.; Bates, F. S. *Macromolecules* **2000**, *33*, 9522-9534.
318. Swaraj, P.; Rånby, B. *Analytical Chem.* **1975**, *47*, 1428-1429.
319. Node, M.; Nishide, K.; Shigeta, Y.; Obata, K.; Shiraki, H.; Kunishige, H. *Tetrahedron* **1997**, *53*, 12883-12894.
320. Greco, A.; Cesca, S.; Bertolini, G. *J. Organomet. Chem.* **1976**, *113*, 321-330.
321. (a) Shreider, V. A.; Turevskaya, E. P.; Kozlova, N. L.; Turova, N. Y. *Inorg. Chim. Acta* **1981**, *53*, L73-L76. (b) Gulino, A.; Casarin, N.; Conticello, V. P.; Gaudiello, J. G.; Marks, T. J. *Organometallics* **1988**, *7*, 2360-2364.
322. (a) Gordon, J. C.; Giesbrecht, G. R.; Brady, J. T.; Clark, D. L.; Keogh, D. W.; Scott, B. L.; Watkin, J. G. *Organometallics*, **2002**, *21*, 127-131. (b) Giesbrecht, G. R.; Gordon, J. C.; Brady, J. T.; Clark, D. L.; Keogh, D. W.; Michalczyk, R.; Scott, B. L.; Watkin, J. G. *Eur. J. Inorg. Chem.* **2002**, 723-731.
323. Fischbach, A.; Herdtweck, E.; Anwander, R.; Eickerling, G.; Scherer, W. *Organometallics* **2003**, *22*, 499-509.
324. Evans, W. J.; Ansari, M. A.; Ziller, J. W. *Inorg. Chem.* **1995**, *34*, 3079-3082.
325. Evans, W. J.; Ansari, M. A.; Ziller, J. W. *Polyhedron* **1997**, *16*, 3429-3434.
326. Giesbrecht, G. R.; Gordon, J. C.; Clark, D. L.; Scott, B. L.; R.; Watkin, J. G.; Young, K. J. *Inorg. Chem.* **2002**, *41*, 6372-6379.
327. (a) Wu, W. L.; Chen, M. W.; Zhou, P. *Organometallics* **1991**, *10*, 98-104. (b) Lin, J.; Wang, Z. *J. Organomet. Chem.* **1999**, *589*, 127-132.
328. Chisholm, M. H.; Gallucci, J.; Phomphrai, K. *Inorg. Chem.* **2002**, *41*, 2785-2794.
329. Hou, Z. M.; Fujita, A.; Yoshimura, T.; Jesorka, A.; Zhang, Y. G.; Yamazaki, H.; Wakatsuki, Y. *Inorg. Chem.* **1996**, *35*, 7190-7195.
330. Rabe, G. W.; Berube, C. D.; Yap, G. P. A.; Lam, K.-C.; Concolino, T. E.; Rheingold, A. L. *Inorg. Chem.* **2002**, *41*, 1446-1453.
331. Deacon, G. B.; Feng, T.; Junk, P. C.; Skelton, B. W.; White, A. H. *Chem. Ber.* **1997**, *130*, 851-857.
332. Deacon, G. B.; Feng, T.; Skelton, B. W.; White, A. H. *Aust. J. Chem.* **1995**, *48*, 741-756.
333. Andersen, R. A.; Wilkinson, G. *J. Chem. Soc. Dalton Trans.* **1977**, 809-811.
334. Dash, A.; Razavi, A.; Mortreux, A.; Lehmann, C. W.; Carpentier, J.-F. *Organometallics* **2002**, *21*, 3238-3249.

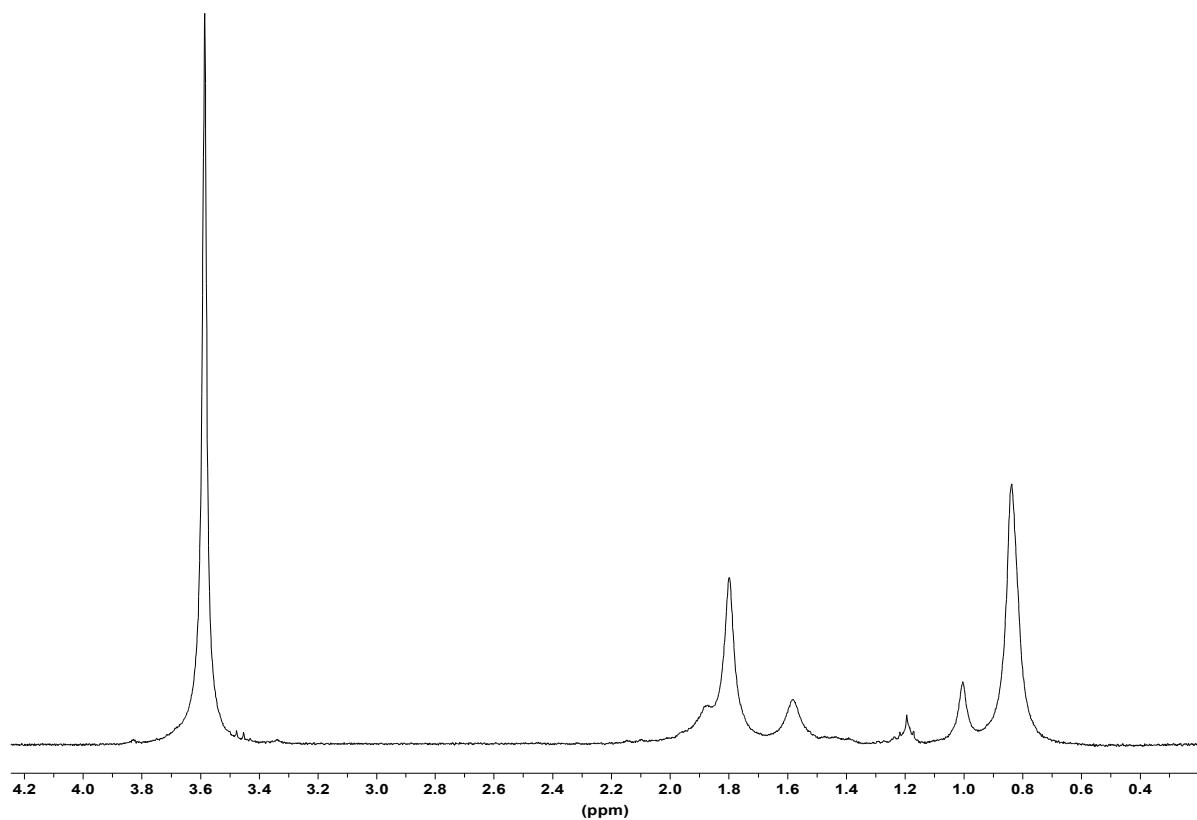


Appendix

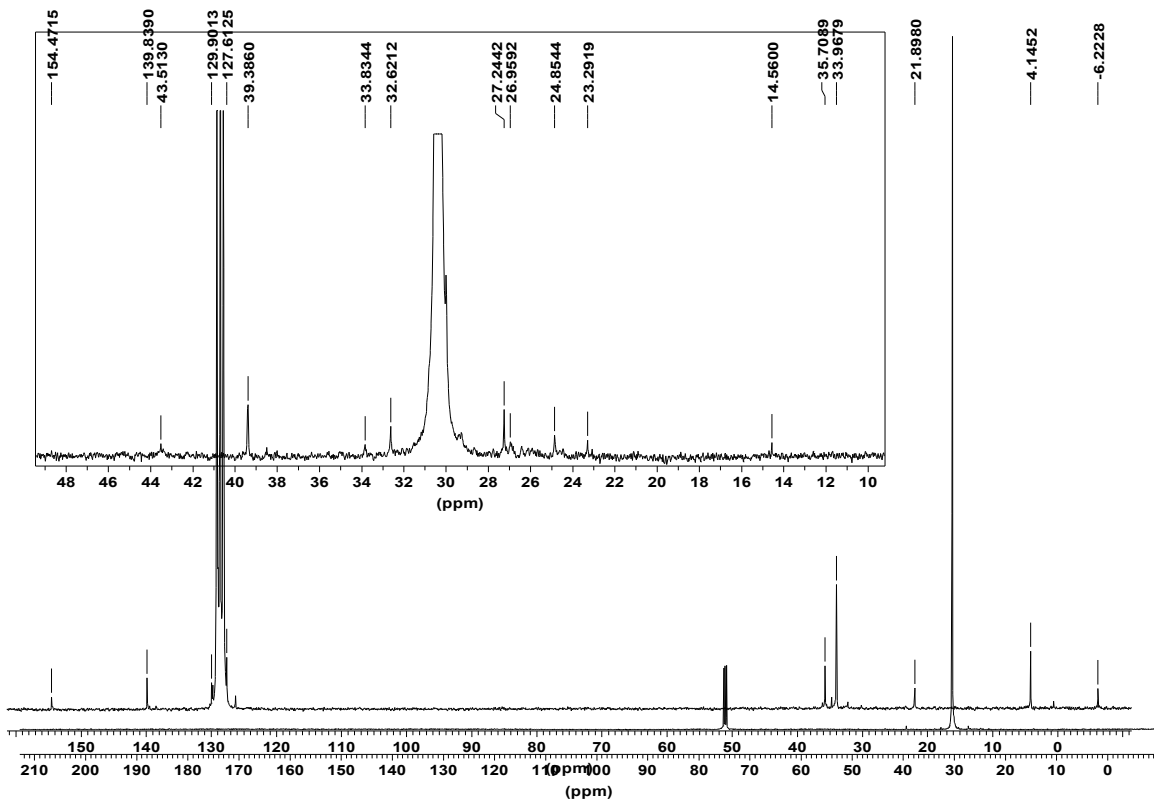


Appendix 1. ^1H NMR spectrum of **1** in toluene- d_8 at various temperatures.**Appendix 2.** ^{13}C NMR spectrum of **12** in C_6D_6 at RT.

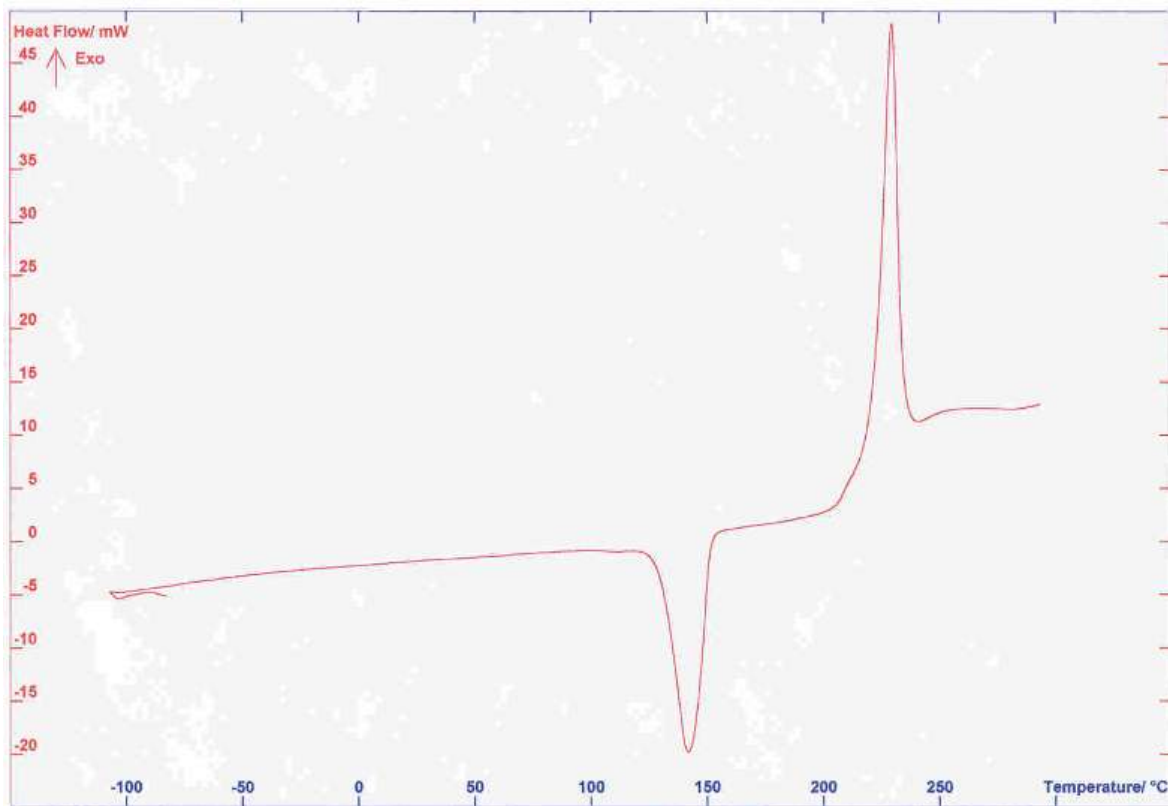
Appendix 3. Typical ^1H NMR spectrum of PMMA obtained with **1**/DHM system (CDCl_3 , 23 °C).



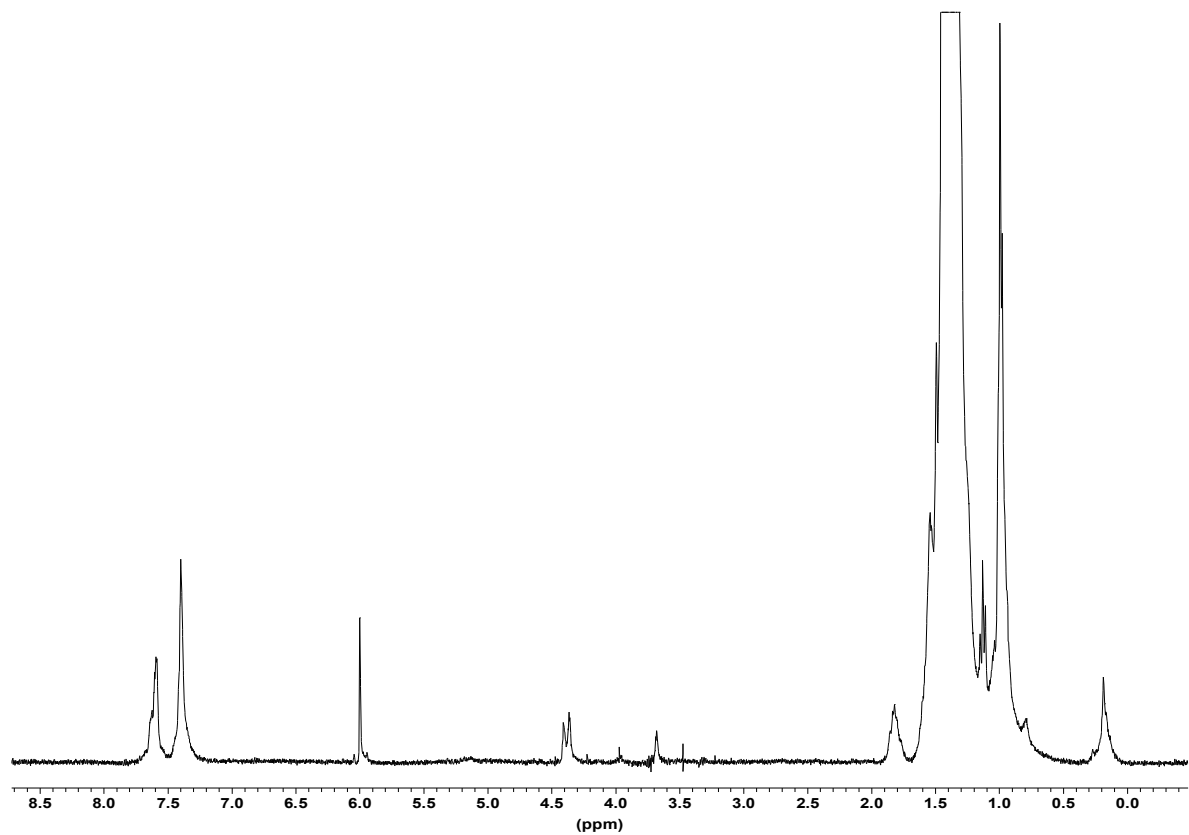
Appendix 4. Typical ^1H NMR spectrum of PE obtained with **1**/DHM system ($\text{C}_2\text{D}_2\text{Cl}_4$, 130 °C).



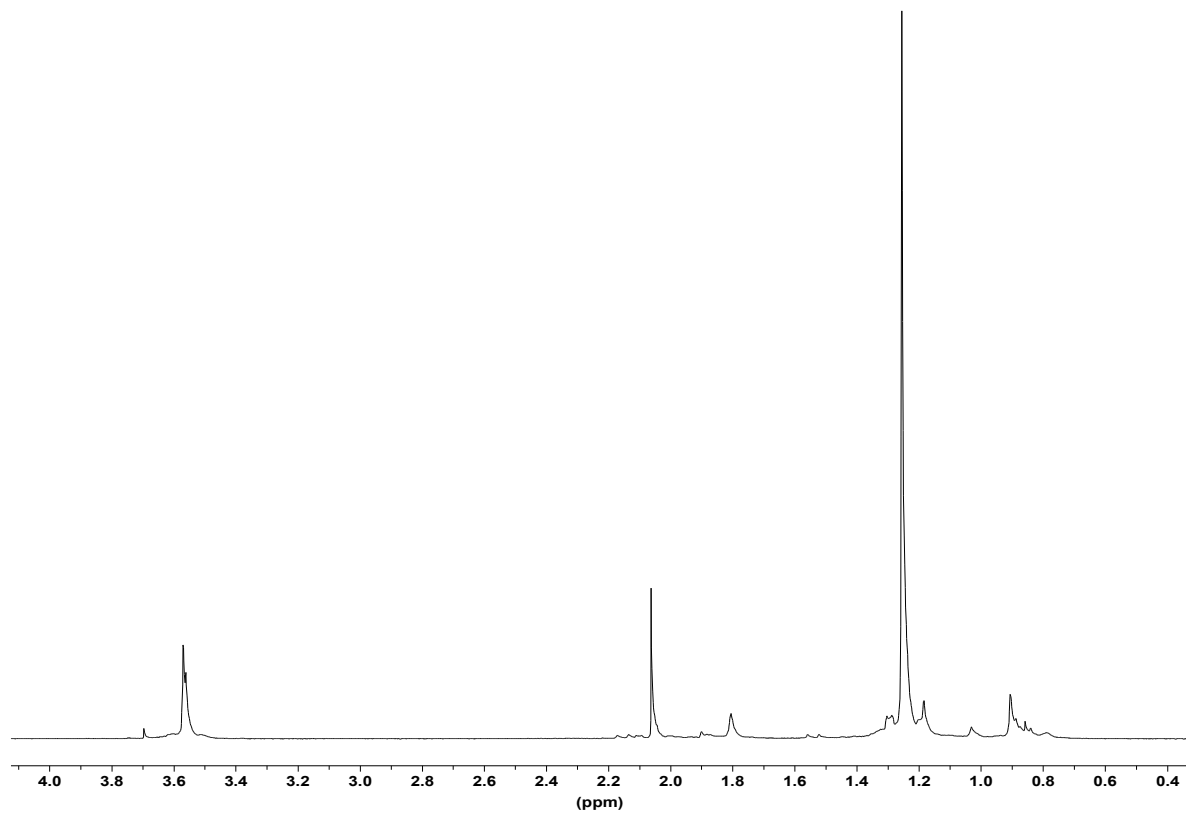
Appendix 5. DSC chromatogram of PE obtained with **1/DHM** system.



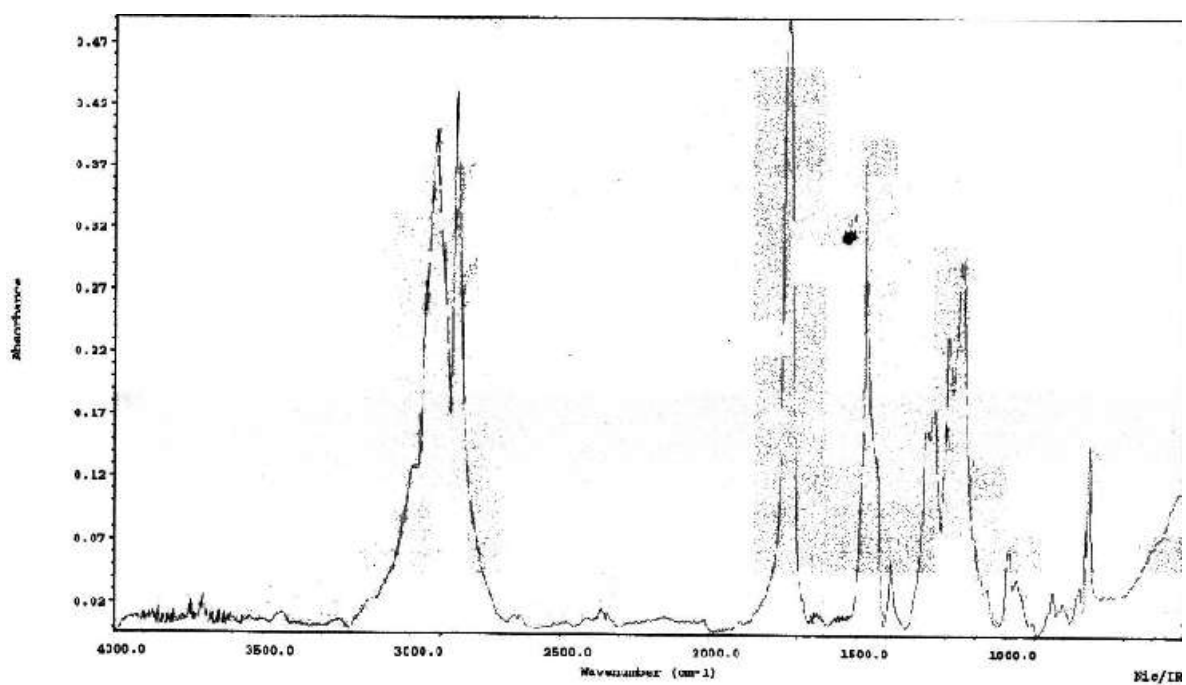
Appendix 6. ^1H NMR spectrum of phenylsilyl-terminated PE ($\text{C}_2\text{D}_2\text{Cl}_4$, 130 °C).



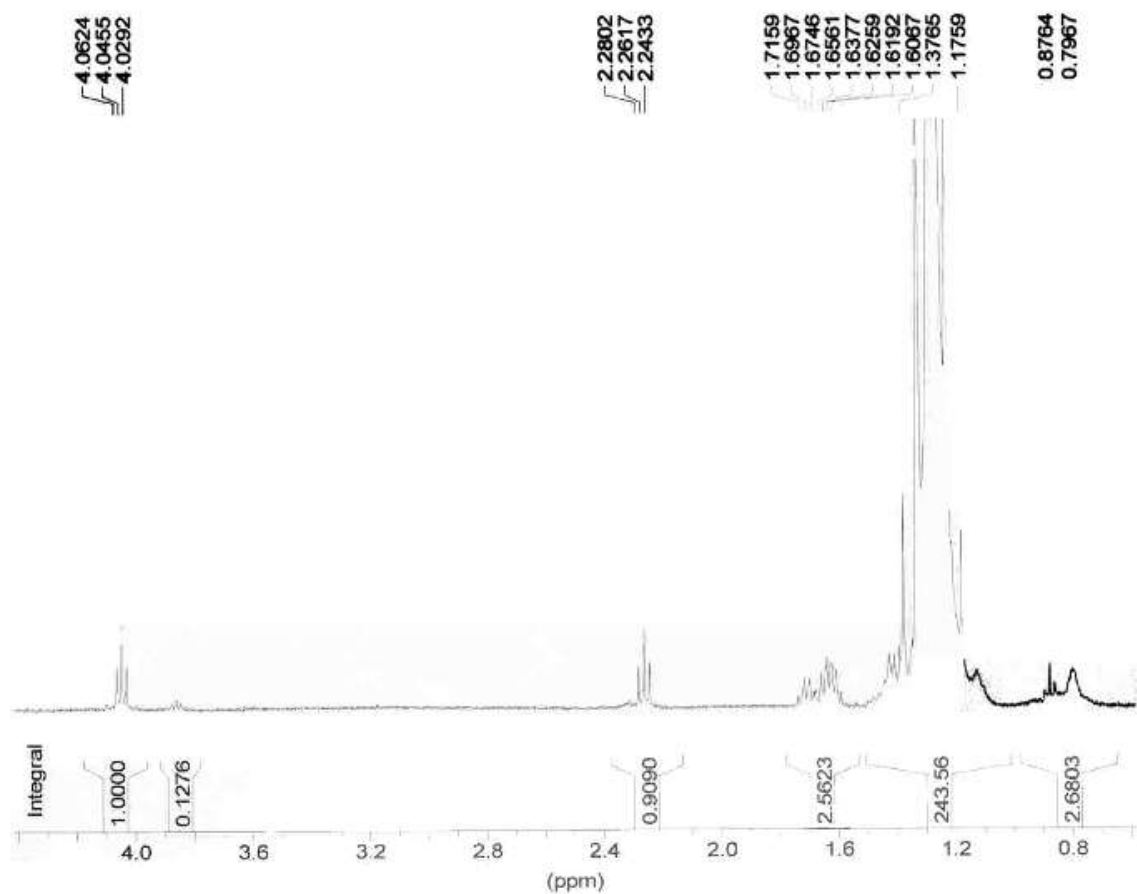
Appendix 7. ^1H NMR spectrum of PE-*b*-PMMA prepared with $\text{La}_3(\text{OtBu})_9(\text{THF})_2/\text{DHM}$ as catalyst system ($\text{C}_2\text{D}_2\text{Cl}_4$, 130 °C).



Appendix 8. IR spectrum of PE-*b*-PMMA copolymer (KBr pellets).

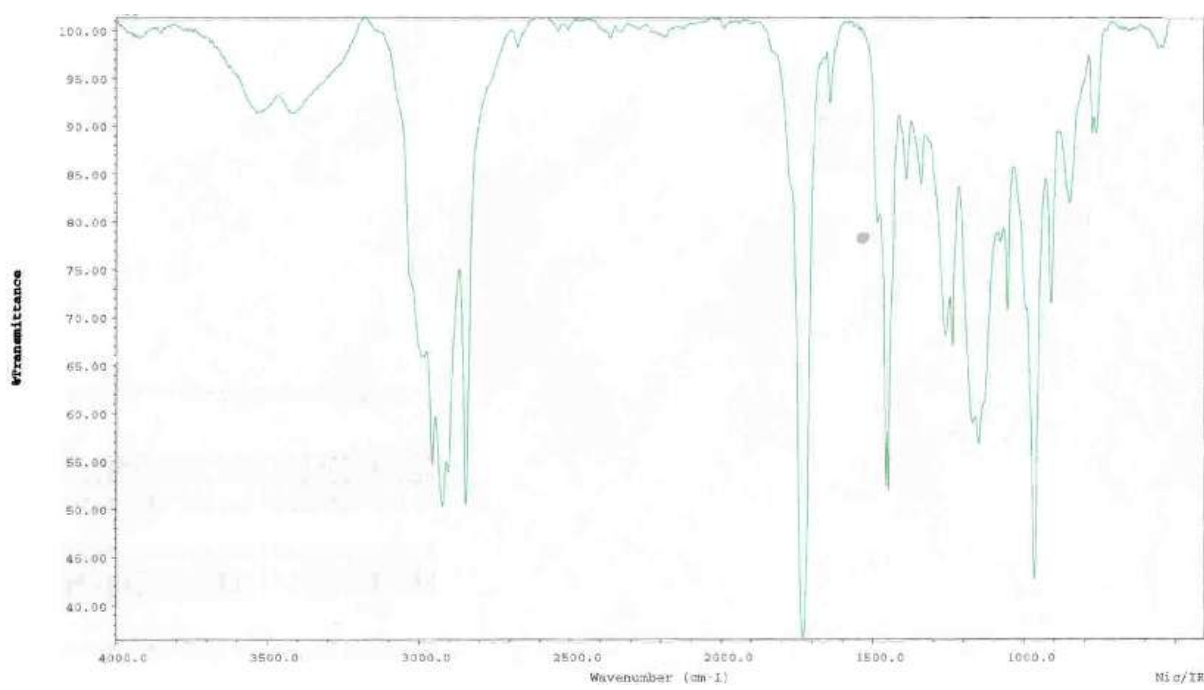


Appendix 9. ^1H NMR spectrum of PE-*b*-poly(ϵ -caprolactone) copolymer ($\text{C}_2\text{D}_2\text{Cl}_4$, 130 °C).



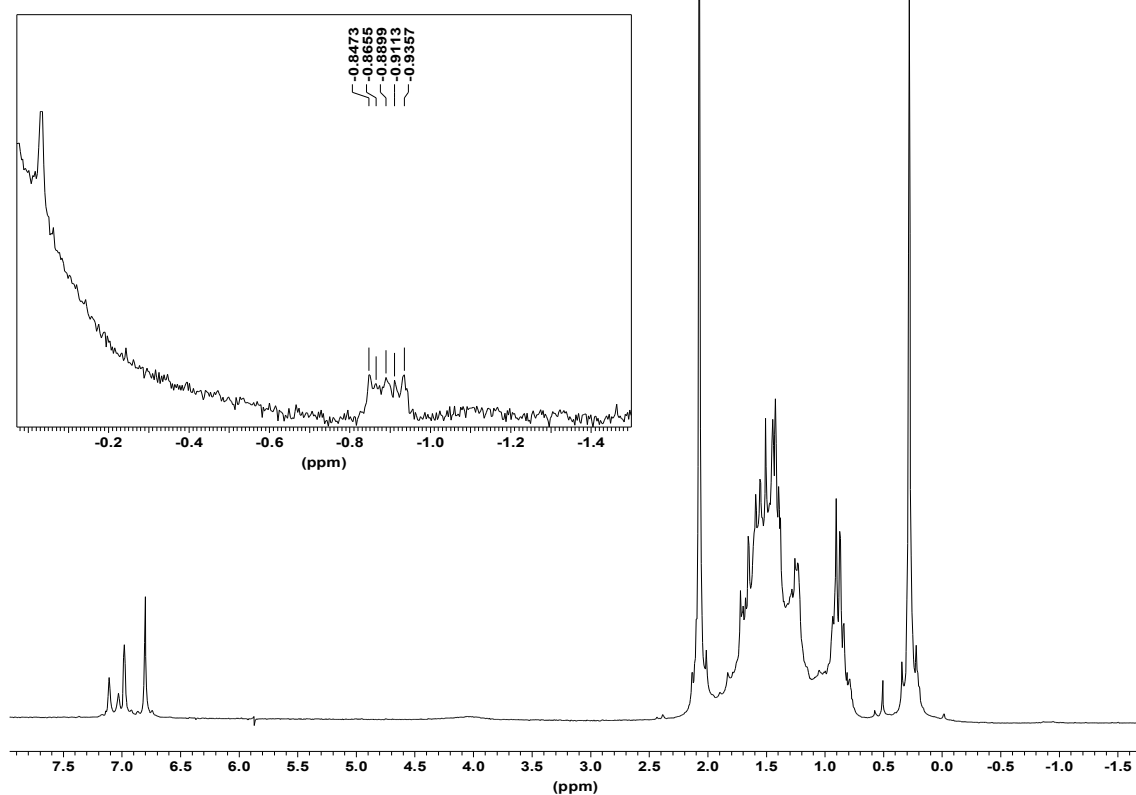
Appendix 10. Typical ^1H NMR spectrum of homopolybutadiene obtained with **12**/DHM as catalyst system (CDCl_3 , 23 °C).

Appendix 11. IR spectrum of PE-*b*-PGA copolymer (KBr pellets).



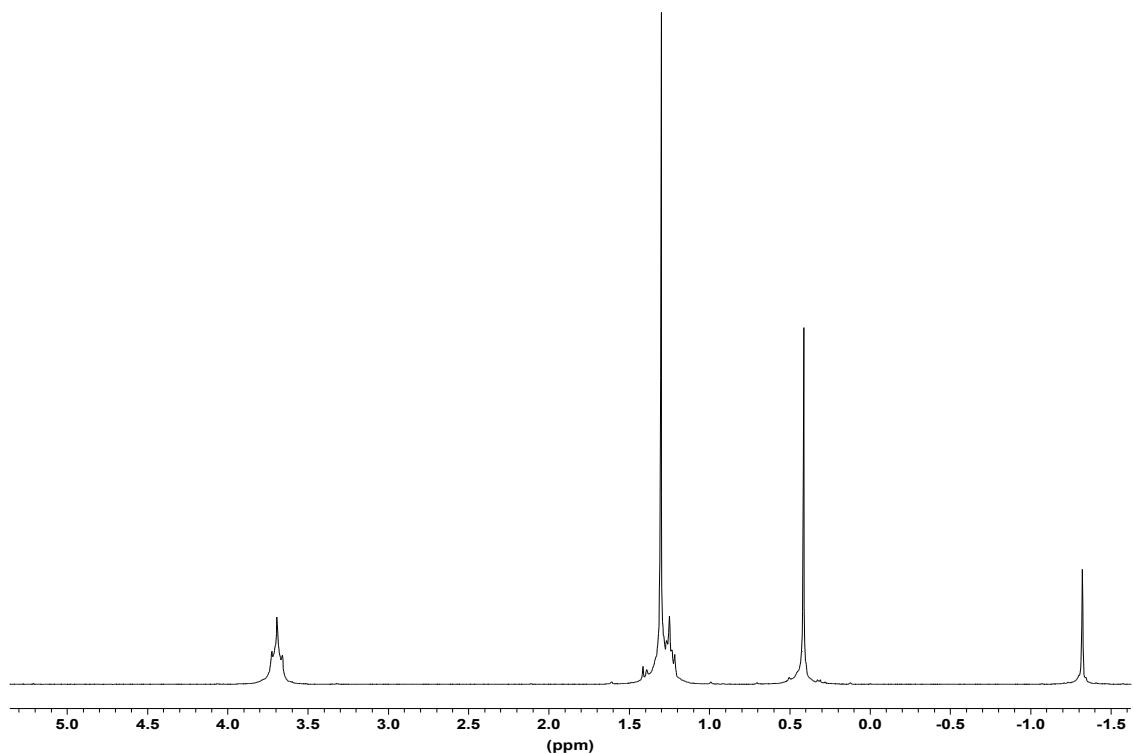
Appendix 12. Formation and consumption of ethylene monitored by ¹H NMR with **1**/BEM system (toluene-*d*₈).

Appendix 13. ^1H NMR spectrum of $\text{La}_3(\text{OtBu})_9(\text{THF})_2/\text{DHM}$ mixture (1:1) at 0 °C in toluene- d_8 .



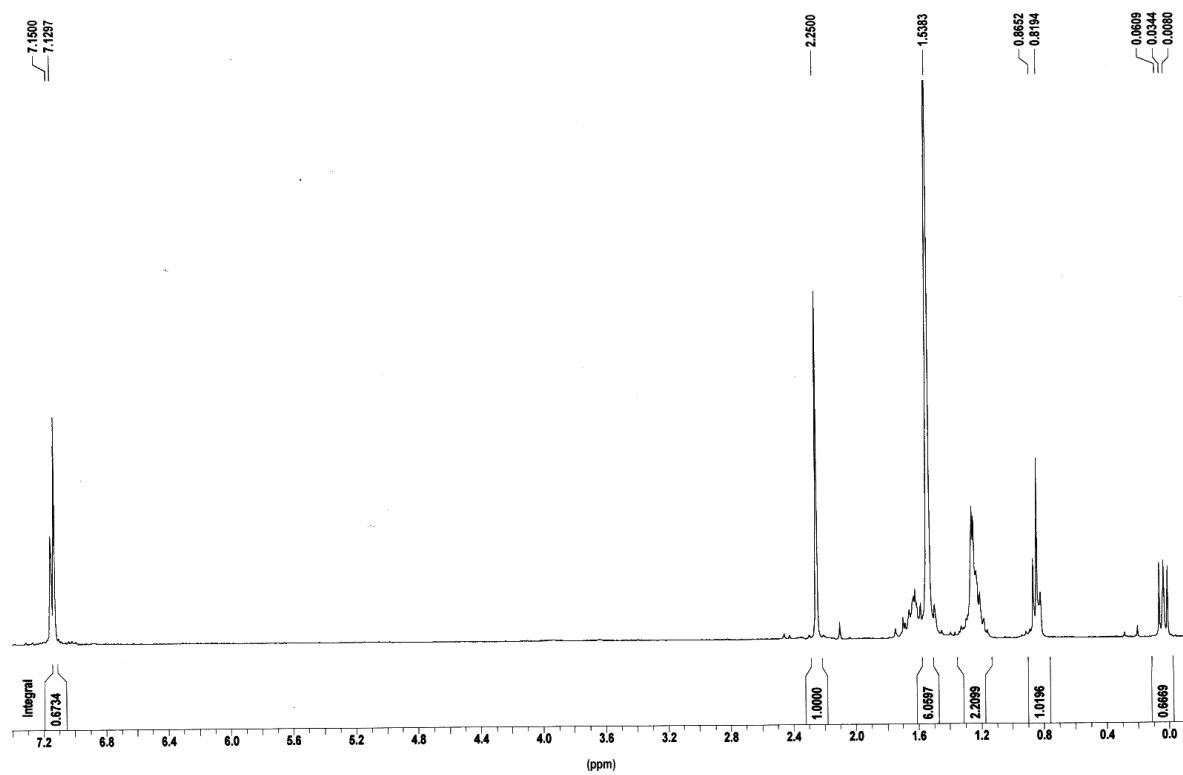
Appendix 14. ^1H NMR spectrum of $\text{Y}_3(\text{OtBu})_8\text{Cl}(\text{THF})_2/\text{DHM}$ mixture (1:1) at 20 °C in toluene- d_8 .

Appendix 15. ^1H NMR spectrum of $[(\text{Me}_3\text{SiCH}_2)\text{Mg(OtBu)}_2(\text{THF})]$ (**15**) in C_6D_6 at 23 °C.

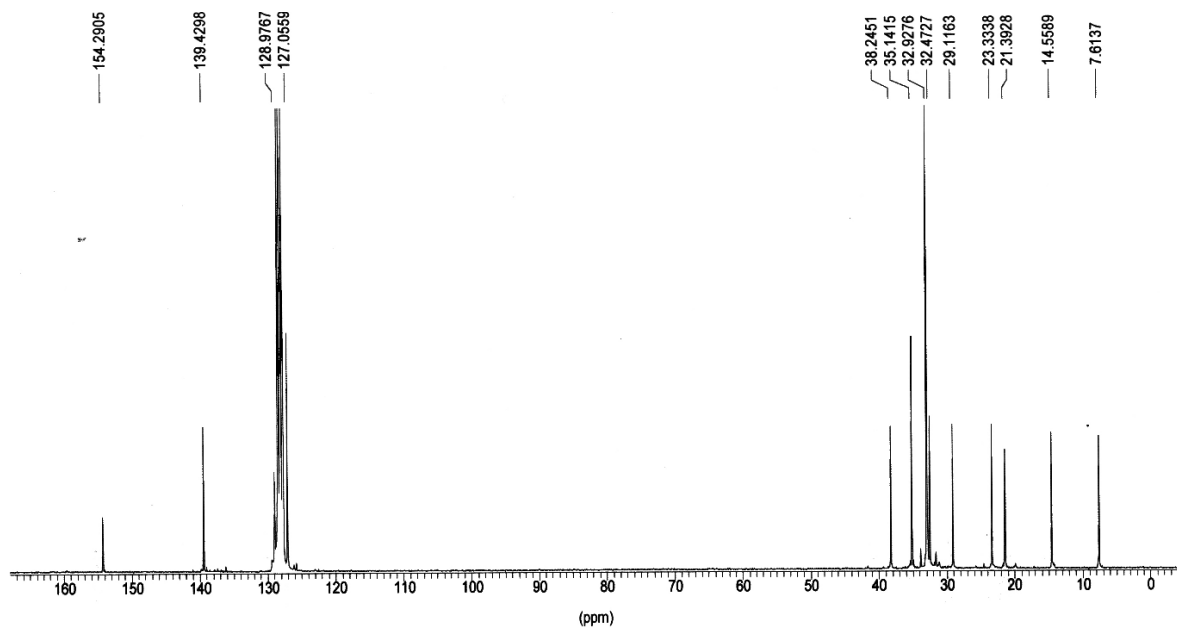


Appendix 16. ^{13}C NMR spectrum of $[(\text{Me}_3\text{SiCH}_2)\text{Mg(OtBu)}_2(\text{THF})]$ (**15**) in C_6D_6 at 23 °C.

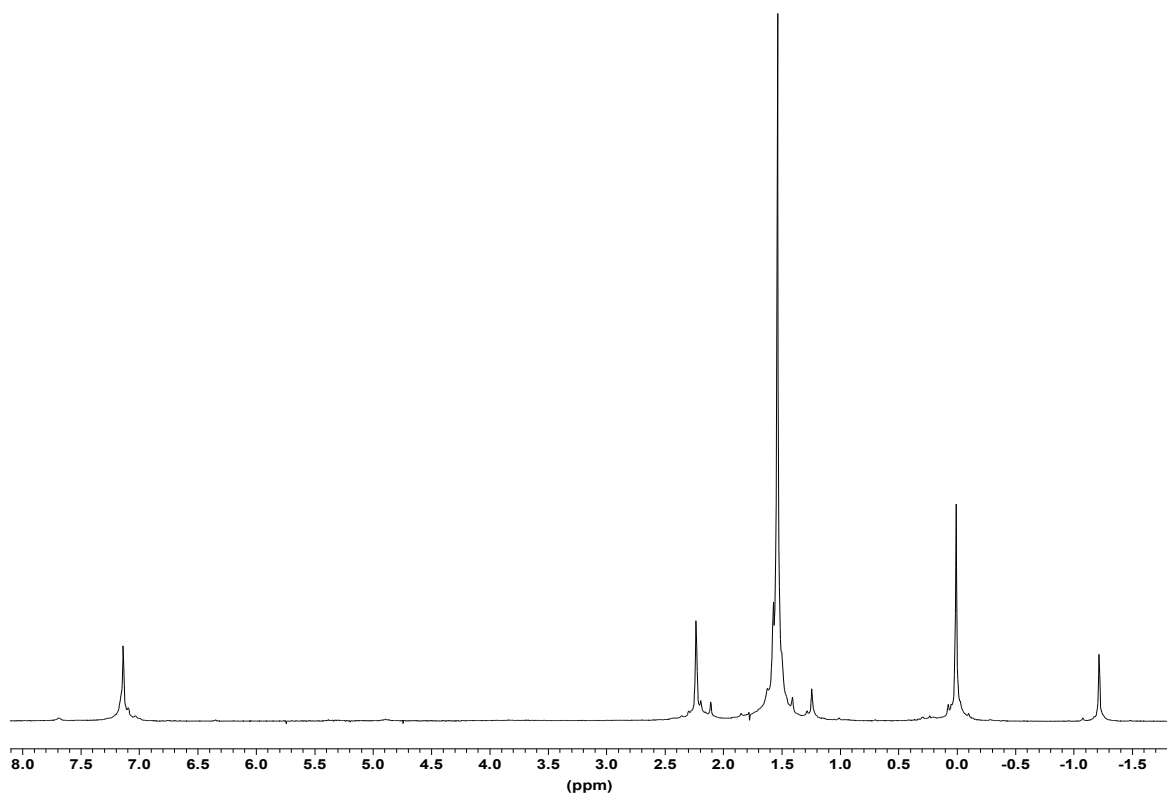
Appendix 17. ^1H NMR spectrum of $[(n\text{-Hex})\text{Mg(O-2,6-}t\text{Bu}_2\text{-4-Me-Ph})]_2$ (**16**) in C_6D_6 at 23 °C.



Appendix 18. ^{13}C NMR spectrum of $[(n\text{-Hex})\text{Mg(O-2,6-}t\text{Bu}_2\text{-4-Me-Ph})]_2$ (**16**) in C_6D_6 at 23 °C.



Appendix 19. ^1H NMR spectrum of $[(\text{Me}_3\text{SiCH}_2)\text{Mg}(\text{O}-2,6-t\text{Bu}_2-4-\text{Me-Ph})]_2$ (**18**) in C_6D_6 at 23 °C.



Appendix 20. ^{13}C NMR spectrum of $[(\text{Me}_3\text{SiCH}_2)\text{Mg}(\text{O}-2,6-t\text{Bu}_2-4-\text{Me-Ph})]_2$ (**18**) in C_6D_6 at 23 °C.

Summary

Since the major discovery of Ziegler and Natta in the 1950's, organometallic polymerization catalysis gave rise to unprecedented industrial and academic interest. The appearance of homogeneous metallocene catalysts ($(\eta^5\text{-C}_5\text{R}_5)_2\text{MR}$, M = Ti, Zr) allowed highly stereospecific polymerizations and new materials to be synthesized. The last decade witnessed the development of lanthanocene catalysts ($(\eta^5\text{-C}_5\text{R}_5)_2\text{LnR}$). Besides a high activity in ethylene polymerization, they allow the living syndiotactic polymerization of methyl methacrylate (MMA) and diblock copolymerization of polar-non polar monomers.

In this context, our work was aimed at developing post-lanthanocene catalysts for olefin polymerization, based on the *in situ* combination of a lanthanide alk(aryl)oxide and a dialkylmagnesium reagent. For this purpose, we synthesized and characterized a set of new neodymium alk(aryl)oxides. Among them, the trinuclear $\text{Nd}_3(\text{OtBu})_9(\text{THF})_2$ complex proved versatile and exhibited the most interesting catalytic features.

Thus, combined with di-*n*-hexylmagnesium, $\text{Nd}_3(\text{OtBu})_9(\text{THF})_2$ enables the pseudo-living syndiotactic polymerization of MMA ($M_w/M_n < 1.10$ and rr = 75-80%). Interestingly, ethylene can also be polymerized with a moderate activity (5-10 kgPE/molNd/atm/h) under mild conditions, yielding highly crystalline linear polyethylenes with high molecular weights ($M_n = 200,000\text{-}2,000,000$). The molecular weights can be reduced on using transfer agents such as molecular hydrogen and phenylsilane. The most remarkable feature of this catalyst system is the synthesis of high molecular weight poly(ethylene)-*b*-poly(methyl methacrylate) diblock copolymers with significant PMMA contents. Furthermore, it provides butadiene polymerization and its diblock copolymerization with glycidyl methacrylate. However, for this application the best results were obtained with $\text{Nd}(\text{O-2,6-}t\text{Bu}_2\text{-4-Me-C}_6\text{H}_2)_3(\text{THF})$ as precursor, which allows also the statistical butadiene-styrene copolymerization.

The existence of alkyllanthanide species, suggested by the polymerization results, was confirmed by NMR studies and X-ray crystal structure determination of isolated products from neodymium alkoxide/dialkylmagnesium combinations. A general mechanism for activation/deactivation pathways observed with this unique catalyst system is proposed based on these results.

Keywords: Polymerization Homogeneous catalysis Lanthanide alk(aryl)oxide
Dialkylmagnesium Ethylene MMA Butadiene
Copolymerization Organometallic complexes

Résumé

Depuis la découverte majeure de Ziegler et Natta dans les années 50, la catalyse de polymérisation utilisant des complexes organométalliques n'a cessé de susciter un vif intérêt dans les centres de recherches académiques et industriels. L'homogénéisation des systèmes catalytiques a permis d'accroître davantage la stéréospécificité des polymérisations et de synthétiser de nouveaux matériaux jusque-là inaccessibles. Parmi ces catalyseurs homogènes, les catalyseurs de type lanthanocénique offrent l'avantage d'être actifs en absence de co-catalyseur tel que le MAO. De plus, ils permettent la polymérisation vivante et hautement syndiotactique du méthacrylate de méthyle ainsi que sa copolymérisation dibloc avec des monomères apolaires.

C'est dans ce contexte que nous avons cherché à développer de nouveaux catalyseurs post-lanthanocéniques. Notre attention s'est portée sur l'utilisation d'alcoolates/phénates de lanthanide, précurseurs qui ont été synthétisés et entièrement caractérisés. L'association de tels alcoolates à un dialkylmagnésien s'est avérée particulièrement efficace, la combinaison $\text{Nd}_3(\text{OtBu})_9(\text{THF})_2/\text{di-}n\text{-hexylmagnésium}$ se révélant la plus intéressante de part sa versatilité et son activité.

En effet, ce système est actif pour la polymérisation pseudo-vivante et syndiotactique du méthacrylate de méthyle. Il conduit aussi à la polymérisation de l'éthylène avec une activité modérée, produisant des polyéthylènes hautement cristallins et de haute masse molaire. Cependant, le principal atout de ce système catalytique réside dans la possibilité de préparer efficacement des copolymères diblocs PE-*b*-PMAM de haute masse molaire. Ces copolymères ont été caractérisés par des méthodes d'analyse classiques (GPC, RMN et DSC) ainsi que par microscopie (AFM et SEM). La polymérisation stéréospécifique 1,4-*trans* du butadiène et sa copolymérisation dibloc avec le méthacrylate de glycidyle ont aussi été étudiées. Toutefois, les meilleurs résultats ont été obtenus avec $\text{Nd}(\text{O-2,6-}t\text{Bu}_2\text{-4-Me-C}_6\text{H}_2)_3(\text{THF})$, qui a permis en plus la copolymérisation statistique butadiène-styrène.

L'étude par RMN et par diffraction RX de produits isolés à partir de combinaisons alcoolate/phénate de néodyme/dialkylmagnésium a confirmé l'existence d'une espèce initiatrice de type alkyl-lanthanide. Un cycle catalytique, rendant compte des processus d'activation/désactivation observés avec ce nouveau système a ainsi pu être proposé.

Mots-clés : (Co)-Polymérisation Catalyse homogène Alcoolate de lanthanide
Dialkylmagnésien Ethylène MAM Butadiène
Complexes organométalliques